■ SESSION: D [DF1]
4월 19일 (목), 12:30 - 14:15
휘닉스1

DF-01(초) **Isomerization of Azobenzene Molecules Studied with Scanning Tunneling Microscopy and Spectroscopy** KUK Young, CHOI B.-Y., CHOI Y.S., KIM H. W.(*School of Physics and Astronomy, Seoul National University, Seoul, 151-747, Korea.*) Isolated or ordered molecules of azobenzene were studied with scanning tunneling microscopy and spectroscopy. Spatially resolved electronic structures give much information on the substrate-molecule interaction and the inter-molecular interactions. The geometric structures, the registries on metal surfaces and dynamics during a conformal transformation were also studied. Depending on the registries on metal surfaces and the transformation pathways in space and time were found to be different for isolated molecules and ordered molecules due to their molecule-molecule interactions. HOMO, LUMO and HOMO or LUMO derive states on metal surfaces were mapped spatially to find the correlation between bonding with neighboring molecules and the conformal transformation. These STM/STS results show good agreement with the DFT calculation results.

1. B.-Y. Choi, S.-J. Kahng, S. Kim, H. Kim, H. W. Kim, Y. J. Song, J. Ihm and Young Kuk, "Conformational Molecular Switch of Azobenzene Molecule: A Scanning Tunneling Microscopy Study," Phys. Rev. Lett. 96, 156106 (2006)

DF-02(초) **Reaction Mechanism of One-Dimensional Molecular Wires on the H-Terminated Si(001) Surface** 조 준형(*한양대학교 물리학과.*) We present a facile method for the self-directed growth of 1D molecular lines on the H-terminated Si(001) surface. The present method overcomes the existing problems in the self-directed growth process. Unlike the previous approach which employed a single dangling bond as the reaction site, we here employ an H-free Si dimer which can be generated with the tip of the STM. For the reaction with the H-free dimer, we chose the O-phthalaldehyde ($C_8H_6O_2$: OP) molecule containing two carbonyl groups. The radical intermediate which is formed with two Si-O bonds between the carbonyl oxygens and the H-free Si atoms is found to be significantly more stabilized as compared to those of various alkenes which have a single Si-C bond. As a result, the present radical intermediate successfully achieves H-atom abstraction without its desorption, thereby allowing the chain reaction. The resulting OP line which is strongly bonded to the Si dimers with two Si-O bonds per molecule will survive heating up to higher temperatures compared to the previously reported alkene lines which have a single Si-C bond per molecule. In addition, we propose a self-assembly technique for fabrication of the heterogeneous molecular wire on the dangling-bond wire generated on an H-passivated Si(001) surface. Here, we choose pyridine and borine as Lewis base and acid molecules, respectively, to demonstrate different behaviors in the chemical reactivity and selectivity on the dangling-bond wire, leading to formation of the heterogeneous pyridine-borine wire.

DF-28(초) **Chemical Sensing Mechanisms of Organic Thin-Film Transistors and Novel Techniques for Analytes Identification** YANG Richard D., GREDIG T., PARK Jeongwon, COLESNIUC Corneliu N., SCHULLER Ivan K., TROGLER William C., KUMMEL Andrew C.(*Departments of Chemistry, Physics, and Materials Science, University of California, San Diego, La Jolla, CA 92093.*) Organic chemically sensitive field-effect transistors (ChemFETs) have shown detection limits to parts per billion (ppb) to gases such as NO_2. However, their chemical sensing mechanisms are still not well understood in. We have developed a basic understanding of the enhancement of sensitivity and selectivity of ChemFETs compared to chemoresistive sensors made from the same sensing material. Low-voltage operating CuPc thin-film transistors have been fabricated for the sensing studies. We have observed that the sensitivity and selectivity of chemFETs can be tuned by the gate voltage. At low gate voltage, the ChemFET sensitivity is found to be dominated by analyte induced changes in the threshold voltage; however, at high gate voltage, the sensitivity is dominated by analyte induced changes in the mobility. We propose a unified sensing model to explain these phenomena: analytes absorbed by CuPc films displaced surface bound oxygen molecules and create trap states and fixed charge. We have taken advantage of the analyte induced change in trap energy by fabricating devices with ultrathin organic channels Compared to thick channel devices, the ultrathin transistors show faster response times, higher baseline stabilities in the presence of analytes, and sensitivity enhancements of 1.5 - 20 for the five analytes tested. The absorption of analytes changes both the surface doping level and trap energies.

The changes in surface trap energies greatly perturb the charge transport properties of the ultrathin devices, thereby, making these devices more sensitive.

DF-03 **Effect of Quantum Well States on Adsorption of Gas Molecules** 김 원동, 한 상욱, 이 도현, 황 찬용, 민 철희[1], 이 한길[2], 김 형도[2](*한국표준과학연구원. [1]서울대학교 물리학과. [2]포항가속기연구소.*) The physical and chemical properties of metal such as superconductivity, magnetism, Kondo effect, gas adsorption, etc. are strongly related with the density of states at the Fermi level. By making an atomically uniform thin film satisfying some specific boundary conditions, quantum well states can be formed in which electrons in that film are bound along the normal direction of the film surface. Then, the intensity of density of states at Fermi level oscillates according to thin-film thickness to show quantum size effect. We investigated the effect of this oscillation on adsorption of CO molecules in case of the Cu/Co/Cu(100) sytem. The formation of quantum well states and resulting oscillation of density of states at Fermi level in wedge-shaped Cu/Co/Cu(100) system were confirmed by high resolution photoemission spectroscopy. After adsorption of CO molecules at the substrate temperature 100 K, we observed the change of binding energies of quantum well states. C 1s core level spectra of adsorbed molecules were also measured as a function of temperature for each Cu thickness. The initial feature of the C 1s spectra show well-known three peak structure similar to that of CO moleucles adsorbed on Cu(100). We could determine the desorption temperature of CO molecules for each Cu thickness, and observed clear dependence of the desorption temerature on the density of states of Fermi level.

■ SESSION: D [DG1]
4월 19일 (목), 12:30 - 13:45
금낭화

D-01 **Relation of First-Order Metal-Insulator Transition and Structural Phase Transition Observed by Synchrotron X-ray in VO_2** KIM Hyun-Tak, KIM Bong-Jun, LEE Yong Wook, LIM Jung-Wook, YUN Sun Jin, SHIN Tae-Ju[1], YUN Hwa-Sick[1](*ETRI. [1]POSTECH.*) It has been well-known that VO_2 undergoes both a structural phase transition (SPT) from monoclinic (insulator phase) to tetragonal (metal phase) and a discontinuous first-order metal-insulator transition (MIT) (Jump) near 68°C. When the MIT and the SPT occurs simultaneously, the MIT can be regarded as the Peierls transition. When both take place separately, the MIT can be interpreted as the Mott transition. Peierls transiton and Mott transition in VO_2 remain controversial. We have investigated a relation of the MIT and the SPT which are simultaneously measured by I-V measurement and synchrotron X-ray of the 1B2 line in pohang accelerator Lab., respectively. A used sample is a VO_2-based two terminal device. The result shows that the MIT and the SPT does not occur simultaneously.
(References on the MIT: New J. Phys. 6 (1994) 52 (www.njp.org), Appl. Phys. Lett. 86 (2005) 242101, Physica B 369 (2005) 76, Phy. Rev. Lett. 97 (2006) 266401, Appl. Phys. Lett. 90 (2007) 023515)

D-02 **Structural Phase Transition and Electrical Conductivity in Cholesterol Crystals** 이 광세, 이 해준[1], 김 일원[1](*인제대 나노시스템공학과. [1]울산대 물리학과.*) Electrical conductivity measurements of polycrystalline anhydrous cholesterol ($C_{27}H_{46}O$) were carried out in the temperature range from 0 to 100 °C under an ambient condition. A step change in the conductivity due to a structural phase transition occurs near the body temperature of 37 °C upon heating. Both phases above and below the transition show the insulating behavior and appreciable thermal hysteresis. The weak anomaly indicates nonferroic nature, i.e., conservation of point-group symmetry of this first-order phase transition. The experimental results are discussed on the basis of crystalline structure with no hydrogen bonds in the network. The pyroelectric current and ferroelectric hysteresis measurements are in progress to determine whether or not the low-temperature phase is ferroelectric.

D-03 **Electric Field-induced Structural Modulation of $BiFeO_3$ Multiferroic Thin Films As Studied Using In-situ X-ray Microdiffraction** 박 정웅, 류 상우, 구 양모, 윤 화식[1], 장 현명(*포항공과대학교 신소재공학과. [1]포항가속기연구소.*) An in situ method, called synchrotron X-ray microdiffraction (XRMD), was introduced to examine the electric field-induced structural modulation of the epitaxially grown pseudo-tetragonal $BiFeO_3$ thin film. To evaluate the d-spacing (d_{001}) from the measured intensity contour in the phi-chi space, the peak position

in each diffraction profile was determined by applying two-dimensional Lorentzian fitting. By tracing the change of d-spacing as a function of the applied electric field and by examining the Landau free energy function for P4mm symmetry, we were able to estimate the two important parameters that characterize the field-induced structural modulation. The estimated linear piezoelectric coefficient (d_{33}) at zero-field limit is 15 pm/V, and the effective nonlinear electrostrictive coefficient (Q_{eff}) is as low as ~$8.0x10^{-3}$ m^4/C^2.

D-05 **Reduction of Ferroelectric Polarization in Perovskite Titanium Oxide Superlattices** LEE Jun Hee, KIM Hanchul[1], WAGHMARE Umesh V.[2], YU Jaejun(*Department of Physics and Astronomy and Center for Strongly Correlated Materials Research, Seoul National University, Seoul, 151-747, Korea. [1]Korea Research Institute of Standards and Science, Daejeon, 305-340, Korea. [2]Theoretical Science Unit, Jawaharlal Nehru Centre for Advanced Scientific Research, Jakkur PO, Bangalore 560-064, India.*) We report a theory of ferroelectric polarization in $(BaTiO_3)_n/(SrTiO_3)_m$ superlattices, which takes account of interface effects in ferroelectric heterostructures. We carried out first-principles density functional theory (DFT) calculations for the short-period $(BaTiO_3)_n/(SrTiO_3)_n$ superlattices with n=1~5 and further performed an effective model analysis based on the Ginzburg-Landau free energy formalism. Contrary to the previous predictions by the macroscopic polarization theory[1,2] based on electrostatic coupling among individual constituents, we found a drastic decline of the average polarization as each component layer of the superlattice is reduced to a single unit-cell-thick layer. The origin of such polarization reduction is identified to be the depolarization field and the anti-ferroelectric reconstruction at the interface. The depolarization field arising from polarization mismatch plays an important role on the enhancement of overall average polarizations in ferroelectric superlattices, while the atomic relaxation at the interface makes a significant contribution to the polarization reduction in the short-period $(BaTiO_3)_n/(SrTiO_3)_n$ superlattices.

■ SESSION: D [DF2]
4월 19일 (목), 12:30 - 14:30
벌개미취1

DF-04(초) **Basic and Application of the Spin Transfer Torque** 유 천열, 이 경진[1](*인하대학교 물리학과. [1]고려대학교 신소재공학부.*) 강자성체에 스핀 분극 된 전류를 인가할 때, 전도성 스핀들과 국소 스핀들 간의 각운동량 보존 법칙에 의해 소위 스핀 트랜스퍼 토크 (STT: spin transfer torque) 현상이 일어난다. 이 STT에 의해 국소 스핀의 방향을 전도성 스핀, 즉 전류를 이용해 조절 할 수 있게 되어 새롭고 흥미로운 물리적 현상들이 발현된다. 강자성층/비자성층/강자성층의 다층박막 구조에서는 인가된 전류에 의해 강자성층의 자화방향을 역전 시킬 수 있는 전류인가 자화역전 (current induced magnetization switching) 및 가변 공명주파수와 높은 Q-factor를 특징으로 하는 마이크로웨이브 발진의 현상이, 나노와이어 구조에서 나타나는 전류인가 자벽이동 현상 등이 이론적으로 예측되고 실험적으로 검증 되었다. 이 흥미로운 STT의 물리적 원인 및 관련된 현상들에 대한 기본적인 고찰과 함께 STT의 다양한 응용 가능성에 대해서 논하고자 한다.

DF-05(초) **Current-induced magnetic domain-wall motion by spin transfer torque: Collective coordinate approach with domain-wall width variation** 이 현우, 정 순욱(*포항공과대학교 물리학과.*) The spin transfer torque generated by a spin-polarized current can induce the shift of the magnetic domain-wall position. In this work, we study theoretically the current-induced domain-wall motion by using the collective coordinate approach [Gen Tatara and Hiroshi Kohno, Phys. Rev. Lett. 92, 86601 (2004)]. The approach is extended to include not only the domain-wall position and the polarization angle changes but also the domain-wall width variation. It is demonstrated that the width variation affects the critical current.

DF-06(초) **CIMS Devices for the Use of STT-MRAM** 신 경호(*한국과학기술연구원.*) 본 발표에서는 '차세대 반도체'가 가져야할 특성 중, 외부전원이 차단된 상태에서도 정보를 유지하는 '비휘발성'과 정보 저장과 처리를 동시에 구현할 수 있는 '유니버설'이라는 특성이 얼마나 중요한가?, 차세대 메모리의 제품군에는 어떠한 것들이 있으며 그 장단점은 무엇인가?, 비휘발성 유니버설 메모리로서 자기식 RAM(이하, MRAM)이 각광을 받고 있는 까닭은 무엇인가?, MRAM을 '고밀도화하기 위해서는 어떠한 장벽을 극복해야 하는가?, 전류구동형 자화스윗칭(이하, CIMS; Current Induced Magnetization Switching)이 MRAM 고밀도화를 성취하는데에 있어서 얼마나 유용한가?, CIMS의 작동원리와 CIMS 소자의 실용화를 위하여 극복해야할 문제점들은 어떠한 것들이 있는가?,

MgO 절연층을 가지는 자기터널접합(MTJ; Magnetic Tunnel Junction)의 출현 배경과 CIMS 소자의 실용화에 미치는 영향은 얼마나 지대한가?, MgO-based MTJ는 어떻게 만들며 그 특성은 어떠한가?, 그리고 STT-MRAM에 대한 기술적, 산업적 전망은 어떠한가?, 등에 대하여 논하고자 한다.

DF-07(초) **Recent studies on spin-torque-related (transport) experiments** JUNG Myung-Hwa(*Quantum Material Research Team, Korea Basic Science Institute, Deajeon 305-333, Korea.*) 스핀토크 기술과 관련된 microwave device 중에서 magnetic nano-oscillator와 spin-torque diode에 관해서 설명하고, straight nanowire, notch를 가지고 있는 straight nanowire, curved nanowire, semicircular nanowire 등에서 보이는 domain wall motion에 대해서 설명하고자 한다. 더불어 최근에 우리팀에서 연구한 스핀토크 관련 실험 결과에 대해서 논의하고자 한다.

DF-08(초) **Experimental Tools for Current-Induced Domain Wall Dynamics** CHOE Sug-Bong(*Seoul National University, School of Physics and Astronomy.*) This talk overviews the recent experimental progress of the current-driven domain wall motion (CIDWM). It will be organized by magnetic-field-assisted CIDWM [1], CIDWM without magnetic field [2], pulsed current CIDWM [3], imaging [4,5] and time-resolved observation [6,7]. Finally, the prospect will be given.

[1] M. Tsoi et al., Appl. Phys. Lett. 83, 2617 (2003).
[2] J. Grollier et al., Appl. Phys. Lett. 83, 509 (2003).
[3] M. Klaui et al., Phys. Rev. Lett. 94, 106601 (2005).
[4] A. Yamaguchi et al., Phys. Rev. Lett. 92, 077205 (2004).
[5] M. Klaui et al., Phys. Rev. Lett. 95, 026601 (2005).
[6] M. Hayashi et al., Phys. Rev. Lett. 96, 197207 (2006).
[7] G. S. D. Beach, et al., Phys. Rev. Lett. 97, 057203 (2006).

DF-09(초) **Direct imaging of domain wall motion driven by spin-torque using X-ray microscopy** KIM Dong-Hyun, MEIER Guido[1], BOLTE Markus[1], EISELT René[1], KRÜGER Benjamin[2], LEE Kyung-Jin[3], FISCHER Peter[4](*Chungbuk National University, Dept. of Physics. [1]Universität Hamburg, Institut für Angewandte Physik. [2]Universität Hamburg, Institut für Theoretische Physik. [3]Korea University, MSE Dept. [4]Lawrence Berkeley National Lab, Center for X-Ray Optics.*) Domain wall motion driven by spin-transfer torque in ferromagnetic structures has been imaged using soft X-ray transmission magnetic microscopy. Domain wall motion with applying ns-pulse of spin-polarized current is visualized for several permalloy patterns such as rings and rectangles with 25-nm spatial resolution and 70-ps temporal resolution, providing a fundamental insight to fast dynamics of domain wall fueled by spin-transfer torque.

■ SESSION: D [DG2]
4월 19일 (목), 12:30 - 13:45
벌개미취3

D-07 **Magnetism in oxide semiconductors** HWANG Chanyong, HAN Sangwook, LEE Dohyun, KIM Wondong, HONG Jisang[1](*Korea Research Institute of Standards and Science. [1]Pukyung National University, Department of Physics.*) There have been a lot of interests in the ferromagnetism of wide band gap oxide semiconductors for the possible application in spintronic device at room temperature. Especially, transition metal doped ZnO or TiO_2 has drawn a lot of attention. However the origin of the ferromagnetic order and the local spin site information is still under debate. Experimental results are controversial; opposite results in the same system. And the corresponding theories cannot be described by the unified picture. We have recently found the local origin of the spin site using MCD. Also this system shows strong magnetic anisotropy. Possible origin of the long range ferromagnetic order will be discussed.

D-08 **A device for polarizing neutrons with a high efficiency** 조 상진, 이 창희, 김 학노, 류 재삼, 박 주환(*한국원자력연구소.*) Using a general polarizing neutron guide, neutrons with only one spin status will be transmitted and used. This work is related to a polarizing neutron guide, solving a problem of a low yield of 50% by employing an ingenious device composed of two different type of polarizing mirrors (normal with FeCo/Si and reverse type with Co/Cu). The simulation results of this device for the neutron gain and divergence will be described in this presentation.

D-09 **Magnetic properties of (Zn,Cu)O dilute magnetic semiconductor** 홍 지상, 김 동유(*부경대학교*

물리학과.) Using full potential linearized augmented plane wave (FLAPW) method, we have investigated magnetic properties of (Zn,Cu) O dilute magnetic semiconductor. It has been found that the physical property of exchange coupling among randomly disctibuted Cu atoms is dependent Cu-Cu distance. In addition, theoretically calculated X-ray magnetic circular dichroism (XMCD) is presented.

D-10 **중희토류 기반의 $(TbBi)_3Fe_5O_{12}$, $(HoBi)_3Fe_5O_{12}$의 4f 궤도모멘트 변화가 미치는 초교환 상호작용 변화에 대한 연구** 박 일진, 고 태준, 김 철성 (*국민대학교, 물리학과.*) 희토류 금속 중 중희토류인 terbium과 holmium을 기본으로 하여 bismuth가 일정량 치환된 iron garnet 분말시료를 졸-겔법을 이용하여 제조하였다. 시료의 조성은 $Tb_2Bi_1Fe_5O_{12}$, $Ho_2Bi_1Fe_5O_{12}$ 으로 두 시료의 bismuth, iron, oxide의 조성은 같게 하고, 중희토류 자리(24c)의 조성만을 다르게 하여 시료를 제조하였으며, 두 시료의 결정학적 및 자기적 특성을 비교 연구하였다. 두 시료의 x-선 회절 분석 결과 결정구조는 Ia3d의 space group을 갖는 cubic 구조임을 알 수 있었고, $Tb_2Bi_1Fe_5O_{12}$의 격자상수는 12.499 Å, $Ho_2Bi_1Fe_5O_{12}$ 12.462 Å로 각각 결정되었다. 상온에서 진동 자화율 측정기(VSM) 측정 결과, 시료의 포화자화 값은 $Tb_2Bi_1Fe_5O_{12}$는 10.234 emu/g, $Ho_2Bi_1Fe_5O_{12}$ 는 14.404 emu/g 로 $Ho_2Bi_1Fe_5O_{12}$ 가 포화자화 값은 다소 크게 보인 반면, 보자력은 $Tb_2Bi_1Fe_5O_{12}$가 56.57 Oe, $Ho_2Bi_1Fe_5O_{12}$가 32.33 Oe로 $Ho_2Bi_1Fe_5O_{12}$의 경우가 다소 작게 측정되었다. 상온에서 자성특성에 영향을 미치는 철의 조성변화가 없음에도 두 시료의 포화자화값과 보자력이 차이를 보이는 것은 두 희토류 금속의 치환에 따라 초교환 상호작용의 세기가 다른 것으로 분석된다. 상온에서의 뫼스바우어 스펙트럼 분석결과, 초미세 자기장의 값이 $Tb_2Bi_1Fe_5O_{12}$가 498 KOe(16a), 413 KOe(24d)로 분석되었고, $Ho_2Bi_1Fe_5O_{12}$가 494 KOe(16a), 409 KOe(24d)로 분석되어 초미세 자기장값은 두 시료가 큰 차이를 보이진 않았다.

■ SESSION: D [DF3]
4월 19일 (목), 16:30 - 18:15
휘닉스1

DF-10(초) **Organic Functionalization of Semiconductor Surface** 김 안순, 김 세훈[1](*한국전자통신연구원, 나노바이오전자소자팀. [1]한국과학기술원, 화학과.*) The organic functionalization of semiconductor surfaces is a burgeoning area of surface science which is poised to play a major role in the creation and development of revolutionary molecule-based semiconductor devices. The incorporation of organic molecules with specific properties at the semiconductor interface has the potential to add novel functionalities to chemical, biological, and electronic devices. In an attempt to understand the reactivity, structure, and interfacial properties of such hybrid organic-semiconductor systems, investigations of the covalent attachment of model organic molecules to vacuum-prepared semiconductor surfaces need to be completed. This presentation will focus on systematic surface reactions of organic molecules with semiconductor surfaces according to various functional groups using vapor phase delivery in a dry processing environment. We will show the surface reactions of simple alkene to form surface-carbon covalent bond and selectivity of bifunctional molecules on the surface. Finally, the layer-by-layer growth method to form an ultrathin film on the surface via spontaneous chemical reaction will be presented.

DF-11(초) **Adsorption of Simple Molecules on Si Surfaces: Long and Cold Look** 여 인환, 정 천형, 정 우진, 염 한웅, 유 병덕[1](*연세대 물리학과. [1]서울시립대 물리학과.*) Understanding gas-surface interaction is crucial not only fundamentally, but also technologically to areas as diverse as molecular electronics to catalysis. Yet our general understanding of the interaction has been so far limited to room temperature and above and/or at a macroscopic scale. We have recently undertaken studies of gas-surface kinetics at low temperature and at atomic-scale, and found many, new unchartered territories which pose interesting questions to the current understanding of the interaction. In this talk, we will present our studies on adsorption of oxygen and ethylene molecules on the technologically important Si(001)-c(4×2) surface using low temperature scanning tunneling microscopy. At the early stage of oxygen adsorption, reactions with Si atoms at S_B steps are dominant over those at terraces by more than 2 orders of magnitude, and they proceed in two distinct stages to high oxidation states, through the formation of -Si-O- chain structures along the step edge. On the other hand, ethylene molecules dosed at 50 K decay thermally to "di-σ" chemisorption states, which exhibits Arrhenius behavior with a small reaction barrier. Surprisingly the decay rate is found 10 orders of magnitude lower than a conventional estimate. Such a large suppression of the reaction

rate is interpreted by the entropic bottleneck at the transition state induced by the free-molecule-like trap state. Our studies suggest that the free-molecule-like trap state may be quite general, including the case of oxygen molecules, and that the entropic bottleneck plays a crucial role at low temperature reactions.

DF-12 **Electronic Structure of Fe-Pt surface alloy** HAN Sang Wook, LEE Dohyun, KIM Wondong, HWANG Chanyong, HWANG Han Na[1], HWANG C. C.[1], HONG J.S.[2], KIM Hanchul(*Korea Research Institute of Standards and Science. [1]Pohang Accelerator Laboratory. [2]Department of Physics, Pukyung National University.*) Previously, we have shown two types of surface alloy structure of FePt on top of Pt(110)-(1x2) surface using scanning tunneling microscopy. The atomic structures of these surface alloys have been also confirmed by the surface core level spectroscopy using synchrotrn radiation. Comparison of these results with the results from the first principles calculation enables the origin of these surface phase transition. More detailed analysis on its valence band from angle-resolved photoemission spectroscopy will be given.

DF-13 **Surface dipole layer induced by pentacene overlayer adsorbed on the silicon substrate: A combined experimental and theoretical study** 정 호진, 정 덕용, 염 한웅(*연세대학교, 원자선 원자막 연구단.*) Pentacene (Pc) is a polyaromatic hydrocabon molecule consisting of five linearly fused benzene rings. It is one of the most important material for the development of organic electronics. Since the energy barrier for charge carrier injection from a substrate to organic molecules open determines the performance of a device, it is a crucial to understand the organic/semiconductor interface. In the present study, we have carefully investigated the electronic structure of Pc on silicon substrates by using the high-resolution photoelectron spectroscopy (PES) combined with density-functional theory (DFT) calculations. From the PES, we have observed that C 1s core level binding energy with respect to the Si 2p is systematically shifted to high binding by ~0.2 eV and the work function of the surface is reduced about 1.0 eV as the Pc coverage increases upto 1 ML. These results imply that the surface dipole moment induced by adsorption of Pc is aligned upward. This is against the simple charge transfer picture since the electronegativity of carbon is much higher than that of silicon. In order to solve this puzzling problem, we have performed DFT calculations for the PC on the Si(001) surface. From the dipole moment calculations and charge density analyses, it is revealed that the unexpected dipole formation originates from the molecular distortion and electron rearrangement due to the di-σ bond formed between C and Si atoms. The detailed experimental and calculated results will be presented.

DF-14 **End group functionalization and electronic transport in organic molecular devices** KIM Gunn, LU Wenchang[1], WANG Shuchun[1], BUONGIORNONARDELLI Marco[1], BERNHOLC Jerzy[1](*Department of Physics, Sungkyunkwan University. [1]Department of Physics, North Carolina State University, Raleigh, NC, USA.*) Using first-principles calculations we have investigated the mechanism of metal/molecule coupling and itsinfluence on the electronic transport properties in the prototypical case of long hydrocarbon (alkane) chainssandwiched between gold contacts. The results show that the end group functionalization (amine vs. thiol) plays acrucial role in controlling the electronic transport through the molecule. The effective contact resistance of theamine/Au system is initially much smaller than that of the thiol/Au one, giving rise to a large difference in thecurrent-voltage (I-V) characteristics at low bias. This order is reverse above a bias of 1V, where weobserve a crossover in the I-V curves for the thiol/Au and amine/Au systems.

■ SESSION: D [DG3]
4월 19일 (목), 16:30 - 17:45
금낭화

D-11 **Thallium Nanodot Arrays on Si(111)-7x7** LEE Geunsik, KIM Jai Sam, JHI Seung-Hoon(*POSTECH, Physics.*) Self-assembled nanoclusters have attracted much research interests due to potential applications in microelectronics, ultrahigh-density recording, and nanocatalysis. In this talk, we present the study on the stability of thallium nanocluster on Si(111)-7x7 for various number of atoms (N=1,2,...,10) within each cluster using DFT total energy calculations. We compare this with clusters of other group III elements (Al, Ga, In). We found that the adsorption energy has minima at N=3, 9

with Tl atoms, whereas N=6 is favored by other group III elements. The energy barrier of Tl atom diffusion for N=9 cluster is 0.02~0.03 eV/Tl which is comparable to the room temperature energy. Our results are consistent with the experiment [Vitali et al., Phys. Rev. Lett. 83, 316 (1999)] in that the Tl cluster consists of nine adatoms and Tl atoms are mobile at room temperature.

D-12 **Molecular Dynamics Study on the Sputtering Characteristics of MgO Surfaces** AHN Hyo-shin, CHO Eunae, HAN Seungwu, CHO Youngmi[1], KIM Changwook[1](*Department of Physics, Ewha Womans University. [1]CAE, Samsung SDI.*) In the plasma display panel (PDP), the protective layer made of MgO thin film is a critical component for lowering the operation voltage and extending the lifetime, and hence tremendous efforts are now being invested toward understanding material properties related to the display performance. One of the most important roles of the MgO film is the protective layer for dielectric substrate. We study sputtering yields of MgO (100) surface due to the low-energy incoming ions such as He, Ne, and Xe atoms by employing molecular dynamics simulations. The low-energy scattering behavior is not accurately addressed by existing pair potentials such as Molière or university potentials. Therefore, the interaction potential between noble gases and magnesium or oxygen atoms are fitted to reproduce the first-principles reference values. We report sputtering yields, which is an important criterion to estimate erosion rate of protective layer, with respect to the energy, incoming directions, and species of impinging ions.

D-13 **First-principles studies of defect-induced electronic states in NiO (001) surface** JEONG Hogyun, YU Jaejun(*Seoul National University.*) Metal-oxide surfaces are important in technological applications such as catalysts and sensors. To probe the electronic and magnetic properties of NiO (001) surface, especially at the presence of vacancies and adatoms, we carried out first-principles electronic structure calculations for the NiO(001) by using the LDA+U method implemented in the LCPAO (linear combination of pseudo-atomic orbitals) method. Our results for the clean surface are found to be consistent with the previous result of LMTO calculations. The detailed electronic and magnetic structures of various defects in NiO (001) surface are presented. From the results, it is shown that the characteristics of defect-induced states vary quite depending on the type of defects, e.g., Ni-vacancy, O-vacancy, Ni-adatom, and O-adatom.

D-14 **Novel Spin-Orbit Coupled Electronic Ground State in Insulating Sr_2IrO_4** JIN Hosub, YU Jaejun(*Department of Physics and Astronomy and CSCMR, Seoul National University, Seoul, Korea.*) We present our first-principles LDA+U calculations and the theoretical model for the insulating Sr_2IrO_4 system. In contrast to thesuperconducting and metallic ground states in Sr_2RuO_4 and Sr_2RhO_4, theinsulating nature of Sr_2IrO_4 has been considered as surprising and unexpected when the extended nature of Ir 5d state is considered. To investigate the electronic structure of Sr_2IrO_4, we performed LDA+U calculations where both on-site Coulomb interactions and spin-orbit couplings are taken into account. From the results, the spin-orbit coupling in Ir 5d is found to play a crucial role in determination of the ground state of Sr_2IrO_4. It is shown that neither the on-site U nor the spin-orbit term only can explain the insulating feature of Sr_2IrO_4. An interesting interplay between the two competing interactions is found to determine the spin and orbital configuration, leading to a novel insulating ground state. To understand the nature ofthe ground state, we suggest a minimal model for the t_{2g} manifold based on the tight binding Hamiltonian.

■ SESSION: D [DF4]
4월 19일 (목), 16:30 - 18:00
벌개미취3

DF-15(초) **Foundation of Quantum Theory and Mesoscopic Physics** 강기천(*전남대 물리학과.*) 양자역학의 근본문제들을 중시계 물리학에서 어떻게 연구할 수 있는가에 대해논의한다. 중시계 간섭계에서의 양자수송 현상을 통해 얽힘(entanglement), 양자측정(quantum measurement), 상보성(complementarity), 비국소성(nonlocality) 등에 대한 탐구를 하는 구체적인 방법을 소개한다 [1-3]. (References: [1] Kicheon Kang and G. L. Khym, Entanglement, measurement, and conditionalevolution of the Kondo singlet interacting with a mesoscopic detector, New J. Phys. (submitted). [2] Kicheon Kang, An Electronic Mach-Zehnder Quantum Eraser, to appear in Phys. Rev. B

(quant-ph/0607031). [3] G. L. Khym and Kicheon Kang, Charge Detection in a Closed-Loop Aharonov-Bohm Interferometer, Phys. Rev. B 74, 153309 (2006).)

DF-16(초) **Non-trivial dc currents: pumps, ratchets, rectifiers** 김 상욱(*부산대학교.*) Everybody know an applied dc bias generates a dc current. Sometimes a non-trivial dc current can occur by breaking a detailed balance in a sophisticated way. I will review several mechanisms to obtain the non-trivial dc currents; quantum pumps, quantum and classical ratchets, quantum rectifiers, and so on.

DF-17(초) **아하로노프-봄 전자간섭계의 전자 행로 탐지에 대한 위상어긋남 특성** 장 동인, 김 경락[1], 강 기천[1], 정 윤철[2], 이 후종, 서 민기[2], MAHALU D.[3], UMANSKY V.[3], HEIBLUM M.[3](*포항공과대학교 물리학과. [1]전남대학교 물리학과. [2]부산대학교 물리학과. [3]Weizmann Institute of Science, Israel.*) 입자가 보이는 파동성은 입자가 택할 수 있는 여러 가능한 행로를 구별할 수 없는 경우에 한해서 발현되는 것으로 알려져 있다. 본 연구에서는, 전자의 파동-입자 이중성을 면밀히 검증하기 위해, GaAs/AlGaAs 이종접합의 이차원전자계에 게이트를 얹어 제작한 닫힌-고리-구조의 아하로노프-봄 형 전자간섭계를 이용하였다. 전자의 행로 탐지기는 전자간섭계의 한 쪽 팔에 삽입시킨 양자점 (quantum dot)과 이와 근접하여 위치시킨 양자점접촉 (quantum point contact)으로 구성하였다. 여기서 양자점은 간섭계의 한 쪽 팔로 통과하는 전자를 일시적으로 가두어 이로 인해 발생하는 양자점접촉의 전도 변이를 측정하여 양자점이 삽입된 팔로 전자가 통과하는 것을 탐지할 수 있게 한다. 이러한 전자의 행로 탐지는 필연적으로 전자 간섭계를 주변환경과 연계시킴으로써 양자점을 통과하는 전자의 상태에 위상어긋남 (dephasing)을 유발하여, 입자 파동성 발현의 징표라고 할 수 있는 전자의 간섭현상을 감퇴시키는 결과를 가져 온다. 그러나 위상어긋남의 메커니즘은 그란 논란이 되어 왔다. 즉, 위상어긋남이 전자 행로에 대한 정보 자체에 의한 것인지, 아니면 행로 탐지 중에 발생하는 운동량 전이에 의한 것인지에 관한 논의가 그것이었다. 후자의 경우는 불확정성 원리를 통한 입자-파동성의 상보성과 관련이 있다. 본 발표에서는 이미 보고된 바 있는 열린-고리-구조의 전자간섭계가 보이는 전자 행로 탐지에 의한 위상어긋남 [1]과 본 연구의 닫힌-고리-구조 전자간섭계가 보이는 위상어긋남의 차이점의 비교에 논의의 초점을 맞출 예정이다.
[1] E. Buks et al. Nature 391, 871 (1998).

■ SESSION: D [DS1]
4월 19일 (목), 20:30 - 22:00
휘닉스1

DS-01(초) **한국 응집물질물리학의 현 위치 및 일류화를 위한 제언: 정책과제 연구결과 발표** 박 용섭(*경희대 물리학과.*)

DS-02(초) **한국의 기초연구 지원: 그 생태계 현황과 문제점** 정 옥희(*순천대 물리학과, 전 과학재단 전문위원.*)

DS-03(초) **일류화로 가는 길: 기초연구 기반 구축의 방향과 대책** 김 승환(*포항공대 물리학과.*)

■ SESSION: D [DT1]
4월 19일 (목), 20:30 - 21:30
토파즈

DT-01(초) **Angle Resolved Photoemission Spectroscopy를 이용한 고체물리 연구** 김 창영(*연세대.*) 지난 15년간 angle resolved photoemission spectroscopy (ARPES)는 많은 발전을 하였다. 이에 따라 ARPES는 고체물리 특히 강상관 물질계 연구에서 중요한 실험 방법으로 자리 잡았으며 ARPES를 이용한 실험 분야에서 중요한 많은 논문들이 나오고 있다. 국외에서 이러한 일이 일어나고 있는 동안, 국내에서는 상대적으로 ARPES가 미개척 분야로 남아 있다. 이번 발표에서는 비 전문가를 대상으로 기본적인 원리, 실제 실험 방법 등을 중심으로 ARPES에 대한 전반적인 소개를 하려고 한다.

■ SESSION: D [DF5]
4월 20일 (금), 09:00 - 10:30
휘닉스1

DF-18(초) **Microphotonic devices for Silicon Photonics** SHIN Jung H.(*KAIST.*) A crucial driving force behind the information revolution of the last 40 years that is often overlooked is the interconnects. However, the traditional metal interconnects are fast approaching their limit, and are predicted to be the bottleneck limiting the future growth. One solution to this problem that

is attracting a great attention of late is integrating photonic functions into silicon integrated circuits. However, the indirect bandgap of Si makes it difficult to develop active photonic devices needed for full integration. Furthermore, the need for small sizes reduces the possible interaction volume, placing a great demand on increasing the light intensity. In this talk, I will talk about the possibility of using erbium silicates as a high-gain material suitable for obtaining optical gain, and how they can be fabricated on a large scale using silicon nanowire templates. For increasing the light intensity, device structures such as micro-resonators and recently suggested slot waveguides are necessary. In this talk, I will present some recent results on fabricating high-Q optical micro resonators employing silicon nanocrystals that suggest that nm-sized silicon nanocrystals do not contribute to scattering losses, and recent results on multi-slot waveguides that confine light on nm-scale.

DF-19(초) **Complete suppression of large InAs island formation on GaAs by metalorganic chemical vapor deposition with periodic AsH_3 interruption** YOON Euijoon(*Department of Materials Science and Engineering, Seoul National University, Seoul 151-742, Korea.*) Self-assembled InAs quantum dots (QDs) on GaAs substrates were grown by metalorganic chemical vapor deposition with periodic AsH_3 interruption (PAI). Contrast to the conventional InAs QD growth method, AsH_3 was interrupted periodically while TMIn was introduced into the reactor continuously. By interrupting AsH_3 periodically, the growth surface is modulated between As-stabilized surface and In-stabilized one, resulting in complete suppression of relaxed large island formation and significant improvement in photoluminescence intensity. With further optimization of growth parameters, we obtained the emission at 1.32 m and narrow linewidth of 32 meV at room temperature. In this presentation, mechanism of PAI will be proposed.

DF-20(초) **Near-field Scanning Phase Interferometer &Its Applications** PARK Seung-Han(*National Research Laboratory of Nonlinear Optics,Yonsei University, Seoul 120-749, Korea.*) Probing instruments such as NSOM, STM, and AFM have been developed to observe more complex structures much smaller than the diffraction limit. In particular, the spatial resolution of near-field scanning optical microscope (NSOM) using tapered fiber probes has improved to up to ~50 nm during the past two decades. Therefore, NSOM has been actively applied to investigate high-density optical disk, optical modification of surface, bio-molecules, etc. In this presentation, we will show a near-field scanning phase interferometer, using the conventional tapered optical fiber probe as a nano-scopic reflective facet. We have employed the tapered optical fiber tip not only as a near-field aperture to obtain optical image but also as a point-like source to detect the ultra-fine relative phase changes. We will demonstrate that conventional topographical images as well as the relative optical phase taken with the near-field scanning phase interferometer, carrying more complex information of the internal structure, can be successfully obtained.

■ SESSION: D [DG4]
4월 20일 (금), 09:00 - 10:00
금낭화

D-17 **Molecular dynamics simulations of the diffusion process of vacanciesin carbon nanotubes.** LEE Tae Kyung, RYU Byungki, LEE In-Ho[1], CHANG Kee Joo(*Korea Advanced Institute of Science and Technology, department of physics. [1]KRISS.*) Vacancies in carbon nanotubes can be generated by ion or electron irradiations. It is known that vacancies diffuse to form clusters, i.e., aggregates of vacancies. In this work, we investigate the structure, energetics, and diffusion process of vacancies in the (5,5) carbon nanotube using both first-principles calculations and tight-binding action-derived molecular dynamics simulations. We examine various diffusion paths of a single vacancy and find that a single vacancy is likely to diffuse along the circumference of tube rather than along the tube axis direction. We also study the coalescence of two single vacancies by testing many diffusion pathways, and find a new stable structure of a divacancy.

D-18 **Adsorption of Hydrogen Molecules on Boron Nitride Nanotubes (BNNT) with a Ti Atom and on Be-doped Carbon Nanotubes (CNT)** JANG Y.-R., DURGUN E.[1], CIRACI S.[1], LEE J. I.[2](*Department of Physics, University of Incheon, Incheon 402-749, Korea. [1]Department of Physics, Bilkent University, Ankara 06800, Turkey. [2]Department of Physics, Inha University, Incheon*

402-751, Korea.) Adsorption of hydrogen molecules on carbon nanotubes (CNT) substituted by Be atoms and on boron nitride nanotubes (BNNT) with a Ti atom were investigated using first-principles pseudopotential plane wave calculations. The binding energies per molecule were calculated to be large enough to adsorb the hydrogen at room temperature and the weight percentage was shown to be greater than the minimum requirement. These results suggests that functionalized nanotubes with light elements would be good candidates for efficient hydrogen storage media.

D-19 **DNA Nucleotide Interaction and Identification of Hybridization with Carbon Nanotubes: Implications to the Bio-Sensors** 공 기정, 장 현주, 이 정오, 부 경호(*한국화학연구원.*) A field effect transistor (FET) sensor consisting of a single-walled carbon nanotube (SWNT) has been actively studied with a view to using them in ultrasensitive sensors. SWNTs functionalized with biomolecular complexes hold great promise as molecular probes and sensors targeted for not only biological species but also chemical species that interact weakly or not at all with unmodified nanotubes. Among the molecules used as a surface functionalization agent, the most popular one is DNA. DNA is regarded as an intriguing candidate for the molecular targeting layer sensing a wide variety of targets, including small molecules and specific proteins, since it can be easily engineered, using directed evolution. Recently, CNTs are proposed to be used as the template for DNA hybridization,[1] electrochemical detection of DNA,[2] and ultrafast DNA sequencing.[3] There was a report that it is possible to discriminate between nucleosides on CNTs based on measurement of electronic features.[4]The sensing mechanism of DNA with CNT-FET sensors is investigated by first-principles electronic structure calculations. We have investigated the interaction of individual DNA nucleobases (especially guanine and cytosine) with SWNTs, and compared the binding energies of various configurations including π-stacking and direct bonding ones. Understanding the interaction between DNA and SWNT is important for the applications and the fundamental science. Secondly, we have also simulated the interaction of the thiolated nucleotides with gold nanoparticles. The gold nanoparticle is used not only as a sensitivity enhancer of SWNT-FET sensor but also as a receptor of DNA via alligating clip atom, sulfur. Comparing the calculated results of above two systems, we tried to propose the mechanism of sensing the binding of single-stranded DNA (ss-DNA) on the SWNTs and the hybridization of complementary DNA on the pre-bound ss-DNA.

[1] Jeng, E. S.; Moll, A. E.; Roy, A. C.; Gastala, J. B.; Strano, M. S., Nano Lett. 2006, 6, 371. [2] Li, J.; Ng, H. T.; Cassell, A.; Fan, W.; Chen, H.; Ye, Q.; Koehne, J.; Han, J.; Meyyappan, M., Nano Lett. 2003, 3, 597. [3] Star, A.; Tu. E.; Niemann, J.; Gabriel, J.-C. P.; Joiner, C. S.; Valcke, C., Prod. Natl. Acad. Sci. U.S.A. 2006, 103, 921. [4] S. Meng, P. Maragakis, C.. Papaloukas, and E. Kaxiras, Nano Lett. 2007, 7, 45.

D-20 **Direct Observation Of Encapsulated Cs Atom Induced Localized Gap State In Carbon Nanotubes.** 최 운이, 김 성헌, 김 건[1], 송 영재, 국 양, 임 지순(*서울대학교, 물리천문학부. [1]성균관대학교, 물리학과.*) Using first principle calculation, we study the electronic structure of Cs atom encapsulated carbon nanotube to elucidate experimentally observed scanning tunneling spectroscopy (STS) data. Encapsulated Cs atom gives one electron to the carbon nanotube and remain as effective +1 charge. One or two of the bound states made by this potential field lie in the gap depending on the dimeter and the eletronic properties of the carbon nanotube. Not only emergence of gap states, the local change of valance and conduction bands are observed and explained. Comparing calculated and experimentally measured STS map, the effects of gold substrate are also discussed.

■ SESSION: D [DF6]
4월 20일 (금), 09:00 - 10:40
벌개미취1

DF-21(초) **양자정보과학(Quantum Information Science) 소개** 이 해웅(*한국과학기술원 물리학과.*) 양자정보과학은 최근 10여 년 동안 눈부신 발전을 하면서 물리학의 첨단중요연구분야로 부상하였다. 이 강연은 양자정보과학의 간단한 소개를 목적으로 한다. 양자정보과학의 핵심 개념인 양자얽힘(Quantum Entanglement)의 논의를 거쳐 양자정보과학의 두 주요 과제인 양자통신(Quantum Communication)과 양자컴퓨팅(Quantum Computation)의 기본 원리를 소개하도록 한다.

DF-22(초) **양자컴퓨터 하드웨어 구현** 이 순칠

(*한국과학기술원 물리학과.*) 양자컴퓨터 시스템으로 연구되는 양자계로서 인공구조로는 양자점, 이온덫, 공진기 QED, 조셉슨소자 등이 있으며 핵자기공명에서는 자연에 존재하는 분자를 이용하고 있다. 현재 양자전산 연구의 초점은 실용적인 양자컴퓨터의 제작에 있다고 할 수 있는데, 이 중 어느 것도 미래에 실용적인 양자컴퓨터가 되기에는 제한이 많다고 생각되고 있다. 실용적인 양자컴퓨터가 되기 위한 양자계의 조건은 (1) 두 개의 잘 정의된 양자상태가 존재할 것 (2) 모든 큐빗의 고유상태로의 초기화가 가능할 것 (3) 모든 단일 큐빗 조작이 선택적으로 가능할 것 (4) 큐빗의 상태를 읽을 수 있을 것 (5) 잘 정의된 상호작용을 켰다 껐다 할 수 있을 것 (6) 결맞춤 시간이 길 것 (7) scalability가 있을 것 등이다. 현재 가장 그럴 듯 하다고 생각되는 양자계로는 반도체에 일정한 간격으로 삽입된 스핀계를 조작하는 고체 양자컴퓨터 시스템이 있다. 소위 Kane모델이라고 불리는데, 이론적으로 제안되었으나 아직까지 실험적으로 구현되지 않았다.

DF-24(초) **양자컴퓨터 개발의 현재와 미래** 최상경(*한국표준과학연구원.*) 양자컴퓨터의 실험적 구현을 위한 여러 접근방식들을 살펴본다. 가장 대표적인 선형광학계, 초전도 소자, 이온덫 방식들의 원리를 설명하고 최근 성과를 요약한다. 기타 방식의 양자컴퓨터들에 대해서도 간략히 소개한다. 이러한 양자컴퓨터 개발 과정이 당면한 기술적 도전 및 미래의 응용 가능성에 관해 논의한다.

■ SESSION: D [DF7]
4월 20일 (금), 09:00 - 10:30
벌개미취3

DF-25(초) **Local structure and Polarization rotation in relaxor ferroelectric Pb(Mg1/3Nb2/3)O3 and (1-x)Pb-(Zn1/3Nb2/3)O3-xPbTiO3 studied using Atomic Pair Distribution Function Analysis** JEONG, IL-KYOUNG (*Pusan National University, Research Center for Dielectrics and Advanced Matter Physics.*) Ultrahigh piezoelectric response of relaxor ferroelectrics is a fascinating phenomenon and has attracted significant interests. Many experimental and theoretical studies suggest that a polarization rotation is a key mechanism for this phenomenon. However, recent studies on local structure of prototypical relaxor ferroelectrics Pb(Mg1/3Nb2/3)O3 (PMN) [1] and Pb(Zn1/3Nb2/3)O3 (PZN) [2, 3] showed that local symmetry is different from that of average structure. These results suggest that the mechanism of the polarization rotation in relaxor ferroelectrics is different from that of typical ferroelectrics like BaTiO3. In this talk, I will discuss structural evolution of relaxor ferroelectric PMN and of (1-x)Pb(Zn1/3Nb2/3)O3-xPbTiO3 (PZN-xPT) as a function of temperature and/or PbTiO3 concentration studied using neutron atomic pair distribution function analysis. In the first part, I'll show the local structure (r <5 A) of PMN and PZN does not change much with temperature but medium-range ordering (5A <r <20A) of local polarizations develops with decreasing temperature. In the second part, I'll show that the local structure of (1-x)Pb(Zn1/3Nb2/3)O3-xPbTiO3 (PZN-xPT) exhibit little changes over the rhombohedral-orthorhombic-tetragonal structural phase transitions with PbTiO3 concentration. These results indicate that the short-range ordering in relaxor ferroelectrics is very stable and not easily affected by temperature and/or composition. Therefore, I propose that the polarization rotation in PZN-xPT is a result of medium-range ordering instead of the change in atomic displacements.

[1] I.-K. Jeong et al., Phys. Rev. Lett. 94, 147602 (2005), Selected for the May 2, 2005 issue of Virtual Journal of Nanoscale Science &Technology.
[2] Jeong, I.-K. and Lee, J. K., Appl. Phys. Lett. 88, 262905 (2006).
[3] Xu, G. et al., Nature materials, 5, 134 (2006).

DF-26(초) **Synthesis and Characterization of Ferroelectric PZT Nanowires/Nanotubes** 부 상돈(*전북대학교, 물리학과.*) We present ferroelectric PZT nanowires/nanotubes by a template-directed growth in conjunction with the sol-gel process and spin-coating technique. A field emission transmission electron microscope (FETEM) image of freestanding PZT nanotubes show that its outer diameter is estimated to be 50 nm with the wall thickness of ~5 nm and its length is in the order of several microns. PZT nanowires exhibit a high aspect-ratio (up to 400) with diameters of 50 nm and lengths of 20 mm. Scanning transmission electron microscope images, along with element mapping, confirm the presence of Pb, Zr, and Ti. The occurrence of the selected area electron diffraction (SAED) ring pattern confirms that the typical PZT nanowires/nanotubes are polycrystalline. Direct observation of lattice fringes by high resolution FETEM shows that they are comprised of crystallites in the size of 2-3 nm. Comparing the direct measurement from the lattice fringe and calculation of the SAED ring

pattern, it is indicated that they mostly consist of the perovskite phase with a tetragonal structure of a=4.036 Å and c=4.146 Å [JCPDS 33-0784].

DF-27(초) **Dielectric response, charge transfer, and Fermi level pinning at metal-oxides interface** 한 승우, 이 보라, 조 은애(*이화여자대학교, 물리학과.*) 첨단소자의 개발 및 미세구조에 대한 관심으로 인하여 물질 사이의 경계면에 대한 연구가 활발해지고 있다. 특히 전자소자로 많이 사용되는 유전체의 경우 강유전성이나 유전율이 인접한 금속의 종류에 의해 달라지는 것을 많이 관측하고 있으나 이에 대한 근본적인 연구가 아직 미진한 상태이다. 본 발표에서는 제일원리계산을 이용하여 금속/유전체 경계면에서 일어나는 다양한 현상을 살펴본다. 우선 경계면에 의한 유전율의 변화를 계산하기 위하여 새로운 방법을 제시하고 경계면에서 유전율이 감소하는 효과를 설명하고자 한다. 또한 다양한 금속과 유전체 사이에서 일어나는 전하이동에 대하여 계산하고 전하이동의 원인을 미시적으로 이해해본다. 반도체 소자에 대한 응용으로써 경계면의 도핑에 의한 Schottky 장벽의 변화를 조절하는 방법도 살펴본다.

■ SESSION: D [DG5]
4월 20일 (금), 11:00 - 12:15
휘닉스2

D-21 **Temperature Dependence of the Radial Breathing Mode and the E_{22} Transition Energy in Single-Walled Carbon Nanotubes** 김 지희, 장 동욱, 한 강전, 김 남제, 이 기주, 임 용식[1], J. Kono[2](*충남대학교, 물리학과. [1]건국대학교, 응용물리학과. [2]Department of Electrical and Computer Engineering, Rice University.*) 분산된 단일벽탄소나노튜브 물질에서 펨토초 Ti-sapphire 레이저를 이용하여 특정 결맞는 radial breathing mode (RBM) 신호 변화에 대해 분석해보았다. 일반적으로 단일벽탄소나노튜브 샘플은 공명 여기 에너지 조건을 만족하는 다수의 진동모드들이 동시에 RBM진동을 일으킨다. Pulse-shaping 방법을 이용하면 공명 여기 조건을 만족하는 다수의 진동모드들 중에 특정 카이럴리티를 갖는 RBM 격자운동을 선택적으로 여기시킬 수 있다. 이러한 상황에 상온에서부터 160C 까지 온도를 올려가며 특정 카이럴리티를 갖는 RBM 격자운동의 진동주파수와 decay time의 변화를 살펴보았다. 또한 190 K 까지 어는점을 낮추기 위해 단일벽탄소나노튜브 샘플에 glycerol을 섞고 상온에서부터 190 K 까지 온도를 낮춰가며 RBM 진동모드의 온도에 따른 특성 변화에 대해 조사하였다. 그리고 다색 펌프-프로브 방법을 사용하여 밴드갭 근처 에너지 영역에서의 결맞는 RBM 신호 세기 변화를 보았고, 또한 온도에 따른 이 신호 세기의 변화에 대해 분석, 논의한다.

D-22 **Eight-fold Shell Filling in a Double-wall Carbon Nanotube Quantum Dot** SONG Woon, MOON Sunkyung, KIM Nam, KIM Jinhee, LEE Soon-Gul[1], CHOI Mahn-Soo[2](*Leading Edge Technology Group, KRISS. [1]Dept. of Applied Physics, Korea University. [2]Dept. of Physics, Korea University.*) We fabricated a quantum-dot device consisting of an individual double-wall carbon nanotube and metal electrodes and studied its electrical transport properties at low temperatures. In the negativebias region, the gate modulation curve exhibited quasi-periodic current oscillations, attributed to the Coulomb blockade of single electron tunneling. We could identify both 4- and 8-fold periodicities in the Coulomb diamond structures. The mirror-symmetric 8-fold periodicity implies that the single particle energy levels of the quantum dot are 8-fold degenerate. Such highly degenerate energy levels require additional symmetry other than the SU(4) symmetry of a single-wall carbon nanotube. We show that the observed 8-fold shell filling is a unique characteristic of a double-wall carbon nanotube quantum dot device.

D-23 **N-type carbon nanotube transistors with large work-function electrodes** MOON sunkyung, SONG woon[1], LEE Joon Sung[1], KIM Nam[1], KIM Jinhee[1], LEE Soon-Gul, PARK Noejung[2](*Korea University, Applied Physics. [1]Korea Research Institute of Standards and Science, Leading-Edge Technology Group. [2]Dankook University, Applied Physics.*) We report that a carbon nanotube field-effect transistor (CNTFET) could exhibit n-type characteristics, even though the electrodes consist of a large-work-function metal such as Co. Our result disproves the well-known understanding that the large-work-function metal in CNTFETs should always lead to p-type behaviors without any further treatment such as doping or annealing. To explain such unexpected results, we performed ab initio electronic-structure calculations for the metal-carbon nanotube junction. It is presented that the Fermi level alignment at the contact could sensitively depend on the microscopic structures of the metal-carbon nanotube interface. This suggests that deposition

method of electrodes as well as the metal type could be utilized to obtain an n-type CNTFET.

D-24 **Single-Electron Transport through Individual Indium Oxide Nanowire** JUNG Minkyung, CHOI Nak-Jin, LEE Hyoyoung, MOON Sunkyung[1], SONG Woon[1], KIM Nam[1], KIM Jinhee[1], JO Gunho[2], LEE Takhee[2](*ETRI. [1]KRISS. [2]GIST, Department of Materials Science and Engineering.*) We have investigated the electron transport properties of individual In_2O_3 nanowire devices. We have found that the gate modulation characteristics depend strongly on the channel length. If the channel length is greater than 450 nm, the gate modulation curve exhibited clear field-effect transistor behavior with dominant n-channel current at room temperature. With decreasing channel length, the threshold voltage shifted to negative voltages and disappeared for a device with a channel length of 180 nm. For most of the fabricated devices, the gate modulation curve exhibited quasi-periodic current oscillations at low temperature, which are attributed to the Coulomb blockade of single-electron tunneling. Some devices even showed two-fold periodicity in the Coulomb diamonds which may arise from the spin degeneracy of the single particle energy levels.

D-25 **전기적 구동이 있는 이중 양자점의 중시계 어드미턴스** 박 희철, 안 강헌(*충남대학교 물리학과.*) 우리는 이중 양자점에 주기적인 마이크로파가 인가된 경우에 대해 플로케 산란이론을 적용하여 진동수에 의존하는 어드미턴스를 계산했다. 이 시스템은 전체 전류와 샷 노이즈를 없애기 위해 한 쪽에만 양자점이 연결된 고리모양의 구조이다. 대신에 전자의 시간 지연으로 인해 대체 전류가 발생하게 된다. 전기적 구동 때문에 전자의 상태는 비 평형이지만 평형상태의 이론으로 잘 알려진 요동-흩어지기 이론이 마찬가지로 적용됨을 보였다. 공명 에너지에서 시간 지연이 커지기 때문에 페르미 에너지의 함수로 쓴 낮은 진동수의 어드미턴스는 피크 모양으로 나타난다. 반면에, 노이즈 파워는 페르미 에너지의 함수로 계단모양이다. 이것은 낮은 진동수 어드미턴스를 결정할 때 페르미 레벨에 있는 전자만 관여하지만, 노이즈 파워는 페르미 레벨 아래 있는 전자도 관여하기 때문이다. 그리고 우리는 낮은 측정 진동수, 낮은 온도에서 어드미턴스가 지연시간의 제곱에 비례하는 것을 보였다. 이것은 뷰티커에 의해 소개된 전하 완화 시간의 개념이 주기적인 시간 포텐셜이 있을 때에도 적용 가능하다는 것을 암시한다.

■ SESSION: D [DG6]
4월 20일 (금), 11:00 - 12:15
금낭화

D-26 **Anomalous Field and Temperature Dependence of Anisotropy Observed in Organic Superconductors with a Torque Method** 강 원, 조 연정[1], 최 은상[2](*이화여자대학교 물리학과. [1]이화여자대학교 물리학과/NHMFL, FL, U.S.A. [2]NHMFL, FL, U.S.A.*) Recent development of piezoresistive torque magnetometry using the commercial microcantilever, originally developed for the AFM probe, has greatly improved the sensitivity of measurement that the anisotropic magnetic properties of microcrystals can readily be studied now. We present the magnetic field and temperature dependence of anisotropy in various ground states of representative organic superconductors studied with the angular dependence of magnetic torque.

D-27 **The determination of ultrathin oxided-layer(SiO_2/AlO_x) thickness using the AR-XPS, TEM and ARCtick** 윤 형중, 박 윤창[1], 손 병철, 임 정란, 이 주한(*한국기초과학지원연구원. [1]나노종합팹센터.*) In this study, we estimated the thickness of ultrathin layer (<5nm) using two procedure for examining the thickness; AR-XPS(Angle-Resolved X-ray Photoemission Spectroscopy), TEM(Transmission Eelctron Microscopy). Both approaches have significant advantage for the determination of thickness. At first, We measured the intensities of Si 2p core-level spectrum with varying the angle of sample(SiO_2;~1.5nm) prepared by CVD and calculated the thickness by the ratio of Si 2p peaks corresponding to SiO_2 in the film and Si in the substrate, where we used the ARCtick program for calculation. To compare the accurate thickness, we observed the TEM image. Secondly, We analyzed another samples, whiche was the SiO_2 with the different thickness(~2.5nm) and AlOx(<4nm) by AR-XPS and TEM. In conclusion, AR-XPS is, non-destructively, a very useful technique for determination of the ultrathin thickness and we have a plan to apply the various metal(Cu, Hf, Zn. etc)-oxide layers.

D-28 **Study of ferromagnetism in Pd nanoparticles** S. Angappane, HWANG Yosun, JANG Y.[1], HYEON T.[1], PARK J.-G.(*BK21 Physics Division, Department*

of Physics, SungKyunKwan University, Suwon-440 746, Korea. [1]National Creative Research Initiative Center for Oxide Nanocrystalline Materials and School of Chemical and Biological Engineering, Seoul National University, Seoul-151 744, Korea.) This study aimed at understanding the origin of ferromagnetism that had been previously reported for Pd nanoparticles [1]. For this work, we prepared nanoparticles of sizes 2, 3, 5, 7 and 10 nm by using the thermal decomposition of the Pd-trioctylphosphine complex. The temperature dependence of the magnetization, after subtracted off the low temperature paramagnetic contribution, shows a behavior similar to those of the magnetic impurities, e.g. Fe_3O_4. Moreover, we note that the magnetization of our samples is about one order of magnitude smaller than that of the earlier reports for Pd nanoparticles. In order to understand the origin of the ferromagnetic signal observed in our samples, in particular to answer whether it is due to intrinsic or extrinsic factors, we intentionally added Fe_3O_4 impurities to Pd nanoparticles and studied their magnetic properties. The results show that the ferromagnetism in Pd nanoparticles is most likely to be of intrinsic in nature. And we will also discuss the similarities and differences between our data and those reported results. [1] B. Sampedro, et al., Phys. Rev. Lett. 91, 237203 (2003); T. Shinohara et al., Phys. Rev. Lett. 91, 197201 (2003).

D-29 **Atomic Geometry and Electronic States on Au/GaAs(111)B** YI Hongsuk, KRATZER Peter[1] (*한국과학기술정보연구원. [1]Univ. Duisburg-Essen.*) We have investigated the stable adsorption sites and simulate scanning tunneling microscopy (STM) images of Au absorbed on the GaAs(111)B surface, using the GGA approximation of density functional theory, and plane-wave pseudopotential calculations. We propose an energetically favorable model for the Au/GaAs(111)B surface with one Au per unit cell located in a threefold hollow site. From the calculated potential energy surface we obtain a diffusion barrier height of 0.2 eV for Au adatoms. In the simulated filled-state STM images the Au atoms appear as triangular structures whose edges point towards neighboring As atoms. The proposed structural model is in agreement with experimental data from low-energy electron diffraction and STM.

D-30 **Clean Si(112) and Si(112) section within the reconstructed Si(557) surface** OH Dong-Hwa, KIM Minkook, AHN Joung Real(*Department of Physics, Sungkyunkwan university.*) We present the structural models for the clean Si(112) surface and the Si(112) section within the reconstructed Si(557) surface using a planewave pseudopotential calculation based on the density functional theory. For the clean Si(112) surface, we examined models, which included one previously proposed and our novel one, adatom-dimer model. We found that our model is the most stable. Based on this model, we could build structural model for the Si(112) section within the reconstructed Si(557) surface by introducing missing dimer and additional adatoms. We have got the simulated scanning tunneling microscopy (STM) image for this, which is good agreement with experimental STM images.

■ SESSION: D [DT2]
4월 20일 (금), 11:00 - 12:00
벌개미취1

DT-02(초) **고체물리학도를 위한 결정학 입문** 정 세영(*부산대학교 나노과학기술대학 나노정보소재공학과.*) 학부 고체물리학 교재의 첫 2-3 Chapter는 대부분 결정의 구조에 관련한 내용이다. 고체 물리학을 공부하는 많은 사람들이 그 정도 수준으로 결정학을 배우고 더 깊은 결정학과 관련한 내용은 대부분 대학원 과정에서 각자 개별적으로 공부하게 된다. 실제 결정의 구조는 7개의 crystal system으로, 32의 point group으로 분류가 되며 또한 230가지의 공간군으로 분류가 될 만큼 복잡한 구조로 나뉘게 된다. 이렇게 복잡하게 분류하는 이유는 그 구조에 따라 결정이 갖는 물성이 다르게 나타나기 때문이다. 실제 물리적 성질은 구조와 떼어서 설명할 수 없는 부분이 많다. 대칭성은 결정의 구조를 설명하는 아주 중요한 요소이다. 결정학을 잘 이해하면 결정의 morphology 만 보더라도 웬만큼 그 물성을 예측할 수 있다. 본 강의에서는 결정에 존재하는 다양한 대칭성과 대칭성의 결합, 대칭에 따른 물리적 성질, 대칭성을 찾는 방법, stereogram 이해법 및 point group 등 물리학에서 배울 수 없는 결정학의 기초를 쉬운 연습 문제를 통하여 직접 배울 수 있는 기회를 갖는다. Tutorial에 사용할 교제는 연습 문제의 형태로 만들어져서 제공될 것이다.

■ SESSION: E [EF1]
4월 19일 (목), 12:30 - 14:00
토파즈

EF-01(초) **Modeling of the Magnetic Behavior for Low Dimensional Magnetic Systems** MARC Drillion (*Director of CNRS-IPCMS, France.*) The use of adapted theoretical tools for modeling the thermodynamical functions of magnetic solids is of prime importance for anaccurate analysis of their experimental behaviors allowing the establishment of detailed structure-properties relationships. A model of "hierarchical superparamagnetism" was developed recently which generalizes the idea of scaling by taking advantage of the non-singular solutions that are introduced, together with the singular ones, when the hypotheses of "critical scaling" are formulated. These non-singular solutions, although they have the same legitimacy, have simply been set aside when the goal was to describe the singularities of phase transitions. They happen to be very useful when correlations exist, but which are not sufficient to trigger a long range order at a finite TC, either because frustration is strong, near e.g. an antiferromagnetic (AF) order, or because we sit at, or below, a lower critical dimensionality. Model systems, such as the 1D or 2D-Heisenberg systems of spin S=1/2, 1,… display such behaviors. For this reason, much effort has been devoted in performing exact calculations on such finite systems of increasing size, and in trying to infer which type of limit is reached when the size diverges. On another hand, the progresses of chemistry have made it possible to design organometallic clusters, chains or planes, of axial, planar or isotropic spins, which are close approximants of the above mentioned systems, and are well appropriate to investigate the properties of interest. We will show on a few examples, that the model of hierarchical superparamagnetism provides the right framework to approach these problems and suggests a strategy adapted to each case.

EF-02(초) **Short period magnetic coupling oscillations in Cobalt/Silicon multilayers** CHRISTIAN Meny(*CNRS-IPCMS, France.*) The discovery of the exchange coupling and giant magnetoresistance effect between ferromagnetic layers separated by nonmagnetic metallic interlayers, attracted attention toward magnetic multilayers. Since then, intensive work has been focused on the magnetic and electronic properties of multilayered systems. More recently, the non-magnetic metallic spacers have been replaced by non-metallic spacers: insulators or semiconductors. While interesting results were obtained with insulator layers (tunnel magnetoresistance) the results obtained with semiconductor spacers are much more controversial. Indeed, when one elaborate nanostructures with ferromagnetic metals and semiconductors, a large mixing of metal and semiconductor atoms occurs at the interfaces. This interfacial mixing influences strongly their magnetic properties. For instance while Enkovaara et al (Phys. Rev. B 2000) have predicted, in Cobalt/Silicon multilayers, the presence of magnetic coupling oscillations between the Cobalt layers, through the Silicon spacer, they where never observed experimentally up to now. In order to reduce the interfacial mixing arising during the growth process, we have chosen to prepare Cobalt/Silicon multilayers at low temperature (90 K). The structural analyses of the samples have shown that low temperature deposition allowed reducing the interfacial mixing to about 1 nm compared to the 5 to 10 nm of interfacial mixing resulting from room temperature elaboration. This allowed us to observe, for the first time, short period magnetic coupling oscillations through the silicon spacer layer. These oscillations are due to the modification of the Si electronic structure when a thin layer is embedded between two ferromagnetic Co layers. These oscillations are consistent with the coupling oscillations predicted by the computations performed by Enkovaara et al. and confirmed by our own computations. Surprisinglythese oscillations are still as strong at room temperature as at low temperature. These results will initiate new research work in the field of semiconductors and ferromagnetic metals.

EF-03(초) **Electric and magnetic properties of metal-organic heterostructures** KIM Tae Hee(*Department of Physics, Ewha Womans University.*) We investigated surface potential profiles for pentacene films as a function of the film thickness and the contact metallurgy (Au and Al) by using a near-field microwave microprobe analysis and Kelvin-probe force microscopy. The surface potential for the Al/pentacene bilayers increased monotonically with the thickness of pentacene while no thickness dependence of the surface potential was for the Au/pentacene bilayers. These results are discussed based on the potential barrier at the metal/pentacene interface due to the space charge.

■ SESSION: E [EF2]
4월 19일 (목), 16:30 - 18:00
토파즈

E

EF-04(초) **Spin Waves : From Fundamentals to Applications** KIM sang-koog(*Department of Materials Science and Engineering, Seoul.*) Spin-wave (SW) excitations in bulk and thin film ferromagnets have long been a fundamentally interesting topic in the research area of magnetism. In recent years, SWs excited or traveling in geometrically confined magnetic elements such as nanodots and nanowires are of revived interest both theoretically and experimentally. Considerable progress in the understanding of spin excitation spectra in restricted geometries has been achieved with the help of theoretical approaches, and sub-nano-second time- and sub-micrometer space-resolving measurement techniques. In this talk, I will report the micromagnetic numerical and analytical studies of strong radiation of spin waves generated via an in-plane magnetic-pulse-field-induced reversal of a magnetic vortex core in a circular dot, as well as the wave behaviors of traveling spin waves in magnetic nanowires. In addition, I will report findings that the radial SWs can be emitted intensively from a vortex core by its field-induced reversal, and then can be injected into nanowires. The results demonstrate: (i) the radiation behavior of SWs produced from a magnetic vortex core associated with its reversal; (ii) the injection behavior of SWs from a circular dot into nanowire waveguides; (iii) how to control the frequencies of SWs using nanowire-type heterostructures. These are key points in understanding the fundamental wave properties of SWs in restricted geometry, such as their radiation, propagation, reflection, transmission, interference, dispersion, and filtering of specific frequencies. All of the three points are crucially important for future technological applications to a variety of SW devices, including logic devices. These results offer a preview of the generation, delivery, and manipulation of SWs in nano-size patterned magnetic elements.
*This work was supported by Creative Research Initiatives of MOST/KOSEF. Special thanks are given to S. Choi, K.-S. Lee, and K. Y. Guslienko for their research works.

EF-05(초) **A novel material system for electrical spin injection and detection: Semi-metallic Bi** 이 우영(*연세대학교 신소재 공학과.*) The spin polarized carrier transport study in a metal or a semiconductor is a challenging field of 'spintronics' to exploit the spin degree of freedom for future electronic applications. The motivation for developing a semimetal-based spin device is to explore the spin injection/transport/detection phenomena to a novel materials system. An understanding of the characteristics of spin dependent transport in a semimetal can not only guide research in semiconductors but also towards the development of spin field effect transistors. This talk is divided into two topics, spin injection in Bi thin films and Bi nanowires. Our experiments on the Bi thin films demonstrate three remarkable results: (i) A spin diffusion length of 230 mm, observed in a semimetallic sample at 2 K, is the longest known spin depth in a thin film sample. (ii) Effects related to the difference in resistivity of F and N, known as the "resistance mismatch" problem, are widely assumed to prohibit spin injection and detection using ferromagnetic metals. Our mismatch factors are the order of 10^5 for all samples, but robust spin injection and detection are observed. (iii) Although the mismatch problem is thereby refuted, the fractional polarization of interfacial currents in semiconducting samples is an order of magnitude smaller compared with semimetallic samples. Our spin injection study has been extended to Bi nanowires. A novel method was found to grow single-crystalline Bi nanowires, which originates from the stress-relief phenomenon of sputtered Bi thin film grown on an oxidized Si substrate during heat treatment. For a 400-nm Bi nanowire, the largest MR (2500%) was found at 110 K, which is the highest value ever reported. MR values of 1580% and 286% were observed at 2 K and 300 K, respectively, indicating the longest mean free path (l)andrelaxation time (τ). Our results provide motivation for exploring spin injection into single-crystalline Bi nanowires.

EF-06(초) **Controlling carrier types and densities in $MnGeP_2$ and $MnGeAs_2$** 조 성래(*울산대학교 물리학과.*) Diluted magnetic semiconductors (DMSs), which are prepared by substituting transition metals into nonmagnetic semiconductors, such as group II-IV, III-V and IV, II-IV-V_2, etc., have attracted the worldwide scientific interests for the possible spintronic devices.[1-3] The ferromagnetic semiconducting material, whit high magnetic moments and high Curie temperature (T_C), was interested by researcher and scientists because of the prac-

tical applications in spintronics. We have synthesized new semiconductors, $MnGeP_2$ and $MnGeAs_2$, whose crystal structure is chalcopyrite, which are "genealogically" related to the more familiar tetrahedral coordinated zinc-blende materials. It showed ferromagnetism with T_C = 320 K and 340 K, and magnetic moment per Mn at 5 K of 2.58 μ_B and 3.42 μ_B, comparable to the calculated 3.2 μ_B. The calculated plane wave (FLAPW) method shows an indirect energy gap of 0.24 eV and 0.06 eV. $MnGeP_2$ and $MnGeAs_2$ thin films show a p-type and n-type carrier density(~10^{20} cm^{-3}), respectively. It is well known that various native defects such as group II and V vacancies and antisite defects are present in II-IV-V_2 chalcopyrite with densities up to 10^{20} cm^{-3}. The p-type behavior of $MnGeP_2$ may arise from native point defects such as cation Mn and Ge vacancies and antisite defects: Mn_{Ge} and the n-type carrier for $MnGeAs_2$ from anion As vacancies and antisite defects: Ge_{Mn}.[4] These defects were depending on the ratio of ambient P and As for the growth of $MnGeP_2$ and $MnGeAs_2$ thin films. In order to control the carrier concentration, we have studied the magnetic and electrical properties of $MnGeP_2$ and $MnGeAs_2$ thin films prepared by changing P and As evaporation ratio. Hall effect, thermopower, and magneto-resistances will be discussed in detail.

■ SESSION: E [ES1]
4월 19일 (목), 20:30 - 21:30
다이아몬드

ES-01(초) **PDP 분야의 물리학** 유 민선(*삼성 SDI.*)

ES-02(초) **OLED 기술과 전망** 한 승진(*두산메가텍.*)

ES-03(초) **물리학도를 위한 LCD 기술과 부품 소개** 최 영석(*엘지필립스.*) LCD는 IT제품을 넘어서 TV로 그 영역을 확대하고 있다. 아직까지는 품위측면과 경제적인 측면에서 도전해야 할 과제가 남아 있으며 공학과 자연과학의 경계에서 해결책이 나와주어야 할 부분이 있다. 이들을 해결하기 위해서는 지금까지의 접근방법과는 다른 좀더 근본적인 고민을 필요로 한다. LCD의 공정기술과 주요부품들의 소개하고 물리학적인 관점에서 어려운점과 접근방향을 소개하고자 한다. 또한 물리적인 지식이 공정과 부품에 어떻게 활용되고 있는지도 함께 소개될 것이다.

E

■ SESSION: E [EF3]
4월 20일 (금), 09:00 - 10:30
토파즈

EF-07(초) **Interface Electronic Structures of OLED studied by Photoemission Spectroscopy** 박 용섭(*경희대학교 물리학과.*) OLED(organic light-emitting diode) 소자는 유기 반도체 물질 박막에 금속 전극을 붙여 전압을 가하면 유기물질에서 빛이 나오는 성질을 이용한 일종의 광전자 소자(optoelectronic device)이다. 본 세미나에서는 이러한 소자의 성능에 중요한 영향을 미치는 것으로 알려진 금속과 유기물질의 계면 전자구조를 X-ray 및 UV 광전자 분광법 (X-ray &UV photoelectron spectroscopy)을 이용하여 연구한 내용을 살펴본다.

EF-08(초) **Device Physics of Organic Light Emitting Diodes** 이 창희(*School of Electrical Engineering and Computer Science, Seoul National Univ.*) 최근 유기 발광 다이오드 (Organic light-emitting diode Display, OLED)가 새로운 광원과 평판디스플레이 기술로서 전 세계적으로 활발하게 연구되고 있다. OLED는 백색 발광 효율이 약 50 lm/W이상으로 아주 높고, 색표현 범위 (color gamut)가 넓고, 구동 전압 및 소비전력이 낮고, 시야각이 넓다는 디스플레이로서의 장점을 가지고 있다. 그리고 소자 구조가 간단하여 제작이 용이하고 궁극적으로 두께 1 mm 이하의 초박형, 초경량 디스플레이 제작이 가능하므로 진정한 의미의 벽걸이형 TV의 구현이 가능하다. 더 나아가서 OLED는 유리기판 뿐만 아니라 플라스틱 기판 등에도 제작할 수 있어서 종이처럼 얇고, 필요할 때 펼쳐 볼 수 있는 플렉시블 디스플레이 (flexible display)에 가장 적합한 기술이다. 현재 OLED는 휴대폰과 디지털 카메라 등 소형 디스플레이에 응용되고 있으나 향후 대형 TV Q뿐만 아니라 다양한 광원에까지 응용될 것으로 예상되고 있다. 본 강의에서는 유기반도체의 기초적인 물성을 설명한 후, OLED 소자에서 전하 주입, 전하 수송, 엑시톤 형성 및 재결합, 전류-전압-휘도 특성, 발광 효율 향상 방법 등의 소자 물리에 대해 설명하고자 한다. 그리고 OLED 소자의 열화 원인 및 수명 향상 방법에 대해서도 간략하게 소개하고자 한다.

EF-09(초) **Self-assembled graded-junction of organic**

layer by "one drop of ink" for bright electro-luminescence 박 병주(*광운대학교 전자물리학과.*) 1987년 코닥(Kodak) 사의 Tang과 VanSlyke가 진공증착 방식으로 이중층 저분자 유기물 박막을 형성하여 유기 전계 발광 소자(OLED, Organic Light Emitting Device)를 제작한 이래, 고효율과 고휘도를 실현시키기 위한 수많은 연구들이 진행되어 왔다. 그러나 기존 진공 증착의 경우, 소자 제작 프로세스가 복잡하다는 단점이 있다. 반면, 고분자 등의 유기물들을 유기용매에 용해하여 소자를 제작하는 습식 방식의 경우, 그 제작 프로세스가 진공 증착에 비해 간단하나, 제작된 소자는 상대적으로 적층구조에 비해 낮은 발광 휘도 및 효율 특성을 보여 왔다. 본 연구에서는 이러한 기존의 습식 방식의 단점을 극복하기 위하여, 휘발성이 상이한 2종 이상의 복합 유기 용제에 용해도가 상이한 저분자 유기물들을 용해한 복합 용액(EL-Ink)을 제조하였으며, 이로 제조된 자기조립성 농도구배형 유기 발광 소자로부터 우수한 전계발광 특성들이 발현될 수 있는 가능성을 보였다. 이러한 결과들을 기반으로, 습식 공정으로 유기 발광 소자를 제작할 수 있는 방법을 더욱 발전시키면, 추후 유기 디스플레이 대형화에 있어 고휘도 발광 및 고효율 확보에 기여할 수 있을 것으로 기대한다.

■ SESSION: E [EG1]
4월 20일 (금), 11:00 - 12:45
다이아몬드2

E-01(초) **실리콘 나노 전자소자 기술** 이 성재(*한국전자통신연구원.*) 쇼트키 트랜지스터는 소스와 드레인의 재료로 금속을 사용함으로써, 기존 MOSFET의 불순물 도핑에 의한 에너지 장벽을 쇼트키 장벽으로 대체하는 신소자 구도이다. 소자의 동작 원리상 쇼트키 장벽에 의한 터널링이 주요 메카니즘으로 작용하며, 나노 스케일 MOSFET의 단점인 단채널 효과를 제어할 수 있는 큰 장점이 있다. ETRI에서 최근 개발한 10nm 크기 이하의 쇼트키 트랜지스터 소자의 제작 방법 및 우수한 전기적 특성을 소개하고 물리학적인 이슈를 소개하고자 한다. 한편 실리콘 나노 소자의 신응용 분야로서 나노 FET 바이오 센서가 최근 각광받고 있다. 이는 동작원리상 단분자 레벨의 단백질을 검출할 수 있을 정도의 고감도, 실시간 모니터링이 가능하며, 센서의 집적을 가능하게 하는 등의 여러 장점이 있기 때문인데, 최근 ETRI에서 수행중인 나노 스케일의 실리콘 구조체 제작 공정 및 실리콘 표면에의 바이오 활성화 기술 개발을 바탕으로 최근 전립선 암의 표지 단백질인 PSA (Prostate Specific Antigen)를 1fg/ml 이하의 농도까지 검출한 특성 결과등을 소개한다.

E-02 **Label-free Immuno Sensor Based on Silicon Field-effect Transistors** 유 한영, 김 안순, 아 칠성, 양 종헌, 백 인복, 안 창근, 박 찬우, 이 성재(*한국전자통신연구원.*) Ultrasensitive, label-free, and selective real-time prostate specific antigen (PSA) sensor was developed using n-type silicon nanowire-based structures configured as field-effect transistors where the conventional "top-down" semiconductor processes were employed to make the nanostructures. To detect the PSA, the surface of silicon was modified with a monoclonal antibody of PSA (anti-PSA) through covalent linkage using specific surface chemistry. Specific binding of PSA with the anti-PSA on the silicon surface leads to a conductivity change in response to variations of electric field at the surface. Concentration- and pH-dependent measurements show that the detection of PSA could be achieved down to 1 fg/mL in solution. This Si-FET biosensor can provide a pathway to high-density and high-reproducible as well as integrated sensors with well-established silicon-based technology and signal processes.

E-03 **Investigation of Solid State Photomultipliers for PET/MRI Scanners** LEE Jae Sung, KWON Sun Il, ITO Mikiko[1], SIM Kwang-Souk[1], HONG Byungsik[1], LEE Kyung Sei[1], LEE Geon Song[2], PARK Kwang Suk[2], MUHAMMAD Jamil[3], RHEE June Tak[3], SONG In Chan[4], HONG Seong Jong[5](*Seoul National University, Department of Nuclear Medicine. [1]Korea University, Department of Physics. [2]Seoul National University, Department of Biomedical Engineering. [3]Konkuk University, Department of Physics. [4]Seoul National University, Department of Diagnostic Radiology. [5]Gachon University of Medicine and Science, Division of Biological Science and Neuroscience Research Institute.*) For a combined PET/MRI scanner, solid state devices are promising devices to detect scintillation photons from PET scanners because they, unlike photomultipliers (PMT), can be used under high magnetic field and radio-frequency environments in MRI scanners. These solid devices consists of a large number of mini-cells, each of which, when stuck by a photon, generates an avalanche of electrons. We have tested solid state photomultipliers (SSPM) with a 556 mini-cells/mm^2, among several different solid state devices in the market. This presentation describes test methods and characteristics of SSPM with an emphasis to be used for PET scanners. We first measured energy and coincidence time reso-

lutions of PMT-LYSO couplings exposed to a ^{22}Na source to check a test setup and to compare these resolutions with those of SSPM-LYSO couplings. Then pulse characteristics of the SSPM-LYSO couplings were compared with those of the PMT-LYSO couplings. After estimating the charge generated in a single mini-cell, the gain at an operating voltage was obtained. We then measured energy and coincidence time resolutions of the SSPM-LYSO couplings exposed to various radiation sources such as ^{133}Ba, ^{22}Na, ^{137}Cs and ^{18}FDG.. We obtained a 25 % energy resolution and a 4.5 ns coincidence time resolution from the SSPM-LYSO couplings, and a 19 % energy resolution and a 0.73 ns coincidence time resolution from the PMT-LYSO coupling. The number of fired mini-cells and the amplification factor were ~150 for ^{22}Na and ~4×10^5, respectively. Even though energy and coincidence timing resolutions of the SSPM-LYSO couplings were worse than those with the PMT-LYSO couplings, newly emerging solid state devices with a higher particle detection efficiency than the tested SSPM could be promising for the combined PET/MRI scanners. We also present preliminary test results obtained under 3-T MRI environments.

E-04 **Improving Spatial Resolution and Sensivity of Small Animal PET Scanners with Three-Layer Scintillation Crystals** HONG Seong Jong, LEE Geon Song[1], PARK Kwang Suk[1], MUHAMMAD Jamil[2], RHEE June Tak[2], ITO Mikiko[3], SIM Kwang-Souk[3], HONG Byungsik[3], LEE Kyung Sei[3], KWON Sun Il[4], LEE Jae Sung[4](*Gachon University of Medicine and Science, Division of Biological Science and Neuroscience Research Institute. [1]Seoul National University, Department of Biomedical Engineering. [2]Konkuk University, Department of Physics. [3]Korea University, Department of Physics. [4]Seoul National University, Department of Nuclear Medicine.*) Improving the spatial resolution without sacrificing the sensitivity is one of the most challenging goals for small animal PET scanners. The 3-layer configuration that we propose consists of 7 mm long $L_{0.2}$GSO and 7 mm long $L_{0.9}$GSO crystals aligned with each other, and 7 mm long $L_{0.9}$GSO crystals with an offset of a half crystal pitch. This presentation describes the design and the Monte-Carlo simulation, along with test results. The 3-layer configuration proposes to distinguish signals of outer $L_{0.9}$GSO from those of $L_{0.2}$GSO using the different timing characteristics and signals of inner $L_{0.9}$GSO from those of outer $L_{0.9}$GSO using the charge-division algorithm. The cross section area 1.5 × 1.5 mm^2 of all the crystals is chosen to obtain a ~3 mm^3 volume resolution at the center of the scanner. The proposed system consists of 6 Hamamatsu H9500 PMTs and about 16000 crystals. To estimate the improvement of the spatial resolution and the sensitivity, we used GEANT4 to compare the 3-layer configuration with the 2-layer configuration of $L_{0.9}$GSO and $L_{0.2}$GSO. Matrix structures made of 3M multilayer polymer were built to provide wrapping and support of crystals. We also built a charge-division circuit to be used with Hamamatsu H9500 PMTs. The Monte-Carlo simulation showed a volume resolution to be ~3 mm^3 at the center and ~5 mm^3 at a 25 mm distance from the central axis with an average sensitivity of ~6 % within the axial direction of $|z|<15$ mm. Flood images of one layer with the charge-division circuit and H9500 showed a clear separation of crystals with a peak-to-valley value of ~8 at the center of a PMT. Initial tests showed that a high resolution of 3~5 mm^3 volume resolution for the size of a mice could be achieved with a sensitivity greater than 6 %.

E-05 **Fabrication and Characterization of organic Bi-stable light-emitting device using α-NPB** KIM Dal Ho, LEE Su Hwan, LEE Gon-Sub, PARK Jea-Gun (*Nano-SOI Process Laboratory, Hanyang University.*) An organic bi-stable device (OBD) was developed and exhibited nonvolatile memory characteristics with a current conduction bi-stability of ~1×10^2 and a threshold voltage of 2 V for the writing state. The OBD was fabricated with the following structure: aluminum (Al) layer / conductive organic layer / Al nano-crystals surrounded by amorphous Al_2O_3 / conductive organic layer / Al layer, where the organic material was N,N'-di(naphthalene-1-yl)-N,N'-diphenylbenzidine (α-NPB). In order to increase the data read-out rate of this type of memory device, an organic light-emitting diode (OLED) has been integrated with the organic bi-stable device, such that it can be read out optically. These features make the organic bi-stable light-emitting device (OBLED). The threshold voltage of OBLED was 5.1 V and during the first bias scan, the device as fabricated shows a very low current in the low-voltage range (0 ~ 5.1 V), indicating the device is at a high impedance state. However, at a critical voltage (~5.1 V), the current density has a sharp increase of nearly 2 orders of magnitude, indicating that the device has had a transition from the high-impedance state to a low-impedance state. When the bias voltage is

further increased, the device shows a very high current density. However, the current density - voltage curve recorded in the second bias scan is totally different from that observed in the first bias scan. Even in the low-voltage range, the device shows very high current density, indicating that the device remains in the low-impedance state. We obtained luminances for low-current conduction state and high-current conduction state of 34 cd/m^2 and 210 cd/m^2 at 4 V, respectively.

*This research was supported by the National Development Program for 0.1-Terabit Non-volatile Memories financed by the Korea Ministry of Commerce, Industry and Energy. We also thank SAMSUNG ELECTRONICS.

E-06 **아르곤 삼중점을 이용한 롱스템형 표준백금저항 온도계용 고정점 제작** 양 인석, 송 창호, 강 기훈, 감 기술, 김 용규(*한국표준과학연구원, 기반표준부.*) 순수한 아르곤은 온도 83.8058 K, 압력 68.8 kPa에서 기체, 액체와 고체가 공존하는 삼중점 상을 가지게 된다. 이 삼중점 상태에서 액체가 고체로 변할 때 생기는 잠열은 1.19 kJ/mol로서 아르곤 삼중점에서 아르곤의 응고나 용융을 실현하면 이를 온도계 교정의 고정점으로 사용할 수 있다. 본 연구에서는 상온에서 기체 상태인 순수한 아르곤을 밀봉형 셀에 60기압 정도 장입한 후 액체질소를 이용한 저온 유지 장치에 담아 삼중점을 실현하고 그 온도를 금속 보호관으로 된 롱스템형 표준백금저항 온도계로 관찰하였다. 저온 유지 장치는 준단열과정에서 삼중점을 실현시키기 위하여 외부의 열유입을 차단할 수 있도록 설계되었다. 실현된 삼중점은 100 분 이상의 긴 시간동안 1 mK 이내의 변화를 보임으로서 롱스템형 표준백금저항온도계용의 고정점으로 사용하기에 적합한 것으로 나타났다.

■ SESSION: E [EG2]
4월 20일 (금), 11:00 - 12:30
토파즈

E-07(초) **ARROW-like Solid Core Photonic Crystal Fibers and the Applications** CHO Min Hyung, CAI Wei[1], HER Tsing-Hua Her[2], LEE YoungPak[3](*Quantum Photonic Science Research Center, Hanyang University. [1]Department of Mathematics and Statistics, Univ. of North Carolina at Charlotte. [2]Department of Physics and Optical Sciences, Univ. of North Carolina at Charlotte. [3]Department of Physics, Hanyang University.*) A system of boundary integral equations based on free-space Green's function and Huygen's principle for the AntiResonant Reflecting Optical Waveguide (ARROW)-like solid core photonic bandgap fiber is formulated from the Maxwell's equations and numerically solved with Nystrom method for the calculation of confinement loss of the fiber. In addition, the preliminary experimental and analytical results from the ARROW model are compared with the simulation ones. The formulations of boundary integral equation for the scattering of electromagnetic wave from the 2-dimensional photonic crystal and magnetic photonic crystal are also described.

E-08 **Compact Design of Coarse Approach Mechanism for low-temperature UHV Scanning Probe Microscope** SEO Yongho(*Sejong University.*) We report a compact design for coarse approach mechanism so-called`walker' for low-temperature ultra-high-vacuum scanning probe microscope. We adapted the slip-stick principle with several actuators driven by time sequential scheme which was suggested by Pan et al. The shear piezo-stack was replaced by single PZT rectangular actuator to reduce the walker volume. Three slip-stick actuators are used rather than six actuators in original design. By using polished sapphire and rough alumina plates, perfect sticking and sliding interface was implemented. Our design minimizes usage of glue or epoxy of which attachment strength would be deteriorated by repeated temperature cycling. By using teflon material, the frictional force of sliding parts was reduced. Without using metallic spring, elasticity was provided by the teflon material against the holding force. We show the experimental data of driving voltage versus moving distance at liquid nitrogen temperature.

E-09 **Formation and Photoluminescence of $CaTiO_3$ and Pr^{3+}-doped $CaTiO_3$ by Mechanochemical Alloying** 박 경화, 김 현구, 명 화남[1](*조선대학교. [1]전남대학교.*) The formation and photoluminescence of the $CaTiO_3$ and Pr^{3+}-doped $CaTiO_3$ by mechanochemical method was investigated by X-ray diffraction, scanning electron microscope, energy dispersive X-ray spectrometer, transmission electron microscope, thermogravimetric /differential thermal analysis, Fourier transform infrared analysis, and luminescence spectrometer. In the XRD experiments, the phase of $CaTiO_3$ in the CaO-TiO_2 mixture improves in crystallinity as the milling times increase. The $CaTiO_3$ single phase can be formed in the

mixture milled for 150 min (500 rpm) or more. For the $CaTiO_3$ mixture milled for 90 min, the crystal of $CaTiO_3$ was formed from thermal annealing for 60 min at the temperature of 600°C. The typical $^1D_2$®$^3H_4$ transition of Pr^{3+}-doped $CaTiO_3$ host by mechanochemical method provided us emission at about 615 nm.
*본 연구는 조선대학교 WISE 광주/전남 지역센터 연구지원으로 수행되었음

E-10 **분광 타원분석법을 이용한 1차원 주기적 구조에 대한 해석** 김 태중, 이 선영, 공 태호, 한 승호, 정 진모[1], 김 영동(*경희대학교 나노광물성연구실 및 물리학과. [1]경희대학교 물리학과.*) 집적회로 기술의 발달은 소자의 크기에 지배되어 왔고, 그 크기가 100 nm 에 이르자 반도체 시장에서는 효과적인 metrology 가 중요시 되고 있다. 따라서 critical dimensional 물질의 제조, 적은 비용과 단시간에 수행할 수 있는 간단한 검사법은 중요한 관심이 되고 있다. 첨단산업기술분야에서는 현재 새로운 성장 및 제조방법의 개발과 더불어 차세대 나노구조 소자들의 성장 및 제조를 위해 비파괴적인 방법으로 분석이 행해지는 실시간 모니터링이 필수적으로 요구되고 있는데, 광학적 방법을 이용한 분광타원편광분석 실시간 모니터링 기술이 가장 적합한 방법으로 인정되고 있다. 타원편광분석법은 주로 균일한 박막의 두께 측정 및 광물성 연구에 사용되어 왔으나 Rigorous Coupled Wave Analysis (RCWA) 방법의 발달로 주기적 회절격자 연구에 있어 중요한 도구가 되고 있다. 본 연구에서는 이를 증명하기 위해 Quartz 기판 위에 Cr 이 주기적인 선을 이루는 1차원 구조의 (높이 약 55 nm, 폭은 500 nm, 패턴 주기 1 μm) 시료를 제작하여 분광 타원분석기로 450 ~ 900 nm 의 파장 구간에서 측정하였다. RCWA 해석법을 이용한 계산 값은 실험오차정도의 오차를 갖는 타당한 값을 얻어내었고, 분광 타원분석기가 소자 구조의 연구와 검사에 뛰어나고 유용하게 응용될 수 있다는 것을 제시하고자 한다.

E-11 **Oxidation process of Ni/Au thin films on p-type GaN** LEE S.P., JANG H.W., NOH D.Y., KANG H.C.[1](*Department of Materials Science and Engineering, Gwangju Institute of Science and Technology. [1]Advanced Photonics Research Institute, Gwangju Institute of Science and Technology.*) Oxidation mechanism of Ni/Au thin films on p-GaN is investigated by scanning electron microscopy, transmission electron microscopy, and synchrotron x-ray diffraction measurements. Up on annealing at 530℃ in air, Ni layer is oxidized to NiO, while Au layer transforms into the continuous Au network. In initial stage, Ni atoms diffuse out through defects to form NiO on the Au layer. Meanwhile, the Au atoms near the defects region occupy the portion of initial Ni layer underneath the Au layer. The process is continued until the Ni atoms are transformed into NiO phase completely. Consequently, Au network is buried under NiO grains and NiO grains fill up the empty space between Au networks.

■ SESSION: E [EG3]
4월 20일 (금), 11:00 - 12:45
에메랄드

E-12 **MC-50 사이클로트론을 이용한 SOBP 형성과 측정** 양 태건, 장 홍석, 채 현식[1](*원자력의학원. [1](주)에스에프테크놀로지.*) 원자력의학원의 MC-50 사이클로트론 빔라인 중 하나에 이온빔 세라피 기초 연구용 라인을 구성하여 in-beam 테스트를 했다. 세라피 연구용 라인은 기본적인 진공 빔라인에 이어 대기 상에서 모듈레이터, 에너지 시프트, 콜리메이터, 노즐 등을 부가적으로 포함하고 있다. 먼저, MCNPX 입자 전송 코드를 사용하여 빔라인 구성 요소들의 배치 조건에 따른 노즐 이후의 빔분포 계산하였고, 그 과정에서 세라피 연구에 적합한 빔분포의 평편도를 갖는 각 요소의 배치 조건을 찾았다. 계산된 각 요소의 배치 조건을 빔라인 설치에 적용한 후, 노즐 뒷단에 간단한 구조의 팬텀을 위치 시켜 in-beam 하에서의 SOBP(Spread Out Bragg Peak) 형성 테스트를 했다. MCNPX 코드의 전산모사로부터 SOBP를 형성을 위한 휠모듈레이터의 두께별 가중치를 구하고, 휠모듈레이터 회전 특성을 고려하여 가중치를 변환한 후 회전 콘트롤러에 적용했다. 본 연구에서는 가속기에서 45MeV 양성자빔을 인출하였고, 아크릴 팬텀에 대해 2mm 폭의 SOBP 영역 형성을 테스트했다. SOBP 형성의 확인은 지난 학회에서 발표했던, 삼각기둥 팬텀과 GAFCHROMIC 필름을 이용한 방법을 활용하였다. 팬텀 내 SOBP 영역의 위치나 폭은 계산 결과와 실험결과가 잘 일치했다. SOBP 영역의 모양은 측정결과 평탄하지 않은 것으로 나타났으나, GAFCHROMIC 필름의 quenching 특성을 계산 결과에 고려해 넣을 때 실험결과와 유사한 선량분포를 형성함을 확인할 수 있었다.

E-13 **편광 액정 홀로그램 격자의 제작과 분석** 최 현희, 우 정원(*이화여자대학교, 물리학과.*) 액정 다중격자의 제작은 광시약각을 위한 액정 디스플레이분야나 프로젝션 디스플레이 그리고 편광 빔스프리터,

광통신에서의 포토닉 디비이스, 편광을 이용한 응용 소자등으로 광범위한 응용성을 가지고 있다. 일반적으로 다중격자는 액정 배향막을 여러번 러빙하는 작업을 통하여 제작되어지지만 본 연구에서는 편광홀로그래픽방법을 이용하여 간섭패턴을 광배향막이 사용된 액정셀에 기록하는 방법을 통하여 편광 비틀림 액정 격자(Twisted Nematic Liquid crystal grating)를 제작하였다. 다중격자 제작에 사용된 편광은 S와P편광이었고 아조분자가 함유된 광배향막과 아조가 도핑된 액정을 사용하여 액정셀을 만들고 여기에 S와 P 편광에 의한 간섭을 기록하였다. 기록광인 S와 P편광에 의해 간섭된 원편광과 타원편광은 스핀 각운동량을 액정 분자에 전달하게 되어 인접한 도메인간의 비틀림각의 비틀림 방향은 서로 다른 방향을 가지게 되었다. 이로 인해 이 액정 격자는 입사광에 관계없는 회절 효율을 보였으며 입사광의 편광에 따라 회절광의 편광이 변조되었다. 또한 본 실험에서는 하이브리드한 셀을 제작하고 특성을 평가하였고 비틀림 액정 편광격자에 대한 이론적인 분석을 제시하였으며 액정의 회전 방향을 결정하는 스핀 각운동량의 중요성을 명시하였다.

E-14 **Double quantum dot system in carbon nanotube crossed junctions** LEE Dong Su, SVENSSON Johannes[1], PARK Seung Joo, KEMELL Marianna[2], RITALA Mikko[2], JONSON Mats[1], CAMPBELL Eleanor[1], PARK Yung Woo(*Nano Systems Institute-National Core Research Center, Seoul National University. [1]Department of Physics, Göteborg University, Sweden. [2]Department of Chemistry, University of Helsinki, Finland.*) Crossed junctions of carbon nanotubes (CNTs) separated by thin oxide layers have been fabricated by combination of chemical vapor deposition growth and dielectrophoresis. In the crossed junction device, the top metallic CNT is used as a local gate to control the electron transport through the lower semiconducting CNT. The explanation of the CNT-gate operation takes into account the presence of Schottky barrier at the interface between the semiconducting CNT and the metal electrodes. Coulomb oscillation was observed on the lower CNTs at low temperatures, where the behavior could not be interpreted by the concept of single quantum dot (QD) system. Instead, we have proposed another possible explanation, a double QD system, i.e. the gating field from the top CNT modulates the band structure in the lower CNT, producing double QDs. The gate dependent conductance data were measured at various temperatures supporting our explanation of double QD systems. In addition, we have intentionally fabricated more CNT crossed junctions without in-between oxide layers. In this case, the contact resistance between two tubes is a potential barrier splitting the initial single QD into two and the back-gate is used to modulate the energy levels of the two QDs. The back-gate dependent data measured from the crossed junctions without oxide layers could be interpreted more clearly by the double QD system.

E-15 **Stability of Quantum Dots Encapsulated into the Membrane Bilayer of Giant Unilamellar Vesicles** 이 규용, 위 행섭, 박 혁규(*부산대학교, 물리학과.*) We present detailed experimental procedures for the preparation of giant unilamellar vesicles (GUVs) with quantum dots (QDs) encapsulated into the membrane bilayer. We used Asolectin lipids and TOPO-coated CdSe QDs with QD core size ranging 3-5 nm. Spin coating method in conjunction with electroswelling technique yields vesicles with highly homogeneous unilamellar structure and large size up to 200 microns. Due to the high quantum yield and long term stability of QDs in the bilayer we obtain very clear fluorescent and confocal images of GUV membrane for an extended period of time. The calculations based on our theoretical model show that the encapsulation of QDs into the membrane bilayer is energetically preferred to the formation of QD-lipid micelles.

E-16 **The in-situ Study on the Transport Dynamics of a Cationic Hydrophobic Molecule across an Anionic Liposome Bilayer: Temperature Effects** 김 준헌, 김 만원(*KAIST 물리학과.*) By using second harmonic generation (SHG), we have studied the transport dynamics of cationic triphenylmethane dyes across anionic liposome bilayers. Because the square root of SH signal is proportional to the difference between the number of dye molecules on both sides of the bilayers, the time dependence of the SH signal provides nondestructive and in-situ information on the adsorption and the transport of these dyes across liposome bilayers. The transport rate can be changed by the lipid bilayer property or the external condition. In this presentation, we show the temperature effect on the transport rate of dyes across two kinds of liposome bilayer, dioleoyl-phosphatidylglycerol (DOPG) and distearoyl-phosphatidylglycerol (DSPG). In the case of DOPG bilayer which is in liquid-crystalline phase at room temperature, the transport rate of dyes significantly increases with temperature. In the case of

DSPG bilayer which is in gel phase at room temperature, dyes did not transport across bilayer in the experimental time scale at room temperature. However as we increase temperature, the transport starts above the gel to liquid-crystalline phase transition temperature which is lowered by the adsorption of dyes on the lipid bilayer. This kind of study can be used for the pharmaceutical application such as design of drug delivery systems.

E-17 **Control of Microstructure in Binary Alloys by Using Local Heat Perturbation** 이 규용, AKAMATSU Silvere[1], LOSERT Wolfgang[2], 박 혁규(*부산대학교, 물리학과. [1]Universites Pierre-et-Marie-Curie and Denis-Diderot, Institut des Nanosciences de Paris. [2]Univ. of Maryland, Dept. of Physics.*) When metallic alloys solidify, various microstructures form inside the alloys depending on the dynamics of the solidification process. The physical properties of alloys are largely influenced by the lengthscales of these structures. Therefore, the understanding and control of microstructure formation in solidification is important in order to achieve desired properties. We used an alloy model system, succinonitrile-coumarin152 (SCN-C152), to experimentally investigate dynamic selection and control of grain boundary structures and dendritic structures in binary alloys. We found that in a temperature gradient the grain boundaries drift toward the high temperature region in addition to the migration due to grain coarsening. We show how we can control grain boundary orientations by generating local temperature gradient through UV or laser heating. We show that perturbations also permit accurate control of the microstructure within a single crystal during the directional solidification process. Dendritic patterns can be controlled either by guiding the initial formation of the pattern or by triggering subcritical transitions between stable microstructures. Using another alloy model system, CBr_4–C_2Cl_6, we investigated the control of lamellar eutectic microstructures. We show that the laser spot perturbation technique can be efficiently used as a tool for mapping out the large range of accessible lamellar spacings and for creation of desired patterns such as smooth spacing gradients or tilt domains.

E-18 **방사선 피폭에 의한 금붕어 장관 평활근의 수축활성에 관한 연구** 문 경희, 김 성부, 옥 치일, 이 종규, 고 혜진[1], 박 남규[1], 길 상형, 조 승일(*부경대학교 물리학과. [1]부경대학교 식품생명공학부.*) 방사성동위원소 ^{18}F을 사용하여 4시간 동안 2Gy의 선량을 금붕어에 피폭시킨 후 시간경과에 따른 금붕어 장관의 수축활성 변화를 피지오그래프로 측정하였다. 수축현상을 관찰하기위하여 10^{-6} M의 아세틸콜린 수용액을 적출한 금붕어 장관에 투여하였으며, 방사선에 피폭되지 않은 금붕어장관의 수축활성을 대조군으로 두고 방사선에 피폭된 금붕어 장관의 수축활성을 비교분석하였다. 결과적으로 방사선 조사 1일 경과 후 장관의 수축활성이 대조군과 비교하여 75%나 줄었으며, 2일 경과 후에는 대조군과 비교하여 38% 수축활성이 줄었으나, 이때부터는 수축활성이 다시 증가하기 시작하여 한달 후에는 원래의 수축활성으로 회복되었다.

■ SESSION: F [FF1]
4월 19일 (목), 12:30 - 14:30
벌개미취2

F

FF-01(초) **Complexity Research in Management** 이 제호(*KAIST Business School.*) Until very recently, researchers in the management field and economics could not work with the structure of complex networks, such as customer interaction networks and organizational structure for learning. They had little choice but to ignore them. For example, Arthur (1989) ignored the complexity of customer interaction networks in studying competition between incompatible technologies. By simply assuming that all customers in the market interact with all the others, he showed that a firm or technology that gets ahead tends to increase its market share, coring the market over time. Recent advances in complexity theory, however, provided economists and management scholars with tools to reexamine the dynamics of customer interaction networks or learning networks for organizational members. The present work will review the progress of complexity research in these areas and highlight how this progress has cast new light on managerial implications.

FF-02(초) **사회연결망 분석의 역사와 전망** 김용학(*연세대학교 사회학과.*) 연결망의 중요성은 사회학이 성립되던 고전사회학에서부터 인식되었다.이 발표는 사회구조를 분석하는 방법으로 발전한 연결망 분석의 역사를되짚어보고 앞으로의 전망을 조망한다. 사회연결망은 사회가 구조화 된 형태를 밝히고 개인들이 이 구조에 놓여 있는 위치 효과를 분석하는 기법으로 발전하였다. 계급 구조에서의 위치, 조직 간 연결망에서의 위치, 인간 관계망에서의 위치 등이 각 개인의 의식과 행동에 영향을 미치고 또 그들의 성과에도 영향을 미치게 된다는 사실을 밝히려는 그 동안의 노력을 분류하여 소개하고, 또 앞으로 남은 과제가 무엇인지를 사회과학의 파라다임과 연관시켜 논의한다.

FF-03(초) **경제적 영역에서의 합리성과 비합리성의 상호작용에 대한 연구** 최 정규(*경북대학교 경제통상학부.*) 경제적 인간은 합리적이고 이기적이라고 가정된다. 하지만 사람들의 경제적 의사결정이 어느 정도 합리적인 토대 위에서 이루어지는지를 둘러싸고 많은 비판이 제기되어 왔다. 진화적 접근에 기초하여 합리적 주체와 비합리적 주체간의 상호작용을 통해 주체들의 합리성이 증진되는 방향으로 움직이게 되는지 그렇지 않은지를 살펴볼 수 있다. 개인들이 시간이 흐름에 따라 점차 합리성을 배워나가는 방향으로 학습과정이 일어나게 되는가 혹은 그렇지 않은가의 여부는, 풀어야 하는 게임의 성격, 주체들의 상호작용의 구조, 그리고 게임의 보수 구조 등에 달려 있다. 본 연구에서는 진화적 경로에서 이들 각각의 조건들이 어떤 방식으로 경제주체들의 선호 형성에 영향을 미치게 되는지를 살펴보고자 한다.

FF-04(초) **Generation of Tripartite Network of Drug-Target-Disease: A Platform for Novel Drug Discovery and Applications** RHO Kyoohyoung, LEE Jason S.M.[1], BAE Tae-Jeong[1], CHO Byunghoon, KIM Sunghoon[2](*Center for ARS Network, College of Pharmacy, Seoul National University. [1]Imagene Co. Biotechnology Incubating Center, Golden Helix, Seoul National. [2]Center for ARS Network, College of Pharmacy, Seoul National University, Imagene Co. Biotechnology Incubating Center, Golden Helix, Seoul National University.*) Since drugs and proteins exert their pharmacological and physiological activities through complex molecular networks, it is important to generate a window to which we can obtain an integrated view on the relationship between drugs, therapeutic targets and diseases. To generate the informatic platform providing comprehensive linkages of these three components. , we have collected the relation data between them from known databases and integrated them by using unique identifier scheme of Entrez GeneID, PubChem ID, and MeSH descriptor to protein, drug and disease, respectively. The assigned unique identifiers were validated by the curation of individual references. The database contains 9,196 proteins (including 1,544 therapeutic targets), 5,106 drugs (2,027 drugs of which have endogenous targets), 764 diseases, 3,820 drug-target interactions, 1,857 target-disease relations, 2,777 drug-disease relations and 31,349 protein-protein interactions. Graphical user interface was designed to provide information in network format, retrieve and extend a sub-network from the global map of drug, target and disease. This database is expected to be applied to drug target identification, drug repositioning, and finding new drug combination.

FF-06(초) **Human Disease Network** 고 광일(*고려대학교, 물리학과.*) Understanding of disease mechanisms is an important goal in human systems biology.

Towards this goal, we construct and study the "human disease network," that summarizes all known disorder-gene associations to provide a global system-level relationship between all human genetic disorders and offers a platform to integrate other human genomic and proteomic informations into single graph-theoretic framework. The obtained human disease network shows local aggregation of disorders of similar type reflecting the common genetic origin of many human disorders. Genes associated with similar disorders show both higher likelihood of physical interactions between their products and higher expression profiling similarity for their transcripts, suggesting the evidence of disease-specific functional modules. Further applications such as to disease gene prediction and drug-target network will also be discussed briefly.

■ SESSION: F [FG1]
4월 19일 (목), 16:30 - 18:15
벌개미취2

F-01(초) **Eigenvalue spectra of weighted Laplacian matrix on scale-free networks** KIM Doochul, KAHNG Byungnam[1](*서울대학교 물리천문학부. [1]서울대학교 물리천문학부 및 BK21 프런티어물리연구단.*) The density of states, or the spectal density, of the weighted Laplacian matrix associated with a random complex network is studied using the replica method. The spectal density is obtained in terms of a solution of non-linear functional equation for the static model of scale-free network in the thermodynamic limit. The link weights are parameterized by a weight exponent β. Explicit analytic results are obtained in the limit of large mean degree for arbitrary degree exponent λ and β. The spectal density shows qualitatively different behaviors depending whether β larger than, less than or equal to 1.

F-02 **Effect of Synaptic Decay on Stochastic Spiking Coherence in Coupled Excitatory Neurons** LIM Woochang, KIM Sang-Yoon[1](*아주대학교 의과학연구소. [1]강원대학교 물리학과.*) We consider a large population of globally coupled excitatory neurons. For the case of instantaneous delta synaptic coupling, stochastic spiking coherence (i.e., noise-induced coherence between neural spikings) is investigated by varying the noise intensity for a fixed coupling strength. The degree of stochastic spiking coherence is found to be maximal for an optimal noise amplitude. The effect of synaptic decay on such stochastic spiking coherence is then studied in the case of non-instantaneous synaptic coupling modelled by the α function with asynaptic time constant τ. (As τ goes to zero, the coupling becomes the instantaneous delta coupling.) Here, we fixthe coupling strength J at some appropriate value, and get the global state diagram through the contour plot of the spiking coherence measure M_s in the τ-D plane. For this case, the value of M_s decreases with increasing τ, eventually it becomes zero, for a threshold value of τ, and then incoherent state appears. Consequently, for the excitatory coupling the degree of stochastic spiking coherence becomes larger for smaller synaptic time constants. To get more insights on the effect of synaptic decay, investigations are also made in the τ-J plane for a fixed D, and similar results are obtained.

F-03 **A High Robustness and Low Cost Model for Cascading Failures** BING Wang, BEOM JUN Kim(*Sungkyunkwan Univ., Dept. of Physics.*) We study numerically the cascading failure problem by using artificially created scale-free networks and the real network structure of the power grid. The capacity for a vertex is assigned as a monotonically increasing function of the load (or the betweenness centrality). Through the use of a simple functional form with two free parameters, revealed is that it is indeed possible to make networks more robust while spending less cost. We suggest that our method to prevent cascade by protecting less vertices is particularly important for the design of more robust real-world networks to cascading failures.

F-04 **Memory-limited Strategies in Evolutionary Prisoner's Dilemma Game** BAEK Seung Ki, KIM Beom Jun(*Sungkyunkwan University.*) Evolutionary game theory studies emergent behaviors arising from strongly interacting elements, each of which determines its move from the past common history. The number of possible strategies, however, increases so rapidly with the number of past steps considered that the main attention has been drawn to the simplest memory one case, where only the last step is referred to. There appear some famous strategies such as Tit-for-tat, Grim Trigger, and Pavlov at this stage in the evolutionary prisoner's dilemma game. We investigate how the selection dynam-

ics changes if the last two steps are taken into consideration. Examining the memory one case closely in terms of transition matrices, we postulate that the equilibrium resulting from replicator dynamics can be a reasonable starting point where one can observe all relevant dynamics. This reduced zoo of memory two strategies exhibits interesting features, including the rise of an error tolerant strategy which contains Tit-for-tat as its fixed point.

F

F-05 **Phase Transitions of Biomaterials and the Possible Glass Formation** 이 광세(*인제대 나노시스템공학과.*) The viscous and glassy states of matter are relevant in many different areas of technology but also in daily life. The advantage of the amorphous modification of some pharmaceuticals over their crystalline counterparts stems from practical aspects such as increased dissolubility and therapeutic activity. Many common drugs contain small molecules and therefore, as glass formers, they are also interesting on their own. In this contribution I report on the structural phase transitions, melting, and freezing phenomena by the differential scanning calorimetry (DSC). This technique is applied to detect supercooled liquids and glasses made from aspirin ($C_9H_3O_4$) and anhydrous cholesterol ($C_{27}H_{46}O$). While in melt crystallization supercooling is inevitable, in solid-state phase transitions both supercooling and superheating are inevitable. The traditional phenomenological asymmetry between melting and freezing is discussed by considering the liquid nucleation behavior during melting and the crystal nucleation behavior during freezing. The possible glass formation is also reported via preliminary study.

F-06 **Spatial Correlations and Extended Self-Similarity in Sandpiles** HA Meesoon, URITSKY Vadim[1], PACZUSKI Maya[1](*Department of Physics. Chonbuk Nat'l University. [1]Complexity Science Group, Department of Physics and Astronomy. University of Calgary, Calgary, Alberta, CA.*) We investigate spatial correlations and extended self-similarity in the metastable states of directed sandpiles with a (1+1)-dimensional non Abelian stochastic directed sandpile model (SDSM) introduced by Hughes and Paczuski [PRL 88, 054302 (2002)]. The non-Abelian SDSM belongs to the same universality class as the Abelain one with respect to the self-organized critical (SOC) behavior avalanches, but it shows totally different structures of the SOC metastable states. We analyze such structures in terms of inter-grain (gap) distribution functions and various two-point correlation functions using Monte Carlo simulations. It is observed that large-scale network of grains has a time-dependent characteristic size of gap between grain clusters, and exhibit extended self-similarity analogous to that found in fluid turbluence when the avalanch propagation is mapped to to (1+1)D interface growth. Scaling arguments for (1+1)D results are also studied as well as additional pattern analysis of the non-Abelian SDSM in (2+1)D, whose results will be compared with recent observations of space plasmas quantitatively.

■ SESSION: F [FF2] / D [DF8]
4월 20일 (금), 09:00 - 10:30
벌개미취2

FF-11(초) **Dynamic Force-Fluorescence Spectroscopy of a DNA Holliday Junction Reveals a Conformational Reaction Intermediate** HOHNG Sungchul(*Department of Physics and Astronomy, Seoul National University.*) As mechanical parameters are being recognized as important determinants of many biological processes, single-molecule manipulation techniques have been continually evolving to break new records in their sensitivity and stability [1-3]. However, one biologically relevant detection regime that has been out of reach is that of high spatial resolution under weak applied forces. We have therefore developed a new single-molecule technique, whereby mechanical manipulation via optical tweezers and observation of molecular motion via single-molecule FRET are combined without compromising their individual capabilities. Using this approach we have studied the conformational dynamics of the Holliday junction under applied stretching force, that has revealed the existence a hidden intermediate state along the reaction coordinate. The length of helical arms is shown to be an important factor determining force sensitivity of the Holliday junction. This suggests that the recombination process occurring in the cell could be extremely sensitive to sub-pico Newton forces that last only milliseconds.

FF-12(초) **Tackling biology molecule by molecule** 이 종봉(*POSTECH, 물리학과.*) The study of a variety

of biological questions by real-time observation and manipulation of individual biomolecules or complexes. The single-molecule techniques allow us to track individual biochemical reactions over time. Through the removal of ensemble averaging in the conventional biochemical methods, single-molecule detections enable us to unravel the salient features of the reaction mechanisms (multiple pathways, time trajectories, and transient intermediates) as well as the fluctuations and distributions of molecular properties involved through the course of the enzymatic activities. I will present a story of using a novel single-molecule technique to study T7 bacteriophage replication machinery, which is the simplest model system of DNA replication.

FF-13(초) **Investigations on biological systems with micromanipulation: from single biomolecule to single cell** HONG SEOK-CHEOL(*Department of Physics, Korea University, Seoul, Korea.*) It is well known that biology has attracted much attention from physicists. For about past fifteen years, biophysics, which studies physical mechanisms behind biological phenomena, has focused on understanding of physical properties of biological molecules such as DNA, RNA, and proteins at single molecule level. Force, one of the most basic physical quantities, has been known to affect the conformation, structure, and function of biomolecules, and to function as an effector in various biological phenomena. Here, we present our researches on biological physics. First, with magnetic tweezers, one of the most versatile tools in mechanical manipulation of biomolecules, we studied conformational changes of DNA molecules when they interact with some chemicals and enzymes. Second, we combined single molecule fluorescence technique to magnetic tweezers to visualize single molecules while manipulating them. Using single molecule fluorescence (or FRET) measurements, we studied structural dynamics of short DNA molecules under external force and torque. Last, we present our studies on single cell biophysics, in which we have extended biophysical studies to single live cells (macrophages) to understand their physical properties and behaviors. We directly measured the force by the cells and their peculiar responses to external force gradient. Our studies showed that biophysical investigations can shed light on and provide useful information in understanding of various biological phenomena.

■ SESSION: F [FF3] / D [DF9]
4월 20일 (금), 11:00 - 12:30
벌개미취2

FF-14(초) **Swimming of Micro-organisms and Propulsion of a Micro-submarine** KIM Yong Woon(*KIAS, school of physics.*) Swimming on the micrometer scale calls for design strategies very different from the ordinary human-scale world, since inertia plays no role and friction is the only way of producing thrust. Cilia and flagella are essential building blocks for locomotion of eukaryotic organisms, and their design principles are the evolutionary answer to the need for generating thrust. Furthermore, recent technical developments in the synthetic manufacture of single-molecule motors raise the question about the minimal design for the effective propulsion of nano-sized machines working in a viscous media. Motivated by this, we study the propulsion efficiency of a system consisting of periodically beating elastic filaments anchored to a solid surface, which resembles the ciliary surface. We find that finite stiffness of the filaments breaks the time-reversal symmetry, showing cilialike beating patterns, and enables propulsion. It also turns out that self-organized synchronization between neighboring filaments occurs autonomously via hydrodynamic coupling, shedding light on metachronal coordination on bacterial surfaces.

FF-15(초) **Fluid Membrane and Quantum dots** PAK Hyuk Kyu, LEE Kyuyong, WI Hanengsub(*Pusan National University, Dept of Physics.*) We present detailed experimental procedures for the preparation of giant unilamellar vesicles (GUVs) with quantum dots (QDs) encapsulated into the membrane bilayer. We used Asolectin lipids and TOPO-coated CdSe QDs with QD core size ranging 3-5 nm. Spin coating method in conjunction with electroswelling technique yields vesicles with highly homogeneous unilamellar structure and large size up to 200 microns. Due to the high quantum yield and long term stability of QDs in the bilayer we obtain very clear fluorescent and confocal images of GUV membrane for an extended period of time. The calculations based on our theoretical model show that the encapsulation of QDs into the membrane bilayer is energetically preferred to the formation of QD-lipid micelles. The possible applications in biological physics will be discussed.

FF-16(초) **Bubble Formation in Topologically Constrained DNAs** 전 재형, 성 우경(*포항공과대학교*)

DNA is a double-helical biomolecule that carries genetic information for living organisms. Two single-stranded DNAs, with complementary sequences, are self-assembled into the stable duplex structure via hydrogen-bonding and stacking interactions. It is known that at physiological conditions the DNAs can be locally disrupted to open, which is called 'bubble' and is relevant to biological processes such as gene transcription and DNA replication. Single-molecule experiments using magnetic tweezers have shown that there is an interplay between the bubble and supercoiling when the DNA is topologically constrained, and a bubble is stably formed along the DNA at certain conditions. Motivated by these facts, we study the DNA bubbles induced by torsional strain or local unwinding in topologically constrained situation. We show that, when the supercoiling is sufficiently suppressed, a bubble is spontaneously formed along the DNA with the torsional strain above critical values which depend on the tension and the length of DNA. The bubble formation relaxes the strain and affects significantly the force-extension relation for the constrained DNA. For the case of torque-induced local denaturation such as the transcription bubble, the bubble formation can be much easier if DNA is initially in an underwound state relative to the relaxed one. Interestingly, a critical torque for bubble formation and the size of bubble sensitively depend on the site where the torque is applied.

■ SESSION: K [KG1]
4월 19일 (목), 12:30 - 14:00
휘닉스2

K-01 **In-situ Doping of $Si_{1-x}Ge_x$ Alloy Nanowires and Their Electrical Propeties** KIM Cheol-Joo, LEE S.H.[1], YANG Jee-Eun, PARK Nae-Man[2], PARK J.H.[2], MAENG Sunglyul[2], JO Moon-Ho(*Dept. of Materials Science and Engineering, Pohang University of Science and Technology (POSTECH), San 31, Hyoja-Dong, Nam Gu, Pohang, Gyungbuk 790-784, Korea. [1]Dept. of Materials Science and Engineering, Yonsei University 134, Shinchon-Dong, Seoul, Korea. [2]Cambridge-ETRI Joint Research Centre, Electronics and Telecommunications Research Institute (ETRI), 161 Gajeong-Dong, Yuseong-gu, Daejeon, 305-700, Korea.*) We show experimental demonstration of successful syntheses and doping of single-crystalline $Si_{1-x}Ge_x$ ($0 \le x \le 1$) nanowires by catalyst assisted chemical vapor deposition process using hydride precursors (SiH_4 and GeH_4) and doped to both p-type and n-type using gas phase dopants (B_2H_6 and PH_3). The relative composition and doping are reproducibly controlled by adjusting the growth conditions such as partial pressures of precursors and dopants. We confirmed that single-crystalline $Si_{1-x}Ge_x$ nanowires in our study are indeed random alloys of Si and Ge by micro Raman scattering study on individual $Si_{1-x}Ge_x$ nanowires. We also for the first time demonstrated the complementary doping of $Si_{1-x}Ge_x$ alloy nanowires for the use of the elemental nanodevice blocks. Specifically we have fabricated both p-type and n-type nanowire field-effect transistors and confirmed corresponding transistor operations in appropriated manners.

K-02 **Temperature Dependence of Chemical States between Amorphous and Crystalline $Ge_1Sb_2Te_4$** 이 영미, 정 민철, 신 현준, 김 형도, 고 창훈[1], 한 문섭[1], 김 기홍[2], 정 재관[2], 송 세안[2], 구 봉진[3], 하 용호[3](*포항가속기연구소. [1]서울시립대학교, 물리학과. [2]삼성종기원. [3]삼성전자.*) As one of promising candidates for next generation phase-change memory device, Ge-Sb-Te system has been intensively investigated in these days. The Ge-Sb-Te system utilizes phase changes from amorphous to crystalline states depending on temperature. $Ge_1Sb_2Te_4$ (GST) is known to have two crystal structures; the rock-salt (fcc) and hexagonal (hcp) structures. When amorphous GST (a-GST) is heated, transition to the fcc structure occurs around 150 ℃, and subsequent transition to the hexagonal structure around 250℃. Yet, chemical states of the GST have not been understood, especially experimentally, mainly because of the difficulty in obtaining oxygen free GST system for high-resolution x-ray photoemission (HRPES) spectroscopy. In this talk, we present HRPES data successfully acquired from an oxygen free a-GST and subsequent crystallized GST upon in-situ annealing the a-GST in ultra-high vacuum. The data show clear evidence of chemical state changes in the Ge and Sb core-levels upon annealing. Meanwhile, the Te core-level spectrum shows negligible changes. The Ge and Sb spectra have been deconvoluted to suggest that the observed chemical structure changes are due to structural changes of Sb and Ge.

K-03 **mask polarization effects for sub 50-nm pattern Generation** 김 상곤(*가톨릭대-정보전자공학부, 한양대-응용물리학과.*) For the larger wavelength then pattern size, mask polarization becomes a major issue: the vector interference forces polarized transmittance of mask and an excellent understanding of how to calculate and optimize polarization dependent mask parameter. In this presentation, it tries to describe how the photomask polarizes radiation in terms of material properties, mask pitch, and mask pattern size by using an analytical approach and the rigorous coupled-wave analysis (RCWA).
*ACKNOWLEDGMENT: This work was supported by the Korea Research Foundation Grant funded by the Korean Government (MOEHRD, Basic Research Promotion Fund) (KRF-2006-003-D00306).

K-04 **Effects of Abrasive Size and Molecular Weight of Poly(acrylic-acid) in Ceria Slurry on Pattern Density and Removal Selectivity of SiO_2/Si_3N_4 Films in STI CMP** CHOI Hyuk-Yul, KANG Hyun-Goo, PAIK Ungyu[1], PARK Jea-Gun(*Nano-SOI Process Laboratory, Hanyang University. [1]Division of Advance Material Science and Engineering, Hanyang University.*) The effects of the molecular weight and concentration of poly(acrylic acid) (PAA) with different primary abrasive sizes in ceria slurry on the nitride film loss, removal rate, film surface roughness, and removal selectivity of SiO_2-to-Si_3N_4 films were investigated by performing chemical mechanical polishing(CMP) experiments using blanket and patterned wafers. In the case of the blanket wafers, we found that for a lower PAA molecular weight, the removal se-

lectivity of SiO_2-to-Si_3N_4 films increased more significantly with increasing PAA concentration in slurry containing a larger primary abrasive size. For the patterned wafers, with a higher PAA molecular weight in the ceria slurry suspension, the erosion of the Si_3N_4 film was less, but the removed amount was also smaller and the surface roughness became worse after CMP. These results can be qualitatively explained by the layer of PAA adsorbed on the film surface, in terms of electrostatic interaction and rheological behavior.

*This work was supported by the Korea Science and Engineering Foundation (KOSEF) through the National Research Lab. Program funded by the Ministry of Science and Technology (No. M10400000436-06J0000-43610).

K-05 **저가 전구체 용액을 이용한 $CuInSe_2$ 박막 제조 연구** 김 재웅, 안 세진, 윤 재호, 이 정철, 윤 경훈(*한국에너지기술연구원.*) CIS($CuInSe_2$)계 화합물은 높은 광흡수계수와 안정성 및 밴드갭 조절의 용이함 등으로 인해 고효율 박막태양전지용 광흡수층 재료로 많은 관심을 끌고 있다. 실제로 CIGS 태양전지의 경우 NREL에서 19.5%가 넘는 에너지 변환 효율을 달성하였다. 그러나 이러한 우수한 성능에도 불구하고 동시증발장치와 같은 진공 공정의 특성상 공정단가가 높고 대면적화가 어렵다는 단점을 가지고 있다. 이런한 관점에서 저가의 전구체 물질을 이용한 비진공 코팅 기법은 CIS 태양전지의 가격을 낮추고 대형화 양산을 가능하게 하는 차세대 기술로 인식되고 있다. 본 논문에서는 비진공 코팅법을 이용하여 CIS 광흡수층을 제조하는 전반적인 과정, 특히 전구체 제조 및 코팅, Se 열처리 각 단계에서 광흡수층 막의 형상, 결정구조, 화학조성의 변화과정을 분석하여 CIS 박막의 형성 과정을 고찰하고자 하였다. 출발물질로는 $Cu(NO_3)_2$와 $InCl_3$를 선정하고, 이를 메탄올 용매에 녹여 전구체 용액을 만들었다. 여기에 유기물 바인더 물질을 첨가하여 닥터 블레이드 코팅에 적합한 점도를 맞춘 후, 이를 Mo/glass 기판에 코팅하였다. 코팅된 Cu,In 함유 유기물 혼합체를 공기중에서 1차 열처리 후 Se 분위기에서 열처리하면 태양전지용 CIS 광흡수층을 얻게 된다. 본 연구에서는 공정 각 단계에서 광흡수층 막의 형상, 결정구조, 화학조성의 변화과정을 분석하여 CIS 박막의 형성 과정을 고찰하고 특히 Se 열처리시 Se flux가 박막 특성에 미치는 영향을 조사하였다.

K-06 **Spectroscopic ellipsometry study of NiO thin films grown on Si substrates by using reactive DC magnetron sputtering** PARK Jun Woo, BAEK Seoung Ho, LEE Hosun, CHOI Kwang Nam[1], CHUNG Kwan Soo[1](*Kyung Hee University, Dept. of Physics. [1]Kyung Hee University, Dept. of Electrical Engineering.*) We deposited nickel oxide (NiO) thin films on silicon (Si) substrates at room temperature and 500℃ using a nickel target by reactive DC sputtering. We annealed the NiO thin films which were deposited at room temperature (RT). Using spectroscopic eillipsometry, we obtained the refractive indexes, extinction coefficients, thicknesses, bandgap energies and broadenings of NiO thin films. We obtained the bandgap energy and the broadening values by using standard critical point (SCP) Model.. We discussed relations of the optical and structural properties of NiO thin films with the oxygen flow rate, substrate temperature and annealing. The NiO films deposited at 500℃ had larger refractive indexes, extinction coefficients, crystallinity, and stability than those deposited at RT. However, the refractive indexes decreased and crystallinity increased when the films grown at RT were annealed. The absorption coefficients k increased as the photon energy decreased at near-infrared range for NiO thin films annealed at 800℃ and 1000℃. This may be the result of the formation of Ni cluster in the NiO thin films.

■ SESSION: K [KF1]
4월 19일 (목), 14:30 - 16:15
휘닉스2

KF-01(초) **Activation Studies of Si-implanted $Al_xGa_{1-x}N$** RYU Mee-Yi, MOORE Elizabeth[1], YEO Y. K.[1], HENGEHOLD R. L.[1](*Kangwon National University, Department of Physics. [1]Air Force Institute of Technology, Department of Engineering Physics.*) Si-ion implantation doping technique was used to produce good n-type conductive $Al_xGa_{1-x}N$ layer for application to the next generation electronic devices such as high frequency, high temperature, and high power electronic devices, and optoelectronic devices workable at short wavelengths in the UV-blue range. Electrical and optical activation studies of Si-implanted $Al_xGa_{1-x}N$ grown on sapphire substrates by molecular beam epitaxial method have been made as a function of ion dose, anneal temperature, and anneal time to obtain maximum possible activation efficiency. Si ions were implanted at 200 keV with doses ranging from $1x10^{13}$ to $5x10^{15}$ cm^{-2}. The samples were proximity

cap annealed from 1100 to 1300 °C for 5 to 25 min with a 500 Å thick AlN cap in a nitrogen environment. The carrier concentration of Si-implanted $Al_{0.18}Ga_{0.82}N$ annealed at 1200 °C increase continuously as the anneal time increases from 5 to 25 min, and nearly 100% electrical activation efficiency was obtained for a dose of $5x10^{14}$ cm^{-2} and 94% for a dose of $1x10^{15}$ cm^{-2} after annealing at 1250 and 1200 °C for 20 min, respectively. Although the activation is lower for the lower dose implanted samples, the activation efficiencies of 84% and 75% were obtained for the $Al_{0.14}Ga_{0.86}N$ after annealing at 1200 °C for 40 min for a dose of $5x10^{13}$ and $1x10^{14}$ cm^{-2}, respectively. Also, nearly 100% activation efficiency was obtained for $Al_{0.24}Ga_{0.76}N$ for a dose of $1x10^{14}$ cm^{-2} after annealing at 1300 °C. Both the sheet carrier concentration and electrical activation efficiency of Si-implanted $Al_xGa_{1-x}N$ increase continuously with anneal temperature and/or anneal time. The mobility also increases along with the increase in sheet carrier concentrations as the anneal temperature and/or anneal time increase, indicating successive damage recovery with increased anneal temperature and/or anneal time. The photoluminescence measurements show an excellent implantation damage recovery after annealing at the optimum anneal conditions, showing a strong near band emission. These optical results correlate well with the electrical results.

KF-02 **Heteroepitaxial Growth of High Quality GaN Thin Films on Si Substrates Coated with Self-assembled Submicron Silica Balls** 안 성진, 홍 영준, 이 규철(*포항공과대학교, 신소재 공학과.*) Heteroepitaxial growth of compound semiconductors on Si substrates has great potential for Si-based optoelectronics applications. Although there have been tremendous efforts to grow heteroepitaxial compound semiconductor films on Si for optoelectronic device applications, it is still very difficult to prepare high quality compound semiconductors on Si substrates if there are large differences in lattice parameters and thermal expansion coefficients between a thin film and a Si substrate. High density of dislocations and cracks are generated for typical lattice-mismatched compound semiconductor systems including GaN films on Al_2O_3 and Si substrates. Although epitaxial lateral overgrowth (ELO) of GaN layers on sapphire and Si substrates with a patterned thin film mask exhibited reduced dislocation density, a micro-patterned mask layer of SiO_2 or SiNx essentially has to be used for lateral growth, and complicated photolithography, thin film deposition, and growth interruption are inevitable. Meanwhile, a simple maskless overgrowth technique without either lithography or interruption can simplify the growth process, which is very helpful for high yield and low cost device fabrications. Here, we present a maskless heteroepitaxial GaN growth on a Si substrate with a self-assembled submicron silica ball layer. Monodispersed submicron-size silica balls were employed as an intermediate layer for heteroepitaxial growth of GaN layers on Si(111) substrates. Meanwhile, GaN thin films were grown on the silica ball-coated Si (SBS) substrates in a horizontal-type metalorganic vapor phase epitaxial growth reactor at low pressure. Prior to the GaN layer growth, AlN buffer layers were deposited on SBS substrates. The typical thickness of GaN epilayers grown for 80 min was 1.4 ㎛. The surfaces were fairly flat, and no pits or cracks were observed. The full-width at half maximum value of the rocking curve was 0.18°, much smaller than that of GaN epilayer on bare Si substrates, 0.30°. Furthermore, transmission electron microscopy and atomic force microscopy (AFM) revealed many enhanced structural characteristics and improved crystallinity for the GaN films on SBS substrates. In particular, for the region on or near the silica balls, no threading dislocations were observed and the total number of surface dislocations of the GaN on SBS substrate was smaller than 10^8 cm^{-2} as determined by AFM.

KF-03 **The stability of cubic GaN doped with transition metal ions** 최 은애, 강 준구, 장 기주 (*KAIST.*) The wurtzite structure is more stable than the zincblende one in bulk GaN. Because of the higher crystal symmetry than for the wurtzite phase, the cubic phase may have different optical and electrical properties. In recent experiments, the cubic phase was observed in GaN doped with 3d transition metals, such as Cr and Mn. Here we investigate the energetics of the hexagonal and cubic phases in GaCrN, GaMnN, and GaFeN alloys through first-principles calculations within the local-density-functional approximation (LDA). Due to the LDA band gap error, the transition metal d-levels are generally mixed with the conduction band of GaN, increasing the stability of the cubic phase. To remove such a mixing, we include strong on-site Coulomb repulsions (U) using LDA+U calculations. We discuss the effect of electron and hole doping on the stability of the cubic phase in GaMnN alloy.

KF-04 **Impact of V/III Ratio on Electrical Properties of GaN Thick Films Grown by Hydride Vapor-Phase Epitaxy** OH Dong-Cheol, HAN Chang-Suk, KOO Kyung-Wan(*호서대학교 국방과학기술학과.*) We have extensive studied electrical properties of GaN thick films grown under different V/III ratios by hydride vapor-phase epitaxy. First, the electrical resistivity of GaN films increases and the electron concentration decreases as V/III ratio increases, while the electron mobility increases. These mean that electron-feeding sources in GaN films are suppressed by enhancing V/III ratio, which is not by generating electron-trapping centers but by reducing donor-type defects. Second, the linewidth of X-ray rocking curves for GaN films decreases as V/III ratio increases. And, the deep-level emission intensity at 2.25 eV in 10 K photoluminescence spectra decreases with the increase of V/III ratio. These mean that higher V/III ratio condition helps for reducing crystalline point defects in GaN films. Third, it is shown that the electron transport of GaN films grown in lower V/III ratio condition is more hampered by the scatterings of ionized impurities and local point defects. It can be found that the three results are consistent to one another. Consequently, it is suggested that higher V/III ratios are very effective in the conductivity control of GaN films in terms of suppressing the generation of donor-type defects and electron-trap centers.

KF-05 **Magnetotransport in AlGaAs/GaAs double quantum well system with self assembled InAs quantum dots** KANNAN E. S., KIM Gil-Ho[1](*성균관대학교, 나노과학기술학부. [1]성균관대학교, 정보통신공학부, 성균나노과학기술원.*) Longitudinal and Hall magnetoresistance studies were carried out for a double quantum well (DQW) structure in which self assembled InAs quantum dots (QD) were embedded in the upper well. An abrupt increase in the Hall resistance is observed when the filling factor in the lower well reaches $\nu = 2$, but no such increase in the Hall resistance (R_{xy}) is observed when the DQW system is in monolayer configuration. Therefore the observed increase in R_{xy} as the DQW system evolves from a single layer to a bilayer is attributed to the tunneling of the edge states which increases the back scattering of the electrons in the edge channels. This edge state tunneling was observed all the way from balanced to far off balanced condition. It is also found that at low carrier densities well developed Hall plateau was observed at fractional filling factor $\nu = 3/2$. The appearance of $\nu = 3/2$ state is attributed to many body correlation effects due to inter-layer electron-electron interaction.

KF-06 **GaAs (111)A면 상에 성장된 InAs 양자점의 광학적 특성** 김 종수, 변 지수[1], 정 문석, 고 도경, 이 종민[2](*광주과학기술원 고등광기술연구소 나노광학연구실. [1]광주과학기술원 고등광기술연구소 레이저분광학연구실. [2]광주과학기술원 고등광기술연구소.*) 본 연구에서는 droplet 방식으로 GaAs (111)A면 위에 성장된 InAs 양자점의 광학적 특성을 photoluminescence (PL) 방법으로 연구하였다. InAs 양자점은 molecular beam epitaxy (MBE) 장치를 이용하여 GaAs (111)A 면 위에 성장하였다. Atomic force microscope (AFM)을 이용하여 양자점의 밀도는 $1x10^{10}/cm^2$ 이고 크기는 30 nm 정도임을 확인하였다. 저온 PL 측정 결과 (111)A 면 위에 성장된 InAs 양자점은 저온 10 K 에서 약 1.2 μm에서 발광을 보여 주었다. 이는 (001) 면 위에 성장된 InAs 양자점에서 보다 적색천이를 나타내었으며, 이는 표면 strain의 차이와 양자점의 aspect ratio에 의한 것으로 해석하였다.

■ SESSION: K [KF2]
4월 19일 (목), 16:30 - 18:15
휘닉스2

KF-07(초) **Control of the exciton by applied vertical electric field and single-photon emission from single InGaN/GaN quantum dots** TAYLOR R. A., JARJOUR A. F., OLIVER R. A.[1], KAPPERS M. J.[1], HUMPHREYS C. J.[1], TAHRAOUI A.[2](*Clarendon Laboratory, University of Oxford, Parks Road, Oxford, OX1 3PU, UK.. [1]Department of Materials, University of Cambridge, Pembroke Street, Cambridge CB2 3QZ, UK. [2]National Centre for III-V Technologies, Department of Electronic and Electrical Engineering, University of Sheffield, Mappin Street, Sheffield, S1 3JD, UK.*) We first present measurements on single InGaN/GaN quantum dots (QDs) under an applied vertical electric field. This is achieved by placing the QDs in the intrinsic region of a p-i-n diode structure [1]. Measurements were made using non-linear excitation spectroscopy. We demonstrated previously [2] that this

allows almost total suppression of the background emission from the underlying wetting layer and yet strong QD emission is still observed. In the present study, we show that an applied electric field along the growth direction results in large blue shifts (up to 60 meV) of the single exciton transition energy (Figure 1). The dependence of the energy shift on the electric field is found to have both linear and quadratic components, which are related to the induced dipole and the polarizability, respectively. Moreover, we show that the applied electric field results in the enhancement of the oscillator strength of the exciton transition due to the increase of the overlap between the electron and the hole wavefunctions. This is achieved via the study of the radiative lifetime dependence on the applied bias. We observe a significant reduction of the lifetime from 32 to 14 ns for an applied field up to half the internal piezoelectric field (Figure 2). In addition, preliminary measurements on the effect of the applied field on multi-excitonic states have been made. The experimental results are compared with theoretical modelling based on semi-empirical tight binding approach. We also present photon-correlation measurements from single InGaN/GaN QDs included in law-Q microcavity for the enhancement of extraction efficiency. The cavity consists of a high reflective AlN/GaN bottom DBR and a law reflective SiO/SiN top DBR. The experimental results (Figure 3) show that second-order correlation function vanishes at zero time demonstrating an almost perfect single-photon emission from these QDs.

[1] R.A. Oliver et al., submitted to Journal of Physics: Conference Series, October (2006). [2] A.F. Jarjour et al., Physica E 32, 119 (2006).

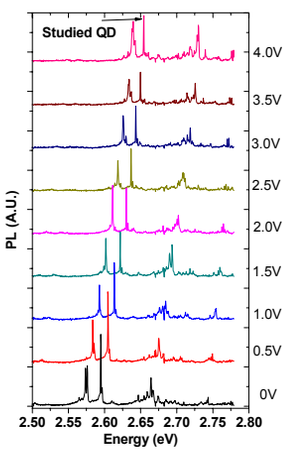

Fig. 1

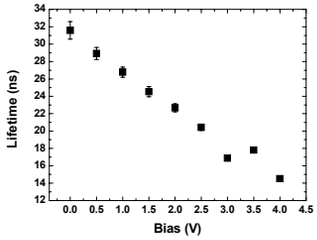

Fig. 2

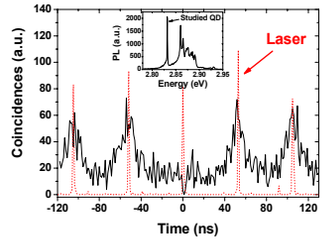

Fig. 3

KF-08(초) **Confined Energy Levels and Charge States of Ge Quantum Dots in Si** CHO Hoon Young (*Department of Physics and QSRC, Dongguk University, Korea.*) Confined energy levels and charge states of self-assembled Ge quantum dots (QDs) embedded in Si have been investigated. We have utilized the photocurrent measurement and deep level transient spectroscopy (DLTS) to study the energy levels of the confined ground states of QDs in Si, and electrostatic force microscopy(EFM) to identify the charge states of them. The sample was grown on (100) p-type Si substrates by rapid thermal chemical vapor deposition (RTCVD) using Silane (SiH_4), Germane (GeH_4), and Boron (B_2H_6) gases as Si, Ge, and p-type dopant sources, respectively. Self-assembled Ge QDs were deposited in the Stranski-Krastanow growth mode. The growth rate of the Ge QDs and Si layers was 1 ML/s at the active layers. Each QD layer was embedded in Si layers at the bottom and a $Si_{0.8}Ge_{0.2}$ QW on the top. A photocurrent signal at T=10 K was observed in the photon energy ranges of 140-400 meV (wavelength range of 3-9 mm) because of the inter-subband transition in the valence band of the self-assembled Ge QDs and the subsequent transport of photo-excited carriers. And the charge states emitted from a ground state in the QD confined state are observed by DLTS and the activation energy is calculated to be E_V+220 meV with the capture cross section of $2.1x10^{-14}$ cm^2, which is corresponding to the energy value obtained by the photocurrent measurement. From EFM images, the charge states were observed after the injection at +5V and -5V for 10s. The EFM results reveals that the charge states of Ge QDs could be electron as well as hole charge states to interact with both charges.

KF-09(초) **Growth and characterization of low density In(Ga)As/GaAs quantum dots** CHOI W. J., SONG J. D., CHO N. K., PARK S. J., LEE J. I., POIZAT J.-P.[1], AUFFEVES-GARNIER A.[1], DANG L. S.[1](*Nano Device Research Center, Korea Institute of Science and Technology, P.O.Box 131, Cheongryang, Seoul 130-650, Korea. [1]Equipe mixte CEA/CNRS/UJF "Nanophysique et Semiconducteurs", Laboratoire de Spectrom?trie Physique (CNRS UMR 5588), Universite Joseph Fourier – Grenoble,140, av de la physique, 38402 Saint Martin d'Heres Cedex, France.*) We have grown low-density (~5 QDs/mm^2) InGaAs/GaAs quantum dots (QDs) by using migration enhanced mo-

lecular beam epitaxy (MEMBE) [1], without any rotation stop during the growth of QDs. The height and width of InGaAs QDs are 5 and 72 nm, respectively, emitting 980-nm and 940-nm wavelengths from their ensemble ground state and the 1st excited state transitions, respectively, at 10 K. The large QDs are thought to be better suited for the study of quantum electrodynamics and quantum logic gate utilizing a single QD in micro-cavity, since they provide larger oscillator strength as well as larger coupling between the optical cavity mode and QD inside the cavity. The spatially resolved CL measurements at 5K showed that the density of QDs is uniform inside regions apart by 1mm from masking edges of the sample holder. This kind of growing technique for the low-density QDs is well matched to the large-area fabrication of single-dot based optical devices such as single photon sources and quantum logic gates. The exciton and bi-exciton peaks were identified from a single QD by using power-dependent micro-PL measurement in a flow-type liquid-He cryostat with a mesa-patterned sample. We have observed the exciton peak up to 40 K without any change in its emission wavelength, which is thought to be due to the large size of QDs. The temperature-insensitive exciton emission wavelength of the large QDs is suitable for the design of temperature-insensitive single photon source adapting micro-cavity including photonic-crystal cavity.

[1] N. K. Cho et al., Appl. Phys. Lett., 88, 133104 (2006).

KF-10(초) Practical application of 1.5 ㎛ QD laser for fiber communication OH D. K., CHOI B. S., SIM E. D., LEE C. W., KWACK H. S, KIM J. S.[1](*IT Convergence &Components Laboratory Laboratory, Electronics and Telecommunications Research Institute, 161 Gajeong-dong, Yuseong-gu, Daejeon, Korea. [1]Division of Advanced Materials Engineering, Chonbuk National University, 664-14 1Ga Deokjin-dong, Jeonbuk, Korea.*) Theoretically, a zero-dimensional quantum dot (QD), which is a three-dimensionally quantum-confined structure, provides the unique properties such as ultra-fast carrier dynamics and an increase in the optical non-linearity compared to other quantum structures. Due to these kinds of intrinsic properties, new-functional quantum devices including optical devices with a high-speed modulation, high output power, low driving current, and broad bandwidth are expected for the future applications. In particular, QD lasers with the emission wavelength of 1.3 ㎛ and 1.55 ㎛ for the fiber optic communications are expected to operate at the continuous-wave mode without a cooling system. QD lasers can also provide the excellent thermal stability and high direct-modulation speed due to the large differential gain. For the high speed modulation more than 10 Gbps by using quantum well (QW) laser, an external modulator is absolutely necessary due to the high chirp values, resulting in the increase in the module size and the price. If we consider the limit of the QW lasers, QD lasers with the distributed feedback (DFB) structure can be the only candidate to meet the demands in the optical communications [1]. Because of the extremely low threshold current and wavelength shift with temperature, QD lasers may provide the breakthrough for the deadlock we have encountered in the future optical devices including communication devices. Therefore, prompt commencement on the nano-QD devices, especially for the fiber optic communications, is necessitated for the prior occupation in the competition of the future technologies.

[1] J.S. Kim et al., Photonics technology letters 18, 595 (2006).

KF-11(초) InGaAs/InP quantum dots grown by MOCVD and their application for optoelectronic devices JEONG W. G., PYUN S. H., LEE D.[1], KIM N. J.[1], LEE E. G.[1], JANG J. W.[2](*Department of Materials Engineering, Sungkyunkwan University, Suwon, Korea. [1]Department of Physics, Chungnam National University, Daejeon, Korea. [2]NanoEpi Technologies, Ansan, Korea.*) InGaAs/InGaAsP/InP quantum dots (QDs) have been grown by Metal-Organic Chemical Vapor Deposition. The areal density of the grown QDs has been controlled up to 10^{11} cm^{-2}. The time-resolved photoluminescence shows that the carrier decay lifetime does not change in the bandwidth larger than 80 nm with a value of 1.8 nsec indicating that the grown QDs are electrically isolated with each other. The cw operation of the QD laser diodes (LDs) at room temperature and up to 75°C has been demonstrated for the ridge-waveguide LDs with QD multistacks of 3~7 QD layers in the lasing wavelength of 1480~1560 nm. The external quantum efficiency of 45 % is measured and the output power reaches higher than 150 mW. These show that the grown QDs are of high crystal quality. However, the threshold current densities are generally higher than those of quantum well LDs, the number of lasing modes increases as the driving current increases,

and the lasing wavelength shifts with the cavity length and ridge width much. These negative effects are due to the inhomogeneous broadening of the gain from the electrically isolated QDs that distribute the carriers into many different subband energies of the QDs and the involvement of excited energy states of the QDs. This inhomogeneity of the gain, however, has been positively utilized for QD semiconductor optical amplifiers (SOAs). The QD SOAs have been fabricated to have tilted mirrors at the angle of 7^{o} and with anti-reflection coatings. The fiber-to-fiber small signal gain of 23 dB, the saturation output power of 10 dBm, and the gain bandwidth of 45 nm have been measured with a fiber coupling loss of 7.2 dB from the QD SOAs with 5~7 QD multistacks. With the increase in the driving current, the gain from the excited states gets larger and this flattens and broadens the gain spectrum. These high gain and high saturation output power, the gain flattening effects by the excited states do show the bright potential of the QD SOAs for practical devices. In addition, there still remains an engineering field where the gain from each layers of the QD multistack can be independently controlled that further flattens and broadens the gain spectrum of the QD SOAs. This possibility has been seen from the QD multistacks intentionally grown to have two different PL peak wavelengths of 1450 nm and 1600 nm.

■ SESSION: K [KT1]
4월 19일 (목), 21:00 - 22:00
에메랄드

KT-01(초) **Recent Progress of InGaN Laser Diodes in Blue and Green Wavelength for Mobile/Portable Laser Projector Applications** NAM O.H., JANG T., HA K.H., LEE S.N., SON J.K., RYU H.Y., KIM K.S., PAEK H.S., SUNG Y.J., KIM H.G., CHAE S.H., KIM Y.H., PARK Y.(*Photonics PRJ. Team, Samsung Advanced Institute of Technology, Suwon, Republic of Korea.*) InGaN has been investigated as a semiconductor material suitable for optical sources emitting in the violet to green spectral range (405nm ~ 520nm). Recently, the market for InGaN laser diode (LD) has been rapidly grown by successful commercializing of the optical storage systems such as Blu-ray and HD-DVD players which has the wavelength of 405nm. In addition, mobile or portable laser projectors that require blue and green (445 nm ~ 520nm) optical sources are the next potential market for InGaN LDs. According to the high color gamut chart, laser based display showed 130% of color representation, higher than that of LED (105%) and Arc lamp (72%). Laser projector would have high resolution, high brightness, small size and low input power comparing to other projection display devices but in order to manufacture the laser projector, RGB (Red/Green/Blue) semiconductor LDs should be obtained.In this paper, InGaN based blue and blue-green LDs were investigated with regard to the characteristics of InGaN semiconductor laser diodes. High power, single mode blue LDs with high COD level (~334mW under CW operation at 25°C, kink-free at 150mW) and long lifetime (~10000 hours under CW operation, 50mW 25°C) were achieved. No significant characteristic differences between blue LDs on LEO-GaN/sapphire and GaN substrate were observed. The blue-green LD which has the wavelength of 485 nm was for the first time successfully fabricated and demonstrated under CW operation 25°C, while it showed poor performances of LD characteristics compared to those of blue LDs. We believe that the poor performance of blue-green LDs were caused by the piezo-electric effect by lattice mismatch along C-axis of GaN, In fluctuation by lattice mismatch and In solubility limit in InGaN QWs and thermal annealing which was performed during the p-layer growth. Further improvement should be required in the future for the development of InGaN green LDs.
[1] O. H. Nam, K. H. Ha, H. Y. Ryu, S. N. Lee, T. Jang, K. K. Choi, J. K. Son, J. H. Chae, S. H. Chae, H. S. Paek, Y. J. Sung, T. Sakong, H. G. Kim, Y. H. Kim, and Y. Park, presented at SPIE, 2006.[2] O. H. Nam, K. H. Ha, S. N. Lee, H. Y. Ryu, J. K. Son, T. Jang, K. S. Kim, H. S. Paek, Y. J. Sung, H. G. Kim, S. H. Chae, Y. H. Kim, and Y. Park, "AlInGaN-based laser diodes in blue and green wavelength," presented at International Workshop on Nitride Semidonductors, Kyoto, Japan, 2006.

KT-02(초) **Technology issues in accelerating the evolution of LED for solid state lighting** HONG Chang-Hee(*Semiconductor Physics Research Center and Department of Semiconductor Science and Technology, Chonbuk National University, 561-756, Korea.*) LEDs exhibit a technological roadmap that far exceeds the luminous efficacy of any traditional lighting sources. The DOE estimates that by 2020 LED light sources will reach up to

200 lm/W. Fortunately the performance of high power LED continued its faster growth in 2006 due to a strong demand of industry for solid state lighting. Nichia have announced a 150 lm/W lamp-type small white LED at the end of last year. However, its performance is decreased dramatically as the current is increased. As you know, the thermal-optical interaction can be strongly related with increase of the driving current. Still we have to improve the external quantum efficiency which can be product by internal quantum efficiency (IQE) and extraction efficiency (EXE) in order to decrease the effect of thermal issue. How can we get 100% IQE? Does it possible to reach it? What is the maximum of EXE value? This present will address the several technology issues to be considered for accelerating the evolution of InGaN/GaN LED for solid state lighting.

■ SESSION: K [KG2]
4월 20일 (금), 09:00 - 10:45
휘닉스2

K-07 **Interaction of Oxygen Vacancy with Hydrogen in ZnO** KIM Yong-Sung(*Korea Research Institute of Standards and Science.*) We have investigated the interaction of oxygen vacancy (V_O) with hydrogen in ZnO using the density-functional theory calculations. Formation energies of hydrogen interstitials, V_O, and various V_O-hydrogen complexes are calculated. We have considered three different V_O-hydrogen complexes; the V_O-atomic-hydrogen complex (H_O; hydrogen substitutional at O site), the V_O-molecular-hydrogen complex (V_O-H_2), and the H-passivated V_O complex. The H_O is a shallow single donor (H_O^+), as recently proposed by Van de Walle [Nature Materials 6, 44 (2007)], forming a multicenter bond with neighboring four Zn atoms. The H-passivated V_O complex consists of two H with V_O in the Zn-H-Zn bonding configurations without any gap states. The V_O-H_2 complex is found to be a double donor [$(V_O\text{-}H_2)^{2+}$] in ZnO. The double donor state is originated from the singlet state of the V_O. However, the double donor level becomes shallower by about 0.5 eV in the V_O-H_2 complex, as compared with that of the V_O. It is due to the suppressed singlet-triplet split of the four Zn 4s orbitals in the presence of H_2 molecule inside the V_O. The H^+ interstitial trapped in V_O^0 forming the H_O^+ gains the energy of 1.1 eV/H, while the H_2 molecule trapped in V_O^{2+} forming the $(V_O\text{-}H_2)^{2+}$ generates the energy of 1.3 eV/H_2. When the $(V_O\text{-}H_2)^{2+}$ complex is formed through combining V_O^0 and two H^+ interstitials, the energy gain is found to be 0.7 eV/H_2. Thus, the H_O^+ is more probable as a H-related donor species in ZnO, and we expect that the $(V_O\text{-}H_2)^{2+}$ species can exist in quenched ZnO samples after hydrogenation in H_2 ambient.

K-08 **Co 이온을 주입시킨 단결정 ZnO의 후속 열처리 온도 따른 구조 및 전자기 특성** 박 강순, 박 광호[1], 이 은경[1], 권 혁란[1], 송 영열[1], 강 희재[1](*충북대학교. [1]충북대학교,물리학과.*) 최근에 발표된 Sato 와 Katayama-Yoshida 등의 논문에 의하면 Co를 주입한 ZnO가 상온에서 강자성특성을 가지고 있다고 이론적으로 보고하였다.[1] 그 후 몇몇 그룹에서 상온에서 $Zn_{1-x}Co_xO$의 강자성특성을 보고 하였으나 아직 완벽하게 이해되지 못하고 있다. 본 연구에서는 350 ℃의 ZnO(0001) 기판에 Co^- 이온 $3 \times 10^{16}cm^{-2}$ 을 80 keV의 에너지로 주입하였다. Co^- 주입 후 700, 800, 900℃ 각각의 온도에서 열처리를 통하여 이온 주입 시 손상된 결정구조를 복구하였다. Co^- 를 주입한 ZnO의 열처리 온도에 따른 시료의 구조 분석은 X-선 회절실험을 통해 수행하였으며, 그 결과 주로 육방정 wurtzite ZnO의 결정구조를 지니고 있었으며 제 이차 상으로 Co(111) 결정구조가 미세하게 포함되어있음을 확인하였다. 이차 상으로 존재하는 Co의 결정구조는 후속 열처리의 온도가 증가할수록 피크의 세기가 상대적으로 증가하고 있음을 확인할 수 있었으며, 이 결과로 Co의 석출이 증가됨을 알 수 있었다. 또한 국소 구조를 확인하기 위한 EXAFS와 XANES 측정 결과에서 시료 내에 Co-Co와 Co-O의 결합이 함께 존재함을 확인할 수 있었으며 이러한 결과는 X-선 회절의 Co 결정의 석출에 부가적으로 Co 산화물의 존재도 확인해 주고 있다. 온도에 따른 자기화를 알아보기 위하여 SQUID를 사용하여 field-cooled(FC)와 zero-field-cooled(ZFC)를 측정하였으며, 열처리 온도가 증가 할수록 bloking temperauture(T_B)도 증가하는 것을 볼 수 있었다. 10 K에서 측정한 PL(photoluminescence) 스팩트럼을 통해서 Co^- 이온을 주입하지 않은 ZnO와 주입 후 열처리를 한 시료 사이에 near-band-edge 와 green-band의 변화를 조사하였다. 또한 Zn자리에 Co가 위치했을 때 anomalous Hall effect (AHE)가 약 50 K 까지 관측되고 있으며 이는 ZnO 내에 일부 Co 금속상이나 산화물 상이 포함되어 있을 지라도 일부 Co^- 이온이 자성 반도체의의 형성에도 기여하고 있음을 나타내고 있다.

[1] K. Sato and H. Katayama-Yoshida, Jpn. J. Appl. Phys.39,L55(2000).

K-09 **RF 마그네트론 스퍼터 법으로 성장한 Al 도핑된 ZnO 박막의 광학적 특성** 김 득영, 성 준제, 김 지훈, 정 의석, 이 아령, 봉 하종, 심 다혜, 이 영민(*동국대학교 이과대학 반도체과학과.*) RF 마그네트론 스퍼터법을 이용하여 Corning 1737 glass 기판에 Al이 2.5 wt% 도핑된 ZnO(순도 99.995%) 타겟을 이용하여 ZnO:Al (AZO) 박막을 성장하였다. AZO 박막은 각각 다양한 온도와 가스 분위기에서 성장하였으며, 각 시료들의 구조적 특징은 XRD, SEM을 이용하여 확인하였고, 전기적 특성을 조사하기 위해 Van der Pauw Hall effect 측정을 하였다. 성장된 박막의 Hall effect 측정 결과에 따르면 모든 시료는 n-type 특성을 보였고, 온도가 변화함에 따라 비저항이 변하는 것을 알 수 있었다. 또한 UV-VIS spectrometer를 이용하여 200nm~800 nm의 가시광 영역에서 광학적 투과 특성을 분석한 결과 90% 이상의 광투과율(transmittance)을 보였으며, 이를 Kramers-Kronig 법을 이용하여 반사율(reflectance), 굴절율(reflactive index)을 계산하였다. 흡수계수(abosorption coefficient)는 흡광도(absorbance)를 측정하여 계산하였고, 이렇게 구한 흡수계수로부터 얻은 광학적 밴드갭 에너지는 약 3.7eV 이었다.

K-10 **Effects of near surface charge on vertically aligned ZnO nanorod growth** PARK SUN HONG, KIM SEON HYO, HAN SANG WOOK, SEO SOO YOUNG, KWAK CHANG HA, LEE YOUNG BYUNG(*포항공과대학교.*) We demonstrate the effects of surface conditions such as surface roughness and charge on the crystallinity and shape of the vertically aligned ZnO nanorods grown on Al_2O_3 substrates with GaN interlayers. ZnO nanorod arrays with a diameter of 40~70 nm were fabricated on various substrates, such as n-GaN, p-GaN and sapphire [0001] by metal organic chemical vapor deposition (MOCVD) at 350 - 500℃. The structural properties of the ZnO nanorods were studied using various techniques. Field emission scanning electron microscope (FE-SEM) measurements demonstrated that vertically well-aligned ZnO nanorods were grown on a smooth GaN interlayer (roughness <0.3 nm) while they became a film as the roughness of the interlayer was larger than 0.3 nm which is comparable to the bond length of Zn-Zn or O-O pairs in the ZnO microstructures. To understand the surface-charge effect on the ZnO nanorod growth, we intentionally implanted H^+ ions on the n-GaN interlayers, with thickness of 2 mm. In general, vertically aligned ZnO nanorods were grown well on n-GaN. The H^+s were mostly implanted on 570 nm depth with a Gaussian distribution. The surface charge was estimated to be 1.5 x 10^{-10} cm^{-2}. Transmission electron microscopy (TEM) measurements confirmed no ionic damage near the surface. The ZnO could not form into nanorods on the H^+-implanted n-GaN interlayers. Our observation of the surface roughness and charge effects on the ZnO nanorod growth strongly suggested that Zn^{2+} ions bonded first on the substrate surface for the ZnO nanorod growth.

K-11 **Selective Growth of ZnO Nanorods on Facet-controlled GaN Micropatterns** HONG Young Joon, AN Sung Jin, JUNG Hye Sung[1], LEE Chul-Ho, YI Gyu-Chul(*포항공과대학교 신소재공학과. [1]포항공과대학교 환경공학부.*) Position-controlled vertical arrays of semiconductor one-dimensional nanostructures offer the ideal geometry for use as functional components in nanometer-scale integrated electronics and optoelectronics. Recently, a few well-controlled semiconductor nanowires have been achieved by either metal catalyst-assisted or catalyst-free methods. For metal catalyst-assisted vapor-liquid-solid (VLS) methods, the choice of materials is limited by the need to form a eutectic, and furthermore, there is the possibility that undesirable metal impurities might be incorporated into the nanowire. Here, we report catalyst-free, selective growth of ZnO nanorods using facet-controlled GaN micropatterns with highly anisotropic surface energies. For the selective growth of ZnO nanorods, position-controlled GaN hexagonal microrods and micropyramids were prepared on GaN/Si substrates with a SiO_2 hole pattern mask by selective MOVPE. ZnO nanorods were selectively grown only on top-surfaces of GaN micropattern arrays by using catalyst-free low-pressure MOVPE. Only one ZnO nanorod was formed on GaN micropyramids with a sharp tip while many ZnO nanorods on GaN microrods with a flat top surface. Electron microscopy and high-resolution synchrotron-radiation X-ray diffractometry indicates that the c-axis-oriented, single crystal ZnO nanorods were heteroepitaxially grown only on GaN(0001) with homogeneous in-plane alignment between the nanorods. Furthermore, these selectively grown ZnO nanorods exhibit excellent photoluminescent characteristics with a free exciton PL peak, resulting from the high-purity process without using any metal-catalyst and pattern mask. The accurate position-control of the nanorods offers an easy way of integrating vertical nanorods for many electronic and optoelectronic integrated circuit applications.

K-12 **CNT를 이용한 ZnO 나노구조의 저온 성장 및 물성평가** 박 승식, 이 진무, 윤 승일, 이 동구, 김 성진, 김 상협[1], 맹 성렬[1], 김 상우(*금오공과대학교 신소재시스템공학부. [1]한국전자통신연구원 Cambridge-ETRI 공동연구센터.*) 최근 nanotube, nanowire, nanobelt, nanowall 그리고 nanorod 등과 같은 1차원 나노구조 물질의 제작 및 특성평가에 관한 연구와 1차원 나노구조의 전기적, 기계적 특징을 이용한 나노스케일의 소자제작에 대한 연구가 많은 주목을 받고 있다. 이중 ZnO는 3.37 eV의 와이드 밴드갭과 60 meV의 높은 exciton binding energy를 가지며, 특히 1차원 ZnO 나노구조물은 나노스케일의 LED, LD, 태양전지, 가스센서 등의 다양한 분야의 차세대 나노소자 응용을 목적으로 활발히 연구되고 있다. 이러한 ZnO 1차원 나노구조를 성장하기 위해 MOCVD, thermal CVD, wet chemical 합성 등의 방법이 이용되고 있다. 그러나 이러한 방법들은 고온(600-1000도) 공정을 수반해야 하는 단점을 가지며, wet chemical 합성의 경우 저온 성장이 가능하나 성장된 나노구조에 상당히 많은 결함을 갖고 있어 소자 활용성에 문제점을 수반하게 된다. 본 연구에서는 이러한 점을 개선하기 위해 스크린 프린팅된 CNT 박막위에 thermal CVD를 이용하여 무촉매 방식으로 저온(400도 및 500도)에서 ZnO 나노구조를 성장 시켰고, 성장된 나노구조의 물성평가를 수행하였다. FE-SEM, XRD 분석을 통해 ZnO 나노구조의 모폴로지 및 결정성을 확인하였고, 저온 및 온도의존 PL 측정을 통해 저온에서 성장되었음에도 불구하고 deep level 발광이 매우 미약함을 확인 할 수 있으며, 이를 통해 성장된 나노구조물이 낮은 defect density를 가짐을 알 수 있었다.

*This work was supported by the Ministry of Information and Communication (MIC), Republic of Korea, under Project No. A1100-0602-0101.

K-13 **Hydrogen Effect on Optical and Electrical Properties of ZnO Thin Films by Pulsed DC Magnetron Sputtering** PARK Young Ran, JUNG Donggeun, KIM Young Sung[1](*Sungkunkwan University, Department of Physics. [1]Sungkunkwan University, Advanced Material Process of Information Technology.*) Transparent conducting nano-structured hydrogen doped zinc oxide (ZnO:H) thin films are deposited on corning 7059 glass substrates by bipolar pulsed DC magnetron sputtering at a substrate temperature of 500℃. During the ZnO:H deposition, H_2 and Ar mixed gas was fed into reaction chamber. We analyze the structural and optical, and electrical properties of ZnO:H using the X-ray diffraction (XRD) measurements, micro Raman spectroscopy, ultraviolet-visible spectrometer in the wavelength range of 200 – 1100 nm and Hall-effect measurements using Van der Pauw method at room temperature, respectively. XRD results show that as H_2-flow continuously increased, the intensity of (0002) peak decreased markedly. The electrical conductivity of ZnO:H thin film increased from insulating to 39 $\Omega^{-1}cm^{-1}$ with n-type behavior being maintained. These results confirmed hydrogen's role as a shallow donor. Micro-Raman was used to investigate the vibration properties of thin films. E_2(low, high), A_1^{LO} ,and week additional mode were observed to located at 95, 432, 573, and 501 cm^{-1}, respectively. Particularly, increasing the intensity of A_1^{LO} mode is observed for increasing the H_2 flow ratio.

** Acknowledgments : This work was supported by the Korea Research Foundation Grant funded by the Korean Government(MOEHRD) (KRF-2005-005-J11902).

■ SESSION: P1
4월 19일 (목), 14:30 - 16:15
스키하우스

Dp-001 **Electron Magnetic Resonance Study of Cu^{2+} Impurity in K_2SnCl_6 Single Crystal** YEOM Tae Ho, LEE Soo Hyung, SEO Yong-Mun[1], SONG Seung-Ki[1](*Applied Science, Cheongju University. [1]Department of Physics, Myongji University.*) The A_2BX_6 compounds show a variety of physical properties depending on the different ions in the unit cells. The magnetic properties, structural phase transitions, and molecular reorientations were investigated. The magnetic resonance spectra of Cu^{2+} ion in K_2SnCl_6 single crystal, grown by aqueous solution method, were obtained by X-band EMR spectrometer. The spectroscopic splitting parameter are determined with the effective spin Hamiltonian. Energy levels of the ground state for the magnetic ion embedded in the K_2SnCl_6 single crystal are calculated. The substitutional site location was also discussed.

Dp-002 **Observation of room temperature ferroelectricity in strained $SrTiO_3$ thin films on $SrTiO_3$ substrate** KIM Yong Su, KIM Dong Jik, CHOI Jin Sik[1], KIM Tae Heon, JO Ji Young, BARK Bae Ho, YOON Jong Gul[2], NOH Tae Won(*ReCOE &FPRD, Department of Physics and Astronomy, Seoul National University. [1]Department of Physics, Konkuk University. [2]Department of Physics, University of Suwon.*) $SrTiO_3$ (STO) is known well as incipient ferroelectric (FE) material. That is, competition between FE instability and intrinsic factors, such as quantum fluctuation or the antiferrodistortive interrupt the FE transition down to 0K. These disturbance factors can be overcome by external operation. Therefore, enhancement of the Curie temperature can be achieved by doping with other atoms, isotopic substitution in the oxygen octahedra, applying external electric fields, or strain. There have been lots of reports for observation of ferroelectric properties in incipient FE material at higher than 0 K, especially on $SrTiO_3$. However, in most previous works, the direct evidences of the spontaneous polarization have been rare. Instead, anomalies of dielectric constant, the second harmonic generation, or changes in the lattice constants were presented as evidences of ferroelectricity. And the enhancement of the Curie temperature is not so large. As far as we know, only one recent report showed the FE P-V loops at higher than 70K, for the first time, on single crystal-like STO on $DyScO_3$ (101) substrate and showed the transition at room temperature.[1, 2] In this presentation, we will report the room temperature FE properties of epitaxial STO thin films placed in between $SrRuO_3$ electrodes on STO (001) substrate. From reciprocal space mapping, we could observe the enhancement of unit cell volume of STO film due to oxygen vacancy. Therefore, STO film has tetragonal structure even on STO substrate. And in the figure 1, the c-axis lattice constant shows strong dependence on deposition oxygen partial pressure. From figure 2, temperature dependence of P-V loops, we could observe the remnant polarization decrease as increase temperature, but it has non-zero value even at room temperature. This is the first observation of P-V loop in compressive strained STO film at room temperature. Figure 3 shows retention for writing domain with piezoresponse force microscopy. Writing to point into the plane, down polarization, disappears fast. On the other hand up polarization shows very slow decay after some time pass. According to the thermodynamic calculation,[3] misfit strain state of our STO film is not large enough to raise the transition temperature up to room temperature. Therefore, we can not explain the room temperature ferroelectricity of STO film by terms of biaxial strain. We will present possible origins of room temperature ferroelectricity and odd behavior of ferroelectric properties of strained STO films.
[1] J.H. Haeni et al. Nature. 430, 758 (2004). [2] M.D. Biegalski et al. Appl. Phys. Lett 88, 192907 (2006). [3] Pertsev et al. Phys. Rev. B 61, R825–R829 (2000).

Dp-003 **Dynamics of $NaHSeO_3$ and $NaHSeO_4$ single crystals by observation of ^1H and ^{23}Na spin-lattice relaxation** 임 애란, 장 서원[1], 장 진해[1](*전주대학교, 과학교육과. [1]금오공과대학교, 고분자공학과.*) The ^1H and ^{23}Na spin-lattice relaxation times of $NaHSeO_3$ and $NaHSeO_4$ single crystals grown by the slow evaporation method were measured. The phase transitions of the two crystals were studied using differential scanning calorimetry (DSC), and the environments of the ^1H and ^{23}Na nuclei in these crystals were investigated by means of ^1H and ^{23}Na NMR spectroscopy. The DSC results show that $NaHSeO_3$ crystals do not undergo phase transitions, whereas for $NaHSeO_4$ crystals there is a small endothermic peak at 419 K. The dimers in $NaHSeO_3$ stabilize its structure to the extent that there are no phase transitions even in the presence of disordered hy-

drogen bonds. In addition, the NMR results indicate that the temperature dependencies of T_1 for the ^1H and ^{23}Na nuclei in the two hydrogen-bonded crystals—the $NaHSeO_3$ crystal with 3-coordinated SeO_3 and the $NaHSeO_4$ crystal with 4-coordinated SeO_4—are significantly different. The different trends in T_1 for Na in the two crystals are accompanied by different shifts of the oxygen atoms from the 3-coordinated SeO_3 and the 4-coordinated SeO_4 species around the Na^+ ions. Thus, although the two crystals have hydrogen-bonded structures, the differences between the hydrogen bonding of the 3-coordinated SeO_3 in $NaHSeO_3$ and the hydrogen bonding of the 4-coordinated SeO_4 in $NaHSeO_4$ result in different T_1 temperature dependences and different phase transitions.

Dp-004 **Superionic phase transitions and nuclear spin phonon relaxation by Raman processes in $Me_3H(SeO_4)_2$ (Me=Na, K, and Rb) single crystals by ^1H and Me NMR** 한 희정, 임 애란(*전주대학교, 과학교육과.*) $Me_3H(SeO_4)_2$ (Me=Na, K, and Rb) single crystals were grown by the slow evaporation method, and the relaxation times of the ^1H and Me nuclei in these crystals were investigated using FT NMR spectrometry. The ^1H T_1 NMR results for $K_3H(SeO_4)_2$ and $Rb_3H(SeO_4)_2$ single crystals were very different from those for $Na_3H(SeO_4)_2$ crystals. Short ^1H relaxation times were found for $K_3H(SeO_4)_2$ and $Rb_3H(SeO_4)_2$ at high temperatures, but not for $Na_3H(SeO_4)_2$, which are attributed to the destruction and reconstruction of hydrogen bonds; thus $K_3H(SeO_4)_2$ and $Rb_3H(SeO_4)_2$ have superionic phases, whereas $Na_3H(SeO_4)_2$ does not. The temperature dependence of the relaxation rate for ^{23}Na nucleus in $Na_3H(SeO_4)_2$ crystals was in accord with a Raman process for nuclear spin-lattice relaxation ($T_1^{-1} \alpha T^2$). In contrast, the spin-lattice relaxation rates for the ^{39}K and ^{87}Rb nuclei in $K_3H(SeO_4)_2$ and $Rb_3H(SeO_4)_2$ single crystals exhibited a very strong temperature dependence, $T_1^{-1} \alpha T^7$. The motions giving rise to this strong temperature dependence may be related to the high electrical conductivities of these crystals at high temperatures.

Dp-005 **Proton NMR study of the effect of paramagnetic impurities in the mixed crystals $[N(CH_3)_4]_2Zn_{1-x}Co_xCl_4$ (x=0, 0.1, and 1) and $[N(CH_3)_4]_2Zn_{1-x}Cu_xCl_4$ (x=0, 0.1, and 1)** 임 애란, 봉 필훈, 정 세영[1](*전주대학교, 과학교육과. [1]부산대학교, 나노학과.*) The effects of adding Co or Cu ions as paramagnetic impurities to $[N(CH_3)_4]_2ZnCl_4$ single crystals were investigated. Specifically, we measured the temperature dependences of the ^1H relaxation times for the mixed crystals $[N(CH_3)_4]_2Zn_{1-x}Co_xCl_4$ (x=0, 0.1, and 1) and $[N(CH_3)_4]_2Zn_{1-x}Cu_xCl_4$ (x=0, 0.1, and 1). We found that addition of these impurities did not affect the phase transition temperatures and the lattice constants of $t_1$the CH_3 groups. The changes in activation energy caused by introducing Co or Cu impurities into the mixed crystals may stem from the Co and Cu ions being smaller than the Zn ions they replace, and also from differences in the electron structures of the metal ions, in particular the structure of the d electrons, which screen the nuclear charge from the motion of the outer electrons. Collectively, our results indicate that introducing Co or Cu impurities into $[N(CH_3)_4]_2ZnCl_4$ single crystals mainly affects the molecular motions at high temperature, and that the molecular motions and activation energy are dependent on whether the paramagnetic impurity is Co or Cu.

Dp-006 **Investigation of the N_4 in $BaO \cdot B_2O_3 \cdot V_2O_5$ Glasses** 김 영훈, 강 재필, 차 유정, 홍 성덕, 서 용문, 송 승기(*명지대학교 물리학과.*) ^{11}B NMR techniques have been employed to investigate the environments of boron atoms as a function of composition in $BaO \cdot B_2O_3 \cdot V_2O_5$ glasses. The ^{11}B NMR spectra consist of a broad resonance line and a narrow resonance line which indicates that these glasses contain both BO_3 and BO_4 units. The N_4,the fraction of four-coordinated boron atoms, were measured by the area method and analyzed, Equations which can predict the behavior of N_4 with changing glass composition are formulated to a simplified model containing the elements for the region $K \leq 2.0$[1,2] (K= BaO mol% / B_2O_3 mol%).

Reference 1. J.Krogh - Moe, Phys.Chem. Glasses, 6,46 (1965). 2. D.J.Cha et al, New Physics, 28, 593 (1988).

Dp-007 **Evidence of the local phase transition in the metal ion doped K_2SnCl_6 observed by the nuclear and electron spin resonance.** 김 영훈, 차 유정, 홍 성덕, 서 용문, 송 승기(*명지대학교 물리학과.*) The non-exponential feature of the nuclear relaxation, characterized by two time constants in the di- and trivalent

metal ion doped K_2SnCl_6 has been attributed to the generation of the ligand deficient octahedra (LDO) through the replacement of the central metal ion, Sn^{4+} by the impurity in the $SnCl_6$-octahedra and their promoting contribution to the lattice dynamics in the high temperature region, the hindered rotation of octahedra [1]. The computer simulation using two time constant parameters showed also a remarkable resemblance to the observed results [2]. On the other hand the existence of the LDO was strongly evidenced by the electron spin resonance measurements of the paramagnetic ions, Fe^{3+} or Cu^{2+}, imbedded in the crystal at room temperature. In the case of Fe^{3+} an intense ESR line was observed without any hyperfine splitting as expected from the zero nuclear spin of the most abundant iron isotope. For Cu^{2+} an intense ESR line was observed overlapped by a few number of hyperfine splittings. Both Fe^{3+} and Cu^{2+} spectra points to the octahedral cubic symmetry of their local sites at room temperature. However the instantaneous local site symmetry is expected to be tetragonal because of the coupled ligand vacancies in the LDO. The tetragonal symmetry is assumed erased by the active jumping motion of ligands in the high temperature region of lattice dynamics above the phase transition temperature. For more detailed structural identification of the LDO an ESR investigation of these crystals at low temperature is planned.
References 1. J. Hypf. Intr. DOI 10.1007 (2005) 2. KPS Meeting / October (2006)

Dp-008 **Dielectric Properties of Proton-Irradiated KH_2PO_4(KDP)** LEE Cheol Eui, OH Byounghoo(*Korea University, Department of Physics.*) KH2PO4 a-axis was irradiated by the proton beam with energy 1.0 MeV with a dose of 1015 ions/cm2. The impedance data were obtained by using the impedance spectroscopy in the temperature range of 11 K ~ 295 K (step size: 1K). From the data we found that the proton irradiation increased the capacitance of the KDP. And we also found that the dielectric constant increases in both the untiferroelectric phase and the paraelectric phase. Proton beam irradiation also showed the change in domain freezing. To discuss the domain freezing we plotted the dielectric loss of KDP irradiated with energy 1.0MeV and dose of 1015ions/cm2.And it is found that the relaxation time of domain freezing in KDP in the kHz range can be described by the Vogel-Fulcher relation.

Dp-009 **Effects of Cosubstitution on the Electrical Properties of $BiFeO_3$ Thin Films Prepared by Chemical Solution Deposition** 김 상수, 이 승우, 박 문흠, 최 은진, 김 진원, 장 기완, 조 현경, 이 호형(*창원대학교 물리학과.*) 강유전 및 강자성 특성을 동시에 가지는 다강체(multiferroic material)는 최근, RAM이나 스핀트로닉스 등의 다양한 응용분야에서 큰 주목을 받고 있다. 이 다강체 중에서 $BiFeO_3$ (BFO)는 높은 큐리 온도 (T_C~850℃) 및 닐 온도 (T_N~370℃)를 가져 상온에서 메모리 소자 등으로의 응용 가능성이 있는 유일한 물질로 알려져 있으며 이에 대한 많은 연구가 이루어지고 있지만, 산소 구성비등의 요인에 의한 누설전류의 증가로 인하여 낮은 분극특성을 보이는 것이 큰 단점으로 보고되어지고 있다. 본 연구에서는 BFO 박막의 낮은 분극 특성을 향상시키기 위해서 $BiFeO_3$의 Fe-site를 Cr으로 부분 치환하고 Bi-site를 Nd나 Sm으로 각각 부분 치환한 BFO박막을 화학 용액 증착법(chemical solution deposition method)으로 제작하였으며, 제작된 박막은 550℃의 질소 분위기에서 30분간 열처리한 후 이들의 미세 구조와 전기적 특성을 측정 분석하였다. 치환에 따른 상(phase) 및 미세 구조의 변화는 X-ray diffraction (XRD)과 Scanning electron microscopy (SEM)을 이용하여 분석하였으며, 박막의 전기적 특성은 강유전성 측정장치(Radiant LC precision)와 미소 전류계(Keithley 6517A)를 이용하여 측정 분석하였다.

Dp-010 **Electrical Properties of $BiFeO_3$ Thin Films Grown on p-type Si(100) Substrate by Chemical Solution Deposition** 김 상수, 박 문흠, 이 승우, 최 은진, 김 진원, 조 현경, 이 호형(*창원대학교 물리학과.*) 강유전체 박막은 차세대 강유전체 메모리 소자로서의 응용 가능성으로 인해 널리 연구되어지고 있다. FeRAM을 구현하기 위하여 metal-ferroelectrics-metal (MFM)형 캐패시터가 다양하게 연구되어지고 있으며, 더불어 또 다른 메모리 응용 구조로서 metal-ferroelectrics-semiconductor field effect transistor (MFS-FET)구조가 주목을 받고 있다. MFS-FET구조는 비휘발성 데이터 저장, 비파괴 readout 그리고 단일 트랜지스터형 cell 구조로 인하여 매우 유망한 메모리 응용 소자로 인식되어지고 있으나 강유전체 박막과 Si 기판 간의 원소들의 확산과 고밀도의 전하 결함등은 개선되어져야 할 요소로 남아 있다. 본 연구에서는 MFS-FET구조의 반도체 메모리 소자로의 응용을 위해서 p-type Si(100) 기판 위에 $BiFeO_3$ (BFO) 박막을 화학 용액 증착법으로 성장시켜 MFS구조로서의 C-V, I-V 특성 등을 측정, 분석하였다. 제조된 BFO 박막의 결정화를 위해서 550℃의 질소 분위기에서 30분 동안 열처리하였고 XRD, SEM을 통해서 상 (phase) 생

성 및 표면의 미세구조 변화 등을 관찰하였으며, 박막의 전기적 특성은 Impedance Analyzer (HP4192A)와 Electrometer (Keithley 6517A)를 사용하여 측정하였다.

Dp-011 **Effects of Excess Bi Content in Precursor Solutions on the Ferroelectric Properties of $BiFeO_3$ Thin Films Prepared by Chemical Solution Deposition** 김 상수, 조 현경, 박 문흠, 이 승우, 최 은진, 김 진원, 이 호형 (*창원대학교 물리학과.*) 강유전성(ferroelectric)과 강자성(ferromagnetic)을 동시에 가지는 다강체 (multiferroics)는 메모리 소자로서의 활용 가능성으로 인해 최근, 많은 연구가 진행되어지고 있다. 다강체 물질 중에서 $BiFeO_3$ (BFO)는 큐리 온도 (T_C~850℃) 및 닐 온도 (T_N~370℃)가 상온보다 높아 상온에서 활용이 가능한 유일한 다강체로 알려져 있다. BFO내의 Bi는 이 물질 내의 다른 원소들에 비해서 상대적으로 낮은 녹는 점과 끓는 점을 가져 열처리 과정에서 쉽게 증발하게 되고 이로 인해서 비화학 당량적이 되고 결국 결함이 생겨 박막의 전기적 특성에 큰 영향을 주게 된다. 따라서 열처리 과정에서의 Bi 성분 조절은 좋은 특성의 강유전체 박막을 얻는데 필수적이며 일반적으로 precursor 용액에 여분의 Bi를 넣어 박막 내의 화학당량을 이루려 한다. 본 연구에서는 BFO 박막의 누설 전류 및 강유전 특성을 향상시키기 위해서 BFO 내의 Fe 중 일부를 Cr이온(3 mol%)으로 치환하고, Bi 를 과량 (0 – 20 mol%) 첨가한 박막을 $Pt(200)/TiO_2/SiO_2/Si(100)$ 기판 위에 화학 용액 증착법으로 제조하였다. 박막의 결정화는 550℃의 질소 분위기에서 30분간 열처리 하였다. 제작된 박막의 Bi 과량에 따른 상(phase)과 미세 구조의 변화는 X-ray diffraction (XRD)과 Scanning electron microscopy (SEM) 측정 결과로부터 분석하였다. 또 Bi 과량에 따른 박막의 전기적 특성 변화는 강유전성 측정장치 (Radiant LC-precision) 및 미소 전류계 (Keithley 6517A)를 사용하여 측정, 분석하였다.

Dp-012 **펄스 레이저 증착법으로 성장시킨 $BiFeO_3$ 박막의 성장 조건에 따른 특성변화** 김 상수, 김 진원, 박 문흠, 이 승우, 최 은진, 조 현경, 이 호형, 정 준기[1], 김 원정(*창원대학교 물리학과. [1]창원대학교 산업기술연구소.*) 다강체의 특성을 응용하는 신개념의 메모리 소자 제조를 위한 연구가 최근, 활발히 진행되고 있다. 특히 $BiFeO_3$ (BFO)는 높은 큐리 온도 (T_C ~ 1103K) 및 Néel 온도 (T_N ~ 643K)를 가져 상온에서 실제 소자로의 응용 가능성이 가장 높은 유일한 다강체로 알려져 있다. 본 연구에서는 BFO 물질의 결정적인 단점인 누설 전류 특성을 향상시키기 위해서 BiFeO3 내 Fe 이온 중의 일부를 Cr 이온으로 치환한 Cr-doped BFO (BFCr)를 고상 반응법으로 제조하여, 열처리 조건을 변화시켜가며 단일상 BFO의 합성을 시도하였다. 또 이렇게 제조된 단일상의 타겟을 이용하여 펄스 레이저 증착법으로 BFCr박막을 제조하여 증착 조건 및 Cr 치환에 따른 BFCr 박막의 미세 구조 및 누설 전류, 잔류 분극 특성을 측정, 분석하였다. 박막은 산소 분압 (1 ~ 100 mtorr) 및 온도 (475°C ~525°C)를 변화시켜가며 증착하였고 증착 조건에 따른 결정성 및 미세구조 변화는 X-ray diffraction (XRD) 및 Scanning electron microscopy (SEM)을 통하여 관찰하였다. 또 박막의 누설 전류 및 잔류 분극 특성의 변화는 미소 전류계(Keithley 6517A) 및 강유전성 측정장치 (Radiant LC-precision)를 사용하여 각각 측정, 분석하였다. 특성 분석 결과, BFCr 박막의 특성은 산소 분압 및 증착 온도에 따라 큰 변화를 나타내었으며, 매우 좁은 증착 조건 범위에서 우수한 강유전 특성을 발현함을 알 수 있었다.

Dp-013 **Dielectric response of metal-oxide interface; an ab initio approach to address interfacial effects** HAN Seungwu, LEE Bora(*이화여자대학교.*) Many experiments indicate that the dielectric constant of the metal/insulator/metal(MIM) structure is affected by interfacial effects between insulator and metal electrodes. Such an interface effect will be very important for nanoscale oxide materials that will be widely used for future electronic devices. However, the microscopic origin of such an interface effect is not fully understood yet. In this presentation, within the first-principles approach, we propose an efficient method to calculate the capacitance of the MIM structure including the interfacial effects. In our approach, the dielectric response of MI model is computed under the finite external electric field, and is used for evaluating capacitance of MIM structures. We apply this method to calculate the capacitances of Au/MgO/Au and $Ni/ZrO_2/Ni$ structures with the oxide thickness of several nanometers. Our results clearly show the presence of interfacial region with dielectric constants significantly different from that of the bulk.

Dp-014 **Correlation between the dynamics of polar nanoregions and temperature evolution of central peaks in PZN-xPT (x=0.09) ferroelectric relaxors** KO Jae Hyeon, KIM Do Han[1], KOJIMA Seiji[1](*Hallym University, Department of Physics. [1]University of Tsukuba, Institute of Materials Science, Japan.*) Acoustic properties of PZN-xPT with x=0.09 have been investigated in a

wide temperature range. The sound velocity of acoustic phonons showed a deviation from its high-temperature linear behavior at the Burns temperature T_B ~ 730K. Upon cooling, acoustic properties exhibited significant changes at about 550K in polarization state and width of the central peak in additionto changes in frequency and damping of acoustic phonons. This finding suggests that, besides T_B, another intermediate characteristic temperature exists in the evolution of relaxor dynamics, which might be related to the formation of long-lived polar nanoregions and associated local strain fields. (*This work was supported by the Korea Research Foundation Grant funded by the Korean Government (MOEHRD, Basic Research PromotionFund) (KRF-2006-003-C00088).)

Dp-015 **Raman analysis of Aurivillius ferroelectric $Bi_{4-x}La_xTi_3O_{12}$ thin film on $Pt/Ti/SiO_2/Si$ substrate** PARK Sungmin, PARK Do-young, SEO chungwon, CHEONG Hyeonsik, PARK Gwangseo(*Department of Physics, Sogang University.*) We investigated Raman spectra of Aurivillius ferroelectric $Bi_{4-x}La_xTi_3O_{12}$ thin films deposited on $Pt/Ti/SiO_2/Si$ substrate using PLD (pulsed laser deposition) methods. The Raman measurement was performed in the quasi-backscattering geometry using 50mW of the 514.5 nm line of an Ar ion laser focused on a line of 100 ㎛ width as the excitation source. The signal was dispersed by a Spex 0.55-m spectrometer with a holographic edge filter and detected with a liquid nitrogen-cooled charge-coupled device (CCD) detector array. In this study, We investigated the distortion of the TiO_6 octahedra for various values of x, the content x of La (x=0, 0.25, 0.50, 0.75, 1.00). The A_{1g} stretching mode (850 cm^{-1}) of the TiO_6 octahedra was not shifted in all films. However, the FWHM (full width at half maximum) of the peak became narrower with increasing post-annealing temperature. For the content of La in the range of $1.00 > x \geq 0.25$, an E_g mode was observed between 200 and 300 cm^{-1}. This mode was splitted into B_{2g} and B_{3g} modes for $x = 1.00$ or $x \leq 0.25$, which indicates an orthorhombic distortion of the crystal. Structural features of Aurivillius ferroelectric $Bi_{4-x}La_xTi_3O_{12}$ will be discussed in terms of Raman modes.

Dp-016 **Nucleation and Domain Wall Motion in Polarization Switching of Ferroelectric $Pb(Zr,Ti)O_3$ Capacitors** KIM D. J., CHEN B., YOON J.-G.[1], NOH T. W.(*ReCOE &FPRD, Department of physics and astronomy, Seoul National University.. [1]Department of Physics, University of Suwon.*) Polarization switching in ferroelectric materials has been studied since the 1950"s intensively. Understanding of switching kinetics is important both for scientific interests and for device applications. However, switching kinetics is net clear yet. Modified piezoresponse force microscope (PFM) was used to observe the domain evolution during switching of polarization. Epitaxial $Pb(Zr,Ti)O_3$ films with $SrRuO_3$ electrodes on $SrTiO_3$ substrate are deposited by pulsed laser deposition method. With external probe tip, ac and dc voltage were applied to top electrode in ferroelectric capacitors. Electric pulses were applied to top electrode for step-by-step switching. At each step of switching, domain patterns were obtained with PFM, like snapshot image. We could obtain reliable and repeatable domain images at each step of switching. Nucleation occurs at certain sites, well-known as nucleation sites. In repeated measurements, nucleation occurs randomly. Domain wall motions can be obtained by comparing domain images before and after applying electric pulse. Reversed domain nucleation is supposed to follow a defect-mediated thermodynamic random process. Domain wall motion has an exponential dependence on electric field. These results are useful to give a criterion for low voltage operation in ferroelectric devices.

Dp-017 **Energy band characteristics of highly elongated $(Ba_{0.5}Sr_{0.5})TiO_3$ thin films for microwave applications.** CHO Kwang-Hwan, KANG Chong-Yun, YOON Seok-Jin, LEE Young-Pak[1](*KIST, Thin Film Materials Research Center. [1]Hanyang Univ., q-psi and Dept. of Physics.*) We have investigated the effect of applied electric field annealing on the structural, microwave properties and band-gap energies of $Ba_{0.5}Sr_{0.5}TiO_3$ (BST) thin films grown on $LaAlO_3$ substrates. The transmission spectra of these BST thin films measured by ultraviolet-visible (UV-VIS) spectrophotometer show that the band-gap energies are strongly dependent on annealing with applied electric field. Based on the structural analyses and microwave, the variation of the band-gap energies and the dielectric constant can be attributed to the combined effects of applied electric filed annealing in highly elongated BST thin films.

Dp-018 **Microstructure and properties of indium tin oxide thin films deposited by sputtering method using moving gun** KIM Jong-Pil, LEE Sang-A[1], BAE Jong Seong, PARK Sungkyun, YOON Jang-Hee(*Nano-Surface Technology Research Team, Korea Basic Science Institute Busan Center, Busan 609-735, Korea. [1]School of Nano-Science and Technology, Pusan National University, Busan 609-735, Korea, Nano-Surface Technology Research Team, Korea Basic Science Institute Busan Center, Busan 609-735, Korea.*) Transparent conductive oxide layers play a very important role in today"s optoelectronic devices applications such as liquid crystal displays, plasma display panels, organic light emitting devices, and solar cells. Among them, indium tin oxide (ITO) thin films are the most widely used materials. Although many deposition techniques, including DC or RF magnetron sputtering, electron beam evaporation, etc., have been successfully developed to produce ITO films, all of them require an elevated substrate temperature between 200 and 500 °C during the deposition, or post annealing in order to improve the electrical and optical properties. Furthermore, the preparation of high quality ITO films on plastic substrates is highly demanded in applications for flexible display devices. However, achieving high quality thin films on polymer substrates are difficult since the substrate heating is limited due to their weak thermal resistance. Therefore, it is desired to develop alternative depostition techniques to obtain high quality film with minimum thermal treatment. In this study, ITO thin films were prepared by unconventional sputtering gun. Unlike conventional sputtering system, the magnetic configuration inside sputtering gun used for film growth was moving during deposition. We examined various effect such as, phase formation, microstructure, chemical bonding state, and resistivity of ITO thin films fabricated using this unconventional sputtering system.

*This work was supported by grant the Korea Institute of Industrial Technology Evaluation and Planning (10023562-2005-01)

Dp-019 **Distribution of Polarization Switching Times and Switching Dynamics in Polycrystalline $Pb(Zr,Ti)O_3$ Films** 조 지영, 한 효섭, 윤 종걸[1], 노 태원(*서울대학교 물리천문학부. [1]수원대학교 물리학과.*) Polarization switching in ferroelectric materials has been investigated intensively for the understanding of domain reversal process. The subject is becoming more important to ferroelectric memory devices for low-voltage/high-speed operation. Kolmogorov-Avrami-Ishibashi (KAI) model, which is based on nucleation and growth of opposite domains, has been successful in describing the switching kinetics of ferroelectric single crystals and epitaxial films. However, the KAI model is not satisfactory for a quantitative explanation of the switching kinetics in polycrystalline thin films. In this work, we will present a quantitative description of switching kinetics in polycrystalline $PbZr_{0.3}Ti_{0.7}O_3$ (PZT) thin films and discuss about Lorentzian distribution of internal field.The switching kinetics in polycrystalline PZT film was investigated at various fields and temperatures by measuring polarization ($\Delta P=P_{sw}-P_{ns}$) with the pulse fields of widths between 200 ns and 1 ms. Application of the KAI model, where normalized $\Delta P(t)=1-\exp[-(t/t_0)^n]$, to our experimental data resulted in unphysical n values smaller than 1. Correct description of switching kinetics was not possible especially for our low-field and low-temperature experiments. As an alternative approach, Lorentzian distribution of $\log t_0$ for the characteristic switching times t_0 in KAI model provided a quantitatively good explanation of our polarization switching data. Since t_0 is sensitive to an applied field, distribution of the switching times might be directly related to the distribution of internal field. We suggest that long-range dipolar interaction between randomly distributed polar regions in polycrystalline films induces variation in local field. The logarithm of center and width of the Lorentzian switching time distribution are proportional to $1/E_{ext}$ in low-field region. We will discuss switching dynamics of ferroelectric domains in conjunction with randomness and switching-field distribution in polycrystalline and epitaxial thin films.

Dp-020 **RF 마그네트론 스퍼터링법으로 제작된 $Gd_2Zr_2O_7$ 박막 특성 연구** 양 호순, 강 준구, 김 종욱[1], 홍 태은[2], 홍 경수[2](*부산대학교 물리학과. [1]부산대학교 기계공학과. [2]한국기초과학지원연구원 부산센터.*) 낮은 열전도도는 열제어장치의 열 차폐코팅 (Thermal Barrier Coating, TBC) 물질이 가져야 하는 중요한 성질이다. 열전도도가 낮은 YSZ (Ytrria-Stabilized Zirconia)이 가장 일반적으로 쓰이고 있는 물질이다. YSZ는 oxygen vacancy로 인하여 평균포논산란 길이가 짧아 그 열전도도가 낮게 나타난다. 형석 (Fluorite)구조에서 산소가 1/8 결핍된 형태의 파이로클로로 (Pyrochlore) 결정구조를 갖는 산화물들은 YSZ (Ytrria-Stabilized Zirconia)

보다 낮은 열전도도를 가진다고 알려져 있다. 차세대 엔진의 높은 가스 온도를 고려하면 이 산화물들은 YSZ를 대체할 열차폐코팅 물질로써 주목받고 있다. 본 연구에서는 Pyrochlore 결정구조를 갖는 산화물들 중에서 $Gd_2Zr_2O_7$ 박막을 RF magnetron sputtering 방법으로 증착하였고, 그 특성에 대하여 조사하였다. 박막은 RF 마그네트론 스퍼터링법으로 증착하였고, 기판 온도, 분압, RF power에 따른 $Gd_2Zr_2O_7$ 박막의 구조적 특성에 대한 연구를 수행하였고 열처리 전과 후를 비교, 분석하였다. 박막의 구조적 결정성과 방향성을 관측하기 위해 x-ray diffraction(XRD)을 이용하였고, grain size와 두께를 각각 Atomic Force Microscope(AFM)와 Scanning Electron Microscope(SEM)을 이용하여 측정하였다. 박막을 두께를 변화시키며 제작하여 두께에 따른 열전도도를 측정하였다. 열전도도 측정에는 3ω방법을 이용하였고 박막과 기판사이의 경계면 효과도 연구하였다.

Dp-021 **Raman Scattering Studies of NiO: Material for Resistance-change Random Access Memory** KIM C., CHO E., CHO E., KIM D. C.[1], SEO S.[1], YOO I. K.[1], SEO C.[2], CHEONG H.[2], YOON S.(*Ewha Womans University. [1]Samsung Advanced Institute of Technology. [2]Sogang University.*) Recently, NiO has attracted much attention mainly because it is known to exhibit resistive memory switching behavior so that it can be applied to non-volatile random access memory. We present Raman scattering measurements on NiO films (with and without IrO_2 buffer layers with different thicknesses) which were deposited by de magnetron reactive sputtering methods. Our Raman measurements of NiO with and without IrO_2 buffer layers corroborated that the addition of a 20 nm-thick IrO_2 layer, which greatly improves dispersion of the switching characteristics, is related to the local crystalline quality. Moreover, our Raman results suggest that the stoichiometry of the NiO compound, which is presumably associated with defects/vacancies might play an important role in switching behavior.

Dp-022 **Measurements of Thermal Conductivities of Diamond Like Carbon Films by using 3 omega method** KIM, J. W., KANG, J. G.[1], HONG, T. E.[2], HONG, K. S.[2], JUN, Y. H.[3], KIM, K. C.[4], YANG, Ho-Soon[1](*Dept. of Mechanical Engineering, Pusan National University. [1]Dept. of Physics, Pusan National University. [2]Busan Center, Korea Basic Science Institute. [3]J&L Tech. Co., Siheung. [4]School of Mechanical Engineering, Pusan National University.*) The interest in diamond-like carbon (DLC) has grown for use in various applications, such as protective coatings, microelectronic systems, optical coatings and biomedical applications since DLC has the particular physical properties such as high hardness, high wear resistance, high transparency in IR range, chemical inertness and biocompatibility. As the technology to produce miniature devices has developed rapidly, the interfacial effect becomes more important. In this study the interfacial effect on thermal conductivity is studied with DLC films deposited on Si substrates and Al_2O_3 substrates. DLC films with the thickness between 600nm and 1800nm are deposited on Al_2O_3 substrate and Si substrates using ion gun method and thermal conductivity of the films is measured using the 3ω method. The thermal conductivities of the DLC are obtained as a function of film thickness. The film thickness dependent thermal conductivity is understood with the interfacial thermal resistance. The intrinsic thermal conductivity of films and the interfacial thermal resistance are estimated by using relationship between the interfacial thermal resistance and the measured thickness-dependent thermal conductivity of films.

Dp-023 **PZ/PT에 의한 PZT 박막의 제작 및 특성조사** 배 세환, 전 기범, 진 병문[1](*동아대학교. [1]동의대학교.*) 이전의 $Pb(Zr,Ti)O_3$ (PZT) 다층박막 연구에서 $PbZrO_3$ (PZ)와 PZT의 stacking과 annealing 방법에 따라 그 특성들이 매우 다르게 나타났다. 이는 PZT 박막 형성에 있어서 반강유전체 즉 PZ의 분포가 특성에 많은 영향을 준 결과이다. 따라서 강유전체로서 PZT의 특성을 유지면서 반강유전체인 PZ의 영향을 분석한 이전의 연구를 $PbTiO_3$ (PT)와 PZ의 stacking sequence에 따른 PZT의 특성과 비교하기 위하여 sol-gel법으로 PZ와 PT를 반복적으로 다층구조가 되도록 만들어 PZT의 생성과정을 살펴보았다. 조사방법으로는 I-V 및 P-E 특성 곡선, X-ray를 이용한 구조분석 및 AFM과 EFM을 이용한 표면 특성 및 memory 효과 등이 포함되며 특히 PZ/PT 다층박막이 PZ/PZT 다층박막과 어떤 차이점을 보이는가에 초점을 맞추어 논의하고자 한다.

Dp-024 **The charge Trap/Detrap Properties in Silicon Nitride/Oxide Layer Investigated by Scanning Probe Microscopy** KIM Jong-Hun, KHIM Z.G (*Physics department of Seoul National University.*) As the Si_3N_4/Oxide-based-nonvolatile memory is getting popular and widely applied to the memory device, the characterization in the scaled down configuration become of

importance. We locally inject the charge into the thin Nitride-Oxide-Silicon structure(NOS) and the trap/detrap mechanism is studied by Scanning Probe Microscopy (SPM). In addition, the local I-V curve and local surface potential is taken on the Nitride with a various thickness and constitution.

Dp-025 **Dielectric and Ferroelectric Properties of $(Na_{0.5}K_{0.5})NbO_3$ Thin Films** 이 재영, 이 해준, 김 일원, 이 재신[1], 정 귀상[2], 이 정식[3](*울산대학교 물리학과. [1]울산대학교 재료공학과. [2]울산대학교 전기공학과. [3]경성대학교 물리학과.*) The $(Na_{0.5}K_{0.5})NbO_3$ (NKN) lead-free ceramics have been studied extensively, because of their good piezoelectric and ferroelectric properties, but few studies have reported on thin films.NKN thin films were grown on $Pt/Ti/SiO_2/Si$ substrates by RF magnetron sputtering methods. The addition of enriched Na_2CO_3 and K_2CO_3 into the target was necessary in order to compensate for the lack of Na and K in the grown NKN films. The films exhibited high remanent polarization of 35 uC/cm^2 and low coercive field of 50 kV/cm at applied electric field of 150 kV/cm. The electrical characterization showed dissipation factor of 0.01 and dielectric constant of 470. The frequency dispersion of dielectric constant was appeared between 1 kHz and 1 MHz. Film exhibited good insulating properties with leakage current density of 10^{-8} A/cm^2 at 300 kV/cm. The NKN film is a promising candidate material for application in memory device, IR sensor, and tunable microwave devices.

Dp-026 **Temperature Dependence of Ferroelectric and Piezoelectric Properties in Textured $Bi_{0.5}(Na_{0.85}K_{0.15})_{0.5}TiO_3$ Lead-free Piezoceramics** 김 일원, 안 창원[1], 김 현규[1], 정 의덕[1], 이 재신[2](*울산대학교, 물리학과. [1]한국기초과학지원연구원. [2]울산대학교, 재료공학과.*) The textured $Bi_{0.5}(Na_{0.85}K_{0.15})_{0.5}TiO_3$ [BNKT] ceramics with $<100>_{pc}$ (where pc denotes the pseudocubic perovskite cell) preferred orientation were fabricated by reactive templated grain growth (RTGG) technique using plate-like $Bi_4Ti_3O_{12}$ particles. The textured BNKT ceramics exhibited relatively high converse piezoelectric coefficient (d^*_{33} = ~400 pm/V) and electric field induced strain levels (S = 0.08% at 20 kV/cm) at room temperature. This strain value is comparable to that of the Pb included PZT (S = 0.05~0.15% at 20 kV/cm) ceramics using actuator device. Therefore, <001>pc textured BNKT ceramics are a strong candidate for Pb-free piezoelectric materials for actuators. And the temperature dependence of ferroelectric and piezoelectric properties in textured BNKT ceramics has also been investigated. The depolarization temperature (T_d) was about 150 °C which is the transition between ferroelectric phase and anti-ferroelectric phase.

Dp-027 **Optical Characterization of Doped $SrTiO_3$ in a Wide Photon Energy Region** KIM S. J., CHOI W. S., MOON S. J., SEO S. S. A., SEO Y. K.[1], HUR N. H.[2], LEE Y. S.[1](*ReCOE &FPRD, School of Physics and Astronomy, Seoul National University, Seoul 151-747. [1]Department of Physics, Soongsil University, Seoul 156-743. [2]Department of Chemistry, Sogang University, Seoul 121-742.*) A large-dielectric transparent band insulator $SrTiO_3$ has attracted much attention due to the usefulness as a substrate for the epitaxial growth of oxide film, and the particular importance from the perspective of fundamental solid-state physics and technological applications. Motivated by this, we investigated the optical properties of doped $SrTiO_3$ and we identified the systematic changes of optical responses with doping: 1) the Drude response appears significantly, together with the significant change of far-IR reflectivity, 2) absorption in mid-IR region develops, and 3) the charge transfer excitation features are drastically suppressed. These behaviors originating from the electron-doping to a band insulator are discussed in relation to intriguing behaviors of doped $SrTiO_3$.

Dp-029 **Electrical properties induced by oxygen vacancies of CeO_2 thin films grown on p-Si(100)** PARK Sung-Min, SONG Sang-Hoon, PAK Jae-Moon, NAM Kwang-Woo, LEE Yong-Woo, KIM Hyun-Jung, PARK Gwang-Seo(*Dept. of Physics, Sogang University.*) We have deposited CeO_2 thin films on p-Si(100) substrates to investigate their electrical properties originated from oxygen vacancies, using pulsed laser deposition(PLD) method. (111) preferential orientation was observed. Raman spectra revealed that a film deposited at 760°C had the smallest distortion of the unit structure due to small quantities of oxygen vacancy.X-ray specular reflectivities were measured to investigate an electron density profile along the thickness. The profile was strongly correlated with oxygen vacancy because total net charges inside the dielectric film should be zero.

As a result, oxide trapped-charge density could be extracted from the electron-density profile. C-V curves depending on frequencies showed that and interface trapped-charge density is not high. Flat band voltage in C-V curves was slightly shifted because of the presence of oxide trapped charge.We will report on a decisive method calculating the shift of flat band voltage.

Dp-030 **Ferroelectric properties of sol-gel derived $Bi_{4-x}La_xTi_3O_{12}$ films prepared on $Pt/Ti/SiO_2/Si$ substrates** PARK Sung-Min, BAEK Jong-Ho, SIN Je-Ho, PAK Jae-Moon, NAM kwangwoo, PARK Do-Young, CHEONG Hyeon-Sik, PARK Gwang-Seo(*Dept. of Physics, Sogang University.*) The ferroelectric properties of $Bi_{4-x}La_xTi_3O_{12}$ (BLT) thin films were studied. The films were coated on $Pt/Ti/SiO_2/Si$ substrates by spin coating method.The crystal structure, chemical composition and internal vibration modes were measured using x-ray θ-2θ scan method, Electron probe micro-analyzer, Raman spectroscopy, respectively. The orientation of the films was (117) and (200). Various type of grains and lattice expansion or reduction was observed in terms of the content of La and the annealing temperature of the films. Raman spectra on the films showed the modes of $271cm^{-1}$(TiO_6 tortional bending) and $849cm^{-1}$(TiO_6 symmetric stretching). The BLT film with x = 0.25 films showed that the peak in the vicinity of $560cm^{-1}$ was splitted into $543cm^{-1}$ and $566cm^{-1}$, which was understood as orthorhombic distortion. In addition, a $476cm^{-1}$ peak appeared remarkably due to Ti-O torsion in TiO_6 octahedra unit cell. The BLT films with x = 0.25 had larger values of polarization and coercive field than other films, and they showed poor fatigue properties. However, the BLT films with x = 0.75 showed a good fatigue property.The ferroelectric properties will be discussed in terms of the microstructure and the distortion of the unit cell in the films.

Dp-031 **Study on the micro-structure of ferroelectric $PbZr_{0.2}Ti_{0.8}O_3$ thin film by Warren-Averbach analysis** 권 대영, ZHANG X. D., 김 창운, 김 복기 (*물리학과, 부산대학교.*) We have analyzed the micro-structure of epitaxial $PbZr_{0.2}Ti_{0.8}O_3$(PZT) thin films with the Warren-Averbach method. The epitaxial film of the PZT with thickness of 30 - 97 nm prepared using off-axis RF magnetron sputtering method on Nb:STO(100) substrate. Grazing Incident diffraction (GID) techniques have been employed to study in-plane diffraction structure of the thin films. We found that the lattice constant c (out of plane) was decreasing from 4.141 Å to 4.128 Å and the lattice constant a (in-plane) was increasing from 3.955 Å to 3.964 Å as increasing the thickness of PZT thin film, showing clear structural evidence of strain relaxation process. The coherent domain size, the root mean square microstrain, and the orientaional spread will be also presented as a function of the film thickness.

Dp-032 **Oxygen Polarization Contribution to the Ferroelectric ordering in $BaTiO_3$** KIM Dong Geun, KIM Jiyeon, OZAKI Taisuke[1], YU Jaejun(*Department of Physics and Astronomy, Seoul National University, Seoul, Korea. [1]National Institute for Advanced Industrial Science and Technology, Tsukuba, Japan.*) We have investigated the ferroelectric instability of the perovskite$BaTiO_3$ by using the local-combination-of-pseudo-atomic-orbital (LCPAO) methods as implemented in the OpenMX code. From the results, theferroelectric distortions are found to be sensitive to the choice of localbasis sets while the dynamical charges of constituent atoms obtained bythe Berry-phase calculations remain intact. The local orbital analysis oftotal energies and charge polarizations reveals that the extrapolarizations at the oxygen sites are critical in the description offerroelectric distortions in $BaTiO_3$. We will discuss the importance ofoxygen polarizations in understanding the ferroelectric ordering inmultiferroic systems.

Dp-033 **Epitaxial growth of p-type ZnO:N thin film with nitrogen diffusion mechanism by co-sputtering magnetron system** LEE Jonghyun, HA Jaehwan, HONG Jin Pyo(*New Functional Materials and Device Lab, Department of Physics, Hanyang University, Seoul 133-791, KOREA.*) The epitaxial p-type ZnO:N thin films were fabricated on Si/Glass/Sapphire substrates with nitrogen diffusion mechanism by double RF co-sputtering method. This mechanism has attractive merits to easily synthesis of p-type ZnO:N thin films at low temperature. First, tungsten-nitride (WN) was deposited as role of the source of nitrogen which was incorporated into ZnO films during the growth and post-thermal annealing process to occupy oxygen part. Second, the amount of activated nitrogen gradually increased in annealing process and exceeded those donor states to realize an effec-

tive compensation, yielding p-type conductivity during the course of post-thermal annealing.

Dp-034 **Orbital Dimerization and Consequent In-Plane Anistropy in Quasi-Two-Dimensional $La_4Ru_2O_{10}$** MOON Soon Jae, NOH T.W., LEE Y.S.[1], KHALIFAH P.G.[2](*ReCOE &FPRD, Department of Physics and Astronomy, Seoul National Uniersity, Seoul 151-747, Korea. [1]Department of Physics, Soongsil University, Seoul 156-743, Korea. [2]Department of Chemistry, University of Massachusetts, Amherst, Massachusetts 01003, USA.*) Recently, quasi-two-dimensional $La_4Ru_2O_{10}$ has attracted much attention due to its exotic spin-singlet ground state. It was theoretically argued that the orbital degree of freedom played an important role to determine the ground state. However, there have been no direct probe on the roles of orbitals in $La_4Ru_2O_{10}$. We investigated polarization- and temperature-dependent optical conductivity spectra of $La_4Ru_2O_{10}$. We observed two correlation-induced peaks at about 1.0 and 2.0 eV. Across the phase transition, optical conductivity spectra undergoes drastic changes. The spectral weight of the lower energy peak was transferred to higher energy peak, and the higher energy peak showed upward shift about 0.3 eV. From the quantitative analysis on the optical spectra, we firstly provide the direct evidence that orbital dimeriztion and ordering play a significant role for the large change of electronic structure.

Dp-035 **뫼스바우어 분광실험을 통한 $AFeO_3$(A= Gd, Tb, Al, Ga) 물질의 초미세상호작용에 관한 연구** 최 동혁, 심 인보, 김 철성(*국민대학교 물리학과.*) 뫼스바우어 분광 실험을 통하여 $AFeO_3$(A= Gd, Tb, Al, Ga) 물질의 초미세 상호작용에 대한 연구를 수행하였다. 또한 X-선회절기(XRD)와 진동형 자화율 측정기(VSM)를 이용하여 결정학적 및 거시적인 자기적 특성을 분석하였다. 모든 시료에 대해서 결정구조는 orthorhombic 구조로써 그 공간군이 Gd(or Tb)FeO_3 시료의 경우 Pbnm, Al(or Ga)FeO_3 시료는 $Pc2_1n$으로 분석되었으며, 온도에 따른 자기 모멘트 측정 결과로부터, T_N은 각각 259 K (246 K) 와 690 K (692 K)로 결정하였다. 뫼스바우어 측정 결과, 모든 시료의 이성질체 이동값 (δ)이 약 0.3 ~ 0.6 mm/s 값으로 Fe의 이온상태는 +3가임을 확인 할 수 있었으며, 온도에 따른 초미세 자기장과 brillouin 이론 곡선의 비교 결과 스핀 값이 5/2의 high spin 상태로 존재함을 알 수 있었다. Gd(or Tb)FeO_3 시료의 경우 극저온인 12 K에서 6개의 공명흡수선이 1 set로 존재하고 초미세 자기장 값 (H_{hf})이 558 (554) kOe로 분석되었다. Al(or Ga)FeO_3 시료의 경우 12 K 에서 6개의 공명흡수선이 4 set로 존재하며 초미세 자기장 값이 430~490 kOe로 분포되어 분석되었다. 이러한 차이는 부격자 사이의 Fe-O-Fe 상호교환작용이 두개의 공간 격자군에서 다르게 작용함을 알 수가 있었다.

Dp-036 **Pyroelectric Study of $LiNbO_3$ doped $(Na_{0.5}K_{0.5})NbO_3$ Lead-free Ceramics** KIM Chang Do, AHN Chang Won, PARK Sung Kyun, BAE Jong Seong, LEE Hai Joon[1], KIM Ill Won[1], LEE Jae Shin[2](*Busan Center, Korea Basic Science Institute, Busan 609-735, Korea. [1]Department of Physics, University of Ulsan, Ulsan 680-749, Korea. [2]School of Materials and Engineering, University of Ulsan, Ulsan 680-749, Korea.*) Pyroelectric materials are well known in their application as room temperature infrared sensors. To develop a high performance pyroelectric IR sensor, the (1-x)NKN-x$LiNbO_3$ lead-free ceramics were synthesized with different $LiNbO_3$ concentrations of x=0~0.1. In previous study, we had investigated dielectric, piezoelectric and dc conductivity. The LiNbO-0.05 modified NKN ceramics showed a high Curie temperature (T_C~410 °C), a large piezoelectric coefficient (d_{33}~200 pC/N), a high electromechanical coupling factor (k_t~45%) and relatively low dc conductivity (s ~ 10^{-12} W^1cm^{-1}). In this study, we have investigated the pyroelectric effect of NKN-LN ceramics. The pyroelectric coefficients are tested using a Byer-Roundy method. Although the pyroelectric coefficient of the LKN-LN is lower than that of PZT system ceramic, the figure of merit of the LKN-LN ceramic is high than that of PZT system ceramics due to its lower dielectric constant and dielectric loss. So, NKN-LT ceramics are shown to be good candidates for developing high performance pyroelectric IR sensors.

Dp-037 **$(Na_{0.5}K_{0.5})_{1-y}Li_yNbO_3$ 세라믹스의 유전성 및 압전성 연구** 박 희진, 김 샛별, 김 은지, 김 유성, 전 병억[1], 최 병춘[1], 정 수태[2], 박 종호[3](*부경대학교 물리학과. [1]부경대학교 기초과학연구실. [2]부경대학교 전자컴퓨터정보통신공학부. [3]진주교육대학교 과학교육.*) $Na_{0.5}K_{0.5}NbO_3$-(NKN)은 비납계 압전체로서 관심이 집중되고 있다. 본 연구에서는 NKN에 $LiNbO_3$을 고용시킨 $(Na_{0.5}K_{0.5})_{1-y}$-Li_yNbO_3(NKN-LNy)를 제작하였고 각 세라믹스 시료의 유전성 및 압전성을 조사하였다. X-선 분석을 통해 NKN-LNy세라믹스는 y가 증가함에 따라 $LiNbO_3$조성

이 증가함을 관찰하였고, SEM분석을 통해 두가지 결정 모양이 혼합된 것을 확인하였다. 임피던스 분석을 통해 실온에서 600℃ 온도 영역에서의 NKN-LNy 세라믹스의 유전성 및 압전성을 조사하였다.

Dp-038 **Interface Resistance Switching Characteristics of Metal/Nb-doped $SrTiO_3$ Junctions** 박 찬우, 정 재욱, 김 동욱(*한양대학교 응용물리학과.*) We report on the transport properties of junctions consisting of metal electrodes (M = Ti, Ni, and Pt) and (001)-oriented Nb-doped $SrTiO_3$ (Nb:STO) single crystals. The junctions with M = Ti, which had a shallow work function, exhibited linear current-voltage (I-V) characteristics without hysteresis. For M = Ni and Pt, with large work function, the junctions showed rectifying I-V characteristics and notable hysteresis upon polarity reversal. The resistance change ratio for M = Ni (Pt) did (not) depend on the doping ratio of Nb:STO. This clearly suggests that the metal work function may not be sufficient to explain the resistance switching.

Dp-039 **An observation of structural distortion in $Bi_{4-x}La_xTi_3O_{12}$ films coated on metal substrate by B-site doping** SHIN Je-Ho, PARK Sung-Min, KIM Hyunjun, PAK Jae-Moon, NAM Kwang-Woo, PARK Do-Young, CHEONG hyeon-Sik, PARK Gwang-Seo(*Dept. of Physics, Sogang University.*) Ferroelectric $Bi_{4-x}La_xTi_3O_{12}$ films which consist of bismuth layered perovskite structure were fabricated on Pt/Ti/SiO_2/Si substrate to study ferroelectric properties by B-site doping with different content of lanthanum(x) as 0.25 and 0.75 using a sol-gel method.The structure of the films was analyzed by x-ray diffraction and Raman spectroscopy. The surface of the films was analyzed by FE-SEM. All films had (117) and (200) oriented grains without any phases. The grain size for x = 0.25 had been larger with increasing annealing temperature. Especially, the film annealed at 750°C had large value of remanent polarization as 37μC/cm^2 where the value of coercive field is 178kV/cm. In the case of x = 0.75, the grain size was almost not changed under various annealing temperatures. It had smaller remanent polarization and coercive field than that of x = 0.25.In this report, the structural distortion, the surfaces and electrical properties of $Bi_{4-x}La_xTi_3O_{12}$ films coated on metal substrate will be discussed..

Dp-041 **Fabrication of Nanodevice Using Single crystalline CoSi Nanowire and Measurements for Transport Characteristics of CoSi nanowire** LEE Sunghun, SEO Kwanyong[1], VARADWAJ K.S.K.[1], KIM Jinhee[2], KIM bongsoo[1](*Interdisplinary program for nano science and technology, KAIST. [1]Department of Chemisty, KAIST. [2]Leading-Edge Technology Group, KRISS.*) Silicide materials have interesting size-dependent characteristics. While CoSi in bulk has diamagnetic property, we found that CoSi nanowire showed ferromagnetic property. Single crystalline CoSi nanowires of 20 ~ 50 nanometer diameter and tens of micrometer length were synthesized by chemical vapor deposition using a modified van-Arkel method. Nano-scale electrodes were patterned by e-beam lithography onto as-synthesized individual CoSi nanowire dispersed on 5 ㎜ × 5 ㎜ Si/SiO_2 wafer. I-V characteristics show ohmic contact between nanowire and electrode. Temperature-dependent resistance measurements show metallic behavior of CoSi. Negative magnetoresistance (MR) was observed in CoSi nanowire at low temperatures. This suggests probable ferromagnetism of as-synthesized CoSi nanowire. MR ratio is about -4 %. With the increase of temperature, MR curve becomes smoothened and the MR ratio is decreased and vanished at 150K.

Dp-042 **준강자성 $MnFe_2O_4$ 스피넬 산화물의 방사광 분광 연구** 김 그라시아, 이 현진, 강 정수, 심 정현[1], 이 순칠[1], 한 상욱[2], 황 찬용[2], 이 한길[3], 김 재영[3] (*가톨릭대학교, 물리학과. [1]한국과학기술원. [2]한국표준과학연구소. [3]포항가속기연구소.*) 준강자성 스피넬 산화물인 $MnFe_2O_4$의 자기적 특성에 관해서는 많은 연구가 보고된 바 있으나, 이들의 전자구조에 대한 연구는 아직까지 거의 이루어지지 않은 실정이다. 본 연구에서는 준강자성 $MnFe_2O_4$ 스피넬 물질의 전자 구조를 연구하기 위하여 방사광을 이용한 연 x선 광흡수 분광법 (soft x-ray absorption spectroscopy: XAS)과 원형자기이색성 (soft x-ray magnetic circular dichroism: XMCD) 실험을 수행하였다. Fe 2p, Mn 2p, O 1s 흡수 근처에서 각각 XAS 와 XMCD 를 측정함으로써 Fe 이온과 Mn 이온의 원자가와, 각각의 Fe 3d 전자들과 Mn 3d 전자들의 스핀 배열 등을 연구하였다. T 2p XAS (T=Fe, Mn) 스펙트럼의 측정을 통하여 대부분의 Fe 이온들과 Mn 이온들은 각각 Fe^{3+}와 Mn^{2+}의 상태에 있지만 Fe 이온의 약 20% 정도는 Fe^{2+}의 상태에 있다는 것을 알 수 있었다. 그리고 T 2p XMCD (T=Fe, Mn) 스펙트럼 측정을 통하여 Fe와 Mn의 스핀 방향이 반평행하게 정렬되어

있다는 것을 알 수 있었다. 본 연구 결과를 토대로 하여 전자구조가 $MnFe_2O_4$의 성질에 미치는 영향을 이해하고자 하였다.

Dp-043 **방사광을 이용한 스피넬 준강자성체 $Fe_{0.9}Mn_{2.1}O_4$ 의 전자 구조 연구** 이 현진, 김 그라시아, 김 혜성, 김 대현, 강 정수, CHEONG S.-W.[1], 한 상욱[2], 황 찬용[2], 정 민철[3], 신 현준[3], 이 한길[3], 김 재영[3] (*가톨릭대학교, 물리학과. [1]Rutgers University. [2]한국표준과학연구원. [3]포항가속기연구소.*) 준강자성(ferrimagnetic) 스피넬 화합물은 합성 온도에 따른 이온들의 위치의 재분배에 의한 결정의 성질이 거시적인 자기적 성질을 결정하는 것으로 알려져 있다 [1]. 예를 들어 Mn_3O_4 에서 Mn 이온 대신 Fe 이온을 치환하면 Fe 이온의 양에 따라 퀴리온도 (Currie temperature: T_C)가 증가하는데 [2], $FeMn_2O_4$의 T_C는 413 K이며 $MnFe_2O_4$ 의 T_C 는 563 K 이고 Fe_3O_4 의 T_C는 858 K 이다. AB_2O_4 형의 정상 스피넬 구조에서 일반적으로 A 금속이온은 2가 상태로 존재한다. $MnFe_2O_4$ 스피넬 산화물의 물성에 대해서는 지금까지 많은 연구가 보고되었으나, $FeMn_2O_4$ 에 대한 연구는 그다지 많지 않으며, 특히 $FeMn_2O_4$의 전자 구조에 대한 연구는 거의 보고된 바가 없다. 본 연구에서는 방사광을 이용하여 $Fe_{0.9}Mn_{2.1}O_4$ 스피넬 준강자성체의 전자구조를 연구하였다. 광전자 분광 (photoemission spectroscopy : PES), 연 x선 광흡수분광 (soft x-ray absorption spectroscopy: XAS), 연 x선 원형 자기 이색성 분광 (soft x-ray magnetic circular dichroism : XMCD) 등의 실험을 수행하여 Fe 이온과 Mn 이온들의 원자가와 각 원소의 상대적인 자기 배열들을 연구하였다. 본 연구 결과를 통하여 $FeMn_2O_4$ 의 전자 구조와 자기적 물성 간의 상관관계에 관하여 논의하고자 한다.

[1] Kh. Roumaih, et al., J. Magn. Magn. Mater. 288 (2005) 267. [2] V. Baron, et al., American Mineralogist, 83 (1998) 786.

Dp-044 **Study of magnetic properties of RB_6 (R=Pr, Gd) and $R^{11}B_4$ (R=Tb, Dy) at milikelvin temperatures** YANG Nam-keun, LEE Seongsu, IGA F.[1], PARK J-G.(*BK21 Physics Division, Department of Physics, SungKyunKwan University, Suwon-440 746, Korea.. [1]Department of Quantum Matter, Hiroshima University, Hiroshima, 739-8530, Japan.*) Despite their interesting magnetic properties, rare-earth borate systems: both RB_4 and RB_6, are not well studied because of difficulties related with making single crystals of good quality. The only exception is CeB_6, which is an archetype Kondo lattice system. Here we report that using a state-of-art mirror furnace we have succeeded in growing several RB_4 and RB_6 single crystals with good quality. As part of our ongoing research on these materials, we have recently made magnetic studies of four single crystals using SQUID. Another noteworthy point is that we used a new ^{3}He option with a base temperature of 0.46 K, which was developed by iQuantum, Japan, in order to measure magnetization below 1.8 K. Here we are going to report and discuss our latest measurements of the magnetization for four single crystal RB_6(R=Pr, Gd) and $R^{11}B_4$(R=Tb, Dy).

Dp-045 **The Spin Canting of Maghemite Nanoparticle Investigated by ^{57}Fe NMR** LEE Seong-Joo, LEE Soonchil(*Department of Physics, Korea Advanced Institute of Science and Technology.*) We investigate 40 nm maghemite to compare the difference between the spin canting of bulk material and that of nano-size material at 4.2 K using ^{57}Fe nuclear magnetic resonance (NMR). Maghemite (γ-Fe_2O_3) is a ferrimagnet of the inverse spinel structure where magnetic Fe ions occupy either the interstitial octahedral or tetrahedral sites of the oxygen lattice. The NMR spectrum shows double peaks in zero external field similar to the bulk case. We split these peaks clearly by applying an external magnetic field. The result showed that the hyperfine field at the nuclear spins in the octahedral site (53.1 T) was larger than that in the tetrahedral site (51.8 T). The field dependence of resonance frequency indicates that the spins at the octahedral site are antiparallel with external field and canted by about 23 °, while those at the tetrahedral site are parallel and canted by about 12 °. However, only the spins at tetrahedral site are canted in the bulk case.

Dp-046 **Mössbauer 분광법을 이용한 $Fe_{0.7}Zn_{0.3}Cr_2S_4$ 의 전기 사중극자 상호작용과 자기 이중극자 상호작용 연구** 배 성환, 김 삼진, 김 철성(*국민대학교 물리학과.*) 직접합성법을 이용하여 제조된 $Fe_{0.7}Zn_{0.3}Cr_2S_4$에 대하여 x-선 회절기(XRD), 진동 시료 자화율 측정기(VSM), Mössbauer 분광기를 이용하여 시료의 결정학적 및 자기적 특성을 연구하였다. Rietveld법을 이용하여 x-선 회절도를 분석한 결과 결정구조는 Fe, Zn 이온이 사면체 자리에 Cr이온은 팔면체 자리에 각각 위치한 normal spinel 구조이며, 공간 그룹은 Fd3m 으로 격자 상수는 a_0 = 9.993 Å로 결정되었다. VSM과 Mössbauer 스펙트럼에 의해 Neel 온도는 134 K로 결정하였다. 100 Oe 인가자장하의 자화곡선(Zero-Field-Cooling:ZFC)에서

는 77 K 지점에서 첨점 형태의 특이현상이 발견되었다. 4.2 K에서의 Mössbauer 스펙트럼은 전기 사중극자 상호작용과 자기 이중극자 상호작용에 의하여 비대칭적인 8-라인 형태를 나타내었고, 온도가 증가함에 따라 Mössbauer 스펙트럼은 전기 사중극자 상호작용 감소에 의하여 8-라인에서 6-라인형태로 나타났다.

Dp-047 **Local Electronic and Magnetic Structure of $LuFe_2O_4$ studied by X-ray Absorption Spectroscopy and Magnetic Circular Dichroism** NOH Han-Jin, KO Kyung Tae[1], PARK B.-G.[1], PARK J.-H.[1], KIM Jae-Young[2], CHEONG S.-W.[3](*Dep. of Phys. Chonnam National University.* [1]*Dep. of Phys. POSTECH.* [2]*Pohang Accelerator lab., POSTECH.* [3]*Rutgers Center for Emergent Materials, Rutgers University.*) We present the local electronic and magnetic structure of $LuFe_2O_4$ revealed by x-ray absorption spectroscopy (XAS) and magnetic circular dichroism (XMCD). The O 1s XAS spectra show that the system has two kinds of Fe cations, Fe2+ and Fe3+, and their electronic configurations are $e_{1g}^3e_{2g}^2a_{1g}^1$ (S=2) and $e_{1g}^2e_{2g}^2a_{1g}^1$ (S=5/2), respectively. The Fe 2p XMCD spectra reveal that the spin alignment in the magnetic state is actually ferrimagnetic in a quite complicated manner. The detailed local magnetic structures and relavant phenomena such as spin-charge-orbital couplings are discussed in this presentation.

Dp-048 **Domain Wall Pinning By Alternating Materials In Current Induced Domain Wall Motion** 이 경진, 김 우진[1], 이 택동[1](*고려대학교, 신소재공학과.* [1]*한국과학기술원, 신소재공학과.*) Current induced domain wall motion by spin transfer torque is of great interest recently. For its application for a high-density storage device [1], sufficiently low threshold current density and high velocity of domain wall (DW) are important. It is equally important to make well-defined pinning positions of DW in the nanostrip with adequate depinning current density. The notch patterned along the edge of nanostrip was suggested as the pinning position [1], and has been used in the experiments [2]. Here we investigate another scheme for pinning DW by inserting the different material into the nanostrip. We studied on the motion of DW in the Permalloy nanostrip of which width and thickness are 60nm and 4nm, respectively. Two identical segments of different material were inserted into the nanostrip. The segments have length of D, and separated by 160nm. The transverse DW was placed in the middle of the segments. We carried out micromagnetic simulation solving the Landau-Lifshitz-Gilbert equation including the adiabatic and the local nonadiabatic spin torque terms [3]. The ratio of nonadiabatic to adiabatic spin torque was assumed to be the same as damping constant. When the saturation magnetization (Ms) of the segment is larger than that of Permalloy, the residual magnetostatic fields from the segments due to the difference of Ms make the magnetic potential in the separation of the segments. Thus, DW is confined in the middle of the segments, and the critical current density (Jc) is needed to move DW through the segment. The potential is deeper for the larger Ms and the longer D of the segments. The variations of Jc as a function of D are different for the various Ms of the segments. Jc's are mostly the same for the different D, for Ms of 1200emu/cm^3 and 1400emu/cm^3. The large difference of Ms disturbs the motion of DW in the segment because the amplitude of spin torque is inversely proportional to Ms, so that it is reduced in the segment of large Ms. For Ms of 1000emu/cm^3, Jc varies with the variation of D, that is, the depth of the potential. The segments with different Ms from that of nanostrip play roles as confinements of DW. Jc can be tuned by changing Ms and D of the segments. More details of the study will be discussed in the presentation.

References [1] S. S. P. Parkin, U.S. Patent No. 6834005 (2004). [2] M. Hayashi, L. Thomas, C. Rettner, R. Moriya and S. S. P. Parkin, Nature Physics 3, 21 (2007). [3] S. Zhang and Z. Li, Phys. Rev. Lett. 93, 127204 (2004).

Dp-049 **The angular dependence of Walker breakdown field** HEO Changhoon, KIM Woojin[1], LEE Taekdong[1], LEE Kyungjin(*Department of Materials Science and Engineering, Korea University.* [1]*Department of Materials Science and Engineering, Korea Advanced Institute of Science and Technology.*) The magnetic domain wall (DW) has attracted a considerable interest because it can be used for logic devices [1] or information storage [2]. The correlation between intensity of magnetic field and velocity of DW differs significantly below and above the Walker breakdown [3]. When a DW is propagated by magnetic field in a nanowire, the velocity of DW decreases above a certain field, i.e. Walker limit. Walker wrote down an exact solution for the motion of the simplest planar DW in a material with uni-

axial anisotropy. Despite well known novel phenomena, there still exist questions about the angular dependence of Walker breakdown field.In this work, we performed micromagnetic studies on the angular dependence of Walker breakdown field in a Permalloy nanowire. The DW velocity as a function of the field intensity shows a dramatic change as the angle varies. However, it falls into an almost universal curve when we normalized the curves by the component (//x) of the magnetic field along the length of nanowire. We also derived a theoretical equation for the angular dependence of the Walker breakdown assuming a one-dimensional rigid DW. In the presentation, we will discuss how angular variation of the applied field leads to increase in the average velocity of DW above the Walker breakdown field.

References [1] D. A. Allwood et al., Science 296, 2003 (2002). [2] M. Tsoi et al., Appl. Phys. Lett. 83, 2617 (2003). [3] N. L. Schryer and L. R. Walker, J. Appl. Phys. 45, 5406 (1974). [4] D. Bouzidi and H. Suhl, Phys. Rev. Lett. 65, 2587 (1990).

Dp-050 **Microwave Generation in Triple-Point-Contact Spin-Transfer Oscillator** 이 경진, 김 우영, 김 우진[1], 이 택동[1](*고려대학교 신소재공학과. [1]KAIST 신소재공학과.*) The spin-transfer torque results from the interaction between the spin-polarized current and the local magnetization [1]. Rippard et al. [2] reported that spin-transfer devices can be used to generate steady-state precession of the magnetization in spin valves with dc electrical current. The precession frequency can be tuned over several gigahertz ranges by varying the applied current. The microwave power of a single spin torque nano-oscillator (STNO) is less than 1nW [3]. To achieve a higher power of the order of microwatts, the two-dimensional arrays of phase coherent emission system were proposed [3]. They reported phase-locking—that is, they synchronize in double-point-contact STNO.. Power output of double-point-contact STNO is about 10 times bigger than that of two single-point-contacts STNO. Here we performed micromagnetic simulation on how STNO works in a multi-point-contact system. The STNO has three 40-nm-diameter point contacts A, B and C separated by 100~150nm and each contact is separately current biased.. Measurements are taken with the device placed in an external 740-mT magnetic field oriented 75° from the film plane. Fig.. 1 shows the power spectral density (PSD) obtained at each STNO. PSDs at each STNO are almost identical when a regular triangular shaped array of three contacts is assumed. However, PSD at the contact C is much enhanced but those at the contact A and B are reduced when a right triangular shaped array of three contacts is assumed. Furthermore, the phase-locked frequency of the right triangular array is lower than that of the regular triangular one. It is because of difference in the spin-wave interactions. In the presentation, we will discuss more details about the spin-wave interactions as a function of array design.

Dp-051 **나노 결정 구조를 가진 CoFeSiB 박막의 줄무늬 자구에 대한 연구** 윤 정범, 박 승영[1], 조 영훈[1], 정 명화[1], 유 천열[2], 김 태완[3], 이 장로[4], 김 영근[5] (*한국기초과학지원연구원, 양자물성팀, 인하대학교, 물리학과. [1]한국기초과학지원연구원, 양자물성팀. [2]인하대학교 물리학과. [3]세종대학교 신소재공학과. [4]숙명여자대학교 물리학과. [5]고려대학교 신소재공학과.*) 비정질 구조와 나노 결정질 구조를 갖고 있는 CoFeSiB 박막의 자성을 연구한 결과, 비정질 박막은 강자성을 보였고 나노 결정질 박막은 반강자성과 유사한 자성을 보였다. 여기서 나노 결정구조 사이의 반강자성 교환작용을 확인하기 위해서 magnetic force microscopy (MFM)로 자구의 모양을 관측하였다. 그 결과 줄무늬 모양의 자구를 확인할 수 있었다. 줄무늬 자구는 Fe-B/Co-Si-B 다층 박막에서 보고된 것과 같이 박막이 나노 구조의 기둥 모양으로 성장함에 따라 스핀이 평면 방향에서 수직 방향으로 주기적으로 위, 아래로 기울어져 수직방향의 자성 성분에 의해서 나타나게 된다. 자기이력곡선과 MFM image를 분석한 결과, 자기장의 세기에 의한 줄무늬 자구의 구조 변화는 자성의 변화와 매우 밀접한 관계가 있음을 확인하였다. 줄무늬 방향에 평행하게 또는 수직으로 자기장을 변화시켰을 때 자구의 모양이 다르게 변한다. 평면상에 자기 이방성이 없음에도 불구하고 줄무늬와 평행한 방향으로 자기장의 세기가 커지면 자구의 폭이 좁아지고 수직으로 자기장의 세기가 커질 때는 자구의 모양이 지그재그로 변한다. 자성이 포화될 때까지 자기장의 세기가 커지면 줄무늬 모양의 자구는 사라진다.

Dp-052 **MnF_2의 결정 및 자기구조 측정에 의한 하나로 FCD 평가 -II** 이 창희, 김 신애, NODA Yukio, 문 명국, 소 지용(*한국원자력연구소 하나로이용기술개발부.*) 하나로 중성자 4축 회절장치(FCD)에 대한 단결정을 이용한 자기구조 연구에의 활용성과 성능을 평가하기 위하여 MnF_2를 이용하여 결정 및 자기 구조 측정, 분석을 보고하였다[1]. 중성자 파장은 0.997Å,

3.9x3.4x3.4 mm^3 크기의 MnF_2 단결정 시료를 관검출기를 이용한 4축 구동모드로 하였다. MnF_2는 정방정계의 단순한 결정구조에 측정 온도 범위에서 구조 상전이가 없으며, Mn^{+2}는 스핀 5/2로서 강한 자기산란을 기대할 수 있어 기기성능 평가에 적절하다. 결정 및 자기 구조 분석을 위한 회절상 수집은 상전이 온도 67K 전후와 상온에서 하였다. 온도에 따른 시료 위치의 정밀 보정을 위하여 극저효율의 2차원 위치민감형검출기를 제작, 적용하였으며 그 결과도 함께 보고한다. 데이타는 회절피크 평가 프로그램 wx-spec.py을 이용하여 전처리를 한 후 흡수 보정은 DABEX, 결정구조 해석은 RADIEL과 SHELX를 이용하여 수행하였고, 이를 바탕으로 자기 구조 분석을 수행하였다.

[1] 이창희 외, 2006년 가을학술논문발표회, 한국물리학회

* 본 연구는 과학기술부 원자력연구개발사업의 일환으로 수행되었으며, 독일 파더본대학에서 육성한 MnF2 단결정을 부산대 단결정은행의 도움으로 가공하여 사용하였음.

Dp-053 **Structural and magnetic properties in GeMn thin films** 김 성규, 박 성균[1], 정 명화[1], 홍 태은[1], 김 종필[1], 성 낙언[2], 조 문호[3], 윤 정범[1](*포항공대/부산대. [1]한국기초과학지원연구원. [2]포항가속기. [3]포항공대, 신소재공학과.*) $Ge_{1-x}Mn_x$ thin films were fabricated on Al_2O_3(0001), Si(100), and glass substrates at the growth temperature ranges up to 500°C by an RF magnetron sputtering system. X-ray diffraction verified that $Ge_{1-x}Mn_x$ thin films grown below 300°C are amorphous. The local structure of $Ge_{1-x}Mn_x$ thin films for their atomic compositions examined by extended x-ray absorption fine structure. We have conformed magnetoresistance by the anomalous Hall effect measurement and showed that the $Ge_{1-x}Mn_x$ thin films grown at 500 °C possess ferromagnetism above room temperature. In this study, we will discuss a possible origin of the ferromagnetism in $Ge_{1-x}Mn_x$ thin films.

Dp-054 **Vortex Dynamics in Submicron Exchange-Biased Disks** 이 경진, 문 정환, 김 우진[1], 이 택동[1] (*Department of Materials Science and Engineering, Korea University, Seoul, Korea. [1]Department of Materials Science and Engineering, Korea Advanced Institute of Science and Technology, Daejeon, Korea.*) Meiklejohn and Bean reported a new type of anisotropy at the interface of the ferromagnet (FM)-antiferromagnet (AFM) in 1956 [1-2].. The directional coupling between FM and AFM called the exchange bias has aroused a considerable interest because it is an indispensable part of magneto-transport devices..Sort et al. reported that a reversal mechanism of magnetic domain in submicron exchange biased disks strongly depends on the angle between the external field and the exchange bias [3]. Recently, Waeyenberg et al. showed that the vortex core polarization is controllable by alternating magnetic field. Since the vortex core polarization can be used as data carriers like an in-plane spiral, it is one of powerful candidates for high density information device [4]. Here, we performed a micromagnetic simulation to understand the vortex dynamics in a submicron exchange biased disk. The diameter and the thickness of the ferromagnetic Permalloy disk is 500nm and 10nm, respectively.. Without exchange bias, a vortex core was formed at the centre of disk. In the exchange biased system, the vortex core was shifted perpendicular to the direction of exchange bias (Fig 1). An external field of 50Oe was applied along the direction of the exchange bias. The vortex core showed precessions around its equilibrium position. The precession frequency increased with the exchange bias field (Fig 2).. We will discuss a correlation between the exchange bias and the vortex dynamics.

Dp-055 **Domain Wall Velocity by Adiabatic Spin Transfer Torque** 서 수만, 김 우진[1], 이 택동[1], 이 경진 (*Department of Materials Science and Engineering, Korea University, Anam-dong 5, Sungbuk-gu, Seoul, 136-713. [1]Department of Materials Science and Engineering, KAIST, Daejeon, Korea.*) Current induced domain wall motion (CIDWM) is a way of manipulating the local magnetization by spin-polarized current [1]. It is of considerable interest because of its novel functions for logic or storage devices [2]. For the application of the current-induced domain wall motion, a continuous domain wall motion at the low current density free from the electromigration issue is strongly desired. Here we performed micromagnetic simulation for the transverse wall (TW) velocity with various aspect ratio (=w/t). We used Landau Lifshitz Gilbert equation with taking into account adiabatic spin torque. The continuous TW motion always accompanies with the periodic injection of the antivortex [3] which was also observed in the field-driven case [4]. We evaluate the TW velocity at which DW moves continuously. When the aspect ratio is a small, TW velocity is shown a perfect sinusoidal function. However, as increasing aspect ratio, its oscillatory wall velocity is not shown a perfect sinusoidal function. We will de-

scribe more detail at the conference.

[1] L. Berger, J. Appl. Phys. 55, 1954 (1984); ibid 71, 2721 (1992). [2] S. S. P. Parkin, U.S. Patent No. 6834005 (2004). [3] A. Thiaville, Y. Nakatani, J. Miltat, and Y. Suzuki, Europhys. Lett. 69, 990 (2005). [4] Y. Nakatani et al, Nature Mater. 2, 521–523 (2003).

Dp-056 **Electronic structure, Magnetism and Half-metallicity of TiZ(Z=Si, Sn)-terminated Co_2TiZ(001) surfaces: A first-principles study** JIN YingJiu, LEE Jae Il (*Dept. of Physics, Inha Univ.*) Half-metallic materials have attracted much attention due to the complete spin-polarization (100%) at the Fermi level and applications for spintronic devices. Recent theoretical investigations showed that the full-Huesler alloy Co_2TiSi and Co_2TiSn are half-metallic ferromagnet [1,2]. In this study, the electronic structure, magnetism and half-metallicity were investigated for the Ti and Z (Z=Si, Sn) atoms terminated (001) surface (TiZ-term) of the Co_2TiZ (Z=Si, Sn) by using the all-electron full-potential linearlized augmented plane wave (FLAPW) method [3] embodied in QMD-FLAPW code within the generalized gradient approximation (GGA) [4]. It was found that both of the TiSi-terminated Co_2TiSi(001) surface and TiSn-terminated Co_2TiSn(001) surface retain the half-metallic character as in the bulk phases. However, the minority-spin band gaps at the surfaces of both terminated systems were reduced compared to the bulk cases. From the calculated density of states (DOS), we found that there are surface states just below the Fermi level in the minority-spin states of the systems, which are responsible for reductions of the band gaps. At the surface, the magnetic moment of Si (Sn) for the TiSi (TiSn) terminated surface were almost same as that of the center layer, but the direction of magnetic moments of Ti atoms were opposite to those of center layers for both of the systems.

[1] X. Chen, R. Podloucky, and P. Rogl, J. Appl. Phys. 100, 113901(2006). [2] S. C. Lee, T. D. Lee, P. Blaha, and K. Schwarz, J. Appl. Phys. 97, 10C307 (2005). [3] E. Wimmer, H. Krakauer, M. Weinert, and A. J. Freeman, Phys. Rev. B 24, (1981) 864, and references therein; M. Weinert, E. Wimmer, and A. J. Freeman, Phys. Rev. B 26, (1982) 4571. [4] J. P. Perdew, K. Burke, and M. Ernzerhof, Phys. Rev. Lett. 77, (1996) 3865.

Dp-057 **CrP thin film: epitaxial growth and magnetic properties** 최 정용, 최 성열, 최 지연, 홍 순철, 조 성래(*울산대학교, 물리학과.*) A NiAs-type transition metal based antimonide and arsenide have considerable interests because of the possible half-metallic characteristics in zinc-blende structure. Among them, the zinc-blende growth and ferromagnetic properties of MnAs, CrAs and CrSb were reported elsewhere. On the other hand, CrP has a orthorhombic crystal structure belonging to the space group Pnma(62) with lattice constant of a=5.348 Å , b=3.109 Å and c=5.997 Å, which is distorted from the NiAs-type hexagonal structure. Several theoretical studies also predicted the half-metallic properties in zinc-blende CrP. We have grown a CrP thin film on semi-insulating GaAs(100) wafer by molecular beam epitaxy(MBE). Standard and cracking effusion cells were used for Cr and P evaporations, respectively. The growth temperature was 500 ℃ and the growth rate of Cr was 0.25 Å/s under the phosphorus ambience. However, the crystal structure of the film on GaAs(100) was orthorohombic with metallic electronic structure.

Dp-058 **Electrodynamics of $La_{1-x}Sr_xCoO_3$ with complexity of orbital ordering and ferromagnetism** SEO Y.K., LEE Y.S., JANG S. Y.[1], MIYAZATO T.[2], ONOSE Y.[2], ASAMITSU A.[2], TOKURA Y.[2](*Soongsil University, Department of Physics. [1]Seoul National University. [2]University of Tokyo.*) Perovskite Co-oxides have attracted much attention due to the complex interplay among charge, spin, and orbital with comparable energy scales between the magnetic exchange and crystal field splitting. Thermal excitation and charge carrier doping for the nonmagnetic ground state of $LaCoO_3$ allow peculiar magnetic interaction and electron-phonon coupling which lead to magnetic transition, orbital ordering, and insulator-metal transition. To get some spectroscopic understanding on these phenomena, we have performed optical measurements of single crystalline $La_{1-x}Sr_xCoO_3$ for x = 0.18 - 0.30 in a wide photon energy region. While the ground states of all samples are ferromagnetic, electric properties varies from insulating to metallic with the increasing x, which are clearly identified in temperature-dependent optical conductivity spectra. These behaviors are discussed in terms of dynamic orbital ordering and related magnetic correlation.

Dp-059 **$YMn_{1.99}Fe_{0.01}O_5$의 자기구조와 유전상수**

의 상관관계 연구 김 동현, 김 철성(*국민대학교, 물리학과.*) Mutliferroic 특성을 지닌 $YMn_{1.99}Fe_{0.01}O_5$를 sol-gel 법으로 합성 후 physical property measurement system(PPMS), vibrating sample magnetometer(VSM)을 이용하여 Multiferroic 특성의 상관관계를 연구하였다. PPMS를 이용한 dielectric constant 측정과 VSM 이용한 M-T curve(Zero-Field Cooled) 측정 결과 50 K 이하 영역인 자기적 특성이 변화하는 Néel temperature(T_N)와 전기적 특성이 변화하는 electric Curie temperature(T_{CE}) 변화의 경향성이 일치하는 모습을 보였다. 또한 second transition anomaly temperature(T_2) 역시 일치함을 알 수 있었다. 이는 자성의 발현과 전기적 분극현상이 서로 강하게 상관(coupling)되어 있기 때문인 것으로 결론지어 진다.

Dp-060 **직접합성법에 의한 $LuFe_2O_4$ 분말시료의 제조 및 자기적 특성 연구** 방 봉규, 김 철성(*국민대학교 물리학과.*) 직접합성법을 이용하여 $LuFe_2O_4$ 단일상을 제조하였으며, 결정학적 및 자기적 특성을 x-선 회절법(XRD), 진동 시료 자화율 측정법(VSM), 뫼스바우어 분광법을 이용하여 분석하였다. 결정구조는 이차원적인 층간구조로 이루어진 R3-mh의 능면체로 결정되었고, 격자상수는 각각 $a_0 = 3.438(3)$ Å, $c_0 = 25.257(3)$ Å이었다. VSM을 이용하여 100 K에서 370 K 구간에서 온도변화에 따른 자기모멘트를 측정하였으며, M-T곡선은 페리자성의 특성을 보이는 것을 확인하였다. 뫼스바우어 스펙트럼은 4.2 K에서 370 K의 구간에서 측정하였으며, 260 K 부근에서 자기적 전이를 확인하였다. VSM결과와 뫼스바우어 분광법에 의하여 Néel 온도는 T_N = 260 K로 결정하였다. 저온 영역에서의 뫼스바우어 스펙트럼은 6라인의 공명흡수선을 갖는 4개의 세트가 중첩된 형태를 보였으며, 240 K부근에서 3개의 세트는 단일 흡수선, 1개의 세트는 이중 흡수선의 형태를 보였다. 분석결과 단일 흡수선은 Fe^{3+}, 이중 흡수선은 Fe^{2+}의 이온 상태를 갖는 것을 확인하였으며, 360 K 이상에서는 날카로운 단일 흡수선의 형태가 나타났다. 이는 260 K 이상에서부터 Fe^{2+} 와 Fe^{3+} 사이의 전자의 빠른 이동이 시작되고, 360 K에서 이러한 전자의 빠른 이동으로 인한 전기적 정렬이 사라짐에 기인된 것으로 해석된다.

Dp-061 **Dependence of the nano-wire temperature on the thermal properties of the substrates for the spin transfer torque** 하 승석, 유 천열(*인하대학교 물리학과.*) 최근 spin transfer torque 현상에 관한 연구가 활발히 진행되고 있으며, 이와 관련된 current induced domain wall motion (CIDWM) 현상도 많은 관심을 받고 있다. 그러나 CIDWM 현상을 관찰하기 위해 요구되는 전류밀도는 매우 크며($\sim 10^{12} A/m^2$) 큰 전류밀도는 나노 와이어에 큰 줄 열을 발생시킨다. 이렇게 시스템의 온도가 높아질 경우 열에너지는 스핀 동역학에 중요한 영향을 미치며, 따라서 CIDWM의 정확한 이해를 위해서는 나노 와이어 구조의 줄 열에 의한 온도의 증가 경향에 대한 이해가 필요하다. 나노 와이어의 온도증가는 Joule heating에 의해 발생되는 열과 발생된 열이 기판을 통해 빠져나가는 정도에 강하게 의존한다는 것을 선행연구의 결과를 통해 알아내었다. 따라서 나노 와이어 구조를 제작할 때 필요한 절연층 물질의 열 특성은 나노 와이어 시스템의 온도 증가 문제 해결을 위해 중요한 요소라고 판단된다. 이에 본 연구에서는 일반적으로 많이 사용되는 다양한 종류의 절연층에 대해서 유한요소법 방법을 통해 수치적으로 열전도 방정식을 풀었다. 또한 나노 와이어 시스템의 온도경향에 대한 해석적인 결과와 본 연구를 통해 얻은 다양한 수치 해석적인 결과를 비교함으로써 절연층을 구성하는 물질의 열 특성과 온도 변화에 대한 상관관계를 분석하였다.

Dp-062 **A first-principles Study of Magnetism and Half-metallicity of Zinc-blende CrSb Interfaced with Simple Cubic Sb** BIALEK B., LEE Jae Il, JANG Y.-R.[1](*Dept. of Physics, Inha Univ.. [1]Dept. of Physics, Univ. of Incheon.*) In the view of possible applications in spintronics, it is very interesting to study the interfaces between different classes of materials, such as half-metals and semiconductors or half-metals and semimetals. It was shown that it is possible to obtain orderly multilayered heterostructures of half-metallic CrSb and a semiconductor material [1]. NiMnSb/Sb is an example of half metal/semimetal heterostructure [2]. In this paper we present the results of ab initio study of the magnetism and half-metallicity of zinc blende (ZB) CrSb/simple cubic (SC) Sb heterostructure. The calculations were carried out with the use of full-potential linearized augmented plane wave method (FLAPW) [3] as embodied in the QMD-FLAPW code. In order to check how the presence of the interface affects the properties of adjacent regions we built a superlattice of 9 layers of ZB CrSb and 3 layers of SC Sb in the unit cell along (001) plane. Through the total energy calculations we found that the minimum energy is obtained when the distance between the interface Cr of CrSb and SC Sb is about 1.5 times of the distance between the Cr and Sb layers in ZB CrSb. We found that the half-metallicity of CrSb is not conserved at the interface region when it is sand-

wiched between Sb layers, but it is maintained in the deeper layers from the interface. On the other hand, the magnetic moment of Cr atom in the layer being in contact with the semimetallic Sb was found to be 3.55 μ_B which means that it is increased comparing to the experimental value obtained for bulk CrSb, that is 3.0 μ_B [4]. At the same time, the atoms of SC Sb are very weekly polarized, which makes the system different from that of NiMnSb/Sb where a long-range Sb spin polarization was observed [2].

[1] J. Kubler, Phys. Rev. B, 67, 220403 (2003). [2] R. Skomski, T. Komesu, C. N. Borca, H.-K. Jeong, P. A. Dowben, D. Ristoiu, and J. P. Nozieres, J. Appl. Phys., 89, 7275 (2001). [3] E. Wimmer, H. Krakauer, M. Weinert, and A. J. Freeman, Phys. Rev. B, 24, 864 (1981). [4] B. G. Liu, Phys. Rev. B., 67, 172411 (2003).

Dp-063 **Micromagnetic Study on Attempt Frequency in Single Domain Particle** 이 경진, 서 홍주, 김 우진[1], 이 택동[1](*고려대학교 신소재공학부. [1]KAIST 신소재공학부.*) As magnetic devices have been developed in small size and high density, thermal stability has become an important issue. Thermal stability is related to the relaxation time (τ), whose equation is $\tau = 1/f_0 \exp(E_b/k_BT)$. The atempt frequency dependent on effective filed. Micromagnetic studies on thermal stability demonstrated attempt frequency (f_0) by direct simulation [1]. Bonerner and Bertram estimate magnetization swtiching time and probability of not switching. This statics show Arrhenius-Néel decay, finding attempt frequency (f_0) using Arrhenius-Néel equation. But This method takes many times for high energy barrier. On the other hand, we calculate attempt frequency (f_0) using the Landau-Lifshiz-Gilbert equation by magnetic variation. We calculate each component of magnetigation at regular time. The magnetic variation allow us to obtain attempt frequency (f_0) by fourier transformation. The result is agreement with Boerner and Bertram's. Therefore we confide in estimating f_o by our method. We will show the attempt frequency (f_0) in low energy barrier(E_b/k_BT <11.4) which is invalid for Brown's equation and in nano structure and various anisotropy.

References [1] Eric D.boerner and H.Neal Bertran, IEEE Transatcions On Magnetics 34(1998)1678[2] William Fuller Brown, Jr., Phys. Rev. 130,(1963)1677

Dp-064 **Electronic and magnetic structures of RB_4 (R=Gd, Tb, Dy, Yb)** 최 홍철, 심 지훈, 권 세균, 민 병일(*Department of Physics, Pohang University of Science and Technology, Pohang, 790-784, Korea.*) Rare-earth tetraboride RB_4 consists of the rare-earth ion (R) planes stacked along the c-axis and two kinds of boron atoms between R ion planes. The first type of the boron atoms forms of B_6 octahedra oriented along the c-axis, which are connected by the second type of boron atoms. A strong structural anisotropy in these compounds gives rise to electrical and magnetic anisotropic properties. RB4 has a complex magnetic ground state except for YbB_4. It is recently proposed that the magnetic state has a strong correlation with the orbital degree of freedom. In this study, we have investigated the electronic and magnetic properties of RB_4 by using both the linearized muffin-tin orbital (LMTO) and the full potential linearized augmented plane wave method (FLAPW). The local spin-density approximation was adopted for the exchange-correlation potential and the spin-orbit coupling term was also considered. We assumed the collinear spin configuration in these calculations. We have found stable magnetic ground states for RB_4 (R = Gd, Tb, Dy), but a non-magnetic ground state for YbB_4. A few bands crossing the Fermi level in YbB_4 indicate a possible mixed valence state

Dp-065 **Si - doped MnP thin film** 최 지연, 최 정용, 조 성래(*울산대학교, 물리학과.*) MnP has been widely studied because of its unique magnetic properties. It is known that a single crystal of MnP, which has a strong magnetic anisotropy, has helicoidal magnetic ordering between 47 K and ferromagnetic ordering between 47 K and T_c = 291.5 K. Furthermore, MnP has the Lifshitz point where paramagnetic, ferromagnetic, and helicodal phases meet. The Lifshitz point which has various magnetic properties has been extensively studied. We have made Si doped MnP thin film grown on GaAs(001) substrate using by solid source MBE (molecular beam epitaxy). The base pressure of growth chamber is below 1.0×10^{-9} Torr and the growth temperatures was 500 ℃. The crystal structure of the grown film was investigated using by XRD measurement. We have observed that the Si doped MnP film had ferromagnetism with T_c = 300 K and its resistivity was metallic behavior. Also, we have showed the disappearance of the helicoidal ordering at low temperature in the Si - doped MnP.

Dp-066 **NMR study of ^{27}Al and ^{55}Mn nuclei on a single crystal of YMn_4Al_8** KANG Kihyeok, MEAN B.J., KIM S.H., KWON S.K., NAM S.K., CHOI S.H., CHOI H.H., KWON D.J., CHO Y.R., LEE Moohee, CHO B.K.[1](*Konkuk university, Dept of Physics. [1]GIST, Department of Materials Science and Engineering.*) We have performed ^{27}Al, ^{55}Mn NMR measurements on a single crystal YMn_4Al_8. Spectrum, Knight shift, spin-lattice relaxation time T_1, and the spin-spin relaxation time T_2 have been measured as a function of temperature for the c-axis parallel and perpendicular direction to the magnetic field 8.0 T using a superconducting magnet. ^{27}Al NMR spectrum showed two different sites with five satellites for each site. ^{55}Mn NMR spectrum exhibited broad five satellites for the nuclear spin of I=5/2. The pseudo-gap behavior with temperature dependence of susceptibility and anisotropy will be discussed in this poster.

Dp-067 **Large magnetoresistance in magnetic tunnel junctions with conventional AlO_x barrier** KIM Ki Woong, KOO Ja Hyun, WOO Seok Jong, HONG Jin Pyo(*New Functional Materials and Devices Lab, Department of Physics, Hanyang University, Seoul 133-791, Korea.*) Magnetic tunnel junctions (MTJs) were fabricated with amorphous AlOx tunnel barrier, deposited by magnetron sputtering and rf remote plasma oxidation method. Rf remote plasma oxidation method demonstrates significant sensitivity to the oxidation process of metallic Al layer. This technique provides a simple method to inspect the AlOx barrier quality of MTJs. The tunnel magnetoresistance (TMR) ratio is about 27 % at room temperature and 78 % at 543 K. By analysis of the voltage and temperature dependence of the resistance and TMR in MTJs, we discuss the effects of the magnetic behavior of the free layer, barrier qualities, and barrier interfaces dependence of annealing temperature with surface plasmon resonance spectroscopy (SPRS) and transmission electron microscope (TEM).

Dp-068 **양성자 주입에 의한 DMS 물질에 대한 연구** 최 강룡, 김 삼진, 이 희민[1], 강 건욱[2], 이 민용[2], 양 태건[2], 김 철성(*국민대학교 물리학과. [1]한국원자력연구소 원자력나노소재응용랩. [2]한국원자력병원 가속기개발실.*) 양성자를 주입한 흑연에서 자기적성질의 변화가 관측되었으며, 산화물 묽은 자성반도체 물질의 경우 산소결핍 및 이온주입에 따라서 상온강자성 특성을 더욱 향상 시킬 수 있다는 결과들이 보고 되고 있다. 본 연구에서는 Fe가 도핑 된 TiO_2에 양성자 주입이 자기적 성질에 미치는 영향을 알아보기 위하여, 양성자를 조사 시간에 변화를 주어, 이에 대한 특성 변화를 연구하였다. Fe가 1 % 도핑 된 시료의 경우, 양성자의 주입에 의한 자기모멘트의 변화를 관측할 수 있었다. 이에 대한 보다 미시적인 자기적 거동을 살펴보기 위하여 상온에서 뫼스바우어 스펙트럼을 취하였다. TiO_2 내에서의 Fe는 모두 Fe^{3+}로 존재하였고, 뫼스바우어 스펙트럼은 doublet (paramagnetic phase)과 sextet (magnetically ordered phase)으로 이루어져 있었다. 이때 상온에서의 작은 자기모멘트 값은 Fe의 일부가 상자성 형태로 존재하기 때문으로 판단된다. 또한 양성자 주입에 따른 그 상대적인 면적비의 변화를 관측할 수 있으며, 이로 인하여 TiO_2 내에서의 Fe이온들의 거동이 양성자의 주입에 따라 변화함을 알 수 있었다.

Dp-069 **Temperature dependence of exchange coupling behaviors in NiFe/IrMn/CoFe structures** WOO Seok Jong, KIM Ki Woong, KOO Ja Hyun, YANG Jung Yup, JUNG Myung-Hwa[1], JO Younghun[1], KWAK June Sik[2], SHIN Il Jea[2], YOON Jungbum[3], HONG Jin Pyo[2](*New Functional Materials and Devices Lab, Department of Physics, Hanyang University, Seoul 133-791, Korea. [1]2Quantum Material Research Team, Korea Basic Science Institute, Daejeon 305-333, Korea. [2]New Functional Materials and Devices Lab., Department of Physics, Hanyang University, Seoul 133-791, Korea. [3]Quantum Material Research Team, Korea Basic Science Institute, Daejeon 305-333, Korea.*) We have investigated temperature dependence of exchange coupling of NiFe/IrMn, NiFe/IrMn/CoFe and magnetic tunnel junctions with Al_2O_3 insulating layer. In the case of MTJs, we measured tunneling magneto-resistance (TMR) and then, calculated exchange bias from curves of TMR obtained by magnetic field sweep. The layer structure of MTJs is typical structure, such as Ta / NiFe / IrMn / CoFe / Al_2O_3 / CoFe / Ta. The Al_2O_3 tunneling barriers were fabricated with optimized oxidation condition measured by surface plasmon resonance spectroscopy (SPRS). The TMR ratio is 33.02 % at room temperature. Before temperature decrease to about 150 K, the TMR ratio increases to 37.55 %. As the temperature decrease more, the TMR ratio decreases to 15.6 % at 10 K. Also, exchange bias has temperature dependence. The exchange bias increases when the temperature decreases for our samples. Before the temperature decreases to about 30 K, the exchange bias in-

creases gradually. Below 30 K, exchange bias increases all of a sudden. So, we fabricated magnetic multi-layers which were exchange coupling layers of the MTJs, such as NiFe/IrMn, NiFe/IrMn/CoFe and NiFe/IrMn/CoFe/Al_2O_3/CoFe; not masked full stack. Then, we investigated temperature dependence of exchange bias by SQUID.

Dp-070 **A mixed magnetic spin cluster system ($Sm_{1-x}Ca_xMnO_3$) with unusual properties** 김 봉주, QIAN Tian, HASSEN Arafa, 우 영수, 정 현석, 김 복기(*물리학과, 부산대학교.*) We have studied the structural, magnetic, and electrical properties of the electron-doped manganites $Sm_{1-x}Ca_xMnO_3$ ($0.85 < x < 0.92$), prepared using solid state reaction method. The samples showed the insulating phase at the low temperature, which is a mixture of the long-range ordered antiferromagnet cluster and the short-range ordered ferromagnet cluster. And this system exhibits history-dependent phenomena with magnetic field. We performed XRD rietveld refinement about the crystal structure, and electric, magnetic experiments under various magnetic fields to understand unusual properties. We discuss the experimental results and possible reasons.

Dp-071 **Ac TEP measurement setup by using two channel function generator** 우 영수, HASSEN Arafa, 김 봉주, 정 현석, 김 병훈[1], 박 영우[1], 김 복기 (*물리학과, 부산대학교. [1]물리학과, 서울대학교.*) An experimental setup was developed for measuring thermoelectric power in the temperature range going from 10 up to 300 K. The system is fully automated and uses two channel function generator as a heating source. It is high accuracy and rapidity that measure an thermo-emf (ΔV) and different temperature (ΔT). Samples are mounted between two thermal blocks which are heated by a sinusoidal frequency v_0 with a 90^o phase difference. The phase difference between two heaters gives a temperature gradient at $2v_0$. The corresponding thermopower can be extracted using a digital signal processing method with quasi-static regime (30 mHz). The calibration process with Pb standard sample has been performed to check the possibilities of our setup. Finally, the experimental results on YBCO and $Sm_{0.5}Sr_{0.5}CoO_3$ will be presented

Dp-072 **스피넬 FeM_2S_4 (M= Cr, Sc, In)물질의 치환 물질에 따른 자성 연구** 손 배순, 김 삼진, 정 명화[1], 조 영훈[1], 김 철성(*국민대학교 물리학과. [1]기초과학지원연구소.*) 스피넬 FeM_2S_4 (M= Cr, Sc, In)를 직접합성법으로 제조하여 시료의 결정학적 및 자기적 특성을 연구하였다. 결정학적 분석결과 Cr 과 Sc이 치환된 시료의 경우 Fe 가 A 자리(A site), Cr, Sc 는 B 자리(B site) 각각 위치하며, 각 이온의 분포도는 $[Fe^{2+}]^A[Cr^{3+}, Sc^{3+}]_2^BS^{2-}{}_4$으로 확인되었으며, In 이 치환된 경우 Fe가 B 자리에 위치하는 역스피넬 이었으며, 이온의 분포도는 $[In^{3+}]^A[In^{3+}, Fe^{2+}]_2^BS^{2-}{}_4$로 확인 할 수 있었다. 격자상수는 Cr, Sc, In의 시료에 대하여 각각 10.01, 10.52, 10.62 Å이었다. 온도에 따른 자화율 측정결과, Cr이 치환된 시료의 경우 온도 증가에 따라 자화율이 증가하다 Néel 온도(175 K)에서 자화율이 급격하게 감소하는 페리자성이었으나, Sc, In의 시료의 경우 온도에 따른 역자화율 그래프에서 상자성 영역에서 Curie-Weiss 법칙을 만족하는 Curie-Weiss 온도가 음의 값을 가지는 반강자성 물질임을 확인할 수 있었다.뫼스바우어 스펙트럼을 비교 분석한 결과, 상온에서의 $FeCr_2S_4$와 $FeSc_2S_4$의 흡수선이 단일선 인데 비하여 $FeIn_2S_4$ 경우 전기사중극자 분열치가 3.22 mm/s로 크게 나타나는 것을 확인 할 수 있었다. Fe^{2+} 이온이 A 자리에 위치하는 $FeCr_2S_4$ 와 $FeSc_2S_4$ 시료의 4.2 K 뫼스바우어 흡수선은 Cr 이 치환된 경우, 자기 이중극자와 전기 사중극자의 상호작용으로 인하여 8 라인 형태이며 Sc 이 치환된 경우 외부흡수선이 비대칭적으로 나타남을 확인할 수 있었다. 이는 Fe^{2+} 이온에 의해 자기 이중극자 상호작용 보다 사중극자 상호작용이 우세하게 작용하여 큰 전기 사중극자 분열치를 유도한 결과라고 할 수 있다.

Dp-073 **Physical characteristics of the flux-grown multiferroic spinel chromite MCr_2O_4 (M = Co and Mn) single crystals** KIM Ingyu, CHUN SaeHwan, OH Yoon Seok, KIM Kee Hoon(*School of physics and astronomy, Seoul National University.*) Multiferroics wherein two or three ferroic orders such as ferromagnetism and ferroelectricity coexist and are coupled to each other has recently attracted renewed attention because of its potential to be used in multifunctional electronic devices. Based on the so-called spin-current model, the chromite spinels, MCr_2O_4 (M=Mn, Co and Fe) have been recently predicted to have a spontaneous electric polarization in a conical spin ordered state stabilized at low temperatures [1]. We have successfully grown $MnCr_2O_4$ and $CoCr_2O_4$ single crystals by the PbO-PbF2 flux up to several milimeters in a lateral size, and have charac-

terized their structure, thermodynamic properties by X-ray and Laue diffraction and specific heat/ magnetization, respectively. Consistent with the previous studies [2], we have found that the conical spin ordering is known to occur at T_s=18 K for M=Mn and T_s=25 K for M=Co, followed by the ferrimagnetic transitions at T_c = 50 K for M = Mn and T_c = 97 K for M = Co, respectively. Based on the spin-current model, it is expected that the spontaneous electric polarization can be induced along [001] for M=Mn and [-110] for M=Co while the magnetization easy axes are along [1-10] for M=Mn and [001] for M=Co, respectively [3]. From the dielectric constant and the polarization measurements along those directions under a magnetic field along the magnetization easy axes, we have investigated the magnetoelectric coupling properties of both $MnCr_2O_4$ and $CoCr_2O_4$. We"ll discuss the difference and similarity of the observed magnetoelectric properties of $MnCr_2O_4$ and $CoCr_2O_4$ in connection with the proper Cr valence and occupation sites.

[1] Y. Yamasaki et al., Phys. Rev. Lett. 96, 207204 (2006) [2] K. Tomiyasu et al., Phys. Rev. B 70, 214434 (2004) [3] H. Katsura et al., Phys. Rev. Lett. 95, 057205 (2005)

Dp-074 **Room temperature ferromagnetism and Transport Properties of Epitaxial Thin Film $Zn_{1-x}Co_xO$ Diluted Magnetic Semiconductor** LEE Hyo Jin, JEONG Yoon Hee(*Department of Physics &Electron Spin Science Center, Pohang University of Science and Technology, Pohang 790-784, S. Korea.*) Many researchers have actively studied oxide based diluted magnetic semiconductor (DMS) for use as the material of spin-based information processing technologies. The cobalt doped ZnO thin films, for example, were reported to show ferromagnetism with Tc above room temperature; however, various subsequent studies including ours do not seem to converge on a definite picture and controversy continues. In this study, $Zn_{1-x}Co_xO$ epitaxial films were grown by using Laser MBE deposition technique. The crystal structures of the $Zn_{1-x}Co_xO$ films were analyzed using x-ray diffraction (XRD). Magnetic measurements were carried out using a Quantum Design PPMS VSM option over a temperature range of 5-350K. In order to investigate how to relate the electrical transport properties with magnetic properties, the Hall effect and magnetoresistance measurements were performed using van der pauw method. The magnetic and transport properties of $Zn_{1-x}Co_xO$ films in detail will be presented.

Dp-075 **AC conductivity and thermoelectric power in magnetic polaron system** 김 범현, 유 운종, 민 병일(*포항공과대학교 물리학과.*) The magnetic polaron is a composite object of a charge carrier and a ferromagnetic (FM) cluster in the paramagnetic (PM) or antiferromagnetic (AF) background. Recently, this concept has attracted enormous attention in relation to the colossal magnetoresistance (CMR) and the spintronic materials research.In this study, we have examined transport and thermoelectric properties of the magnetic polaron system employing the double-exchange model. Based on the linear response theory, we have obtained current operator (J), energy current operator (J_E) and their correlation functions. We have derived the expression of the AC conductivity ($\sigma(\omega)$) and thermoelectric power (S) in the double-exchange model, and examined behaviors of ($\sigma(\omega)$) and S as a function of temperature.

Dp-076 **Anisotropy magnetotransport properties of MnAs epitaxially grown on GaAs(001)** 조 성운, 최 형국, 정 채임, 최 우석, 오 윤석, 노 태원, 김 기훈, 박 윤(*서울대학교 물리 천문 학부.*) Magnetotransport properties of MnAs are studied considering magnetic anisotropy between easy axis along MnAs[11$\bar{2}$0] and hard axis along [0001] with various thicknesses. Both easy and hard axes of magnetization lie in the film plane. 30, 80, and 320 nm MnAs thin films are grown on (001) SI-GaAs substrate by using low temperature molecular beam epitaxy (LT-MBE). And their magnetization properties are investigated over the phase transition temperature of MnAs between ferromagnetic α phase, α-β phase coexistence, and paramagnetic β phase as the functions of temperature (M vs. T) and external magnetic field (M vs. H) along easy and hard axes by Vibrating Sample Magnetometer (VSM). With the bar shape piece of MnAs cleaved along GaAs[110] and [11$\bar{2}$0] direction, electrical transport measurements are conducted from 5 K to 350 K under the applied magnetic field that is parallel and perpendicular to the current. Distinct MR behavior changes from the negative to the positive are observed for all of magnetic field directions as the temperature decreased. In the case of observing negative MR behavior, easy axis MR shape is linear and hard axis MR shape depend ~B^2. Additionally, the transition of slope from near IR ab-

sorption data is observed at the region of 80 K.

Dp-077 **Cr이 도핑된 반도체 MnTe 박막에서의 강자성 발현** 김 우철, 문 승재, 김 삼진, 김 철성, 김 광주[1], 윤 정범[2], 정 명화[2](*국민대학교 물리학과. [1]건국대학교 물리학과. [2]한국기초과학지원연구원.*) 분자선 증착법(Molecular beam epitaxy)을 이용하여 희박 자성반도체 $Mn_{1-x}Cr_xTe$ (x=0.05, 0.1, 0.15) 박막을 Si(100):B의 기판위에 성장을 시켰다. Mn과 Te이 들어있는 두개의 K-cell과 Cr원자를 위한 E-beam을 동시에 사용하여 박막을 합성하였다. 성장과정 동안 Te이 풍부한 상태와 기판온도 400 ℃를 유지하였다. 이경우 증착비율은 1.1 Å/s이였고 성장된 층의 두께는 1000 Å 정도였다. 합성된 $Mn_{1-x}Cr_xTe$ 박막을 x-선회절(XRD), 초전도 양자 간섭계(SQUID)및 광전자 분광기(XPS)를 사용하여 박막의 구조적 및 자기적 특성을 조사하였다. X-선회절 실험결과 Si(100):B 기판위에 성장된 $Mn_{1-x}Cr_xTe$는 다결정의 hexagonal 구조를 나타내었다. 자기적 특성 실험결과, 외부자기장에 따른 자화(M-H)측정은 5 K에서 강자성의 자기이력곡선을 보여주었다. Zero-field-cooling (ZFC)과 field-cooling (FC) 조건에서 취해진 온도에 따른 자화측정에서 ZFC와 FC 자화 사이의 큰 불가역성을 보여주었다. 이러한 행위는 보통 spin-glass 또는 superparamagnetism의 자기적 무질서계에서 관찰된다. Arrott-plot 분석으로부터 평가된 강자성 전이온도 (T_c)는 x=0.05일 때 175 K, x =0.15일 때 235 K로 Cr 농도가 증가함에 따라 증가함을 보였다. 광전자 분광 실험결과 $Mn_{1-x}Cr_xTe$의 valence band 스펙트럼은 MnTe의 valence band 스펙트럼에 비해 더 낮은 binding energy 쪽으로 약간 이동하였음을 알 수 있었다.

Dp-078 **Structural and magnetic properties of spin- and charge-doping $Sr_{0.9}La_{0.1}Ti_{0.9}Co_{0.1}O_3$** YANG Jie, LEE YoungPak, LEE BoHwa[1](*q-Psi and BK21 Program Division of Advanced Research and Education in Physics, Hanyang University, Korea. [1]Department of Physics, Hankuk University of Foreign Studies, Yongin, Kyungki 449-791, Korea.*) The structural and the magnetic properties of $Sr_{0.9}La_{0.1}Ti_{0.9}Co_{0.1}O_3$ have been investigated. The sample shows a cubic structure belonging to space group PM3M at room temperature, and the lattice parameter of $Sr_{0.9}La_{0.1}Ti_{0.9}Co_{0.1}O_3$ turns out to be a = 3.9009(5) Å. The temperature dependence of magnetization (M) of $Sr_{0.9}La_{0.1}Ti_{0.9}Co_{0.1}O_3$ in both zero-field-cooled (ZFC) and field-cooled (FC) modes at H = 0.01 and 0.1 T was measured. It is found that the sample undergoes the paramagnetic-ferrimagnetic (PM-FIM) phase transition at 180 K, which is suggested to originate from the superexchange interaction between Co ions in the Co^{3+}-O-Co^{3+} chain. Moreover, the FC- and ZFC-M (T) curve exhibit a distinct upturn below 50 K arising from the PM background contribution, which is proved by a linear behavior of the M (H) curve at 5 K of $Sr_{0.9}La_{0.1}Ti_{0.9}Co_{0.1}O_3$.

Dp-079 **Magnetic Properties of V thin films on the fcc Co(001) Surface** 김 원동, 한 상욱, 이 도현, 황 찬용, HOSSAIN Mohamed Bellal[1], 이 한길[2], 김 재영[2](*한국표준과학연구원. [1]충남대학교 재료공학부. [2]포항가속기연구소.*) Magnetic properties of Vanadium thin films deposited on the fcc Co(001) surface was studied using Surface Magneto-Optical Kerr Effect (SMOKE) and X-ray Magnetic Circular Dichroism (XMCD) method. Submonolyer V thin filmes were deposited on the fcc Co(001), which was prepared by deposition of 5 ML Co on the Cu(001) surface. SMOKE results showed the reduction of coercivity after Vanadium deposition. However, unlike the theoretical prediction of Vanadium-induced perpendicular magnetic anisotropy[1], the magnetic easy axis of the system remained at inplane [110] direction after Vanadium deposition. XMCD experiment was performed at EPU6 beamline at Pohang Light Source. Induced magnetic moment of V was clearly confirmed from XMCD spectra, even at 0.25 ML V thickness. From V and Co XMCD spectra, element specific hysteresis loop were measured, and the results showed the anitiferromagnetic coupling between V and Co. The post-annealing up to 470 K was tried after deposition but no remarkable change of magnetic properties was observed after annealing.

[1] Jisang Hong, Surface Science 600, 2323(2006)

Dp-080 **1-D Magnetic Chain Fragmentation Effect on Multiferroic $DyMn_2O_5$** 김 일원, 강 선희, 이 해준, 장 태환[1], 정 윤희[1], 구 태영[2](*울산대학교, 물리학과. [1]포항공과대학교, 물리학과. [2]포항가속기연구소.*) The competition between inversion symmetry broken spin density waves became the key issue of magnetism driven ferroelectricity and concomitant giant magnetodielectric effect observed in $DyMn_2O_5$ system. The basic crystallographic and magnetic structural building blocks are turned out to be two different types of magnetic 1-dimensional (1-D) Mn chains: (1) edge-shared $Mn^{4+}O_6$ octahedral chain along the c-axis and (2) zigzag shaped

chain consisting of dimmer-like $Mn^{3+}O_5$ bypyramids connected by double stacked $Mn^{4+}O_6$ octahedra running along the a-axis. In this presentation, we investigate the robustness of these 1-D chain structures, even the dimmer formation itself and multiferroicity of $DyMn_2O_5$ by fragmenting two magnetic chains selectively with substitution of nonmagnetic Ga^{3+} and Ti^{4+} into Mn^{3+} and Mn^{4+} sites, respectively.

Dp-081 **^{53}Cr NMR evidence of double mixed valence state by self doping in half-metallic CrO_2**
SHIM Jeong Hyun, LEE Soonchil, DHO Joonghoe[1], ASTHANA Saket[1], KIM D.H.[1](*Department of Physics, Korea Advanced Institute of Science and Technology. [1]Department of Physics, Kyungpook National University.*)
We have investigated the local electronic and magnetic propertiesof Cr ions in half-metallic CrO_2 using zero-field ^{53}Cr nuclear magnetic resonance (NMR). Remarkably, the ^{53}Cr NMR spectra displayed two peaks with similar intensity instead of single peak anticipated from an uniform single valence state of Cr^{+4}. Both Cr peaks exhibited a strong anisotropy in the hyperfine field and the same magnitude of enhancementfactor and T_2 relaxation time, while their T_1 relaxationtime and field dependence were slightly different. These results strongly suggest the presence of a double mixed valence state of $Cr^{(+4\ +\ x)}$ and $Cr^{(+4-x)}$ by a self doping effect, which is probably the origin of the metallic ferromagnetism in CrO_2.

Dp-082 **Cluster calculation and XAS of LuFe2O4**
박 재훈, 고 경태, 박 병규, 김 태영, 노 한진[1](*포항공과대학교 물리학과. [1]전남대학교.*)
Recently, LuFe2O4, hexagonal layered structure, was reported to exhibit ferroelectricity. However, in this material, all Fe sites are crystallographically equivalent and mixed valence. The most adaptable scenario is the charge ordering, but the nature of charge ordering is not unequivocal. To investigate the electronic structure of LuFe2O4, polarization dependent XAS and cluster calculation were performed. The polarization dependent XAS were carried in Fe-L edge and O-K edge and the cluster calculation was followed. In the calculation, we considered the Fe2+ and Fe3+ ion, separately. We also took in the realistic hybridization and crystal field potential. With reliable physical parameters, XAS results are well interpreted by the calculation, and further investigations are now ongoing.

Dp-083 **반강자성 물질인 $NiGa_2S_4$의 연구**
명 보라, 김 삼진, 김 철성(*국민대학교 물리학과.*)
직접합성법으로 제조된 $NiGa_2S_4$ 시료를 X-회절기(XRD), VSM (Vibration Sample Magnetometer)를 이용하여 시료의 결정학적 및 자기적 성질을 연구를 하였다. 각각의 시약 Ni, Ga, S 분말을 정확한 당량비로 석영관 바닥에 놓고 10^{-6} torr 진공으로 봉입하였고, 1000 ℃에서 열처리하였다. X-선 회절도를 분석한 결과 결정구조는 trigonal구조이며, 공간그룹은 임을 확인하였다. 각 이온위치의 parameter는 Ni은 (0,0,1/2), Ga, S_1, S_2는 (1/3,2/3,x) (x=0.215, 0.420, 0.874)인 구조로 C 축을 따라서 Ga, S_1, S_2 가 순차적으로 ordering을 이루고 있음을 밝혀 냈다. 이는 얻어진 결정구조가 2차원적인 결정성을 띠고 있으며, C 축으로 성장된 육각판상구조를 이루고 있기 때문이다. 상자성 영역에서 자기감수율 측정 결과 이 물질의 경우 약한 반강자성적 질서가 존재하는 것으로 확인되었다.

Dp-084 **How to Suppress the Breakdown of Domain-Wall Velocity in Nanostripes? : Using Magnetic Underlayers with Strong Perpendicular Anisotropy**
KIM sang-koog, LEE Jun-Young(*Research Center for Spin Dynamics &Spin-Wave Devices, Seoul National University, Nanospintronics Laboratory, Department of Materials Science and Engineering, College of Engineering, Seoul National University, Seoul 151-744, Republic of Korea.*)
The domain wall (DW), which is the transition region where the orientation of local magnetizations (M) gradually changes between neighboring magnetic domains of different M orientation, has long been one of the fundamentally interesting topics in the research area of magnetism and magnetic thin films [1]. Recently, the DW motion driven by applied magnetic fields or spin torques in magnetic nanostripes is of considerable interest because it is essential to the performance of information storage and logic devices [2]. However, the velocity of DW movements in nanostripes remarkably reduces at applied magnetic fields whose strength is larger than a threshold field- the so-called Walker field (H_w) [3][4]. This phenomenon is known to be related to a complex behavior of oscillatory DW motion, that is, the turbulent motion above H_w. From a technological point of view, the DW velocity determines the operating speed of such devices mentioned above. Thus, it is a key issue how to prevent the velocity breakdown above H_w in

order to achieve its required level for the technological applications.Here, we provide a better understanding of the complex DW motion in the turbulent regime, as studied by micromagnetic simulations. In a certain range just above H_w, the motions are not turbulent but rather periodic with different periodicities in the dynamic transformation between the different types of DW internal structures. The found characteristic motions of DWs in the turbulent regime are caused not only by the periodic transformations of internal DW structures from the transverse wall (TW) type to the antivortex (AVW) or vortex wall (VW) type, and back, but also by the backward and forward motion for the VWs or vice versa for the AVWs due to their gyrotropic motion, which gives rise to a significant reduction in the DW velocities [5]. We also propose a means of preventing the nucleation of the VWs or AVWs during the dynamic transformation to them from the TW type by using magnetic underlayers with strong perpendicular anisotropy. The perpendicularly magnetized underlayer plays a crucial role in the suppression of the velocity breakdown above H_w by introducing magnetostatic and exchange interactions, which prevents the nucleation of the cores of the VW or AVW near the edges of nanostripe. Thus, the field region for the steady-state DW motion of the TW in ferromagnetic nanostripes placed on the perpendicularly magnetized underlayer is extended to a higher-field region. These results offer not only a new understanding of the complex DW dynamics in patterned thin films, but also a means to suppress the remarkable drop in velocity in fields above H_w [6].

*This work was supported by Creative Research Initiatives (ReC-SDSW) of MOST/KOSEF.

[1] A. Hubert and R. Schafer, Magnetic Domains (Springer, Berlin, 2000). [2] D. A. Allwood, G. Xiong, C. C. Faulkner, D. Atkinson, D. Petit, and R. P. Cowburn, Science 309, 688 (2005). [3] Y. Nakatani, A. Thiaville, and J. Miltat, Nature Mater. 2, 521 (2003). [4] G. S. D. Beach, C. Knutson, C. Nistor, M. Tsoi, and J. L. Erskine, Phys. Rev. Lett. 97, 057203 (2006). [5] J.-Y. Lee, K.-S. Lee, S. Choi, K.Y. Guslienko, and S.-K. Kim (unpublished). [6] J.-Y. Lee and S.-K. Kim (unpublished).

Dp-085 **Theoretical X-ray Resonant Magnetic Scattering Study of Soft X-ray Circular Reflectivity Near the Brewster's Angle**

KIM Sang-Koog, JEONG Dae-Eun(*Research Center for Spin Dynamics and Spin-Wave Devices, Seoul National University, and Nanospintronics Laboratory, Department of Materials Science and Engineering, College of Engineering, Seoul National University, Seoul 151-744, Republic of Korea.*) Soft or hard x-ray resonant magnetic scattering (XRMS) measurement techniques have been widely used to investigate charge, orbital, and spin degrees of freedom in multi-component magnetic materials, because those techniques take advantages of the exceedingly enhanced, element-specific sensitivity to different such orderings at energies close to the absorption edges of a selected element [1]. Due to a variety of microscopic interactions between incident photons and each of the different orderings, and their angular and polarization dependence in the XRMS process, the initial polarization state of incident photons is converted to various polarization states of the scattered photons [2, 3], which in turn makes it possible to determine element-specific charge, orbital, spin orderings by analyzing the changed polarization states of the scattered soft x rays and their angular and polarization dependence. Any arbitrary polarized states of photons can in principle be described in terms of the orthogonal right- and left-handed circular polarization (RCP and LCP) modes (or opposite photon helicities). Since the RCP and LCP modes are not only the basis of an irreducible representation of rotational symmetries in atomic transition processes, but are also the eigenmodes of photon beams interacting with the different kinds of orderings in broken symmetries, such circular polarizations are useful in the determination of the fundamental atomic transition spectra in the x-ray resonant region for magnetic materials [4]. Thus, in order to obtain better or deeper insight into not only the interactions of incident photons with different scattering sources of charge, orbital, and spins, but also their polarization and angular dependences, theoretical interpretations of XRMS in the framework of the RCP-and-LCP-modes basis is more fundamental than the linear-polarization-modes basis. In this presentation, we first report a novel phenomenon that shows colossal difference in soft x-ray reflectivity from ferromagnetic transition-metal films between the LCP and RCP modes at the resonance near the normal Brewster's angle. Theoretical and numerical studies of XRMS using the circular-polarization-mode basis reveal that this effect arises from a totally destructive interference of photons scattered individually from charge, orbital, and spin degrees of freedom in magnetized thin films that selectively occurs only for one helicity of the opposite circular modes when the required criteria are fulfilled. Across the normal

Brewster's angle the polarization state of scattered soft x rays is continuously variable from the RCP to LCP mode or vice versa through the linear s polarization by changing the incidence angle of a linearly p-polarized x rays at the resonance.

*This work was supported by Creative Research Initiatives (ReC-SDSW) of MOST/KOSEF.

References [1] J. B. Kortright, D. D. Awschalom, J. Stöhr, S. D. Bader, Y. U. Idzerda, S. S. P. Parkin, Ivan K. Schuller and H. -C. Siegmann, J. Magn. Magn. Mater. 207, 7 (1999). [2] D.-E. Jeong, K.-S. Lee, and S.-K. Kim, J. Korean Phys. Soc. 46, 1180 (2005). [3] D.-E. Jeong, K.-S. Lee, and S.-K. Kim, Appl. Phys. Lett. 88, 181109 (2006). [4] G. van der Laan, Phys. Rev. B 57, 112 (1998).

Dp-086 **Total Reflection and Total Refraction of Dipole-Exchange Spin Waves** KIM sang-koog, CHOI sangkook(*Research Center for Spin Dynamics &Spin-Wave Devices, Seoul National University; Nanospintronics Laboratory, Department of Materials Science and Engineering, College of Engineering, Seoul National University, Seoul 151-744, Republic of Korea.*) Waves in nature exhibit reflective and refractive behaviours when they encounter an interface between two different media. For example, for the case of light waves, the laws of reflection and refraction are analytically well described based on Maxwell equations, and are experimentally well verified. In contrast, for dipole-exchange spin waves (DESWs), which can be described by Landau-Lifshitz-Gilbert (LLG) equation, those behaviours in nano-size magnetic media are not well described due to the difficulty of simultaneous consideration of exchange, magnetic dipolar interactions, and their boundary conditions in the governing LLG equation. Technologically, the reflective and refractive properties of DESWs are of importance in terms of signal delivery via SW propagation in the next-generation logic devices [1-4]. Here, we report on micromagnetic modeling of the reflective and refractive behaviors of DESWs traveling in two-dimensional thin films that consist of two dissimilar ferromagnetic media. From micromagnetic simulation results, the laws of reflection and refraction of DESWs are analytically derived, which are in quite agreement with light waves. Surprisingly, not only omnidirectional total reflection but also total refraction of DESWs are also found. We present analytical interpretations of these novel behaviors based on the dispersion relation of DESWs in ferromagnetic thin films.

*This work was supported by Creative Research Initiatives (ReC-SDSW) of MOST/KOSEF.

References [1] R. Hertel, W. Wulfhekel, and J. Kirschner, Phys. Rev. Lett. 93, 257202 (2004). [2] K.-S. Lee, S. Choi, and S.-K. Kim, Appl. Phys. Lett. 87, 192502 (2005). [3] S. Choi, K.-S. Lee, K. Y. Gu slienko, and S.-K. Kim, Phys. Rev. Lett. 98, 087205 (2007). [4] S. Choi, K.-S. Lee, and S.-K. Kim, Appl. Phys. Lett. 89, 062501 (2006).

Dp-087 **Electric-current driven phase control of spin waves propagating in a nanowire interferometer** KIM Sang-Koog, LEE Ki-Suk(*Research Center for Spin Dynamics and Spin-Wave Devices, Seoul National University, and Nanospintronics Laboratory, Department of Materials Science and Engineering, College of Engineering, Seoul National University, Seoul 151-744, South Korea.*) Spin waves (SWs) travelling along magnetic nanowires at ultrafast speeds are highly promising for their applications to information processing technology [1-3]. Recently, it has been reported that the phase of SWs can be modified when they propagate through a 180° or 360° domain wall that is present in magnetic nanowires [3,4] However, it is not easy to practically manipulate the presence of a well-established domain wall in the nanowire waveguide. From a technological point of view, using electric currents is mostly promising for control of the SW phase. It is well known from theoretical and mciromagnetic simulation studies that SW dispersion relation varies with magnetic field applied to magnets where SWs propagate. Consequently, the phase of SWs is readily controllable with the Oersted magnetic field produced via electric currents flowing in a conducting wire. Here, we report on micromagnetic modelling of a spin-wave interferometer, based on the Mach-Zender-type interferometer, which is made of Permally thin-film nanowire waveguides. This SW interferometer is composed of a bifurcated nanowire with 30 nm width and 10 nm thickness, and a conducting wire of 270 nm diameter located in between two branches of the bifurcated nanowire waveguide. We calculated the distribution of the strength of the Oersted fields induced by currents along the conducting wire. On the two different branches of the bifurcated nanowire, the applied magnetic field is oppositely oriented, thus this opposite field direction leads to the phase difference between separately travelling SWs passing through the two different channels. This phase difference depends on current density (J). With theoretically and numerically calculated

dispersion relations of SWs at given magnetic fields in a Wentzel-Kramers-Brillouin (WKB) approximation, we can determine the phase difference of the separately travelling SWs along the two different channels. As example, for J = $2x10^{11}$ A/m^2, SWs of 17 GHz frequency destructively interfere after passing the two channel branches of the bifurcated nanowire waveguide because they are 180° out of phase, thus the amplitude is strongly suppressed. This effect can be applicable to an electric-current controlled SW interferometer.

*This work was supported by Creative Research Initiatives (ReC-SDSW) of MOST/KOSEF.

[1] K.-S. Lee, S. Choi, and S.-K. Kim, Appl. Phys. Lett. 87, 192502 (2005). [2] S. Choi, K.-S. Lee, K. Yu. Guslienko, and S.-K. Kim, Phys. Rev. Lett. 98, 087205 (2007). [3] R. Hertel, W. Wulfhekel, and J. Kirschner, Phys. Rev. Lett. 93, 257202 (2004). [4] C. Bayer et al., IEEE Trans. Magn. 41, 3094 (2005).

Dp-088 **자성반도체 Co-doped ZnO 박막의 성장조건에 따른 결정성 및 물리적 특성 조사** 이 창민, 최 석철, 사켓 아스타나[1], 도 중희[1], 손 상호[1](*경북대학교 나노과학기술학과. [1]경북대학교 물리학과.*) ZnO는 대표적인 투명 전도성 산화물(Transparant Conducting Oxides: TCO)로서 기존의 투명 전극재료을 대체하기 위한 많은 응용연구가 되어왔다. 또한 최근에는 3d 전이금속이 미량 첨가된 ZnO가 반도체성과 자기적 성질을 동시에 갖는 소위 자성반도체(Diluted Magnetic Semiconductor: DMS)로서의 기능성을 가짐에 따라 스핀전자공학(spintronics)에의 응용성 관련 연구도 많이 진행되고 있다. Co-doped ZnO의 경우, 상온에서 강자성(ferromagetism)을 나타낸다는 실험적 보고가 있었으나 그 특성이 실험조건에 따라 가변적인 경향을 보여왔으므로 정확한 물리적 근원에 대해서는 여전히 불명확한 상태이다. 본 연구에서는 화학적 정량이 맞춰진 Co-doped ZnO 타겟을 만들고 rf-스퍼터링 방법으로 기판온도와 가스분위기을 다르게 하며 다양한 Co-doped ZnO박막을 제작하였다. (0001) Al2O3 기판 위에서 에피탁시 ZnO 박막으로 성장되는 것처럼 유리 기판(glass substrate)에 제작된 Co-doped ZnO의 경우 다결정성 박막임에도 불구하고 (002) 방향성 성장(oriented growth)이 강하게 일어남을 알 수 있었으며 기판온도와 가스분위기에 따라 전기전도성,자기적 성질, 그리고 광학적 특성이 민감하게 의존함을 알 수 있었다.

Dp-089 **Magnetodielectric effect and Transport study in LuFe2O4 single crystal** JANG Tae-Hwan, KOO Tae Yeong[1], KIM Sung Baek[2], JEONG Yoon Hee, CHEONG Sang-Wook[3](*eSSC and Department of Physics, Pohang University of Science and Technology, Pohang, Korea. [1]Pohang Accelerator Laboratory, Pohang University of Science and Technology, Pohang, Korea. [2]Laboratory of Pohang Emergent Materials and Department of Physics, Pohang University of Science and Technology, Pohang, Korea. [3]Rutgers Center for Emergent Materials and Department of Physics &Astronomy, Rutgers University, Piscataway 08854, New Jersey, USA.*) Layered compound LuFe2O4 system have attracted due to the electronic based ferroelectricity from the charge ordering and multiferroicity point of view. In this material, ferroelectricity results from the charge ordering of Fe ions with valence fluctuations. Recently, some experimental and theoretical approaches about charge ordering and room-temperature magnetodielectric effect have been studied. In this presentation, we investigated magnetic, dielectric, and transport properties to try to clarify the 2D-3D charger ordering transition and low temperature magnetodielectric effect. Magneto-resistance and high temperature resistivity behavior are also discussed.

Dp-090 **InP based half metallic ferromagnetic materials: Density functional theory calculations** GUL Rahman, CHO Sunglae, HONG Soon Cheol(*Department of Physics, University of Ulsan.*) It is desirable in spintronics to control the magnetic properties by an electric filed through the application of gate voltage. Half metal ferromagnets are ideal candidates for spintronic devices. In order to search ideal materials, here we chose systems based on InP which plays an very important role in high speed devices. Magnetic and electronic properties of zinc-blende bulk (TM, TM= Ti, V, Cr, Mn, Fe, Co, Ni, Cu)P and InP/(TM)P superlattices in detail. Full-potential linearized augmented plane wave (FLAPW) method based on density functional theory in generalized gradient approximation are used to study the magnetic and electronic properties of (TM)P and InP/(TM)P. The exchange energies of these superlattices, which are the measure of T_C, are found to be larger than bulk (TM)P. Detailed properties will be discussed in this meeting.

*Supported by grant (No. R01-2004-000-10957-0) from the Basic Research Program of KOSEF

Dp-091 **Mn이 델타 도핑된 GaSb의 전자구조와 자성에 대한 제일원리계산** 권 오룡, 윤 원석, 최 정

용, 조 성래, 홍 순철(*울산대학교 물리학과.*) 묽은 자성반도체(DMS)는 일반적으로 Ⅲ-Ⅴ과 Ⅱ-Ⅵ 반도체에 자성 원소를 도핑하여 제조하고 있다. 스핀트로닉스에의 응용 가능성을 타진하기 위해 이들 물질들의 전자구조, 자성, 스핀 분극된 수송 현상에 대한 연구가 활발하게 진행되어 왔다. 이들 물질의 자성이 자성반도체에 기인하는지 아니면 제 2의 상에 기인하는지는 최근까지도 논란의 대상이 되고 있다. 뿐만 아니라 지금까지 구현된 DMS의 가장 높은 큐리 온도는 110 K이어서 상온 DMS를 실현하기까지는 아직도 많은 연구가 요구되고 있다. 큐리 온도를 높이고 스핀분극 전류 문제를 해결하기 위한 방안의 하나로 자성물질을 반도체에 델타 도핑하는 방법이 제안되고 있다. 본 연구에서는 GaSb에 Mn을 델타 도핑한 계에 대해 제일원리계산을 수행하였다. Mn이 Ga 자리를 치환한다고 가정하였고 도핑 농도가 전자 구조 및 자성에 미치는 영향을 보기 위해 Ga:Mn의 비율을 1:1, 3:1, 5:1, 7:1로 하였다. Vienna Ab-initio Simulation Package (VASP)를 사용하여 원자구조를 결정하였고 최종적인 자성에 대한 연구는 교환상관전위에 대해 GGA를 도입한 full-potential linearized augmented plane wave (FLAPW) 방법을 이용하였다. 이 구조에서 가장 안정된 자성구조를 찾기 위하여 상자성(PM), 강자성(FM), 반강자성(AFM)에 대해 계산을 수행하였으며, GaSb층과 관계없이 FM 상태가 가장 안정한 것으로 밝혀졌다.

Dp-092 **Electronic structure and magnetism of NiAs and zinc-blende MnTe: First-principles study** YUN Won Seok, CHA Gi-Beom, HONG Soon Cheol(*Dept. of Physics, University of Ulsan.*) Recently, magnetic semiconductors and diluted magnetic semiconductors (DMSs) have attracted considerable attention for applications in spin electronic devices, especially when they exhibit magnetic properties at room temperature. Among stable binary manganese compounds, only MnTe exhibits semiconductor properties. A stable phase of MnTe is a hexagonal NiAs (NA) structure below 1040 °C. MnTe has indirect energy gap close to E_g=1.27 eV at room temperature. Experimentally, Durbin et al. and Anno et al. succeeded in a growth of zinc-blende (ZB) MnTe film and measured its optical properties.In this work, we investigate electronic structure and magnetism of the MnTe with ZB and NA structures, using the highly precise all electron full-potential linearized augmented plane-wave (FLAPW) method based on general gradient approximation (GGA) for exchange-correlation potential. The lattice constants of NA MnTe were taken as experimental values, a = 4.143 Å and c = 6.711 Å. The total energy of ZB MnTe was calculated as a function of the lattice constant in range from 6.10 Å to 6.60 Å and was determined to be equilibrium lattice constant 6.31 Å. Antiferromagnetic states were found to be energetically more stable, compared to ferromagnetic states for both of NA and ZB structures.

Dp-093 **^{11}B 핵자기 공명 측정방법을 이용한 반강자성 DyB_4 단결정 시료의 국소 전자 구조와 4f전자의 스핀동역학 연구** 민 병진, 강 기혁, 현 일남, 김 정훈, 김 성훈, 권 세근, 남 승관, 최 성훈, 최 헌화, 권 달중, 조 용래, 이 무희, 조 병기[1](*Konkuk university, Dept of Physics. [1]GIST, Department of Materials Science and Engineering..*) 반강자성 DyB_4 단결정 시료의 국소 전자 구조와 4f전자의 스핀동역학을 ^{11}B 펄스 핵자기 공명 방법으로 측정하였다. 8 T의 외부 자기장에서 4.3 K까지 온도를 변화시키며 선모양, 공명선 이동, 스핀-격자 완화율 및 스핀-스핀 완화율의 측정실험을 수행하였다. 선폭과 공명선 이동은 Dy 4f전자 스핀의 영향으로 강한 온도 의존성을 보였다. 또한 이 두 양은 자화율에 비례하는데 이것은 붕소위치의 초미세자기장이 Dy의 4f전자로부터 왔음을 나타낸다. 반강자성 상전이온도 T_N = 20 K이하에서 폭이 넓은 하나의 공명선이 여러 개로 갈라지는 것은 스핀의 반강자성 정렬에 의해 나타나는 국소 자기장을 반영한다. T_N이상에서 스핀-격자 완화율과 스핀-스핀 완화율은 매우 크며 온도에 무관하나 T_N이하에서는 급격히 감소한다. 이것은 Dy의 4f전자 스핀이 반강자성 정렬에 관련하여 스핀 요동이 감소하고 스핀 동력학의 급격하게 변화하기 때문인 것으로 확인된다.

Dp-094 **^{11}B 핵자기 공명 측정방법을 이용한 반강자성 HoB_4 단결정 시료의 국소 전자 구조와 4f전자의 스핀동역학 연구** 민 병진, 강 기혁, 김 정훈, 현 일남, 김 성훈, 권 세근, 남 승관, 최 성훈, 최 헌화, 권 달중, 조 용래, 이 무희, 조 병기[1](*Konkuk university, Dept of Physics. [1]GIST, Department of Materials Science and Engineering.*) 희토류-4붕소 화합물은 휘토류 원소를 치환함에 따라 비자성체, 강자성체, 반강자성체로 자기적 성질이 다양하게 나타난다. HoB_4는 Ho이온의 자기 쌍극자 모멘트가 결정의 c축에 평행 및 반평행하게 정렬하는 반강자성체이다. HoB_4 단결정 시료의 국소 전자구조와 4f전자의 스핀동역학에 대하여 밝히고자 ^{11}B 핵자기 공명 실험을 수행하였다. 실험에 사용된 초전도자석의 자기장은 대략 8 T이며, 3.5 – 300 K의 온도 범위에서 선모양, 공명선 이동, 스핀-격자 완화율 및 스핀-스핀 완화율을 측정하였다. Ho 이온의 4f 전자의 스핀 자기모멘트의 영향으로 선폭과 공명선 이동은 대단히 큰

온도 의존성을 갖는다. 스핀-격자 완화율은 반강자성 상전이 온도 T_N = 8 K이상에서 온도에 무관하나 T_N이하에서는 온도가 감소함에 따라 급격히 감소한다. 이것은 Ho 이온의 4f 전자의 스핀의 요동이 매우 크게 제한됨을 가리킨다. 스핀-스핀 완화율 또한 반강자성적 정렬에 관련된 4f 전자 스핀 동역학의 특성을 보인다.

Dp-095 **Raman scattering spectroscopy of $Nd_{1+x}Ba_{2-x}Cu_3O_7$ coated conductors grown by pulsed laser deposition** UM Yu Mi, JO. W, SEO. C.W[1], CH. H.S[1], WEE. S.H[2], YOO S.I[2](*Department of Physics and Division of Nanosciences, Ewha Womans University, Seoul 120-750, Korea. [1]Department of Physics, Sogang University, Seoul 121-742, Korea. [2]School of Materials Science and Engineering, Seoul National University, Seoul 151-742, Korea.*) We explore optimal growth conditions of superconducting $Nd_{1+x}Ba_{2-x}Cu_3O_7$ (NdBCO) coated conductors on ion-beam assisted deposition (IBAD) yttria-stabilized zirconia templates deposited in various growth temperature at the range of 750 ~ 830 °C with 1% O_2/Ar gas. It has been addressed to investigate growth orientation, cation disorder, Ba-Cu-O second phases, and oxygen deficiency of NdBCO coated conductors by using Raman scattering spectroscopy. The films grown at 750 °C show c-axis orientation with a-axis grains and degraded superconducting properties with critical temperature (T_c) of ~ 83 K. The samples grown in the higher growth temperature show a strong c-axis orientation and good superconducting properties with T_c of 88 ~90 K and critical current (J_c) of ~ 1.8 MA/cm^2. Through the Raman scattering studies, the growth factors that lead to high T_c and J_c are elucidated.

Dp-096 **Relation between the Critical Current and the n-Value of ReBCO Thin Films: A Scaling Law for Flux Pinning of ReBCO Thin Films** OH Sangjun, CHOI Heekyung, LEE Chulhee, LEE Sangmoo[1], YOO Jaeun[1], YOUM Dojun[1](*National Fusion Research Institute, Material Research Team. [1]Korea Advanced Institute of Science and Technology, Department of Physics.*) Detailed field and angle dependences of the critical current and the n-value for a SmBCO coated conductor have been measured. It was found that the field dependence of the n-value can be fitted by an empirical power law with three parameters including the irreversibility field. We also found that there is a correlation between the critical current and the n-value which can be describe by the Kramer model including thermal activation. The model fits the field dependence of the empirical critical current data at various angles and temperature with three fitting parameters, the pinning force maximum, the g-factor and the upper critical field. The upper critical field found from fitting was higher than the irreversibility field and the angular dependence of the upper critical field is in agreement with the Tinkham model. The pinning force maximum does not show a correlation with the upper critical or the irreversibility field which is attributed to the difference in the pinning mechanism with a variation of the angle. It was further shown that the angular dependence of the critical current can be calculated by the Kramer model including thermal activation with empirical angular dependence expressions of each parameter. The critical current data reported by Yamada et al. for YBCO thin films on various substrates deposited by pulsed laser deposition method also can be described by the Kramer model including thermal activation and the angular dependences of each parameter were compared with the SmBCO coated conductor fitting results.

Dp-097 **Square Helmholtz coil system for SQUID evaluations** KANG Chan Seok, CHANG Jung Won, OH Soo-Ho, HONG Sung-Hak, LEE Soon-Gul(*Korea University.*) We have designed and fabricated a uniaxial square-loop coil system to calibrate second-order SQUID gradiometers. The coil system consists of 2 pairs of identical square loops, a Helmholtz pair for generation of uniform fields and the second pair for the 2nd-order gradient in combination with the Helmholtz pair. Full expressions of the axial components of the field were calculated by using Biot-Savart"s law. To understand the behavior of the field near the coil center, analytical expressions were obtained up to the 4th-order in the midplane and along the coil axis. The Helmholtz condition for generating uniform fields was calculated to be d/a=0.544505643, where d is the inter-coil distance and a is the side length of the coil square. The pure second-order gradient field can be generated by subtracting the Helmholtz field from the field of the 2nd pair with equal magnitudes of the center fields of the two pairs. We fabricate. These features are very useful for balancing and sensitivity test of second-order SQUID gradiometers. Details of experimental results will be discussed

Dp-098 **Effect of Co and Fe doping on Structure and Superconductivity of $(Ga_{1-x}M_x)Sr_2(Tm_{1-y}Ca_y)Cu_2O_z$ (M= Co, Fe) samples** LEE H.K., KWON O.-H., BAE S.M.(*Department of Physics, Kangwon National University.*) We investigated the effects of Fe and Co doping on the structural and superconducting properties of $(Ga_{1-x}M_x)$-$Sr_2(Tm_{1-y}Ca_y)Cu_2O_z$ (M = Co, Fe) samples. X-ray diffraction revealed that, for a fixed Ca content y, the phase purity of the samples increases as the M-doping concentration increases. In contrast to the Co-substituted samples, which show superconductivity at appropriate Co-doping content, the corresponding Fe-substituted samples do not exhibit superconductivity. The superconducting behavior of the Fe-substituted samples is discussed in connection with the structural properties characterized by using neutron powder diffraction and transport measurements. *This work was supported by the Korea Science and Engineering Foundation(M2-0602-00-0018).

Dp-099 **고에너지 전자빔 조사에 의한 초전도 박막 열화 연구** 장 정원, 김 윤원, 홍 성학, 이 순걸, 김 민완[1], 한 영환[1](*고려대학교. [1]한국원자력연구원.*) $YBa_2Cu_3O_7$ 박막과 MgB_2 박막에 고에너지 전자빔을 조사하여 초전도 특성 열화 정도를 연구하였다. 사용한 전자빔은 1 MeV의 에너지와 약 10^{13} e/cm^2×sec의 선량으로, 2시간 20분 조사하여 총 조사량이 $0.8'10^{17}$ e/cm^{2}이었다. YBCO 박막의 경우, 실리콘, 사파이어, 포토리지스트 세 가지 마스크로 보호한 시료와 보호막 없이 조사한 시료를 비교한 결과, 임계특성 열화가 아주 작게 나타나, 보호막 없이 노출한 시료의 경우 비저항 값이 약 50 % 증가하는데 그쳤으며, 임계온도는 거의 변하지 않은 것으로 관측되었다, 반면, MgB_2 박막의 경우, 보호막 없이 전자빔이 조사된 시료는 임계온도가 0 이었으나, 포토리지스트 마스크로 보호한 박막은 임계온도가 18 K로 관측되었다. 전자빔 조사 전의 MgB_2 박막은 임계온도가 36 K 였으며, 전자빔 조사 후에는, 포토리지스트 마스크를 씌운 시료는 비저항 값이 약 100 배 증가한 금속성을 보인 반면, 보호막 없이 노출된 시료는 비저항 값이 최소 만 배 이상으로 반도체 저항-온도 특성을 보였다. 이 결과로부터, 포토리지스트 마스크와 고에너지 전자빔을 이용한 MgB_2 박막의 접합 제작 가능성이 있음을 알 수 있다.

Dp-100 **Magnetic susceptibility in a superconducting coaxial cylindrical multi-shell structure** LEE J. H., KIM Y. C., KO Rock-Kil[1], JEONG D. Y.[1], AHN S. S., PARK I. S., KIM D. J., JANG M. S.(*부산대학교 물리학과. [1]한국전기연구원.*) Generally, magnetic signals of type II superconductors such as magnetic hysteresis, M(H), or temperature dependence of magnetic susceptibility, χ(T), have been analyzed by critical state models.The critical state models are based on the assumption that pinning force and Lorentz force applied to flux bunbles are balanced. However, in principle, the assumption cannot give an information on the first local field distribution just after applying external field, because there is no field inside the sample at the first moment that external field (H) is applied. We suggest a new model on the first local field distribution which can be applied to finite type II superconductors. We calculated M values of a superconducting coaxial cylindrical multi-shell structure and applied the calculation results to χ(T) curves of a $YBa_2Cu_3O_x$ bulk superconductor. The shells are assumed to be type I superconductors. Since each shell has different demagnetization factors, fields that each shell allows entering are different. Calculated χ(T) curves agree well with experimental data, and obtained parameters are $J_{cg}(0)=2.6\times10^7$ A/cm^2 and $J_{cJ}(0)=1.3\times10^3$ A/cm^2, where $J_{cg}(0)$ and $J_{cJ}(0)$ are intra- and intergranular critical current densities.

Dp-101 **Tunneling Density of States in Superconductor-Ferromagnet Hybrid Structures.** 이 나영, 최 한용(*성균관대학교, 물리학과.*) 우리는 Eilenberger 방정식을 사용해서 초전도체(superconductor, S)와 강자성체(ferromagnet, F)의 다양한 접합체들의 온도가 0일 때의 터널링 상태밀도(tunneling density of state)를 계산했다. 여기서 초전도체와 강자성체의 경계면은 스핀에 의존하지 않은 경우를 고려했고, 강자성체/초전도체/강자성체(F/S/F) 접합체는 두 강자성체의 자기화 방향이 서로 평행, 반 평행(antiparallel), 그리고 직각을 이루는 경우에 대해서 계산했다. 이번 계산에서는 S/F, F/S/F 접합체들의 근접효과(proximity effect)와 F/S/F 접합체에서 강자성체의 자기화 방향 등이 상태밀도에 미치는 영향을 설명하고자 한다.

Dp-102 **Systematic treatment of a non-perturbative method for the correlations in two-dimensional vortex liquid systems** PARK Hyunjoon, KIM Younghee, YEO Joonhyun(*건국대학교 물리학과.*) Ginzburg-Landau 모델을 바탕으로 초전도체 내의 2차원 vortex 액체를 기술하는 비섭동적인 방법 중에 parquet diagram을 이용한 방법에 대해 체계적으로 연구한다. 특히 최

근 논문에서 non-parquet 기여가 포함된 첫번째 근사 방법이 vortex liquid가 온도가 낮아지면서 격자화되는 과정을 이전의 방법들에서 보다 더 명확하게 보일 수 있었다는 사실이 밝혀졌는데, 이번 논문에서는 이 방법을 좀 더 확장하여 이전 보다 더 많은 non-parquet diagram을 단계적으로 포함하는 새로운 iteration 방법을 제시하고 이의 수치적 계산 결과를 보인다. 특히 포함되는 Feynman diagram의 범위가 단계적으로 어떻게 주어지는지 이미 알려져 있는 정확한 섭동전개 결과와 비교하여 연구한다.

Dp-103 **V_2O_3를 첨가한 BiPbSrCaCuO 초전도체의 활성화에너지에 대한 연구** 손 인호, 김 영국, 이 상찬, 주 유환, 오 재근[1](*경남대학교. [1]국립과학수사연구소.*) 높은 임계온도를 가지는 Bi-2223초전도체의 성장을 위하여 $Bi_2Pb_{0.3}Sr_2Ca_2Cu_3O$ 혼합물에 V_2O_3를 첨가하여 self flux방법으로 성장하였다. 그리고 Pb보다 더 나은 초전도 특성을 보인다고 알려진 V_2O_3를 소량 첨가하여 초전도상의 형성에 대한 영향을 조사하였다. Bi-2223상을 성장시키기 위하여 $Bi_2Pb_{0.3}Sr_2Ca_2Cu_3O$ 조성으로 1차소결후 V_2O_3를 첨가하였으며, V_2O_3의 Bi-2223상형성에 대한 영향을 알아보기 위하여 원형 성형체로 만들어 830℃와 850℃에서 24시간 2차소결한후 830℃와 860℃에서 72시간동안 3차소결하였으며, 시료를 XRD와 SEM, EDS를 이용하여 미세구조 및 결정성을 관찰하였으며, 비저항 측정하였다. Bi계 초전도시료의 비저항을 외부자기장에 대해 구하여 Arrhenius 방법으로 활성화 에너지 및 상부 임계자기장의 온도의존성과 V_2O_3의 첨가로 형성된 상들의 영향을 조사 하였다.

Dp-104 **Ti doping in MgB2 superconductor** 정 창욱(*한국외국어대학교, 전자물리학과.*) MgB2의 Mg 자리에 도핑을 통해서 초전도 물성을 개선 및제어하려는 시도는 MgB2의 발견직후 시작되었다. Al 경우에는 도핑에는 성공하였으나 초전도 전이온도가 매우 감소함을 발견하였다. 한편 Ti의 경우는 성공적인 치환자체가 불가능했고 따라서 Ti도핑을 통한 물성의 개선이나 제어는 그 시도조차 아직까지 제대로 이루어지지 못했다. 본 연구에서는 Mg, Ti, 그리고 B을 다양한 정량비대로 혼합한 초전도체인 (Mg,Ti)B2 polycrystal을 제작하였다. 약 3만 기압의 고압에서 생성된 다결정 시료들은 밀도가 매우 치밀하였다. 초전도양쟈간섭장치로 magnetization을 측정한 결과 초전도 전이온도와 superconductinv volume fraction이 원하는바 대로 도핑이 성공적으로 이루어졌음을 보여 주었다. 따라서 본 연구에서 시도된 초고압합성법은 도핑을 통한 MgB2의 물성변화의 연구에 적극적으로 사용될 수 있을 것으로 기대된다

Dp-105 **Growth of Epitaxial MgB_2 Thick Films with Columnar Grains by HPCVD** SEONG WON KYUNG, HUH JI YOUNG, KANG WON NAM, KIM JEONG WOON, KWON YONG SUNG, YANG NAM KEUN, PARK JE-GEUN(*Sungkyunkwan University, BK21 Physics Division and Department of Physics.*) Epitaxial MgB_2 thick films were grown on c-cut Al_2O_3 substrates at 600℃ by using hybrid physical-chemical vapor deposition (HPCVD) technique. In order to obtain a high magnesium vapor pressure around substrate at low temperature, we used specially designed susceptor having susceptor cap and we achieved very high growth rate of 1700 Å/min at low temperature. The x-ray diffraction patterns showed epitaxial growth of MgB_2 thick films. C-axis oriented columnar grains with 100 - 500 nm in diameter were observed by cross-sectional view of scanning electron microscope (SEM) images after milling by dual beam-focused ion beam (FIB). Critical current density calculated by Bean's critical state model was 4×10^6 A/cm^2 at 30 K and zero field, and superconducting transition temperature (T_c) was ~ 40.5 K.

Dp-106 **Effect of Sm substitution on magnetic and transport properties of $Eu_1Ba_2Cu_3O_7$** AHMAD DAWOOD, LEE JUNHO, KIM YOUNG CHEOL, KIM GUN CHEOL, AN SEUNG SU(*Pusan National University.*) We have studied the effect of Sm substitution on $Eu_1Ba_2Cu_3O_7$ sample at different temperatures and applied fields. SmEu series was made by usual heating method. The T_c's of series samples are almost the same. This research was carried out in order to investigate the effect of Sm on Jc and pinning force of $Eu_1Ba_2Cu_3O_7$ sample. Our results show that Jc is increased continuously by increasing Sm substitution. We have also observed the increment in pinning force in our systems parallel with Jc.

Dp-107 **초전도 상변이 온도계를 이용한 X-선 검출기** 권 용대, 이 영화, 이 상준, 김 용함, 이 경범, 이 민규(*한국표준과학연구원.*) 초전도 미소열량계를 이용한 고분해능 x-선 검출용 온도센서(transition edge sensor: TES)를 개발하였다. TES는 초전도 상전이의 급격한 저항변화 특성을 이용하여 x선 흡수에 의한 미세 온도변화를 측정한다. 본 연구에서는 사진식각법 및 전자선(e-beam) 증착법으로 Ti/Au bilayer 박막 센서를 형성시켰고, 흡수체로는 Au를 사용하였다. 또한, 센서부에

서 Si 기판으로의 열확산을 최소화하고 센서 자체의 열용량을 최소화하기 위하여 후면을 비등방 식각, SiN_x-membrane 위 구조를 이루도록 하였다. 제작된 센서의 기본 물성인 상전이온도(T_C)를 Au의 두께를 100 nm로 고정시키고 Ti의 두께를 변화시켜 측정하였다. Ti/Au bilayer의 상전이 온도는 근접효과(proximity effect)로 인하여 두 막의 두께비에 의존한 다양한 값을 나타내었다. TES형 x선 검출기는 반도체 x-선 검출기에 비해 매우 우수한 분해능을 보여준다. 따라서 미소 영역의 성분분석 및 기타 여러 미세 검출 분야에 널리 응용될 수 있다.

Dp-108 **Thermally activated critical current distribution in intrinsic Josephson Junctions of $Bi_2Sr_2CaCu_2O_{8+x}$** PARK Jung-Hwan, BAE Myung-Ho[1], LEE Gil-Ho[2], LEE Hu-Jong[3], KHIM Zheong Gu(*Department of Physics and Astronomy, Seoul National University, Korea. [1]Department of physics, University of Illinois at Urbana-Champaign, USA. [2]Department of Chemistry, Pohang University of Science and Technology, Korea. [3]Department of physics, Pohang University of Science and Technology, Korea.*) We have measured the tunneling critical current distribution of the $Bi_2Sr_2CaCu_2O_{8+\delta}$ intrinsic Josephson junctions (IJJs). According to the resistively and capacitively shunted junction (RCSJ) model, the dynamics of Josephson junctions can be described by the motion of a phase particle in a tilted washboard potential. The escape of a phase particle from the washboard potential determines the tunneling critical current of a Josephson junction. The sample system employed in this study was a stack of IJJs (with the lateral dimension of 2x10 μm^2) fabricated on a $Bi_2Sr_2CaCu_2O_{8+\delta}$ single crystal by electron-beam lithography, ion-beam etching, and double-side cleaving technique. Considering the stochastic nature of the escape of a phase particle the critical current distribution was obtained by repeating measurements for 1000 times at a temperature. The distribution obtained while lowering the temperature down to 4.2 K is interpreted in terms of the thermal activation of the escape of the phase particles from the washboard potential. The result will be discussed in connection with the feasible observation of the macroscopic quantum tunneling in IJJs.

Dp-109 **Measurement of magnetic flux in thin film and coated conductor strips using Scanning Hall Probe Microscope(SHPM)** YOON WonSik, JANG YongSik, LEE NamMi, PARK SangKook(*경북대학교, 물리학과.*) Strip pattern을 가지는 고온초전도체 YBCO thin film 및 coated conductor에 전류와 자기장을 인가하여 전류수송 특성을 연구한다. 시료 표면에서의 국소 자기장 분포를 측정하기 위해 제작한 SHPM을 이용한다. 이 장비는 시료와의 거리를 유지하는 Capacitance sensor와 50μm x 50μm의 active area를 가지는 Hall sensor, 이 센서들을 이동시킬 Piezo xyz scanner 및 시료를 200mm x 200mm x 200mm 이동시킬 수 있는 시스템, 그리고 cryogenic system으로 구성되어 있다. strip pattern이 있는 thin film 및 coated conductor에 직류전류 및 외부 자기장을 인가하여 그 세기를 변화시키면서 주변의 자기장 변화를 측정한다. 이 결과를 criticla state model을 이용하여 분석한다.

Dp-110 **4μm 두께의 MgB_2 박막에 대한 박막 두께별 구조적 특성 및 고주파 특성 변화** 박 은규, 이 재훈, 양 우일, 정 호상, 최 윤옥, 이 상영, 성 원경[1], 강 원남[1] (*Department of Physics and Center for Emerging Wireless Transmission Technology. [1]성균관대학교, 물리학과.*) 사파이어 기판 위에 4μm 두께로 증착된 MgB_2 박막의 두께별 구조적 특성 및 고주파 특성의 변화를 연구하였다. Ar-ion milling을 이용하여 MgB_2 박막을 식각하는 방법으로 MgB2 박막의 두께를 변화시켰으며 이러한 MgB2 박막의 표면저항을 마이크로파 영역에서 비파괴적 측정법인 유전체 공진기법으로 측정하였다. 또한 두께에 따른 MgB_2의 구조적 특성 변화 및 조성의 변화를 확인하기 위해 X-ray diffraction 측정 실험을 수행하였다. As-grown MgB_2의 Tc는 약 41 K로 단결정 시편에 대해 관측되는 39 K 보다 상당히 높은 값을 보였지만 normal-state resistivity는 약 $2.1x10^{-8}$ (Ohm-m)로 대단히 작은 값을 지니는 것으로 관측되었는데, 이러한 사실은 두껍게 성장된 MgB_2 박막의 표면이 Mg-rich phase와 같이 금속적 특성을 지니고 있음을 말해준다. Ar-ion milling에 의해 두께가 변할 경우 이러한 측정값 들 간의 상관 관계가 논의될 것이다.

Dp-111 **An Influence of Potential Impurity on the 1-Dimensional Antisymmetric Spin Filter** LEE Hyun C., PARK Jaeshin(*Sogang University, Department of Physics.*) An influence of potential impurity on the transport properties of one-dimensional antisymmetric spin filter is investigated using the methods of bosonization and renormalization group. The tranport properties are qualitatively similar to those of Lutttinger, however, the exponents of temperature dependence and the coeffients of conductances depend sensitively on the spin-orbit coupling and the parallel magnetic field.

Dp-112 **Secondary electron emission from doped MgO; an ab-initio study** CHO Eunae, HAN Seungwu, CHO Youngmi[1], KIM Changwook[1](*Department of Physics, Ewha Womans University, Seoul 120-750, Korea. [1]CAE team, Samsung SDI, Co., LTD, Yongin 446-557, Korea.*) In plasma display panel(PDP), the protective layer made of MgO thin film is a critical component for lowering the operation voltage and extending the lifetime, and hence tremendous efforts are now being invested toward understanding material properties related to the display performance. One of the most important roles of the MgO protective layer is the emission of secondary electron. The surface orientations, morphology, dopants and electronic property of MgO thin film influence the secondary electron emission. In an effort to understand the secondary emission properties depending on the surface electronic structures and various dopants, we present in this poster presentation first-principles analysis on the doped MgO (100) surface. We find that localized states for each dopant play an important role in determining the work function and electron affinity. The connection with the secondary emission performance will also be discussed.

Dp-113 **First-principles study on phase stability and electronic structures of tantalum mononitride** HAN Seungwu, KIM Tae-Eun, SHIN Seokmin[1], SON Won-joon[1] (*이화여자대학교, 물리학과. [1]서울대학교, 화학과.*) Using the density functional methods, we study electronic and structural properties of various phase of tantalum mononitrides (TaN). The ε phase is found to be most stable. We also find that the cubic phase of stoichiometric TaN undergoes spontaneous distortion. The presence of cation or anion vacancies stabilizes the cubic phase. The change in the electronic structures with respect to the off-stoichiometry are discussed in detail.

Dp-114 **Exact calculation of the optical conductivity of disordered quasi-one-dimensional Peierls systems and its universal behavior** 조 영권, 김 기홍(*아주대 에너지시스템학부.*) We consider the Peierls-Frolich ground state of quasi-one-dimensional materials with static Gaussian random potential due to impurities and lattice fluctuations. Starting from a Dirac-type equation for the wave functions describing electrons moving in one direction and another, we derive an infinite number of coupled ordinary differential equations describing electronic properties. We solve these equations numerically using a truncation method and use the result in calculating the exact frequency-dependent conductivity. Our results are substantially different from previous approximate calculations. The scaled conductivity follows a universal curve when it is plotted against a scaled frequency. We compare our results with previous experiments in detail.

Dp-115 **Exact calculation of the disorder-averaged resistance and its fluctuations in one-dimensional disordered conductors** 이 광진, 김 기홍(*아주대 에너지시스템학부.*) We consider the electrical conduction in one-dimensional disordered conductors at low temperatures. According to the well-known Landauer formula, the electrical resistance is given by the ratio of the reflectance and the transmittance. Using the invariant imbedding method for studying the wave propagation in one-dimensional disordered media, we calculate the disorder-averaged resistance and its fluctuations exactly, for unitary, absorbing and amplifying cases. In these calculations, the disorder effect is introduced by adding a delta function correlated Gaussian random potential to the Schroedinger equation. For small disorder, the averaged resistance increases exponentially in an oscillatory manner as the frequency increases. We find a surprising result that both absorption and amplification enhance the averaged resistance.

Dp-116 **물분해 광촉매 Titania(TiO_2) 표면에 대한 전자구조 연구** 박 찬현, 공 기정, 장 현주, 백 진욱, 문 상진(*한국화학연구원.*) Titania(TiO_2)는 광촉매 물질로서 환경, 에너지 등 많은 분야에 연구되고 있다. 특히, 수소에너지에 대한 관심이 높아지면서 태양빛을 이용한 물분해 수소 발생용 광촉매로서 Titania(TiO_2)에 대한 많은 연구가 수행되고 있다. 우리는 제일원리 계산 방법(VASP)을 이용하여 Rutile TiO_2 표면(110)에서 H_2O가 어떻게 반응하는지 알아보았다. 결함이 없는 Rutile TiO_2 (110) 표면은, Ti(Titanium)와 O(Oxygen)이 같은 평면에 위치하는 부분(Ti-O)과 O만이 돌출된 부분, 이 두 가지 영역으로 이루어진다. 이러한 TiO_2 표면 위에 H_2O가 위치하면, Ti-O 부분의 Ti 위에 H_2O의 O가 자리할 때 낮은 에너지로 안정된 구조를 보인다. Rutile TiO_2 표면에 O 결함이 생기면 그 자리에 H_2O의 O이 자리하여 안정된 구조를 가진다. 이 상태에서 H_2O가 해리되면 더 낮은 에너지를 가지게 되는데, 해리되는 과정에서 에너지 장벽이 있음을 확인하였다.

Dp-117 **멀티스케일(Multiscale) 방법을 이용한 탄소나노튜브의 전자구조에 대한 연구** 박 찬현, 공 기정, 장 현주, 박 종연[1], 임 세영[1](*한국화학연구원. [1]KAIST.*) 탄소나노튜브(CNT)등을 나노디바이스에 이용하기 위해서는 탄소나노튜브의 형태에 따라 전자구조를 알아보는 것이 중요하다. 제일원리계산은 이러한 전자구조를 알아보는데 많이 사용된다. 하지만 제일원리계산은 다룰 수 있는 원자 수에 제한이 있다. 그래서 우리는 멀티스케일(Multiscale) 방법을 이용하여 큰 크기의 탄소나노튜브를 계산하였다. 우리가 연구한 모델은 (10, 0) 단일벽 탄소나노튜브(SWNT)로써 1200개의 C(Carbon) 원자로 이루어져 있고 약 129.05Å의 길이를 가진다. 연구 결과 멀티스케일방법에 포함된 양자 현상의 기술에 의해서, 결함 있는 탄소나노튜브에 나타나는 오각형 구조등을 볼 수 있어, 더 정확한 구조를 구할 수 있음을 확인하였다. 하지만 상태밀도(DOS : density of states)를 보면 페르미 에너지(Fermi energy)에 에너지 상태들이 몰려있고 띠틈(band gap)이 더 커 보인다. 이는 양자 현상을 기술을 위해 클러스터(cluster)를 이루면서 가장자리의 C 원자에 나타나는 현상이 중심까지 영향을 주기 때문이다. 그래서 클러스터 크기를 변화시키면서 상태밀도를 서로 비교하여 보았다. 그 결과, 같은 평면에 있는 탄소나노튜브 10개의 원자를 한 층으로 보았을 때, 10층 이상이 되어야 중심에서 에너지 상태들이 몰려있는 현상이 거의 나타나지 않고 띠틈이 비슷해짐을 확인하였다.

Dp-118 **Monte Calro Study of Orientational Ordering of Electric Quadrupoles in FCC Structure** SHIN H. D., LEE S. H., KWON Y.(*Konkuk University, Department of Physics.*) Due to requirements on the symmetry of the wave function, hydrogen molecule has two species: para-H_2 and ortho-H_2. One of interesting features of this molecular solid is that ortho-hydrogen experiences the orientational order-disorder phase transition to the Pa3 structure even at zero pressure, as the temperature lowers. This orientational ordering is due to the anisotropic interaction between ortho-hydrogen molecules, most of which can be explained by an electric quadrupole-quadrupole interaction. In order to study this phenomenon, we have performed Monte Carlo simulations on a system of electric quadrupoles localized at FCC lattice sites and found the orientationally-ordered structure at low temperatures.

Dp-119 **First-Principles Investigation of Extended Line Defects in $SrTiO_3$** KIM Jiyeon, JIN Hosub, YU Jaejun(*Department of Physics and Astronomy and CSCMR, Seoul National University. Seoul, 151-747, Korea.*) Recently an extended O-vacancy defect in $SrTiO_3$ (STO) single crystal has been suggested to be responsible for the resistance switching behavior in STO-based devices [1]. As a step toward understanding the electronic and structural properties of extended defects in STO, we carried out first-principles electronic structure calculations for the several line defect configurations in $SrTiO_3$. Since the oxygen vacancy may provide an excess charge at the Ti-site leading to the significant d-orbital occupation, we employed the LDA+U method as implemented in the OpenMX code. To model the line defects in STO, we consider the configurations with the lines of O-Sr-O, Sr-O, and O atoms removed from bulk $SrTiO_3$. From the results, it is found that the defect states induced by each line of vacancies are closely related to both the bonding characters and the local environments of the removed atoms. While the O vacancies induce an impurity band consisting of the Ti d e_g-character, the Sr-O vacancies seem to bring in a mid-gap state derived from the O p valence band. Further the electronic ground states are found to vary from insulator to metal, depending on the types of line defects, e.g., O-Sr-O, Sr-O, and O vacancies.
[1] K. Szot et al., Nature materials 5, 312 (2006).

Dp-120 **Adsorption Pt atom on defective carbon nanotube walls: Density functional approach** PARK YONGJIN, LAHAYE ROB, KIM SUNGJIN, LEE YOUNGHEE(*CNNC, Dept. of Physics, Sungkyunkwan University.*) The choice of supporting electrodes for the Pt catalyst is important to the performance of fuel cells. Pure CNTs have shown to produce low loading amounts of Pt catalyst particles, to the weak adsorption of Pt on CNT walls. However, defective CNT surfaces seem to be more promising. In present work we have applied density functional theory for studying the adsorption of a single Pt atom on defective single-walled carbon nanotubes (SWCNTs), for both semiconducting and metallic SWCNTs. Stable adsorption site, bonding distance, binding energy, and electronic structure are analyzed by comparing Pt adsorption property differences between pure, Stone-Wales, and vacancy SWCNTs. On pure SWCNTs, the Pt binding energy is about 2.5 eV and 2.7 eV for (5,5) metallic and (8,0) semiconducting nanotubes, respectively. On vacancy sites, the binding energies become about 6.6 eV and 6.4 eV, respectively. In general the Pt binding energy on defective SWCNTs

is always larger than on pure SWCNTs and for vacancy SWCNTs the binding energy is largest.

Dp-121 **Mechanism of transition metal-H_2 binding** 이 훈경, 임 지순(*서울대학교 물리천문학부.*) We show mechanism of transition metal atoms (i.e., Ti)-H_2 molecules binding using first-principles electronic structure calculations based on the density functional theory. A single Ti atom attached to cis-polyacetylene (PA) adsorbs up to five H_2 molecules with the binding energy of 0.46 eV/H_2. The origin of binding between Ti and H_2's is derived from hybridization between the unoccupied d orbitals of Ti atom and the σ orbitals of H_2's (donation) or the occupied d orbitals of Ti atom and the σ* orbitals of H_2's (backdonation) which is explained by Kubas model. We observe that the hybridization is the respective e_g and t_{2g} orbitals of the Ti atom with the respective σ and σ* orbitals of the H_2"s in octahedral coordination. We also present orbital anaylsis for other metal-decorated structures in terms of hybridization between the d orbitals and σ and σ* orbitals

Dp-122 **Local Moment Approach to the Anderson Impurity Model with Spin-Dependent Hybridization** KIM Choong H., YU Jaejun(*Department of Physics and Astronomy and CSCMR, Seoul National University, Seoul, Korea.*) We report an extended local moment approach (LMA) method for the solution of the Anderson impurity model with spin-dependent hybridization, which may serve as a prototype of the quantum dot coupled to magnetically polarized leads. The two self-energy description, originally proposed by Logan and collaborators, is extended for the case with spin-dependent hybridization, where the generalized version of the symmetry restoration condition is required. The self-consistent ground state is determined through the variational minimization of the ground state energy with respect to several self-consistent solutions. Our method of the spin-dependent local moment approach is applied to a quantum dot system coupled to ferromagnetic leads. The qualitative feature of results arefound to be in good agreement with the numerical renormalization group method. The finite splitting of Kondo peaks is found for the case of the asymmetric Anderson model.

Dp-123 **First principle study of defect formation energy and migration energy in NiO** JEON Sang Ho, PARK Bae Ho, PARK So Hee[1], LEE Bora[1], HAN seungwu[1](*Department of Physics, Konkuk University. [1]Department of Physics, Ewha Womans University.*) Reversible resistance switching phenomena in transition metal oxide such as NiO, TiO_2, and $SrTiO_3$, have attracted considerable interest owing to a potential application for the Resistance Random Access Memory (ReRAM) device. Despite of many studies, the microscopic origin of reversible resistance-switching is yet to be revealed. Several phenomenological models have been proposed, but they cannot demonstrate the microscopic origin of resistance-switching sufficiently. the results of experimental about NiO, binary oxide material, showed that the phenomena of switching in NiO could explain as forming conductive path at grain boundary. Recently, the oxidation owing to migration of oxygen ions as electric field bias at interface between metal and oxide material is proposed as switching modeling. In this presentation, we report a first-principle study on NiO in the presence of the oxygen vacancy. We find that defect formation energy is changed as the position of oxygen vacancies near surface and that defect migration energy at surface is lowered than the value in bulk.

Dp-124 **First-principles Investigation of Interfacial Electronic Structure and Conductance of Fe/MgO/Fe Tunneling Junction** KIM Nam Wook, OZAKI Taisuke[1], KINO Hiori[2], YU Jaejun(*Department of Physics and Astronomy, Seoul National University, Seoul, Korea. [1]National Institute for Advanced Industrial Science and Technology, Tsukuba, Japan. [2]National Institute for Materials Science, Tsukuba, Japan.*) As the dimension of electronic devices shrinks to the nanometer scale, the interfaces between different parts of the device become critical in determination of the device performance. To understand physics at the device interfaces, it is desired to develop an accurate model for interfaces between metals, oxides and semiconductors, and thus to be able to calculate the effect of the different interfaces. As an application of our non-equilibrium Green's function (NEGF) implemented in density functional theory (DFT) methods, we carried out quantum transport calculations for the MgO layers coupled to Fe electrodes. Our calculation results are compared with the recent work [1], where the electronic states at the Fe-MgO interface were identified to be responsible for tunneling magneto-resistance behaviors in Fe/MgO/Fe junctions. It is hoped that our approach to

the interface physics will give a new insight into the physical mechanism of quantum transport in nano-scale devices.

[1] W.H. Butler, X.-G. Zhang, T.C. Schulthess, and J.M. MacLaren, Phys. Rev. B 63, 054416 (2001)

Dp-125 **Superfluidity of Small Hydrogen Clusters Doped by a Single Deuterium Molecule** 권 용경, 추 정민(*건국대학교, 물리학과.*) Path-integral Monte Carlo calculations have been performed to study superfluid behaviour of small para-H_2 clusters doped by a single impurity molecule of ortho-D_2 at low temperatures. It is found that the heavier D_2 molecule is located around the geometric center of the cluster with negligible thermal effects on its density distribution below 2 K, where a cluster with less than 20 H_2 molecules are shown to be in superfluid state. In addition, we have found that around the onset temperature (~2.5 K) of superfluidity of H_2 clusters the presence of D_2 significantly reduces the hydrogen superfluidity since the exchange propensity among H_2 molecules is suppressed near the impurity. However, the addition of D_2 has little effect at lower temperatures where hydrogen superfluidity is almost complete.

Dp-126 **Bond Operator Approach to the Doped Mott Insulator on Shastry-Sutherland Lattice** PARK Kwon, YANG Bohm-Jung[1], KIM Yong Baek[2], YU Jaejun[1] (*School of Physics, Korea Institute for Advanced Study,. [1]School of Physics and Astronomy and Center for Strongly. [2]Department of Physics, University of Toronto, Toronto.*) The Shastry-Sutherland lattice is a two-dimensional frustrated spin system which has a valence-bond solid ground state with a spin gap. To describe the physical properties of the system, the nature of the dimerized singlet state should be carefully considered. In this context a bond operator formalism is a promising way to describe the correct physical characteristics of the system. We describe the doped Mott insulator on the Shastry-Sutherland lattice via t-J-V model. When the inter-site Coulomb repulsion is smaller than the critical value, there is always finite density of holon which prevents the emergence of D-wave superconductivity. However, under the inter-site Coulomb repulsion larger than the critical value, the holon density goes to zero at finite doping and we can observe the emergence of D-wave superconductivity which shows an interesting real space pattern.

Dp-127 **Ellipsometric study of the poling effect on nonlinear-optical side-chain polymers containing disperse red 1** 이 호석, 강 태동, 이 호선, 이 상규[1], 김 주희[1], 최 동훈[1](*경희대학교 물리학과. [1]고려대학교 화학과.*) We measured the complex refractive index of corona-poled nonlinear-optical polymers grown on glasses using spectroscopic ellipsometry at room temperature at various angle of incidences. We attached nonlinear-optical (NLO) active dye and photo-crosslinkable moieties as side chains of poly(4-hydroxystyrene), deposited the polymer thin films on glass substrates by spin-coating, and corona-poled it along the surface-normal direction to align dipole moments of the chromophores along the electric field direction. In detail, PSDR1-25 designates a poly(4-hydroxystyrene) where 25% of side chain is substituted by disperse red 1 (DR1), and PSDR1-50 means the same except for 50% substitution. PSDR1 has the NLO property, which is expected to show ascentric ordering by poling electric field. We observed the absorption spectral change using UV-Vis spectroscopy before and after corona poling. We used parametric optical constant model to estimate the complex refractive index of the polymers. We found that the poling induced the uniaxial property of the complex refractive index of the polymers by aligning the chromophores along the poling direction. With increased poling voltage, we found that the oscillator strength of the major peak near 2.4 eV (designated as E_a) peak decreases in the surface-parallel direction (x), whereas that of the surface-normal direction (z) increases. Moreover, detailed analysis of the dielectric functions using standard critical point model showed that the poling induced a new peak E_c (~2.6 eV) between dominant E_a (~2.3 eV) and weak E_b (~2.9 eV) peaks for PSDR1-50 polymers. With increased poling voltage, the E_c peak strength increased compared to those of E_a and E_b peak.

Dp-128 **X-ray reflectivity study of thermal capillary waves on propanol-water mixture** JEON Yoonnam, SUNG Jaeho, KIM Doseok, VAKNIN David[1], BU Wei[1] (*Sogang University, Department of Physics and Interdisciplinary Program of Integrated Biotechnology. [1]Iowa State University, Ames laboratory and Department of Physics and Astronomy.*) Surfaces of propanol-water mixtures at different concentrations were studied by surface tension measurement and X-ray reflectivity. As more propanol is added to the mixture, the reflectivity dropped more rapidly with

the increase in the incidence angle, indicating the surface became rougher with more propanol in the mixture. The roughness of the surface deduced from the reflectivity measurement along with the roughness of the upper wavelength cutoff determined from the average size of the molecule (~1.9 A for pure water and ~2.7 A for pure propanol) allowed unambiguous determination of the intrinsic roughness of the surface at different concentrations.

Dp-129 **Charge Inversion at the Surface by Adsorption of Trivalent Cations on Langmuir Monolayer** SEOK Sangjun, KIM Doseok(*Department of Physics and Interdisciplinary Program of Integrated Biotechnology, Sogang University.*) IR-visible sum-frequency generation (SFG) spectroscopy was used to study cation adsorption and charge inversion behavior at the water/lipid interface of dimyristoylphosphatidic acid (DMPA) monolayer. At low subphase salt ($LaCl_3$) concentrations, the sum-frequency signal from interfacial water molecules decreased as the negative charges at the headgroup of DMPA are compensated by the cations. It is because the cations from the solution adsorbed more to the surface molecules, reducing the surface charge-density of the monolayer. At around ~10 μM of bulk $LaCl_3$ concentration the SFG signal was at the minimum, suggesting the charge neutrality at this specific salt concentration. With the further increase in the salt concentration, small amount of SFG signal from the interfacial water molecules showed up again. This phenomenon was explained by the overcompensation of the surface charges by trivalent cations causing the inversion of surface charges, which caused the alignment of interfacial water molecules at high salt concentration.

Dp-130 **Dye-induced alignment of liquid crystals detected by fluorescence enhancement** SHIM Taekyu, KIM Doseok, OH-E Masahito[1](*Department of Physics and Interdisciplinary Program of Integrated Biotechnology, Sogang University. [1]Yokoyama Nano-structured Liquid Crystal Project, ERATO, and Liquid Crystal Nano-system, SORST.*) Fluorescence from the hemicyanine dye molecules doped in liquid crystal (4,4'-n-pentylcyanobiphenyl, 5CB) was investigated at various temperatures. Fluorescence lifetime decreased monotonically with the increase of temperature irrespective of the thermodynamic phase of the host medium, and was explained in terms of increased nonradiative decay of the excited dye molecules due to the increased mobility of the host medium. However, fluorescence intensity from the dyes in nematic liquid-crystalline phase was ~3 times larger than that in crystalline or liquid phase. This fluorescence enhancement was found to be from the anisotropic alignment of dye molecules along the polarization direction of excitation beam, which was caused by the alignment of host liquid crystal molecules enhanced by the guest dyes preferentially excited along the polarization direction. Order parameter of the dyes in liquid crystalline phase deduced from fluorescence anisotropy with polarized-beam excitation was ~0.33.

Dp-131 **Control Microtubule Growth inside Vesicles** PARK HYUNJOO, KIM MAHNWON(*KAIST.*) Microtubule inside ~10 μm cell-sized vesicles is a major component which determines shape of living cell. We observed quasistatic deformation of lipid vesicles from within, due to the polymerization of confined microtubulesa. A pair of long, narrow membrane sleeves appears, sheathing the microtubule ends as they grow. Spontaneous buckling reveals that the force generated can be several pN. The evolution of shape and magnitude of force are consistent with a simple theory for the membrane free energy. We try to study effects of various ligands (GMPCPP, taxol and MAP) which alter mechanical properties for biological relevant circumstances.

Dp-132 **Effect of Charged Amphiphiles on Structural Properties of C12E5 Nonionic Cylindrical Micelles in Aqueous Solution** KIM Sanghyun(*KAIST.*) Reversible self-assembly of surfactant monomers into cylindrical micelles shows the micellar growth and branch formation with increasing surfactant concentration or temperature. Those phenomena depend on the conformational defect energies of cylindrical micelle. In this study, we have studied the nonionic cylindrical micellar solutions(Penta-ethyleneglycol mono n-dodecyl ether, $C_{12}E_5$) in dilute region using small angle neutron scattering as a small amount(1~7mol%) of the cationic surfactant (Dodecyltrimethylammonium Bromide, DTAB) is added and the temperature is changed. Unlike the neutral lipid as an added amphiphiles, when the cationic surfactant is added to cylindrical micellar solution the tendency of micellar growth and rheology properties is complicate. At the doping level of 6 mol% or more, a rigid cylindrical micelle forms and the cylindrical local structure of the doped micelles shows no variation ac-

cording to the whole doping level covered in this study (0 mol% » 10 mol%).

Dp-133 **Size Relations and the Driving Factor in Coalescence** WEON Byung Mook, JE Jung Ho, HWU Yeukuang[1], MARGARITONDO Giorgio[2](*X-ray Imaging Center, Department of Materials Science and Engineering, Pohang University of Science and Technology, Pohang, Korea. [1]Institute of Physics, Academia Sinica, Nankang, Taipei 11529, Taiwan. [2]EPFL, CH-1015 Lausanne, Switzerland.*) We investigated the equation that links the sizes of bubbles or droplets in coalescence phenomena on the microscopic scale. Experimentally, we found a cubic relation for gas bubbles whereas for mercury droplets the relation is intermediate between cubic and quadratic. We could explain these results with a simple model that predicts a general form for the equation, whose limit is a cubic relation for ideal gas bubbles. The model also predicts that the ratio between the total energy change and the surface energy change only depends on the parameter that characterizes the pressure dependence on the density. The model could be used for other cases of coalescence and in general to clarify the links between size-related properties and the driving factor for these phenomena.

Dp-134 **Energy Dissipation Dynamics During Jamming of Granular Media** WEON Byung Mook, JE Jung Ho, POURNIN Lionel[1], RAMAIOLI Marco[1], LIEBLING Thomas M.[1](*X-ray Imaging Center, Department of Materials Science and Engineering, Pohang University of Science and Technology, Pohang, Korea. [1]Mathematics Institute, EPFL, CH-1015 Lausanne, Switzerland.*) Jamming is an immobile state that emerges from mobile systems as a consequence of energy dissipation. We here focus on the transition frominitially fluid to completely jammed states in granular media. The energetic behavior of such transition is monitored using numericalexperiments carried out with the Distinct Element Method. From simulations, we find three regimes in energy dissipation dynamics: i)accelerated, ii) decelerated, and iii) jammed regimes. We present a physical model to compute the transition times between the regimes. Themodel is well in agreement with the simulated experiments.

Dp-135 **Surface Waves at an Air-Water Interface Covered by Charged Lipids Adsorbed by Polyelectrolytes** YUN Sungyoung, KIM Mahn Won(*KAIST, 물리학과.*) We have measured complex surface wave frequency using thermally excited surface wave spectroscopy at an air-water interface. The interface is covered by positively charged lipids (dioleoyl trimethylammonium propane chloride-DOTAP) adsorbed by poly-anions(Poly Styrene Sulfonic Acid,Sodium Salt) with different chain length and monomer. From the data, we obtain informations about comprssibility and dilational and shear surface viscosities.

Dp-136 **On the Shape-Change of the Complex of Cationic Micelles and Anionic Polyelectrolytes** MOON Jun Hyuk, SHIBAYAMA Mitsuhiro[1], KIM Mahn Won (*Department of Physics, KAIST. [1]Neutron Science Labortory, Institute for Solid State Physics, The University of Tokyo.*) We investigated the complex of cationic micelles with anionic polyelectrolytes. The cationic micelles were consisted of C14E8 (Octa-ethyleneglycol mono n-tetradecyl ether) and TTAB(Tetradecyltrimethylammonium Bromide), the molar ratio of which is 8:2. This micelle is spherical (radius=38A) and has effective charges +15e. And, NaPSS 80k (Poly Styrene Sulfonic Acid, Sodium Salt; Mw=73,900, Mn=60,000) was used as the anionic polyelectrolyte. SANS (Small Angle Neutron Scattering) results showed that the change of the shape of complex was induced by polyelectrolyte. As the concentration of NaPSS 80k increased, the maximum length of complexes became smaller. And the complexes became the spherical shape from necklace-like shape. This shape-change supported the simulation result which showed that the more the salt concentration the smaller the attraction between particles due to the polyelectrolytes is [J. Dzubiella et al. Macromolecules 36, 1741 (2003)]. And SANS experiments using the deuterated NaPSS80k supplied that the hydrophobic backbone of NaPSS80k penetrated the core of micelles. So, the stiffness and the hydrophobicity of polyelectrolytes play an important role in the clustering of complexes

Dp-137 **Effect of surfactants on shrinkage of an optically trapped oil droplet in de-ionized water** 박 창영(*한국과학기술원 물리학과.*) 일반적으로 활성계면제들은 물 속의 오일이나 오일 속의 물을 안정화시키고 각각의 닫힌 시스템을 만든다고 알려져 있다. 일반적으로 모든 오일들은 물에 대한 solubility가 있어 시간에 대한

오일 방울들의 크기 변화가 일정한 갑으로 나오는데 활성계면제들에 의해 오일 방울이 물에 녹아들어가는 속도가 어떻게 변하는지 연구해보았다. 오일 방울의 크기 및 물 속의 오일 분자들의 오일 방울 사이의 영향을 없애기 위해서 광학 집계를 사용하여 물 속에 오직 하나의 오일이 들어있는 시스템을 만들었으며 활성계면제가 녹아있는 물을 흘려주면서 이 오일 크기의 변화를 관찰하였다.

Dp-138 **The measurement of electrical resistance during the elongating of a multi walled carbon nanotube** JANG Hoon-Sik, LEE YUN-HEE, BAEK UN-BONG, PARK JONG-SEO, NAHM SEUNG-HOON(*한국표준과학연구원, 안전그룹.*) The response of multi walled carbon nanotubes (MWCNTs) to mechanical strain, applied using a tungsten tip via a nano-manipulator controlled by a personal computer, was investigated inside a scanning electron microscope. The contact resistance between a MWCNT and the tungsten tip decreased during exposure to the electron beam. The electrical resistance was significantly changed until fracture occurred. When the nanotube was fully elongated, the value of resistance increased to ~1.34 times as the initial value was measured. In the beginning of fracture, the resistance increased abruptly. As the nanotube was further fractured, the electrical resistance was finally measured to be infinite.

Dp-139 **Electron transport in small bundles of carbon nanotubes: intertube interaction and effects of the electric field** KIM Gunn, KIM Taekyung[1], ZUO Zin-Min[1], BUONGIORNONARDELLI Marco[2], BERNHOLC Jerzy[2](*Department of Physics, Sungkyunkwan University. [1]Department of Materials Science and Engineering, UIUC, IL, USA. [2]Department of Physics, North Carolina State University, Raleigh, NC, USA.*) In small bundles of carbon nanotubes, an external electric field can effectively tune the electronic behaviorof the system. Semiconducting tubes can be switched to metallic or semimetallicdepending upon the direction of the field in a field-effect transistor (FET).This is demonstrated experimentally using a FET which allows precise structure determinationof tube bundles by electron diffraction. Ab initio simulation shows that the screening of the electric field breaksthe cylindrical symmetry of the bundles and changes their band structure in agreement with experiments.These results prove the importance of intertube interaction in electrical transport of bundled nanotubesin external electric fields.

Dp-140 **Single-electron transport observed in ZnMgO/ZnO coaxial nanorod heterostructure** JEONG Dongchan, KI Dongkeun, BAE Myung-ho[1], LEE Chul-ho[2], YOO Jinkyung[2], YI Gyu-Chul[2], LEE Hu-Jong(*Department of Physics, Pohang University of Science and Technology. [1]Department of Physics, University of Illinois at Urbana-Champaign. [2]National CRI Center for Semiconductor Nanorods and Department of Materials Science and Engineering, Pohang University of Science and Technology.*) We report on the fabrication and the electrical characterization of ZnO/ZnMgO coaxial nanorod heterostructure at 50 mK. A few 40-nm-radius nanorods were deposited on the oxidized Si substrate and Ti/Au electrodes were prepared on the nanorods by employing the conventional single-layer e-beam lithography technique. The contact resistances were 300 and 70 kΩ at room temperature for two samples with the inter-electrode distances of 217 and 266 nm, respectively. An attempt was made to measure the Altshuer-Aronov-Spivak (AAS) oscillation in a cylindrical shell of electron gas formed at the interface of ZnO and ZnMgO layers. A Coulomb-blockade behavior was observed, instead, in these samples. The overall shape of Coulomb diamonds, however, did not match the single quantum-dot one and the size of Coulomb diamonds varied with changing the gate voltage. This nonuniformity in the size of Coulomb diamonds indicates the formation of multi-dots in the most range of the gate voltages. The mechanism of the multi-dot formation and the observation condition of the AAS oscillation in this system will be discussed.

Dp-142 **Atomic Trapping By Decoherence** YI Sangyong, KIM Sang Wook(*부산대학교 물리학과.*) We present a scheme for trapping two level atoms induced by decoherence in a ring interferometer. If the decoherence takes place in the ring, two partial waves in the ring no longer interfere with each other. In such a case we found that the sum of both the transmission and the reflection probability becomes less than unity so that part of the atoms are trapped in the ring.

Dp-143 **The Quantization of Current Induced by Surface Acoustic Wave Through a Quantum Point Contact** 김 남, 우 병칠, 김 진희, 서 민기[1], 정 윤철[1](*한국표준과학연구소. [1]부산대학교 물리학과.*) The acousto-electric current through a quantum point contact induced by

surface acoustic waves was observed. It has been found that the current is quantized at integer multiples of ef, where f is the frequency of surface wave. By using the interdigitated transducer with 500nm spacing between the gates, we produced the surface acoustic waves at 2.456GHz. The results in 1.18nA of quantized current when 3 electrons are transferring from source to drain at a time. Also, it has been found that the quantization is related with a presence of a static quantum dot unintentionally formed in a quantum point contact.

Dp-144 **Electron Transport Induced by Moving Array of Two Dimensional Potential Wells Using Acousto-Electric Effects** 김 남, 서 민기[1], 김 하나[1], 정 윤철[1](*한국표준과학연구원. [1]부산대학교 물리학과.*) Surface acoustic wave(SAW) induced current devices have used so far quasi 1D channels made of either GaAs/AlGaAs hetero-structures or carbon nanotubes. We propose new type of SAW-induced current device using the so called 'moving quantum dots'. We suggest that moving quantum dots or moving array of potential wells could be formed on the GaAs/AlGaAs hetero-structrues by combining the piezo-electric effects and the superposition principle of two independent but phase-correlated SAW's whose directions are perpendicular each other.

Dp-145 **Interference in a Two-Level Quantum Dot with a Bridge Channel** 이 우람, 김 재욱, 심 흥선(*한국과학기술원 물리학과.*) We investigate Fano interference in a two-level quantum dot with a bridge channel directly connecting two reservoirs, for both cases of non-interacting and interacting electrons. For the non-interacting case, we find that the Fano line shape strongly depends on the relative signs of the left and right couplings of each level. It is because in the (+-) symmetry, there is no inter-level correlation, whereas in the (++) symmetry, there is strong inter-level correlation. We also discuss the modification of the Fano line shape due to the Coulomb interaction between the two levels in a Hartree-Fock approach.

Dp-146 **Electronic Structure of Graphene in Spatially Nonuniform Magnetic Fields** 박 성훈, 심 흥선(*한국과학기술원, 물리학과.*) We investigate energy spectrum of graphene sheet in the presence of an electrostatic step-like potential and a perpendicular spatially nonuniform magnetic fields. By solving the Dirac equation that describes low energy properties of graphene, we obtain energy levels of massless Dirac particles for different nonuniform spatial distributions of magnetic fields. We compare the energy spectrums with those of conventional two-dimentional electrons. We also discuss edge channels propagating in a spatially nonuniform magnetic field region, based on the Landauer-Büttiker formalism

Dp-147 **Coherent Lattice Vibrations in Various Micelle-Suspended Carbon Nanotubes** LIM Yong-Sik, AHN Jae-Geum[1], KIM Ji-Hee[2], YEE Ki-Ju[2], E. H. Haros[3], J. Shaver[3], J. Kono[3], R. H. Hauge[3], R. E. Smalley[3](*Konkuk Univ; Rice Univ. [1]Konkuk Univ. [2]Chunnam Univ. [3]Rice Univ.*) We have generated and detected coherent lattice vibrations in single-walled carbon nanotubes corresponding to the radial-breathing mode (RBM) using ultrashort laser pulses. Because the band gap is a function of diameter, these RBM-induced diameter oscillations cause ultrafast band gap oscillations thereby modulating the interband excitonic resonances at the phonon frequencies (3-10 THz). Excitation spectra show a large number of pronounced peaks allowing the determination of the chiralities present in a particular samples and relative population differences of particular chiralities between samples.We also measured coherent lattice vibrations in single-wall carbon nanotubes prepared by different growth methods, such as CVD, CoMoCAT, HipCo, and compared the differences between them. The observed RBMs of CVD sample were found to have similar chiral distribution to HipCo sample, but CoMoCAT sample showed less chiral distribution with a distinct (9,1) chirality compare to other samples. Finally, when viewing the excitation profiles of several RBMs, we found a two-peak resonance, which we attribute to this technique acting as a modulation spectroscopy over the whole samples. We will also show the coherent lattice vibrations in miscelle-suspended double-walled carbon nanotubes.

Dp-148 **Raman scattering studies of CdS nanostructures** 이 경연, 노 희석, 최 영진[1], 최 경진[1], 박 재관[1](*전북대학교, 물리학과. [1]한국과학기술연구원, 나노재료연구센터.*) 펄스 레이저 증착 방법을 이용해 성장된 CdS 나노선, 나노벨트, 나노시트에 관한 라만 산란 연구를 보고한다. 나노선의 직경은 약 50 nm이다. 나노벨트와 나노시트의 너비는 각각 1 μm와 5 μm 정도이

며 두께는 나노선과 비슷하다. 각각의 앙상블 시료로부터 얻어진 라만 산란 결과는 크게 두 가지로 요약된다. 첫째는, 나노선-나노벨트-나노시트로 그 크기가 증가할수록 격자진동 에너지의 증가가 관측되었다. 이러한 결과는 격자수축과 연관이 있다. 둘째는, 나노선으로부터 얻어진 라만 산란 반응과는 달리 나노벨트와 나노시트로부터 얻어진 라만 산란 반응에서는 현격하게 증가된 부가적인 산란 반응이 나타났다. 그 세기가 증가된 라만 산란 반응은 다중격자진동과 연관이 있는 것으로 보이며 이는 나노벨트와 나노시트에서 나타나는 향상된 결정성이나 엑시톤-격자진동 상호작용 세기의 증가와 연관이 있는 것으로 보인다. 보다 심화된 연구를 위해 단일 나노선, 나노벨트, 나노시트로부터 라만 산란 반응을 얻었다. 나노구조 앙상블로부터 얻어진 라만 산란 반응과 비교했을 때 단일 나노구조로부터 얻어진 라만 산란 반응에서 보다 세부적인 다중격자진동에 관한 반응을 관측할 수 있었다.

*이 논문은 2006년 정부(교육인적자원부)의 재원으로 한국학술진흥재단의 지원을 받아 수행된 연구임(KRF-2006-005-J00302). 한국과학기술연구원에서의 연구는 기관고유사업(2E19440)의 지원을 받아 수행되었음.

Dp-149 **Electron Spin Resonance of Vanadium Oxide Nanorods** LEE Cheol Eui, PARK Jitae, LEE Eunmo, LEE Kyu Won[1](*Korea University, Department of Physics. [1]Korea University, Institute for Nano Science.*) Vanadium oxide-based low dimensional products have been widely studied. In this work, the vanadium oxide nanorods (VO_x–NRDs) obtained from V_2O_5 xerogel after hydrothermal treatment were investigated by various methods such as X-ray diffraction (XRD), Scanning Electron Microscopy (SEM), and Electron Spin Resonance (ESR) spectrometer. From the XRD data, it seems to be VO_2 phase is dominant in as grown VO_x–NRDs. Meanwhile, ESR spectra results show complex line shapes which fitted by three Lorentzian lines through wide range of temperatures (140 ~ 300 K). The three Lorentzian lines may indicate each of electronic structures of VO_x–NRDs.

Dp-150 **Polarized Raman Scattering Studies of $InGaP_2$ Structures** 노 희석, 민 경인, 이 경연, 임 정란[1], 이 주한[1], 송 진동[2], 최 원준[2], 김 종민[3], 이 용탁[3](*전북대학교, 물리학과. [1]한국기초과학지원연구원 전주센터, 유기나노소자연구팀. [2]한국과학기술연구원, 나노소자연구센터. [3]광주과학기술원, 정보통신공학과.*) 다양한 $InGaP_2$ 구조에 대한 라만 산란 반응에 관한 연구 결과를 보고한다. 모든 시료는 분자선 켜쌓기 방법을 이용하여 InP 층과 GaP 층을 교대로 성장함으로써 얻어졌다. 특정 성장 온도 및 층 두께에 따라 성장 방향에 수직한 방향으로 In이 많은 InGaP, Ga이 많은 InGaP 띠가 교대로 나타나는 측면방향으로의 성분변조가 관측되었다. 이러한 시료에서는 측면 성분변조와 CuPt-유형의 정렬이 공존하는 것으로 보인다. 측면 성분변조가 형성된 시료에서는 띠 방향으로 매우 강하게 편광 된 발광 반응이 관측된다. CuPt-유형의 정렬의 형성 유무와 상관없이 측면 성분변조가 형성되지 않은 시료에서는 발광 반응의 편광성이 관측되지 않는다. 측면 성분변조가 형성된 시료와 형성되지 않은 시료로부터 편광 라만 산란 반응을 얻음으로써 측면 성분변조에 따른 라만 산란 대칭성을 연구한다. 성장 온도 및 성장 층 두께 변화에 따른 측면 성분변조의 형성과 연관된 시료의 결정 구조의 대칭성에 관한 연구 결과를 보고한다.

*이 논문은 2006년 정부(교육인적자원부)의 재원으로 한국학술진흥재단의 지원을 받아 수행된 연구임(KRF-2006-312-C00183).

Dp-151 **Field Emission Characteristics of Point Emitters Fabricated by Multi-Walled Carbon Nanotube Yarn** JUNG SEUNG IL, SHIN DONG HOON[1], KIM KWANG SUB[2], LEE CHEOL JIN[1](*Department of Nanotechnology, Hanyang University. [1]School of Electrical Engineering, Korea University. [2]Program in Micro/Nano Systems, Korea University.*) We fabricated point-emitters of multi-walled carbon nanotube(MWCNT) yarn made by a thermal CVD and demonstrated their field emission properties. The long MWCNT yarn was made out of the super-aligned array of very long MWCNTs using a simple spinning thechnique. The field emitter was fabricated by cutting the long MWCNT yarn into a small segment and attaching it on a sharp metal tip. The gap between the anode and the MWCNT yarn was about 1 mm, 1.5 mm. The field conversion factor of the MWCNT yarn point-emitter was inversely proportional to the gap. The maximum field emission current density, which can be extracted just before the destruction of MWCNT yarn emitter, was about 75 A/cm^2 for the MWCNT yarn emitter. The emission properties of the MWCNT yarn emitter were changed during the initial subsequent voltage sweeps, and this change of emission properties can be explained by the effect of the adsorption and desorption of adsorbates on the MWCNT yarn.

Dp-152 **일차원 나노전기역학계에서의 자기폴**

라리톤 김 경중, 안 강헌(*충남대학교 물리학과.*) 일정한 두께를 갖는 1차원 구조의 전도체가 자기장 속에 놓여 있을 때의 전기전도를 이론적으로 연구하였다. 전류와 도체의 역학적 움직임을 모두 양자역학적으로 기술하였으며 전자의 상호작용은 루틴저 액체 모델을 이용하여 기술하였다. 탄소나노튜브와 실리콘 빔 과 같은 두께가 있는 실제 일차원 구조가 본연구의 대상이다. 기존의 이상적으로 가는 일차원 도체의 경우를 연구했던 결과(Ahn and Yi, Europhys. Lett. 67, 641 (2004)) 와 마찬가지로 되먹임 작용으로 두 개의 보오존 모드 중의 하나가 들뜸 간격이 생긴다. 이 간격은 $\omega_B=(v_F e^2 / 2\rho h)^{1/2}$ B으로 나타나고 여기서 B는 자기장, 는 도체의 선형 질량 밀도이다. 일정한 두께가 있는 경우에는 두 보오존 모드의 분산 관계에서 교차점이 발생하여 자기 폴라리톤이 생성됨을 보였다. 이때 교차점에서의 파수는 $q_c \sim v_F(\rho/EI)^{1/2}$으로 나타난다. 여기서 E는 영률이며 I 는 면적관성모멘트 이다.

Dp-153 **Fabrication of n-type carbon nanotube transistor by the in-situ controlled Al decoration technique.** 김 효숙, 김 병계, 김 주진, 이 정오[1](*전북대학교 물리학과. [1]한국화학연구원.*) We have fabricated n-type carbon nanotube field effect transistors by the "in-situ" controlled Al decoration technique. Three different device configurations were used for Al decoration; contact-shielded, channel shielded, and open devices. All three types of devices turned into n-type transistors after decoration, and goes back to p-type transistor again in ambient atmosphere.While channel-shielded devices show improved p-type characteristics in air, contact shielded devices show decreased conductance and negative shift of gate threshold voltages. In case of open device or contact-shielded devices, doping control was possible by controlling the amount of Al particles

Dp-154 **CCD detector based x-ray reflectivity measurement** AHN Kangwoo, KIM Sangsoo, KIM Soonam, NOH Doyoung(*GIST, Meterial science & Technology.*) X-ray diffraction (XRD) techniques are widely used to characterize nano-scale materials. One-dimensional point detectors, typically used in the conventional XRD, provide a reasonable angular resolution, but limited in measuring extended area in reciprocal space with high resolution. As an alternative method, we employed a two-dimensional charge-coupled device (CCD) detector having better angular and temporal resolution than a point detector. In order to verify the performance of CCD, we investigated the structural properties of Ta nano-trenchs on Si(100) substrate as a model system in low angle reflectivity geometry. We will present the simulation and experimental results obtained by the CCD, which will be compared to those of the point detector.

Dp-155 **Synthesis of Thin Multiwalled Carbon Nanotubes using Fe-Mo/MgO Catalyst Produced by a Gel-Combustion Method** CHOI SANG KYU, PARK SANG MIN[1], CHOI JI HOON[1], LEE CHEOL JIN[1] (*Department of Nanotechnology, Hanyang University. [1]School of Electrical Engineering, Korea University.*) We have studied synthesis of thin multiwalled carbon nanotubes (t-MWCNTs) using catalytic chemical vapor deposition (CCVD) method. To synthesize the t-MWCNTs, we used methane carbon source and Fe-Mo/MgO catalyst which produced by gel-combustion method. Gel-combustion method have many advantages to get an uniform distribution of metal particle sizes over the support material. In this work, the gelation process is a main role to realize t-MWCNTs with an uniform diameter. TEM analysis shows that high quality t-MWCNTs have a narrow diameter range of 6-7nm and graphene layers about 5 numbers. The purity of as-grown t-MWCNTs was observed with about 70% by Thermogravimetric analysis and Raman spectroscopy analysis showed the I_G/I_D of 6.92.

Dp-156 **Field Emission Properties of Carbon Nanotube Point Emitters** SHIN DONG HOON, JUNG SEUNG IL[1], KIM KWANG SUB[2], LEE CHEOL JIN(*School of Electrical Engineering, Korea University. [1]Department of Nanotechnology, Hanyang University. [2]Program in Micro/Nano Systems, Korea University.*) We fabricated probe type carbon nanotube (CNT) point emitters by attaching single-walled CNTs (SWCNTs) and double-walled CNTs (DWCNTs) onto the tip of atomic force microscope probe using a dielectrophoresis method. High purity SWCNTs and DWCNTs were synthesized by a hydrogen arc discharge method in a stainless steel chamber. The field emission current from SWCNT point emitter was 4.9 uA at 750 V, which is corresponding to the emission current density of at least 1.2×10^3 A/cm^2. Emission current of 1.7 uA was achieved from DWCNT point emitter at 1050 V. The Fowler-Nordheim plots showed that the SWCNT bundle consists of more individual CNTs than DWCNT bundle. We suggest that

the probe type CNT based point emitter can be used in the applications such as a microwave amplifier tube which requires a large emission current density.

Dp-157 **Beating of Aharonov-Bohm Oscillations in a Closed-loop Interferometer** JO Sanghyun, KHYM Gyong Luck[1], CHANG Dong-In, CHUNG Yunchul[2], LEE Hu-Jong, KANG Kicheon[1], MAHALU Diana[3], UMANSKY Vladimir[3](*Department of Physics, Pohang University of Science and Technology, Korea / National Center for Nanomaterials Technology, Korea. [1]Department of Physics and Institute for Condensed Matter Theory, Chonnam National University, Korea. [2]Department of Physics, Pusan National University, Korea. [3]Department of Condensed Matter Physics, Weizmann Institute of Science, Rehovot 76100, Israel.*) One of the issues with closed-loop-type interferometers is beating in the Aharonov-Bohm (AB) oscillations. Recent observations suggest the possibility that the beating results from the Berry-phase pickup by the conducting electrons in materials with the strong spin-orbit interaction (SOI). In this study, we also observed beats in the AB oscillations in a gate-defined closed-loop interferometer fabricated on a GaAs/AlGaAs two-dimensional electron-gas heterostructure. The beats showed noticeable characteristics that the h/2e period oscillation, imposed by Onsager relation, appeared only in the nodes of the beats and showed a parabolic distribution for varying voltages applied to one of the gates forming the interferometer. Since the GaAs/AlGaAs heterostructure has very small SOI the recently claimed Berry-phase-pickup mechanism of beats is ruled out. The often-cited multiple transverse sub-band effect is also ruled out because, unlike the case of mesa-defined interferometers, we tuned a single transverse sub-band in each arm of our gate-defined interferometer. We show all our observed results are well interpreted by the multiple-longitudinal-modes (MLM) effect in a single transverse sub-band mode, without resorting to the SOI effect. In addition, the Fourier spectrum of measured conductance, despite showing the magnetic-field-dependent multiple h/e peaks that are very similar to those from strong-SOI materials, can also be interpreted by the MLM effect.

Dp-158 **Study the Effect of Fuel Agents on the Fe-Mo/MgO Catalysts by Combustion Method for Synthesis of Thin MWCNTs** LUO TAO, CHEN LU YANG, CHOI SANG KYU[1], CHOI JI HOON, PARK SANG MIN, LEE CHEOL JIN(*School of Electrical Engineering, Korea University. [1]Department of Nanotechnology, Hanyang University.*) Thin multi-walled carbon nanotubes (t-MWCNTs) have been synthesized by catalytic decomposition of methane over Fe-Mo/MgO catalyst at 900℃. To fabricate the catalysts, we employed the combustion method, which has the advantage to form uniform distribution of catalytic nanoparticle over the support material. The effects of various fuel agents on the fabrication of Fe-Mo/MgO catalysts were studied, where hydrazine, glycine, and oxalic acid were used as fuel agents in the combustion method. Using hydrazine as fuel agent, we found that the molar ratio of hydrazine to metallic ion, gelation process, and the combustion atmosphere played important roles in the fabrication of high quality catalysts. Using glycine as fuel agents, we investigated the effect of pure glycine and glycine with a little amount of citric acid on the preparation of the catalysts. With regard to oxalic acid, it can be used as not only the fuel agent but also the coordinate agent with molybdate ion to avoid the precipitation $Fe_2(MoO_4)_3$, which is in favor of forming homogeneous catalyst. SEM observation showed that the as-synthesized t-MWCNTs had high quality and a narrow diameter distribution.

Dp-159 **Formation of Au nano-crystals on sapphire(0001) substrates by rapid thermal annealing** RYU Ki Hyeon, KANG Hyon Chol[1], LEE Sung Pyo, NOH Do Young(*Department of Materials Science and Engineering, Gwangju Institute of Science and Technology. [1]Advanced Photonics Research Institute, Gwangju Institute of Science and Technology.*) We report the formation of Au nano-crystals on sapphire(0001) substrates during thermal annealing. Au thin films with a thickness of 15nm were deposited on sapphire(0001) substrates by electron-beam evaporation, and then annealed in air at temperatures of 300℃, 700℃, and 800℃, respectively. Structural evolution was characterized using atomic force microscopy and X-ray diffraction measurements. Upon annealing, Au thin films transformed into Au nano-crystals. We observed a two-step transition process; generation and ripening (coarsening) of Au nano-crystals. In the initial stage, polygonal-shape holes, mostly triangle and hexagonal shapes, were nucleated in the films. Such holes then grew and contacted each other that resulted in the formation of Au nano-crystals having a well-defined flat-top surface with the <111> surface nor-

mal direction and the facets in the in-plane direction. Au nano-crystals became larger and thicker during the ripening process as the annealing proceeded further.

Dp-160 **Field Emission Properties of In Situ Potassium Doped SWCNT Synthesized Using Hydrogen Arc-Discharge** KIM KWANG SUB, HA BYEONG CHUL[1], SHIN DONG HOON[2], LEE CHEOL JIN[2] (*Program in Micro/Nano Systems, Korea University. [1]Department of Nano Science, Cheongju University. [2]School of Electrical Engineering, Korea University.*) In situ potassium(K)-doped single-walled carbon nanotubes (K-doped SWCNTs) were synthesized by hydrogen arc-discharge method. X-ray photoelectron spectroscopy analysis showed that the work function of K-doped SWCNTs is 3.99 eV which is less than that of the undoped SWCNTs (4.21 eV), and K-doped SWCNTs consist of 0.12 % K mass composition after purification that includes thermal oxidation and acid treatments. In their field emission properties, the K-doped SWCNTs indicated much lower turn-on electric field (2.0 V/mm at 10^{-9}A/cm^2) and higher emission current density (3.0 mA/cm^2 at 4.6 V/mm) than those of the undoped SWCNTs. These results are mainly caused by the lower work function and their electronic structure.

Dp-161 **DLC 박막의 열처리를 통한 탄소 Nanofiber 합성** 김 지영, 윤 지혜, 전 혜영, 김 미경, 박 홍준, 이 재열, 김 용(*동아대학교 물리학과.*) 촉매금속(Ni, Fe)이 이미 증착된 p-type Si(100) 웨이퍼에 RF-PECVD 법을 이용하여 DLC(Diamond-Like Carbon) 박막을 증착하였다. 이렇게 얻은 DLC/촉매금속/Si 샘플을 열 반응로에서 수소(H_2) 와 질소(N_2) 기체를 주입하면서 촉매의 종류와 두께, DLC Film두께에 따른 탄소 Nanofiber의 성장을 관찰 하였다. DLC는 RF-PECVD 장치에서 메탄(CH_4)기체를 사용하여 바이어스 -600V를 인가한 상태에서 증착하였다. 증착 시간을 달리 하여 DLC 박막의 두께에 변화를 주었다. 이렇게 얻은 DLC/Ni/Si 샘플과 DLC/Fe/Si 샘플을 이용하여 반응로에 장착하고 1000℃에서 열처리하여 탄소 Nanofiber를 성장시킨 후, FE-SEM을 이용하여 구조변화와 성장메커니즘에 대해 조사하였다.

Dp-162 **HFCVD 장치를 이용한 탄소 whisker 증착 및 특성** 김 미경, 심 성빈, 전 혜영, 김 지영, 박 홍준, 이 재열, 김 용(*동아대학교 물리학과.*) 다이아몬드 합성 시 사용되는 HFCVD 장치를 이용하여 다이아몬드 결정입자가 아닌 whisker 형태의 탄소를 성장하였다. 탄소 원자의 공급원으로 CH_4기체를 사용하였다. 이 때 바이어스, 메탄농도, 기판온도에 따른 탄소 whisker의 성장을 조사하였다. 본 실험으로 얻은 whisker를 FE-SEM을 이용하여 구조변화와 성장메커니즘 및 전기적 특성에 대해 분석하였다.

Dp-163 **HFCVD법을 이용한 나노다이아몬드 합성** 전 혜영, 김 미경, 심 성빈, 김 지영, 박 홍준, 이 재열, 김 용(*동아대학교, 물리학과.*) Fe 촉매금속을 p-type Si 웨이퍼에 증착시킨 후 RF-PECVD법을 이용하여 DLC (Diamond-Like Carbon) 박막을 그 위에 합성하였다. 이렇게 얻은 DLC/Fe/Si 기판을 HFCVD 장비에 장착하고, Ar 혹은 H_2 기체를 흘리며 열처리하여 나노다이아몬드가 성장하는 조건을 찾았다. DLC 박막의 두께, 열처리 온도와 시간에 따른 나노다이아몬드의 구조, 크기와 밀도의 변화를 조사하고 그 성장 메카니즘에 대해 분석하였다.

Dp-164 **Effect of surface treatment on the electronic and structural properties of in situ lateral grown Si nanowire bridge** 이 윤희, 권 혁상, 박 성림, 노 지영(*고려대 물리학과.*) Silicon nanowires are one of the promising 1-D materials for studying nanoscience and technology of nanoscale devices. There are many methods that the electronic properties of the Si nanowires can be modified. In this work, we investigate the electronic and structural properties of in situ lateral grown Si nanowire bridge by coating B(boron) and annealing in C_2H_2 (acetylene) ambient. We found that the B dopants migrate to the edge of the Si nanowire by high resolution TEM observations and increase current level in substantial. In case of C_2H_2 treated Si nanowire, we observed an appearance of energy gap widening from gate voltage response characteristics due to surface coating of carbon as well as reduction effect of oxidized surface.

Dp-165 **수소와 메틸기를 이용한 graphene 표면의 자기화** 김 승철, 임 지순, 손 영우[1](*서울대학교 물리천문학부. [1]고등과학원, 건국대학교 물리학과.*) 탄소 기반의 물질에 금속을 사용하지 않고도 자성을 띄는 구조에 대한 연구에서 최근에 몇가지 주목할 만한 성과들이 있었는데, 이런 구조들을 graphene의 zigzag edge의 flat band에 의해서 자기화 되거나 탄소의 빈자리 때문

에 생기는 dangling bond에 의한 것이 대부분이다. 이와는 다른 구조로서, 수소나 메틸기(-CH3)가 흡착된 graphene을 제시하고자 한다. 제일 원리적 전자구조 계산을 이용하여 수소 원자나 메틸기가 결함이 없는 graphene 표면의 동일한 부분격자에 화학적으로 결합하면 graphene이 자화됨을 알아냈다. 서로 다른 부분격자에 결합된 수소 원자나 메틸기의 개수의 차이만큼 전자가 편극되며, graphene의 탄소 원자당 최대로 1/2까지 편극된다. 페르미 레벨의 바로 위와 아래에 서로 다른 스핀의 밴드가 생긴다.

Dp-166 **Magneto-transport behavior of in situ lateral grown single wall carbon nanotube bridge with gate electrode** 이 윤희, 노 지영, 이 종희(*고려대 물리학과.*) We present the results of gated magneto-transport measurements of in situ grown single wall carbon nanotube bridge with transparent contact electrodes. The suspended SWNT bridge between transparent oxide contacts exhibits an on-to-off current ratio of 10^4 10^6 and a subthreshold slope of 120~270(mV/dec) at room temperature. Under the parallel and perpendicular magnetic field the bridge show signature of phase-coherent transport at 3.8K and magneto-conductance that shows a gate controlled behavior. The observed result provides a step toward the understandings of the transparent one dimensional magneto-electronics.

Dp-167 **Spin Coherence in a Quasi-one-dimensional Electron Gas with a Quantum Point Contact** JEONG Jae-Seung, LEE Hyun-Woo(*Pohang University of Science and Technology, Department of Physics.*) We study spin coherence and relaxationin a quasi-one-dimensional electron gas including a quantum point contact(QPC) in the presence of Rashba and Rashba + Dresselhaus spin-orbit coupling. Electron transport properties such as spin-resolved conductance and polarization are investigated numerically using a recursive Green function method, with attention to the quantum effects of spin-charge transport channels. Scattering by spin-independent impurities are also addressed. It is found that when the conductance is examined as a function of the Rashba spin-oribt coupling strength, the conductance modulation ratio, defined as the ratio between the maximum and minimum conductances,can be enhanced by introducing a QPC in the ballistic and the weakly diffusive regime as well. Decaying rate of the spin-polarization can be also reduced due to the existence of the QPC.

Dp-168 **Ti을 기본으로 하는 준결정체의 성분비에 따른 안정성** 김 재용, 김 남혁, 전 재균, 이 윤만(*한양대학교 물리학과.*) Ti을 기본으로 하는 준결정체는 구조학적인 기초학문으로서의 가치뿐 아니라 많은 양의 수소를 저장할 수 있는 가능성이 최근 알려지면서 활발한 연구가 진행되고 있다. 본 연구에서는 기존에 알려진 성분비로 제작된 $Ti_{45}Zr_{38}Ni_{17}$ 시료를 기본으로 Ti의 비율을 33~50 at. % 범위내에서 변해가며 시료를 제작하여 X-ray diffraction으로 분석한 결과 비교적 넓은 조성비 내에서 준결정체가 형성됨을 확인하였다. 먼저, Ar 분위기 내에서 arc-discharge 방법으로 합금을 만들어 이를 냉각시켰는데 스테인레스 휠의 회전속도는 0~3000 rpm 으로 하였다. 이렇게 만들어진 구조를 분석한 결과 결정에 해당하는 C-14 Laves phase (hcp) 에서부터 비결정체까지의 다양한 구조체가 형성되는 됨을 확인하였다. 특히 $Ti_{50}Zr_{31}Ni_{19}$ 조성비로 제작한 경우, 준결정체로만 이루어진 시료를 얻을 수 있었다. 현재까지의 결과를 종합하여 볼 때, Ti을 기본으로 하는 준결정체는 비교적 넓은 성분비 내에서 형성됨을 알 수 있었고, 이는 추후 대용량 수소저장 매체로서의 손쉬운 활용가능성이 있음을 시사한다.

Dp-169 **Local structural properties of ZnO nanorods and ZnO nanoparticles** JEONG, E.-S, YU, H.-J., PARK, S.-H.[1], KIM, S.-H.[1], KIM, Y.-J.[1], YI. G.-C.[1], HAN, S.-W.(*전북대학교 과학교육학부. [1]포항공대.*) We present the local structures of ZnO nanorods and ZnO nanoparticles, comparing ZnO powder counterpart. The ZnO nanorods were synthesized with metal-organic chemical vapor deposition and the ZnO nanoparticles were fabricated with a Solution method. Extended x-ray absorption fine structure (EXAFS) was employed to investigate the structural properties of the ZnO nanomaterials. EXAFS revealed that the ZnO nanorods were elongated along the c-axis while the ab-plane of the ZnO nanorods was shrunken slightly, comparing with the ZnO powder. From the EXAFS measurements on the ZnO nanoparticles with average diameter of 5 nm, we found that the Zn-O pairs had a tight bond but the Zn-Zn bonding had a large amount of disorder. Moreover, only the half of the Zn sites around a Zn atom was filled and the last were occupied by oxygen atoms. We will discuss the detail structural properties of the ZnO nanostructures.

Dp-170 **Memory effect from the Si1-xGex alloy**

nanworie field effect transistors 전 은경, 성 한규[1], 최 헌진[1], 김 병계, 소 혜미[2], 김 주진[3], 이 정오[2](*한국화학연구원, 전북대학교. [1]연세대학교. [2]한국화학연구원. [3]전북대학교.*) We have fabricated field effect transistors (FETs) by using high quality Si1-xGex alloy nanowires. To obtain stable contacts between Si1-xGex alloy nanowire and Ni/Au electrodes, we conducted rapid thermal annealing (RTA) of the samples at 400℃ or at 500℃ with N2 atmosphere. The behavior of the samples changed dramatically with annealing. When annealed at 400℃, Si1-xGex alloy FETs showed p-type gating effect and bias-dependent hysteresis regardless of the Ge contents. The bias-dependent hysteresis was highly reproducible so that the device can be used as a memory. Devices annealed at 500℃ show either metallic conductance with a small resistance (~10kΩ) or infinite resistance. Metallic conductance from the device can be explained by the formation of metallic silicide nanowires, and confirmed by ultra-high resolution SEM (UHR-SEM) and electron diffraction analysis.

Dp-171 **Photoluminescence characteristics of $La_{1-x}Gd_xAlO_3:Eu^{3+}$ phosphors** 문 병기, 권 일민, 심 규성, 정 중현, 전 병억[1], 최 병춘, 김 중환[2], 최 혜영[2], 이 성수[3](*부경대학교 물리학과. [1]부경대학교 기초과학연구소. [2]동의대학교 물리학과. [3]신라대학교 전자재료공학과.*) $La_{1-x}Gd_xAlO_3$ doped with Eu^{3+} was synthesized by solvothermal reaction with aluminum isopropoxide and lanthanum or gadolinium nitrate solution. Both X-rays diffraction (XRD) and scanning electronic microscope (SEM) show that these phosphors exhibit the homogenous particle distribution in the range of 20-30 nm. As the content of Gd^{3+} increased, crystal structure changes from $LaAlO_3$ to $GdAlO_3$ and lattice constant decreased. The photoluminescence property of $La_{1-x}Gd_xAlO_3:Eu^{3+}$ was compared to investigate as a function of Gd^{3+} ions concentration, which revealed that these phosphors showed charge transfer band (CTB) became narrower and shifted shorter wavelength, the number of magnetic dipole transition ($^5D_0$ -> $^7F_1$) and electric dipole transition ($^5D_0$ -> $^7F_2$) peaks split, and the intensity between them inversed.

Dp-172 **Parametric amplification and synchronized oscillation in nanomechanical coupled nonlinear oscillator** 심 승보, IMBODEN Matthias[1], MOHANTY Pritiraj[1], 박 윤(*서울대학교 물리 천문학부. [1]Department of Physics, Boston University.*) For the ultimate realization of microwave frequencies and beyond oscillators, mechanical structures need to approach nanometer dimensions. However, amplitudes of mechanical motion in nano-scale structures is often too small to detect, even with state-of-the-art detection techniques. Toward this end, on-chip amplification of small forces is a natural solution. Here, we demonstrate the mechanical amplification utilizing parametric modulation and nonlinear response. We have realized coupled nanomechanical oscillator from single crystal silicon using electron beam lithography and surface machining. With two electrically isolated resonators, we demonstrate the phase sensitive mechanical gain with parametric modulation and the synchronized oscillation in coupled nanomechanical oscillator. We will also discuss nonlinearity in nanomechanical structures of differing material systems.

Dp-173 **Nanoelectromechanical systems (NEMS) torsional resonators of carbon nanotube network and metal-carbon nanotube composites** 김 영덕, 홍 승새, 박 정훈, 이 병양, 조 성운, 홍 승훈, 박 윤(*서울대학교 물리천문학부.*) Carbon nanotubes have been spotlighted for its great potential as a promising material as well as the future candidate for nanoelectronics, with CNT's unique electrical and mechanical properties. NEMS structure combined with CNT can be applied to elucidate the nanotube's physical properties as well as further applications. Furthermore, metallic based nanoelectromechanical systems (NEMS) resonator structures are of interest due to higher optical reflectivity, ductility, and conductivity compared to insulator- and semiconductor-based NEMS structures. We present NEMS torsional resonator structures fabricated from aluminum-carbon nanotube(CNT) and palladium-CNT composites. In addition, we realize NEMS structures suspended by carbon nanotube on GaAs surface by adopting highly selective wet-etching and reactive ion etching techniques. The resonators are electrostatically driven and are detected at room temperatures under moderate vacuum conditions using optical modulation techniques. We will also discuss the characterization of mechanical properties of the structures by AFM force deflection spectroscopy.

Dp-174 **Magnetic properties of ferritin embedded in nanofiber** HYUN YoungHoon, PARK SangYoon, LEE YoungPak, SHIN MinKyoon[1], KIM SeonJeong[1] (*q-Psi and BK21 Program Division of Advanced Research and*

Education in Physics, Hanyang University, Korea. [1]*Center for Bio-Artificial Muscle and Department of Biomedical Engineering, Hanyang University, Korea.*) The magnetic properties of ferritin embedded into polyvinyl alcohol (PVA) fibers with a diameter of about 100 nm were investigated as a function of process-temperature (T_p) of the mixed PVA-ferritin solution. The ferritin-embedded fibers were synthesized by electrospinning at room temperature. The dependences of diameter-size and the distribution on T_p were determined by transmission electron microscopy. The results of M(T) and M(H) measurements show that the ferritin-embedded fiber at a low T_p exhibits a mixed magnetic phase of the superparamagnetic and the anti-ferromagnetic states. On the other hand, the magnetic properties of the ferritin-embedded fiber at a T_p revealed a ferromagnetic behavior.

Dp-175 **Synthesis of ZnO nanotube via thermal evaporation** WANG DuoFa, LEE YoungPak(*q-Psi and BK21 Program Division of Advanced Research and Education in Physics, Hanyang University, Korea.*) By forming a well-controlled temperature gradient in the tube furnace, high density ZnO nanotubes were synthesized by thermal evaporation without catalyst. The nanotube sample was characterized by scanning electron microscopy (SEM), transmission electron microscopy (TEM), and selected area electron diffraction (SAED). The SEM image shows that the sample is in a tubular structure and the density is very high. The TEM results reveal that the nanotube has a diameter of 270 nm and the wall thicknesss is about 45 nm. The SAED image demonstrates that the nanotube is single-crystalline.

Dp-176 **Morphology control of CNT cold cathode using plasma treatments** 이 규, 이 일하[1], 임 성주[2], 이 영희[3](*성균관대학교 물리학과, 나노튜브 및 나노복합구조 연구센터.* [1]*성균관대 성균관 나노과학 기술원.* [2]*성균관대 나노튜브 및 나노복합구조 연구센터.* [3]*성균관대 물리학과, 성균관대 성균관 나노과학 기술원, 성균관대 나노튜브 및 나노복합구조 연구센터.*) 화학 기상법을 이용하여 다층벽 탄소 나노튜브를 성장하였다. 이렇게 성장된 나노튜브는 기판과 수직하게 정렬되어있어 전계 방출시 인가 전압을 낮출 수 있다. 하지만, 튜브의 길이가 일정하지 않아 강한 점 발광을 보인다, 이러한 이유는 주변의 튜브보다 길게 자란 튜브 들이 우선적으로 전자를 방출하기 때문이다. 점 발광을 억제하기 위하여 수직 성장된 탄소나노튜브 냉음극을 플라즈마에 노출하여 길게 자란 튜브를 선택적으로 식각하여 제거하였다. 이러한 평탄화 과정을 거친 후 냉음극의 전계방출 특성을 측정 하였다. 플라즈마 처리 후 탄소나노튜브 냉음극의 표면은 플라즈마 파워, 노출 시간, 사용된 가스의 종류 및 혼합비율 등에 따라서 커다란 차이를 보였다.

Dp-177 **안티몬 텔루라이드 화합물을 이용한 측면접촉방식 상변화 소자에 대한 연구** 이 상엽, 배 병택, 안 영근, 장 민영, 정 광호(*연세대 물리및응용물리.*) 텔루리움 원소가 정량 조정된 이원 켈코게나이드 안티몬 텔루라이드를 이용한 측면 접촉 방식 상변환 소자의 스위칭 특성을 연구하였다. 텔루리움 원소가 정량 조정된 안티몬 텔루라이드 박막은 열처리 과정중의 각 온도에서의 결정화 양상과 결정화 후 상태의 옵티컬 밴드 갭 에너지에서 차이를 보였다. 우리는 이러한 결과에서, 상변화 물질인 안티몬 텔루라이드를 이용한 소자는 스위칭 특성이 조절될 수 있다고 충분히 예상할 수 있었다. $Sb_{1.0}Te_{0.3}$ and $Sb_{1.0}Te_{2.7}$ 두개의 안티몬 텔루라이드 박막들이 소자응용에 상변환 물질로 사용되었다. 실리콘 (001) 기판위에 결정화된 박막의 화학적 조성비와 결정성 분석을 위해서 PIXE와 XRD를 이용한 RSM(reciprocal space mapping)을 이용하였다. 텔루리움 양이 정량 조절된 안티모니 텔루라이드 소자들은 완전히 다른 스위칭 특성을 보였다. 첫번째로, $Sb_{1.0}Te_{2.7}$ 박막을 사용한 소자는 두개의 인접한 V_{th}(threshold voltage)를 갖고, 동적 전류-전압 곡선상에서 도전상태(conducting state)의 기울기가 더 급한 것을 보이는 스위칭 특성을 보였으며, 이러한 것은 소자내의 켈코게나이드 박막의 기하학적 접촉 형상내에서 급격한 열집적 효과와 이전의 XRD측정에서 보였던 향상된 결정성에 의한 것으로 해석되었다. 반면에 $Sb_{1.0}Te_{0.3}$를 이용한 소자는 전형적인 부도체의 성질을 보였는데, 이것은 밴드 갭이 조정된 전기적 물성으로 이해되었으며, $Sb_{1.0}Te_{0.3}$ 박막의 경우 초기 전도성 경로 형성과정을 거치는 동안 소자내에서 상변환 현상이 제한되는 것으로 해석된다. 이것은 열처리 과정에서 다른 결정상으로의 상변환 현상이 억제되는 것을 보였던 XRD실험에서 유추될 수 있었다. 두 경우 사이의 이러한 큰 차이는 텔루리움 원소의 정량 조절에 의한 것이전부이다. 이상의 결과에서, 우리는 이원계 켈코게나이드 안티모니 텔루라이드 박막내에서의 텔루리움 량의 조절이 상변환 현상 특성을 조절할 수 있으며, 이원계 켈코게나이드 물질을 이용한 상변환 소자의 상변환 거동 특성을 부여하지 않게 하는 텔루리움 양의 임계값이 존재할 것이라는 것을 제안한다.

Dp-178 **Development of Spin-polarized Positron Source from ^{18}F for Electron Spin Structure** 김 재홍,

이 종용[1](*원자력의학원, RI 및 방사성의약품개발실. [1]한남대, 광전자물리학과.*) Recently, positrons are becoming unique probe tools to the measurement of electronic structures of surface and point-like defects, including spin structures of electrons in magnetic materials. Like an electron, a positron has a spin, which can be used to investigate magnetism, electron spin states of both surface and bulk. Along with ^{22}Na, a radionuclide of ^{18}F has been interested as an intense slow polarized positron source, which produced by a proton cyclotron through ^{18}O(p,n)^{18}F reaction. Positron beams are to be promised a very powerful probe for observing submicroscopic defect structures, as well as the medical diagnosis, such as Positron Emission Tomography (PET). Positrons in materials have lifetimes that are governed by the electron density in the material; the higher the electron density, the shorter the positron lifetime. If the defect density is lower than the bulk density, then the defects contain fewer electrons, so positrons in the defect have a longer lifetime. Thus, positron spectroscopy is a sensitive probe of electron density in materials. In this study, we investigate a positron-emitting radionuclide, ^{18}F can be produced a highly polarized positron beam.

Dp-179 **Surface and Luminescent Properties of Pulsed Laser Ablated $Sr_2SiO_4:Eu^{3+}$ Thin Film Phosphors.** 배 종성, 김 종필, 박 성균, 박 종호[1], 정 중현[2], 이 성수[3] (*한국기초과학지원연구원, 나노표면기술연구팀. [1]진주교육대학교, 과학교육과. [2]부경대학교, 물리학과. [3]신라대학교, 광전자공학과.*) $Sr_2SiO_4:Eu^{3+}$ thin film phosphors have been grown on MgO (100) substrates using the pulsed laser deposition. Luminescence and X-ray photoelectron spectroscopy (XPS) measurements were used to investigate the variation of optical properties and chemical state of the as-grown sample with various substrate temperature and oxygen pressure. Based on X-ray diffraction patterns, the as-grown sample has the orthorhombic structure, crystallizing in the Pmcn space group. The films grown on various growing condition exhibit different crystallinity, surface morphology, and luminescent properties indicating the importance of the crystallinity and photoluminescence of the samples are highly dependent on the deposition conditions; in particular, the substrate temperature and the oxygen pressure. XPS measurements showed two Gaussian components of O1s spectrum assigned to Sr-O and Si-O, respectively, in $Sr_2SiO_4:Eu^{3+}$ thin film. The $Sr_2SiO_4:Eu^{3+}$ films exhibit a broadband emission extending 565 to 670 nm, peaking at 582, 597, and 620 nm, which are composed of several overlapping emission bands. The brightness of PL depends on not only crystallinity, but also surface roughness. The PL intensity reaches a maximum at 150 mTorr and the peak positions and FWHMs of two major bands were not varied with increasing of oxygen pressures. The films grown at 600^o C exhibited superior luminescence characteristics, as compared to the films grown at 500 and 700^o C.

Dp-180 **Study of Pt Clusters and CO Molecules on Pt(110)-(1x2) Surface Using STM** CHOI Eunyeoung, JUNG Woojin, LYO In-Whan(*Yonsei University, Institute of Physics and Applied Physics.*) The design and performance of a variable-temperature scanning tunneling microscope (STM) is presented. STM operates from 8 to 350 K in ultra-high vacuum. The thermally compensated Besocke-type STM is suspended by springs from the cold top of a continuous flow cryostat and is fully surrounded by two radiation shields. The design allows in situ dosing and irradiation of the sample as well as the exchange of samples and STM tips. The enhanced stability and low-noise performance of the home-built STM was utilized in the study of one dimensional diffusion of Pt clusters and CO molecules in the missing rows on a reconstructed Pt(110)-(1x2) surface. Recent results thus obtained will be discussed during the talk.

Dp-181 **중성자 반사율 측정장치 이용 PNR 기법 연구** 이 정수, 이 창희, 홍 광표, 김 기연, 김 학노(*한국원자력연구소.*) 한국원자력연구소의 30MW 연구용 원자로인 하나로의 ST3 수평공에 중성자 반사율 측정장치(REF-V)를 개발, 설치하였다. 이러한 REF-V를 이용한 자성 박막의 특성 측정이 가능하도록 하는 PNR 기법 및 PNR 구현 기구에 대한 기초 연구를 수행하였다. PNR 기법은 편극 중성자를 이용하여 첨단 스핀트로닉스 분야의 자성 박막 또는 초전도 박막 등의 수직 및 수평 방향의 자화 밀도 분포를 비파괴적으로 평가할 수 있는 방법이다. 이러한 PNR 기법의 구현을 위해서는 편극 중성자를 얻기 위한 편극기와 편극 중성자의 방향을 반전하기 위한 스핀 반전기 및 가이드 필드 등이 필요하다. 또한 측정 박막 시료에 자기장 인가를 위한 전자석 및 극저온 시료 환경이 가능하도록 하는 시료환경장치의 개발이 필수적이다. 한편 박막 시료의 반사율 측정시에 중성자 편극, 자기장 및 온도변화 등의 복잡한 구동 변수들을 정밀 구동할 수 있는 통합 ICP의 개발이 요구된다. 이를 위하여 우선 전자석, 스핀반전

기, 극저온시료환경장치 등의 PNR 구현 기구들을 개발하였으며 이들에 대한 일부 성능 시험을 수행하였다.
* 본 연구는 과학기술부 원자력연구개발사업의 일환으로 수행되었습니다.

Dp-182 **Surface vs. Bulk Characterizations of Electronic Inhomogeneity in a VO_2 Film** CHANG Y. J., CHAE S. C., KIM D.-W.[1], OH E[2], KAHANG B.[2], NOH T. W.(*ReCOE &FPRD, Department of Physics and Astronomy, Seoul National University, Seoul 151-747, Korea. [1]Department of Applied Physics, Hanyang University, Ansan, Kyeonggi 426-791, Korea. [2]School of Physics and Center for Theoretical Physics, Seoul National University, Seoul 151-747, Korea.*) We investigated the inhomogeneous electronic properties at the surface and interior of VO_2 thin films that exhibit a strong first-order metal-insulator transition (MIT). Using the crystal structural change that accompanies a VO_2 MIT, we used bulk-sensitive X-ray diffraction (XRD) measurements to estimate the fraction of metallic volume p^{XRD} in our VO_2 film. The temperature dependence of the p^{XRD} was very closely correlated with the dc conductivity near the MIT temperature, and fit the percolation theory predictions quite well: $\sigma \sim (p - p_c)^t$ with $t = 2.0\pm0.1$ and $p_c = 0.16\pm0.01$. This agreement demonstrates that in our VO_2 thin film, the MIT should occur during the percolation process. We also used surface-sensitive scanning tunneling spectroscopy (STS) to investigate the microscopic evolution of the MIT near the surface. Similar to the XRD results, STS maps revealed a systematic decrease in the metallic phase as temperature decreased. However, this rate of change was much slower than the rate observed with XRD, indicating that the electronic inhomogeneity near the surface differs greatly from that inside the film. We investigated several possible origins of this discrepancy, and postulated that the variety in the strain states near the surface plays an important role in the broad MIT observed using STS. We also explored the possible involvement of such strain effects in other correlated electron oxide systems with strong electron-lattice interactions.

Dp-183 **Electronic Structure of Carbon-incorporated Si(001) Surfaces** LEE Seung Mi, KIM Wondong, KOO Ja-Yong, KIM Hanchul(*Korea Research Institute of Standards and Science.*) The electronic structure of carbon-incorporated Si(001) surfaces are studied using density functional theory calculations. Each incorporated carbon atom is known to form the so-called DV41 defect which is the fourth-layer substitutional carbon under a surface Si dimer vacancy [PRL 89, 106102 (2002)]. The DV41 defects tend to align linearly across the dimer row direction at low concentration (2xn superstructure). In contrast, the DV41 defects are two-dimensionally arranged at higher concentration, forming a c(4x4) superstructure [PRL 94, 076102 (2005)]. In this presentation, we report a detailed theoretical analysis on the electronic band structure and the projected density of states for the carbon-incorporated Si(001) surfaces, to elucidate the effects of the carbon-induced structural modification on the electronic properties.

Dp-184 **Fabrication of high quality Polymer film (Di-Chloro-Para-Xylylene) and its surface characterization** LEE YOUNGMI, LEE SANGMIN, LEE InJae(*Department of physics, Chonbuk national university.*) 고분자 박막 형성에 많이 쓰이는 패럴린은 내마모성, 내화학성, 내수성, 내열성의 우수한 특성으로 인하여 많은 분야에서 사용되고 있다. 패럴린은 진공 상에서 가스 형태로 승화되어 모노머 분자들이 사슬의 끝과 반응하여 긴 체인형태의 반복단위를 형성하며 중합체로 표면에 증착이 되게 되는데 우리는 Cl치환기를 가진 패럴린C (Di-Chloro-Para-Xylylene)를 화학기상증착법(chemical vapor deposition: CVD)을 사용하여 Si표면에 thin film 형태로 증착하였다. 증착된 패럴린 박막에 다양한 표면처리를 하여 박막표면의 물리적, 화학적 특성의 변화를 XPS (X-ray Photoelectron Spectroscopy)와 AFM(Atomic Force Microscopy)을 통하여 연구하였다

Dp-185 **Magnetron sputtering으로 증착한 Au 박막의 증착 기판 온도에 따른 grain size와 표면거칠기** 최 혁철, 유 천열(*인하대학교 물리학과.*) 우수한 전도성과 내산화성으로 널리 사용되는 Au 박막의 전도성은 박막의 증착조건에 따라 달라진다. 증착 조건에 의해 grain size가 달라지면 grain boundary 가 산란의 주요원인으로 작용하기 때문에 박막의 전도도는 grain size의 크기에 영향을 받게 된다. 본 연구에서는 박막을 증착하는데 magnetron sputtering 방법을 사용하여 증착시 기판온도에 따른 Au grain size의 변화를 연구하였다. Si(111) 또는 Si(100) 기판위에 Au을 30nm 또는 Ta/Au를 5nm/30nm의 두께로 기판의 온도를 바꾸어 가며 증착하고, x-ray diffraction 의 rocking curve측정법으로 grain size를 측정하였다. 또 표면거칠기는 AFM (atomic force microscope)를 이용해서 측정하였다. 기판의 온도가 증가함에 따라 시료의 grain size가 증가하였

고 박막 표면거칠기 또한 증가함을 확인하였다. Si/Ta/Au 구조에서의 표면거칠기가 Si/Au구조에서의 표면거칠기보다 더 완화됨을 관측하였고 Si(111) 기판보다 Si(100) 기판에서 시료의 표면거칠기가 다소 완화됨을 확인하였다. Si(100)/Au구조에 Ta으로 얇은 buffer layer를 삽입하여 표면거칠기 정도를 낮춤과 동시에 기판 온도를 적절히 조절함으로서 grain size를 증가시킬 수 있었다.

Dp-186 **Pulsed DC magnetron sputtering을 사용하여 Polyether Sulfone 위에 성막된 Indium Tin Oxide 박막의 특성 연구** 김 용기, 장 덕우, 김 덕수, 홍 재석, 이 병로, 김 종재, 박 승환, 홍 우표, 김 화민(*대구가톨릭대학교,전자공학과.*) 최근, 투명전도 산화막 (TCO film : Transparent Conductive Oxide film)의 기판 물질을 기존의 투명 유리 대신 PET (polyethylene terephthalate), PC (poly carbonate) 그리고 PES (polyether sulfone)와 같은 플라스틱 기판으로 대체하려는 연구가 진행되어 오고 있다. 그 이유는 유리 기판 대신 플라스틱 기판을 사용할 경우, 플랙서블 디스플레이를 가능하게 함으로써, 평판표시 (Flat Panel Display) 장치의 무게 감소는 물론 가격 경쟁력에서도 유리하기 때문이다. 지금까지 가장 많이 사용되고 있는 투명전도막은 DC 마그네트론 스퍼터링 방법에 의해 유리 기판 위에제작되는 ITO 박막이다. 하지만, 플라스틱 기판의 경우, 유리 기판과는 달리 열적 내구성이 작기 때문에, 박막 성막 시 기판에 전달되는 열을 최소화 할 수 있는 공정이 요구된다. 본 연구에서는 ITO 박막 성막 시 플라즈마에 의해 발생되는 열을 최소화하기 위하여 50 KHz 이하의 bipolar pulsed DC 전압을 사용하여 PES 기판 위에 ITO 박막을 제작하였다. ITO 박막의 공정 조건으로는 5～30 KHz의 bipolar pulse와 340～360 volt의 범위에서 pulse 주파수와 전압을 변화시켰으며, 각각의 공정 조건에 의해 제작된 ITO 박막의 전기적 특성으로 Hall Effect 측정을 통해서, 비저항과 이동도를 조사하고, 광학적 특성으로는 200 ～ 900 nm의 파장 범위에서 광투과도를 측정하였다. 한편, PES 위에 성막된 ITO 박막의 외부 스트레스에 의한 안정성 평가를 위해, bending과 급격한 온도 변화 그리고 습열 (moist heat)에 대한 전기적 안정성과 표면 morphology 변화 등도 제시된다.
*본 연구는 한국산업기술재단의 지역혁신인력양성사업의 지원에 의해 수행되었음.

Dp-187 **고주파 마그네트론 스퍼터링에 의해 성막된 Al이 첨가된 ZnO 박막의 전기적 및 광학적 특성** 장 덕우, 김 용기, 고 현규, 류 성원, 이 병로, 김 종재, 박 승환, 홍 우표, 김 화민(*대구가톨릭대학교, 전자공학과.*) 디스플레이 산업과 전지 산업이 발달함에 따라, 투명 전도막(TCO film : Transparent Conductive Oxide film)의 응용 분야가 태양전지, TFT-LCD, OLED와 같은 평면표시소자, 광전소자 및 가스센서 등에 적용이 되고 있으며, 고품질, 저가, 고 효율성을 가진 투명전도막이 요구되어지고 있다. 현재 투명 전도막으로 ITO (indium tin oxide)를 많이 사용하고 있으나, 소자의 전극으로 사용할 경우, 전기적 불안정성이 문제가 되고 있으며, In_2O_3가 고가의 물질이어서 제작비가 높은 것도 문제로 대두되고 있다. 이와 같은 문제점을 해결하기 위해 전기적으로 안정적이고, 값이 저렴한 ZnO에 3가 원소를 도핑하여 제작한 투명 전도막에 대한 연구가 많이 진행되고 있다. 본 실험에서는 고주파 마그네트론 스퍼터링 방법을 사용하여, Al-doped ZnO (AZO) 박막을 유리기판 위에 제작하였다. AZO 박막 제작을 위한 sputter용 타겟은 ZnO 분말에 Al_2O_3 분말을 2 wt.% 혼합하여 1000 ℃에서 소결하고, 압착을 한 후, 다시 1000 ℃에서 고형화 시켜 2인치 타겟을 제작하였다. AZO 박막은 타겟과 기판 사이의 거리와 활성화 가스 량의 변화에 따라 성막되었으며, 이렇게 제작된 AZO 박막의 전기적·광학적·구조적 특성을 알아보았으며, 전기적 특성으로는 4-point probe에 의한 면 저항과 van der Paw 방법에 의한 Hall Effect 측정으로부터 비저항 (resistivity)과 이동도 (mobility)를 조사하고, 광학적 특성으로는 200 ～ 900 nm의 파장 범위에서 측정된 광투과도 스펙트럼으로부터 굴절률과 밴드갭이 조사된다. 또한 AZO 박막의 후열처리 특성으로서 공기 중 450 ～700 ℃의 열처리에 의한 전기적 또는 광학적 특성 변화가 조사되고, 이 결과들은 AZO 박막의 구조변화와 함께 설명된다.
*본 연구는 산업자원부의 부품·소재 기술개발사업의 지원에 의해 수행되었음.

Dp-188 **STM Study of Atomic Chains on the In-induced Si(557)1x3 Surface** SONG I.K., NAM J.H.[1], KIM M.K., PARK J.-Y., AHN J.R[1](*BK21 Physics Research Division, SungKyunKwan University, Suwon 440-746, Korea, Center for Nanotubes and Nanostructured Composites (CNNC), SungKyunKwan University, Suwon 440-746, Korea. [1]BK21 Physics Research Division, SungKyunKwan University, Suwon 440-746, Korea, Institutes of Basic Science, SungKyunKwan University, Suwon 440-746, Korea.*) We have investigated the In-induced one-dimensional (1D) surface reconstruction on the Si(557) surface using low energy electron diffraction (LEED) and scanning tunneling microscopy (STM). One-dimensional electron systems have showed exotic phenomena such as Jahn-Teller distortion, non-Fermi liquid behavior, and Peierls instability. Recently, stepped Si surfaces have attracted much atten-

tion as templates for formation of one-dimensional structures. Some examples that have been extensively studied are the Au/Si(553), Au/Si(557), Pb/Si(557) surfaces. The In-induced 1D structure on the Si(557) surface was prepared by depositing In on the RT Si(557) surface and subsequent annealing at 500℃. LEED show the In-induced surface reconstruction to have 1×3 phase, where the direction of the ×3 period is perpendicular to the step direction. In STM images, we found two kinds of atomic wires located at the step edge and within the terrace, respectively. The atomic chain within the terrace has obviously ×3 period along the chain direction, while the atomic chain at the step edge seems to have ×1 period along the chain direction. The atomic chains on the In-induced Si(557)1×3 is quite similar with those on the Au/Si(557) and Au/Si(553) surface. We will explain the In-induced Si(557)1×3 surface in comparison with the Au/Si(557) and Au/Si(553) surface.

Dp-189 **양성자 빔을 조사한 금속산화물 분말의 Ar 흡착 표면분석** 김 재용, 이 정길, 김 병욱, 김 의권, 윤 상필[1], 김 계령[1](*한양대학교 물리학과. [1]원자력연구소, 양성자기반공학기술개발사업단.*) 개스 분자를 이용한 흡착연구는 기존의 첨단장비로 측정할 수 없는 미세범위까지 시료의 표면 구조를 탐색할 수 있다는 점에서 최근 들어 활성화되고 있다. 본 연구에서는 rf-induction 방법으로 제작한 나노 크기의 MgO 금속산화물 시료에 고 에너지 (35 MeV) 양성자빔을 조사하여 표면 구조변화를 분석하였다. 분석방법으로는 불활성기체인 Ar의 삼중점온도 (83.78K) 근처에서 흡착곡선 결과를 얻었고, 동시에 양성자를 조사한 MgO시료에 대해서도 같은 방법으로 측정하여 결과를 비교 분석하였다. X-ray와 TEM을 이용하여 MgO시료의 구조를 분석한 결과 양성자를 조사하여도 구조에는 변화가 없음을 확인하였다. 양성자를 조사한 MgO의 Ar 흡착실험 결과의 경우, 삼중점 이하의 온도에서는 개스 평형증기압이 (final equilibrium vapor pressure) 포화단계에 이르러 불연속적으로 변화하였다. 특히, 75K이하에서는 양성자를 조사하지 않은 시료와 달리 second 혹은 third isotherm step이 생기는 것을 관찰할 수 있었다. 이것은 양성자를 조사함으로써 MgO 표면이 더 균일하게 형성 되었다고 해석할 수 있다. Isotherm step 형성은 compressibility와 heat adsorption 값을 계산한 결과에서도 확인할 수 있었다. 85K 이상 온도에서 측정한 Ar 흡착곡선은 시료에 흡착된 개스량이 증가할수록 포화증기압이 asymptotic하게 증가하였고, 이는 흡착량이 많아질수록 Ar 개스분자와 MgO(100) 표면과의 상호작용이 점진적으로 줄어든다고 해석할 수 있다.

Dp-190 **Cr의 도핑비율에 따른 SrZrO3 박막표면에서의 전자구조변화** 신 효섭, 조 수연, 박 원구, 오 세정(*서울대학교 물리천문학부.*) 차세대 비휘발성 저항성메모리소자로 전이금속산화물이 많이 연구되고 있는데, 그 정확인 원리는 아직 규명되지 않고있다. 최근의 여러 실험을 통해 전극과 산화물의 경계에서 중요한 변화가 일어나고 있음이 확인되었고, 이는 기존의 이론들에 의해 지지, 보완되고 있다. 특히 내부 multi-filamentary 현상과 전극과의 계면 효과가 복잡하게 얽힌 가운데 내부결함과 외부불순물의 역활이 중요하게 부각되고 있다. 최근의 실험에서 0.2mol%Cr도핑된 SrZrO3 표면에서 electric forming전후로 Cr의 valence state가 변한다는 사실이 발표되었고 우리는 Cr과 Zr, O의 연관성에 대해서 조사한 바 있다. 여기서는 더 나아가 Cr의 도핑농도를 다양하게 변화시킬때 표면영역내의 Cr이 주변의 O, Zr, Sr과 어떤 반응을 하는지를 광전자방출실험(XPS)를 통해 조사하였으며 또 어떤 전류-전압특성을 보이는지 측정하였고 x-선 흡수실험(XAS)를 통해 forming전후 Cr의 valence state변화를 확인해보았다. 더불어 기존에 아랫쪽 전극으로 사용되던 SrRuO3를 Nb도핑된 SrTiO3로 대체해서 XAS와 I-V특성을 조사하였다.

Dp-191 **실온에서 마그네트론 스퍼터링 방법으로 제작한 ITO/SiO_2/PEN 기판의 투습특성 조사** 이 성호, 김 영태, 이 도경, 오 지훈, 최 수호, 정 상권[1](*구미전자기술연구소. [1]경북대학교 물리학과.*) 본 연구에서는 Flexible 디스플레이용 기판의 투습방지막 형성을 위하여 실온에서 RF(13.56 MHz) 마그네트론 스퍼터링 방법으로 PEN(Polyethylenenapthalate) 필름 위에 SiO_2 (Silicon oxide)와 ITO(Indium tin oxide) 박막을 증착하였다. 박막 증착에 사용된 고상 타겟의 직경, 두께, 순도는 각각 3 inch, 6 mm, 99.99%이며 타겟과 기판 간의 거리는 90 mm로 고정하였다. ITO/SiO_2/PEN 기판의 투습율, 표면거칠기, 전기전도도는 각각 MOCON permeability tester(Permatran-W 3/33), AFM(Atomic force measurement), 4-point probe로 조사하였다. Flexible 기판의 투습율은 SiO_2 박막의 표면거칠기에 따라 증가하였으며 ITO 박막의 두께 200 nm 이하에서 최소값을 가졌다. 그러나 그 이상에서는 오히려 증가하는 경향을 나타내었으며 전기전도도도 감소하였다. 이는 박막의 스트레스 증가에 따른 결함에 기인한 것으로 여겨진다. 제작된 Flexible 기판의 투습율은 ~0.1gm/[m^2-day]@38℃의 값을 가졌다.

Dp-192 **Cr surface diffusion effect study on annealing of Cr:Nb_2O_5 films** 이 상, 박 원구[1], 오 세정[1]

(*서울대학교 물리학부. [1]CSCMR, School of Physics, Seoul National University.*) Cr-doped niobium oxide films are fabricated by pulsed laser deposition. Films are made as a standard of two conditions. One of them is that $Cr:Nb_2O_5$ films are grown directly on p-type silicon substrates, and the other is samples are made as a method of patterning platinum on chromium-added Nb_2O_5 films. In order to deposit Pt, molybdenum mask and Pt sputtering equipment in Inter-University Semiconductor Reserch Center are used. When these samples by two defined conditions are deposited by PLD, film growth is performed under same substrate temperature, ambient oxygen pressure, and deposition time. And then, each sample including two conditions is annealed to various temperatures. After fabrication, the binding energy about each element in oxidation film is measured by x-ray photoelectron spectroscopy. I have 200℃, 400℃, 600℃ -annealed and no-annealed samples which is grown to platinum and not measured. Finally, after the chemical composite ratio of niobium and oxygen is analyzed from XPS fitting program, the diffusion degree onto the surface of chromium in oxide is represented on annealing temperatures.

Dp-193 **Sm^{3+} ion concentration and substrate effect on the luminescent characteristics of Sm-doped YVO_4 thin films grown by pulsed laser deposition** 양 현경, 심 규성, 정 예란, 정 종원, 문 병기, 최 병춘, 정 중현, 이 성수[1], 김 중환[2](*부경대학교, 물리학과. [1]신라대학교, 전자재료공학과. [2]동의대학교 물리학과.*) YVO_4 and Sm^{3+} ion have been attracted as a host material and an activator for phosphor, respectively. YVO_4 thin films with various Sm^{3+} ion concentrations have been grown on various substrates using a pulsed laser deposition technique. The Sm^{3+} concentration was varied from 1.0 to 7.0 mol %, and the MgO(100), Si(100), Al_2O_3 (0001), and Fused Sillica substrates were used. Thin films were grown under the oxygen pressures of 150 mtorr and substrate temperatures of 600 °C. The crystalline structure, surface morphology characteristics, chemical states, and photoluminescence properties of the Sm-doped YVO_4 films were analyzed using X-ray diffraction, scanning electron microscope, X-ray photoelectron spectroscopy, and spectrophotometer, respectively. The films grown at various Sm^{3+} contens and substrates show the different crystallinity, surface morphology, and luminescent properties. The room temperature photoluminescence spectra were dominated by the red emission peak at 603 nm radiated from the transition of $^4G_{5/2}$-$^6H_{7/2}$ within Sm^{3+} ions. We found that the luminescence spectra of the films are highly dependent on the crystallinity and surface roughness of the films. And the surface roughness and luminescence intensity of the films showed similar behavior as a function of Sm^{3+} concentration.

Dp-194 **Photoluminescence characteristics of pulsed laser ablated $Y_xGd_{1-x}VO_4:Eu^{3+}$ thin film phosphors grown on Al_2O_3 (0001) substrate** 심 규성, 양 현경, 정 예란, 정 종원, 문 병기, 최 병춘, 정 중현, 이 성수[1], 김 중환[2] (*부경대학교, 물리학과. [1]신라대학교, 전자재료공학과. [2]동의대학교 물리학과.*) Red emitting $Y_xGd_{1-x}VO_4:Eu^{3+}$ oxide luminescent thin films were grown on Al_2O_3 (0001) substrates using pulsed laser deposition. The microstructure and surface morphology of $Y_xGd_{1-x}VO_4:Eu^{3+}$ films grown under different deposition conditions have been analyzed by X-ray diffraction (XRD) and atomic force microscope(AFM), respectively. The crystallinity and the surface morphology of the films are highly dependent on the molar ratio of Y/Gd. Photoluminescence spectra have been measured at room temperature using a luminescence spectrometer and excitation by a broadband incoherent ultraviolet light source with a dominant excitation wavelength of 312 nm. The luminescent characteristics of $Y_xGd_{1-x}VO_4:Eu^{3+}$ presented that the photoluminescence spectra depended not only on the crystalline phase but also the surface roughness of the films. The phosphor thin films showed a strong red emission at 619 nm radiated from the hypersensitive transition $^5D_0$ – $^7F_2$ of Eu^{3+} ions. In particular, the incorporation of Y into Gd_2O_3 lattice could induce a remarkable changeof PL. The highest emission intensity was observed with $Y_{0.4}Gd_{0.6}VO_4:Eu^{3+}$ films, whose brightness was increased by a factor of 1.5 in comparison with that of $GdVO_4:Eu^{3+}$ films.

Dp-195 **Relationship of Lattice Relaxation and Local Structure for ZnO Thin Films** 유 청종, 성 낙언, 이 익재, 주 만길[1], 김 형국[2](*포항가속기연구소, 빔라인부. [1]포항산업과학기술연구원. [2]부산대학교, 나노기술과학대.*) The epitaxial growth of ZnO thin films on Al_2O_3 (0001) substrates have been achieved at a low-substrate temperature of 200℃ using a dc reactive sputtering technique. ZnO films were grown on Al_2O_3

(0001) substrate at several temperatures ranging from 200 °C to 600 °C. We observed that the crystal quality of ZnO films were considerably sensitive to the growth temperatures. The crystal structure of the ZnO thin films were characterized using x-ray diffraction (XRD). XRD θ-2θ scan, ω scan and ϕ scan indicate that the ZnO films have a good c-axis orientation and in-plane epitaxy. The local structure of the ZnO thin films were studied using angle-dependent x-ray absorption fine structure (XAFS) at the Zn K edge. Also, we can describe the angle and distances of neighboring atoms from a probe atom to investigate the angle-dependent residual strain in ZnO films.

Dp-196 **Li-doping Effect on The Luminescent Characteristics of $CaTiO_3:Pr^{3+}$ Thin Films** 양 현경, 정 예란, 심 규성, 정 종원, 문 병기, 최 병춘, 정 중현, 이 성수[1], 김 중환[2](*부경대학교, 물리학과. [1]신라대학교, 전자재료공학과. [2]동의대학교, 물리학과.*) Li-doping has been interested to improve the luminescent characteristics of thin-film phosphors. Li-doped $CaTiO_3:Pr^{3+}$ luminescent thin films have been grown on Al_2O_3 (0001) substrate using a pulsed laser deposition technique at various oxygen pressure and substrate temperature. The Li^+ ion concentration was varied from 0.5 to 20 wt.%. The crystallinity and surface morphology of the films were investigated using X-ray diffraction (XRD) and atomic force microscope (AFM), respectively. Crystalline phase and surface morphology of thin films have been very important factors to determine luminescent characteristics of thin films. The crystallinity of $CaTiO_3:Pr^{3+}$ films were improved by Li-doping as shown the relatively intense and sharp peaks in the X-ray diffraction pattern. Photoluminescence (PL) spectra have been measured at room temperature using a luminescence spectrometer and excitation by a broadband incoherent ultraviolet light source with a dominant excitation wavelength of 332 nm. The emitted radiation was dominated by the red emission peak at 614 nm radiated from the transition of $^1D_2$-$^3F_4$ of Pr^{3+} ions. In particular, the incorporation of Li^+ ions into $CaTiO_3$ lattice could induce an increase of photoluminescence. The enhanced luminescence results not only from the improved crystallinity but also from the reduced internal reflections caused by rougher surfaces. The luminescent intensity and surface roughness exhibited similar behavior as a function of Li^+ ion concentration.

Dp-197 **Quasi-Persistent Photocurrent in $V_2O_5nH_20$ thin flim** LEE Cheol Eui, KWON Hyocheon, LEE Kyu Won[1](*Korea University, Physics. [1]Korea University, Institute for Nano Science.*) $V_2O_5nH_20$ flims, which has a layered structure of vanadium oxide layers intercalated with waters, were obtained by spin casting gels of V_2O_5 and hydrogen peroxide. The electrical property was studied in air and in vacuum. The current-voltage characteristics were measured along the directions parallel and perpendicular to the vanadium oxide layer. On all occasions, the conductivity measured along the parallel direction to the vanadium oxide layer was larger than that measured along the perpendicular direction. The photocurrent was measured as a function of the light-irradiation time. The photo-conductivity showed a remarkable enhancement in vacuum. The photocurrent decay measured just after the light switching off, namely quasi-persistent photocurrent, did not depend on the irradiation in vacuum but did in air.

Dp-198 **^1H nuclear magnetic resonance study of $(TMTSF)_2ReO_4$ organic conductors** LEE Cheol Eui, KIM Se Hun, LEE Kyu Won[1](*Korea University, Physics. [1]Korea University, Institute for Nano Science.*) We have studied the anion-ordering phase transition in the organic conductors $(TMTSF)_2ReO_4$, where TMTSF indicates tetramethyltetraselenafulvalene by means of ^1H nuclear magnetic resonance (NMR). The ^1H NMR spin-lattice (T_1) and spin-spin relaxation time (T_2), representing dynamics of the TMTSF donor molecules, manifested an anomaly associated with the anion-ordering phase transition around 180 K. The spin-latteic relaxation curve was a single-exponential form above the transition temperature but becomes a non-exponential form below the transition temperature, indicating that an additional contribution to the spin-lattice relaxation occurs in the anion-ordered phase.

Dp-199 **황색 형광체 $Y_3Al_5O_{12}:Ce^{3+}$와 $(Ba, Sr)_2SiO_4:Eu^{2+}$의 열 특성 비교 분석** 최 남식, 이 성훈, 박 부원, 김 종수(*부경대학교 화상정보공학부 이미지시스템공학전공.*) 백색 LED는 가장 유망한 고체광원중 하나로서 우수한 성능을 바탕으로 디스플레이 및 조명용 광원으로 그 비중을 높이고 있지만 많은 열이 발생된다는 문제점을 가지고 있기 때문에 백색 LED에 사용되는 형광체 또한 그에 맞는 열 특성이 요구된다. 본 연구는, GaN

청색 LED위에 청색광을 흡수하여 황색을 발광하는 형광체을 패키징한 가장 대표적인 백색 LED 구조에 사용되는 형광체인 $Y_3Al_5O_{12}:Ce^{3+}$(YAG)와 $(Ba, Sr)_2SiO_4:Eu^{2+}$(BOS)의 열 특성을 비교 분석하였다. 일반 적인 발광 특성을 알아 보기 위하여 광발광(PL)과 색좌표를 측정하였다. 그리고 온도에 따른 발광특성 분석하기 위하여 30℃에서 300℃까지 가열, 냉각시의 온도의존 광발광(PL)과 그에 따른 색좌표의 변화를 측정하였다. 그 결과 YAG 형광체는 BOS 형광체에 비하여 quenching 온도가 우수하고, 온도에 따른 색좌표의 변화가 거의 없이 안정하지만, 300℃까지 가열후에 냉각 시켜도 본래의 밝기를 회복하지 못하는 열퇴화가 발견되었다. 이는 YAG 형광체에 도핑되는 Ce^{3+}이온이 열에 의해서 Ce^{4+}이온으로 산화되기 때문인 것으로 생각되어진다. 그리고 BOS 형광체는 YAG 형광체에 비하여 quenching 온도가 떨어지며, 온도가 증가함에 따라 색좌표가 황색에서 녹색으로 발광색이 급격히 변화하는 것이 관찰되었다. 이는 BOS 형광체의 2가지 발광 피크 중에서 황색영역의 피크가 녹색영역의 피크보다 온도에 대한 영향을 크게 받기 때문이라 여겨진다. 그러나 YAG 형광체에서와 같은 열퇴화는 발견되지 않았다.

Dp-200 **대향타겟식 스퍼터 (FTS) 제작 및 SiO_xN_y 박막 공정 특성** 안 병철, 우 병재, 홍 재석[1], 류 성원[1], 박 승환[1], 김 종재[1], 홍 우표[1], 김 화민[1]*((주)AVACO. [1]대구가톨릭대학교,전자공학과.)* 본 연구는 OLED의 passivation 박막을 증착하기 위한 공정 방법으로서, 기존의 sputter 방법에 의한 치밀한 구조의 박막을 형성할 수 있는 잇점을 살리고, 플라즈마나 열에 의한 유기 층의 손상을 방지하기 위한 대안으로써, 대향타겟식 스퍼터링 (FTS : Facing target sputtering) 방법을 제시한다. 이를 위해서 OLED 용passivation 방식의 system 최적 공정 기술 개발을 목표로 기존의 개발되어 있는 Laminator System과 연계하여 고속 저온증착이 가능한 FTS 시스템 (370×470 ㎟)을 직접 제작하였다. 제작된 FTS의 공정 특성을 평가하기 위하여 먼저, 캐소우드 자기장 배열에 따른 플라즈마 안정성과 타겟과 타겟 사이와 타겟과 기판 사이의 거리 변화에 따른 최적 공정 특성 그리고 가스 유입에 따른 방전 전압의 hysteresis 특성이 매우 안정하며, 재연성이 우수함을 보여 줌으로써, 본 시스템의 공정에 대한 신뢰성을 확보한 후, 규격 200 x 200 mm^2의 유리 기판 위에 성막된 SiN_x 박막의 광학적 특성과 구조적 특성을 평가하여 ± 5% 이하의 uniformity와 550 nm에서 광투과율이 85 % 이상인 양질의 박막과 아울러 N_2 가스 분위기에서 고 밀도의 실리콘 질화 박막이 형성됨을 제시하고, 특히 400 nm 이상의 두께를 갖는 박막 성막 시 80 °C 이하의 공정 대응이 가능함을 보여 준다. 또한 FTS 공정을 사용하여 실제 OLED 소자에 SiN_x 박막을 passivation 층으로 성막한 결과, 영구자석의 배열이 순방향일 때, OLED 소자의 damage를 최소화 할 수 있었으며, 그 결과 passivation 박막 성막 후 OLED 소자의 휘도가 크게 영향을 받지 않는 것을 확인하였다.
*본 연구는 대구테크노파크의 차세대선도산업기술 연구개발사업의 지원에 의해 수행되었음.

Dp-201 **Probe Designs for In-Situ NMR Analysis of Direct Methanol Fuel Cells** HAN Kee Sung, HAN Oc Hee[1], PAIK Younkee[1], KIM Seong Soo[1], LEE Moohee(*Deparment of Physics, Konkuk University. [1]Daegu Center, Korea Basic Science Institute.*) Fuel cells convert the chemical energy of fuels directly into electricity by oxidation of the fuels. There are several kinds of fuel cells such as direct methanol fuel cells (DMFCs), solid oxide fuel cells (SOFCs), polymer electrolyte fuel cells (PEFCs), and phosphoric acid fuel cells (PAFCs), etc. Among them, a DMFC appears to be the most promising as battery replacement for portable applications such as cellular phones and laptop computers due to its higher power density at lower temperature, rather simple structure and easy management. However, it is difficult to get reasonable power density to commercialize the DMFC because methanol crossover from the anode to the cathode through the membrane and catalysts poisoning formed during methanol oxidation result in performance reduction of the DMFC with operating time. To improve the DMFC performance in the viewpoint of electrocatalysts, it is necessary to investigate dynamic aspect of direct methanol oxidation and of oxygen reduction reaction in Pt based electrocatalysts of a DMFC in real operating conditions. Here, our NMR probe head designs for in-situ analysis of a single cell of DMFC will be introduced and recent results obtained with the probe head will be presented.

Dp-202 **Preparation and characterization of Gd_2O_3:Eu Ceramic scintillator** 노 용석, 김 수호, PHAN Van Cuong, 강 승렬[1], 박 정병[2], 이 충화[2], 김 도형(*경북대학교. [1]한국전자통신연구원. [2]디알젬.*) The polycrystalline Gd_2O_3:Eu ceramic scintillator was synthesized by solid-state-reaction with varying the synthesis temperature. We investigated the effects of crystallinity and phases of Gd_2O_3:Eu on the excitation and emission spectra. From the XRD spectra, we observed that the structural transition from α-Gd_2O_3(cubic) to β-Gd_2O_3(monoclinic) is oc-

curred at the 1250°C. Gd_2O_3:Eu synthesize below 1250°C have cubic structure, and show a strong red emission at 612nm originating from the hypersensitive transition $^5D_0 \rightarrow ^7F_2$ of Eu^{3+} ions by the excitation charge transfer state(CTS). However, monoclinic Gd_2O_3:Eu synthesize over 1250°C, and show a emission peak at 628nm ($^5D_0 \rightarrow ^7F_2$) with a different main excitation of gadolinium $Gd^{3+}(^8S_{7/2} \rightarrow ^6I_{11/2})$.

Dp-203 **Luminescence of $Gd_{1-x}Y_xEu_{0.06}O_3$ ceramic scintillator and their optimum synthesis condition** 노 용석, 김 수호, PHAN Van Coung, 강 승렬[1], 박 정병[2], 이 충화[2], 김 도형(*경북대학교. [1]한국전자통신연구원. [2]디알젬.*) $Gd_{1-x}Y_xEu_{0.06}O_3$ ceramic scintillator was prepared for the application of the x-ray imaging system. We investigated the effect of the yttrium doping in Gd_2O_3 matrix on the crystal structure and luminescent intensity by the measurements of x-ray diffraction (XRD), X-ray Excited Luminescence Spectroscopy (XELS), Photoluminescence (PL). $Gd_{1-x}Y_xEu_{0.06}O_3$ ceramic scintillators have both phases of Gd_2O_3 and Y_2O_3 at the optimized temperature in the synthesis of Gd_2O_3:Eu ceramic scintillator. However, the increase of the synthesis temperature is required for a single phase of $Gd_{1-x}Y_xEu_{0.06}O_3$ ceramic scintillator. It is suggested that the synthesis temperatures have to be optimized for better crystallinity and light output corresponding to yttrium doping rate.

Dp-204 **UV laser를 이용한 용액 중 C_{60} aggregates의 광중합 반응에 관한 연구** 여 승준, 박 소라, 차 정옥, 신 진호, 김 화민[1], 안 정선(*경희대학교 물리학과. [1]대구카톨릭대학교 전자공학과.*) Fullerene(C_{60})은 아크 방전법을 이용한 거시적 스케일의 생산기술이 개발된 이후 현재까지도 다양한 분야에서 활발한 연구가 진행 중이며, 그 동안 C_{60}의 독특한 분자 구조에 기인한 많은 특성들이 밝혀졌다. 그 중에서도 광, 압력 그리고 도우핑된 금속에 의해 쉽게 플러렌 중합체(polymerized fullerene)를 형성하는 현상은 C_{60}의 독특한 분자 구조에 기인한 대표적인 특성 중의 하나라고 하겠다. 기존에는 쉽게 중합체를 형성하는 이러한 특성을 이용하여 주로 bulk 상태에서 중합체 형성이 시도 되었으며 이때 형성된 C_{60} 중합체는 나노 크기의 구조체 형성에 있어 크기를 제어하기가 불가능하고 생성된 C_{60} 중합체를 bulk 물질에서 분리하기가 어려운 단점이 있다. 나노 크기의 구조체 형성을 기본 목적으로 하는 본 연구는 bulk 상태의 C_{60}에서 중합체를 형성한 기존 방법과는 달리 용액 중에서 나노미터 크기의 C_{60} aggregates을 형성하고 C_{60} aggregates내에서의 광중합 반응을 이용하여 나노 구조체를 형성하려는 시도로서 이때 형성된 광 중합체는 그 사이즈가 C_{60} aggregates의 사이즈에 의해 제한될 것으로 기대되며, C_{60}의 광중합 반응을 이용한 나노 구조체 형성을 위해서는 나노미터 크기의 C_{60} aggregates을 용액 중에서 생성하는 것이 필요 불가결한 사항이다. 최근 우리는 C_{60}의 PL 스펙트럼을 측정하여 용액 중에서 나노미터 크기의 C_{60} aggregates의 형성을 보고한 바 있다. 나노미터 크기의 C_{60} aggregates은 특정 농도 이상의 C_{60} 용액을 냉각하는 과정에서 용액의 어는점에서 생성되며, C_{60} aggregates 내부의 C_{60}분자 간의 결합이 약하여, 상온에서는 분자상태로 복귀하는 weakly bound cluster 이다. 또한 이전 연구에서 톨루엔 용액 중 생성된 C_{60} aggregates의 PL 스펙트럼을 분석한 결과, C_{60} aggregates의 직경이 C_{60} 분자 3개에 크기에 해당되는 나노미터 영역의 aggregates임을 제안한 바 있다. 본 연구에서는 이들 용액 중에서 형성된 나노미터 크기의 C_{60} aggregates의 광중합 반응을 이용하여, 나노 크기의 안정된 결합을 가진 구조체 형성의 가능성을 조사하였다. C_{60} aggregates에 UV pulse laser(Nd:YAG laser, 355 nm)를 조사하는 과정에서의 PL 스펙트럼의 변화를 측정하여 광중합 반응 여부를 조사하였다. UV pulse laser의 조사 전후의 스펙트럼 변화를 비교한 결과 광중합 반응 전과 후의 스펙트럼의 형태는 큰 변화를 보임을 알 수 있었다. 특히 광중합 반응 후의 스펙트럼은 가시광 영역 전반에 걸친 넓은 스펙트럼 폭을 갖고 있는 백색 발광 특성을 보이고 있음을 알 수 있었다. 광중합 반응에 의하여 형성된 나노 구조체는 상온에서도 안정하였으며, High-Resolution TEM image를 이용하여 관측한 결과 구형의 나노 입자임을 확인 할 수 있었다.

Dp-205 **Site-selective fluorescence spectroscopy를 이용한 protein dynamics의 광학적 특성 연구** 신 진호, 차 정옥, 여 승준, 박 소라, 안 정선(*경희대학교.*) Natural optical probe를 지닌 chromoprotein을 대상으로 한 protein dynamics의 광학적 연구가 꾸준히 진행되고 있다. 이는 chromoprotein의 optical spectrum으로부터 단백질 구조(conformation)의 정보(Fluctuation, Relaxation, etc)들을 얻을 수 있고, 그 성질은 저온에서 amorphous mtrices 의 분석결과와 매우 유사한데, 이는 충분히 낮은 온도에서의 chromoprotein이 glass-like 한 특성 때문이다. 그러나 chromophore과 polypeptide chain의 위치가 glass-like choromoprotein에서는 잘 정의 되어지나, dye-doped polymer의 경우 dye-molecule의 microscopic environment를 정확히 정의할 수가 없다. 이는 inhomogeneous broadening이라 불리는 spectral broadening이 야기되기 때문이다. 이때 동일한 optical transition energy를 갖는 각 microenvironment를 site라 부른다.

Protein 분자에서 필요한 정보를 얻기 위해서는 inhomogeneous broadening를 야기하는 the site-energy distribution과 inhomogeneous broadening의 영향이 없는 homogeneous spectrum을 구별해야 한다. 우리는 site-selective fluorescence method를 이용하여 single-site fluorescence에 대한 중요한 정보뿐만 아니라, WDOS 에 대한 정보를 얻음으로써 site-selective fluorescence method의 높은 효율성을 검증했다. 그러나 실험에 있어서, exiting light의 wavelength와 fluorescence spectrum의 resonance line의 wavelength가 동일하여 resonance line을 spectrum상에서 정확히 구별하기가 어렵다는 문제가 있었다. 이를 해결하기 위하여 time-correlated single-photon counting technique과 CW mode locked laser의 repeatative short light pulses를 이용하였다. Chromoprotein으로는 protein dynamics 연구에 널리 사용되는 myoglobin을 선택하였고, Fe-protoporphyrin을 chromophore로 가진 native myoglobin의 경우 fluorescence spectrum을 관찰할 수 없기 때문에 Chromophore로서 Fe를 다른 Zn으로 대체한 Zn-substituted myoglobin과 Mg으로 대체한 Mg-substutyted myoglobin을 사용하였다.

Dp-206 **황녹 형광체 $(Sr_{1-x-y}Ba_xEu_y)_2SiO_4$의 x/y에 따른 광학적 특성 연구** 서 광일, 이 성훈, 박 부원, 최 남식, 김 상지, 김 종수(*부경대학교 화상정보공학부 이미지 시스템공학과.*) 질화물반도체(GaN)를 이용한 청색 혹은 근자외선에서 여기되어 백색광원으로 사용할 수 있는 $(Sr_{1-x-y}Ba_xEu_y)_2SiO_4$ 형광체의 x의 따른 광학적 색변환 특성에 대해 연구하였다. 고상반응법으로 $(Sr_{1-x-y}Ba_xEu_y)_2SiO_4$를 제작하고, XRD(X-ray diffraction)를 이용 단일상을 확인하였고, 광발광(PL) 측정결과를 토대로 광발광 스펙트럼에서 활성제(Eu^{2+})의 소광농도를 찾는다. $(Sr_{1-x-y}Ba_xEu_y)_2SiO_4$에서 x의 값이 증가할수록 광발광 스펙트럼의 위치는 장파장 발광에서 단파장 발광으로 이동한다. 따라서 모체의 조성비에 따라 발광 파장을 제어 할 수 있으며, 또한 활성제의 소광농도(y)에 따른 발광휘도도 제어할 수 있다. 한 격자내의 두 개의 Eu^{2+} sites에 따른 황색과 녹색 발광 스펙트럼이 형성되고, x의 양이 증가함에 따라 $Ba_2SiO_4:Eu^{2+}$의 특성이 크게 나타나 활성제의 소광농도가 감소되는 것을 확인하였다.

Dp-207 **Probing Hydrogen Dynamics in Nano-Channels of THF Clathrate Hydrate** PARK Sungil, CHOI Yong Nam, YEON Sun-Hwa[1], PARK Youngjune[1], LEE Huen[1](*KAERI. [1]KAIST.*) Inelastic neutron scattering is a powerful tool to probe hydrogen dynamics, especially of the hydrogen molecules trapped inside nano-scale voids of caged compounds. With the need to learn hydrogen dynamics ever rising thanks to the push toward the hydrogen economy, we have studied a binary THF-H2 Clathrate Hydrate by using an inelastic neutron scattering technique. At a low temeprature of 2 K, a well defined ortho (J=1) to para (J=0) hydrogen transition was observed at 13.6 meV. Additional peak apears at 14.7 meV, a free hydrogen value, above 10 K. Quasi-elastic neutron scattering (QENS) signal has also been observed above 65 K. We discuss the behavior of hydrogen molecules in the nano-channels of THF Clathrate Hydrate based upon these observations.

Dp-209 **Discrete thermal patterns on the neutron diffraction of THF+X_2(X=H, D, N, O) clathrate hydrate** CHOI Yong Nam, YEON Sun-Hwa[1], PARK Youngjune[1], CHOI Sukjeong[1], LEE Huen[1](*HANARO Utilization and Technology Development Division, Korea Atomic Energy Research Institute. [1]Department of Chemical and Biomolecular Engineering, Korea Advanced Institute of Science and Technology.*) The clathrate hydrate formed by the tetrahydrofuran(THF) was known as a structure II (sII) hydrate which has 8 large cages and 16 small cages composed by 136 water molecules within the unit cell. And this material has been known as a nano-caged system which can accomodate small guest molecules such as H_2, D_2, N_2, O_2 and CH_4 within the cage. From the temperature dependence of the neutron diffraction patterns obtained from the THF+gas (H_2, D_2, N_2 and O_2) clathrate hydrates, discrete thermal dehaviors were analyzed and compared. Heavy water and deuterated THF were used for the sample synthersis to get rid of high incoherent scattering from the hydrogen nuclei. The dynamic behavior of each guest molecules will be discussed by the temperature dependence of the lattice parameter and the scattering intensities.

Dp-210 **Electromagnons in Lattice-coupled Triangular Antiferromagnets** 한 정훈, 김 정훈(*성균관대학교 물리학과.*) We investigate the influence of the spin-phonon coupling in the triangular antiferromagnet where the coupling is of the exchange-striction type. The magnon dispersion is shown to be modified significantly at wave vector $(2\pi,0)$ and its symmetry-related points, exhibiting a roton-like minimum and an eventual instability in the dispersion. Various correlation functions such as equal-time phonon correlation, spin-spin correlation, and local magnetization are calculated in the presence of the coupling.

■ SESSION: P1
4월 19일 (목), 14:30 - 16:15
스키하우스

P1
포스터세션
Ep

Ep-001 **Magneto-optical Kerr Effect of Magnetic Gratings** KIM J. B., LEE G. J., LEE Y. P., RHEE J. Y.[1], YOON C. S.[2](*Quantum Photonic Science Research Center and BK21 Program Division of Advanced Research and Education in Physics, Hanyang University, Korea. [1]BK21 Physics Research Division and Institute of Basic Science, Sungkyunkwan University, Korea. [2]Division of Advanced Materials Science, Hanyang University, Korea.*) The magneto-optical properties of one-dimensional magnetic-grating structure of Co_2MnSi film were investigated. Amorphous Co_2MnSi films were prepared by rf-magnetron sputtering on a glass substrate at room temperature. The as-deposited films exhibit no magnetic response at room temperature. By using the interference pattern of two femtosecond-laser beams, a selective-area annealing of the as-deposited Co_2MnSi film was achieved and one-dimensional magnetic-grating structures were fabricated. The atomic-force-microscopy and the transmission-electron-microscopy results confirmed that regularly-spaced alternating lines with a periodicity of 2 μm were produced, and the magnetic-force-microscopy studies reveal the same periodic patterns of magnetic domains. The longitudinal Kerr rotations of the zeroth- and the first-order diffracted beams were measured. The longitudinal Kerr rotation of the first-order diffracted beam is nearly 18 times larger than that of the zeroth-order beam.

Ep-002 **유기첨가제에 의한 전기도금 연자성 박막의 GMI효과 향상** 방 원배, 홍 기민, 이 희복[1](*충남대학교 물리학과. [1]공주대학교 물리교육과.*) 연자성 박막의 GMI(Giant Magnetoimpedance) 효과를 향상시키기 위해서는 표면 거칠기가 낮은 기판, 낮은 보자력 값, 그리고 높은 투자율이 필요하다. 본 연구에서는 니켈-철 Permalloy 연자성 합금박막을 전기도금 방법으로 제작하였다. 유기첨가제 SNPS를 Permalloy 도금용 전해액에 미량 첨가하여 도금한 박막들의 경우 SNPS의 농도 증가에 따라 VSM(Vibration Sample Magnetometer)으로 측정한 보자력 값이 0.92 Oe에서 0.29 Oe 로 감소하였고, AFM(Atomic Force Microscopy)으로 표면을 관찰한 결과 표면 거칠기는 7.6 nm에서 2.7 nm로 감소하였다. 이에 따라 실제 GMI 변화를 측정한 결과 주파수 영역에 따라 최대 약 20 %의 증가를 보였다. 유기첨가제 SNPS는 전기도금 시 확산거리를 줄여주고, 용액내의 grain 크기를 작게 하여 표면 거칠기를 감소시키는데, 그 결과로 보자력 값이 감소하고 GMI 효과가 증가하는 것으로 판명되었다.

Ep-003 **감마선 피폭에 의한 HDPE의 중성자 감속능 변화 평가** 박 광준, 주 준식, 강 희영, 신 희성, 김 호동(*한국원자력연구소.*) 고밀도 폴리에틸렌(HDPE)은 사용후핵연료 처리시설에서 특수 핵물질 계량을 위한 중성자 검출시스템의 중성자 감속재로 사용된다. HDPE 감속재의 방사선 피폭 효과는 습식재처리와 같이 최종 산출물인 우라늄과 플루토늄에 감마선을 방출하는 핵분열 생성물이 포함되지 않는 경우의 핵물질 계량에서는 별 문제가 되지 않는다. 그러나 건식처리에서와 같이 최종 산출물의 핵물질내에 핵분열 생성물이 잔존하는 경우, HDPE 감속재는 핵분열 생성물에서 방출되는 감마선에 의해 영향을 받게 된다. 그래서 중성자 감속능은 HDPE분자구조의 변화, 팽윤(swelling), 방사선유도 산화 등으로 인해 변화될 수 있다. 그러므로, 핵물질 측정에서 얻은 자료를 정확하게 분석하기 위해서는 방사선 피폭에 따른 HDPE의 중성자 감속능 변화량을 확인하는 것이 필요하다. 본 연구에서는 HDPE 중성자 감속재의 방사선 피폭 선량에 따른 중성자 감속능 변화량을 실험적으로 검증하기 위하여 여섯 개의 동일한 HDPE 구조물을 제작하여 10^5 rad, 10^6 rad, 10^7 rad, 10^8 rad 및 10^9 rad 로 감마선에 조사시켜 시간 경과에 따른 중성자 측정시험을 수행하였다. 중성자 측정시험 결과, 10^5 rad 조사시킨 HDPE의 감속능이 감마선조사를 시키지 않은 순수한 HDPE에 비해 약 7% 감소된 것을 확인하였다. 반면에 다른 조사선량의 HDPE의 중성자 감속능은 순수한 HDPE에 비해 큰 변화가 없었다. 이러한 결과는 감마선조사 HDPE의 중성자 감속능은 집적선량에 의존하지 않고, 특정 피폭선량에서 주로 변한다는 것을 의미한다. 이러한 실험적인 결과의 원인을 규명하기 위해서 비조사 및 조사 HDPE 구조물로부터 시편을 채취하여 물성분석을 수행하였으며, 물성분석 결과, HDPE 의 분자구조 변화를 확인하였다.

Ep-004 **Fe60Mn40 기계적 합금의 자성 및 구조분석** 양 동석, 김 나영, 유 성초(*충북대학교.*) 기계적 합금법으로 제조된 Fe60Mn40의 미세구조 및 자기적특성을 분석하여 구조 및 자기적 특성과의 관련성을 조사하였다. 기계적 합금화 시간은 1, 2, 4, 6, 12, 24이었으며 각 시료의 구조는 XRD 및 EXAFS 에 의해 분석 되었다. XRD 분석에 의하여 시료의 long range order이 조사 되었고, EXAFS에 의하여 시료의 local structure가 조사되었다. XRD 분석 결과 1시간 이내에

시료들의 Mn peak들이 현저히 줄어들고 12시간이 지나면서 시료가 거의 비정질화 되는 것이 관측되었다. EXAFS 분석 결과 12시간에서 local structure가 급격히 변화하는 것이 관측되었다. 시료의 자기적 특성은 VSM에 의해 측정되었고 시료의 자화는 기계화합금 시간이 경과함에 따라 점차 감

Ep-005 **Dielectric anomalies at the magnetic transition in a bismuth ferrite.** 송 기명, 허 남정, 이 재일, THOMPSON J. D.[1], 박 영안(*Department of Physics, Inha University. [1]Los Alamos National Laboratory, Los Alamos, NM 87545, USA.*) We will report the magnetic and dielectric properties of $Bi_2Fe_4O_9$ single crystals in this presentation. Observed dielectric anomalies at the magnetic transition and their frequency dependence will be discussed in terms of the exchange interaction effect on the dielectric function. It was found that both the magnetic properties and the dielectric anomalies at T_N are strongly anisotropic, suggesting a strong correlation between magnetism and dielectric properties in these compounds.

Ep-006 **Study Of The Droplet''s Motion In Aqueous Solution** SONG Chaeyeon, MOON Jong Kyun(*Soft Condensed Matter Physics Lab, Physics.*) Our work is a fundamental study on the movement of micro-liter droplets on a liquid's surface subjected to interfacial tension gradients. The interfacial tension gradients were induced by using laser heating. The droplets using Nitrobenzene oil contain I_2 and KI to achieve very high absorbance of the light inside the oil droplet. The droplets showed two types of motion. Directed motion of an oil droplet floating in an aqueous solution can be switched between forward and backward by changing the optical path of the laser through the droplet. The other motion of oil droplet is a periodic pumping. The induced surface tension caused the changing of the droplet's shape. This generated restoring force and resulted in periodic pumping of oil droplet. This pumping motion of droplet was changed by the laser intensity and the optical position of the laser.

Ep-007 **전하트랩층과 전하저지층을 이용한 고효율 유기발광소자 제작 및 발광특성** 곽 병찬, 추 동철[1], 김 태환[1], 서 지현[2], 김 영관[2](*한양대학교 정보디스플레이공학과. [1]한양대학교 전자통신컴퓨터공학부 디스플레이공학연구소. [2]홍익대학교 정보디스플레이공학과.*) 정공의 이동도를 줄여주는 전하저지층을 정공수송층에 삽입하고 정공과 전자의 재결합 확률을 높이는 전하트랩층을 발광층에 삽입하여 고효율 유기발광소자를 제작하였다. 전하저지층은 전자나 정공의 주입을 방해하는 에너지 장벽으로 작용하는 물질로 1,3,5-tris(N-phenylbenzimidazol-2-yl)benzene (TPBi)를 정공수송층에 삽입하였고 전하트랩층은 전자나 정공을 포획하여 전하의 흐름을 조절할 수 있는 물질로 5,6,11,12-tetraphenylnaphthacene (rubrene)을 발광층에 삽입하였다. 전하저지층과 전하트랩층이 삽입되지 않은 소자, 전하트랩층만이 삽입된 소자, 전하저지층과 전하트랩층이 모두 삽입된 소자를 제작하여 전류밀도-전압, 휘도-전압, 전류밀도-발광효율을 측정하였다. 전하저지층과 전하트랩층이 모두 삽입된 소자는 동일전압에서 가장 높은 전류밀도를 보이며 가장 낮은 개시전압을 나타낸다. 전하트랩층이나 전하저지층의 삽입으로 인한 개시전압의 증가는 보이지 않으며 발광효율도 개선되었다. 발광층 영역에 삽입된 전하트랩층은 정공과 전자가 발광층으로 주입될 확률을 향상하고 정공수송층에 삽입된 전하저지층으로 인해 발광층에서 전자와 정공수의 균형을 이루어 낮은 개시전압 특성과 높은 발광효율을 나타내는 고효율 유기발광소자를 제작할 수 있었다. 제작된 유기발광소자의 전기적 및 광학적 특성으로부터 고효율 발광메카니즘을 제시하였다.

*이 논문은 2006년도 정부재원(교육인적자원부 학술연구조성사업비)으로 한국학술진흥재단의 지원을 받아 연구되었음 (KRF-2004-005-D00166).

Ep-008 **Study of structure and dynamics of thin diblock copolymer films** LEE Heeju, LEE Young Joo, SONG Sanghoon[1], BYUN Youngsuk[2], KIM Hyunjung[3], JIANG Zhang[4], SINHA S. K.[4], RUEHM A.[5](*Dept. of Physics, Sogang University. [1]Interdisciplinary Program of Integrated Biotechnology, Sogang University. [2]Dept. of Physics, Sogang University. [3]Dept. of Physics and Interdisciplinary Program of Integrated Biotechnology, Sogang University. [4]Dept. of Physics, UC San Diego and LANSCE. [5]Metallforschung, MPI.*) We have investigated the dynamics of thin block copolymer films of poly(styrene)-b-poly(dimethylsiloxane) using X-ray Photon Correlation Spectroscopy (XPCS). The films were prepared on Si substrates and examined at melt (170℃-210℃). Block copolymer exhibit internal interactions and therefore an internal structure (in our case spherical micelles). This ought to have a strong influence on the surface dynamics of the thin films. The incident angles were chosen at 0.14° and 0.2° for studying selectively dynamics from surface and micelles in

films. The results was compared with the theory of over-damped thermal capillary waves on polystyrene films. We also obtained surface tensions and viscosities of block copolymer films.
*This research was supported by International Coorperation Research Program of Ministry of Science &Technology of Korea, Seoul Research &Business Development Program.

Ep-009 **유한차분시간구역 계산을 이용한 초해상 ROM 광디스크 재생 신호 연구** 김 준서, 유 천열, 곽 금철[1](*인하대학교. [1]LG Electronics Institute of Technology.*) ROM 형태의 광디스크의 재생신호는 디스크 표면의 피트의 유무에 따라 변하는 반사율을 이용하기 때문에, 회절한계보다 작은 크기의 피트에서는 아무런 재생신호를 얻을 수 없게 된다. 회절한계를 극복하기 위해서는 소위 초해상 현상이라고 알려진 방법을 이용해서 회절한계 이하의 피트에 대해서도 재생신호를 실험적으로 얻을 수 있지만, 초해상 현상의 물리적 이해는 매우 부족하다. 본 연구에서는 회절한계이하에서 재생신호를 얻기 위해서 온도에 따라서 굴절률이 변하는 GeSbTe (GST)층을 삽입하는 방법을 사용하였다. 본 연구에서는 GST층을 고려한 ROM 광디스크 구조에서 재생신호를 FDTD(finite-difference time-domail) 시뮬레이터를 이용하여 전산모사를 하였다. GST층의 온도에 따른 굴절률의 변화를 고려하여 전산모사를 한 결과, 회절한계 이하에서 재생신호를 얻을 수 있었으며, 최대 재생신호를 발생시키는 피트의 깊이는 GST층의 마크의 크기와 재생피트의 크기 그리고 마크와 재생피트의 상대거리에 따라서 다르다는 것을 확인하였다.

Ep-010 **Exact calculation of the optical response in simple structures made of nonlinear negative index media** KHUONG Phung Duy, 김 기홍, 임 한조[1](*아주대 에너지시스템학부. [1]아주대 전자공학부.*) Recently, it has been pointed out that in representative negative index media fabricated using split ring resonators, nonlinearity in the dielectric response causes stronger nonlinearity in the magnetic response. When dealing with these kinds of media, one needs to solve electromagnetic wave equations containing nonlinear dielectric permittivity and magnetic permeability. We have developed a new version of the invariant imbedding method for wave propagation in arbitrary stratified media where both dielectric permittivity and magnetic permeability depend on the intensity of the wave field. This method allows an exact calculation of all wave propagation characteristics. In particular, we consider the wave propagation in simple layered structures made of nonlinear negative index media and calculate the reflectance, the transmittance and the field distribution as a function of the electric field intensity exactly. We find that strong hysteresis occurs in these systems and the reflectance and transmittance curves show several kinks at some critical values of the field intensity. We explain this phenomenon by calculating the spatial distribution of the effective magnetic permeability.

Ep-011 **$(Zn, Mg)_2SiO_4$:Mn 형광체의 제조와 물성** LEE Ji-Young, YU Il(*동의대학교, 물리학과.*) Mn을 0.8mol% 첨가한 $Zn_xMg_{1-x}SiO_4$:Mn 형광체를 1300℃에서 4시간 동안 열처리하여 제조하였다. X-ray diffraction pattern의 측정 결과 Mg를 첨가함에 따라 $Zn_xMg_{1-x}SiO_4$:Mn 형광체는 Willemite 구조에서 Orthorhombic 구조로 결정이 변함을 관찰하였다. Photoluminescence측정결과, $Zn_xMg_{1-x}SiO_4$:Mn 형광체는 x의 양이 감소함에 따라 532nm였던 PL피크가 장파장대로 이동함을 관찰 할 수 있었고, 그에 따라 색좌표가 변화됨을 확인하였다.

Ep-012 **Phase-Contrast X-ray Imaging with Synchrotron Radiation for Medical Applications** KIM Ki-Hong, PARK Sung Hwan[1], KIM Hong-Tae[2], KIM Jong-Ki[3], JHEON Sanghoon[4](*Department of Visual Optics, Kyungwoon University. [1]Department of Surgery, College of Medicine, Catholic University of Daegu. [2]Department of Anatomy, College of Medicine, Catholic University of Daegu. [3]Department of Radiology and Biomedical Engineering, College of Medicine, Catholic University of Daegu. [4]Thoracic and Cardiovascular Surgery, College of Medicine, Seoul National University.*) The medical applications of synchrotron radiation(SR) continues to develop rapidly with new results and new techniques in a diverse range of programs. The different contrast mechanisms in image by x-ray are described. The phase-contrast X-ray imagings with SR from ex-vivo coronary angiograpy, breast cancer, lung, bone and nerve were obtained with an 8 Kev monochromatic beam and 20-μm thick CsI(Tl) scintillation crystal. The visual image was magnified using 20x microscope objective and captured using an analog CCD camera. The results showed more structural details and high contrast images with SR imaging system than conventional X-ray radiography system. The SR imaging system may have a potential for imaging in biological researches, material applications and clinical radiography

Ep-013 **식물 잎의 건조스트레스가 지연발광에 미치는 영향** 소 광섭, 강 준호[1], 김 대식[1], 정 대웅[1], 이 훈식[1], 박 상현(*서울대학교 물리학과. [1]한국과학영재학교.*) 모든 살아 있는 생물의 세포와 조직은 그 생명활동으로 자외선과 가시광선 및 적외선 영역(200nm-800nm)의 빛을 방출하는 것으로 알려져 있으며, 이를 생물광자(biophoton)라 한다. 물리학적 측면에서 생물광자의 중요성은 양자 결맞음(quantum coherence)특성을 보이므로 큰 관심을 끌게 되었다. 생물광자 중 외부의 빛 자극이 없이 세포수준에서 방출되는 것을 자발광(spontaneous photon emission)이라 하고, 외부에서 빛을 조사한 후 차단했을 때 방출되는 것을 지연발광(delayed luminescence)이라 한다. 이러한 생물광자의 발광 메커니즘에 대해서는 많은 가설들이 제시된바 있으나, 아직 정확히 입증된 메커니즘은 없다. 본 연구는 첫째, 식물에 건조스트레스(dehydration stress)가 주어짐에 따라 지연발광양이 어떠한 변화양상을 보이는지 관찰하였다. 건조스트레스는 일정한 온도, 습도에서 시료 채취 후 경과시간을 달리하며 조절하였다. 일반적으로 엽록체가 지연발광에 많은 영향을 준다고 알려져있는데, 이를 확증하기 위해 둘째, 엽록체가 존재하지 않는 꽃잎(flower)과, 엽록체가 존재하는 잎(leaf)의 지연발광 비교실험을 수행하였다. 엽록소가 지연발광의 주된 원인이므로, 시료가 건조됨에 따라 지연발광양이 변하는 것은 엽록소의 손상에 있다고 추론하였다. 대상 시료로는 장미(rosa hybrida, rosa hybrida cv.calibro)를 사용하였다. 셋째, 광합성을 일으키는 색소들 중에서도 가장 많은 양을 차지하는 chlorophyll이 식물 잎의 지연발광의 주된 원인이라고 알려져 있으나, chlorophyll이 지연발광에의 주 영향인자로 작용하는지 확인하기 위하여, 녹색과 적색단풍잎(Acer Palmatum)의 지연발광양과 파장별 지연발광 형태를 비교하였다. 지연발광양 측정은 텅스텐-할로겐램프를 광원으로 사용하여, 시료에 일정시간 조사하였다. 파장별 지연발광형태실험의 광원부는 직접 제작하였는데, 먼저 텅스텐할로겐램프의 파장의 빛을 monochromater(CM-110)를 이용하여 450-600nm 범위에서 10nm간격으로 단파장을 선택할 수 있게 하였다. 텅스텐-할로겐램프의 단파장의 빛의 강도(intensity)를 일정하게 하기위하여, 두개의 편광판의 각도를 달리하여서 그 강도를 일정하게 조절하였다. 지연발광 측정은 생물광자-PMT (Photo Multiplier Tube) 검출기 (R331-05s, Hamamatsu)로 100ms 간격으로 연속 검출하였다. 지연발광양은 빛을 조사한 후 150초간 측정한 생물광자 중, 10초까지의 값을 더하여 cps(count per second)의 단위로 나타내었다. 본 실험으로 얻은 결과는 다음과 같다. 첫째, 건조스트레스로 인한 지연발광양의 변화실험 중 장미잎(Rosa hybrida)의 경우, 채취 후 24시간까지 지연발광양의 변화를 관찰하였다. 지연발광양의 감소곡선의 형태가 예상과는 달리 단조감소형태를 보이지 않았다. 관찰된 지연발광양의 변화 양상은, 초기에는 천천히 증가하는 추세를 보이다가 2시간 후에 초기보다 120%정도로 증가하여 최대값을 갖고, 그 후 약 3시간동안은 급격히 감소하다가 점차 천천히 감소하여 측정 후 8시간에는 초기값의 약 20%가 되었다. Rosa hybrida cv.Calibra의 경우도 지연발광양이 Rosa hybrida의 경우와 같이 초기에는 증가하다가 감쇠하는 형태를 보였다. 이 경우, 지연발광양은 6시간정도에 최대값을 나타냈고, 그 이후 초기에는 급격한 감소를 보이다가 점차 완만한 감쇠로 18시간에는 거의 건조가 완료되었다. 두 시료의 지연발광감쇠경향을 비교한 결과 Rosa hybrida의 지연발광양이 Rosa hybrida cv.Calibra보다 훨씬 급격하게 감쇠하였다. 본 실험으로 수분의 부족으로 엽록체에 가해지는 약한 스트레스는 오히려 지연발광양을 증가시키고, 그 후 스트레스가 계속 축적되어 지연발광양의 감쇠를 만들어낸다는 것을 발견하였다. 둘째, 엽록소가 존재하는 잎과 존재하지 않는 꽃잎의 지연발광양 비교실험에서는 잎은 강한 지연발광을 나타내었으나, 꽃잎은 지연발광이 거의 관찰되지 않았다. 이를 통하여 엽록소가 지연발광의 주요 인자로 작용하는 것으로 추측되어 엽록소가 지연발광의 주요 원인이라는 이전 연구보고와 일치함을 확인할 수 있었다. 이전 연구에 따르면 엽록소의 가장 많은 부분을 차지하는 Chlorophyll이 지연발광의 주요 원인이라고 보고된바 있으나 본 연구에서는 다음 실험을 통하여 다른 결과를 얻었다. 셋째, 녹색 단풍잎과 적색 단풍잎의 광조사 파장별 지연발광양의 패턴을 측정해 본 결과, 두 시료에 대한 지연발광양의 패턴이 동일함을 알 수 있었다. 또한 녹색 단풍잎과 적색 단풍잎의 절대적인 지연발광양을 측정하여 비교하였을 때 그 절대적인 양 또한 동일함을 볼 수 있었다. 이는 두 시료의 지연발광 특성의 같다는 것을 의미하고, 또한 녹색 단풍잎에는 있고 적색단풍잎에는 없는 Chlorophyll이 지연발광에 영향을 주지 않는다는 이전 연구와는 다른 결과를 알 수 있다. 결과적으로, 지연발광의 원인이 되는 물질은 광합성 색소들이지만, 이 중 Chlorophyll은 지연발광에 전혀 영향을 미치지 않는 다는 사실을 알아내었다. 본 연구를 통하여, 지연발광은 식품에 대하여 절대적인 기준이 없는 신선도를 흔히 일반적으로 신선도를 평가하는 기준인 겉보기 색에 비해 보다 정확하고 정량적인 지표로서 활용될 수 있음을 제시할 수 있다고 판단된다. 또한 지연발광은 동물이나 사람에 대해서도 노화와 생명력의 정도를 측정하는 지표로서 활용가능할 것이라 생각되어 더 많은 연구가 추진되어야 할 것이다.

Ep-014 **Controllable switching behavior of defect**

modes in one-dimensional heterostructure photonic crystals LU YueHui, PARK SangYoon, LEE YoungPak, KIM KiWon[1], RHEE JooYull[2](*q-Psi and BK21 Program Division of Advanced Research and Education in Physics, Hanyang University, Korea. [1]Department of Physics, Sunmoon University, Korea. [2]BK21 Physics Research Division and Institute of Basic Science, Sungkyunkwan University, Korea.*) A dimerlike-positional-correlation heterostructure is used in one-dimensional photonic crystals to introduce the defect mode with the perfect transmittance. The switching behavior of the transmittance at the defect mode is demonstrated theoretically. When the normal incident beam is tilted, the perfect transmittance peak vanishes even at a negligibly small angle. It is found that this condition causing this behavior can be easily met and controlled. This finding is significant for the potential applications to high precision filters and optical switches.

Ep-015 **Investigation of Spectral Characteristics of Gold Nanoparticles for the Application of SPR Biosensors** YUK Jong Seol, JUNG Jaeyeon[1], HYUN Jinho[1], HA Kwon-Soo(*Kangwon National University, College of Medicine. [1]Seoul National University, Department of Biosystems &Biomaterials.*) The first bioanalytical application of 5-50 nm gold colloids, also called gold nanoparticles was electron-dense probes in electron microscopy. Gold nanoparticles have been employed as molecular-recognition elements and amplifiers in sensors. We have investigated spectral properties of 3.5-20 nm gold nanoparticles with both Mie's theory in the quasi-static regime and UV-VIS spectrophotometer. To introduce size effects, we assume that as the size of the particle diminishes, the rate of scattering from the particle surface begins to exceed the bulk scattering rate. The experimental dielectric function of bulk gold was decomposed into two terms, a free-electron term and an interband term. Gold nanoparticles of diameter 3.5 - 20 nm were synthesized by citrate reduction method, which were confirmed by TEM images. Absorption spectrum of the 20 nm gold nanoparticles was observed around 520 nm, which was similar to the theoretical result. Experimentally, blue shift was monitored according to the decrease of size. In this study, we have successfully investigated the spectral characteristics of gold nanoparticls below 20 nm for the application of SPR optical biosensor as a signal amplifier.

Ep-016 **양극산화 다공성 알루미나 박막에 의해 제작된 나노점 배열 구조의 Al과 Cu 박막에 대한 전계방출 특성** 김 동현, 진 원배(*동아대학교 신소재물리학과.*) 알루미늄 양극산화법에 의해 양극전압 조건을 변화시킴으로서 세공 크기가 서로 다른 다공성 알루미나 박막을 제작하였다. 이렇게 제작된 다공성 알루미나 박막을 주형으로 이용하여 저항 가열방식의 진공증착에 의해 크기가 서로 다른 나노점 배열 구조의 알루미늄과 구리 박막을 합성하였다. 합성된 나노점의 형태는 반구형이면서, 크기는 주형으로 사용된 다공성 알루미나 박막에 따라 각각 직경이 약 59, 69, 79 ㎚이었다. 이렇게 제작된 나노점 배열 구조의 알루미늄과 구리 박막을 전자 방출 원으로 사용하여 이들 박막의 전계 방출 특성을 측정하였다. 알루미늄 나노점 배열 구조에서는 나노점 크기에 따라 동작 전기장은 6, 8, 14 V/㎛이었고, 구리 나노점 배열 구조에서는 12, 16, ~10 V/㎛이었다. 이들 방출 전류에 대한 Fowler-Nordheim 곡선은 좋은 선형성을 보여주었다.

Ep-017 **상호작용 퍼텐셜에 따른 CNT 내 수소 저장 분자동역학 시뮬레이션** 임 의순, 윤 달호[1], 임 승환[2], 소 철호[3](*세명대학교, 컴퓨터학부. [1]청주대학교, 나노과학과. [2]배재대학교, 광혼돈제어 창의연구단. [3]동신대학교, 광전자공학과.*) CNT 내 수소 저장 가능성을 여러 퍼텐셜들에 대하여 분자동역학 시뮬레이션하여 그 효과를 관찰하였다. 시뮬레이션은 다양한 CNT 시뮬레이션에 폭넓게 사용되는 탄화수소 공유결합에 대한 실험 퍼텐셜인 Tersoff-Brenner potential과 이 Tersoff-Brenner potential에 근접 산란에 대한 Biersack-Zeigler potential을 적절히 결합한 복합 퍼텐셜이다. 이 시뮬레이션을 통하여 Tersoff-Brenner potential에 Biersack-Zeigler potential을 결합하면, 퍼텐셜의 척력 영역은 줄어들고 인력의 깊이는 증가하여 Tersoff-Brenner potential만을 고려한 시뮬레이션보다 CNT 내로 수소원자가 투과할 확률이 증가됨을 알 수 있었다. 또한 근접 산란의 경우 Biersack-Zeigler potential을 고려한 경우 Tersoff-Brenner potential만 고려한 경우와 전혀 다른 수소원자 궤적을 확인할 수 있었다.

Ep-018 **SWNT 내로 수소분자 주입에 대한 분자동역학 시뮬레이션** 임 의순, 윤 달호[1], 임 승환[2], 소 철호[3](*세명대학교, 컴퓨터학부. [1]청주대학교 나노과학과. [2]배재대학교 광혼돈제어 창의연구단. [3]동신대학교, 광전자공학과.*) SWNT 내로 수소분자 주입에 대하여 분자동역학 시뮬레이션을 수행하였다. 근접 산란에 대한 Biersack-Ziegler potential을 포함하는 Tersoff-Brenner

potential을 사용한 시뮬레이션을 통하여 초기 운동에너지를 갖고 정지한 SWNT를 향하여 발사된 수소분자의 행동을 다양한 에너지와 방향에 대하여 조사하였다.

Ep-019 **Single-crystalline Bismuth Telluride Nanowires for high-efficiency Thermoelectric Devices** HAM Jinhee, SHIM Wooyoung, LEE Seunghyun, LEE Wooyoung (*Department of Materials Science and Engineering, Yonsei University, 134 Shinchon, Seoul 120-749, Korea.*) High efficient thermoelectricity requires materials with a large figure of merit, ZT, defined by $ZT = \sigma S^2 T/\kappa$, where σ is the electrical conductivity, S the thermoelectric power, and κ the thermal conductivity. However, due to the interdependence of σ, S, and κ, the optimization of thermoelectricity remains challenging. It is well known that there are two approaches to enhanced ZT value. One is to utilize quantum confinement effects of nanostructures, providing an opportunity to individually control σ and S, and thus to promote ZT [1] because of increase of the density of states (DOS). The other is to reduce κ without having an effect on σ and S by using semiconductors of high atomic weight such as bismuth telluride (Bi_2Te_3) with much lower atomic vibration frequencies [2]. In this work, we present a new method to grow high-quality, single-crystalline Bi_2Te_3 nanowires for use as a thermoelectric material with high ZT. Bi_xTe_{1-x} (x = 0.35 ~ 0.55) thin films were grown on an oxidized Si substrate using a co-sputtering system with a Bi (99.999%) and a Te target (99.99%). For the growth of Bi_xTe_{1-x} nanowires, the co-sputtered films were transferred to a furnace for heart treatment in the temperature range 300 - 450 ˚C. Scanning electron microscopy (SEM) and high-resolution transmission electron microscopy (HRTEM) were employed for the structural characterizations of the nanowires. Interestingly, uniform and straight Bi_2Te_3 nanowires with high aspect ratios were found to grow on the surface of the co-sputtered films after heat treatment. The growth of the Bi_2Te_3 nanowires is attributable to the relaxation of stress, originating from a thermal expansion mismatch between the film and the substrate. This mismatch is due to the large difference in the coefficient of thermal expansion of Bi_xTe_{1-x} (~19 × 10^{-6}/℃), SiO_2 (0.5 × 10^{-6}/℃) and Si (2.4 × 10^{-6}/℃). Elemental mapping profiles show the uniform distribution of Bi and Te along the length of the nanowire without appreciable segregation. Quantitative analysis of composition variation by line profiles also reveals that the Bi and Te are homogeneously distributed through the nanowire. The composition of Bi_xTe_{1-x} nanowires were found to be adjusted by tailoring the composition of co-sputtered films from x = 0.35 to 0.55. A high-resolution TEM study reveals that the Bi_2Te_3 nanowire with d = 100 nm grown along the <110> direction is high-quality single crystalline. The diffraction pattern recorded perpendicular to the long axis of the nanowire can be indexed to the hexagonal lattice of Bi_2Te_3 (a = 4.43Å, c = 29.91Å) with [001] zone axis. The Bi_2Te_3 nanowires were found to have diameters ranging from 50 nm to 500 nm depending on the thickness of the co-sputtered Bi_xTe_{1-x} films, indicating that the diameter of Bi_2Te_3 nanowires is controllable. The thermoelectric properties of individual single-crystalline Bi_2Te_3 nanowires are discussed in detail. Our results demonstrate that single-crystalline Bi_2Te_3 nanowires can be grown by the stress-relief method, providing a motivation for exploring the high-efficiency thermoelectric properties of single-crystalline Bi_2Te_3 nanowires.
[1] Y. Lin et. al., Phys. Rev. B 62, 4610 (2000)[2] A. Majumdar, Science 303, 777 (2004)

Ep-020 **Irradiation Induced Defects Study in Reactor Pressure Vessel Steel by SANS** 한 영수, 성 백석, 이 창희, 박 덕근(*한국원자력연구소.*) The irradiation induced defects of irradiated reactor pressure vessel(RPV) steel were investigated by small angle neutron scattering(SANS). The degradation of the mechanical properties of RPV steels during irradiation in a nuclear power plant is closely related to the irradiation induced defects. The size of these defects is known as a few nanometer, and the small angle neutron scattering technique is convinced as the best non destructive technique to characterize the nano sized inhomogeneities in bulk samples. The RPV steel was irradiated at HANARO reactor in KAERI. The small angle neutron scattering experiments were performed at SANS instrument in HANARO reactor. The nano sized irradiation induced defects were quantitatively analyzed by SANS. The relation between irradiation induced defects and the mechanical properties, especially yield strenght was discussed.

Ep-021 **The structural stability of Graphite Oxide** LEE yunpyo, AN kayhyuk[1], LEE younghee[2](*Department of Physics, Sungkyunkwan university. [1]R&D Department, Jeonju Machinery Research Center. [2]Department of Physics, Center*

for Nanotubes and Nanostructured Composites, Sungkyunkwan university Advanced Institute of Nanotechnology, Sungkyunkwan University.) Graphite oxide (GO) has been known since the 19th century. Recent interest grew due to proposed application as material for battery electrodes or membrane models. The various structural characterization of GO researched over the years, but the stability of GO was not studied yet. First, GO was synthesized from needle shaped cokes and natural graphite by oxidation with $HNO_3/NaClO_3$, according to the Brodie method. After annealing treatment, the structure of GO was investigated by elemental analysis, X-ray diffraction, infrared Fourier transform spectroscopy, X-ray photoelectron spectroscopy.

Ep-022 **Catalytic Synthesis of Thin Multiwalled Carbon Nanotubes for Mass Production** LEE ILHA, KIM EUNSUNG[1], KIM SUNGJIN[1], JUNG SEUNGYOL[1], LEE YOUNGHEE[1](*Department of Nanoscience and Nanotechnology, Sungkyunkwan University. [1]Department of Physics, Sungkyunkwan University.*) We have synthesized thin multiwalled carbon nanotubes (t-MWCNTs) by catalytic chemical vapor deposition (CCVD) with FeMoMgO catalyst. The large-capacity CVD system of a quartz tube with a diameter of 25 cm and length of 150 cm was designed for mass production. Methane (CH_4) and Hydrogen (H_2) gases have been used for the growth of t-MWCNTs. Carbon dioxide (CO_2) has also been used to avoid catalyst poisoning as an etching agent. We observed that the yield of t-MWCNTs increased with the addition of CO_2. The number of tube walls are 3~7 with the corresponding diameter of 3~7 nm. T-MWCNTs are characterized by high-resolution transmission electron microscopy (TEM), Raman analysis, and Thermogravimetric analysis (TGA).

Ep-023 **Bias Voltage Dependence of TMR In Ferromagnetic Amorphous CoSiB DMTJ and SMTS** 이 장로, 이 선영, 이 서원, 황 재연, 임 혜인, 김 태완[1], 이 상석[2], 황 도근[2], 이 희복[3], 유 성초[4](*숙명여자대학교, 물리학과. [1]세종대학교, 나노신소재 공학과. [2]상지대학교, 컴퓨터 전자 물리학과. [3]공주대학교, 물리교육과. [4]충북대학교, 물리학과.*) 자기터널접합(MTJ)를 사용하는 고밀도자기메모리(MRAM)는 높은 터널 자기저항(TMR)과 낮은 스위칭자기장(H_{sw})를 필요로 한다.[1] 이 문제를 해결하기위하여 자기터널접합의 강자성 전극으로 비정질 재료를 사용하였다.[2] 본 실험에서는 MTJ의 자유층으로 비정질 강자성 $Co_{75}Si_{15}B_{10}$을 사용하였다. CoSiB 자유층을 사용한 MTJ의 자기저항효과와 스위칭 특성을 $Co_{75}Fe_{25}$, $Ni_{80}Fe_{20}$ 및 비정질 강자성 $Co_{70.5}Fe_{4.5}Si_{10}B_{10}$ 자유층을 사용한 MTJ 것과 비교하여 조사하였다. CoSiB 자유층을 사용한 MTJ는 이것의 높은 스핀 분극도 때문에 다른 자유층을 사용한 MTJ보다 높은 TMR비와 낮은 저항-면적(RA)를 나타내었다. CoSiB은 낮은 포화자화도(M_S)와 높은 자기이방성 상수(K_u)를 가지므로 CoSiB 자유층을 사용하는 MTJ는 외부 자기장에 대해서 낮은 스위칭자기장(H_{sw})과 높은 민감도를 나타내었다. CoSiB 합성반강자성(SAF) 자유층을 사용한 MTJ는 단일 CoFeSiB 자유층을 갖는 MTJ보다 낮은 스위칭자기장(H_{sw})를 가질 뿐만 아니라, 다른 합성반강자성(SAF) 자유층을 갖는 MTJ보다 더 낮은 값을 가졌다.[3,4] 그리고 CoSiB를 사용한 이중자기터널접합(DMTJ)과 단일 자기터널접합(SMTJ)의 바이어스전압 의존성특성도 조사하였다.

Ep-024 **A High-mobility Field-effect Transistor based on Single-crystalline Bi Nanowire** SHIM Wooyoung, HAM Jinhee, LEE Seunghyun, LEE Wooyoung(*Department of Materials Science and Engineering, Yonsei University, 134 Shinchon, Seoul 120-749, Korea.*) Semimetallic bismuth (Bi) is a group V element with unusual transport properties due to a unique band structure of −38 meV in band overlaps. In particular, single-crystalline Bi nanowires exhibit the electrical properties of both semimetal and semiconductor due to quantum confinement effect (QCE) [1], which takes an advantage of maximizing electric field effect. These interests of gating effect in Bi nanowires lie in the realization of high-speed field-effect transistor (FET) arising from high mobility due to low resistivity and low carrier concentration in Bi nanowires. In the present work, we report the demonstration of high-mobility FET based on an individual single-crystalline Bi nanowire at room-temperature. Bi nanowires were grown onto the sputtered-Bi thin films by heat treatment at 270 °C for 10 hours, resulting from thermal expansion mismatch between the film and substrate. For fabricating the devices, nanowires were dispersed onto thermally oxidized silicon substrates with the underlying conducting Si used as a back gate. Electrical contact to the nanowires was defined using a combination of photo- and electron beam lithography. The dependence of conductance on gate voltage was found in a field effect transistor (FET) based on an individual single-crystalline Bi nanowire with d = 120 nm. The conductance (G) values were

measured as an external gate voltage V_g is swept from – 50 V to + 50 V, and these exhibit the symmetric dependence of G on V_g. The observed behavior is attributed to the unique property of Bi that the number of holes is equal to the number of electrons without an external electric field, deriving the carrier concentration of 2.1 × $10^{17}cm^{-3}$ at room-temperature. A lower carrier concentration of our 120-nm Bi nanowire by one order, relative to the bulk of 10^{18} cm^{-3} at 300 K, can be explained by a lower Fermi wave-vector k_F, caused by a small wire diametner d_w.The measured value for n_e reported herein, the electron mobility μ_e and mean free path ℓ_e are found to be $\mu_e = (en\rho)^{-1} \approx 367{,}000$ cm^2/Vs with $\rho \approx 8.1 \times 10^{-5}$ Ω·cm and $\ell_e = (h/2e)(3n_e/\pi)^{1/3}\cdot\mu_e \approx$ 4.4 μm at room-temperature. The results show that the mobility and concentration are 3 and 2 order of magnitude is larger, respectively, for our single-crystalline Bi nanowire relative to polycrystalline Bi nanowire [2], and this value exceeds those for all known semiconductors, including semiconducting carbon nanotubes (>100,000 cm^2/Vs) [3]. Our results provide motivation for exploring novel physics, e.g., high-speed transistors and high-performance thermoelectric devices based on the single-crystalline Bi nanowires.

References[1] J. Heremans, C. M. Thrush, Y. Lin, S. Cronin, Z. Zhang, M. S. Dresselhaus, and J. F. Mansfield, Phys. Rev. B , 61, 2921 (2000). [2] A. Boukai, K. Xu, and J. R. Heath, Adv. Mater. 18, 864 (2006). [3] T. Dulrkop, S. A. Getty, E. Cobas, and M. S. Fuhrer, Nano. Lett. 4, 35 (2004)

Ep-025 **$Y_{1-x}La_xAlO_3$ 나노입자에 첨가된 Eu^{3+} 이온의 형광특성** 김 중환, 최 혜영, 문 병기[1], 양 현경[1], 정 중현[1], 심 규성[1], 이 성수[2](*동의대학교 물리학과. [1]부경대학교 물리학과. [2]신라대학교 광전자공학과.*) Yttrium aluminum perovskte는 레이저 및 신틸레이터에 좋은 특성을 보이는 물질이다. 이 결정에 희토류이온을 첨가하면 점군 C_s 대칭에 자리한 Y^{3+} 이온 자리에 치환된다. Field emission display 와 신틸레이터에 관한 응용을 목적으로 이 물질에 첨가한 Eu^{3+} 이온의 발광 특성을 조사하였다. 나아가 lanthanum 의 첨가량에 따른 형광의 특성을 조사하였다. $Y_{1-x}La_xAlO_3:Eu^{3+}$ (YLaAP:Eu) 나노결정은 solvothermal법으로 제조하였으며, 결정구조와 결정의 형상 및 형광스펙트럼은 각각 X-ray diffraction, scanning electron microscopy, transition electron microscopy 및 time resolved spectroscopy를 사용하였다. La 또는 Al의 첨가량에 따라 그리고 소결온도에 따라 입방구조와 육방구조 및 단사구조가 혼재되어 있는 비율이 달라지며, 이에 따라 형광의 특성이 다소 달라졌다. 그리고 La의 첨가량이 증가함에 따라서 Eu^{3+} 이온의 전하이동띠 (charge transfer band)가 점차 낮은에너지 쪽으로 이동하는 일관성을 보였다.

Ep-026 **Shubnikov-de Haas Oscillations in an Individual Single-crystalline Bi Nanowire** KIM Jeongmin, SHIM Wooyoung, LEE Wooyoung(*Department of Materials Science and Engineering, Yonsei University, 134 Shinchon, Seoul 120-749, Korea.*) Semimetallic bismuth (Bi) is a particularly favorable material with which to study its unusual electronic properties of quantum wires due to its highly anisotropic Fermi surface, low carrier concentrations, long carrier mean free path l and small effective carrier mass m*[1]. In single crystals, these characteristics lead to very large ordinary magnetoresistance (OMR) effects and pronounced quantum oscillations including Shubnikov-de Haas (SdH) Oscillations and related effects [2]. For these studies, materials with lower dimensions such as nanowires are often required, and 4-probe measurement of an individual nanowire is necessary to obtain quantitative information such as the charge density and the anisotropic of Fermi surface. In the present work, we report the observation of Shubnikov-de Haas oscillations in an individual single-crystalline Bi nanowire. We have successfully grown the single-crytalline Bi nanowires via heat treatment at 270 ˚C for 10 hours by utilizing the relaxation of stress from the Bi films. For a 400-nm-diameter Bi nanowire, the largest transverse and longitudinal OMR of 2496% at T = 110 K and −38% at T = 2 K were observed, indicating that the Bi nanowires grown by the proposed method have the longest mean free paths l, and these are high-quality, single crystalline. Mean free path l is directly related to the observation of SdH oscillations that is characterized by an exponential decay, exp (– 1/$w_c\tau$), where relaxation time τ is defined $\tau = el / m^*$. The observation of robust SdH oscillations proves that the Bi nanowire is the high quality, single-crystalline. Oscillations with the field of perpendicular to the nanowire exhibit higher amplitude by one order than those of parallel to the nanowire. The results show good qualitative agreement with the large transverse MR data, defined by $w_c\tau$. The observed period of SdH oscillations with the field perpendicular to the nanowire (n = 3) is small, relative to those with the field perpendicular to the nanowire (n = 6), therefore ensuring that Bi nanowire is oriented along the trigonal direction, i.e., (00ℓ).

These results are consistent with TEM analysis and the preferred orientation of (00ℓ) in films where nanowires start to grow [3]. Further description of the cyclotron behavior in terms of SdH oscillations in the single-crystalline Bi nanowire in the ballistic regime will be discussed in detail.

References [1] J. Heremans, C. M. Thrush, Y. Lin, S. Cronin, Z. Zhang, M. S. Dresselhaus, and J. F. Mansfield, Phys. Rev. B, 61, 2921 (2000).
[2] F.Y. Yang, K. Liu, K. Hong, D.H. Reich, P. C. Searson, and C. L. Chien, Science 284, 1335 (1999).
[3] W. Y. Shim et al., to be publihsed

Ep-027 **Nanorods of $La_{1-x}Sr_xMnO_3$ by microwave irradiation method** PHAN Van Cuong, 노 용석, 김 도형(*경북대학교.*) $La_{1-x}Sr_xMnO_3$ nanorods(NRs) were synthesized by microwave irradiation method. The method has a shorter reaction time and a simpler process compared with hydrothermal method. X-ray diffraction of NRs shows that they are pure, cubic perovskite structure and single crystalline. Field emission scanning electron microscope (FE-SEM) images demonstrate that lengths of the NRs are in the range of several to several tens of micrometers, and diameters are in the range of 50–200 nm. High-resolution transmission electron microscopy (HR-TEM) analysis indicates that these NRs grow along [110] and clean surface. The magnetization behaviors of the NRs were discussed in detail.

Ep-028 **Field Emission Properties of CNT-emitters on Conducting Films/Si with Thermal Treatment** PARK Chong-Yun, RYU Dong Heon, LEE Seung Youb, SONG Woo Seok, HONG Jun Yong, YEOM Min Hyung, SHIN Yong Sook, YANG Ji Hoon[1](*성균관대학교 물리학과. [1]포항산업과학연구원.*) Since carbon nanotubes (CNTs) have been discovered, they showed unique electrical, mechanical, and geometric properties for nanoelectronic devices such as field emitters, interconnects, and field effect transistors. We have investigated field emission properties of the sprayed CNTs on the conducting films/Nb/Si substrate. To improve the adhesion between the conducting films and Si wafer, the Nb(thickness : ~30㎚) has been deposited on Si wafer by using magnetron sputtering system. Then, the conducting films(thickness : ~500㎚) have been deposited on the substrate by using magnetron sputtering system. The solutions with thin-CNTs(ILJIN : CMP-310F) have mixed 1,2-dichloroethane (DCE)[(1)]. The dispersion process consists of the sonication and centrifugation to remove the undissloved CNTs and some amorphous carbon. After this solutions were blown into the substrate by the spray method, the sample was annealed with ambient Ar at ~700℃. As the CNTs on the conducting films were heated, they have been penetrated into the molten conducting films. As a result of the heating process, the CNTs were tightly combined with the conducting films.[(2)] Moreover, the conducting films are provided with characteristics as a electrode, high electrical conductivity, low contact resistance. Then, we measured the field emission current, turn-on voltage, I-V curve and field emission stability. Furthermore, we observed the morphology of the embedded CNTs by scanning electron microscopy (SEM).

[Reference]1. Hee Jin Jeong et. al, Fabrication of efficient field emitters with thin multiwalled carbon nanotubes using spray method, Carbon 44, 2689(2006) 2. Lingbo Zhu et. al, Well-aligned open-ended carbon nanotube architectures: An approach for device assembly, Nano Lett. 6, 243(2006)

Ep-029 **Raman Spectroscopic Study of Electric Field Effect on the Absorption Property of ZrO_2 Thin Films** KIM Hyun Kyu, PARK June, SEONG Maeng-Je, KIM Soo Hong[1], HWANG In Rok[1], PARK Bae Ho[1], SEO Sunae[2], YOO In-Kyeong[2](*Chung-Ang Univ., Dept. of Physics. [1]Konkuk Univ., Dept. of Physics. [2]Samsung Advanced Institute of Technology, Semiconductor Device Lab..*) ZrO_2 is a promising candidate for the thin oxide layer of the next generation CMOS and RRAM due to its high dielectric constant and wide bandgap. Polycrystalline ZrO_2 thin films have been deposited on $Pt/Ti/SiO_2/Si$ substrates by DC magnetron sputtering. When proper voltages were applied to the ZrO_2 thin films they showed On/Off resistance switching behaviors. Raman measurements were performed on both the pristine ZrO_2 layers and the ZrO_2 layers whose resistance status had been switched by applying an electric field. We have observed strong Si substrate Raman signature at ~ $520cm^{-1}$ for the switched ZrO_2 layers whereas the Si Raman peak was not observed from the pristine ZrO_2 layers. This indicates that electric field applied to the ZrO_2 layers can drastically change their absorption coefficient at the energy of the Raman excitation laser energy 2.54eV.

Ep-030 **Noble-metal 코팅을 통한 탄소나노튜브의 전계방출 특성향상** 박 종윤, 이 승엽, 류 동헌, 염 민형, 홍 준용, 송 우석, 양 지훈[1], 최 원철, 신 용숙, 권 명희[2](*성균관대학교 물리학과. [1]포항 산업과학연구원. [2]인천대학교 물리학과.*) 전계방출 디스플레이어에 사용되는 전계방출소자는 낮은 문턱전압, 높은 전류밀도, 장시간안정적인 전계방출이 요구된다. 탄소나노튜브는 큰 지름 대 길이 비와 뛰어난 전기적 특성(1), 화학기상 증착을 통한 선택적인 성장가능성 때문에 차세대 전계방출소자로 주목받으며 많은 연구가 이루어져 왔다. 하지만 이러한 탄소나노튜브도 단일 특성을 갖는 나노튜브의 합성이 어렵고 patterning을 하지 않으면 밀도조절을 하는데 어려움 있다. 그래서 이런 문제점을 해결하기 위하여 여러 가지 방법들이 연구되어 왔다. 그 방법으로 플라즈마 식각을 통해 밀도를 낮추는 방법, 알칼리족 금속이나 7족 원소를 증착하여 전기전도성을 향상시키는 방법, 이종원소를 도핑하여 나노튜브를 단일 특성화 하는 방법, 열처리를 통하여 결정성을 높이는 방법 등이있다. 본 연구에서는 noble metal을 증착하여 탄소나노튜브의 전계방출특성 향상을 연구 하였다. 위에서 언급하였던 알칼리족 금속이나 7족원소를 증착하는 방법에서는 여러 가지 장점이 있었지만 낮은 열적 안정성과 공기 중에서의 산화 때문에 실제 응용에 문제가 있었다. 하지만 noble metal은 화학적으로 안정적이여서 산화반응이 잘 발생하지 않으며, 전기전도성이 우수하기 때문에 알칼리족 금속이나 7족원소를 증착하는 방법보다 좋은 결과를 나타낼 것으로 예상을 하였다. 또한 이전의 연구에서 은과 구리의 합금을 나노튜브에 코팅함으로써 문턱전압이 낮아지고, 전류밀도가 증가하며, 열악한 분위기에서 안정적으로 전계방출이 이루어지는 것을 확인 하였다. 하지만 이러한 전계방출특성의 향상이 단순히 전기전도성의 향상에 의한 것인지 전계차폐효과의 감소에 의한 것인지 emission site증가에 의한 것인지는 명확하게 밝힐 수가 없었다. 그래서 본 연구에서는 이러한 전계방출특성향상의 명확한 이유를 알아보고 은과 구리의 합금 외에 다른 noble metal의 코팅을 통하여 탄소나노튜브의 전계방출 특성변화에 대하여 연구 하였다.

[참고문헌] 1. Walt A. de Heer, science 270, 1179 (1995) 2. Nilsson, APL 76, 2071 (2000)

Ep-031 **Fe catalyst의 Diffusion Process를 이용한 선택적인 위치에서의 탄소나노튜브의 합성** 박 종윤, 송 우석, 홍 준용, 류 동헌, 이 승엽, 염 민형, 신 용숙, 전 철호, 양 지훈[1], 최 원철(*나노튜브 및 나노복합구조센터, BK21 물리연구단, 성균관대학교. [1]포항산업과학연구원.*) 탄소나노튜브(carbon nanotubes : CNTs)는 뛰어난 전기적, 물리적인 특성을 가지고 있기 때문에 device분야에서 이를 활용하려는 노력들이 활발히 이루어지고 있다. 그 중에서 CNTs의 기하학적 구조를 제어하고, 원하는 위치에 선택적으로 합성시키는 기술은 CNTs를 이용하여 electronic device를 구현하는 데 있어서 가장 중요한 사항이라 할 수 있을 것이다. 단일벽 탄소나노튜브(Singlewalled carbon nanotubes : SWCNTs)나 얇은 다층벽 탄소나노튜브(Thin-multiwalled carbon nanotubes : Thin-MWCNTs)등의 작은 직경을 가진 튜브의 합성에서는 촉매의 크기가 튜브에 직경에 큰 영향을 미치기 때문에, 최근에는 촉매금속과 촉매의 크기를 작게 유지 시켜 줄 수 있는 다공성 물질을 powder의 형태로 혼합하여 spin coating한 후, CNTs를 성장시키는 방법들이 보고되었다.(1) 하지만 이러한 방법은 device 분야로의 활용이 어려운 단점이 있다.(2) 따라서, 이러한 단점을 보완하기 위해서 Si 기판위에 film의 형태로 catalyst를 증착하는 다양한 방법이 연구되어지고 있다.(2),(3) 또한, CNTs를 원하는 위치에 선택적으로 합성시키는 방법은 photolithography를 이용하여 원하는 위치에 촉매를 pattering하여 CNTs를 합성하는 방법들이 보고된 바 있다.(4) 이러한 방법 역시 촉매의 size를 작게 유지하는 것에 대한 문제와 원하는 위치에 CNTs를 성장시키는 것에는 한계를 가지고 있다. 본 연구에서는 Si 기판위에 Al_2O_3를 증착하고, Fe catalyst를 증착 후 그 위에 다시 Al을 증착하여 sandwich-like한 형태의 구조물을 만든 후 열처리 과정을 통하여 Fe catalyst가 Al층 위로 diffusion 하는 것을 이용하여 Fe 촉매의 aggregation 없이 작은 크기의 Fe을 유지시키고, 또한 diffusion barrier의 역할을 해주는 금속을 patterning하여 선택적인 위치에서만 Fe particle이 diffusion 되어 원하는 위치에서 CNTs를 합성하였다. Al과 Fe catalyst의 두께, 처리 온도에 따라 Fe catalyst가 diffusion 되는 정도를 X선 광전자 분광법(X-ray photoelectron spectroscopy : XPS)과 투과전자현미경(Transmission electron microscopy : TEM)을 통하여 확인하였고, 성장된 CNTs의 길이와 직경을 주사전자현미경(Scanning electron microscopy : SEM)과 라만 분광법(Raman spectroscopy)을 통해 측정하였다.

참고문헌 1. Avetik R. Harutyunyan et al, Nanoletters 2002 Vol.2, No.5 525 2. H. Hongo et al, Chemical Physics Letters 380(2003) 158 3. Quofang Zhong et al, J. Phys. Chem. B 2007 111(8) 1907 4. Ant Ural et al, Applied Physics Letters Vol. 81, 18

Ep-032 **Properties of Direct Current Sputtered Titanium Thin Films** B. Karunagaran, 김 서군, 서 은경(*전북대학교 반도체과학기술학과/반도체물성연구소.*) Titanium (Ti) thin films were deposited by DC magnet-

ron sputtering at conventional conditions with different cathode power (75 to 150 W), sputtering pressure (1.1 to 3.3 Pa) and base vacuum (4 to 13 × 10^{-4} Pa). The compositional properties of the films were studied using four point probe, XPS and spectroscopic ellipsometry techniques. Additionally, the structural properties of the Ti films were obtained using XRD, SEM and AFM techniques and also derived from ellipsometry data. Deposition conditions with low cathode power (75 W) and high base pressure (13 × 10^{-4} Pa), independent of the other parameters, yielded significant nitridation in the films and that condition, together with high sputtering pressure (3.3 Pa), resulted in transparent Ti oxide film. The films prepared under these conditions were amorphous. Otherwise, under deposition conditions of higher cathode power and lower sputtering and base pressures, only oxidation in the films was observed. The concentration of the oxide phase decreased with an increase in the cathode power and decrease in the sputtering and base pressures. Furthermore, under these conditions the films crystallized. The crystallinity increased with increase in cathode power (100-150 W) and sputtering pressure (1.1-2 Pa) and eventually was found to be amorphous with a slight increase in the base vacuum from the lowest of 4 × 10^{-4} Pa. However, the morphological properties of the Ti films were least influenced by the preparation conditions. The films were uniform and void free exhibiting densely packed morphological characteristics with similar smooth surface roughness. A strong relation existed between the composition and structural properties in the films. From this dependence the optimum deposition conditions is obtained to prepare metallic and crystalline Ti films under conventional conditions.

*Acknowledgements This work was supported by the Korea Research Foundation Grant funded by the Korean Government (MOEHRD) (KRF-2005-005-J07501).

Ep-033 **Novel synthesis process of MWCNT using double zinc and nickel catalytic layer (DCL) at low temperature** HA Jaehwan, LEE Jonghyun, HONG Jin Pyo(*New Functional Materials and Device Lab, Department of Physics, Hanyang University, Seoul 133-791, KOREA.*) Multi-wall carbon nano tubes (MWCNTs) were synthesized with zinc (Zn) and nickel (Ni) double-catalytic-layer (DCL) by plasma enhanced chemical vaporized deposition systems. The thickness of nickel and zinc double layer was varied from 10nm to 15nm. The DCL was treated by ammonia (NH_3) with 60 W at 400℃ for 4 minutes. It could be expected to be easily applied on the hetro-structure device between CNTs and oxide materials such like back-light unit and other emitters. Compared to the diameter of MWCNTs which were synthesized with single-catalytic-layer (SCL), the diameter of MWCNTs could be decreased as much as about 10-15nm. Moreover, the number of wall was also decreased with DCL than the number of wall with SCL. The properties of MWCNTs were investigated with scanning electron microscopy (SEM), scanning-transmission electron microscope (s-TEM) and Raman spectroscopy.

Ep-034 **Self-assembled $NiSi_2$ nanocrystals for nanoscale non-volatile memory application** CHO Chi-Won, CHOI Sung-jin[1], HWANG Hyundeok, LIM Chaehyun[1], MIN Dong-hoon[1], KIM Sangsig[2], LEE Seung-Beck[1] (*Division of Electronics and Computer Engineering, Hanyang University, Seoul, 133-791. [1]Department of Nanotechnology, Hanyang University, Seoul, 133-791. [2]Division of Electronics and Computer Engineering, Korea University, Seoul, 136-701.*) We investigated the nanoscale floating-gate characteristics of $NiSi_2$ self-assembled nanocrystals for non-volatile memory by rapid thermal annealing(RTA) on p-type silicon substrate. The $NiSi_2$ films with thickness of few nanometers (from 3nm to 5nm by 1nm increasment) were deposited onto substrate by RF sputtering. The films were subjected to RTA for various time durations (from 30 s to 90 s. by 30 s. increasement) at 800 °C. We fabricated the doping of source and drain electrodes using phosphorous solid-phase by thermal diffusion. The most significant features of this device at room temperature were its use of low voltages (3V for write/read/erase), large threshold-voltage shifts (about 2V) with the source-drain bias at 1V. When higher gate voltage was applied, the threshold-voltage hysteresis was increased significantly. The results demonstrate that self-assembled $NiSi_2$ nanocrystals by RTA is a useful method for nanoscale floating-gate nonvolatile memory application.

Ep-035 **Capacitance-Voltage characterized of $NiSi_2$ nanocrystal with High-K gate oxide** CHOI Sung-Jin, JEON Hyeong-Seok, CHO Chi-Won[1], PARK Bonghyun, LIM ChaeHyun, MIN Dong-Hoon, KIM Sangsig[2], LEE Seung-Beck(*Department of Nanotechnology, Hanyang University, Seoul, 133-791. [1]Division of Electronics and Computer Engineering,*

Hanyang University, Seoul, 133-791. [2]Department of Electrical Engineering, Korea University, Seoul, 136-701.) We investigated the charge capacitance of $NiSi_2$ nanocrystals with High-K gate oxide. The $NiSi_2$ films with thickness of few nanometers were deposited onto Si wafers using RF sputtering method. They were subjected to rapid thermal annealing (RTA) for various time durations (from 30 s to 90 s by 10 s. increasement) at 800 temperature in Ar ambient. The High-K gate oxide was deposited onto $NiSi_2$ nanocrystals using ALD. The morphologies of the $NiSi_2$ were characterized by scanning electron microscopy (SEM) and transmission electron microscopy (TEM). The capacitance-voltage (C-V) measurements were performed to study the electron charging and the discharging effects of the $NiSi_2$ nanocrystals. We investigated the hysteresis of the C-V characterized depend on RTA time.

Ep-036 **In-situ patterning of carbon nanotube thin film devices by selective vacuum filtration** LIM Chaehyun, LEE Seung-Beck[1], PARK Bonghyun, MIN Dong-hoon(*한양대학교 나노공학과. [1]한양대학교 전자통신컴퓨터공학부.*) Recently, interest in mechanically stable, low power consuming and highly selective gas sensor has increased. We present the fabrication process of flexible and transparent carbon nanotube gas sensor on PDMS substrates using selective vacuum filtration. SWCNT thin film device structures were fabricated during deposition by using pre-patterned membrane filters. The in-situ patterned nanotube device structures were transferred to a flexible PDMS substrate by direct molding method. We found that the lower SWCNT density network thin film had higher sensitive to NH_3 or NO_2 gas exposure. We also have investigated the degassing characteristics of the trapped gas molecules on the CNT surfaces. Depending on the heat generation by current flow through the CNT film.

Ep-037 **Contrast Enhancement of Back Scattered Electrons in a Micro-Column Scanning Electron Microscope** PARK Bonghyun, LIM Chae Hyun, MIN Dong-Hoon[1], YOSHIMOTO Takatoshi[2], KIM Ho-Sub[2], LEE Seung-Beck[3](*Department of Nanotechnology, Hanyang University, Seoul, Korea 133-791. [1]Division of Electronics and Computer Engineering, Hanyang University, Seoul, Korea 133-791. [2]Department of Physics and Advanced Materials Science, Sunmoon University, Asan, Korea 336-708. [3]Department of Nanotechnology and Division of Electronics and Computer Engineering, Hanyang University, Seoul, Korea 133-791.*) For electron-beam imaging applications that require large field size and variable observation angles, position controlled micro-column electron-beam systems are being researched due to their inherent maneuverability, which originates from their small size and light weight. The micro-column also has advantages of reducing substrate charging effects and sample surface damages since the low acceleration energy results in shallow electron beam penetration. Here, we report on the contrast enhancement of back scattered electron images produced using a low energy micro-column SEM system. We were able to enhance the back scattered electron image contrast between insulating and conducting parts of the sample, by applying electric field induced contrast(EFIC) imaging techniques. The EFIC image clearly shows enhanced contrast between the SiO_2 substrate and the carbon nanotubes bridging gold electrodes. We will report on the bias voltage dependence of the EFIC images and also compare them with electron-beam induced current images.

Ep-038 **External Pressure Dependent Conductance Changes of SWCNT Network film on Elastomer (PDMS)** WOO Chang-Seung, LIM Chae Hyun, PARK Bonghyun, MIN Dong-Hoon, LEE Seung-Beck[1](*Department of Nanotechnology, Hanyang University, Seoul. [1]Division of Electronics and Computer engineering, Hanyang University, Seoul.*) There have been several reports of strain sensing devices based on single-walled carbon nanotubes (SWCNTs), recently. In this study, we focused on the conductance change of SWCNT network film (SCNF) due to applied indirect external pressure. Once SCNF was made by vacuum filtration process, it was transferred to the poly dimethyl siloxane (PDMS) elastomer surface using a dry stamping method. Then, the SCNF-elastomer hybrid was bonded between two parallel electrodes (Cr/Au) separated 6 ㎜ pre-deposited on glass substrate. As pressure was applied to the sample surface, the conductance of the SCNF was increased. The conductance increase of the SCNF was as much as 10 % at 0.3 MPa pressure and the responses were reproducible. These results may be used for flexible pressure sensor applications.

Ep-039 **Transparent thin film transistor using low density single-walled carbon nanotube bundles**

HWANG Yoon-Sun, MIN Dong-Hoon, CHOI Won-Il, LIM Chae Hyun, PARK Bonghyun, LEE Seung-Beck[1] (*Department of Nanotechnology, Hanyang University, Seoul,. [1]Division of Electronics and Computer engineering, Hanyang University, Seoul,.*) The fabrication of carbon nano tube(CNT) thin film transistor(TFT) is difficult, because CNTs display high metallic properties in bundling. We presented here, a method to fabricate low density uniform distribution single-walled carbon nano tube(SWCNT) network films which have low bundle concentration. We immerged an anodic aluminum oxide(AAO) membrane, which has pores with average diameter 0.02um, into the well dispersed SWCNTs suspension in a bottle, which was then bathsonicated. The suspended CNTs were traped by AAO membrane pores during the sonication. Scanning electron microscope(SEM) was used to evaluate the density of SWCNT bundles which were 7~12ea./㎛2. We compared the TFT performance of network structure fabricated by the vacuum filtering method and demonstrated that the sonication filtering method showed higher on/off ratio, lower leakage transistor performance

Ep-040 **Deposition and Optical Properties of High Quality CdSe Nanocrystalline Thin Films by a NH_3-free Chemical Route** 이 현주, 이 수일(*조선대학교 과학(물리)교육학부.*) High-quality CdSe nanocrystalline thin films were prepared by a ammonia-free chemical method on the slide glass at room temperature. As prepared thin films were characterized by scanning electron microscopy (SEM), X-ray diffraction (XRD), UV-vis absorption and Raman scattering spectroscopy. The Surface morphologies of CdSe thin films revealed a sperical-like structure formed by the smaller particles. The UV-vis absorption spectrum shows a first sharp excitonic transition peaked at about 2.1 eV (589 nm). This peak was blue-shifted about 0.4 eV compared to bulk CdSe exciton energy (E_g=1.7 eV) due to the strong quantum confinement effect. We also found that the excitonic peak shifted to the higher energy levels with increasing CdSe thin film thickness. Raman spectrum shows a well-resolved vibrational mode at about 207 cm^{-1}, which is shifted to lower frequency about 3 cm^{-1} compared to the 1LO phonon of the CdSe bulk material (210 cm^{-1}).

Ep-041 **Dispersion Stability of Single-Walled Carbon Nanotubes using Nafion in Bisolvent** LEE Young Hee, KIM Ki Kang, AN Kay Hyeok[1], PARK Min Ho[2], YANG Cheol Woong[2], LEE Jin Hyon[3], PAIK Ungyu[3], YOON Seon Mi[4], LEE Jeonghee[4], KIM Byung Ki[4], KIM Jong Min[4], CHOI Jae Young[4] (*Department of Physics, Sungkyunkwan University. [1]Chonju Mechanics Research Center, Chonju. [2]School of Advanced Materials and Engineering, Sungkyunkwan University. [3]Hanyang University. [4]SAIT.*) We have investigated the effect of Nafion and its resulting interaction with single-walled carbon nanotubes (SWCNTs) on solubility and dispersion properties of SWCNTs in bisolvent. Nafion was used as a polymeric dispersant, providing both electrostatic and steric stabilization in preparation of stable and homogeneous suspension of SWCNTs. Correlation was made between solubility and nanodispersion of SWCNTs. It was found from the optical spectroscopy that solubility and nanodispersion of SWCNTs increased with an addition of 1-propanol and was maximum at a volume mixture of water / 1-propanol (80/20). We propose a mechanism of improved solubility and nanodispersion of SWCNTs, which is strongly correlated with an adsorption behavior of Nafion on SWCNTs, surface potential of SWCNTs, and solubility of Nafion in liquid medium, i.e., amphiphilic Nafion enhances dispersion of SWCNTs in the mixture of hydrophilic water and relatively hydrophobic 1-propanol.

Ep-042 **Defect-induced loading of Pt nanoparticles on carbon nanotubes** LEE Young Hee, KIM Sung Jin, PARK Yong Jin, RA Eun Ju, KIM Ki Kang, AN Kay Hyeok(*성균관대, 물리학과.*) Carbon nanotubes (CNTs)-supported Pt nanoparticle catalysts were prepared by a microwave technique for fuel cell. Pt nanoparticles were loaded under a microwave oven on the defective carbon nanotubes generated by an additional oxidant during acid treatment. Our Raman spectra and X-ray diffraction analysis demonstrated that the defects created during oxidation and microwave treatment acted as nucleation seeds for Pt adsorption. The generated Pt nanoparticles had the size distributions of 2~3 nm and were uniformly distributed on the defects of carbon nanotubes. Our density functional calculations showed that the adsorption strength of Pt atom on the vacancy defect of nanotube was significantly stronger by s-p hybridization with carbon atoms near the defect site.

Ep-043 **Direct writing of NiO nanostructures using an electron beam for nonvolatile memory application** JANG A-Rang, KIM Ki-Chul[1], LEE Sang-Hoon[2], PARK Sungho[2], KANG Dae Joon[3](*BK 21 Physics Research Division, SKKU Advanced Institute of Nanotechnology, Sungkyunkwan University. [1]BK 21 Physics Research Division and Institute of Basic Science, Sungkyunkwan University. [2]Department of Chemistry, Institute of Basic Science and SKKU Advanced Institute of Nanotechnology, Sungkyunkwan University. [3]BK 21 Physics Research Division, Institute of Basic Science, Center for Nanotubes and Nanostructured Composites and SKKU Advanced Institute of Nanotechnology, Sungkyunkwan University.*) In recent years, much attention has been paid to the development of resistive random access memory (ReRAM) due to its excellent memory characteristics such as low power operation, high density integration, and high-speed write and erase operations. Binary oxide systems such as Al_2O_3, TiO_2, Nb_2O_5, NiO and Ta_2O_5 have been extensively studied for their potential application in nonvolatile ReRAM. In this study, a spin-coatable NiO electron beam resist were developed for ReRAM application, We have attempted to realize sub-100 nm nanostructures of NiO using a high resolution electron beam lithography. These nanostructures were characterized by SEM, XRD, and Raman spectroscopy. Current-voltage (I-V) characteristics of NiO nanostructures were also measured to verify its resistance switching behavior.

Ep-044 **High quality single crystalline NiO nanowires grown by a thermal CVD technique** JANG A-Rang, KIM Ki-Chul[1], LEE Sang-Hoon[2], PARK Sungho[2], KANG Dae Joon[3](*BK 21 Physics Research Division, Institute of Basic Science, Center for Nanotubes and Nanostructured Composites and SKKU Advanced Institute of Nanotechnology, Sungkyunkwan University. [1]BK 21 Physics Research Division, and Institute of Basic Science, Sungkyunkwan University. [2]Department of Chemistry, Institute of Basic Science, and SKKU Advanced Institute of Nanotechnology, Sungkyunkwan University. [3]BK 21 Physics Research Division, Institute of Basic Science, and SKKU Advanced Institute of Nanotechnology, Sungkyunkwan University.*) Resistive RAM (ReRAM) is promising for advanced system on a chip in terms of high density and low power consumption. Among the various candidate materials for ReRAM applications, NiO is one of the most promising materials due to its large resistance change and simple constituents. High quality single crystalline nickel oxide (NiO) nanowires were successfully synthesized by a thermal CVD. The structure, morphology and properties of as-grown nanowires were examined by scanning electron micrscopy (SEM), X-ray diffraction (XRD), transmission electron microscopy (TEM), and raman spectroscopy. Our nanowires showed its resistance switching behavior. The results of the electrical measurements made on these nanowires are also discussed. Our results based on high quality single crystalline nanowires may hint about an operative switching mechanism

Ep-045 **Control synthesis of silver nanosheets, chainlike sheets and microwires via a simple solvent-thermal method** DU Jimin, KANG Dae Joon(*BK 21 Physics Research Division, Institute of Basic Science, Center for Nanotubes and Nanostructured Composites and SKKU Advanced Institute of Nanotechnology, Sungkyunkwan University.*) In this work, we present a facile method to synthesize silver nanosheets, chainlike sheets and microwires via decomposition of the $AgNO_3$ in ethanol in the presence of ammonia. All products are characterized by X-ray diffraction (XRD), whose results show that all the diffraction peaks can be indexed to the face-centered cubic (fcc) silver. Scanning electron microscopy (SEM) and transmission electron microscopy (TEM) results indicate that the amount of ammonia plays the key role in controlling the morphologies of the obtained products According to the experiments results and literatures, we propose an ammonia-tuning Oswald ripening mechanism to elucidate the formation of different morphologies of silver structures such as the nanosheets, chainlike sheets, and microwires. Furthermore, the I-V curve of the silver wires was recorded with Probe Station (Wentworth Company MP1008) and Semiconductor Parameter Analyzer (Hewlett-Packard 4140B), showing the metallic characteristics.

Ep-046 **Energetic electron irradiation induced formation of patterned SERS-active films** 조 성오, 김 용남(*한국과학기술원, 원자력및양자공학과.*) 초산은(silver acetate)에 전자빔을 조사함으로써 패턴화된 SERS (Surface Enhanced Raman Scattering) active 필름을 제조하였다. 초산은을 유리나 실리콘 기판 위에 코팅하여 약 100nm 두께의 균일한 필름을 만들고, 50keV의 에너지를 가진 전자빔을 진공에서 TEM grid를 마스크로 이용하여 선택적으로 조사하면, 조사된 부분의 초산은만

화학적 결합이 분해되어 나노 입자로 변환된다. TEM grid의 mesh 크기에 따라 패턴의 크기 조절이 가능하며, 제조된 필름이 50~100 nm 크기의 은 나노 결정입자로 구성되어 있음을 SEM, TEM, EDX, XRD를 이용하여 확인하였다. 패턴화된 필름의 SERS 효과를 측정하기 위해 benzenethiol과 632.8nm 파장의 레이저를 이용하여 Raman 스펙트럼 및 영상을 얻었으며, 약 10^4~10^6의 표면증강 강도를 나타내었다.

Ep-047 **양극산화 전압에 따른 균일한 다공성 알루미나의 구조적 및 광학적 특성의 변화** 이 광섭, 오 세웅[1], 김 태환[1], 우 덕하[2], 정 미[2](*한양댜학교, 정보디스플레이공학과. [1]한양대학교, 전자컴퓨터통신공학부. [2]한국과학기술연구원 광기술센타.*) 균일한 다공성 알루미나는 제작방법이 단순하고 높은 균일성을 얻을 수 있어 다양한 분야에 응용이 가능하다. 다공성 알루미나를 제작하기 위하여 전해연마 처리한 순도 99.99%의 알루미늄(Al) 호일을 양극전극으로 하고 음극전극에 백금전극을 사용하여 알루미늄을 양극산화한다. 전해질로는 0.3M의 옥살산($H_2C_2O_4$)용액을 이용하며, 항온조를 이용하여 3℃ 저온을 유지시킨다. 전압 공급장치를 이용하여 일정한 전압을 걸어주면 다공성 알루미나 박막을 만들 수 있다. 1차 양극산화로 형성된 다공성 알루미나는 매우 불균일하여 0.4M의 인산(H_3PO_4)과 0.2M의 크롬산(H_2CrO_4)을 혼합한 식각용액을 이용하여 식각하고 1차 양극산화와 동일한 방법으로 2차 양극산화를 실시하여 균일한 다공성 알루미나를 형성할 수 있었다. 양극산화 전압이 증가할수록 다공성 알루미나의 동공크기가 50~150 nm의 다양한 크기의 다공성 알루미나의 크기 및 비율을 조정할 수 있으며, 이러한 현상을 원자힘 현미경으로 관측할 수 있다. 형성된 다공성 알루미나를 유기발광소자의 광추출효율을 높이기 위한 구조로 사용하기 위하여 다공성 알루미나 박막의 광학적 특성에 대한 조사를 하였다. 다공성 알루미나의 양극산화 전압에 따른 구조적 특성과 광학적 특성에 대한 변화를 투과도 측정으로 다공성 알루미나의 동공크기에 의해 투과도가 증가 및 감소하는 것을 관측 할 수 있었다. 이 결과로부터 유기발광소자의 광추출효율을 향상하기 위해 요구되는 다공성 알루미나박막의 최적화된 제작조건을 결정하였다.

*이 논문은 2006년도 정부재원(교육인적자원부 학술연구조성사업비)으로 한국학술진흥재단의 지원을 받아 연구되었음 (KRF-2004-005-D00166).

Ep-048 **Comparative study of ZnO nanowires growth using Au catalysts in terms of preparation condition of catalytic materials.** LEE Suok, KANG Dae Joon[1](*BK 21 Physics Research Division, Institute of Basic Science, and Center for Nanotubes and Nanostructured Compositions, Sungkyunkwan University. [1]BK 21 Physics Research Division, Institute of Basic Science, and Center for Nanotubes and Nanostructured Compositions, and SKKU Advanced Institute of Nanotechnology, Sungkyunkwan University.*) ZnO nanomaterials are promising candidates for nano electronics and photonics. It is known that well aligned ZnO nanowires can be grown by thermal chemical vapor deposition method using metal catalysts such as Au, Ni, Cu etc. In this study, we attempted to elucidate the growth mechanism of ZnO nanowires by comparing its different growth behaviors in terms of preparation conditions of Au catalysts We synthesized ZnO nanowires from a very thin Au layer deposited on Si substrate following a literature recipe while varying different thermal decomposition temperature, time and the thickness of Au film. We then attempted to grow ZnO nanowires from sub 5 nm diameter Au nanoparticle arrays deposited on Si substrates for a comparison,. Structural and Optical Characterization were carried out on both samples by SEM, TEM and RAMAN spectroscopy. The results demonstrated that the growth behavior is not quite the same depending on the preparation condition of Au catalyst. We will attempt to compare their different growth behaviors and elucidate its possible growth mechanism carefully based on our results.

Ep-049 **화학적 습식 방법으로 성장된 ZnO 나노구조물의 특성 평가 및 이의 응용** 이 선영, 김 상협, 명 혜진, 맹 성렬(*한국전자통신연구원 캠브리지-ETRI공동연구센타.*) ZnO 는 Eg = 3.35 eV의 반도체 물질로 FET, 바이오 및 화학센서, 발광 소자, 태양전지 등 나노 소자로서의 응용이 기대되는 물질로 각광을 받고 있다. 그러나 ZnO 나노 구조물은 Au와 같은 귀금속 촉매 위에 고온 기상 증착법에 의하여 ZnO의 핵 생성 및 성장이 일어난다. 이러한 방법은 고온에서 성장하고 장비의 한계로 대량의 ZnO 나노 구조물을 성장 할 수 없는 단점이 있다. 최근 화학적인 습식 방법으로 ZnO 나노 구조물을 성장시키는 방법이 널리 연구되어지고 있다. 본 연구에서는 화학적인 습식방법으로 대기압, 저온의 조건에서 간단한 공정으로 Si, ITO, glass 등의 기판위에 수직 성장 시켰으며 이의 특성 평가를 수행하였다. 또한 화학적인 습식방법으로 성장시 생기는 부산물을 분석하여 대량의 ZnO 나노로드 분말을 얻어 이의 특성 평가를 수행하였다. 기판위에 성장된 나노와이어 및 ZnO 나노로드 분말의 구조적, 광학적 분석을 위해 FE-SEM, TEM, PL 등의 측정을 수행하였다. 또한 성장

된 나노 구조물을 이용하여 유무기하이브리드 solar cell 로서의 응용 가능성을 보았다.

Ep-050 **Bismuth박막의 임계두께와 박막물성 변화에 대한 연구** 안 영근, 이 상엽, 장 민영, 김 현종, 최 진문[1], 정 광호, 박 상윤[2], 신 상원[3](*연세대학교 물리 및 응용물리. [1]연세대학교 학부대학. [2]한양대학교 물리학과. [3]한국과학기술원.*) 고진공 환경(High Vacuum environment)에서 열증착방법으로 Si(001) 및 fused glass 기판에 상온 형성된 나노 스케일의 Bismuth thin film에 대해서 두께에 따른 표면morphology와 이와 관계된 결정 structure의 변화, 그리고 이러한 물성이 급격히 변화하는 임계두께를 관찰하였다.본 연구에서는 Bismuth박막의 표면, 구조적 특성을 구분할 수 있는 임계두께(critical thickness)의 존재를 검색할 수 있도록, 다양한 두께(1.8nm ~ 273nm)의 Bismuth 박막시편의 표면, 구조적 특성 변화 연구에 초점을 맞추었다. 그 결과, Atomic force microscopy(AFM) 측정을 통해 Silicon 기판과 fused glass 기판에 형성된 Bismuth박막 시편에서 두께가 9nm인 경우를 경계로 비정형의 Bismuth cluster들이 hexagonal structure로 예상되는 다각형의 결정립(crystalline domain)으로 변하기 시작하였으며, 두께가 18nm인 경우에서부터 박막의 결정화가 급격히 진행되고 있음을 X선회절실험(XRD)과 AFM을 통해서 발견했다. 박막의 두께가 45.5nm~273nm의 경우에서는 상온의 증착 과정에서 이미 결정화가 대부분 이루어진 것으로 보이는 0.2㎛~0.4㎛크기의 결정립들이 관찰되었다. 박막의 두께는 저각X선반사(low angle X-ray reflectivity, XRR)측정을 통해서 결정하였고, 2theta 10 ° ~90°의 고각XRD(high angle XRD) 측정결과로부터 박막두께가 18nm이상인 경우에서부터 crystalline structure가 형성되기 시작하여, 그 이상 두께의 경우에서 결정상(crystalline phase)은 유지한 상태로, 결정상의 크기(crystallite size)가 두께가 증가함에 따라 증가하는 것을 보여, 결과적으로 상온의 증착 조건에서 Bismuth 박막의 두께에 따른 결정화가 임계두께 이상의 나노스케일 영역에서는 연속적으로 이루어지고 있으며, 반면에 임계두께 이하에서의 Bismuth cluster는 amorphous phase를 형성하고 있음을 알 수 있었다. 이와 같은 Bismuth의 두께에 따른 박막 결정상과 morphology의 급격한 변화는 박막의 전기적 성질의 변화에 큰 영향을 미치는 요소이며, 이에 대한 추가적인 연구를 통해서 이미 알려진 Bismuth 박막의 양자효과에 대한 보다 많은 정보와 Bismuth를 이용한 spintronics 및 superconductivity, thermoelectric effect 등의 분야에 도움을 줄 것으로 기대된다.

Ep-051 **Effect of Electrode Thickness on the Bottom Contact Pentacene Thin Film Transistors** CHAEHO Kim, D. Jeon(*Seoul National University.*) In organic thin film transistors(OTFTs), a bottom contact is widely used because it can be made easily by photolithography. The performance of OTFTs using bottom contact in general is poor compared to the top contact. This difference probably is due to the geometry and bonding of the metal-organic interface. We fabricated pentacene OTFTs with bottom contact of various electrode thickness and measured I-V characteristics and cross-sectional scanning electron micrographs. We found that there was a microscopically observable gap at the boundary between the thick electrode and pentacene film, which was the main reason for the reduced performance. On the other hand when the electrode was too thin, the channel current was also reduced because of the high electrical resistance. At the meeting we will discuss I-V characteristics and corresponding microscopic images of the device with different electrode thickness. This work was supported by the Korea Science and Engineering Foundation through the Nano Systems Institute-National Core Research Center at Seoul National University.

Ep-052 **Growth and characterization of high quality single crystal organic semiconductor: TMTSF (tetramethyl tetraselena fulvalene)** KIM Ja-Yeon, LEE InJae(*Department of Physics of Chonbuk National University.*) We present an overview of making and analyzing high quality single crystal organic semiconductor TMTSF. The starting material is a powder type of TMTSF. The source material has been purified several times in a high-vacuum horizontal tube system at sublimation temperature with a temperature gradient. Subsequent recrystallize has been made on the purified TMTSF with a deliberate inert carrier gas flow at the same conditions. Both forced and buoyancy driven convections possibly occur at the same time for making organic crystals. The lattice structure of the TMTSF crystals has been analyzed by using XRD. We expect that the single crystal TMTSF will be a good material as an active layer for field effect transistors.

Ep-053 **음극금속이 혼합된 이중전자수송층을 포함한 고효율 유기발광소자 제작 및 특성** 차 한뫼, 추 동철[1], 김 태환[1], 서 지현[2], 김 영관[2](*한양대학교, 전자컴퓨터통신공학부. [1]한양대학교, 전자컴퓨터통신공학부*

디스플레이공학연구소. [2]홍익대학교, 정보디스플레이공학과.) 혼합되지 않은 순수한 전자수송층위에 전자주입층 물질 또는 음극금속물질이 혼합된 층으로 구성된 이중전자수송층을 가진 유기발광소자를 제작하였다. 이중전자수송층은 다음과 같은 두 가지 구조로 전자주입층으로 사용되는 Lithium quinolate (Liq)와 전자수송층으로 사용되는 tris-(8-hydroxy quinoline) aluminum (Alq_3)의 혼합층과 Alq_3 층으로 구성된 구조 (소자1) 또는 Alq_3 와 음극전극물질인 알루미늄(Al)이 혼합된 층과 Alq_3 층으로 구성된 구조 (소자2)와 이중전자수송층을 갖지 않는 기준 소자를 제작하여 전류밀도-전압 특성, 휘도-전압 특성, 전계발광 및 발광효율 특성을 측정하였다. 소자 1과 2는 이중전자수송층을 갖지 않는 기준소자보다 높은 효율을 보였다. 소자 1은 기준소자보다 전류밀도가 증대되는 특성을 보였으며 이는 전자주입층으로 사용되는 Liq의 혼합으로 전하의 주입효율이 향상하였음을 나타낸다. 그러나 발광효율면에서는 Alq_3 와 Al의 혼합층으로 구성된 소자 2는 효율이 전류밀도 200 mA 이하에서 가장 높게 나타난다. 전류밀도가 낮은 영역에서 혼합된 Al 이 포함된 층은 전자뿐만 아니라 정공의 주입을 방해하여 발광층에서 전자와 정공의 균형을 조절하는 역할을 하여 효율을 향상하나 전류밀도가 높은 영역에서는 전자의 주입이 증가하여 전자와 정공수의 불균형을 초래하여 발광효율이 감소하는 특성을 나타낸다. 이중전자수송층을 사용한 유기발광소자의 발광메카니즘의 변화는 전압변화에 대한 전계발광특성 결과로부터 확인할 수 있었다.

*이 논문은 2006년도 정부재원(교육인적자원부 학술연구조성사업비)으로 한국학술진흥재단의 지원을 받아 연구되었음 (KRF-2004-005-D00166).

Ep-054 **전도냉각방식 고온초전도 도체의 임계전류 측정 장치 개발** 손 명환, 김 석호, 심 기덕, 이 언용, 성 기철, 김 호민, 권 영길(*한국전기연구원 초전도기기연구그룹.*) 오늘날 고온초전도 도체를 이용한 초전도 응용기기들이 속속 개발되고 있다. 사용 목적에 따라 운전온도가 다르다. 운전온도 근처에서 고온초전도 도체의 특성 특히 임계전류(Ic)는 매우 중요하고 가장 일반적인 측정방법은 고온초전도 도체에 전류를 흘리면서 가운데 부분에서 전압을 측정하는 4-단자법이다. 이 때 보통의 경우 일정온도를 유지하기 위해 냉매를 사용하는데 액체질소 온도(77K)나 액체헬륨온도(4.2K)에서만 측정이 가능하다. 그리고 고온초전도 도체의 응용측면에서 볼 때 액체질소온도에서는 고온초전도 도체의 임계전류가 낮아 실용성이 없고 액체헬륨을 사용할 경우 냉매가 비싸고 취급하기 어렵다. 또한 냉동기의 성능이 우수해짐에 따라 전도냉각방식으로 초전도응용기기들이 개발되고 있다. 따라서 액체질소온도와 액체헬륨온도 사이에서 전도냉각이 된 고온초전도 도체의 특성을 평가할 수 있는 장치가 필요하다. 본 연구에서는 2단 GM 냉동기를 사용한 고온초전도 도체의 Ic 측정장치를 제작하였으며, 본 장치를 이용한 Bi-2223 고온초전도 도체의 각 온도에 따른 Ic 결과들을 소개한다.

*"본 연구는 과학기술부 지원의 한국전기연구원 기본연구사업 연구비로 수행되었습니다."

Ep-055 **분무열분해법으로 성장된 p-형 ZnO 박막의 구조와 광학적 전기적 특성** 서 동주, 이 관교, 임 수경, 김 건호[1](*조선대학교. [1]경상대학교.*) p-형 ZnO 박막을 분무열분해법으로 유리기판위에 성장시켰다. 이 때 유리기판은 450℃의 온도로 일정하게 유지시켰다. 불순물로 첨가한 인(P)의 변화에 따른 ZnO : P 박막의 결정구조는 X-선회절(XRD) 무늬로부터 분석하였으며, 표면의 형태와 화학적 조성은 주사전자현미경(SEM)과 에너지분산 X-선분석기(EDS)로 분석하였다. ZnO : P 박막의 광투과율과 광흡수 스펙트럼을 측정하였고, ZnO : P 박막의 광학적 에너지 띠 간격을 구하였다. 또한 불순물로 첨가한 인(P)의 변화에 따른 ZnO : P 박막의 비저항과 운반자 농도는 van der Pauw법으로 측정하였다.

Ep-056 **HfO_2-SiO_2 계 나노 박막의 두께 분석** 김 창수, 조 용재, 조 현모, 조 만호, 박 재환[1], 윤 지연[1], 오 병성[1], 최 용대[2](*한국표준과학연구연 전략기술연구부. [1]충남대학교 물리학과. [2]목원대학교 광전자물리학과.*) 실리콘 소자의 고집적화에 따라 게이트 산화막의 두께가 수 nm 정도로 극히 얇아지고 따라서 고유전율 박막을 이용하는 노력이 이루어지고 있다. 차세대 게이트 산화막으로 기대되는 고유전율의 HfO_2 및 $Hf(Si)O_4$ 계열의 나노 박막의 두께를 XRR(X-Ray Reflectivity), TEM, SE(Spectroscopic Ellipsometry), MEIS(Medium Energy Ion Spectroscopy) 등을 이용하여 분석하고 그 특성을 평가하였다. 실리콘 기판 위에 성장한 3.5, 5, 8 nm 두께의 HfO2와 Si의 조성이 다른 5 nm 두께의 $Hf(Si)O_4$ 박막 3종을 준비하였다. XRR 결과의 Fourier Transform과 TEM 분석을 통하여 기판과 HfO_2 사이의 SiO_2 중간층을 확인하였고 이 결과를 바탕으로 SE 및 XRR 분석 시 중간층을 고려하였다. XRR과 MEIS에 의한 두께 결과는 대체적으로 잘 일치하였으나 SE에 의한 결과와는 다소 차이를 보여주었다. 특히 중간층은 고려한 SE 분석 결과는 고려하지 않은 경우에 비해 XRR과 MEIS 결과에 대하여 크게 개선되었다. 본 연구에서는 각 분석방법에 의한 두께 결과를 비교 분석하고 그 차이점을 논하였다.

Ep-057 **Spectroscopic Ellipsometry as Surface Plasmon Resonance Mode for Detection of Cancer Protein** KIM yunbog, WOO minah[1], CHO Myunghaing[1], JEON dongryul(*Seoul National University, Department of Physics Education. [1]Seoul National University, College of Veterinary Medicine.*) Since the first application of surface plasmon resonance (SPR) for biosensing almost two decades ago, SPR has made great strides in terms of both the instrumentation and the application. We used spectroscopic ellipsometry as an SPR sensor to detect the reaction between HER2 protein extracted from SKBR3 breast cancer cells and HER2 antibody. Since the Psi value of ellipsometry is related to the reflectivity of p wave, the surface plasmon signal can be measured using spectroscopic ellipsometry. The experiment was done as follows : a glass plate coated with a 50 nm-thick gold film was shaked in HER2 antibody solution for 2 hour. After this, the substrate was dipped in a soup of SKBR3 protein to induce the antibody-antigen reaction. The gold film exhibited a typical plasmon peak at 2.06 eV. After the HER2 antibody introduction, the peak showed up at 2.04 eV, and after the reaction with the protein of SKBR3 a new peak appeared at 1.99 eV. We believe the 1.99 eV peak is a plasmon signal arising from the binding of HER2 proteins of SKBR3 to HER2 antibody. Our result adds an example to the possibility of using spectroscopic ellipsometry as SPR mode for the detection of cancer cells.

Ep-058 **Fabrication of LCO and LSCO Thin Films by Pulsed Laser Deposition for Metal-Insulator Transition** PARK Seongtae, KANG Weekyung, YUN Sun Jin[1], KIM Hyun-Tak[1](*Soongsil University, Dept. of Chemistry. [1]ETRI, IT Convergence and Components Research Laboratory.*) The phenomenon of metal-insulator transition (MIT) attracts much attention due to its scientific implication and possibility to be used in variety of applications. The parent compound, La_2CuO_4 (LCO) is classified as a Mott insulator. A controlled hole-doping of LCO with substitution Sr^{2+} at La^{3+} sites makes it the ideal system to study the mechanism of MIT in cuprates. In underdoped region of $La_{2-x}Sr_xCuO_4$ (LSCO), resistivity measurements have revealed the field-induced normal state to be a charge insulator. High quality thin film of LCO and LSCO are required for a variety of fundamental studies. A large number of techniques have been used in recent years to synthesize thin films of this material. Pulsed laser deposition (PLD) technique is a rather novel method for a wide range of materials including metals, alloys and oxide films. The MIT properties of LCO and LSCO thin film prepared under various conditions by PLD technique will be discussed in this presentation.

Ep-059 **Chemical Bath Deposition(CBD)에 의해 성장된 CdS/ITO 박막의 Near-Field Scanning Microwave Microscope 특성 연구** 김 미정, 정 원호, 차 덕준, 조 승곤[1], 정 양준[1], 이 기진[2](*군산대학교, 물리학과. [1]목포대학교, 물리학과. [2]서강대학교, 물리학과.*) ITO 유리 기판에 CBD 방법으로 200℃~ 500℃ 범위에서 2μm의 두께로 다결정 CdS를 적층 성장하였다. 성장된 박막의 구조와 표면특성 측정을 위해 XRD와 SEM(scanning electron microscopy), AFM(atomic force microscopy)을 이용하였으며, 4단자 접촉방식으로 표면전기저항을 측정하였다. 측정된 구조 및 표면특성을 비파괴, 비접촉방식인 near-field scanning microwave microscope 을 이용하여 CdS/ITO박막의 표면저항특성과 비교 연구하였다.

Ep-060 **타원 편광분석법을 이용한 $In_xAl_{1-x}As$ alloy 유전함수 연구** 윤 재진, 김 영동, STOUTE N. A.[1], ASPNES D. E.[1], 김 혜정[2], CHANG Y. C.[2], 송진동[3](*경희대학교 나노 광물성 연구실 및 물리학과. [1]Department of Physics, NC State University. [2]Research Center for Applied Sciences. [3]한국과학기술연구원(KIST)*) InAlAs alloy는 InP계 및 GaAs계의 고 전자이동도 트랜지스터(HEMT)와 IC응용기술등에 사용되고 있고 전자 통신 및 디바이스 산업에서 넓은 응용범위를 갖고 있지만 다른 화합물에 비해 전이점 연구 및 광 특성 연구가 미흡한 실정이다. 본 연구에서는 타원 편광 분석법을 이용하여 1.5 ~ 6eV의 분광 영역에서 인듐 조성비가 각기 다른 InAlAs alloy의 유전함수를 측정하였다. 또한 표면에 자연 산화막을 제거하기 위하여 Methonol과 DI Water로 표면을 세척 하고 NH_4OH, BrM등으로 적절한 화학적 에칭을 하여 산화막을 제거함으로서 순수한 유전함수를 측정할 수 있었다. 측정된 InAlAs 유전함수를 Standard analytic CP line shape 방법으로 인듐 조성비에 따른 에너지 전이점을 얻을 수 있었다. 또한 얻어진 에너지 전이점 값을 이용하여 Davenport와 그의 연구진들이 발전시킨 LASTO 방법으로 밴드구조 계산을 하였고, 이를 바탕으로 E_2 전이점 지역의 여러 전이점 특성을 정확히 정의할 수 있었다. 타원 편광 분석법을 이용한 전이점 연구 및 물성 분석은 InAlAs alloy의 광학적 데이터베이스를 확보하는 성과와 더불어 초고속 전자 디바이스기술 및 전자 통신 산업에도 유용한 정보가 될 것이다.

Ep-061 **Exchange bias in epitaxial Fe/CrSb bilayer** 김 재휘, 최 정용, 황 영훈, 최 지연, 조 성래(*울산대학교, 물리학과.*) The exchange bias effect, which shifts not only the magnetic hysteresis but also induces the various interesting magnetic properties between the ferromagnetic (FM) and antiferromagnetic (AFM) layers, was discovered about fifty years ago.[1] The exchange bias has been widely applied to the spintronic devices such as spin-valve and MTJ, and so on. Many scientists have studied noble FM/AFM bilayer structures because of increasing importance in pinning layer. Antiferromagnetic FeMn, IrMn, and NiO have widely been used as a pinning layers in the devices.[2] On the other hand, CrSb has a antiferromagnetism with T_N of 710 K and has NiAs-type hexagonal structure with lattice constant of a=4.122 Å and c=5.464 Å.[3,4] In this talk, we will present the exchange bias effect in epitaxial Fe/CrSb system.We have grown Fe/CrSb bilayer by molecular-beam epitaxial (MBE). Firstly, we grew 1000 Å thick GaAs buffer layer at 550 °C, followed by 1000 Å thick GaSb at 550 °C, 200 Å CrSb at 350 °C and 200 Å Fe at room temperature. Finally, we capped the Fe/CrSb bilayer with 100 Å thick GaAs in order to protect the surface. From the magnetization and transport measurements, we have observed the exchange bias phenomena between Fe and CrSb layers, which will be discussed in detail.

Ep-062 **Spectroscopic Ellipsometry를 이용한 $Zn_xCd_{1-x}Se$ 화합물 반도체의 광특성과 밴드 구조 연구** 변 준석, 정 용우, 김 영동, 김 혜정[1], CHANG Y.C.[1](*경희대학교 나노 광물성 연구실 및 물리학과. [1]Research Center for Applied Sciences.*) 본 연구는 $Zn_xCd_{1-x}Se$ 화합물 반도체의 유전함수를 실온에서 0.7~9 eV의 분광영역을 가진 Vacuum Ultra-Violet Spectroscopic Ellipsometry (VUV-SE)를 이용하여 측정하였다. VUV-SE는 6 eV 이후의 유전함수를 측정할 수 있는 장비로써, 기존의 ellipsometry 가 측정할 수 없었던 ZnCdSe의 E_2 peak 보다 큰 밴드갭을 얻을 수 있었다.측정된 유전함수를 이용하여 에너지 밴드갭을 얻기 위해 standard analytic dielectric function line shape를 이용하였고, 이 데이터를 통해$Zn_xCd_{1-x}Se$의 밴드 구조를 계산하였다. 계산 방법은 Davenport와 그의 연구진들이 발전시킨 LASTO 방법을 이용하였으며, 끝점 물질인 CdSe 및 ZnSe 의 밴드 구조는 local density approximation으로 계산 되었고, 실온 밴드 구조 생성을 위해 scissor operator 가 적용되었는데, 이는 전도대를 완고하게 이동시키기 위해서이다. 이 밴드 계산을 통해, 0.7~9 eV 부근에서 에너지 전이점 (E_0, $E_0+\Delta_0$, E_1, $E_1+\Delta_1$, E_2, E_0', $E_2+\Delta_2$, E_2', $E_0'+\Delta_0'$)들을 정의할 수 있었다. 결과적으로 이 연구를 통하여 임의의 함량 x에의한$Zn_xCd_{1-x}Se$의 광특성을 측정할 수 있었고, 이러한 추론은 광전자 공학 산업의 데이터베이스와 같은 $Zn_xCd_{1-x}Se$의 광특성에 대한 학문적 및 산업적 접근에 유용할 수 있다고 하겠다.

Ep-063 **Fabrication of GaAs on Si Heterostructures by He Ion Implantation at Room Temperature and Wafer Direct Bonding** HYUNG-JOO WOO, HAN-WOO CHOI, GI-DONG KIM, WAN HONG, JOON-KON KIM(*Ion Beam Application Group, Korean Institute of Geoscience and Mineral Resources.*) Transfer of GaAs layers onto Si by helium ion implantation and direct wafer bonding was investigated. The influence of the 100 keV He ion fluence and subsequent annealing on sudden avalanche-type exfoliations was studied by RBS/channeling, optical microscopy and cross-sectional TEM analysis, and the optimum conditions for achieving splitting only after post-implantation annealing were experimentally determined. Our results suggest that the optimum fluence for the GaAs ion-cut is in the range of 2 ~ 5 x 10^{16} He^+/cm^2 at room temperature, which is markedly lower than that in case of hydrogen implantation (1.2 ~ 1.5 x 10^{17} He^+/cm^2) at a specific high temperature window (120 ~ 140℃). Thin 4" GaAs layer was successfully transferred onto silicon after bonding of helium implanted GaAs and Si wafer via a spin-on-glass layer and subsequent low temperature splitting annealing at 190 ~ 200°C (10 ~ 14 hrs). FE-SEM analysis revealed no detectable defect at GaAs/SOG/Si bonding interfaces, and the transferred layer thickness (and surface roughness) depends on the implant fluence.

Ep-064 **Cobalt Thin Films Fabricated by Plasma Enhanced ALD** NOH S. J., LEE D. H., KWON S. R., KIM H. S., KIM Y. M.(*Dankook University, Applied Physics.*) We developed a PEALD(Plasma Enhanced Atomic Layer Deposition) system adopting an ICP (Inductively Coupled Plasma) source with an ALD system. Cobalt thin films were fabricated by ALD and PEALD. $Co_2(CO)_6$ was used as a cobalt precursor, NH_3 as a reactant, and Ar as a carrier and purge gas. The deposition characteristics and film properties were investigated using four-point probe, field emission scanning electron microscopy (FESEM), atomic force microscopy

(AFM), and auger electron spectroscopy(AES). The detailed results will be reported.

*This work was supported by HANBIT Users Cultivation Program of National Fusion Research Center, and also by Seoul Development Institute(SDI) as a project of "Cluster for Advanced Information Display with enhanced Human Sensibility Ergonomics" (2006).

Ep-065 **X-ray Diffuse Scattering Study of the Polystyrene Films with Temperature Dependence.** BYUN Youngsuk, EOM Daeyong[1], LEE Young-joo, LEE Heeju, SONG Sanghoon[1], KIM Hyunjung[2](*서강대학교, 물리학과. [1]서강대학교, 바이오융합과정. [2]서강대학교, 물리학과 &바이오융합과정.*) We have measured x-ray diffuse scattering of thin polystyrene films at melt. We carried out the measurement with varying thickness and molecular weights as a function of temperature(150~220℃,in-situ). We observed a deviation from conventional capillary wave theory for viscous liquids when the film thickness is close to the radius of the polymer. We shall discuss the deviation and modification of liquid theory with the model considering elastic effect.

Ep-066 **Diffusion of LiF into Al Cathode in Alq3 Based OLED** LEE Young Joo, BYUN Youngsuk, EOM Daeyong, PARK Seong-Sik[1], IM Woobin[2], KIM Jinwoo[3], KIM Hyunjung(*Sogang University. [1]Samsung Corning Co., Ltd. [2]Neoview Kolon. [3]Gwangju Institute of Science and Technology.*) We measured interfacial diffusion of LiF into Al cathode in tris-(8-hydroxyquinoline) aluminum (Alq3) based organic light emitting device (OLED) by X-ray reflectivity. The thickness of LiF was varied from 5Å to 25Å. We adopted Al/LiF/Alq3 on ITO-coated glass and Alq3/LiF/Al on ITO-coated glass samples in order to investigate dependence of diffusion of LiF on the order of deposition of Al and Alq3. We pre-annealed the OLED samples from room temperature to 180℃. We found a thin mixed layer of Alq3 and LiF and another mixed layer of LiF and Al in the process of estimating dissociative reaction and diffusion of LiF. We will discuss LiF diffusion between Al cathode and Alq3 as a function of LiF thickness, order of deposition of Al and Alq3, and annealing temperature in more detail.

Ep-067 **Nondestructive Sensing of Metallic flaws Using AC Magnetic Fields by Single Excitation Coil** LEE Jun Sik, JANG Do Kuen, KIM Nan Yong, KIM Ki Hyeon, KIM Jong Ho[1], SHON Jong Sik[1], YOO Young Kuen[1](*Dept. of Physics, Yeungnam Univ. [1]Research Institute of Nova Magnetics.*) The role of electromagnetic-based non-contact and nondestructive evaluation (NDE) of metallic components in engineering industry is increasing [1, 2]. It has been mainly applied for inspection of metal constructions, pipes, parts of plains, etc.. Among the electromagnetic based NDE, eddy current testing (ECT) probes combine an excitation coil that induces eddy currents in a specimen and a detection element that identifies the perturbation of currents caused by cracks or other defects. Therefore, we have performed the nondestructive testing (NDT) to detect the metallic surface flaws using the simplified eddy current sensing system.The simplified eddy current testing (ECT) sensor was composed of the commercial tape recording magnetic inductive head as a sensing component and single coil with straight and circular shape as an excitation coil. The excitation coil was generated the AC magnetic fields with the frequency range of 30 kHz to 60 kHz which were applied to the artificial cracks specimen. This sensor was moved on surface of the artificial cracks specimen with 4 mm of flying height and 4 mm/s of scan speed which controlled by X, Y, Z-axis scanner. And then the signals were amplified and filtered by the pre-amplifier and Lock-in amplifier, respectively. The artificial crack specimens were prepared with the various shape of cracks (slit and hole), size (minimum depth and width; 0. 5 mm) and materials (Al, Cu; nonmagnetic, Fe, FeC; magnetic), respectively. As results, the signals at crack position were obtained with high S/N ratio for the magnetic and nonmagnetic materials.

Ep-068 **Spectral Characteristics of a Self-developed SPR Sensor** YUK Jong Seol, HONG Duk-Geun[1](*Kangwon National University, College of Medicine. [1]Kangwon National University, Department of Physic.*) We present a self-constructed biosensor with an angular interrogation based-surface plasmon resonance (SPR) spectroscopy for the purpose of analysis of antigen-antibody interactions on protein chips. SPR intensity, resonance angle and full width at half maximum (FWHM) were significantly affected by the thickness of gold film.

Optimal gold film thickness as an active metal for surface plasmons was determined as an approximately 45 nm, considering SPR intensity and FWHM of SPR spectrum. The detection limit of the sensor based on the minimal refractive index variation was calculated to be 1.4×10^{-4}. The interaction of C-reactive protein (CRP) with anti-CRP antibody on a 45 nm-thick gold film was successfully analyzed by the self-constructed SPR sensor. We suggest that the SPR sensor can be used as a useful tool for analysis of immunoreactions.

Ep-069 **나노 구조를 갖는 다공질규소를 이용한 알부민 검출에 관한 연구** 김 한중, 박 선화, 이 기원, 김 영유(*공주대학교 물리학과.*) 다공질규소(Porous Silicon)는 상온에서 제작공정이 간단하고, 부피에 비해 대단히 큰 비표면적을 가진 나노 구조로 되어 있어 센서(Sensor), 발광다이오드(LED), 도파관(Waveguide) 등으로 응용을 위한 연구가 지속적으로 이루어지고 있다. 최근에는 다공질규소를 질병의 진단과 예방에 응용하기위한 생물학적 분야로의 이용이 기대되고 있다. 질병의 발현이 유전자 수준이 아닌 단백질 수준에서 규명되기 때문에 질병의 진단과 치료를 담당하는 단백질 바이오칩(Protein Biochip)이 크게 주목받고 있는 실정이다. 본 연구에서는 다공질규소를 알부민(Albumin)과 같은 단백질을 검출하는 센서로 응용하기 위한 몇가지 기본 실험을 수행하였다. 연구결과 특정 단백질에 대해 광학적 및 전기적 특성의 변화가 감지되었다.

Ep-070 **Stair Current Output Power Supply For Switching Magnet** 성훈 정, 기현 박, 흥식 강, 동언 김, 진혁 최(*PAL.*) The switching magnet for beam distribution is served with Digital Signal Processor (DSP) controlled PWM switching-mode power supply (SMPS). This SMPS is employed phase-shifted parallel (PSP) operation of IGBTs. This technique allows ± 350 A, 2.5 Hz stair output, and ± 350 A at bipolar mode operation. Current feedback and input voltage feed-forward control schemes are applied to improve the output current stability. Experimental results showed that the implemented converter achieved a useful versatile power supply.

Ep-071 **Rubrene thin-film transistors with crystalline and amorphous channels** IM Seong il, PARK Se Woung, HWANG Jung Min, CHOI Jeong Min, HWANG Do kyung, KIM Jae Hoon(*Yonsei University Institute of Physics and Applied Physics.*) We report on the fabrication of rubrene organic thin-film transistors (OTFTs) with crystalline and amorphous channels, which were achieved by patterning a rubrene thin film deposited under a specific condition. The deposited film was mostly covered by amorphous rubrene matrix with smooth surface except many crystalline rubrene discs embedded with rough surface, as characterized by optical and atomic force microscopes. When the channel of OTFT covers some portion of crystalline discs, our OTFT displayed a typical field effect behavior while it showed little drain current with the channel covered with amorphous background. Typical field mobility obtained from OTFT with crystalline discs was 1.23×10^{-4} cm^2/V s with an on/off current ratio of $\sim 10^3$ and a high threshold voltage of -30 V.

Ep-072 **Ultraviolet-enhanced device properties in pentacene-based thin-film transistors** IM Seongil, CHOI Jeong-Min, HWANG Do Kyung, HWANG Jung Min, KIM Jae hoon(*Yonsei University, Institute of Physics and Applied Physics.*) We report on the ultraviolet (UV)-enhanced device properties in pentacene-based thin-film transistors (TFTs). Pentacene-TFTs showed a degraded mobility and lowered saturation current after illumination by a high energy UV with 254 nm wavelength. However, under 364 nm UV these devices surprisingly displayed enhanced saturation current and also showed threshold voltage shift toward lower values, maintaining their mobilities. The saturation current increase and threshold voltage shift were further related to the negative fixed charges excessively formed at the pentacene/dielectric interface by the low-energy UV. We thus conclude that a low energy UV could rather enhance the pentacene TFT performances and also control the threshold voltage of the device.

Ep-073 **대형 LCD TV backlight unit용 외부전극형광램프의 구동조건에 따른 전기광학 특성 변화** 최 재영, 김 영엽, 고 재현(*한림대학교, 물리학과.*) 대형 LCD TV의 backlight unit용 광원 중의 하나인 EEFL(외부전극형광램프)은 뛰어난 수명과 높은 효율, 병렬 구동으로 인해 주목을 받아 왔다. 본 연구에서는는 EEFL을 구동시는 여러 변수들을 변화시킬 경우 이러한 변화가 EEFL의 전기광학적 특성에 어떤 변화를 주는지를 확인하고자 하였다. 램프의 외부 전극에 구형파 전압을 인가할 경우 램프 전류는 인가된 구형파의

전압인가 주파수 및 Duty에 영향을 받는다. 램프의 전류를 고정시킨 상태에서 구동 주파수 및 Duty 변화에 따른 휘도, 전압, 전류를 측정하여 발광효율의 변화를 분석하였다. 그 외에도 램프 발광부분(양광주)에 형성되어 있는 전압의 분포를 측정하여 양광주 전기장의 세기를 정량화하였다. 이러한 전기광학적 특성이 백라이트의 백샤시와 유사한 램프 외부의 도체 유무에 따라 어떻게 변화하는지도 분석하였다.

Ep-074 **Simulation And Experiment Study To Improve Ion Transfer Efficiency Through The Ion Transfer Optics For An External Ion Injection FTICR-MS** 최 명철(*한국기초과학지원연구원.*) The FTICRMS(Fourier Transform Ion Cyclotron Resonance Mass Spectrometry) is one of the most precise mass spectrometry. That can measure the heavy ion or macromolecular mass. The FTICRMS has been improved to make higher sensitive instrument. To do this, the ion transmission efficiency in octopole RF ion guide has to be improved for external ion injection. A new ion optics system has been also designed in front of the gate valve which is installed between an external ion source and the high vacuum region of a mass spectrometer. Installing the gate valve in the middle of the octopole ion guide can reduce the transmission efficiency because the gate valve gap space can increase the ions radial position, this radial position have an relation to the transfer of ion. From this relation, if the radial position is increased, relatively low mass ion can be ejected. Moreover, if we use high magnetic field magnet, these magnetic field also effect on the transmission efficiency of ion. Both effects will decrease the overall ion transmission efficiency. To increase the ions transmission efficiency of the gate valve gap space and high magnetic field, ions need to be focused before entering the octopole ion guide, and also if there is gap space in the middle of octopole ion guide system, ions have to be focused to reduced the radial position in the octopole ion guide. The proper operation condition of octopole ion guide was discussed to deliver the relation between ions radial position and ion transfer, and then compared with simulation results.

Ep-075 **Detection of Magnetic Nanoparticles and Red Blood Cell by Using a Highly Sensitive Spin Valve Bio-sensor** PARK Sang-Hyun, AHN Myung-Cheon[1], HWANG Do-Guwn[2], SOH Kwang-Sup, LEE Sang-Suk[1] (*Biomedical Physics Laboratory, School of Physics, Seoul National University. [1]Dept. Of Oriental and Western Medical Engineering, Graduation, Sangji University. [2]Dept. Of Applied Physics and Electronics, Dept. of Oriental Biomedical Engineering.*) In this study, a high sensitive giant magnetoresistance-spin valve (GMR-SV) bio-sensing device with high linearity and very low hysteresis was fabricated by photolithography and ion beam deposition sputtering system. Detection of the Fe-hemoglobin inside in a red blood cell and magnetic nanoparticle using the GMR-SV bio-sensing device was investigated. A red blood cell includes hemoglobin, and the nanoparticles are the Co-ferrite magnetic particle coated with a shell of amorphous silica which the average size of the water-soluble bare cobalt nanoparticle was about 9 nm with total size of about 50 nm. When 1mA sensing current was applied to the current electrode in the patterned active GMR-SV devices with areas of 5*10 m^2 and 2*6 m^2, the output signals of the GMR-SV sensor were about 100 mV and 14 mV, respectively. The magnitude of output of voltage signals was obtained from four-probe magneto resistive measured system, and the picture of real-time motion images was monitored by optical microscope. Even one drop of human blood and nanoparticles in distilled water were found to be enough for detecting and analyzing their signals clearly.

Ep-076 **LCD 백라이트용 평판형 형광램프의 출광 패턴 조절에 관한 연구** 박 지희, 이 지영, 김 영엽, 고 재현(*한림대학교, 물리학과.*) Backlight 기술의 발전은 고휘도, 대면적화, 저 소비전력, 친환경 대응 등 LCD 업계가 요구하는 고품위 Backlight 의 필요성에 맞추어 진전되고 있으며, 이러한 추세에 맞추어 최근 신 광원으로 대두되고 있는 평판형 평광램프(면광원, FFL)에 대한 연구와 기술은 주목될 만하다. 현재 출시되고 있는 수은형 면광원은 다채널 구조를 띠고 있으며 상하판에 형광체가 도포되고 하판형광체 밑면에는 반사막이 형성되어 있다. 면광원 BLU는 기존 선형적인 형광램프를 사용하는 BLU와 같이 광원 위에 여러 광학적 기능을 수행하는 광학필름들이 배치되어 있다. 기존의 광학필름은 비즈/반구형 확산필름, 일차원적인 배열을 띠는 프리즘 필름 등으로써 후면의 광원으로부터 조사되는 빛에 대한 확산 및 집광기능을 담당하여 BLU의 균일화 및 고휘도화에 기여한다. 본 연구에서는 기존 BLU에서 광학필름을 사용함으로써 얻을 수 있는 확산 및 집광 기능의 광학적 특성을 면광원의 평판 glass위에 여러 가지 패턴을 형성함으로써 대체할 수 있는 가능성을 모색해 보았다. 다양한 광학적 패턴을 면광원의 상

판 유리 위에 배열하여 광학필름을 사용하지 않고서도 광원 자체만으로 확산 및 집광 기능을 수행할 것이라 예상하여 광 추적 시뮬레이션(ASAP)을 이용하여 새로운 면광원을 설계해 보았다. 시뮬레이션은 면광원의 상판 유리에 아무런 패턴이 들어가지 않은 결과를 기준으로 패턴이 들어간 경우의 각각의 출사광 분포를 비교해 보았다. 그 결과 상판 유리에 광학적 특성을 고려하여 패턴을 배열한 면광원은 광학필름을 사용하여 얻을 수 있는 출광분포의 변화 및 이에 의핸 고휘도화가 가능함을 확인할 수 있었다.

Ep-077 **Theoretical Study Of A Field Emission Enhanced Semiconductor Thermoelectric Cooler** BAE Hae Kyung, JANG Yu Jin, LEE Han Na, CHUNG Moon Sung(*울산대학교 물리학과.*) There is a continuing and widespread need for a compact, reliable, long life, low cost, low power consumption and low maintenance cooler. Most useful thermoelectric cooler materials have a value of ZT(dimensionless figure of merit) between 0.4 and 1.3. Although there is no theoretical limit to the value of ZT, it has not been significantly increased in spite of continuous efforts since the early 1960s. This is due to the fact that all good thermoelectric materials also have relatively good thermal conductivity resulting in backflow of heat from the hot to the cold plate. To circumvent this difficulty in the solid-state thermoelectric cooler, we have made a novel approach using two element field emission sources within a standard thermoelectric cooler configuration to enhance the performance of the device. The presence of these field emission sources in the semiconductor paths constitute thermal breaks without significantly affecting the electric/thermoelectric behavior of the cooler. Thus this composite thermoelectric device has the property of a good electric conductor with little or no phonon conduction. The proposed cooler is shown to have an efficiency that exceeds standard thermoelectric coolers.

Ep-078 **네마틱 액정에서의 이온양과 그 효과 측정** 오 유미, 임 지영, 김 종현(*충남대학교, 물리학과.*) 액정디스플레이에 있어 해결해야 할 많은 과제들 중 한 가지는 바로 잔상과 관련된 문제이다. 액정디스플레이에는 유리 기판에 복잡한 반도체공정과 액정공정을 거쳐, TFT, 전극, 배향막들을 형성하고 배향막, 액정 등의 유기물질에 적절한 전기장을 가해 주어 구동을 한다. 이러한 패널을 만드는 과정에서도 매우 미량의 불순물들이 삽입되며, 구동과정에서도 분자들의 해리되어 이온을 생성한다. 이러한 이온들은 구동과정에서 배향막과 액정의 사이에 흡착 또는 막을 형성하고, 셀 사이를 이동하며 미세한 액정 제어에 영향을 미친다. 이는 잔상을 일이키는 중요한 원인으로 그 정확한 영향을 이해하여 이온효과를 감소시켜야 한다. 일반적으로 이온효과를 알기위한 방법으로는 잔류전하측정 방법이 있다. 이는 액정 셀에 DC전압을 가해줄 경우 축전용량의 그래프는 이력곡선을 나타내게 되며, 전압의 차이는 이온에 의한 전류 손실 정도를 보여 준다. 또한 직접적으로 외부 전기장에 의한 전류를 측정하는 방법도 있다. 이는 액정이 외부 전압에 의해 구동되는 과정에서의 전류를 보여준다. 우리는 이온의 양과 그 영향을 알기위하여 비교적 잘 만들어진 네마틱 액정 셀에 불순물의 역할을 하는 색소를 첨가하여 전극부분의 이온 양을 조절하였다. 또한 DC 전압을 주어 전하량을 계산하였다. 이온의 증가 정도와 전하량을 비교하면 이온의 양을 상대적으로 계산이 가능 할 것이다. 동시에 축전용량을 측정하여 잔류전하의 변화를 비교하여 액정과 이온의 움직임을 동시에 알아보고자 한다.

Ep-079 **Pd Nanowire Hydrogen Sensors Fabricated by Electron-Beam Lithography** JEUN Minhong, LEE Eunsongyi, LEE Wooyoung(*Department of Materials Science and Engineering, Yonsei University, 134 Shinchon, Seoul 120-749, Korea.*) Pd nanostructures such as nanowires, nanochains, and nanotubes, are well recognized to detect hydrogen gas at room temperature as well as to be highly sensitive and to respond very fast [1,2]. In this work, we present a simple method to fabricate Pd individual nanowires patterned by electron-beam lithography from sputtered Pd thin films and their hydrogen sensing performance dependent upon the dimension of the patterned nanowires. Pd thin films were deposited on a thermally oxidized Si(100) substrate in a dc magnetron sputtering system with a base pressure of $4x10^{-8}$ Torr. A combination of electron beam lithography and a lift-off process has been utilized to fabricate Pd single nanowires (w = 300 nm, l = 10 mm) from continuous Pd films with t = 60 – 400 nm. The patterned Pd nanowires with w = 300 nm and t = 60 – 400 nm were found to detect hydrogen in the H_2 concentration range 20 – 20,000 ppm at room temperature by measuring the change of electrical resistance in the nanowires. With respect to the detection limit of H_2 concentration, the Pd nanowires with t = 60 nm and t = 100 nm were found to sense 20 ppm, the lowest concentration in Pd

nanostructures reported in the literatures. The response time was also found to decrease with decreasing thickness of the nanowires in the thickness range 60 – 400 nm. In this work, the fastest response time of ~ 20 seconds was obtained in the nanowire with t = 60 nm. The low detection limit and the fastest response time are likely due to larger high surface-to-volume ratio of the smaller Pd nanowires. Interestingly, the sensitivity ($\Delta R/R$) for the single nanowires with t = 60 – 400 nm was found to be independent of the nanowire thickness in the H_2 concentration 20 – 20,000 ppm. The sensitivity for the nanowire with t = 60 nm is 25 % and 0.35 % for the concentrations of 20,000 ppm and 20 ppm, respectively. The power consumption of the Pd nanowire sensor for hydrogen detection was found to be as low as a few nW. The hydrogen sensing properties of Pd nanowires arrays are compared with that of single Pd nanowires. The annealing effects of the Pd nanowires on the hydrogen sensing performance are also discussed.

[1] F. Favier et al., Science 293, 2227 (2001) [2] Y. Im et al., Small 2, 356 (2006)

Ep-080 **대형 LCD TV 백라이트용 평판형 형광램프의 전기광학 특성 평가** 김 영엽, 최 재영, 고 재현(*한림대학교, 물리학과.*) 최근 LCD TV backlight unit용 평판형 형광램프(면광원, FFL)은 높은 수명과 효율, 단일 인버터의 사용을 통한 구조적 단순화 등 많은 장점으로 인해 주목을 받고 있다. 면광원은 형광체를 여기시키는 자외선 발생원에 따라 수은(Hg)형과 제논(Xe)형으로 구분된다. 본 연구에서는 최근 상용화에 성공한 수은형 32" FFL의 전기광학 특성에 대해 보고한다. 본 연구의 대상인 면광원은 유리성형기술을 이용해 형성된 28개의 채널들이 나란하게 배열된 상판 유리와 평판형의 하판유리가 결합된 구조를 가지고 있는 수은형 면광원이다. 면광원의 방전공간 내에는 Ne:Ar 혼합가스와 소량의 액체 수은이 주입되어 있다. LCD TV 내에서 일반적으로 사인파 인버터로 구동되던 램프를 구형파를 이용하여 구동하고 Duty와 주파수를 변화시켜 측정함으로써 사인파와 구형파간의 비교, Duty, 주파수 변화에 따른 전기광학 특성을 자세히 측정하였다. 주파수 50kHz, Duty 50%를 가지는 구형파로 실온 25°C에서 구동할 경우 관전압 1215 V, 관전류 140 mA에서 확산판 위의 9-point 평균 휘도가 약 5300 nit였고 이를 발광효율로 변환할 경우 약 60 lm/W 였다. 이 때 휘도균일도는 93%, 확산판 위에서의 색 좌표는 x=0.247, y=0.241 로 측정되었다.

Ep-081 **Evidence for Electrical Spin Injection into a Semi-metal in FM/Al_2O_3/Bi/FM Junctions** LEE Kyoung-Il, LEE Kiyoung, SHIN Kyung-Ho[1], JOHNSON Mark[2], LEE Wooyoung(*Department of Materials Science and Engineering, Yonsei University, Seoul, Korea. [1]Korea Institute Science and Technology, Seoul 136-791, Korea. [2]Naval Research Laboratory, Washington DC, USA.*) The electrical spin injection, transport and detection in non-magnetic materials has continued to be of central importance over the past decade in the field of spintronics. A typical device structure for spin-injection experiment is a lateral spin-valve system consisting of laterally separated ferromagnetic electrodes and a spin-transport channel layer. It is essential to rule out plausible artifacts, e.g. anisotropic magnetoresistance (AMR), local Hall effect and other geometrical effects, in the lateral spin devices. By contrast, a magnetic tunnel junction (MTJ) is a kind of a vertical structure in which the geometrical artifacts may not be involved with the spin-dependent transport. There have been several reports on the spin-dependent tunneling and the spin decay length in non-magnetic interfacial layers in magnetic tunnel junctions (MTJs) [1, 2]. In this work, we present the spin-dependent tunneling effect in Bi inserted MTJs as a function of thickness of the Bi layer. A 100 Å-thick Bi inserted MTJ was found to show 4.8 % tunneling magnetoresistance (TMR) at room temperature, indicating that effective spin tunneling into the Bi layer as well as spin transport via the inserted Bi layer give rise to the electrical spin detection in the MTJ. It was also found that TMR values exponentially decreases with the thickness of the inserted Bi layer. Interestingly, a MTJ with 200Å-thick Bi layer was found to still exhibit larger than 1 % TMR. The spin decay length (λ_{Bi}) in the Bi inserted MTJs was quantitatively estimated to be approximately 41 Å. It should be noted that the λ_{Bi} value is five times larger than that in a Cu inserted MTJ. Our results contrast with a previous study [2] reporting that the estimated spin decay length in interfacial metallic layers is limited to only a few monolayers. The origin of the very long spin decay length in the Bi inserted MTJs will be addressed. Our results demonstrate an extension of successful spin tunnel injection and electrical detection of spins to a novel material system, semi-metallic Bi.

[1] S. Yuasa, T. Nagahama, and Y. Suzuki, Science 297, 234 (2002) [2] P. LeClair, H. J. M. Swagten, J. T. Kohlhepp, R. J. M. Van de Veerdonk, and W. J. M.

De Jonge, Phys. Rev. Lett. 84, 2933 (2000)

Ep-082 **전자기파의 간섭에 의해 생기는 RFID 음영지역 분석** 정 대민, 양 형우, 양 정국, 김 진영[1], 강 준희(*인천대학교 물리학과. [1]인천대학교 물리학과, (주)키스컴.*) RFID(Radio Frequency IDentification)은 유비쿼터스의 가장 기본이 되는 기술이다. 바코드를 대체할 수 있으며 다양한 응용분야에 접목이 가능하여 많은 연구가 진행되고 있다. 현재 RFID의 광범위한 응용에 있어서 가장 걸림돌이 되고 있는 것은 태그의 인식률이다. 본 연구에서는 태그의 방향에 둔감한 원형편파 side feed 안테나를 설계, 제작하여 태그가 인식되지 않는 음영지역을 분석하였다. 제작된 안테나는 147MHz의 대역폭을 가지고 있으며 중심주파수인 912 MHz에서 -25.7dB의 반사계수 특성을 나타내었다. 축비는 2.1dB 이고 Gain은 8.25dBic 였다. 정량적인 측정을 위해 2차원 평면 스캐너를 개발하여 측정하였다. 현재 가장 많이 사용되고 있는 EPC C1G2 프로토콜을 지원하는 태그를 사용하였으며 태그와 안테나 사이의 거리와 높이에 따른 음영지역을 분석 하였다. 또한 파동의 특성을 갖는 RF신호에 의해 필연적으로 생기는 음영지역을 줄이기 위한 안테나 쉐이킹 기법을 사용하여 음영지역의 변화를 비교분석하였다.

Ep-083 **Real-time Detection of Superparamagnetic Beads using Highly Sensitive Spin-Valve Sensors for a Chip-cytometer** ROH Jong Wook, LEE Young Taek, SUN GU Yi, LEE Kyoung-Il, SON Ohtaek[1], JUNG Hyo-Il[1], LEE Wooyoung[2](*Department of Materials Science and Engineering, Yonsei Univ., Seoul, South Korea. [1]School of Mechanical Engineering, Yonsei Univ., Seoul, South Korea. [2]Department of Materials Science and Engineering, Yonsei Univ., Seoul, South Korea.*) The development of a chip-cytometer detecting magnetic beads using a spin-valve sensor has recently attracted great interest since it is capable of realizing both cell-separation and cell-counting on a chip [1]. In order to realize a chip-cytometer, the detection of magnetic labels flowing in the microfluidic channel is one of the key issues. For this reason, sensors with high sensitivity and large signal to noise ratio, i.e. giant magnetoresistance (GMR) spin-valve sensors, are prerequisite to detect directly flowing magnetic beads in the microfluidic channel. In this work, we report on the real-time detection of flowing magnetic beads using a highly sensitive spin-valve sensor integrated in a microfluidic channel.The generic structure of a spin-valve was $Co_{84}Fe_{16}$(20)/NOL/Ni_81Fe_{19}(25)/$Co_{84}Fe_{16}$(10)/Cu(17)/$Co_{84}Fe_{16}$(20)/$Ir_{22}Mn_{78}$(75)/Ta (50) (Å). In this work, nano-oxide layers(NOLs) were employed in order to enhance the sensitivity and to enlarge the range of a magnetic field resolved by a spin-valve sensor. The spin-valve was observed to exhibit about 10 % magnetoresistance(MR). A combination of photo lithography and a lift-off process has been utilized to fabricate a spin-valve sensors (w = 6 μm, l = 30 μm). A polydimethylsiloxane(PDMS) microfluidic channel with a height of 25 μm and a width of 30 μm was fabricated and integrated in order to transport superparamagnetic beads with d = 2.8 μm(Dynalbead 280) toward an active area of the spin-valve structure. In order to generate a magnetic dipole field of magnetic beads, a DC magnetic field of 34 Oe was applied to the longitudinal direction of the spin-valve structure during the measurement experiment.The real time detection of a single-bead was observed by the direct measurement of a magnetic dipole filed from a moving magnetic bead using a spin-valve sensor. It was found that the real-time signal voltage of 0.3 μV sharply dropped when a magnetic bead approached the active area of the spin-valve sensor. The signal voltage output recovered the initial voltage as the magnetic bead completely passed over the active area. This signal voltage drop is attributed to a fringe field of the magnetic bead, which partially cancels the applied field in the free layer of the spin-valve structure [2]. We extend our study to the real-time detection of animal cells coated with magnetic beads for the biological application. Our results demonstrate the possibility of implementing a chip-cytometer for biological applications using high-sensitive spin-valve sensor integrated with a microfluidic device.

Reference [1] W. Shen et al., Appl. Phys. Leet. 86, 253901 (2005) [2] D. L. Graham et al, Trends Biotechnol. 22, 455 (2004)

Ep-084 **Introduce of TL/OSL dating system at Chungcheong cultural properties research Institute.** SONG KiWoung, KIM MyungJin, HONG DukGeun[1] (*Chungcheong Cultural Properties Research Institute. [1]Dept. of Physics, Kangwon national University.*) We introduce the procedures used for luminescence dating at Chungcheong cultural property research Institute. Luminescence dating is based upon the premise that several commonly occurring minerals (e.g. quartz and feldspar) can be used as natural dosimeters, recording the amount of radiation to which they have been exposed. Two quantities are re-

quired for luminescence dating: the radiation dose to which the sample has been exposed since the event that is being dated (i.e. equivalent dose); and the radiation dose to which it is exposed per year (i.e. dose rate). Equivalent dose is estimated by luminescence measurement using an automated TL/OSL system (Model TL/OSL-DA-20). The dose-rate is obtained by using a high-purity germanium detector.

Ep-085 **Design of portable nanotube-based biosensors.** 박 동원, 소 혜미, 김 병계[1], 전 은경[1], 부 경호, 공 기정, 장 현주, 김 범수[2], 이 정오(*한국화학연구원 융합바이오기술연구센터. [1]전북대학교 물리학과. [2]충북대학교 화학공학과.*) We have fabricated single-walled carbon nanotube field effect transistor (SWNT-FET) arrays as a sensor platform for tumor marker detection. SWNT was grown by patterned catalyst growth technique and Ti/Au electrodes were generated on the SWNT using a photolithography method. For biosensor applications, SU-8 negative photoresist patterns were used as an insulation layer. For the simultaneous detection of multiple tumor markers, tumor-specific antibodies were immobilized either by micro-spotting or photosensitive cross-linkers. PDMS microfluidic channels for sample delivery were fabricated by using laserjet printed transparent films as a mask. To make portable sensor platforms, micropump was used to deliver the sample to the sensor surface. Detailed design principles will be presented.

Ep-086 **Fabrication of hybrid sensor using microcantilever combined with SWNT devices** 김 병계, 소 혜미[1], 공 기정[1], 장 현주[1], 부 경호[1], 이 광철[2], 김 민석[2], 이 정아[2], 김 주진, 이 정오[1](*전북대학교 물리학과. [1]한국화학연구원 융합바이오 기술연구센터. [2]한국 표준연구원.*) In recent years, highly sensitive and selective detection of biomolecules (e.g. virus, bacteria, DNA and proteins) by MEMS/NEMS (Micro-/Nano Electro-Mechanical-System) structures have attracted extensive attention for its importance in clinical diagnostics. Many of the cantilever based sensors use optical techniques to measure deflection coming from the binding of biomolecules. Recently, Shekhawat et al. showed that CMOS transistor combined cantilever can be used as a sensitive biosensor, where deflection of cantilever can be transduced as an electrical conductance from the transistor. We fabricated single-walled carbon nanotube (SWNT) devices on microcantilever to interpret the deflection of cantilever by measuring the electrical conductance from SWNT device. Preliminary measurement shows that the deflection of microcantilever can be scaled with the electrical conductance of SWNT device. Detailed mechanisms of the signal transduction and possible applications for biosensors will be discussed.

Ep-087 **Three-dimensional Particle-in-cell Simulations of 300GHz Reflex Klystrons** 전 석기, 김 정일, 진 윤식, 김 근주, 손 채화(*한국전기연구원 (KERI).*) Three-dimensional (3D) particle-in-cell simulations of 300GHz reflex klystrons are presented. 300GHz electromagnetic wave generation in a resonant cavity is analyzed by using a 3D simulation model in which all the geometric parameters (such as the grid thickness, repeller shape, beam radius, etc.) are described. When an electron beam of an energy of 1.0 keV and a net current of 8.9mA is used, the maximum electronic efficiency of energy transfer is observed when the gap transit angle is 0.7π rad, and the efficiency sturates when the beam current is over 10mA. Space charge forces produce a shift in the optimum repeller voltage. It is also shown that the effect of the beam temperature is not critical, even though the bunching wavelength of the electron beam is several times smaller than that in conventional vacuum electron devices. Our simulation results show that a microfabricated 300GHz reflex klystron can directly generate electromagnetic waves with output power levels of several tens of milliwatts.

Ep-088 **Fabrication of Nano-Floating Gate Memory Device with In_2O_3 Nano-Particles Embedded in Polyimide Layer** LEE DongUk, KIM SeonPil, KIM Jae-Hoon, KIM Eun Kyu, KOO Hyun-Mo[1], CHO Won-Ju[1], KIM Young-Ho[2](*Quantum-Function Spinics Laboratory and Department of Physics, Hanyang University, Korea. [1]Department of Electronic Materials Engineering, Kwangwoon University, Seoul, Korea. [2]Department of Materials Science and Engineering, Hanyang University, Korea.*) The nano-floating gate memories (NFGM) with nano-particles are very attractive because they are promising candidates for low operating voltage, long retention time and fast program/erase speed. Few studies concerning on the formation of metal or metal-oxide nano-particles embedded in an organic layer for applications to nonvolatile flash memories have been achieved. A fabrication method of

metal-oxide nano-particle in a polymeric matrix was developed. In this study, we fabricated the silicon-on-insulator (SOI) NFGM n-MOSFET device with In_2O_3 nano-particles embedded in polyimide layer. Self-assembled In_2O_3 nano-particles were created by chemical reaction between the polymer precursor and indium film. The current-voltage curves (I-V) and retention times of In_2O_3 NFGM were characterized by semiconductor parameter analyzer HP 4155B. The memory window was measured about 1.3 V at initial status of writing and erasing operations.

Ep-089 **Characteristics of amorphous Indium zinc tin oxide film grown by RF-sputtering system in pure Ar ambient** 김 한기, 최 광혁, 정 진아, 배 정혁, 문 종민, 정 순욱(*금오공과대학교, 정보나노소재공학과.*) To substitute conventional ITO anode in OLEDs and flexible OLED, various transparent conducting oxide (TCO) materials, such as Al-Zn-O (AZO), Ga-Zn-O (GZO), Zr-Zn-O (ZZO), In-Ga-O (IGO), In-Zn-O (IZO), In-Ga-Sn-O (IGTO), Zn-In-Sn-O (IZTO), have been suggested as anode materials. Among various multi-component-TCO materials, IZTO films recently have been recognized as alternative anode materials in OLEDs or flexible OLEDs due to its high work function, good conductivity, high transparency, and low deposition temperature. In this work, electrical, optical, structural and surface properties of indium zinc tin oxide (IZTO) films grown by a radio-frequency magnetron sputtering in pure Ar ambient were investigated as a function of RF power and working pressure. The IZTO anode films on glass substrate have conductivity and transparency comparable to a commercial crystalline ITO (c-ITO) anode prepared at high temperatures (200~300 ℃). A sheet resistance of ~ 11 Ohm/sq., average transmittance above 85% in visible range, and root mean spare roughness of 5 nm were obtained even in the IZTO layers deposited at room temperature without reactive oxygen gas. Due to the specially designed oxygen-rich IZTO target, we can obtain high quality IZTO film without addition of reactive oxygen gas. This indicates that the IZTO film is a promising transparent conducting oxide material that can be used as a substitute for a conventional ITO anode for OLED and flexible OLEDs.

Ep-090 **Top emitting organic light emitting diodes passivated by catalyzer enhanced chemical vapor deposition** 김 한기, 정 진아, 문 종민, 정 순욱, 김 명수[1](*금오공과대학교, 정보나노소재공학과. [1]삼성 SDI.*) We report on specially designed catalyzer enhanced chemical vapor deposition(CECVD) system for high-quality SiNx thin film passivation layer on top-emitting organic light emitting diodes(TOLED). This system was equipped with high efficient W catalyzer and bipolar type electrostatic chuck (ESC) system for low temperature deposition of passivation layer on TOLEDs. The CECVD system not only has several advantages, such as high deposition rate, low growth temperature, low hydrogen concentration of the films, simply apparatus, and low cost, but also obviates the plasma damage effect on films. In this work, we report on characteristics of SiNx passivated TOLEDs by CECVD technique. Using a tungsten catalyzer connected in series, a high-density SiN_x passivation layer was deposited on TOLEDs and bare polycarbonate (PC) substrates at a substrate temperature of 50 ℃. Despite the low substrate temperature, the single SiN_x passivation layer, grown on the PC substrate, exhibited a low water vapor transmission rate of $2\sim6\times10^{-2}$ g/m^2/day and a high transmittance of 87 %. Furthermore, J-V-L characteristic and accelerated lifetime of TOLEDs passivated by the SiNx grown by CECVD exhibit that CECVD could be a useful deposition technique for AMOLEDs and possible applying to the flexible displays.

Ep-091 **Electrical and optical properties of phosphorescent OLED fabricated on amorphous IZTO anode** 김 한기, 배 정혁, 최 광혁, 문 종민, 정 진아, 정 순욱, 강 재욱[1], 김 장주[1](*금오공과대학교, 정보나노소재공학과. [1]서울대학교, OLED센터.*) The preparation and characteristics of a transparent conducting indium zinc tin oxide (IZTO) anode for phosphorescent organic light-emitting diodes (OLEDs) are described. The electrical and optical properties of the IZTO anode were comparable to those of commercial ITO anode films even though it was prepared at room temperature (~50 ℃). In addition, the work function of the ozone-treated amorphous IZTO anode (5.12± 0.02 eV) is much higher than that of ozone-treated commercial ITO anode (4.96± 0.02 eV). It was found that the current-voltage-luminance characteristics and efficiencies of OLEDs prepared on the IZTO anode are critically dependent on the sheet resistance of the IZTO anode. Furthermore, both the quantum efficiency and power efficiency of the OLED

fabricated on the amorphous IZTO anode were much higher than those of an OLED with the commercial ITO anode due to high work function of IZTO anode. This indicates that IZTO is an alternative anode material for substituting conventional ITO anode in OLEDs. To explain improved electrical and optical properties of amorphous IZTO based OLEDs, possible mechanism is given.

Ep-092 **Characteristics of flexible IZO/Ag/IZO anode on PES substrate for flexible organic light emitting diodes** 김 한기, 조 성우, 정 진아, 문 종민, 최 광혁, 정 순욱(*금오공과대학교, 정보나노소재공학과.*) IZO/Ag/IZO (IAI) stacks on PES substrate were evaluated as transparent conductors for flexible organic light-emitting diode (OLED) displays. Even though IAI stacked film were prepared at room temperature by DC sputtering (IZO) and thermal evaporator (Ag), it showed high conductivity and transparency comparable to IZO/PES and ITO/PET which is conventionally used in flexible displays. Low sheet resistance of 10.2 Ω/□ and high transmittance of above 75 % in visible range, especially above 80 % in 550 nm, were obtained from IAI anode films with a thickness of Ag-10nm. However, the IAI stacked films showed dramatically improved mechanical properties when subjected to bending both as a function of number of cycles to a fixed radius. Moreover, to investigate structural and surface properties of IAI stacked films, x-ray diffraction (XRD) and scanning electron microscopy (SEM) were used, respectively. Flexible OLED fabricated on IAI stacked anode shows comparable optical and electrical properties to flexible OLED fabricated ITO/PET substrate. This indicated IAI stacked anode film is promising anode structure for flexible organic light emitting diodes and flexible solar cells.

Ep-093 **Plasma damage free sputtering of Al cathode using twin target sputtering system for Organic Light Emitting Diodes** 김 한기, 문 종민, 이 상현[1](*금오공과대학교, 정보나노소재공학. [1]탑엔지니어링, 핵심기술개발팀.*) Sputtering is a commonly used deposition method because of its simplicity, high throughput, and improved adhesion. However, the bombardment of energetic particles during the sputtering process can result in damage to the underlying organic layers. Therefore, the development of a direct sputtering method for an Al cathode layer on organic layer is imperative in finding a solution of the problems of Al thermal evaporation and applying a sputtering process to the fabrication of organic-based optoelectronic devices. In this work, we report on plasma damage free sputtering technique of Al cathode on organic light emitting diodes (OLEDs) using specially twin target sputter (TTS) system. Characteristics of high-density plasma in TTS system are investigated as a function of working pressure, dc power, and target-to-substrate distance in order to optimize Al sputtering condition. Due to the effective confinement of high density plasma and the off-axis geometry of twin target gun, we can grow Al cathode on organic layer at low substrate temperature with deposition rate of ~10 nm/min. In particular, the OLED with TTS-grown Al cathode shows low leakage current density at reverse bias comparable to a OLED with only thermally evaporated Al cathode. This suggests that there is no plasma damage caused by the bombardment of energetic particles during Al sputtering using the TTS system.

Ep-094 **Effects of dispersed single-walled carbon nanotubes in conjugated polymer for photovoltaic cells** LEE Cheol Eui, YOON Sung Min, PARK Jitae, LEE Eunmo, LEE Kyu Won[1](*Korea University, Department of Physics. [1]Korea University, Institute for Nano Science.*) We studied the effects of dispersed single-walled carbon nanotubes (SWNTs) in poly[3-hexylthiophene] (P3HT) conjugated polymer. The blend ratio of P3HT/SWNT composites for photovoltaic cells ranged from 0 wt% to 1 wt% of SWNTs. The power conversion efficiency increased with increasing the weight percent of SWNTs. These results may have implications for the understanding of bulk junctions in conjugated polymer.

Ep-095 **Characteristics and process of ultra thin silicon membrane using B-doped Si wafer** YANG Hee-Doo, LEE Su Hwan, LEE Gon-Sub, PARK Jea-Gun(*Nano-SOI Process Laboratory, Hanyang University.*) Previous research, we had investigated the etching selectivity between silicon and oxide designed SOI wafer to produce an ultra thin silicon membrane. The buried oxide layer in a nano-SOI wafer had been able to designed for a etching-stop layer because the etching selectivity between oxide and silicon layer using KOH at 80℃ was 1:400. In addition, we focus on the advanced etching-stop layer of silicon. We investigated a nano-SON wafer which consists of a nitride layer. But

ITO anode must be sputtered to the SOI and SON wafer than additional process needed. To solve this problem, we implant boron into Si wafer and demonstrate B-doped (p-type) Si wafer instead of ITO. In this presentation, fabrication methods and performances of the ultra thin silicon membrane using B-doped Si wafer with high transmittance, better clean interface, and higher quality will be discussed. We have fabrication technology of B-doped SON wafer with ultra thin silicon (top-silicon: 214 nm). In case of 214 nm thickness top-silicon of optical transmittances of 93 %, 91 % and 91 % are obtained for the R(660 nm), G(520 nm) and B(440 nm) wavelengths, respectively.

*This work was supported by the Korea Science and Engineering Foundation (KOSEF) through the National Research Lab. Program funded by the Ministry of Science and Technology (No. M10400000436-06J0000-43610).

Ep-096 **열반사율법에 의한 부분 불소계 블록공중합체의 열전도도 측정** 박 경민, 김 석원, 이 민영[1], 임 권택[1](*울산대학교, 물리학과. [1]부경대, 화상정보공학부.*) 최근 고분자는 여러 장점 때문에 포토닉스 응용분야에서 열광학 스위치. 도파관 회절격자 멀티 플렉스 등과 같은 여러 소자의 응용에 매우 우수하며 유망한 것으로 인식 되기 시작하였다. 응용분야가 활발해짐에 따라 고분자의 물성이 연구되기 시작하였으며, 물성 중 소자에 가장 민감한 열화현상에 대한 연구가 필요하게 되었다. 본 연구에서는 박막의 두께 방향 열전도도 측정을 통하여 부분 불소계 블록공중합체가 소자 응용에 적합함을 확인하고자 하였다. 블록공중합체는 벤젠과 TFT solvent를 합성한 PEO-b-PFOMA(polyethylene-b-polyfluorooctyl methacrylate)를 3~4㎛ 두께로 합성을 하고, 그 위에 Bi(bismuth)를 150㎚ 두께로 금속 박막을 입혔다. 그리고 파장이 514.5 ㎚인 Nd:YVO_4 laser 빔을 광원으로 한 Thermo-Reflectance법을 이용하여 블록공중합체의 열전도도를 측정함으로써 부분불소계블록공중합체가 소자의 응용에서도 활용가능함을 확인하였다.

Ep-097 **Effect of Ultra-thin Al_2O_3 layer to Hole Injection with Organic Light-Emitting Diode** LEE Su Hwan, KIM Dal Ho, LEE Gon-Sub, PARK Jea-Gun (*Nano-SOI Process Laboratory, Hanyang University.*) A gold and aluminum layer was investigated as an anode for organic light-emitting devices (OLEDs). And we have shown that a Au and O_2 plasma treated Al anode can be used as an effective anode for bottom-emitting OLEDs. The O_2 plasma treatment of the Al could greatly enhance the hole injection ability as compared with anodes using only Au or Au:Al without plasma treatment. We demonstrated that the injection of holes occurred by tunneling across the thin insulating Al_2O_3 layer. In addition, the driving voltages of our devices with the only Au, Au:Al and Au: pretreatment Al anode devices are about 18.5 V, 16 V and 5.8 V, at a current density of 100 mA/cm^2, respectively. And, the voltages to obtain a luminance of 1000 cd/m^2 for only Au and Au: pretreatment Al anode devices are needed approximately 18.7 V and 6 V, respectively.

*This work was supported by the Korea Research Foundation Grant funded by the Korean Government (MOEHRD) (KRF-2004-005-D00166)

Ep-098 **Highly efficient Red electro-phosphorescent OLEDs** 전 우식, 박 태진, 박 정주, 이 용균, 장 진, 권 장혁(*경희대학교, 정보디스플레이학과.*) 현재 OLED는 차세대 디스플레이 및 차세대 조명기술로서 각광을 받고 있다. OLED는 크게 fluorescent OLEDs와 phosphorescent OLEDs (PHOLEDs)로 나뉘어지는데, fluorescent OLEDs는 유기분자의 singlet states만 발광에 이용하여 최고 외부양자효율이 약 5%로 제한되는 반면, PHOLEDs는 singlet states와 triplet states 둘 다 발광에 이용하여 외부양자효율이 20~25% 정도로 나타난다고 알려져 있다. 이러한 PHOLEDs는 high external efficiency and power efficiency때문에 최근 몇 년 동안 다양한 연구가 활발히 진행되고 있다. PHOLEDs는 triplet exciton lifetime이 길고 host 물질의 band gap이 크기 때문에 fluorescent OLEDs에 비해 그 구조가 복잡해고 1~2V 정도의 높은 turn-on voltage를 가지는 단점이 알려져 있다. 본 연구에서는 기존의 이러한 문제점을 극복하기 위하여 새로운 개념의 band gap이 작고, 전자이동성이 있는 host 물질을 발굴하였고, 이를 이용하여 매우 간단한 유기물 2층 구조의 고효율 red PHOLEDs 소자를 개발하였다. 본 연구에 사용된 소자구조는 ITO/α-NPB(40nm)/CBP(device 1) or new host(device 2): $Ir(piq)_3$(30nm)/BAlq(5nm)/Alq_3(20nm)/ LiF/Al와 ITO/α-NPB(40nm)/new host (device3):$Ir(piq)_3$ (50nm)/LiF/Al를 사용하였다. 그 결과로는 500cd/m^2에서 device 1의 경우 5.05cd/A(1.80 lm/W)을 나타내고, new host 사용한 유기물 5층 구조인 device 2의 경우 8.67cd/A(4.00lm/W)을 나타내어 30%정도의 향상을 나타내었고, 유기물 2층 구조를 적용한 device 3의 경우 9.66cd/A(6.90lm/W)를 나타났다. 본 연구에서는 new phosphorescent host를 사용하여 저전압 구동 및 고효율를 나타내는 유기물 2층 구조의 단순한 red PHOLEDs를 개발하였다.

Ep-099 **변조기술을 이용한 고감도 광대역 스핀밸브 자기저항 센서** 박 승영, 조 영훈, 윤 정범, 정 명화, 김 지원[1], 조 순철[1](*한국기초과학지원연구원. [1]숭실대학교 전자공학과.*) 본 연구에서는 변조기술을 이용하여 보자력이 없으면서도 수십 Oe 까지 넓은 영역의 자장을 감지하는 것을 목표로 소자를 설계하고, 그 가능성을 살펴보았다. 이를 위해 여자도선이 있는 스핀밸브 자기저항 센서를 제작하고, 그 도선에 10 KHz의 교류 전압을 인가하여 자기저항 곡선의 경향을 조사하였다. 그 결과 도선에 인가된 교류 전압의 진폭에 의존하여 자화반전 자장이 감소되는 현상과, 오프셋에 의존하여 자기저항 곡선이 천이되는 결과를 얻을 수 있었다. 또한 스핀밸브 소자의 출력 신호를 주파수 영역에서 관찰한 결과 도선에 인가한 교류 신호의 주파수인 10 KHz에서 뚜렷한 피크를 관찰할 수 있었으며, 이는 1/f 잡음 대역으로부터 멀리 떨어져 있어 잡음 감소 효과 또한 기대할 수 있었다. 소자 제조시 열에 의한 자기저항 곡선의 왜곡을 최소화 할 수 있는 공정을 도입할 경우, 본 변조기술을 이용하면 1 Oe 이하의 분해능으로 20 Oe 이상의 자장을 선형 및 저잡음으로 측정할 수 있는 고감도 광대역 자장 검출 센서의 구현이 가능하며, 나노입자 검출, 위폐감별 등 국부적인 저자장 검출 분야에 응용이 가능하다.

Ep-100 **저주파 마그네트론 스퍼터링방식으로 유리 기판 및 고분자 필름에 증착된 투명전극 특성에 미치는 산화물버퍼층의 영향** 김 충수, 정 상권, 이 상목, 박 이순[1], 손 상호(*경북대학교, 물리학과. [1]경북대학교, 고분자학과.*) 본 연구는 마그네트론 스퍼터링 방법으로 Glass 및 PES (Polyethersulfone) 필름 위에 ITO/Buffer Layer/Glass, ITO/Buffer Layer/PES 박막을 제작하였다. Buffer Layer의 재료는 SiO2, TiO2, Al2O3 등이고, RF 마그네트론 스퍼터링 방법으로 증착하였으며, Buffer Layer 위에 LF 마그네트론 스퍼터링법으로 ITO 박막을 증착하였다. 동일 증착 조건(진공도, Ar분압, 인가전압, 증착시간, 두께)에서 기판 온도만 다르게 하여, 버퍼층을 삽입한 것과 하지 않은 것을 샘플로 만들어 증착온도에 따른 특성(광학적, 전기적, 구조적)을 조사하였다. 본 연구에서의 OLED 용 전극으로 활용하기 위해 박막의 평가는 80 % 이상의 높은 가시광 투과도, 50 Ω/□ 이하의 낮은 면저항, 1 nm 이하의 표면 거칠기 (Ra)를 요구한다.

Ep-101 **Adapted Wavelet Packet Transformation 에서 다양한 Filter를 이용한 Speech Enhancement의 비교에 관한 연구** 김 원현, 조 경현, 원 종성, 권 영헌 (*한양대학교 응용물리학과.*) 본 논문은 실질적인 환경에서 발생하는 non-stationary 잡음을 Adapted wavelet packet transformation 방법으로 제거를 할 때, 사용되는 Filter들의 종류에 따라 잡음이 개선되는 정도를 비교 분석하는 연구이다. 잡음 데이터는 f16, leopara, pink, volvo, white 잡음이 이용되었고, 음성 데이터는 DARPA TIMIT 데이터베이스(DR6, 남성화자 10명, 여성화자 10명)를 사용하였다. Haar, Beylkin, Coiflet, Daubechies, Symmlet, Vaidyanathan, Battle등의 다양한 Filter를 사용하여 각 Filter들에 대한 잡음 개선 정도를 분석하였다.

Ep-102 **Retardation 물질을 이용한 선택적인 투과 액정셀 제작** 강 동한, 박 원훈[1], 안 기완[1], 오 재환[1], 장 진[1](*경희대학교 물리학과. [1]경희대학교 정보디스플레이학과.*) 최근 각광받는 평판 디스플레이로서 LCD를 들수 있다. LCD 의 장점은 크기가 작고 가벼우며, 소비전력이 작고 저전압 구동 (5V이하)이 가능다는 것이다. 하지만 다른 디스플레이에 비해 좁은 시야각을 가진다는 단점을 가지고 있다. 현재 이 단점인 좁은 시야각을 개선하기 위한 방법들이 활발히 연구되고 있다. 광시야각 개선의 방법으로는 보상필름을 액정 셀 외부에 라미네이팅 방식으로 붙이는 방법과 배향막의 멀티도메인을 통하여 시야각을 개선하는 방법등이 있다. 그러나 최근에는 액정 셀 내부에 retardation 물질을 코팅하여 보상필름의 역할을 하면서, 그 물질 자체를 패턴화 하여 선택적으로 투과 영역과 비투과 영역으로 나눌 수 있는 방식이 활발히 연구중이다. Retardation 물질을 이용할 경우 기존의 방식에 비해서 더 얇고, 가벼우며, 투과도를 더 높일 수 있다는 장점이 있다. 본 연구에서는 Retardation 물질로서 Reactive Mesogen 을 사용하였으며, 액정 셀 내부에 스핀코팅 하여 투과 빛을 1/2λ, 1/4λ 원편광 시키는 박막을 제작하였다. 또한 이 Reactive Mesogen 물질의 UV polymerization 특성을 이용하여 패턴화를 할 수 있었다. 이 Reactive Mesogen 물질은 열적 안정성과 UV polymerization 이후의 안정성 등이 이미 검증 되어진 물질이다. 이를 이용하여 Passive Matrix 방식으로 액정 구동을 하여, 선택적인 투과를 하는 액정 셀을 제작하였다.

Ep-103 **배향 기술에 따른 액정 배향의 특성 연구** 임 지영, 오 유미, 김 종현(*충남대학교 물리학과.*) 본 논문에서는 배향 기술이 액정 배향의 특성에 어떠한 영향을 주는지 알아보고자 한다. ITO (Indium Tin Oxide)가 코팅된 유리 기판에 main-chain-substituted poly-amic acid 의 동일한 배향물질을 사용하여 배향층을 형성했다. 러빙법, 광배향법 (Argon laser, Hg-Xenon

lamp)의 배향 기술을 이용하여 액정 배향을 하였다. 러빙은 거시적인 러빙 파라미터로 정의된 러빙세기, 광배향은 에너지를 조절하면서 그 차이를 관찰하였다. 그리하여 극각 방향의 배향력 (anchoring strength), 이방성 (anisotropy), AFM을 이용한 topology를 측정, 관찰하고 이들이 액정 배향에 어떤 영향을 주는지 알아보았다.

Ep-104 **네트워크 형태의 탄소나노튜브 가스센서에서의 가스흡착 특성 및 폴리머코팅 효과** 김 상훈, 이 형락, 윤 용주[1], 윤 완수[1], 하 동한[1](*경북대학교 물리학과. [1]한국표준과학연구원 전략기술연구부.*) 네트워크 형태의 탄소나노튜브 가스검출 소자를 제작하고, 단층분자흡착(monolayer adsorption)에서 다층분자흡착(multilayer adsorption)에 이르는 범위의 농도에 대하여 가스 흡착특성을 관찰하였다. 이산화질소(NO_2)와 암모니아(NH_3) 가스흡착의 경우, 소자의 전기전도도의 변화율은 저농도에서는 Langmuir isotherm을 따르고, 고농도 즉 다층분자흡착 영역에서는 가스농도에 비례한다. 탄소나노튜브에 polyethyleneimine(PEI)를 코팅할 경우 코팅전에 비하여 초기저항이 커지므로 NO_2에 대한 감도(sensitivity)는 크게 증가하지만, 결합에너지(binding energy)나 흡착계수(sticking coefficient)와 같은 기본적인 흡착특성들은 특이할 만한 변화를 보이지 않는다. Nafion을 코팅한 경우에는 NH_3에 선택적으로 반응하지만 감도나 흡착특성은 전혀 변화가 없었다. 전기전도도의 변화율 결과로부터, 탄소나노튜브 네트워크상에서 NO_2와 NH_3의 결합에너지는 각각 0.55 eV, 0.47 eV 임을 알 수 있었다. NO_2의 결합에너지는 이론값과 잘 일치하지만, NH_3의 결합에너지는 이론값보다 다소 크다. 이는 실온에서 NO_2는 탄소나노튜브의 표면에 흡착되지만, NH_3는 번들(bundle)을 구성하는 탄소나노튜브 사이의 빈 공간에 들어가서 여러 개의 탄소나노튜브와 동시에 결합하기 때문이라고 생각한다.

Ep-105 **열반사율법에 의한 As_2S_3 박막의 열전도도 측정** 최 병민, 박 경민, 김 석원(*울산대학교, 물리학과.*) 열반사율법(thermo reflectance method)은 박막의 주기적 온도변화에 의한 박막 표면의 반사율 변화를 이용하는 방법으로 실리콘 웨이퍼 위에 입혀진 측정하고자 하는 박막 시료 위에 넓은 금속 박막을 얇게 입혀 이를 주기적으로 줄-가열하면서 금속 박막 표면의 가운데 점의 수직한 방향으로 레이저 광을 입사시켜, 교류 온도 변화(ω)에 따른 반사율 변화(2ω)를 측정하고 이를 기판-박막시편-금속박막으로 이어지는 3층 시스템에 적용하여 열전도도를 구하는 방법이다. 본 실험에서는 광원으로 632.8 nm의 He-Ne 레이저를 사용하였다. 광원에서 나온 레이저 광은 빔 분리기로 나누어져 입사되고 시료를 거치지 않은 입사광과 진공챔버 내부에 장착된 시료에서 반사된 광을 실리콘 광검출기로 검출하고, lock in amp를 사용하여 반사율을 측정하여 측정된 반사율을 1차원 열전달방정식에 대입하여 박막의 열전도도를 구하였다. 실험에 사용된 As_2S_3 박막 위에 두께 150 nm, 크기 10 mm×4 mm 로 증착하여 열전도도를 측정하였다. 본 실험에서는 에너지 2.4 eV를 가지고 빛을 쪼이게 되면 As_2S_3 박막에서 미세구조변환이 일어난다는 점을 이용하여 증착된 As_2S_3 박막에 2.4 eV에 근접한 에너지를 가진 파장 532 nm의 반도체 레이저로 각각 2분~8분의 시간간격으로 입사시켜 미세구조변환된 박막의 열전도도를 측정하였다.

Ep-106 **Thickness and chemical identification of imbedded polymer films based on multiplex CARS microscopy using photonic crystal fiber** 최 대식, 남 정림[1], 이 흥순[1], 전 병혁[1], 정 세채[1], 조 동현[2](*한국표준과학연구원, 고려대학교 물리학과. [1]한국표준과학연구원. [2]고려대학교 물리학과.*) 최근에 재료, 생물 그리고 의학분야에 걸쳐 주목 받고 있는 새로원 간섭성 반 스톡스 라만 산란 현미경 (CARS)이 개발되었다. 본 현미경은 공초점 형광 현미경과는 달리 색소를 샘플에 착색하지 않고 분자 진동 분광 영상을 얻는 장점이 있다. 또한 CARS는 3차 비선형 광학 현상을 이용하므로 핀 홀 없이도 고 분해능을 갖는 3차원 영상 획득이 가능하다. 본 연구에서는 최근 전자 산업 분야에서 많은 요구가 있는 수십 nm에서 수 um까지 두께를 갖는 다중 층 고분자 필림에 대한 multiplex CARS 현미경 응용 기술 가능성을 검증 하였다.

Ep-107 **Bipolar HOST materials for Red and Green phosphorescent OLEDs** 박 태진, 전 우식, 박 정주, 이 용균, 권 장혁, 장 진(*경희대학교 정보디스플레이학과.*) 현재 OLED는 공정가격이 저렴하고 자체발광을 하며 flexible하게 제작이 가능한 특성을 가지고 있어 차세대 디스플레이 소자로서 각광을 받고 있다. 하지만 operation voltage, efficiency, lifetime면에서 그 특성을 개선하여야 하며 이에 현재 연구가 활발이 진행되고 있다. 그 중에서 효율은 소자의 수명과 소자의 발열, 소비전력에 영향을 미치기 때문에 매우 중요하게 인식된다. 효율을 높이기 위한 방법 중에 내부양자효율 100%를 내기 위하여 Ir, Pt, Os같이 무거운 금속을 포함하는 물질을 Guest로 사용하여 인광소자를 널리 활용하고 있다. 보편적으로 사용되는 HOST 물질인 CBP는 Bipolar의 특성을 가져 hole과 electron이 잘 이동되는 장점이 있으나 큰 band gap을 가지고 있어 carrier가 잘

주입되지 않는 단점이 있다. 이 연구에서는 CBP의 단점을 보완하기 위하여 carrier가 원활이 주입되도록 band gap이 작고, Bipolar 특성을 가진 두 물질 CTP(green), CQP(red)를 HOST 물질로 개발하여 인광 Red와 Green에 연구하였다. 소자구조는 green의 경우 ITO/α-NPB (40nm)/CBP(device 1) or CTP(device 2):Ir(ppy)$_3$(30nm) / BAlq(5nm) / Alq$_3$(20nm) / LiF/Al으로 제작하였고, Red의 경우 ITO/α-NPB(40nm)/CBP(device 3) or CQP(device 4):Ir(piq)$_3$(30nm) / BAlq(5nm) / Alq$_3$(20nm) / LiF/Al으로 제작하였다. 효율을 비교한 결과 Green 소자의 경우 1000cd/m^{2}에서 Device 1은 20.18 cd/A(7.1 lm/W)를 나타내고, CTP를 적용한 Device 2의 경우 21.90 cd/A(10.75 lm/W)을 나타내어 효율 증가를 나타냈고, Red 소자의 경우800cd/m^{2}에서 Device 3은 5.81 cd/A(2.6 lm/W)를 나타내고, 새로운 물질을 적용한 Device 4의 경우 7.20 cd/A(2.83 lm/W)을 나타내어 20% 효율 증가를 나타냈다. 따라서 CTP와 CQP의 경우 AMOLED 또는 PMOLED에 저전압 및 고효율을 위한 적절한 특성을 가진 물질로 나타났다.

Ep-108 **청색 고분자 LED의 효율과 색좌표 변화에 관한 연구** 이 용균, 박 태진, 전 우식, 박 정주, 권 장혁, 장 진(*경희대학교 차세대 디스플레이 연구센터 &정보디스플레이학과.*) 최근, OLED(Organic Light-Emitting Device)는 휴대전화의 보조화면과 MP3 플레이어의 표시장치로 많이 사용되고 있으며, 휴대용 기기의 디스플레이로 사용될 수 있는 2인치급 AMOLED가 곧 양산될 예정이다. 또한, OLED의 백색광을 사용한 조명이나 LCD(Liquid Crystal Display)의 백라이트(Backlight)로의 응용도 대두되고 있다. OLED에서 풀컬러를 구현함에 있어서 우수한 색표현을 나타내기 위해서는 적색, 녹색, 청색의 색좌표가 NTSC 색좌표에 근접해야한다. 적색과 녹색 OLED의 경우 NTSC 색좌표에 근접한 특성을 보이고 있지만, 청색의 경우 아직 부족한 면이 있다. OLED 소자를 제작할 경우 소자의 효율과 발광특성은 발광층이나 기능층의 두께변화에 따라 달라진다. 본 연구에서 동일한 청색 발광재료를 사용한 PLED 소자는 발광층의 두께 변화에 따라 효율과 CIE 색좌표 특성이 변화하였다. 특히, 고분자 발광재료의 PL 관찰에서 발광파장은 발광층의 두께 변화와는 무관한 특성을 보였지만, PLED 소자의 EL 관찰에서는 두께 변화에 따라 발광파장이 크게 달라졌다. 제작된 청색 고분자의 발광층 두께가 110에서 65 nm로 변화함에 따라 CIE 색좌표는 (0.165, 0.236)에서 (0.147, 0.098)로 sky blue에서 deep blue 영역으로 변화하였으며, 소자의 효율 또한, 2.4에서 3.9 cd/A를 나타냈다. 따라서 효율과 색좌표 특성이 우수한 PLED를 제작하기 위해서는 박막의 두께, 소자의 효율 및 색좌표 변화에 대한 상관관계를 잘 이해할 필요가 있다.

Ep-109 **증착 조건이 co-sputtering법으로 형성된 AuSn 솔더박막의 조성에 미치는 영향** 김 동진, 성 규준, 이 택영, 이 종원, 김 건남[1], 이 홍기[2](*한밭대학교 신소재공학부. [1](주)우리정도 부설연구소. [2]한국생산기술연구원 생산기반기술본부.*) 본 연구는 multi-gun rf-magnetron sputter를 사용하여 Au와 Sn을 동시에 증착하는 co-sputtering 방법으로 AuSn솔더 박막을 Ti/Ni/Au (UBM layer)이 증착된 Si기판 위에 성장하였다. 알려진 바와 같이 AuSn 합금은 조성의 변화에 따라 융점의 변화가 나타나는데, co-sputtering으로 증착된 AuSn 역시 조성의 변화에 따라 융점의 변화가 크게 나타났다. 따라서 Au와 Sn의 조성을 정확하게 조절할 수 있어야 원하는 융점의 솔더를 얻을 수 있다. 본 연구는 이 문제를 해결하기 위해 조성을 결정하는 공정조건 (성장온도, 성장시간, rf 전원, 동작압력)에 대하여 각각의 조건을 독립적으로 변화시키면서 실험하였으며, 조성의 변화를 야기하는 조건에 대한 분석을 진행하였다. 분석에는 EDX을 통하여 조성의 변화를 조사하고, 또한 공정 조건에 의한 표면 형상의 변화 분석에 SEM을 사용하였으며, cross-section SEM과 FIB를 사용하여 증착층 내부의 단면을 관찰함으로서 void 형성 여부 및 UBM Au의 확산 여부를 확인하였다.

Ep-110 **고진공과 Ar가스 분위기에서 PLD방법으로 제작된 TiNi박막의 조성 및 결정성에 관한 연구** 차 정옥, 안 정선, 신 진호, 여 승준, 박 소라(*경희대학교 물리학과.*) Ti-50 at. % Ni 합금 타깃으로 PLD(pulsed laser deposition)방법을 사용하여 TiNi 형상기억합금 박막을 제작하였다. 고진공(5×10^{-6} Torr)과 Ar 가스 분위기(200mTorr)에서 TiNi 박막을 제조하여. 조성 및 결정성의 변화를 조사하였다. TiNi 박막의 조성은 EDXS(Energy Dispersive X-ray Spectroscopy – HORIBA, EMAX-5770)을 이용해 분석하였으며, XRD(X-Ray Diffractoins)를 이용하여 상온에서 600℃의 범위의 기판온도에서 제작된 TiNi 박막의 결정성을 분석하였다. 박막의 조성은 기판과 타깃의 거리에 의존되었지만, Ar 분위기에서 플럼 안쪽에 기판이 위치하였을 때 표적의 조성에 화학량론적으로 더 근접함을 알 수 있었다. 또한, Ar 가스 분위기에서 증착 된 TiNi 박막은 고진공 분위기에서 증착된 박막보다 더 낮은 온도(약 400℃)에서 in situ로 결정화됨을 알 수 있었다. 이들 결과는, PLD방법으로 TiNi 형상기억합금 박막을 제작할 때 분위기 가스의 압력이 조성조절을 용이하게 하고, 결정화 온도를 낮추어 주는 중요한 역할을 할 수 있음을 시사한다.

Ep-111 **탄소나노튜브 첨가를 통한 Epoxy의 인장강도 향상** HONG Jun Yong, PARK Chong Yun (*성균관대학교 물리학과.*) Resist Ink는 원판, 화학약품 등과 함께 전자산업의 기구부품중의 하나인 Printed Circuit Board(PCB) 제조용 핵심소재로서, 전자산업의 발전방향인 System화 Soft화, Multimedia 화에 따른 시장에서 전자제품의 경박단소화, 고기능화 요구에 부응하는 소재로서의 물성확보가 중요하다.Epoxy는 Resist Ink를 이루는 주요한 물질로써, 약한 인장강도로 인하여 Resist Ink의 Soft화를 이루는데 있어서 장애가 되고있다. 본 연구에서는 Epoxy의 보강제로 탄소나노튜브(Carbon Nanotube)를 첨가함으로써 Epoxy의 인장강도를 크게 향상시켰다.

Ep-112 **Reactive sputtering으로 제작한 가스채색 박막의 내구성 연구** 김 나라, 서 충원, 정 현식 (*서강대학교 물리학과.*) 수소는 친환경적인 요소와 자원의 무한함을 장점으로 많은 연구가 진행되고 있다. 하지만 폭발성이 강한 수소에너지를 상용화하기 위해서는 수소의 누출을 검지할 수 있는 센서의 개발이 필수적으로 필요하다. 본 연구실에서는 Pd/WO_3와 같은 박막에 수소가 흡착될 때 박막의 색깔이 변하는 가스채색 현상을 이용해 수소검지 광센서를 연구해왔다. 기존의 thermal evaporation 방법으로 제작한 가스채색 박막의 경우 광투과도 변화에서 좋은 특성을 보였지만 내구성 면에서 좋지 않은 특성을 보였다. 본 연구에서는 thermal evaporation으로 증착한 Pd/WO_3 복층박막과 reactive sputtering으로 증착한 Pd/WO_3 복층박막의 특성을 비교하였다. 2×10^{-6} torr의 base pressure와 1.1×10^{-2} torr의 working pressure에서 Tungsten target을 사용하여 mass flow controller(MFC)로 아르곤의 유량은 8 sccm으로 고정시키고 산소유량을 바꿔주며 WO_3 박막을 증착하였다. 산소의 유량을 0.5 sccm에서 2.5 sccm까지 변화시켜가면서 증착한 WO_3의 Raman spectrum을 측정하여, 1.5 sccm에서 기존의 thermal evaporation으로 증착한 WO_3의 Raman spectrum과 가장 유사한 결과를 얻을 수 있었다. 서로 다른 방법으로 만든 가스채색박막의 반응성과 내구성을 알아보기 위해 밀폐된 chamber 안에 박막을 고정시킨 후 MFC로 1% 수소가스와 공기를 번갈아 주입하였다. 박막에 632.8 nm He-Ne Laser를 조사하고 투과된 빛을 high speed photo detector를 이용해 광투과도 변화율을 측정하였다. 기존의 thermal evaporation으로 제작한 Pd/WO_3 박막은 수소 주입 후 수초 이내에 급격한 광투과도 변화를 보였으나 수소와 공기 주입을 반복할 경우 일정 시간이 지나면 광 투과도의 변화율이 급격히 줄어드는 결과를 얻었다. 하지만 위의 조건으로 최적화시킨 WO_3 박막 위에 sputtering으로 Pd를 증착한 Pd/WO_3 박막의 경우 수소 주입 후 500회 이상 수소와 공기 주입을 반복하여도 광투과도의 변화율이 일정하게 유지되었다. 이 결과로 thermal evaporation으로 증착한 박막에 비해 sputtering으로 증착한 박막의 내구성이 향상되었음을 알 수 있었다.

Ep-113 **Enhanced resistive switching properties of polycrystalline TiO_2 nano-layer using a WN diffusion barrier layer** KWAK June Sik, DO Young Ho, JEONG Koo Woong, PARK Min Su, KIM Chae Ok, HONG Jin Pyo(*New Functional Materials and Device Laboratory, Dept. of Physics, Hanyang University, Seoul, Korea.*) The resistive switching properties were observed in a polycrystalline TiO_2 nano-layer with a WN diffusion barrier layer sandwiched between Pt electrodes. A fabricated memory cell was measured voltage-current characteristics in order to investigate the transport properties of Low and High resistance state by using four-point probe method. A TiO_2 memory cell using a WN barrier layer shows not only stable switching voltage value in "Set" and "Reset" process, but also enhanced curve plot in semi-log voltage-current characteristics. A low resistance state was achieved by applying a positive 2.5V under 3mA current compliance condition, and a high resistance state was achieved by applying a positive 0.5V. A resistance switching was repetitively observed with a resistance ratio $>>10^3$. It is possible that this enhanced switching property is due to the decrease of oxygen vacancy between Pt electrode and TiO_2 nano-layer interface under voltage bias. The WN barrier layer plays a crucial role in blocking a diffusion of oxygen ion from the TiO_2 nano-layer interface.

Ep-114 **Temperature dependence of resistive switching characteristic of binary oxide TiO_2 thin films for the nonvolatile applications** DO Young Ho, KWAK June Sik, JEONG Koo Woong, PARK Min Su, KIM Chae ok, HONG Jin Pyo(*New Functional Materials and Devices Lab. Department of Physics, Hanyang University, Seoul 133-791, Korea.*) Many materials have been reported to switch from a high to a low resistance state when subjected to an electric field. However, the mechanism of such resistive switching phenomenon is still not clear. It is the purpose of this work to discuss temperature dependent current - voltage characteristics of binary oxide TiO_2 thin films to elucidate the relation between resistive switching and current conduction

mechanisms. The binary oxide polycrystalline TiO_2 thin film has been prepared by a conventional rf magnetron sputtering system. The experiment was done as a function of oxygen pressure. Structural properties of the TiO_2 thin films are characterized utilized XRD and TEM. In order to analyze the temperature dependence switching properties, the 4-point probe method was used as a function of temperature for temperatures from 10 K up to 300 K with Keithley 236 source measure unit.

Ep-115 **Switching properties of various metal-insulator-metal sandwich structure with binary oxide layers for the ReRAM applications** JEONG KooWoong, KWAK JuneSik, DO Young Ho, PARK Min Su, HONG Jin Pyo(*New Functional materials and devices lab., Department of Physics, Hanyang University, Seoul, KOREA.*) The switching property of MgO for resistance random access memory application was studied about the defect, crystallinity, temperature dependence. We have prepared MIM, Pt/MgO/Pt, structure on $Ti/SiO_2/Si$ substrate by a reactive sputtering system at room temperature, and annealed with rapid thermal annealing system in oxygen ambience. In result of term, the resistive switching behaviors in metal-insulator-metal structure as insulator MgO clearly have revealed. In addition, we observed experimentally that these resistive switching phenomena would be strong dependence of oxygen vacancies. In conclusion, we suggest that the oxygen vacancies with the trapped charge would perform an important role for the resistive switching mechanism in MgO sandwich structure.

Ep-116 **Nonvolatile memory characteristics in metal-oxide-semiconductor containing the metal silicide heteronanoparticles fabricated by unique laser irradiation method** KIM JooHyung, YANG JungYup, KWAK JuneSik, DO Young Ho, HONG Jin Pyo(*New Functional materials and device lab. Department of Physics, Hanyang University Seoul 133-791, Korea.*) We have investigated metal-oxide-semiconductor (MOS) capacitors which embedded the metal silicide heteronanoparticles. The metal silicide heteronanoparticles were fabricated by utilizing an external laser exposure technique and were formed on HfO2, high permittivity, for the application of non-volatile memories. Images of transmission electron microscopy(TEM) revealed that the metal silicide heteronanoparticles clearly embedded in gate oxide layer. The results of energy dispersive x-ray(EDX) and x-ray photoelectron spectroscopy(XPS) were confirmed to make the metal silicide. Hysteresis results of C-V, I-V measurement for memory characteristic showed typical charging and discharging effects with a large flat band shift. In addition, excellent long-term retention rendered it feasible for the near-future development of the metal silicide-based floating gate memory.

Ep-117 **근접장 마이크로파 현미경을 이용한 과당에 따른 S11 변화 및 당도 측정 연구** 김 송희, 유 형근, 윤 영운, 김 종철, 이 기진(*서강대학교, 물리학과.*) 오늘날 과체중으로 인한 비만인구의 증가는 우리가 먹는 음식물이 갖고 있는 열량에 대해 관심을 갖게 했다. 더불어 맛과 건강을 위한 올바른 선택을 위한 노력이 시도 되고있다. 본 연구에서는 여러 종류의 과일이 가지고 있는 당분에 대해 근접장 마이크로파 현미경을 이용하여 마이크로파 반사계수를 측정하여 변화를 알아보고 상용의 당도계를 사용하여 과당을 측정하여 그 변화를 비교하여 보았다. 이러한 당도 비교 측정연구는 포도, 사과, 감, 귤, 배, 오렌지에 대해 이루어 졌다. 이 외에도 포도당의 농도변화에 따른 변화를 알아보기 위하여 농도가 다른 포도당 용액에 대해서도 반사계수 변화를 측정하여 보았다. 이를 통해, 근접장 마이크로파 현미경을 이용한 과일 및 포도당의 반사계수 측정 연구에서 반사계수의 여러 가지 변화원인에 대해 고찰해 보았다.

Ep-119 **금이 첨가된 전통한지의 구조적 특성 및 항균성 효과 연구** JEON, jong-sul, 한 상욱(*전북대학교 과학교육과.*) 전통한지는 pH 7.5-9.0인 중성지로 일반종이에 비해 오래 보존할 수 있고 통기성, 유연성, 방음성, 단열성, 습도조절능력, 자외선 차단 능력이 우수하여 여러 분야에 이용되고 있다. 이러한 우수한 소재인 전통한지를 다양한 기능의 기능성 한지로 개발하기 위하여 전통한지에 미세한 금 (Au) 입자를 첨가하여 전통한지의 항균효과를 연구하였다. 금입자가 첨가된 전통한지는 전통한지의 제작방법에 따라 주원료인 닥나무와 부원료인 황촉규를 이용하여 제작하였으며, 금입자를 첨가하여 항균성 기능한지를 개발하였다, 금이 첨가된 기능성 한지의 광 투과성을 측정하였으며, 금입자의 구조적인 특성은 엑세프 기법을 이용하여 금입자 내 금원자 주위의 미세구조를 연구하였다. 금이 첨가된 한지의 항균효과는 여러 가지 균을 한지 위와 주위에 뿌리고 활성화 정도를 관찰하였으며, 전통한지와 다른 종이에서 활성화된 균과 비교하였다. 금입자가 첨가된 전통한지에서는 균이 대부분 괴멸된 것으로 관

찰되었으며, 금이 첨가된 전통한지가 좋은 항균재료로 이용될 수 있음을 보여 주었다. 항균효과와 금의 구조적, 광학적 특성을 비교할 것이다.

Ep-120 **Highly Sensitive Dual Spin-valve Sensors for Detection of Nano-sized Magnetic Beads in Biosensors**

LEE YoungTeak, ROH Jong Wook, YI Sun gu, LEE Kyoung-Il, JUNG Hyo-Il[1], SON Ohtaek[1], LEE Wooyoung (*Department of Materials Science and Engineering, Yonsei Univ., Seoul, South Korea.. [1]School of Mechanical Engineering, Yonsei Univ., Seoul, South Korea..*) In the last few years, spin-valve sensors have been proposed as the potential detection components in biosensors and biochips based on superparamagnetic labeling [1]. Nano-sized magnetic labels have the advantage of being sufficiently small that they do not hinder biomolecular recognition/interaction processes. In spite of this advantage for biological applications, magnetic labels with nano-size generally have much smaller magnetic moments than micron-sized ones, which give rise to the difficulty in the detection. Therefore, spin-valve sensors with much higher sensitivity are prerequisite to detect the nano-sized magnetic beads. Compared with single spin-valve sensors, dual spin-valve sensors offer larger giant magnetoresistance (GMR) ratios and therefore higher sensitivity at low fields. In this work, we report the fabrication of dual spin-valve sensors to detect nano-sized magnetic beads for biosensors. The generic structure of a dual spin-valve sensor was Ta(50)/$N_{81}Fe_{19}$(25)/$Ir_{22}Mn_{78}$(60)/$Co_{84}Fe_{16}$(35)/Cu(18)/$Co_{84}Fe_{16}$(10)/$N_{81}Fe_{19}$(25)/$Co_{84}Fe_{16}$(10)/Cu(18)/$Co_{84}Fe_{16}$(35)/$Ir_{22}Mn_{78}$ (60)/Ta(50)(Å), a combination of photo lithography and a lift-off process has been utilized to fabricate a dual spin-valve sensor (w = 6 μm, l = 30 μm). The dual spin-valve sensors are composed of two pined layers ($Co_{84}Fe_{16}$), two spacer layers (Cu), and a free layer ($Co_{84}Fe_{16}$/$N_{81}Fe_{19}$/$Co_{84}Fe_{16}$). Spin-dependent scattering of the electrons takes place at the interfaces of two pinned layer/spacer layer, two free layer/spacer layer in the dual spin-valve structure, while it occurs only at the interface of free layer/spacer layer and pinned layer/spacer layer in the typical single spin-valve structure. The dual spin-valve sensor was observed to exhibit about 10 % magnetoresistance (MR) ratio. The detection of the nano-sized magnetic beads was performed by applying a dc magnetic field in the longitudinal direction of the dual spin-valve sensors. The MR curves of the sensor were measured before and after the nano-sized magnetic beads with d= 200 nm were located on the active area of the sensor surface. We found that MR curves of the sensor with nano-sized magnetic beads slightly shift. The differences in the resistance are attributed to a fringe field of the magnetic beads, which partially cancels the applied field in the free layer of the spin-valve structure [2]. We extend our study to the detection of DNA or virus coated with the nano-sized magnetic beads. Our results demonstrate the potential for using dual spin-valve sensors in order to detect the nano-sized magnetic beads for highly sensitive biosensors.

Reference[1] G. Li et al, J.Appl. Phys. 99, 08P107 (2006)[2] D. L. Graham et al, Trends Biotechnol. 22, 455 (2004)

Ep-121 **Highly Sensitive Electrical Detection of Biomolecules using Si Nanowires for Cancer Diagnosis**

LEE Seung-Hyun, KIM Cheol-Joo[1], CHOI Ahmi[2], JO Moon-Ho[1], JUNG Hyo-il[2], LEE Wooyoung(*Department of Materials Science and Engineering, Yonsei University, Seoul. [1]Department of Materials Science and Engineering, POSTECH, Pohang. [2]Department of Mechanical Engineering, Yonsei University, Seoul.*) Field-effect biosensors based on semiconductor nanowires (NWs) have extensively been investigated due to their practical advantages for real-time, label-free and highly sensitive detection of a wide range of biological and chemical species. For the realization of bio-sensors, the semiconductor nanowires such as Si are desirable since they are able to create a large variation in charge at the surface associated with binding and/or dissociation of analyte molecules, which is based on the well-established methods for the modification of the surfaces[1]. In the present work, we report on the detection of an protease enzyme, MMP (Matrix Metallo Protease)-9, in individual single-crystalline Si NWs for the use of a cancer marker.Si NWs used in this work were p-type with lightly boron-doped using a Si:B ratio of 1000:1 during growth. Si NWs with an average diameter of 70 nm were dispersed on oxidized Si substrates with the underlying conducting Si used as a back gate. Electrical contacts were made to NWs ends using electron-beam lithography, followed by Ti(100)/Au(200) (in nm) deposition and rapid thermal annealing (RTA) for ohmic contacts[2]. Si NW surfaces have been modified by applying one drop of telomerase solution onto a nanodevice in order to detect MMP-9.The dependence of current between source and drain (I_{SD}) on gate voltage (V_G) was found in a field-ef-

fects transistor (FET) device based on an individual single-crystalline Si NW with d = 70 nm. Linear gate-dependent current of the FET increases (decreases) with negatively (positively) increasing V_G, showing that Si NW is typical p-type. Similarly, I_{SD} versus V_G curves are shown to be characteristic of a p-channel FET, implying that the conductance modulation of the Si NW FET is demonstrated by changing the applied electric field. These results enable us to derive the carrier concentration n_e and electron mobility μ_e of 2.17×10^{17} ㎝$^{-3}$ and 13.6 ㎠/Vs at room temperature, respectively. The variation of conductance recorded from a p-type Si NW modified with telomerase was investigated after applying MMP-9 down to 5 nM solution. After binding telomerase with MMP-9, a decrease in conductance was observed. This decrease can be attributed to the reduction of the incorporation of negatively charged units on the NW surface during the binding process. Our results demonstrate that Si NW biosensors can be sued to detect MMP-9 down to a concentration of 5 nM, exhibiting the potential to impact the cancer diagnosis as well as new tools for research of biosensors based on semiconducting nanowires.

[1] C. M. Lieber, Nature Protocols. 1, 1711~1724 (2006)[2] J. R. Heath, Appl. Phys. Lett. 76, 2068~2070 (2000)

Ep-122 **싸이클로트론용 초전도 자석 개념 설계** 이 병섭, 김 동락, 양 형석, 최 연석, 강 준선[1], 채 종서[1](*한국기초과학지원연구원, 고자기장개발팀.* [1]*원자력의학원.*) 의료용 초전도 싸이클로트론 개발을 목적으로 3.5 T 초전도 자석에 대한 개념 설계를 진행하였다. 중입자 치료, 단수명 방사선 동위원소 생산을 위하여 계획된 초전도 싸이틀로트론은 기존 전자석을 이용한 싸이클로트론에 비교하여 상대적으로 크기가 작고 저전력 소비의 장점을 가지고 있다. 초전도 자석 냉각문제와 관련하여 소형 냉동기를 이용한 냉각방식을 채용함으로 헬륨 소비를 최소화하고 운영 편의성을 고려하였다.

Ep-123 **유기 발광소자 내 Alq3의 박막 열처리 조건에 따른 특성연구** 이 후능, 윤 영운, 김 송희, 유 형근, 김 종철, 김 승완, A. Babajanyan, 이 한주, 김 기언, 이 승호, 이 기진(*서강대학교 물리학과.*) 녹색 발광소자인 Alq_3 유기물 증착시 기판의 온도에 따른 특성 변화를 연구 하였다. 상온과 기판의 온도를 150~180℃로 변화시켜가며 증착하여 박막 특성의 상전이 현상을 관측하였다. 증착 시, 소자를 증착하기 전에 열을 가하여 소자를 증착하는 전열처리 방법과 소자를 증착 한 후 기판에 열을 가하는 후열처리 방법을 통해서 Alq_3 박막의 phase transition현상을 근접장 현미경(NSMM)을 이용하여 관측하였다. 또한 UV를 통해 파장 대에 따른 absorption특성 및 X-ray diffraction을 통한 구조 변화를 통해 상전이 현상을 관측하였다.

Ep-125 **Hydrogen sensing properties in Pd-Ni thin films** LEE Eunsongyi, JEUN Minhong, LEE Wooyoung(*Department of Materials Science and Engineering, Yonsei University, 134 Shinchon, Seoul.*) Palladium (Pd) has attracted much attention for its ability that absorbs large amount of hydrogen compared with its volume [1]. Hydrogen absorption has been known to give rise to biaxial stress at the interface between a Pd thin film and a substrate, causing 'peeling off' of the thin film from the substrate. Pd alloy with Ni, Ag or Au has been found to be useful in order to prevent 'peeling off'. Pd-Ni is of particular interest since it delays the formation of β-phase related to irreversible behavior in sensing mechanism [2]. In the present work, we report the effects of Ni content on demonstrate the hydrogen sensing performance in Pd-Ni thin films. Pd and Ni were simultaneously deposited on a thermally oxidized Si(100) substrate in a dc magnetron sputtering system with a base pressure of 4×10^{-8} Torr. The Pd and Ni co-sputtered thin films were subsequently heat-treated. Ni contents in the Pd-Ni thin films were found to vary from 4.3 % to 42.0 % by controlling the deposition power of a Ni target. The 20-nm-thick Pd-Ni thin films with Ni contents up to 42 % were found to operate as hydrogen sensors in the concentration range 0.05 – 1 % at room temperature by measuring the electrical resistance change in the films. The response time of Pd-Ni films was found to dramatically decrease with increasing Ni content. The response time of a Pd-Ni film with Ni content of 7.2 % was found to be 20 seconds, whereas that of a pure Pd film was observed to be 121 seconds. The sensitivity of the Pd-Ni films for H_2 sensing is defined as $S\ (\Delta R/R) = (R_H - R_N)/ R_N \times 100$ %, where R_H and R_N are the resistances in the presence of H_2 and N_2 gas, respectively. The sensitivity of Pd-Ni films was found to slightly decrease with increasing Ni content. However, the Pd-Ni films was observed to effectively prevent hydrogen embrittlement according to cycles of absorption and desorption of hydrogen, as compared to pure Pd films, which is vulnerable to cycles of absorp-

tion and desorption of hydrogen. The effects of Ni content in the Pd-Ni thin films on the hydrogen embrittlement are addressed.
[1] F.A. Lewis, The Palladium Hydrogen System, Academic, New York, 1967 [2] R.C. Hughes, et. al., Thin films of Pd/Ni alloys for detection of high hydrogen concentrations, J. Appl. Phys. 71 (1992) 542-544

Ep-126 **HIGH-PRECISION MEASUREMENTS OF THE QUANTIZED HALL RESISTANCE USING A CRYOGENIC CURRENT COMPARATOR BRIDGE SYSTEM** 김 완섭, 유 광민, 김 문석, 김 규태, 정 연욱, 박 포규, 김 영균, 원 성호(*한국표준과학연구원, 기반표준부.*) A cryogenic current comparator bridge system has been developed to fulfill the needs of national standards for an improved uncertainty level in the resistance measurements. The bridge system is served to compare with the best accuracy and control the two tracking currents with an accuracy of 10^{-9} using a SQUID sensor as a null detector. The quantized Hall resistance value of plateau i = 2 of GaAs-based heterostructure device $R_H(2)$ = 12.9064035 kΩ generated at a temperature of 1.45 K with a current of 30 μA and with a magnetic flux density of 10.0 T is used to calibrate standard resistors of 100 Ω (Tinsley, Type 5685A). The results of the comparison, $R_H(2)$ vs. 100 Ω, reveal that the measurement uncertainty is typically less than 5.9 parts in 10^9. The high-precision resistance measurement technique will be described in detail along with the measurements uncertainty budget.

Ep-128 **자기냉각에 의한 저온 발생** 김 동락, 이 병섭, 염 성호, 양 형석, 최 연석, 박 장현[1], 박 진홍[2] (*한국기초과학지원연구원 고자기장 개발팀. [1]한국천문연구원. [2]KAIST 물리학과.*) magnetocaloric effect를 이용한 냉각방식은 magnetic cooling이라고 하며 한제를 사용하지 않고 저온을 얻을 수 있다. 본 연구는 0.1K 온도영역을 얻기 위한 예비냉각단계로 4K~1K 사이의 온도에서 냉각하기 위해 GGG를 이용하여 magnetic cooling 실험을 수행한 결과에 대해서 보고한다.

Ep-129 **Pattern growth of carbon nanotubes on stainless plate for field emitters** KIM Chang-Duk, KANG Jun-Tae[1], LEE Sung-Youp, SHIN Byong-Wook[1], KIM Sanghun[1], LEE Hyeong-Rag(*Department of Nano-science &Technology, NPTL, Kyungpook National University. [1]Department of Physics, NPTL, Kyungpook National University.*) In order to use with the field emitter synthesized the carbon nanotube(CNT) on stainless plate of 5mm diameter. Vertical alignment is essential in achieving a high geometrical enhancement factor in field emitters. It is well known that the mutual shield effect between neighbouring CNTs leads to the suppression of field emission properties in densely packed CNTs. We studied in vertically aligned pattern growth for reduction shield effect of CNT emitters, which is encouraging for applications in field emitters and nanoelectrodes.

Ep-130 **Study of discharge characteristics according to conditions of dielectric layer in a mercury-free flat discharge fluorescent lamp** RYU Hyun-Woo, KIM Chang-Duk[1], KIM Young-Jin[1], CHUNG Kyu-Yong[2], KANG Jun-Tae, KIM Jae-Bum, LEE Hyeong-Rag (*Department of Physics, NPTL, Kyungpook National University. [1]Department of Nano-science &Technology, NPTL, Kyungpook National University. [2]Department of Physics, Kyungpook National University.*) Generally mercury is used in fluorescent lamp because it provide high efficacy . The use of mercury, however, leads to difficulties in lamp ignition at low temperature and a relatively long build-up time is necessary for the lamp to reach the saturated luminance level . Further, for environmental reason, there has been an increasing effort to reduce and eliminate mercury in fluorescent lamps. These problems preclude the use of mercury lamps for liquid crystal display (LCD) backlighting. So a mercury-free discharge fluorescent lamp has been developed for LCD backlighting. In this experiment we used flat fluorescent lamp of coplanar electrode type in Xe atmosphere. Especially, the dielectric layer plays a important role in dielectric barrier discharge (DBD). It protects electrodes to have stable discharge and emits the secondary electron to decrease firing voltage. The aim of this work is to study discharge characteristics according to several different condition on dielectric layer fabrication. From this experiment, we could understand effect of dielectric on discharge characteristic.

Ep-132 **Performance Improvement by Surface Modification of Indium Tin Oxide in the Method of Self-Assembled Monolayer** 김 경석, 김 영훈[1], 한 정인[1], 정 관수[2](*KETI IDRC, 경희대학교. [1]KETI IDRC. [2]경희대학교.*) Organic thin-film transistor (OTFT) is of in-

creasing interest for applications such as smart cards, identification (ID) tags and flexible displays. OTFTs are likely to have suitable applications requiring large-area coverage, structural flexibility and low-cost. However, there are still many issues to be addressed for practical organic electronics. In the paper, pentacene triisopropylsilyl (TIPS)-based organic thin film transistors have been fabricated with and without the presence of a modifying monolayer at the interface between the ITO source-drain and the organic semiconductor. The monolayer consists of Chlorophenyl dichloro-phosphate (CPDP) is deposited by spin coating. The interface modification by the CPDP monolayer has resulted in improved device performance, including 12% higher effective mobility, threshold voltage from 5 V to 1.3 V, and on/off ratio from 1.0×10^3 to 8.7×10^3. The presence of this monolayer appears to improve the interface characteristics of the deposited pentacene layer, as modifying to surface of ITO.

Ep-134 **Low-pass filter가 무선전원용 렉테나의 파워 변환효율에 미치는 영향 연구** 정 호상, 이 재훈[1], 박 은규, 허 정[2], 이 상영[3](*건국대 물리학과. [1]건국대 차세대무선전원센터. [2]건국대 전자공학부, 차세대무선전원센터. [3]건국대 물리학과, 차세대무선전원센터.*) 유비쿼터스 기술의 발전과 함께 무선으로 전원을 공급할 수 있는 장치의 필요성이 여러 분야에서 커지고 있다. 특히 이러한 무선전원의 응용성은 인체 내에 삽입되어 사용되는 의료보조기기에서 큰 효용성을 찾을 수 있는데, 이는 이러한 삽입형 의료보조기기의 경우 전원이 소모된 경우 반드시 수술을 통해 전원을 교체해야 하기 때문이다. 마이크로파 신호를 직류신호로 변환시켜주는 렉테나(rectenna)는 antenna와 rectifier의 기능을 동시에 지니는 소자로 무선전원을 실현하기 위한 핵심요소이다. 이러한 렉테나의 구성요소는 안테나, 필터 그리고 GaAs Schottky 다이오드로서 이러한 구조는 RFID의 tag와 유사하지만, tag의 경우 일정한 거리 내에서 통신이 가능하면 되고 렉테나의 경우 무선전원으로 사용하기 위해 파워 변환효율을 크게 해야 한다는 것이 중요한 차이이다. 본 연구에서는 렉테나에서 필터의 유무가 파워 변환효율에 어느 정도 관계를 가지는지를 살펴보고자 한다.

Ep-135 **주류의 알코올도의 측정불확도요인분석과 알코올도의 국제표준과 국내 주류분석규정과의 비교에 관한 연구** 이 용재, 장 경호(*한국표준과학연구원.*) 주류의 알코올도는 주류의 완제품을 증류하여 얻어진 알코올을 소정의 물로 희석하여 시료용액을 만들고 이 용액의 밀도를 측정하여 알코올도를 측정한다. 시료용액의 밀도측정기로서 Hydrometer와 Density meter를 사용하여 측정하고 있다. 그러나 측정기의 성능과 사용방법 그리고 증류중 또는 측정과정 가운데 발생하는 증발로 인하여 측정불확도의 요인이 발생하게 된다. 본 연구에서는 이 측정불확도요인과 부액계 사용시 측정불확도모델를 제시하고 이를 분석한다. 또한 알코올도의 국제표준과과 국내주류분석규정과의 표준을 비교하고 국내 주류의 국제경쟁력향상을 위하여 국내 알코올도를 국제표준으로 전환을 제안하고저 한다.

Ep-136 **Improvement of SNR in Magnetic Resonance Force Microscopy by Phase-cycled Average** WON Soonho, SAUN Seung-Bo, KIM Changsoo, LEE SangGap, LEE Soonchil(*Department of Physics, Korea Advanced Institute of Science and Technology, 373-1 Guseong-dong, Yuseong-gu, Daejeon 305-701, Korea.*) Magnetic resonance force microscopy (MRFM) is a powerful method of detecting electron spin resonance (ESR) for subsurface investigations on the spin properties and interactions of a small number of doping impurities or point defects in thinly-layered devices beyond the sensitivity problem of conventional ESR. In MRFM, a magnetic-resonant change of the force exerted by the spin polarization in the presence of a magnetic field gradient is monitored by using a micromechanical cantilever. In this study, MRFM was demonstrated using the fast-relaxing electron spins of the standard ESR marker DPPH. Signals were detected in frequency-modulation (FM) mode by a phase-locked loop FM detector. We used a spin-modulation protocol where the spin polarization is cyclically saturated at the cantilever's fundamental resonance frequency in some phase with respect to the cantilever vibration. We report that a practical signal-to-noise ratio of MRFM can be improved drastically when two signals, each of which is obtained while the phase is 0 and p respectively, subtract each other and a common baseline included in the signals is subsequently removed.

Ep-137 **Electro-optical characteristics of Mercury-free Flat Fluorescent Lamp with various mixture ratio of Xe-Ne and Xe-He.** CHUNG. K.Y., KIM. Y.I., KIM. Y.J.[1], KIM. C.D.[1], MOON. H.S., LEE. S.M., SOHN. S.H.(*Dept. Physics, Kyung-pook Nat. Univ. [1]Dept. Nano Sci &Technol, Kyung-pook Nat. Univ.*) We fab-

ricated the opposed discharge type FFL (Flat Fluorescent Lamp), which is composed of transparent and metal electrodes, dielectric layers, phosphor layers, and discharge space. We studied on the electro-optical properties of the FFL as a function of mixture gas ratio of Xe-Ne and Xe-He, in these studies, we fixed the total gas pressure in 300 torr. We got the maximum result at Xe (90%)-Ne (10%), the luminance is 9,289 cd/m^2.

Ep-138 **유기발광소자에서 전극 변화에 따른 내장 전압** 이 은혜, 윤 희명, 한 원근, 김 태완, 장 경욱[1], 정 동희[2], 임 종태[3], 안 준호[4](*홍익대학교, 정보디스플레이공학과. [1]경원대학교, 전기공학과. [2]신천중학교. [3]성균관대학교, 재료공학과. [4]홍익대학교, 과학기술연구소.*) 유기발광소자에서의 내장 전압을 분광학 흡수를 이용하여 측정하였다. 소자 구조는 양극/Alq_3/음극으로 제작하였으며, 양극으로는 ITO와 ITO/PEDOT:PSS을 사용하고, 음극으로는 Al, LiF/Al, Li_2O/Al을 이용하였다. 이 때 사용한 LiF와 Li_2O의 두께는 0.5nm, 0.8nm, 1nm로 하였다. 소자 내의 내장 전압은 기본적으로 양전극과 음전극의 일함수 차이로 인하여 발생된다. 본 연구에서는 이 차이를 전기광학적 방법으로 측정하였다. 실험 장치로는 500W Xenon 램프, Keithley 236 SMU, Stanford SR530 lock-in amplifier를 사용하였다. 소자에 빛을 인가하여 발생되는 미세 광전류를 lock-in amplifier를 통하여 측정하였다. 이 때 사용한 chopping 진동수는 20Hz로 하였다. lock-in amplifier에서는 미세 광전류의 크기와 위상을 측정하며, 이들의 변화를 통하여 내장 전압을 측정하게 된다. 실험 결과, PEDOT:PSS를 사용한 소자는 사용하지 않은 소자에 비해서 내장 전압이 증가함이 측정되었다. LiF와 Li_2O를 사용한 소자의 내장 전압에 대한 결과도 발표하고자 한다.

Ep-139 **유기 발광 소자에서 Li_2O/Al 음전극의 효과** 신 은철, 안 희철, 한 원근, 김 태완, 이 원재[1], 송 민종[2](*홍익대학교, 정보디스플레이공학과. [1]경원대학교, 전자통신공학부. [2]광주보건대학, 의료공학과.*) OLED의 소자의 효율을 높이기 위해서는 음극 방향에는 전자 주입층과 수송층, 양극 방향에는 정공 주입층과 수송층이 있어야 한다. 우리는 Alq_3와 Al 전극 사이에 Li_2O의 재료를 삽입하여 소자(ITO/ TPD(40nm)/ Alq_3(60nm)/ Li_2O(xnm)/ Al(100nm))를 제작하였다. Li_2O의 두께를 0.5nm부터 2nm까지 변화시켰으며, 유기물과 음전극은 모두 열증착하여 제작하였다. Li_2O의 역할은 LiF에서와 같이 음전극의 일함수 변화에 영향을 줄 것으로 판단된다. Li_2O/Al 음전극의 효과를 알아보기 위하여 I-V-L, 효율을 상온에서 측정하였다. 측정한 결과, Li_2O를 사용한 소자는 전반적으로 사용하지 않은 소자에 비해 특성이 우수하게 나타났다. 특히, Li_2O(0.5nm)/Al 의 소자는 Al 소자보다 휘도, 효율, 구동전압면에서 향상된 결과를 보이고 있다. 이는 Li_2O층이 음극의 일함수를 낮추어 전자주입이 강화되어 효율을 높이는데 기여한 것으로 판단된다.

Ep-140 **방사선조사 후 금붕어 장관 평활근 수축활성 변화 측정** 길 상형, 문 경희, 김 성부, 이 종규, 조 승일, 김 동원[1], 이 미란[1](*부경대학교 물리학과. [1]부산대학교병원 방사선종양학과.*) 방사선 조사시 생체에서는 방사선의 직접적인 작용, 자유산소기의 간접적인 작용에 의해 손상이 일어나는 것으로 알려져 있다. 방사선 발생장치(LINAC)를 이용하여 방사선(10 Gy)을 금붕어에 전신조사 후 10^{-5} M의 Acetylcholine 용액을 투여 한 다음 시간경과에 따른 장관 수축활성 변화를 생리기록기(physiograph)를 사용하여 평활근의 장력을 측정하였다. 방사선조사 후 시간 경과에 따른 금붕어 장관 수축활성 변화는 조사전 평활근의 수축활성이 1.15±0.15(g중)이었던 것이 조사 후 2시간, 1일, 2일, 3일, 4일까지는 0.76±0.10(g중), 0.52±0.10(g중), 0.53±0.17(g중), 0.55±0.07(g중), 0.67±0.14(g중)으로 유의수준 $p<0.05$로 유의성 있게 감소하였다. 방사선조사 후 6일, 9일, 15일, 40일에는 평활근 수축활성이 0.92±0.18(g중), 1.02±0.16(g중), 0.82±0.10(g중), 1.07±0.15(g중), 0.83±0.26 (g중)으로 방사선 조사전보다 평활근의 수축활성은 감소하였으나, 유의수준 $p>0.05$로 유의성은 없었다. 방사선조사 후 6일, 9일, 40일에는 금붕어 장관 평활근의 수축활성이 가장 많이 감소한 방사선 조사 1일후 보다 각각 43.2%, 48.7%, 51.1% 유의수준 $p<0.05$로 유의성 있게 증가하였으며, 방사선 조사전의 평활근의 수축활성과 비슷한 회복을 보였다.

Ep-141 **Synthesis and Photophysical Properties of Transition Metal Ions-Doped Nanocrystalline Titanium Oxidefor Photocatalytic Applications** 홍 경수, 홍 태은, 김 현규, 진 종성, 하 명규, 박 설진, 정 의덕(*한국기초과학지원연구원 부산센터.*) Chromium-doped nanocrystalline titanium oxide was synthesized using the sol-gel and hydrothermal synthesis methods in order to understand the operating principles of transition metal-doped photocatalytic materials active under visible light irradiation. After heat treatment for the samples, we characterized their structures and basic properties using conventional X-ray diffraction patterns, UV-visible absorption spectrum, and high resolution transmission emission microscopy. The photoluminescence spectra in

visible region at room temperature were taken to study the photophysical properties of synthesized nanoparticles. We showed that chromium-doped nanocrystalline titanium oxide is a promising candidate for visible light photocatalytic applications.

Ep-142 **BTL(blue thermoluminescence)을 이용한 석영에 대한 Activation Energy 와 Frequence factor 결정** 송 기웅, 홍 덕균[1](*충청문화재연구원. [1]강원대학교 물리학과.*) 열 루미네선스(TL;thermoluminescence)는 석영이나 장석 등과 같은 무기결정이 외부에서 어떠한 형태의 에너지를 받아 흡수된 에너지가 열에 의해서 빛으로 바뀌어 외부에 방출하는 물리적인 현상이다. 측정 결과는 몇 개의 peak로 나타나며, 이때 peak의 모양과 위치, 세기는 석영 격자결함(trap)의 물리적 특성과 밀접한 관련이 있다. 석영의 격자 결함에 포획된 전자는 Activation energy보다 큰 빛 또는 열 에너지를 흡수해야만 여기됨으로서 루미네선스를 방출한다. Activation energy 와 Frequency factor를 산출하는 측정 방법에는 여러 가지가 있지만 Peak shape method와 Isothermal decay method가 주로 사용 된다. 본 연구에서는 위 두 방법을 이용하여 서로 다른 기원의 자연 석영 입자에 대해서 청색 계열의 열 루미네선스(BTL)를 이용하여 Activation energy 와 Frequency factor를 구하였다.

Ep-143 **국가킬로그램 원기의 질량 변화** 정 진완, 이 성준, 이 우갑, 김 광표(*한국표준과학연구원.*) 질량의 단위인 킬로그램은 국제킬로그램의 질량으로 정의되어 있다. 질량표준의 소급성 유지를 위하여 각 국가의 표준기관에서는 킬로그램 원기를 보유하고 있다. 한국의 표준기관인 한국표준과학연구원은 킬로그램 원기를 3개 (No. 39, No. 72, No. 84) 보유하고 있는데 이 중 No. 72를 국가킬로그램원기로 사용하고 있다. No. 72는 5년에 한번씩 국제도량형국(BIPM)에서 보조 국제킬로그램원기와 비교교정을 통하여 질량표준의 소급성을 확인하고 있다. 2002년도에 이어서 금년 초에 다시 교정이 이루어질 예정이다. 이 결과를 바탕으로 한국표준과학연구원에서 보유하고 있는 킬로그램원기의 질량 변화를 분석하여 발표하려고 한다.

Ep-144 **프레스 가공에서의 불량품 검출을 위한 음향방출(AE: Acoustic Emission)신호의 분석** 김 동훈, 박 상진, 이 원규, 김 인구[1], 이 민성[1], 김 석원[1](*울산대학교,기계자동차학과. [1]울산대학교,물리학과.*) AE 센서를 이용한 기술들은 10여년전부터 활발하게 적용되어 비파괴적 재료의 내부 탐색, 밀링이나 드릴링 작업 시 공구 마모 등을 감시하기 위한 용도로 널리 사용 되어 왔으나 프레스 작업 시 제품의 불량을 자동으로 판별하기 위한 용도로 쓰인 경우는 없었다. 따라서 본 연구에서는 프레스 공정(예를 들면 오일 팬 생산 공정)에서 AE를 이용하여 성형이전의 각 공정에서의 프레스 장치에 부착시킨 AE센서에서 발생되는 음향 파를 수집하고 분석하여 양호한 신호와 불량일 때의 신호를 판단, 제품의 양/불량뿐만 아니라 데미지의 정도와 위치까지 파악했다. 이를 위한 실험 장비로는 PHYSICAL ACOUSTICS CORPORATION의 R15α Sensor, 2/4/6 프리앰프, PCI-2 AE 보드를 사용하였고, 프로그램은 AE WIN을 사용하였다. 본연구의 결과를 토대로 AE 센싱 시스템을 개발하고 현장에 적용함으로서 향 후 프레스작업 시 불량품을 실시간 검출 및 예방하여 생산성을 높이는데 기여 할 것이다.

Ep-145 **Thermoluminescence of Au-Ion Implanted Al_2O_3 Single Crystal** KIM Taekyu(*Jeonju National University of Education, Department of Science Education.*) Three-dimensional thermoluminescence spectra were measured from x-ray excited Al_2O_3 single crystals implanted with Au ion. Au ion implantations were carried out with the energy range of 50 keV ~ 100 keV and the dose range of 1×10^{14} ions/cm^2 ~ 5×10^{16} ions/cm^2 at room temperature. The thermoluminescence spectrum shows the thermoluminescence peak with 415-nm emission band at 390 K and 502 K, and thermoluminescence peak with 685-nm emission band at 381 K. Glow curve of 60 keV x-ray excited Al_2O_3 implanted with 80 keV Au ion was divided into 308 K, 346 K, 385 K, 413 K, and 503 K peaks. The kinetic order, activation energy, and frequency factor of dominant 385 K peak were calculated with the peak shape method, the initial rise method and curve fitting with numerical method. The 385 K peak intensity decreased with increasing Au ion dose. Emission spectrum at 385 K was split into 1.81-eV emission band and 3.0-eV emission band associated with the excited Cr^{3+} impurities and F center, respectively. As Au ion doses increased, the intensities of 1.81-eV emission bands monotonously decreased but the intensities of 3.00-eV emission bands abruptly decreased. Because Cr impurities were intrinsically involved in Al_2O_3, the implantation of Au ions did not deeply affect on the intensities of 1.81-eV emission bands. On the contrary, the intensities of 3.00-eV emission bands were influenced on implanted Au ions, which played a role to kill the F-centers.

Ep-146 **자동차 휠하우스 PET 흡음 소재의 물성 연구** 이 재란, 김 형영, 박 경민, 김 석원(*울산대학교, 물리학과.*) 자동차가 정속 주행시 타이어 마찰 소음, 물 또는 모래가 튀는 소음 등으로 인해 실내 소음이 발생하게 된다. 자동차 휠 하우스는 이를 개선하기 위하여 타이어 둘레를 감싸기 위한 제품으로서 소음을 흡수하기 위하여 흡음성이 좋은 재료들로 만들고자 한다. 기본적으로 구성소재는 원가 절감과 재활용성이 고려된 재활용된 PET, 잡사와 최소한의 LM PET 등을 혼합하여 성형성을 갖추어야 한다. 그러나 이러한 소재의 기계적 강도, 열적특성, 흡음성에 대한 연구결과가 아직 충분하지 않아, 이에 대한 정확한 물성치를 알지 못하면 충분한 성과를 거두지 못하게 된다. 따라서 본 연구에서는 PET를 방사하여 만든 펠트와 시트 소재를 관내법을 이용하여 1000~3000 Hz 진동수 영역에서 지름이 29 mm 내외인 원반형 시편의 흡음율을 비교하였다. 그리고 UTM 장비를 이용하여 두께가 3 mm인 아령 모양 시편의 인장강도를 측정·분석하였다.

Ep-147 **Finite Size Effects on the Surface Structure and Properties of Films Made of Wedge-Shaped Molecules** SONG Jinsuk, KIM Mahn Won(*Korea Advanced Institute of Science and Technology.*) We have studied the structure and properties of the film made of wedge-shaped molecules by varying the size of a film using Monte Carlo simulation. The structure of the film shows transition from the isotropic phase to the nematic phase as decreasing the size of the film. The lateral size at this transition is the length where the radial correlation function of particles stops oscillating and becomes constant. The surface properties like diffusion constant and fluctuation of surface tension changes sharply at this point, too. This transition divides the length scale into two regimes in one of which the capillary wave theory fails and in the other it succeeds.

Ep-148 **Measurement of Thermophysical Properties of IC Packaging Materials** 박 경민, 이 제홍, 김 석원(*울산대학교,물리학과.*) In order to apply the polymer and ceramic compounds to the packaging of IC (integrate circuit) chip the variation of thermal conductivity and coefficient of thermal expansion were studied. The thermal diffusivity, specific heat and coefficient of thermal expansion of the epoxy and liquid crystal polymer samples which were filled by 40～70 volume % of SiO_2, α-Al_2O_3 and AlN fillers were measured by laser flash method, DSC(differential scanning calorimetry) and TMA (thermo-mechanical analyzer), respectively. The thermal conductivity was obtained by the multiplication of thermal diffusivity, specific heat and density of the samples and it agrees with the predicted values which were calculated on the Bujard's model(percolation threshold : 30%, threshold : 1) within ± 15 %. Also, the result shows us that the coefficient of thermal expansion linearly decreased as the volume fraction of filler increased and the sample of AIN filler and liquid crystal polymer matrix showed the optimized thermophysical properties as IC packaging materials.

Ep-149 **Measurement of Raman spectral differences between normal and cancer tissues using confocal micro Raman spectroscopy** PARK Do-young, NAM Jungwoo, YOON Doohee, CHEONG Hyeonsik, LEE Jungwoon[1], KIM Jungho[1](*Department of physics, Sogang University. [1]Department of life science, Sogang University.*) Confocal micro-Raman spectroscopy provides a powerful tool for biochemical changes in cells and tissues causing cancer and detailed information about biochemical molecular vibration frequencies of cells. Confocal micro-Raman spectroscopy of tumor and normal tissues were perfomed with the 514.5 nm line of an Argon ion laser with a spatial resolution of approximately 1 μm^2 as determined by the size of focused laser beam. The signal was dispersed by a Spex 0.55-m spectrometer with a holographic edge filter and detected with a liquid nitrogen-cooled charge-coupled device (CCD) detector array. Since tumor cells are accompanied with changes in the distribution of biochemical compounds (such as Amide, lipid and C-H bonding), Changes in molecular vibration frequencies of such compounds are revealed by Raman spectroscopy. We examine Raman spectral difference between normal and tumor tissues.

Ep-150 **극저상점 습도 발생장치 개발 및 성능평가** 최 병일, 남 현수, 우 상봉, 김 종철, 권 수용, 유 형근(*한국표준과학연구원.*) 극 저습의 환경에서 습도의 조절은 첨단산업의 진보에 있어 매우 중요한 문제이다. 반도체 공정, 디스플레이 산업 그리고 가스 산업 등 과 같이 첨단기술을 필요로 하는 많은 공정에서는 오염물질 특히 수분은 재품의 물성에 크게 영향을 미쳐 제품의 품질을 좌우하게 된다. 극 저노점 영역의 습도 표준 확립을 위하여 새로운 저노점 발생장치를 개발하였고, 성능평가 및 유효성 평가를 마쳤다. 이는 이단 압

축 냉동기에 의한 열전달 방식과 열전소자를 이용하여 온도조절을 하는 새로운 개념의 고체 평형 저노점 발생장치이다. 습도의 발생영역은 (-95 ~ -40) ℃ D.P. 이며, 포화조의 온도 안정도는 5 mK 이내 이었다. 제작된 발생장치는 유효성 평가를 위하여 KRISS의 다른 표준기인 이온도 발생장치와 (-80 ~ -40) ℃ D.P.에서 비교되었으며, QCM에 의한 평가를 -91 ℃ 까지 수행 하였다.

Ep-151 **무수은 평면형광램프(Flat Fluorescent Lamp)의 제작과 상판 형광막 형성에 따른 전기 광학적 특성** 문 희송, 정 규용, 정 진구[1], 손 인호[1], 이 상목, 손 상호(*경북대학교, 물리학과. [1]유엔아이.*) LCD는 Back Light와 같은 광원을 필요로 하는 수광형 디스플레이다. 이에 이용되는 Back Light 중에서 무수은 평면형광램프는 수은타입의 결점인 외부온도에 따라 특성이 변하는점과 환경문제의 측면에서 그 대체로 여겨지는 광원이다. 본 연구에서는 대향형 무수은 평면형광램프(FFL)를 제작하였다. 하판은 Glass를 Sand Blast로 식각한 다음 Ag전극을 형성하고 방전 셀 안에 Dispenser를 이용하여 형광체를 토출하여 형성하였다. 상판은 ITO Glass에 Screen Print로 형광막을 형성한 다음 상하판을 합착하여 제작 하였다. 램프를 제작할 때 상판의 형광막 형성을 각각 달리 하였다. 완성된 램프에서 Xe 및 Ne 가스 분압별로 전기 광학적 특성을 연구 하였다.

Ep-152 **열린 공간 음파 전달 모사를 위한 PML (Perfectly Matched Layer) 경계조건** 박 석현, 이 형원[1] (*인제대학교, 컴퓨터응용과학과. [1]인제대학교, 컴퓨터응용과학부, 수리과학 연구소.*) 도로에서의 소음의 전파는 실내 공간에서의 음파의 전달과는 달리 음이 반사하는 경계와 무한히 퍼져나가는 경계가 공존한다. 대부분의 음향 시뮬레이션 프로그램들은 닫힌 공간에 관한 것으로 도로와 같은 열린 공간에 적용하기에 적절하지 못하다. 따라서 본 연구에서는 열린 공간에서의 음파의 전달을 정확하게 모사하기 위해 전파의 전달에서 사용하는 PML(Perfectly Matched Layer)경계를 적용하는 수치 모델을 개발하고자 한다.

Ep-153 **Spatial filter를 이용한 공초점현미경의 공간분해능 향상 연구** 윤 두희, 정 현식(*서강대학교 물리학과.*) 공초점 현미경을 이용한 microscopy 연구에 있어서 공간분해능은 매우 중요한 요소이다. 본 연구실에서는 공초점 현미경을 이용하여 photoluminescence, Raman spectra mapping image를 얻는 연구를 진행하고 있는데, 보다 선명한 image를 얻기 위한 노력으로 spatial filter 이용한 공초점현미경의 분해능 향상 연구를 진행하였다. 공간분해능은 대물렌즈에 의해 모아진 레이저 beam spot의 크기에 의해 결정된다. Beam spot의 크기를 줄이기 위해서는 NA (numerical aperture) 값이 큰 대물렌즈를 사용하여야 하는데 NA값이 높은 대물렌즈는 working distance가 작은 단점을 지닌다. 저온에서 microscopy를 하기 위해서는 시료와 대물렌즈 사이에 진공을 만들고 온도를 내릴 수 있는 저온장치가 들어가야 하므로 어느 정도 이상의 working distance를 유지하여야 한다. 현미경 대물렌즈의 제한된 NA값에서 공간분해능을 향상시키는 위해서 시료와 대물렌즈 사이에 SIL (solid immersion lens)을 사용하여 고 분해능을 기대할 수 있으나 시료의 제작 및 정확한 위치 제어가 어렵기 때문에 이번 연구에서는 spatial filter를 이용하여 레이저의 경로 전환 및 진행에 있어서 발생하는 spatial noise를 제거하고 동시에 beam expander의 역할을 함으로써 공간 분해능을 향상시키는 비교적 간편한 방법을 연구 하였다. Ar ion 레이저의 514.5 nm 파장과 He-Cd 레이저의 325 nm 파장을 사용하였으며 achromatic 과 Schwarzschild식 현미경 대물렌즈를 사용하였다. Beam spot의 크기는 knife-edge 방법을 통해서 측정하였다. Spatial filter를 사용하기 전과 후를 비교해 보았을 때 레이저 beam spot의 크기가 줄어듦을 확인할 수 있었다. Spatial filter에 사용되는 pinhole의 크기, 렌즈의 조합에 따른 레이저 beam spot의 크기 변화를 조사하였다.

■ SESSION: P1
4월 19일 (목), 14:30 - 16:15
스키하우스

Fp-001 **Multifractal detrended fluctuation analysis of derivative and spot markets** 임 규창, 김 수용, 김 경식[1](*한국과학기술원, 물리학과. [1]부경대학교, 물리학과.*) We investigate the multifractal properties of price increments in the cases of derivative and spot markets. Through the multifractal detrended fluctuation analysis, we estimate the generalized Hurst and the Renyi exponents for price fluctuations. By deriving the singularity spectrum from the above exponents, we quantify the multifractality of a financial time series and compare the multi-fractal properties of two different markets. The different behavior of each agent-group in transactions is also discussed. In order to identify the nature of the underlying multifractality, we apply the method of surrogate data to both sets of financial data. It is shown that multifractality due to a fat-tailed distribution is significant.

Fp-002 **Dynamical mechanism of two-phase phenomena in financial markets** 임 규창, 김 수용, 장 기호[1], 김 경식[2](*한국과학기술원, 물리학과. [1]KMA. [2]부경대학교, 물리학과.*) Two-phase behavior of the Korean treasury bond (KTB) futures in the Korean exchange market is investigated in this study. To show that the two-phase phenomena are due to heavy-tailed behavior of distribution of price returns, actual data from the KTB futures market with shuffled data and a generated time series are examined according to the Brownian process. In addition, we study the correlation inherent in the KTB futures and its Brownian walk, describing the extent to which the volatility clustering plays a crucial role in equilibrium and nonequilibrium states of financial markets. It is shown that the two-phase behavior essentially results from heavy-tailed behavior of the distribution of price returns. This two-phase behavior does not appear to be relevant to volatility clustering.

Fp-003 **Volatilities, traded volumes, and the hypothesis of price increments in derivative securities** 임 규창, 김 수용, 김 경식[1], SCALAS E.[2](*한국과학기술원, 물리학과. [1]부경대학교, 물리학과. [2]East Piedmont Univ.*) A detrended fluctuation analysis (DFA) is applied to the statistics of Korean treasury bond (KTB) futures from which the logarithmic increments, volatilities, and traded volumes are estimated over a specific time lag. In this study, the logarithmic increment of futures prices has no long-memory property, while the volatility and the traded volume exhibit the existence of the long-memory property. To analyze and calculate whether the volatility clustering is due to a inherent higher-order correlation not detected by with the direct application of the DFA to logarithmic increments of KTB futures, it is of importance to shuffle the original tick data of futures prices and to generate a geometric Brownian random walk with the same mean and standard deviation. It was found from a comparison of the three tick data that the higher-order correlation inherent in logarithmic increments leads to volatility clustering. Particularly, the result of the DFA on volatilities and traded volumes can be supported the hypothesis of price changes.

Fp-004 **Analysis of Price Fluctuations in Futures Exchange Markets** 임 규창, 김 수용, 김 경식[1](*한국과학기술원, 물리학과. [1]부경대학교, 물리학과.*) We study the fluctuation of returns from tick data of the Korean treasury bond (KTB) futures in a futures market, which can be described in terms of the Fokker-Planck equation (FPE). We calculate the corresponding drift and diffusion coefficients and argue that they can contain some information pertaining to the market state. Particularly, the fourth Kramers-Moyal coefficient we presented is compared with other calculated findings.

Fp-005 **Bipartite network analysis on protein complexes in Saccharomyces cerevisiae** LEE Sang Hoon, JEONG Hawoong(*Dept. of Physics, KAIST.*) Proteins in organisms usually form protein complexes to perform cellular functions rather than act alone. We study the structure of protein complexes and their component proteins in the budding yeast in terms of the bipartite network, where the complexes and proteins are its two distinct components. From the bipartite network, weighted networks among complexes and among proteins are constructed, corresponding to one-mode projections of the bipartite network. In contrast to conventional protein-protein interaction networks where the degree distribution follows the power-law, the complex-mode and protein-mode projection of the bipartite network show the exponential degree and strength distributions. Nevertheless, complexes and proteins re-

lated to the ribosome have rather large values of degrees and strengths in their projection networks. Two classes of component proteins, classified as cores and attachments in the database, are shown to be distinct by the number of complexes they participate in.

Fp-006 **Conformation and Dynamics of a DNA with Hydrodynamic Interaction** KIM WON KYU, KUM OYEON[1], SUNG WOKYUNG[2](*Department of physics, Pohang University of Science and Technology (POSTECH), Pohang 790-784, South Korea. [1]Combinatorial and Computational Mathematics Center, POSTECH. [2]POSTECH Center for Theoretical Physics(PCTP) and Department of Physics, POSTECH.*) We study static and dynamic correlation functions of segmental charge density and orientation in a DNA in an ionic fluid. The polymer semi-flexibility is described by the worm-like chain model, where the effective Hamiltonian incorporates bending and stretching energies. Furthermore, we incorporate the Coulomb and hydrodynamic interaction between the beads screened and mediated respectively by ionic fluid environment. Within small undulation approximation, we analytically calculate the correlation functions and discuss how conformation and dynamics are affected by net charge value, segmental charge fluctuation, and persistence length. We also discuss the possibility for undulation instability leading to collapse transition and how it depends different parameterization of the DNA conformation. The Brownian dynamic simulations are performed to support and extend the analytical results.

Fp-007 **Effects of Stacking interactions on DNA bubble and Denaturation** 김 재열, 전 재형, 성 우경 (*포항공과대학교, 물리학과.*) It is well-known that DNA stably exists as a double-stranded structure due to the hydrogen-bonding and stacking interaction between bases. The stacking interaction is strengthened when DNA is paired, which contributes to the huge difference of DNA stiffness between double-stranded (ds) and single-stranded DNAs. We study the effects of this stacking-induced stiffness difference on DNA denaturation and bubble (i.e., local denaturation). To this end, we model dsDNA as a duplex of two semiflexible chains whose persistence length varies depending upon the base-pair distance. Using this model, we perform the Langevin dynamics simulation to examine the characteristics of denaturation transition, and the statistics and dynamics of bubbles. We find that the stacking interaction causes the denaturation transition to be much sharper. At physiological temperatures, the initiation of bubble formation becomes difficult due to the stacking interaction, but, once the DNA opens, large size bubbles can be easily formed.

Fp-008 **Jamming Transition in the Internet with Priority-Based Protocol** KIM Kanghoon, KAHNG Byungnam, KIM Doochul(*Department of Physics and Astronomy, Seoul National University, 151-747, Korea.*) We study the packet transport on a scale-free network using two different processing protocols, one being the first-in-first-out (FIFO) and the other priority-based protocol. Each packet is given its own priority x that is distributed uniformly in the interval [0,1]. The packet with highest priority is treated firstly in each queue. We find that when packet generation ratio p is small, mean travel time between every pair of nodes is the same irrespective of the FIFO and priority-based protocols. However, it is significantly different when p is large beyond the jamming transition point. The mean travel time is reduced drastically for packets with high priority, however, it remains unchanged for those with low priority. Thus, the new protocol based on the priority enhances capability of packet transport in the Internet and could be applied to commercial download services or paid mail delivery system and so on.

Fp-009 **Phase transition of spin model for market dynamics** YOON Sooyeon, KIM Hong-Joo, YOOK Soon-Hyung, KIM Yup(*Kyung Hee Univ., Dept. of Physics.*) We study the phase transition for a spin model of market dynamics based on the Bornholdt"s model [Int. J. Mod. Phys. C {f 12}, 667(2001)]. The spin dynamics is governed by a ferromagnetic couplings connecting each spin to its local neighborhood and an antiferromagnetic coupling of each spin to the global magnetization. The Hamiltionain of the spin system is $H=-sum_{} J_{ij}S_{i}S_{j}+sum_{i}alpha S_i^2left|Might|$, where the state of agent on each site is defined as a spin variable, $S_i=pm1$ and the magnetization $M(t)=rac{1}{N}sum_{j=1}^{N}S_j$ ($J_{ij}>0$, $alpha>0$). We consider the phase transition from the ferromagnetic phase to an oscillating phase on a 2-dimensional regular lattice, random network, and scale-free network. In the oscillating phase an intermittent behavior between

bubbles and crashes of magnetization $M(t)$ is controlled by the global coupling constant $alpha$ and the temperature. We also check the distributions of returns formagnetization.

Fp-010 **The Change In Information Flow Patterns Of EEG Channels In Human Brains At Different Mental States** HWANG Eunjin, KIM Seunghwan(*The Asia Pacific Center for Theoretical Physics and Nonlinear &Complex Systems Lab./Brain Research Center, Dept. Physics, POSTECH, Pohang, Korea 790-784.*) The Electroencephalogram (EEG) signals can provide the information on the different cognitive states of the brain. With the help of the evolution map approach proposed by M. Rosenblum, we measure the asymmetry of information flow between EEG signals recorded in anesthetic experiments. We introduce the concept of weighted directionality, which combines phase synchrony and normalized directionality, and calculate average whole-channel weighted directionality matrices for the periods before, during and after the administration of anesthetic drugs to the subjects. The dissimilarity between each matrix is defined and the clustering analysis is carried out. We found that the human brain in anesthetic and awakened states exhibit functional differences in information flow patterns between EEG channels.

Fp-011 **Folding Network In Conformation Space** LEE JONG SANG, PARK JIYONG, KAHNG BYUNGNAM(*Seoul National University, Department of Physics and Astronomy.*) Proteins are complex macromolecules with many degrees of freedom and have to fold to a unique three-dimensional structure for working their function. Protein folding is a complex process governed by non-covalent interactions involving the entire molecule. Here, we use network analysis to study the conformation space and folding of Trp-cage (NLYIQWLKDG GPSSGRPPPS), a designed 20 residue peptide whose solution conformation has been investigated by NMR spectroscopy. To build the folding network in conformation space, the Trp-cage conformations and transitions sampled by molecular dynamics were considered as nodes and links. The conformation space network describes the significant free energy minima and their dynamic connectivity. In this work, to define the nodes and links of the network the secondary structure was calculated for each snapshot saved along the molecular dynamics trajectory. The protein structures were assigned to one of eight secondary structure states. A "conformation" is a single string of secondary structure. Conformations are nodes of the network and the transitions between them are links. We focus on the analysis of topology to study the conformation space network of Trp-cage, the connectivity between different conformations. The connectivity distribution P(k) is the probability that a node(conformation) has k links (neighbor conformations). The clustering coefficient C describes the cliques of a node. Free energy minima and their connectivity emerge without requiring projections onto arbitrarily chosen reaction coordinates. The conformational space network of Trp-cage is a scale-free network, that is, the distribution of the number of possible connections of a conformation follows a power law. Complex network was used to analyze the conformation space of a structured peptide and that of a random heteropolymer of the same residue composition. The network analysis seems to be particularly useful to study the conformation space and folding of structured peptides.

Fp-012 **On community detection using q-state Potts model** 이 재성, 강 병남[1], 김 두철[1](*서울대학교 물리천문학부. [1]서울대학교.*) We study the Ising spin Hamiltonian which is associated with the modularity for detecting a community structure of a network and whose antiferromagnetic interaction strength is controlled by aparameter η. We obtain the phase diagram analytically based on the replica symmetric solution on a random scale-free network, static model, with the degree exponent γ. In the diagram the system orders into a ferromagnetic(F) or a spin glass(SG) phases in low temperatures. We determine the respective transition temperatures analytically. The ferromagnetic phase transition temperature T_c is infinite when $2<\gamma<3$ for all η and finite when $3<\gamma$ for some range of η. We also study the dependence of the critical exponent of ferromagnetic order parameter, m, and spin glass order parameter, q, on γ. They depend on γ when $3<\gamma<5$($3<\gamma<4$) at the F(SG) boundary and coincide with the result of D.-H. Kim et.al. (Phys. Rev. E 71, 056115).

Fp-013 **Statistics of Waiting-Time-Distribution for Bak-Sneppen model** LEE KYOUNG EUN, LEE JAE WOO(*Inha University, Physics.*) We investigate the statistics of a self-organized criticality (SOC) system when

the avalanches organize a hierarchical sequence, i.e. the strong-overlapping regime in which individual avalanche is no longer distinguishable. Bak-Sneppen (BS) model is one of the simplest SOC systems that exhibit avalanche overlapping. The method is based on the analysis of the statistics which waiting or quiet time distribution was constructed for avalanche and activity of BS model. The statistics of durations between avalanche (or activity) changes from Poisson to scale invariance on increasing the threshold for probing instantaneous activity. For accuracy of the fit, the distributions are tested by the chi-square merit function and Pearson coefficient. Lastly, we compare waiting-time distribution with other data (earthquake, sandpile, solar flare etc.)

Fp-014 **먹이그물망의 구조와 특징** 황 준경, 이 재우(*인하대학교, 물리학과.*) 자연의 많은 생태시스템은 먹이그물망을 통해 연결되어 있다. 그래서 생태학에서는 먹이그물망의 구조와 특징을 이해하는 것이 중요하다. 하지만 먹이그물망의 구조와 특징을 분석하는 것은 그 구조의 복잡성 때문에 매우 어렵다. 몇몇 먹이그물망은 좁은세상 그물망, 척도없는 그물망 구조를 가지지만 일반적으로 먹이그물망은 평균 최단거리가 작고, 낮은 결집계수를 가지는 특징을 보인다. 여기에서는 실제 먹이그물망 데이터를 토대로 링크 수 분포, 결집계수, 평균 최단거리등 그물망 분석에 사용하는 물리량을 계산하고 먹이그물망 구조에 대해 알아본다.

Fp-015 **Broadcasted Nodes And Local Islands In Complex Networks** SHIN Jeongkyu, KIM Seunghwan (*The Asia Pacific Center for Theoretical Physics and Nonlinear & Complex Systems Lab./Brain Research Center, Dept. Physics, POSTECH, Pohang, Korea 790-784.*) Diverse methods have been proposed to model the real-world networks from the perspective of complex networks. We introduce a complex network model with broadcasted nodes and measure network characteristics as the broadcast threshold varies. We find that the average shortest path length of the network rises drastically above a critical broadcast threshold, while the assortativity index decreases. This reflects the loss of shortcuts and the creation of local islands, which can be often found in real-world networks, for example, metabolic networks.

Fp-016 **Thermodynamic free energy of GNNQQNY peptide β-sheet bilayers** PARK Jiyong, KAHNG Byungnam, HWANG Wonmuk[1](*Department of Physics and Astronomy, Seoul National University. [1]Department of Biomedical Engineering, Texas A&M University.*) Diverse oligopeptides have been reported to self-assemble into ordered β-sheet filaments. Those oligopeptides were derived from pathogenic proteins causing fatal neuro-degenerative disorders such as Alzheimer's disease and other diseases known as amyloidosis. The filaments constructed by the oligopeptides preserve structural fingerprints of original proteins, misfolded and accumulated in patients suffering the diseases. Because of growing number of evidences showing intimate correlation between the progress of the diseases and the formation of the filaments, the detailed structure of the filaments and the underlying principles of the self-assembly process have been of great interest in biomedical literature. However, owing to insolubility and lack of crystalline order, detailed structural information is limited yet. Consequently, computational approaches emerge as promising complementary to bio-chemical experiments. We combine molecular dynamics (MD) simulation and normal mode analysis (NMA) to compare detailed structure and thermodynamic free energy of possible β-sheet bilayer conformations comprised of a 7-residue peptide (GNNQQNY) derived from yeast prion protein Sup35. We prepare in-register parallel β-sheets based on previous experiments. Eight different conformations out of two β-sheets are simulated for 2.5 ns to give conformational energy (E_S) and solvation free energy (G_S) of each of them. Normal modes of each conformation are computed and vibrational enthalpy (H_V) and entropy (S_V) values are calculated. By comparing Gibbs free energy ($G=E_S+G_S+H_V-TS_V$), we are able to select three probable bilayer configurations. One of selected pattern coincides minutely with recent x-raycrystallographic experiments of Nelson, et. al. (Nature 435), where a simulated peptide has very small RMS deviation (1.18 Å) to the PDB coordinate (ID: 1YJP)and 'steric zipper' pattern of side chains at the interfacial region is correctly reproduced. Based on our computational results, we realize the vibrational free energy terms (H_V-TS_V) contribute essential role in the stability of the bilayers. We are trying to extend our methodology to various β-sheet bilayers whose exact structural information and the origin of stability are not yet understood.

Fp-017 **Phase diagrams of quasispecies theory with**

recombination and horizontal gene transfer PARK, Jeong-Man, DEEM, Michael W.[1](*The Catholic University of Korea. [1]Rice University.*) We consider how transfer of genetic information between individuals influences the phase diagram and mean fitness of both the Eigen and the parallel, or Crow-Kimura, models of evolution. In the absence of genetic transfer, these physical models of evolution consider the replication and point mutation of the genomes of independent individuals in a large population. A phase transition occurs, such that below a critical mutation rate an identifiable quasispecies forms. We show how transfer of genetic information changes the phase diagram and mean fitness and introduces metastability in quasispecies theory, via an analytic field theoretic mapping.

Fp-018 **Sub-block Order Parameter in a Driven Ising Lattice Gas Using Block Distribution Function** KWAK Wooseop, YANG Jae-Suk, SOHN Jang-il, KIM In-mook, LANDAU D.P.[1](*고려대학교 물리학과. [1]Univ. of Georgia.*) We inverstigate the order parameter of the standard Ising lattice gas and a driven Ising lattice gas. The sub-block order parameter is introduced to these conserved model as an order parameter using block distribution functions. We also intruduce the sub-block order parameter of damage using the block distribution functions of damage. We measure the sub-block order parameters using the Metropolis and the heat-bath rates. These order parameters are working well for the non-equilibrium conserved model as well as the equilibrium conserved model. We obtain the critical exponent of order parameter $\beta=1/8$ for the standard Ising lattice gas and $\beta=1/2$ for a driven Ising lattice gas using the Metropolis and the heat-bath rates.

Fp-019 **Critical Behavior of the XY Model on Growing Scale Free Network** YANG Jae-Suk, KWAK Wooseop, SOHN Jang-il, KIM in-mook(*고려대학교 물리학과.*) We study the ferromagnetic XY model on growing scale free networks with various degree exponents $lambda$. In this model, we find there is no phase transition on growing scale free networks as system goes infinite for $lambda<=3$. But, for $lambda=8$, we obtained the critical temperature T_c and the critical exponents for XY model on growing scale free network.

Fp-020 **Relaxation Dynamics of Coupled Oscillators on Complex Networks** SON Seung-Woo, KIM Beom Jun[1], JEONG Hawoong, HONG Hyunsuk[2](*Korea Advanced Institute of Science and Technology, Dept. Physics. [1]Sung Kyun Kwan University, Dept. Physics. [2]Chonbuk National University, Dept. Physics.*) We study collective synchronization in a system of coupledoscillators on various type of networks; globally coupled network, small-world (SW) network, and scale-free (SF) network. In particular, we pay attention to the relaxation dynamics of the synchronization, which is important in the point of view of information transfer and exploring the recovery dynamics from perturbation. We measure the time it takes to establish global synchronization from random initial phases, varying the structural properties of the networks. It is found that the relaxation time exhibits the logarithmic dependence on the network size N in the case of the coupling strength above critical strength, which is attributed to the contribution from the initial random phase distribution, which gives the initial phase order parameter r_0 to $O(N^{-1/2})$. Under the removal of such effects, the relaxation time is found to be independent of the system size, which is striking and implies that the local interaction is irrelevant in the network synchronization. The scaling form of the relaxation dynamics is derived, and it shows a good consistency with the numerical simulations.

Fp-021 **Critical Properties of Majority Voter Model and Their Dependence of the Dynamics** SOHN Jang-il, KWAK Wooseop, YANG Jae-Suk, KIM In-mook (*고려대학교 물리학과.*) The critical properties of the two dimensional majority voter model with two different transition rates (the Glauber rate and the Metropolis rate) are studied by Monte Carlo simulations. The majority voter model with the Glauber rate can be mapped to the previous work using the noise parameter. The critical temperature and the exponents are obtained from finite size scaling analysis. The critical temperature is found to depend on a transition rate. However, the critical exponents are the same for both transition rates, and the obtained critical exponents belong to the two dimensional Ising class.

Fp-022 **The Quenched Mullins-Herring Equation and Directed Percolation** KIM Jin Min, SONG Hyun

Suk(*Soongsil University, Department of Physics.*) We study the pinning-depinning transition of a discrete surface growth model following the quenched Mullins-Herring (qMH) equation with an external driving force. At the critical force F_{c}, the growth velocity v of the average surface height follows a power-law behavior $v(t) \sim t^{-\delta}$ with $\delta \approx 0.158 (d=1+1)$ and $\approx 0.460 (d=2+1)$ and the surface width W shows a scaling behavior $W^{2}(t,L)~L^{2\alpha}f(t/L^{z})$ with $\alpha \approx 1.350 (d=1+1)$ and $\approx 1.026 (d=2+1)$, $\beta \approx 0.844 (d=1+1)$ and $\approx 0.577 (d=2+1)$, and $z \approx 1.60 (d=1+1)$ and $\approx 1.778 (d=2+1)$. Near F_{c}, the steady-state velocity v_{s} follows $v_{F} \sim (F-F_{c})^{\theta}$ with $\theta \approx 0.278 (d=1+1)$ and $\approx 0.575 (d=2+1)$ for $F>F_{c}$. Also, we obtain ν_{t} and ν_{x} through the finite-size scaling of the velocity v. These exponents are dramatically similar to them of Directed Percolation (DP) class in both 1+1 and 2+1 dimensions.

Fp-023 **GCMC Study of Argon Monolayer Adsorbed on a Continuum Graphite** HAN Kyu-Kwang, KOOK Hyungtae[1](*Pai Chai University, Department of Physics.* [1]*Kyungwon University, Department of Physics.*) Argon layers physisorbed on a graphite substrate were studied at coverages near monolayer completion on an isotherm by simulating a small, simple model system using the grand canonical Monte Carlo method. The results consistent with a picture of monolayer argon melting via two-stage process involving the existence of an intermediate phase, which has been reported in recent thermodynamic measurements, are presented. Snapshots of monolayer configurations indicate that thecreation and dissociation of a dislocation pair are involved in the melting mechanism.

Fp-024 **Monte Carlo Study of the J1-J2 antiferromagnetic XY model on the triangular lattice** HAN Jung Hoon, PARK Jin Hong(*SungKyunKwan University.*) We study the antiferromagnetic J1-J2 XY model on triangular lattice using the Monte Carlo simulation. We find a clear separation of magnetic (T1) and nematic (T2) phase transition for x close to one, where x is parameterized as J1=1-x, J2=x (0<x<1). Quite remarkably, the staggered chirality order sets in at T=T2, where the nematic order occurs. This is the first demonstration of the clear separation of the chiral phase transition and the magnetic phase transition in XY-like models.

Fp-025 **Conserved mass aggregation model with mass-dependent fragmentation** YOON Sooyeon, LEE Dong-Jin, KWON Suncghul, KIM Yup(*Kyung Hee Univ., Dept. of Physics.*) We study a conserved mass aggregation with mass-dependent fragmentation in one dimension. In the model, the whole mass m of a randomly selected site isotropically diffuse to the one of the nearest neighboring sites with rate D. With rate ω, a mass of m^{λ} is fragmented from the site and moves to the one of the nearest neighbors. Since the fragmented mass is smaller than the whole mass for $\lambda <1$, the on-site attractive interaction presents for the case. The model undergoes phase transitions from the fluid phase into the condensed phase as the density of masses increases for a given λ. We numerically investigate the$\rho -\omega$ phase diagram and the critical behavior of the mass distribution $P(m)$

Fp-026 **Percolation transition in scale-free networks with degree correlation** NOH Jae Dong, KIM Sang-Woo(*University of Seoul.*) We introduce a model for scale-free networks with degree correlation. The model is a variation of the so-called static model [1]. Initially the network consists of N nodes, which are assigned to weights $w_i = i^{-\alpha}$. Links are then added iteratively between two nodes, one of which is selected according to the weight and the other of which is selected randomly among nodes with the same degree as the former. The resulting network is scale-free with degree exponent $\gamma = 1 + 1/\alpha$ and has positive degree correlation. We study numerically the percolation phase transition in our model as varying the link delsity. Measuring the giant cluster density and mean cluster size, we investigate the nature of the percolation transition

Fp-027 **Invasion percolation between two sites in two, three, and four dimensions** SANG B. Lee(*Department of Physics, Kyungpook National University.*) We study the nontrapping invasion percolation between two sites, one an injection site and the other an extraction site. We cosider the fractal nature and the mass distribution of the invaded clusters following the in-

vasion rule; the lowest-pressure site among the neighboring sites to the invaded cluster is invaded in each invasion step until the extraction site is reached. The fractal dimension of the invaded clusters is the same as that of the ordinary percolation cluster at criticality, i.e. at p_c, independent of the pressure on the extraction site p_e. The mass distribution exhibited a power-law behavior $P(m) \propto m^{-\alpha}$. the index α for $p_e<p_c$ appears to be independent of the value of $p_e$and also independent of the lattice dimensionality. When $p_e=p_c$, on the ohter hand, the index α appears to be weakly dependent on the lattice dimensionality. However, the conjecture in the earlier work [Phys Rev E 72, 041404 (2005)] $\alpha=\tau-1$, τ being the exponent characterizing the cluster size distribution, $n_s \propto s^{-\tau}$, appears to be incorrect.

Fp-028 **Fisher Zeros of Six-state Clock Model on a Square Lattice** 황 치옥, 김 승연[1], 김 진민[2](*국가수리과학연구소. [1]충주대학교. [2]숭실대학교.*) We investigate the phase transitions of the six-state clock model with nearest neighbour interactionson a square lattice. We obtain the density of states via Wang-Landau algorithms and study Fisher zerosto get phase transition temperatures.

Fp-029 **Strange Nonchaotic Bursting in Quasi-periodically Forced Neural Oscillators** LIM Woochang, KIM Sang-Yoon[1](*아주대학교 의과학연구소. [1]강원대학교 물리학과.*) We study the neural bursting activity (alternating between a silent phase and a bursting phase of repetitive spiking) in are presentative Hindmarsh-Rose model. In addition to the usual periodic and chaotic burstings, a new type of strange nonchaotic burstings are found to occur in the quasiperiodically forced case. This strange nonchaotic bursting state may appear through at ransition from a silent state. Using a rational approximation to the quasiperiodic forcing, the mechanism for the occurrence of such a strange nonchaotic bursting is investigated. These strange nonchaotic burstings are characterized in terms of the interburst intervals, the bursting length (i.e., the time interval between the first and last spikes in each burst), the number of spikes in each burst, and the peak to base ratios in the power spectra. The effect of noise on this strange nonchaotic bursting state is also studied. Finally, a transition from a bursting to a beating (continuous spiking) is briefly discussed.

Fp-030 **The Effect of Mode Coupling in Coupled Dielectric Microdisks** RYU Jung-Wan, KIM Sang Wook(*부산대학교.*) We study the mode coupling between quasi-eigenmodes in coupled dielectric microdisks. The positions in complex energy plane of modes and the corresponding mode distributions in real spaceis obtained according to variation of inter-disk distance and size difference between two microdisks. The interesting phenomena such as the directional emission and avoided resonance crossing can be explained by mode coupling.

Fp-031 **Modeling and Solutions of Queue Systems in Human Dynamics** KIM Jin S., KAHNG Byungnam, KIM Doochul(*Department of Physics and Astronomy, Seoul National University.*) The dynamics of queue has been intensively studied by the needs in the fields of computer sciences, massive manufacturing managements, and so on. In traditional models, the number of events coming into the system in unit time is assumed to be randomly distributed and thus well approximated by Poisson processes. On the other hand, the analysis of real human activity data such as e-mail corresponding logs and wireless communication archives shows that the number of input events follows power law, and hence here we introduce a generalized queue model whose number of input tasks is given by a power law. Also we consider the case that the queuing dynamics is performed based on priority instead of first-in-first-out protocol. We present numerical result and compare it with the first passage time distribution of Levy flight random walks.

Fp-032 **Influence of ocean bottom topography on the characteristics of edge waves** 유 대중, 김 기홍(*아주대 에너지시스템학부.*) As an ocean surface wave approaches a plane sloping beach, some of its energy is trapped near the shoreline and excites an edge wave at well-defined resonance frequencies. We investigate the influence of ocean bottom topography on the characteristics of edge waves, using an exact method based on the invariant imbedding theory. When the ocean depth increases linearly with the distance from the beach, our results agree very well with known analytical solutions. We find exact solutions for the edge wave frequencies and field distributions, when the ocean

depth is given by a power law function of the distance from the beach, for the first time. When the exponent is smaller (larger) than 1, we find that all edge wave frequencies shift to higher (lower) values in a systematic manner.

Fp-033 **Liquid Nanodroplets on Patterned Surfaces** JUNG Youngkyun(*KISTI, Supurcomputing Center.*) The spreading of liquid Nanodroplets on chemically patterned surfaces are investigated by means of molecular dynamics simulations. We measure the spreading rate of the precursor foot and the time evolution of the contact angle and compare them with the results for the homogeneous surfaces.

Fp-034 **The Effect of Ionic Size in Charge-Correlation Between Two Charged Membranes** GONZALEZ Omar, 성 우경(*포항공과대학교.*) The charge correlation and the resulting interaction between membranes are of fundamental importance in a variety of cellular process including cell fusion and membrane transport. Lots of theoretical approaches have addressed the problem using the mean field theory like the Poisson-Boltzmann equation and the other continuum theory that incorporates the fluctuations and correlations. Here we employ the hypernetted chain (HNC) theory for the primitive model that treat ions in solution as charged hard spheres and the solvent as a dielectric continuum. The charge density profiles and membrane pressure are investigated as functions of surface charge, intermembrane distance, and concentration of salt and divalent counterions. It is shown that the HNC results differ significantly from those of previous theoretical approaches which treats the ions as points. Most interestingly, the charge inversion can occur on surfaces, which diminishes as the intermembrane distance decreases to nanoscale one. A Monte-Carlo simulation is carried on to support these theoretical results.

■ SESSION: P2
4월 20일 (금), 11:00 - 12:45
스키하우스

Kp-001 **Phonon mode of ternary BeZnO** 유세기(*한국외국어대학교, 전자물리학과.*) Optical phonon modes of wide-band gap alloy of $Be_xZn_{1-x}O$ were investigated. Calculation based on the modified random element isodisplacement model (MREI) indicates that phonon behavior of ternary BeZnO exhibits the two mode behavior. This result is explained by the mass difference of each component atom.

Kp-002 **Temperature dependence of energy band gap for ZnSe Single Crystal grown by sublimation method** 홍 광준(*조선대학교 물리학과.*) We investigated the electrical and the optical properties of a ZnSe single crystal of good quality which was grown by a sublimation method in which the pressure in the growth tube was controllable with a reservoir. From the measurement of the temperature-dependent photocurrents, the energy band gap as a function of temperature was found to be where the spin-orbit splitting gap was 0.42 eV. It was also found from the measurement of the temperature-dependent photoluminescence that for T<100K, the luminescence peak near the band gap was due to excitons whereas for T>100K, it was due to band-to-band transitions. An analysis of the Self-activated (SA) peak by using a configuration coordinate model gave Δ E=0.0191 eV and =0.0314eV.

Kp-003 **Optical properties of Ge-doped ZnO thin films studied with spectroscopic ellipsometry** BAEK Seoung Ho, KANG Tae Dong, LEE Hosun, LEE Do Kyu, EOM Seung Hwan, CHOI Suk-Ho(*Dept. of Physics, Kyung Hee University.*) We grew Ge-doped ZnO thin films on four different substrates (Quartz/ /glass/Si) by RF sputtering and measured pseudo-dielectric functions between 1 eV and 6 eV by using variable angle spectroscopic ellipsometry (VASE). The effect of doping concentration and gas ratio on the dielectric function of the Ge-doped ZnO thin films has been investigated by means of layer modeling analysis. We obtained the dielectric function by using parametric semiconductor model and acquired the refractive indexes, extinction coefficients, thicknesses, and surface roughnesses. We also use standard critical point (SCP) model and determined the SCP parameters (amplitude, excitonic phase angle, band gap and broadening) by fitting the numerically obtained second derivative spectra of the fitted Ge-doped ZnO dielectric function.

Kp-004 **다른 차원을 가진 $Cd_xZn_{1-x}Te$/ZnTe 나노구조에서 구조적, 광학적 특성** 이 홍석, 김 현종, 김 태환[1], 최 진철, 박 홍이(*연세대학교, 물리학과. [1]한양대학교, 전자통신컴퓨터공학부.*) 현재 반도체 나노구조의 전기적, 광학적 특성을 이용한 적외선 검출기, 레이저, 메모리 등 반도체 소자로의 응용연구가 활발히 진행되고 있다. 다양한 나노구조 중에 III-V/III-V 나노구조는 활발히 연구 되고 있으나 II-VI/II-VI 나노구조는 복잡한 성장 과정 때문에 III-V/III-V 나노구조에 비해 연구하는데 어려운 문제점을 가지고 있다. 본 연구에서는 분자 선속 에피 성장법성장법으로 ZnTe 완충층 위에 $Cd_xZn_{1-x}Te$ 나노구조의 두께를 변화시켜 구조적, 광학적 특성을 연구 하였다. 저온 광루미네센스 (PL) 측정 결과 $Cd_xZn_{1-x}Te$ 나노구조의 두께가 커질수록 $Cd_xZn_{1-x}Te$ 나노구조의 피크가 낮은 에너지로 이동함을 알 수 있었고 원자 힘 현미경 (AFM) 측정 결과 $Cd_xZn_{1-x}Te$ 나노구조의 두께가 커질수록 양자점에서 양자선으로 변화되는 것을 볼 수 있었는데 이는 $Cd_xZn_{1-x}Te$ 나노구조의 두께가 커질수록 양자점이 병합현상이 일어나기 때문이다. 또한 온도 의존 광루미네센스 측정 결과 $Cd_xZn_{1-x}Te$ 나노구조에서 $Cd_xZn_{1-x}Te$ 양자점의 열적 활성화 에너지가 가장 커짐을 알 수 있었다. 이와 같은 결과는 $Cd_xZn_{1-x}Te$/ZnTe 나노구조에서 차원에 따른 구조적, 광학적 특성을 이해하는데 도움을 주었다.

Kp-005 **GaAs(111) 기판위에 성장된 h-CdS 박막의 특성연구** 김 대중, 박 재환[1], 최 용대[2], 이 종원[3], 윤 만영[4](*목원대학교 테크노과학연구소. [1]충남대학교 물리학과. [2]목원대학교 광전자물리학과. [3]한밭대학교 신소재공학부. [4]중부대 정보통신학과.*) 열벽적층 성장법을 이용하여 고품질의 h-CdS/GaAs(111) 박막을 성장시켰다. 성장된 박막들은 X-선 회절 패턴을 분석한 결과 육방정 구조(hexagonal structure)를 갖는 것으로 확인되었다. 또한 박막의 표면상태를 알아보기 위하여 Nomarski 간섭현미경과 AFM을 이용하여 관측하였고, 박막들의 광학적 특성을 알아보기 위하여 분광학적 엘립소미트리를 사용하여 실온에서 1.5-8.7 eV 사이 포톤에너지 범위에서 측정하였다. 측정된 데이터들은 유사유전함수 스펙트럼 $\langle\varepsilon(E)\rangle=\langle\varepsilon_1(E)\rangle+i\langle\varepsilon_2(E)\rangle$에 나타난 E_0, E_1, $E_1+\Delta_1$, E_2, 와 같은 임계점 구조에 관하여 연구하였다. 특히, $E_1+\Delta_1$ 구조에 대한 기판온도의 함수로서의 변화를

연구하였다. 또한 박막의 복소 유전함수와 밀접한 관계를 가지고 있는 굴절지수 n(E), 소광계수 k(E), 반사계수 R(E) 그리고 흡수계수 α(E)와 같은 광학적 특성 등을 연구하였다.

Kp-006 **Optical Properties of ZnSe Epilayer on GaAs Substrate by Molecular Beam Epitaxy** 조 현준, 심 준형, 배 인호, 김 종수[1], 변 지수[1](*영남대학교 물리학과. [1]광주과학기술원 고등광기술연구소.*) The optical properties of ZnSe epilayer grown on GaAs (001) substrate were investigated by photoluminescence (PL) and surface photovoltage (SPV). The ZnSe epilayer showed two sharp PL lines and one broad emission band. The emission energy of two sharp PL lines are 2.77 and 2.60 eV. The broad emission band covers from 1.5 to 2.5 eV. The 2.77 and 2.60 eV emission lines might come from the free exciton and complex dislocation tangles, respectively. The temperature and excitation power dependence of PL measurement revealed that the broad band is superposition of deep level emissions of ZnSe epilayer. And we verify that a differential surface photovoltage (DSPV) technique is a effective method of analyzing characterization of epilayer grown by MBE.

Kp-007 **Deep Level Transient Spectroscopy Study on Defect States in ZnO Thin Films Grown by Pulsed Laser Deposition Technique** SONG Hooyoung, KIM Jae-Hoon, KIM Eun Kyu(*Quantum-Function Spinics Lab. and Department of physics, Hanyang University.*) Recently, ZnO is widely investigated as a promising material for the optical application because of its high optical transmittance and wide band gap (3.4 eV at 300K) with high exciton binding energy(60 meV). Also ZnO is very attractive for the diluted magnetic semiconductor which has high Curie temperature in theoretical prediction. To realize device applications, it is necessary to develop reliable ohmic contacts and understand about defects in order to make p-type single crystallized thin film. In this study, ZnO films were grown by pulsed laser deposition on sapphire (0001) substrates and then Ti/Au and Al_2O_3 were deposited on the ZnO thin films for forming metal-insulator-semiconductor structure. For ohmic contacts, rapid thermal annealing was done at temperature of 500 ^{o}C. To investigate the defect states in ZnO films, capacitance-voltage and deep level transient spectroscopy were performed.

Kp-008 **Optical properties of CdSe quantum dots depending on growth conditions** 정 순일, 윤 일구, 이 주인[1](*연세대학교 전기전자공학과. [1]한국표준과학연구원 첨단산업측정그룹.*) We report the synthesis of colloidal CdSe quantum dots using high-temperature organometallic reagents by a one-step single-flask method. In order to modify the size and quality of CdSe quantum dots, we controlled the growth temperature and the relative amount of precursors to be injected into the coordinating solvent, e.g. trioctyl phosphine oxide. Moreover, an effective surface passivation of monodisperse CdSe nanocrystals was performed by overcoating them with a higher-band-gap material such as ZnS. Synthesized CdSe and CdSe/ZnS quantum dots were studied by using transmission electron microscope, and photoluminescence measurement.

Kp-009 **RF 스퍼터링을 이용하여 Si(100) 기판에 기판온도를 변화시켜 성장한 ZnO 박막의 열처리 온도 변화에 따른 발광특성 및 전기적 특성 연구** 이 도규, 김 성, 정 필성, 김 창오, 최 석호, 엄 승환[1](*경희대 전자정보대학 물리 및 응용물리. [1]Total Equipment Solution.*) RF 스퍼터링 성장기법을 이용하여 Si(100) 기판위에 상온에서 600℃까지 성장 온도를 달리하여 ZnO 박막을 성장하였고, 600-1000°C까지 열처리 변화에 따른 광루미네센스(photoluminescence; PL) 특성과 전기적 특성을 연구하였다. 상온에서 600°C까지 성장 온도를 변화시켜 성장한 ZnO 박막의 PL은 ZnO 에너지띠 근처의 자외선 영역(ultraviolet; ~380nm)과 결함(defect)과 관련한 가시광선(Visible; 500-700nm) 영역에서의 PL 띠가 관찰되었으며, 성장온도 400℃에서 자외선 세기가 가장 우세하게 관찰되었다. 또한 600에서1000°C까지 열처리 온도가 증가함에 따라 PL 세기가 증가하였으며, 질소와 산소 분위기에서의 열처리에 따라 각각 다른 PL 및 전기적 특성을 나타냈다. XRD를 통하여 열처리 온도 800℃에서 구조적으로 c-축 (002) 면으로의 뛰어난 배향성을 확인하였고, PL은 900℃의 열처리 온도에서 결함대비 자외선 영역 세기가 가장 우수하게 관찰되었다. PL의 온도 의존성 실험을 통하여 상온에서 UV 발광에 기여하는 주된 ZnO의 엑시톤 (exciton)을 구분할 수 있었으며, 온도에 따른 엑시톤의 변화를 관찰하였다. 홀 효과(hall effect) 측정을 통해 열처리 온도 800-900℃에서 낮은 저항과 이동도의 큰 변화가 관찰되었다. 본 연구에서는 ZnO박막의 성장온도, 열처리 조건에 따른 XRD, Hall 측정, PL등의 연구를 통하여 불순물이 들어가지 않은 ZnO 박막의 다양한 특성을 규명하고자 하였다.

Kp-010 **Micro-structural and electrical properties of Al doped ZnO films** 서 수영, 박 순홍, 곽 창하, 이 용병, 김 선효, 한 상욱(*포항공과대학교, 신소재공학과.*) We present the structural and optical properties of Al-doped single-crystal ZnO films synthesized on Al2O3 substrates by a RF-magnetron sputtering procedure. The structural properties of the films were characterized by x-ray diffraction (XRD) measurements. The XRD measurements demonstrated that the films had a hexagonal wurtzite phase with a strong c-axis orientation. We did not observed any extra peak from the XRD measurements. The lattice constant c was linearly increased with Al doping ratio. These strongly implied that Al atoms were randomly substituted for the Zn atoms. The optical and chemical properties of the Al-doped ZnO films were investigated by photoluminescence(PL) and x-ray photoelectron spectroscopy measurements, respectively. We will compare the structural and optical properties with electrical properties of the films.

Kp-011 **Characteristics of p-type ZnO thin films doped with phosphorus** KIM Jun Kwan, LIM Jung Wook[1], KIM Hyun Tak[1], YUN Sun Jin[1](*University of Science and Technology, Department of next generation device engineering. [1]Basic Research Laboratory, Electronics and Telecommunications Research Institute.*) In order to study the influence of post-annealing treatment on the conductive type conversion of ZnO films, we investigated electrical properties and crystalline quality of P-doped ZnO thin films at annealing temperature ranging from 600 to 800℃. The ZnO thin films were deposited on 100 nm-SiO_2 coated Si substrates at 200℃ using rf magnetron sputter deposition technique. The rf power, substrate temperature, and working pressure were 150 W, 200 ℃, and 50 mTorr, respectively. The thickness of as-deposited ZnO thin films was approximately 150 nm. Depth profiling of ZnO films using secondary ion mass spectrometry indicated that post-annealing at 800℃ for 1 hr resulted in considerable reduction of ZnO film thickness due to the intermixing of ZnO with under-layer. A p-type ZnO thin film annealed at 700 ℃ showed a hole concentration of 1.9 X 10^{14} cm^{-2} and a hole mobility of 10.8 cm^2/V-s. X-ray diffraction measurements showed that p-type ZnO thin films had the preferential orientation of (002) plane after post-annealing.

Kp-012 **Luminescent characteristics of ZnO/$Mg_{0.2}$-$Zn_{0.8}$O nanorod double-quantum-wells** 유 진경, 이 규철, 천 봉환[1], 주 태하[1](*POSTECH, 신소재공학과. [1]POSTECH, 화학과.*) Recently, semiconductor quantum structures embedded in a single semiconductor nanorod have attracted much attention due to their feasible manipulation of physical properties and nanophotonic device applications such as resonant tunneling devices, field effect transistors, and light-emitting devices. Furthermore, coupled quantum structures having narrow separation lengths have been considered as essential parts for nanophotonic switches. For realization of various quantum devices based on nanorod quantum structures, the sizes of quantum structures must be controlled accurately, and their physical properties should be investigated thoroughly. In this presentation, we report on the fabrication and optical measurements of ZnO nanorods embedding ZnO/ZnMgO double-quantum-wells (DQWs) and demonstrate optical spectroscopy as a powerful tool for probing quantum structures in semiconductor nanorods. ZnO/$Mg_{0.2}Zn_{0.8}$O nanorod DQWs with various well and barrier widths were fabricated on Si and Al_2O_3 (0001) substrates by catalyst-free metal-organic chemical vapor deposition (MOCVD). The optical properties of ZnO/$Mg_{0.2}Zn_{0.8}$O nanorod DQWs were investigated using time-integrated (TI) and time-resolved (TR) photoluminescence (PL) spectroscopy. TIPL spectra of ZnO/$Mg_{0.2}Zn_{0.8}$O nanorod DQWs exhibit strong near band-edge emission originated from quantum wells. The PL emission from DQWs exhibits the dependence on the barrier widths. From temperature-dependent PL and TRPL spectra, exciton localization energy and recombination lifetime of QW PL emission peak are estimated. The luminescence behaviors in excitonic emissions of ZnO/$Mg_{0.2}Zn_{0.8}$O nanorod DQWs will be also discussed.

Kp-013 **Photoluminescent Properties of $Zn_{1-x}Li_xO$ (x = 0 ~ 0.10) nano-particles by Wet Chemical Synthesis** 최 병춘, 전 병억[1], 김 샛별, 김 유성, 박 희진, 정 중현, 문 병기(*부경대학교 물리학과. [1]부경대학교 기초과학연구소.*) Pure and Li-doped ZnO nano-particles were synthesized by the solvothermal method and the crystalline morphologies of them were confirmed by the transmission electron microscopy (TEM). The Li doping effects on the optical, structural and chemical properties of ZnO nanoparticles were observed by the photoluminescence (PL), X-ray diffraction and X-ray photo-

electron spectroscopy method. There were two PL peaks centered at around 430 nm and 540 nm, respectively. The TEM images of $Zn_{1-x}Li_xO$ nanoparticles displayed as a hexagon, but the nano-sized pore-like image contrasts were observed through the sub-micro sized Li-doped ZnO particles. It was observed that the PL peak at around 540 nm was increased by Li doping from the normalized PL graph. It was considered that Li ions substitute Zn sites resulting in formation of the nano-sized $Zn_{1-x}Li_xO$ clusters in the sub-micro sized ZnO particles.

Kp-014 **PLD 법으로 증착한 $Zn_{1-x}Li_xO$(X= 0.001 ~ 0.005) 박막의 특성변화** 김 유성, 박 희진, 김 샛별, 김 은지, 전 병억[1], 최 병춘, 정 중현, 문 병기, 양 현경(*부경대학교 물리학과. [1]부경대학교 기초과학연구소.*)
리튬을 도핑한 ZnO 박막을 PLD법을 이용하여 제작하였다. Target은 Li이 치환된 ZnO로서 치환 농도의 따른 구조적, 표면적 변화를 관찰하였고 특히 SEM 측정으로 극미량의 Li이 Zn의 입자구조와 그레인 사이즈에 어떠한 영향을 미치는지 관찰할 수 있었다. Li의 농도가 증가함에 따라 Zn의 결정이 치밀화가 이루어져 구조에 관여하지만 Li의 일정농도 이상에서는 다시 조성의 치밀성이 낮아지는 특성도 관찰이 되었다. 이러한 Target을 PLD법으로 제작한 ZnO:Li박막을 AFM, FE-SEM을 통하여 morphology와 roughness 그리고 hole측정을 통해서 투명전극의 가능성도 관찰하였다.

Kp-015 **Fe, Co, Ti, Nb를 도핑한 ZnO의 유전율 및 자기적 특성 조사** 김 샛별, 김 유성, 박 희진, 김 은지, 전 병억[1], 최 병춘, 양 현경, 정 중현(*부경대학교 물리학과. [1]부경대학교 기초과학연구소.*) ZnO는 구조적 이방성, 넓은 에너지 영역, 가시광선 영역에서 투명성과 높은 굴절률을 가지는 재료이며, II-VI족 화합물 반도체 소자의 물질로 연구되어지고 있다. 본 연구에서는 ZnO에 Fe, Co, Ti, Nb 을 각각 10mol %첨가하여, 세라믹을 제조하고 제조된 세라믹의 유전율 및 자기적 특성을 조사하였다. 각 세라믹스의 결정성 및 결정모양을 XRD 및 SEM을 이용하여 관찰하였으며, 특히, XRD패턴을 통해 ZnO가 Wurzeit 결정구조를 가짐을 확인할 수 있었다. ZnO에 Fe,Co,Ti,Nb를 도핑한 각 세라믹스의 유전율을 측정하였고, 자기적 특성을 관찰하여 이 물질들이 ZnO의 강자성 현상에 어떤 영향을 주는지 논의하고자 한다.

Kp-016 **Electrical characteristics of vertically aligned ZnO nanocolumn grown by solution method.** 김 민석, ULHAQ Ahsan[1], 양 하용[2], 김 정현[2], 윤 창주[2], 한 윤봉[1], 이 정수(*전북대학교 반도체과학 기술학과. [1]전북대학교 화학공학과. [2]전북대학교 반도체 과학 기술학과.*)
We report on the electrical characterization of vertically aligned zinc oxide nanowire grown by solution method. The electron-beam lithography(EBL) make something of SEM and the zinc oxide film deposition put to use RF sputter. The zinc oxide nanowire growth by solution method. The zinc oxide before growing the nanowire, measurement price and characteristic it compared a kind measurement price tightly. The growth kind electric characterization improved result.

Kp-017 **전극물질 변화에 따른 ZnO 나노막대 소자의 전기적 특성 연구** 오 영무, 이 경문[1], 박 경호[2], PARK Ji-Yong(*아주대학교 에너지시스템학부. [1]아주대학교 물리학과. [2]나노소자특화팹센터(KANC).*) 본 연구에서는 ZnO 나노막대의 전기적특성을 밝히기 위하여 전기수송측정, 원자힘현미경(AFM), 전자현미경(SEM)을 이용하였다. 화학기상증착법으로 합성한 지름 30~50nm, 길이 5~10um인 ZnO 나노막대를 메탄올에 분산한 후 SiO2/Si 기판에 뿌려준 후 광리소그래피, lift-off공정을 통하여 금속전극을 형성하는 방법으로 소자를 제작하였다. 제작된 ZnO 나노막대소자는 n형 반도체특성을 나타내는 것을 전기수송측정법을 통하여 확인하였고 전극물질의 변화에 따른 I-V 특성을 조사하여 ZnO 나노막대와 금속사이의 접합특성을 연구하였다. 또한 이를 정전기힘현미경(EFM), 주사게이트현미경(SGM)법과 같은 AFM기법과 SEM을 이용한 음극형광(CL), 전자빔유도전류방법(EBIC)을 이용하여 나노스케일에서 그 상관관계를 조사하였다.

Kp-018 **Free-Standing ZnO Nanorod와 Nanowall의 제작 및 물성평가** 김 대희, 이 삼동, 박 현규, 김 상우(*금오공과대학교 신소재시스템공학부.*) ZnO 나노구조물은 차세대 나노스케일 UV LED, 화학-바이오 센서, 태양전지 등의 구현에 있어서 매우 각광을 받고 있는 재료로서, 나노구조의 구현 및 물성평가에 대한 활발한 연구가 진행되고 있다. 그러나 ZnO 나노구조 제작에 있어서 대부분의 연구그룹에서 고온 공정인 화학기상증착법을 이용하여 기판 위에 나노구조물을 구현하고 있다. 최근의 연구에서 습식 화학합성법을 이용하여 ZnO 1차원 나노구조물의 합성이 가능하며, 이를 통해 화학기상증착법의 단점인 대량 생산, 기판의 선정, 고온 성장 등의 문제점을 간단히 해결하려는 노력이 전세계적으로 진행되고 있다. 본 연구에서는 습식 화학합성법

을 이용하여 ZnO 나노구조 중에서 나노로드(nanorod)와 나노월(nanowall)구조를 성장시켰으며, 물성평가를 수행하였다. 습식 화학합성법을 이용하여 대기압, 상압, 저온의 조건에서 간단한 공정으로 ZnO 나노로드와 나노월을 성장시켰다. 습식 화학합성법에 있어서 온도는 매우 중요한 변수이며, 간단한 온도 조절을 통하여 산화아연 나노로드와 나노월을 성장시켰다. 상대적으로 고온(100-150도)에서 산화아연 나노로드가 성장이 되었으며, 산화아연 나노월은 상온에서 성장되었다. 성장된 산화아연 나노로드와 나노월의 모폴로지, 구조적-광학적 분석을 위해 FE-SEM, TEM, PL, CL 측정을 수행하였다.

*이 논문은 2006년도 정부재원(교육인적자원부 학술연구조성사업비)으로 한국학술진흥재단의 지원을 받아 연구되었음(KRF-2006-003-D00312).

Kp-019 **GaN/Sappahire 기판 위의 ZnO 나노와이어 성장에 대한 Ramping Time 효과** 이 삼동, 박 현규, 이 득희, 김 상우(*금오공과대학교 신소재시스템공학부.*) 최근 ZnO 나노와이어의 우수한 광학적·전기적 성질 때문에 ZnO 나노와이어의 제작 및 물성평가에 관한 연구가 활발히 진행 중에 있다. 이에 본 연구에서는 열화학기상증착법을 이용하여 ramping 시간에 따른 GaN/sappahire 기판위에 ZnO 나노와이어의 성장변화를 확인하였다. 촉매로써 Au 3nm를 thermal evaporator를 이용하여 GaN/sappahire기판 위에 증착시킨 후, ZnO와 C을 1대 1로 혼합한 파우더를 반응원료로 사용하여 대기압 하 900도, 800 sccm 아르곤 분위기에서 ZnO 나노와이어 성장온도의 ramping 시간과 holding 시간을 각각 변수로 하여 열화학기상증착법을 이용해 vapor-liquid-solid 방식으로 ZnO 나노와이어를 수직 성장시켰다. 그 결과 ZnO 나노와이어의 길이 변화에 대한 holding 시간의 영향은 미비하고 ramping 시간의 변화에 따라 ZnO 나노와이어의 성장 길이가 크게 영향을 받음을 명확히 확인할 수 있었다. 즉 holding 시간의 변화에는 나노와이어의 길이 변화가 거의 없었으며 ramping 시간의 증가에 따라 나노와이어의 길이가 증가함을 관찰하였다. 성장된 ZnO 나노와이어의 물성평가를 위해 FE-SEM을 측정하여 표면구조를 관찰하였고, EDS를 이용하여 조성분석을 하였다. 또한 HRTEM을 이용해 나노와이어가 단결정 구조를 가짐을 확인할 수 있었다.

*이 논문은 2006년도 정부재원(교육인적자원부 학술연구조성사업비)으로 한국학술진흥재단의 지원을 받아 연구되었음(KRF-2006-003-D00312).

Kp-020 **Controlled growth of ZnO nanoflower arrays on glass substrate by a wet chemical process** 권 병화, 김 용진, 이 규철(*POSTECH, 신소재공학과.*) Zinc Oxide, a direct wide band gap (3.37eV) semiconductor with a large exciton binding energy (60meV), is one of the most promising materials for electronic and photonic device applications. Selective growth which can control the position and size of 1D nanostructures on many types of a substrate is prerequisite for the integration of nanoscale devices. Among 1D nanostructures, we synthesized unique ZnO nanoflowers composed of some taper-like nanowires in the same growth condition of ZnO nanowires. Recently, ZnO nanostructures have been demonstrated for an electrode of the dye-sensitized solar cell. The position- and size-controlled ZnO nanoflower arrays have a large surface area capable of the dye loading and diverse inorganic materials loading by changing their inter-distance. They can also show the enhanced electron transport in a single crystalline nanowire of ZnO nanoflower arrays. Furthermore, the progress in the fabrication of heterostructures including coaxial and longitudinal 1D nanostructures enables the solar cell to light in a wide range of wavelength and improve the charge transport. For photocatalyst, the flower-like morphology can increase the reaction area of organic compounds, which results in the enhanced photocatalytic activity. The size- and position-controlled growth of 1D nanostructures has been achieved using selective area metal organic chemical vapor deposition (MOCVD) and catalyst-assisted vapor-liquid-solid (VLS) methods. But these methods require both expensive single crystalline substrates and a high growth temperature in the range of 800-1000 °C. On the contrary, in the hydrothermal method we can use glass and polymer substrates because 1D nanostructures were synthesized at the temperature as low as 80-100 °C. In particular, it was on the glass substrate that we made ZnO nanoflower arrays selectively. It has a great significance that 1D nanostructures are synthesized economically in the large area for industrial mass production. Here, we report on the position- and size-controlled growth of ZnO nanoflower arrays on transparent conducting glass substrate by a wet chemical process. The structural and optical properties of ZnO nanoflowers were investigated using X-ray diffraction, transmission electron microscopy and photoluminescence spectroscopy.

Kp-021 **Effect of ZnO buffer layer on ZnO nanorods growth by MOCVD** 곽 창하, 박 순홍, 서

수영, 이 용병, 김 선효, 한 상욱[1](*포항공과대학교 신소재공학과. [1]전북대학교 과학교육학부.*) We present the growth and structural properties of ZnO nanorod arrays on ZnO buffer layers. Previous studies reported the observation of a natural buffer layer between the nanorods and substrates in the beginning of ZnO nanorod growth by a catalyst-free metal organic chemical vapor deposition (MOCVD) procedure. To understand the role of the homo-buffer layer in the ZnO nanorod growth, we intentionally deposited a ZnO film with thickness of 200nm on the Al_2O_3 substrates by MOCVD, and subsequently, synthesized ZnO nanorods on the pre-grown film in-situ. The ZnO nanorods had the lengths of 0.2, 0.3 and 0.7 mm. The structure properties were characterized using various techniques, x-ray diffraction (XRD), polarization-dependent x-ray absorption fine structure (XAFS) and tunneling electron microscopy (TEM). XRD measurements on the ZnO (0002) Bragg peaks of the ZnO nanorods grown on ZnO-buffer layer/Al_2O_3 and on bare sapphire revealed that the crystal quality of the ZnO nanorods was little difference. However, q-rocking curves at the ZnO (0002) peak showed that the FWHM of the ZnO nanorods with the homo-buffer layer had a smaller value than that of the nanorods without the buffer layer. It implied that the homo-buffer layer didn't affect on the crystal qualities of ZnO nanorods much but contributed to the mosaicity of the nanorods. FE-SEM image confirmed the XRD q-rocking measurements, showing that the ZnO nanorods with the homo-buffer layer vertically better aligned than without the buffer layer. Orientation-dependent x-ray absorption fine structure (XAFS) measurements revealed that ZnO nanorods with about 0.1 μm had substantial amounts of disorders and distortion in the bonding lengths of Zn-O pairs in the ab-plane as well as along the c-axis. When the nanorod length became longer than 0.1μm, the disorder of the Zn-O pairs in the ab-plane reduced, however, the disorder of the Zn-O pairs located along the c-axis was still observed. TEM measurements corresponded with the XAFS results. Our observation of the ZnO nanorod growth on the ZnO homo-buffer layer with unchanging the crystal quality strongly suggested that this technique can be widely applicable to synthesize ZnO nanorods on various substrates with the ZnO homo-buffer layer.

Kp-022 **Effect of Calcination Process to Control the Abrasive Particles in Nano Ceria Slurry for STI CMP** LEE ByongSeog, KANG Hyun-Goo, PAIK Ungyu[1], PARK Jea-Gun(*Nano SOI Process Laboratory, Hanyang University. [1]Department of Ceramic Engineering, Hanyang University.*) In contemporary ULSI fabrication, chemical mechanical polishing (CMP) is an essential process, and shallow trench isolation (STI) process is one of the most important applications of CMP technology. Recently, it is the ceria slurry that enables the application of STI-CMP, in which the selectivity of removal rate between oxide (SiO_2) and nitride (Si_3N_4) layers is a critical factor. Ceria slurry with an organic additives shows higher oxide-to-nitride selectivity than fumed silica based slurry. However, the ceria slurry has a major disadvantage, defects on wafer surface, which can be induced with sharp exterior of particles and only a small amount of large particles. In this study, we have been investigated the effect of calcinations process to control the abrasive particles in ceria slurry on slurry characteristics, such as the particle shape, the particle size distribution, the large particle count and defects on wafer surface during the STI-CMP. Hence, we controlled the amount of adding oxygen during calcination process, according to reduce the scratch on film surface of a wafer, such as morphology and hardness problems were exceedingly improved. In addition, the abrasive particles in ceria slurry suspension were enhanced by crystal orientation and modified calcinations process with different temperature. In the CMP evaluation, as a result, defects on wafer surface were significantly restrained, while maintaining the reasonable oxide removal rate and removal selectivity between oxide and nitride films.

*This work was supported by the Korea Science and Engineering Foundation (KOSEF) through the National Research Lab. Program funded by the Ministry of Science and Technology (No. M10400000436-06J0000-43610). We thank SUMCO Corp. and Hynix Semiconductor, Inc. for helping us with our experiments.

Kp-023 **DC sputtering법에 의한 NiO 박막의 구조적 광학적 특성연구** 신 유리미, 황 영훈, 조 성래(*울산대학교, 물리학과.*) NiO는 4.194 Å의 격자상수 값을 가지는 입방구조로써, 3.6 ~ 4.0 eV 근처에서 띠 간격 에너지를 가지는 반도체 물질로 알려져 있다. 한편, NiO는 523 K 이하에서 반강자성의 자기적 특성을 나타낸다. 본 연구에서는 NiO 박막의 열처리 온도 변화에 따른 구조적 광학적 성질을 조사하였다. 박막성장은 Ar 분위기에서 dc sputtering법으로 quartz 기판위

에 증착하였다. 성장된 박막은 산소 분위기에서 다시 300에서 1000 ℃까지 온도를 변화시켜가면서 열처리 하였다. XRD 측정으로부터 성장된 박막의 결정 구조는 입방구조임을 확인하였고, 격자상수의 변화는 열처리 온도가 600 ℃까지는 감소함을 600 ℃ 이상에서는 증가하는 것을 관측하였다. 또한, XRD 결과로부터 FWHM과 입자 크기를 계산하였다. 광흡수 측정으로부터 열처리 온도에 따른 에너지 띠 간격은 3~4 eV 근처에서 나타나는 것을 확인하였다.

Kp-024 **Photocurrent study on the splitting for $ZnIn_2S_4$ thin film grown by using hot wall epitaxy** 홍광준, 김 장복, 이 상열(*조선대학교 물리학과.*) The stochiometric mixture of evaporating materials for the $ZnIn_2S_4$ single crystal thin film was prepared from horizontal furnace. To obtain the $ZnIn_2S_4$ single crystal thin film, $ZnIn_2S_4$ mixed crystal was deposited on throughly etched semi-insulating GaAs(100) in the Hot Wall Epitaxy(HWE) system. The source and substrate temperature were 610 ℃ and 450 ℃, respectively and the growth rate of the $ZnIn_2S_4$ single crystal thin film was about 0.5 ㎛/hr. The crystalline structure of $ZnIn_2S_4$ single crystal thin film was investigated by photoluminescence and double crystal X-ray diffraction (DCXD) measurement. The carrier density and mobility of $ZnIn_2S_4$ single crystal thin film measured from Hall effect by van der Pauw method are 8.51×10^{17} cm^{-3}, 291 cm^2/V-s at 293。K, respectively. From the photocurrent spectrum by illumination of perpendicular light on the c-axis of the $ZnIn_2S_4$ single crystal thin film, we have found that the values of spin orbit splitting ΔSo and the crystal field splitting ΔCr were 0.0148 eV and 0.1678 eV at 10 。K, respectively

Kp-025 **Temperature dependence of energy band gap for $CuAlSe_2$ thin film by hot wall epitaxy** 박 창선, 홍 광준[1](*조선대학교 금속재료공학과. [1]조선대학교 물리학과.*) Single crystal $CuAlSe_2$ layers were grown on thoroughly etched semi-insulating GaAs(100) substrate at 410℃ with hot wall epitaxy (HWE) system by evaporating $CuAlSe_2$ source at 680℃. The crystalline structure of the single crystal thin films was investigated by the photoluminescence(PL) and double crystal X-ray diffraction (DCXD). The carrier density and mobility of single crystal $CuAlSe_2$ thin films measured with Hall effect by van der Pauw method are 9.24×10^{16} cm^{-3} and 295 cm^2/V-s at 293K, respectively. The temperature dependence of the energy band gap of the $CuAlSe_2$ obtained from the absorption spectra was well described by the Varshni's relation, $E_g(T) = 2.8382\ eV - (8.86 \times 10^{-4}\ eV/K)T^2/(T + 155K)$.

Kp-026 **방사광을 이용한 GeTe의 상변화에 따른 화학적 상태 분석** 정 민철, 고 창훈, 이 영미, 신 현준, 한 문섭[1], 김 기홍[2], 정 재관[2], 송 세안[2](*포항가속기연구소. [1]서울시립대학교 물리학과. [2]삼성종기원.*) Giga 바이트급 Phase-change RAM (PRAM) 소자의 기술개발에 있어서 상변화 재료에 대한 물성 분석은 상변화 원리 및 제어 메커니즘을 이해하는데 폭 넓은 정보를 제공할 수 있다. 본 연구는 상변화 물질 중 비교적 구조가 간단한 GeTe에 대하여 비정질과 결정질(fcc)의 구조 변화에 따른 화학적 상태 변화를 분석하는데 그 목적이 있다. 실리콘 웨이퍼 위에 증착된 GeTe의 표면 산화막을 Ne^+ ion sputtering 기법을 이용하여 화학적 조성비가 유지된 상태에서 제거하였고, 열처리 이후 GeTe의 상변화에 따른 화학적 상태변화를 방사광을 이용한 HRXPS(High-Resolution x-ray photoelectron spectroscopy) 측정을 통해 분석하였다. Te 3d와 Ge 3d의 core-level 및 valence structure의 spectra를 통해 GeTe의 상변화 메커니즘에 대한 이해를 시도하였다. 본 연구는 현재 활발히 연구되고 있는 $Ge_2Sb_2Te_5$(GST) 물질의 물성분석에 대하여 높은 신뢰성을 가지는 기초 자료로서의 활용 및 상변화 물성 분석의 전반적인 분석 기술로서의 적용이 가능하다.

Kp-027 **Impact of Silicon Wafer Nanotopography on Poly-Si Chemical Mechanical Polishing** PARK Keum-Seok, PARK Jin-Hyung, PARK Hyung-Soon[1], PAIK Ungyu[2], PARK Jea-Gun(*Nano SOI Process Laboratory, Hanyang University. [1]Hynix Semiconductor Inc. [2]Department of Ceramic Engineering, Hanyang University.*) Recently, NAND flash memories beyond 60 nm have been fabricated using the self-aligned chemical-mechanical polishing (CMP) of floating-gate poly-silicon. The remaining thickness variation of floating-gate poly-silicon after CMP is directly influenced by the wafer nanotopography. In this study, we investigated how the material property of poly-silicon CMP slurry affects the remaining thickness variation of floating-gate poly-silicon which is determined by the wafer nanotopography. After the CMP of floating-gate poly-silicon, the remaining poly-silicon thickness variation induced by the wafer nanotopography increased with the root-mean-square (rms) of the wafer nanotopography. The amount of the remaining film

thickness variation for using the poly-silicon slurry was higher than that for using inter-layer deposition (ILD) slurry but was less than that for using ceria slurry. It was found that the remaining poly-silicon thickness variation induced by the wafer nanotopography was well correlated with the simulated result proposed with "wear-contact model".

* This work was supported by the Korea Science and Engineering Foundation (KOSEF) through the National Research Lab. Program funded by the Ministry of Science and Technology (No. M10400000436-06J0000-43610).

Kp-028 **EUV resist의 Monte Carlo 방법에 의한 노광 후 열처리에 대한 전산모사.** KIM Jong-Sun, PARK Joon-Min, KIM Eun-Jin, CHANG Wok, KANG Young-Min, PARK Seung-Wook, OH Hye-Keun(*한양대학교 응용물리학과.*) International Technology Roadmap for Semiconductor (ITRS)에 의하면 resist 패턴의 선폭이 2010년에는 45 nm 2013년에는 35 nm로 줄어들고 있다. 현재까지 반도체 제조 공정에서는 주로 ArF(193nm) laser를 사용하고 있는데, 45 nm 이하 급의 patterning을 하기 위해 193 nm immersion과 13.5nm의 파장을 사용하는 EUVL이 연구되어지고 있고, 상당한 연구의 발전을 이루고 있다. 아직까지는 많은 문제점들로 인해 양산공정에 적용되고 있지 않지만 조만간 적용될 것으로 예측된다. 그러나 EUVL 에 있어서 22 nm 의 작은 CD를 갖는 패턴을 형성하기 위해서는 아직까지도 많은 연구가 이루어져야 한다. 본 연구에서는 해상도 32 nm 급 sensitivity ~ 5 mJ/㎠ 인 resist의 개발을 위해 다양한 type의 고분자 합성을 확립하고, EUV resist 에 대해 정확한 CD 예측을 위한 노광후 열처리 시의 산 확산 공정을 전산모사 하고자 한다. 이를 위해 Monte Carlo 방법을 사용하였다. 이 연구는 45 nm 급 뿐만 아니라 32 nm 급 이하의 작은 패턴을 형성하는 데 필요한 감광제와 현상액의 개발에 응용할 수 있을 것이다.

Kp-029 **Mn 치환된 Magnetite 박막의 자기저항 특성 연구** 이 희정, 김 광주, 최 동혁[1], 김 철성[1](*건국대학교 물리학과.* [1]*국민대학교 나노전자물리학과.*) Magnetite (Fe_3O_4)는 반금속(Half Metal) 물질로서, 높은 큐리온도 (T_C = 860 K) 및 열적 안정성을 바탕으로 하는 스핀트로닉스 소자로의 응용성에 기인하여 지속적인 연구가 진행되고 있으며, Fe 자리에 전이금속을 치환하여 그 물리적 성질을 개선하려는 연구 또한 최근까지 활발히 진행되고 있다. 본 연구에서는Mn 치환된 $Mn_xFe_{3-x}O_4$ (x £ 1.0) 박막을 졸-겔 스핀코팅 방법으로 제작하였으며, X-ray Diffraction(XRD), X-ray Photoelectron Spectroscopy (XPS), Scanning Electron Microscopy(SEM), Vibrating Sample Magnetometry(VSM), 자기저항 측정 등을 이용하여 그 결정학적, 전자기적 특성에 대하여 조사분석하였다. 제작된 박막들에 대한 XRD 측정 결과, 입방구조의 단일상이 형성되었음을 확인할 수 있었으며, Mn 치환량이 증가함에 따라 격자상수는 선형적으로 증가함을 알 수 있었다. 이는 사면체 자리를 선호하는 Mn^{2+} 이온의 반경이 사면체 Fe^{3+} 이온의 반경보다 큰 것에 기인하는 것으로 해석된다. 또한, Scherrer Formula를 이용하여 박막들의 Grain Size를 계산한 결과 20~30 nm 범위에 있음을 알 수 있었다. XPS 측정을 통하여 Mn의 이온가를 유추할 수 있었으며, VSM을 통한 자기적 특성 측정 결과, Mn 치환량이 증가함에 따라 보자력은 급격히 감소하였다. 상온에서의 자기저항(MR) 효과 측정 결과, Mn 치환량이 증가함에 따라 MR 비는 감소하였으며, 제작된 박막의 열처리 시간 증가에 대해서도 MR 비는 상대적으로 감소하였다. 한편, $Mn_{0.1}Fe_{2.9}O_4$ 박막의 경우 온도에 따른 비저항 변화를 측정한 결과, Verwey Transition Temperature 근처에서 저항이 급격히 증가하는 현상을 확인할 수 있었다.

Kp-030 **a-Si:H/μc-Si:H 적층형 박막 태양전지의 터널접합 특성분석** 장 지훈, 이 정철, 이 지은, 송 진수, 윤 경훈(*한국에너지기술연구원.*) 비정질 실리콘(a-Si:H) 박막 태양전지는 원재료 가격이저렴하고 대면적 및 대량생산 제조가 가능하여 많은 연구가 진행되고 있다. 하지만, a-Si:H 박막 태양전지는 상용화되어 있는 c-Si 태양전지에 비하여 효율이 매우 낮은 것이 단점이며, 최근 이를 극복하기 위하여 a-Si:H/μc-Si:H 적층형(tandem) 태양전지가 많이 연구되고 있다. Tandem 태양전지에서 효율을 결정하는 중요한 기술 중 하나는, 상부전지(top-cell)의 n a-Si:H와 하부전지(bottom cell)의 p μc-Si:H의 사이에서 접합기술(tunnel junction)로, 투명전도막 물질을 중간층으로 삽입하여 접합을 실시한다. 본 연구에서는 ZnO를 중간층으로 삽입하여 a-Si:H/μc-Si:H 적층형 태양전지 tunnel junction의 특성을 향상하고자 하였다. SnO2:F glass 기판위에 PECVD로 n a-Si:H과 p μc-Si:H을 차례로 증착하고, 두 층 사이의 저항을 측정하였으며, n-type과 p-type Si층 사이에 ZnO 중간층을 삽입하여 저항을 측정하여 그 값을 비교한 결과, ZnO를 첨가하지 않은 cell의 경우 그 값이 600Ω-㎠로 측정되었으나, ZnO를 첨가한 cell의 경우 1Ω-㎠로 현저히 낮아졌다. 또한, SnO2:F/p a-SiC:H/i a-Si:H/n a-Si:H/p μc-Si:H/Ag 구조의 태양전지와 SnO2:F/p a-SiC:H/i a-Si:H/n a-Si:H/ZnO:Al/p μc-Si:H/Ag 구조의 태양전지에서 ZnO:Al 중간층 유무에 따른 특성을 분석한 결과, ZnO 중간층의 삽입한 경우 개방전압은 57%, 변환효율은 50%가 증가한 것으로 분석되었으며, 이러한 특성향

상은 a-Si:H/ZnO:Al/μc-Si:H 적층형 태양전지에서도 동일하게 나타나는 것으로 확인되었다.

Kp-031 **Current aging effect of CNTs field emitter array** 김 기서, 유 제황[1], 문 종현[2], 안 정선[3], 장 진[1], 박 규창(*경희대학교 물리학과, 차세대디스플레이연구센터. [1]경희대학교 물리학과, 정보디스플레이학과, 차세대디스플레이연구센터. [2]경희대학교 차세대디스플레이학과. [3]경희대학교 물리학과.*) 본 연구에서는 성장된 CNT에 지속적인 전류방출 인가를 통하여 전자방출특성 및 방출전류 안정도를 향상시켰다. 실험에 사용된 탄소나노튜브는 RAP(Resist Assisted Patterning)방법을 이용하여 성장하였으며, 전류특성측정을 위한 FEA(Field Emitter Arrays)는 직경 5 μm의 디스크타입이 40μm 거리의 주기를 가지는 패턴을 이용하였다. 실험 결과 임계전압(@ 0.1 μA/cm^2)의 경우 탄소나노튜브에 인가된 Aging 전류가 증가함에 따라 감소되는 특성을 보였으며 100 μA/cm^2 이상의 Aging전류밀도서부터는 일정한 값을 유지하는 것을 볼 수 있었다. 전자방출특성의 경우는 Aging 전류가 증가함에 따라 전자방출특성이 증가되는 경향을 보이다 500 μA/cm^2 이상의 Aging전류밀도에서는 약간 감소되는 경향을 나타내었다. 본 실험을 통하여 직접 성장한 CNT의 경우, 일정한 Aging전류를 가하면 보다 낮은 임계전압과 높은 전자방출특성을 가지며 안정적인 전자방출특성을 보인다.

Kp-032 **Electrochemical lithium insertion properties of boron-doped diamond** M. Anbu Kulandainathan, A. Manuel Stephan, CHRISTY maria[1], 서 은경[1], 황 운주[2], 남 기석[2](*Central Electrochemical Research Institute. [1]전북대학교 반도체과학기술학과/반도체물성연구소. [2]전북대학교 화학공학부.*) The ambit of application of lithium batteries is being extended from laptops, digital cameras and portable memory devices to the transport sector, where they may be the sole power source or may be part of a hybrid with supercapacitors or fuel cells. In the last two decades much effort has been made to find alternatives to carbonaceous anodes with larger capacities and better cycling performances. These materials include alloys with an active component, tin-based oxides and layered materials. Recently, boron-doped diamond has drawn the attention of many researchers as a possible anode material for lithium batteries due to its appealing properties like mechanical robustness, chemical inertness and electrochemical activity over a large potential window. In the present study, boron-doped diamond produced by chemical vapor deposition is investigated as a lithium-insertion anode material. The structural and electrochemical characteristics of the diamond materials are correlated.
*Acknowledgements This work was supported by the Korea Research Foundation Grant funded by the Korean Government (MOEHRD) (KRF-2005-005-J07501).

Kp-033 **스퍼터링 방법에 따른 Nickel Oxide 박막의 광학 및 전기적 특성 연구** 최 광남, 박 준우[1], 이 호선[1], 정 관수(*경희대학교 전자공학과. [1]경희대학교 물리학과.*) 많은 금속산화물들은 외부 전압 혹은 전류에 의해서 전도성이 변화하는 현상을 보이며, 이러한 전도성 전이 현상은 가역적이며 비휘발성이기에 resistance random access memory (RRAM) 라는 새로운 개념의 차세대 비휘발성 메모리의 핵심 소재로 급부상하고 있다. 이러한 산화물 중에서 Nickel Oxide(NiO)는 그 저항의 변화가 크고 비교적 간단한 구조를 가지고 있기 때문에 최근 가장 주목받는 연구 대상 중 하나이다. 이러한 NiO 박막을 다양한 스퍼터링법으로 제조해 보았으며 각 박막의 광학적, 전기적 특성을 분석하였다. 스퍼터링 조건으로는 크게 DC와 RF로 나눌 수 있으며, 각각의 전원에서 반응성 스퍼터링법으로 산소의 분압에 따른 NiO 박막을 연구하였다. 또한 NiO 타겟을 사용하여 RF 스퍼터링법으로 NiO 박막을 증착하여 반응성 스퍼터링법으로 제작한 NiO 박막과도 비교하였다. 광학적 특성은 ellipsometry를 이용하였으며, 전기적 특성은 I-V 특성곡선을 분석하였으며, 박막의 구조는 X-ray diffraction(XRD)으로 분석하였다.

Kp-034 **실리콘 박막 태양전지용 ZnO:Al 투명전도막의 전기*광학적*구조적 특성 분석** 김 영진, 왕 진석[1], 이 정철, 송 진수, 윤 경훈(*한국에너지기술연구원. [1]충남대학교 전자전파정보통신공학부.*) 흔히 전면 투명 전도막 (Transparent Conductive Oxide : TCO)에는 FTO(SnO_2:F), ITO(In_2O_3:Sn), AZO(ZnO:Al) 등이 있으나, 플라즈마 내에서 화학적 안정성이 우수하고, 높은 투과도와 우수한 전도도로 인해 AZO(ZnO:Al) 많이 사용하고 있다. 실리콘 박막 태양전지의 투명전도막은 박막이 얇고, 실리콘의 흡수계수가 작고, 또한 장파장의 빛을 흡수하지 못하기 때문에 효율을 증가시키기 위해 ZnO:Al 투명전도막을 etching 한다. 본 연구에서는 압력의 변화에 따른 ZnO:Al 투명전도막의 물리적 성질을 전기, 광학적, 구조적 특성으로 분석했고, 압력의 변화에 따른 ZnO:Al 투명전도막의 etching 전*후의 특성을 비교, 분석하였다. 먼저, 압력의 변화에 대한 ZnO:Al 투명전도막의 특성은 AFM, SEM으로 표면형상을 분석했을때, 증착압력이 낮아질수록 결정립 크기가 크고, 빽

빽하고 조밀한 구조의 박막이 형성됨을 알 수 있다. 투과도와 총투과도, 비저항은 증착압력이 높아질수록 증가하는 것을 알 수 있고, 캐리어 이동도와 캐리어 농도는 증착압력이 높을수록 감소하는 것을 알았다. etching 후의 ZnO:Al 박막 특성은 etching 전과 비교하여 볼 때 면저항(Sheet Resistance) 비저항(Resistivity) 특성이 상당히 좋아졌다. 증착압력이 증가할수록 식각율과 투과도가 증가했고, 반대로 Haze는 감소했다. ZnO:Al 박막의 etching 으로 빛의 이동경로가 증가하기 때문임을 알수 있다. 앞으로의 실험방향은 온도변화를 통해서 ZnO:Al 박막의 물성에 어떠한 영향을 주는지 알아보고, 온도변화에 따른 etching 전*후의 특징에 대해 비교해 볼 것이다. 또한 미세결정 실리콘(yc-si:H)박막 태양전지를 만들어 ZnO:Al와 어떠한 차이를 나타내는지 알아보고자한다.

Kp-035 **Touch panel application을 위한 Poly silicon photo sensor와 TFT에 대한 연구** 이 승훈, 김 응범, 이 은영, 김 세환, 장 진(*경희대 정보디스플레이 학과.*) 최근 디스플레이 소자 재료가 비정질 실리콘(amorphous silicon)에서 다결정 실리콘(polycrystalline silicon)으로 대체하려는 움직임이 활발이 진행되고 있으며, 디스플레이는 점점 고화질과 초박막 형으로 발전하고 있다. 비정질 실리콘 트랜지스터의 낮은 이동도(~1 cm^2/Vs)에 비해 다결정 실리콘 트랜지스터는 10 ~ 400 cm^2/Vs 의 높은 전계 효과 이동도(field effect mobility) 특성을 가지므로 화소용 스위치 뿐만 아니라, 게이트 구동회로 및 데이터 구동 회로를 값 싼 유리 기판에 제작할 수 있는 장점이 있다. 본 연구에서는 touch panel application을 위해서 ELA 박막을 이용하여 TFT와 photo diode sensor를 제작하였다. ELA 박막을 이용하여 제작된 TFT는 20~80 [Cm^2/Vs]의 mobility를 얻을 수 있었고, PIN photo diode sensor의 경우는 0 ~ 2000 lux 사이의 빛에서 photo current의 변화를 확인한 결과, -5 V에서 약 10^{-12} A로 매우 작은 전류가 흐르며 2000 lux 의 빛에서는 약 10^{-10} A의 전류가 흐르는 것을 확인하였다.

Kp-036 **VLS 기법을 통한 SnO_2 나노와이어의 선택성장 및 물성평가** 이 득희, 박 현규, 이 삼동, 이 진무, 김 상협[1], 맹 성렬[1], 김 상우(*금오공과대학교 신소재시스템공학부. [1]한국전자통신연구원 Cambridge-ETRI 공동연구센터.*) SnO_2는 상온에서 3.6eV 의 넓은 밴드갭을 가지는 n-type 반도체 물질로서 화학 센서, 광소자, 투명 전극 및 태양 전지 등 다양한 분야에 응용되어지고 있으며, 이에 더해 고효율, 고감도, 고집적성을 보장하는 나노구조 제작에 대한 연구도 활발히 진행되고 있다. 본 연구에서는 3nm Au 박막이 패터닝 된 c-Al_2O_3 기판 위에 열화학기상증착 공정을 통해 SnO_2 나노와이어를 패턴 된 영역에 선택 성장을 구현시켰다. 나노와이어의 합성을 위해 두께가 3nm인 Au 박막이 나노와이어 성장촉매로 이용되었으며 SnO_2 나노와이어의 성장을 위해 순수 SnO 파우더를 반응 원료로 사용하였다. SnO_2 나노와이어의 합성은 대기압 하 900-1000도 600-800 sccm 아르곤 분위기에서 60-90분 동안 이루어졌다. 성장조건에 따른 선택 성장된 SnO_2 나노와이어의 모폴로지 변화 및 물성평가를 위해 FE-SEM, XRD, EDS, HRTEM 분석이 이루어졌으며, PL 분석을 통한 광특성을 확인하였다. 본 연구에서는 Au 박막이 패터닝 되어있는 부분에서만 SnO vapor의 화학 반응이 일어남을 확인함으로써 SnO_2 나노와이어가 vapor-solid-liquid (VLS) 기법을 통해 구현되었음을 확인할 수 있었다.

*This work was supported by the Ministry of Information and Communication (MIC), Republic of Korea, under Project No. A1100-0602-0101.

Kp-037 **동시증발법을 이용한 Wide Bandgap $Cu(In_xGa_{1-x})Se_2$ 박막태양전지 연구** 송 진섭, 윤 재호, 김 재웅, 안 세진, 윤 경훈(*한국에너지기술연구원.*) CIS계 화합물 태양전지는 빛의 광흡수계수가 매우 높기 때문에 CIGS를 광흡수층으로 사용할 경우 19% 이상의 고효율을 나타내고 있다. 따라서 연구초기에는 실리콘 박막 태양전지에 비해 탠덤구조 태양전지에 대한 요구가 크지 않았다. 하지만 결정질 실리콘 및 기존의 화석연료에 의한 발전 방식을 뛰어넘어 상용화되기 위해서는 20%이상의 고효율 태양전지 개발이 필요하기 때문에 세계적인 선진 연구기관들을 중심으로 탠덤구조 태양전지에 대한 연구가 진행되고 있다. 본 연구에서는 탠덤구조 태양전지의 Wide Bandgap $Cu(In_xGa_{1-x})Se_2$를 만들었다. 기판은 soda-line glass를 사용하였고 뒷면 전극으로는 Mo를 스퍼터링법으로 증착하였다. 또한 버퍼층으로는 기존에 쓰이고 있는 CdS를 CBD법으로 증착시켰으며, 윈도우층으로는 i-ZnO/n-ZnO를 스파터링 법으로 증착하였다. 그리고 앞면전극으로는 Al을 E-beam으로 증착하였다. 위 실험에서 얻은 Wide Bandgap $Cu(In_xGa_{1-x})Se_2$ 박막태양전지의 Ga 조성에 따른 박막 특성과 광전압 특성을 조사하였다.

Kp-038 **Growth and Hall effect properties for $ZnGa_2Se_4$ thin film by hot wall epitaxy** 백 승남, 홍 광준[1], 김 도선[1](*조선대학교 금속재료공학과. [1]조선대학교 물리학과.*) The stochiometric mix of evaporating materials for the $ZnGa_2Se_4$ single crystal thin films were prepared from hot wall epitaxy(HWE). To obtains the

single crystal thin films, $ZnGa_2Se_4$ mixed crystal were deposited on throughly etched Si(100) by the Hot Wall Epitaxy (HWE) system. The temperates of the source and the substrate were 590℃ and 450℃, respectively. The crystalline structure of single crystal thin films was investigated by the double crystal X-ray diffraction (DCXD). Hall effect on this sample was measured by the method of van der Pauw and studied on carrier density and mobility dependence on temperature.

Kp-039 **전면 투명전도막과 p층 물성에 따른 비정질 실리콘 박막 태양전지 특성 분석** 이 지은, 이 정철, 오 병성[1], 송 진수[2], 윤 경훈[2](*한국에너지기술연구원 태양광발전연구단. [1]충남대학교, 물리학과. [2]한국에너기기술연구원 태양광발전연구단.*) 유리를 기판으로 하는 superstrate pin 비정질 실리콘(a-Si:H) 박막 태양전지에서 전면 투명전도막 (Transparent Conducting Oxide : TCO)은 태양전지의 효율을 결정하는 중요한 요소 중 하나이다. 현재 가장 흔히 사용되는 SnO_2:F와는 달리 ZnO:Al 박막은 전기·광학적 특성이 우수하고 입사광의 회절 정도를 나타내는 안개율(haze ratio)이 높으며, 수소 플라즈마에 대한 안정성이 높은 장점을 가지고 있다. 그러나 ZnO:Al를 전면 TCO로 사용할 경우 p층으로 사용되는 a-SiC:H 박막과의 접촉저항이 커 비정질 실리콘 박막 태양전지의 충진율(fill factor)과 개방전압(Voc)을 감소시키는 것으로 보고되고 있으나 정확한 원인은 밝혀지지 않고 있다. 본 논문에서는 ZnO:Al과 SnO_2:F를 각각 사용하여 TCO/p-Si/i a-Si:H/n a-Si:H/Ag 구조의 태양전지를 제조하고 TCO와 p층(p-Si) 물성에 따른 태양전지의 동작특성을 분석하였다. 일반적으로 보고된 바와 같이 ZnO:Al/p a-SiC:H 구조를 갖은 태양전지의 충진율은 65-70%로 SnO2:F/p a-SiC:H의 충진율 75%에 비해 낮은 값을 보였는데, 이는 ZnO:Al과 p a-SiC:H의 높은 접촉저항에 의한 태양전지 직렬저항 증가에 의한 것으로 분석되었다. ZnO:Al/p a-SiC:H 접합특성을 분석하기위해 p μc-Si:H/p a-SiC:H의 이중 p층을 사용하거나 p a-SiC:H 증착시 B_2H_6의 유량을 증가시켜 박막의 케리어 농도를 증가시킨 결과 ZnO:Al과의 접촉저항은 현저히 감소하였으며 70% 이상의 높은 충진율을 얻을 수 있었다. 이상의 결과로부터 ZnO:Al/p a-SiC:H의 접촉저항은 n형의 ZnO:Al 박막에 의한 p a-SiC:H 박막의 공핍(depletion)과 그에 따른 전위장벽에 의한 것으로 분석되었다.

Kp-040 **OVPD(유기기상증착)방식을 이용한 N형 유기박막트랜지스터의 제작에 관한 연구** 이 기정, 한 승훈, 이 선희, 손 영래, 최 민희, 김 용희, 장 진(*경희대학교 정보디스플레이학과, 차세대디스플레이연구센터.*) 펜타센으로 대표되는 고성능 P형 유기박막트랜지스터(OTFT)에 비해 N형 OTFT는 낮은 전자친화도 값으로 인해 공기 중에서 쉽게 산화되어 상대적으로 고성능을 확보하지 못하고 있다. 최근에 연구되고 있는 N형 OTFT의 경우 전자이동도 1 cm^2/Vs 를 넘는 값이 보고 되었으나 이 역시 진공 중에서 얻어진 값으로 공기 중에서는 매우 낮은 전기적 특성을 보이거나 TFT의 동작 특성을 보이지 않았다. 이 연구에서는 bottom contact구조의 N형 OTFT를 유기기상증착(OVPD)법으로 제작하였고 parylene 보호막을 통해 외기를 차단함으로써 공기 중에서 우수한 이동도 및 점멸 비를 확보할 수 있었다. 제작된 N형 OTFT의 초기 성능은 전계 효과 이동도 0.012 cm^2/Vs, 문턱 전압 21.8 V, 점멸 비 ~10^6로 우수한 특성을 나타내었고 모든 측정은 공기 중에서 실시되었다.

*Acknowledgement 이 연구(논문)는 산업자원부의 21세기 프론티어기술개발사업인 차세대정보디스플레이기술개발사업단의 기술개발비(F0004082-2006-22)지원으로 수행되었습니다.

Kp-041 **잉크젯 방식을 이용한 유기TFT 제작에 관한 연구** 최 민희, 한 승훈, 이 선희, 손 영래, 이 기정, 김 용희, 장 진(*경희대학교 정보디스플레이학과, 차세대 디스플레이 연구센터.*) 잉크젯 프린팅은 디스플레이 및 전자소자 제작에 적용할 경우 기존의 포토리소그래피 방법을 대체할 수 있게 되고 원하는 곳에만 패턴을 만들 수 있기 때문에 제작 공정이 간단하고 공정 비용에 있어서 절감이 가능하다. 최근에 연구되고 있는 잉크젯 방식을 이용하여 제작된 TFT의 경우, 전극과 반도체를 형성하는 데 있어서 spin coating 이나 drop cast의 방식도 함께 사용하여 제작한 것으로 보고되고 있다. 이 연구에서는 bottom contact구조의 P형 OTFT를 잉크젯 프린팅 방식으로 제작하였다. 실버 나노 입자 잉크 및 유기 반도체 잉크를 프린팅 기술을 이용한 유기박막트랜지스터(OTFT)를 제작하여 소자 특성을 확인하였다. 제작된 OTFT의 초기 성능은, 전계 효과 이동도 9.21×10^{-4} cm^2/Vs, 점멸비 ~10^5, 문턱전압 -15V의 우수한 전기적 특성을 나타내었다.

*Acknowledgement 이 연구(논문)는 산업자원부의 21세기 프론티어기술개발사업인 차세대정보디스플레이기술개발사업단의 기술개발비(F0004082-2006-22)지원으로 수행되었습니다.

Kp-042 **Nonvolatile Memory Effects in Device Using Ag Nanocrystals Embedded in poly(N-vinycarbazole) with Indium Tin Oxide Electrode** HAN Byeong

Il, SEUNG Hyun Min, LEE Jong Dae, PARK Jea-Gun(*Nano SOI Process Laboratory, Hanyang University.*) Memory effect in organic molecules is based on electrical bistability of the materials and the bistable phenomenon was observed in poly(N-vinylcarbazole) (PVK) layer, containing many small discrete Ag nanocrystals, sandwiched between Al and indium tin oxide (ITO) electrodes. More importantly, a forward bias may switch the device to a high conductivity state, while a reverse bias is required to restore it to a low conductivity state. It may be found that the current at the low conductivity state is space-charge limited and the bistability is attributed to the electron traps at the Ag nanocrystals. Also, since the bistability shown in current-voltage characteristics is reproducible, the device has the potential in the application for nonvolatile memory.

*This research was supported by Korea ministry of commerce industry and energy for the 0.1 Terabit Non-volatile Memory Development.

Kp-043 **Organic Light Emitting Devices with In-doped ZnO thin Films as Anodic Electrode** PARK Young Ran, NAM Eunkyoung, JUNG Donggeun, KIM Young Sung[1](*Sungkyunkwan University, Department of Physics. [1]Sungkyunkwan University, Advanced Material Process of Information Technology.*) Transparent In-doped (4 at.%) zinc oxide (IZO) thin films are deposited with variation of substrate temperature and pulsed DC power at Ar atmosphere on corning 7059 glass substrate by pulsed DC magnetron sputtering. Organic Light-emitting diodes (OLEDs) with IZO/N,N'-diphenyl-N, N'-bis(3-methylphenl)-1, 1'-biphenyl-4,4'-diamine (TPD)/ tris (8-hydroxyquinoline) aluminum (Alq_3)/LiF/Al configuration were fabricated. LiF layer inserted is used as a interfacial layer to increase the electron injection. Under a current density of 100 mA/cm^2, the OLEDs show an excellent efficiency (10 V turn-on voltage) and a good brightness (12000 cd/m^2) of the emission light from the devices. These results indicate that IZO films hold promise for anode electrodes in the OLEDs application.

** Acknowledgments : This work was supported by the Korea Research Foundation Grant funded by the Korean Government(MOEHRD) (KRF-2005-005-J11902).

Kp-044 **Transparent Anodic Properties of In-doped ZnO thin Films for Organic Solar Cells** PARK Young Ran, KIM Geumjoo, JUNG Donggeun, KIM Young Sung[1](*Sungkyunkwan University, Department of Physics. [1]Sungkyunkwan University, Advanced Material Process of Information Technology.*) Transparent In-doped (4 at.%) zinc oxide (IZO) thin films are deposited on corning 7059 glass substrate by pulsed DC magnetron sputtering at different $H_2/(H_2+Ar)$ ratio (R) between H_2 and Ar gas-flow rates with a fixed total (H_2+Ar) flow rate during the sputtering. The electrical, optical, and structural properties of these films were investigated as variation of H_2 flow ratio. Organic solar cells with IZO/poly (3,4-ethylenedioxythiophene)(PEDOT)/poly[2-methoxy-5-(20-ethylhexyloxy)-p-phenylene vinylene](MEH-PPV) + [6, 6]-phenyl C_{61}-butyric acid methyl ester (PCBM)/LiF/Al configuration were fabricated. LiF and PEDOT layer inserted is used as a interfacial and transport layer, respectively. The photovoltaic cells were studied in ambient atmosphere by recording the initial values of open circuit voltage (V_{OC}) and current density (I_{SC}). The results of this experiment were good compared with the case of using commercial ITO.

** Acknowledgments : This work was supported by the Korea Research Foundation Grant funded by the Korean Government(MOEHRD) (KRF-2005-005-J11902).

Kp-045 **ALD를 이용한 3D Multi-gate FET의 Source/Drain contact 저항 특성** 지 진욱, 이 헌복[1], 백 경흠[1], 장 재형[1], 양 충모[1], 윤 상원[1], 조 현익[1], 하 종봉[1], 나 경일[1], 이 정희[1], 함 성호[1](*경북대학교, 전자공학과. [1]경북대학교,전자공학과.*) 고성능화 고집적화를 위해 지속적으로 소자의 크기를 축소시키는 연구가 진행되면서 반도체 소자의 소형화는 물리적, 기술적 한계에 도달할 것으로 예상되고 있으며, 이러한 CMOS의 물리적, 기술적 한계들을 극복하기 위한 연구가 활발히 진행되고 있다. ITRS(International Technology Roadmap for Semiconductor)에 따르면 FinFET, Tri-gate FET, and multiple-gate FET 이 35nm이하의 소자에 적용되어 우수한 특성을 나타낼 것으로 보고 있다. 하지만 Fin 폭의 감소에 따른 몇가지 문제가 발생하게 된다. 그 중에 극복해야 할 문제점 중의 하나가 소스-드레인의 실리콘과 금속간의 접촉 비저항에 관한 것이다. 지금까지의 금속과 소스-드레인 접촉은 Silicide를 형성하여 낮은 접촉 비저항을 구현하였다. 하지만 Silicide만으로는 65 nm급이하의 소자에 적합한 $10^{-8}\Omega\cdot cm^2$ 이하의 접촉저항을 구현하기 어려운 한계에 직면할 것으로 알려지고 있다. 이런 Silicide 형성시의 문제점을 극복하기 위해서 소스-드레인에 Silicide를 형성하기 전에 선택적으로 SiGe (strained Si/SiGe)을 에피텍시한 후 Silicide를 형성하는 구조가 연구되고 있다. 하지만 이러한 구조는 복잡한

공정과 비용 측면에서 큰 단점을 가지고 있다. 본 실험에서는 다양한 Fin폭을 갖는 소스-드레인을 형성 후, Fin 측면과 Fin spacer 사이에 oxidation을 통해 트랜치를 형성하고, ALD로 Ni을 deposition하였다. Ni etching 후, Fin측면과 Fin spacer 의 좁은 공간에 빈 공간 없이 Ni이 채워지는 것을 확인했다. 열처리를 통해 Fin측면에 Ni Silicide를 형성했으며, 향후 contact metal을 deposition해서 소스-드레인의 접촉 비저항의 감소를 기대한다. 이와 같은 Source/Drain의 구조는 Fin과 Fin spacer 사이의 폭에 따라 접촉저항의 개선은 물론 면저항의 개선도 기대 할수 있다. 또한 소스-드레인의 면적을 줄일 수 있기 때문에 고집적이 가능한 장점이 있다.

Kp-046 **Multi Level Cell Nonvolatile Memory Fabricated with Stacked Structure of Organic Bi-stable Device** NAM Woo Sik, KIM Yool Guk, PARK Jea-Gun, KIM Young Min[1](*한양대학교 나노 SOI 공정 연구소. [1]Korea Basic Science Institute.*) We developed organic nonvolatile memory fabricated with the device structure of Al/Alq_3/Al nano-crystals surrounded by Al_2O_3/Alq_3/Al. Al nano-crystals surrounded by amorphous Al_2O_3 were included in conductive organic material Alq_3. We obtained the best conduction bi-stability and threshold voltage at the Alq_3 thickness of 30nm and the middle Al layer thickness of 30nm, the evaporation rate of 1.0Å/sec. These devices showed excellent bi-stable memory characteristic; i.e., V_{th} of 2.7V, V_p (program) of 5.1V, V_e (erase) of 8V, I_{on} (program)/I_{off} (erase) of ~$9.3x10^1$. We fabricated with stacked structure of these device and confirmed similar characteristic in each devices; i.e., V_{th} of 2~3V, V_p (program) of 4.5~5V, V_e (erase) of 8~8.2V, I_{on} (program)/I_{off} (erase) of ~$1x10^2$, and erase/program cycles of $1x10^5$. In the same way, each device demonstrated four level nonvolatile memory behavior, so we realized multi level cell. These devices can indicate total 8 levels, namely 3 bits on $4F^2$ dimension. As a result, that is a great use to integration improvement of organic bi-stable devices.

Kp-047 **금속 촉매를 이용한 In2O3 가스센서의 제작 및 특성** 이 홍진, 이 윤수[1], 송 갑득[2], 이 상문[3], 주 병수, 이 덕동(*경북대학교 전자공학과. [1]경북대학교 모바일 디스플레이 센터. [2]경북대학교 첨단 디스플레이 제조공정및장비 연구센터. [3]경북대학교 모바일 디스플레이 산학연 센터.*) 가스센서는 인간의 오감 중 후각 기능을 대신하는 소자로서 산업용, 가정용 등 그 응용범위가 다양하며 사용범위가 확대되고 있다. 특히 많은 가스 중에서 휘발성 유기화합물(VOCs:volatile organic compounds)가스는 상온 · 대기압 상에서 쉽게 휘발할수 있는 탄화수소계 화합물로서 주로 연료의 불완전 연소와 유기용제의 증발등으로 형성되기 때문에 배출원이 매우 다양하며 날로 그 발생량이 증가하고 있다. 뿐만 아니라 VOCs는 200 ㎍/㎥·h이 넘으면 인체에 영향을 미치기 시작해 300~3000 ㎍/㎥·h이면 불쾌감, 두통, 인후두부 염증 등을 초래할뿐만 아니라 대표적인 발암물질로 알려져 있다. 따라서 휘발성 유기화합물 가스를 신뢰성 있게 측정할수 있는 소자의 개발이 요구되어진다. 본 연구에서 제작된 센서는 기본적으로 금속산화물 반도체식 가스센서이다. 소자는 8mm×10mm크기의 Al_2O_3기판위에 IDT(inter digitated transducer)구조의 Pt 감지전극을 형성하였고 back side에 역시 Pt로 heater를 구성하였다. 감지막 형성을 위한 원료물질로는 Aldrich 社에서 제공되는 In(Indium wire 1.0mm diam, 99.999%) 시료를 사용하였고 열증착법을 이용하여 In박막을 증착한 다음 전기로(electric furnace, LINDBERG 社, 1-800-657-0770)를 사용하여 600 ℃의 온도에서 O_2 가스를 주입한 후 열산화하여 In_2O_3를 형성하였다. 또한 촉매효과를 확인하기 위하여 Ion coater(Eiko 社)를 사용하여 Sn을 얇은 두께로 코팅하였다. 제작된 센서는 대상 가스와 감지막의 접촉에 의해 전도도가 변하는 가변 저항성 소자로서 LabVIEW(National Instrument 社) 프로그램으로 저항의 변화를 측정하였으며 DC power supply를 사용하여 heater의 온도를 제어하였다. 감지 가스로는 CH_4, CH_3COCH_3, C_7H_8, C_6H_6가스에 대한 감응특성 및 재현성 · 장기안정도를 조사하였다. 각각의 가스는 100 ppm의 농도에서 측정되었으며 이 중 200 ℃동작온도에서 대표적인 폭발성가스 중의 하나인 CH_4에 대하여 우수한 선택성을 가짐을 확인할 수 있었다.

Kp-048 **Nonvolatile Memory Fabricated with Al nano-crystals Embedded in Conductive Organic Layer using Cu Electrode** SEO Sung-ho, OH Young-hwan, PARK Jea-gun, KIM Young-min[1](*Hanyang University. [1]Korea Basic Science Institute.*) We developed stack type organic nonvolatile memory fabricated with the device structure of Top Cu electrode / Alq_3 / Al nano-crystals surrounded by Al_2O_3 / Alq_3 / middle Cu electrode / Alq_3 / Al nano-crystals surrounded by Al_2O_3 / Alq_3 / bottom Cu electrode where Alq_3 is Aluminum tris (8-hydroxyquinoline). Al nano-crystals surrounded by amorphous Al_2O_3 were included in conductive organic material Alq_3. These devices showed unstable bi-stable memory characteristic; i.e., V_{th} of 2.9V, $V_{program}$ of 4V, V_{erase} of 7.3V, and I_{on} / I_{off} of ~ $1X10^2$ for bottom NVM. Top NVM showed similar characteristic; i.e., V_{th}

of 2.7V, $V_{program}$ of 4V, V_{erase} of 6.5V, and I_{on}/I_{off} of ~ $1X10^2$. They presented seven different reversible current paths approving electron charge or discharge on Al nano-crystals. Both top and bottom NVM showed asymmetric and unstable I-V characteristics. So we examined Cu electrode diffusion to conductive organic layer by Auger electron spectroscopy (AES). But our device showed Negative Differential Resistance (NDR) region, thus our device demonstrated multi-level nonvolatile memory behavior.

Kp-049 **Interface Traps and Charge Traps in ONO (Oxide –Nitride-Oxide) Structures** 김 태근, 서 유정, 김 경찬, 김 재무, 조 훈영[1], 서 명원[1], 오 종수[1], 주 문식[2], 피 승호[2], 양 홍선[2](*고려대학교, 전기전자전파공학부. [1]동국대학교, 물리학과. [2]하이닉스 반도체.*) The oxide-nitride-oxide (ONO) structure has been used as a dielectric film in non-volatile memory devices. and known to contain a large number of charge traps. The charge traps in the ONO structure are referred to electron or hole energy levels associated with impurities or defectsThe origin(s) of the traps in the ONO structure grown on n-type Si substrate are investigated by deep level transient spectroscopy (DLTS) and capacitance voltage(CV). Typically, two electron traps were observed at 0.27 and 0.52eV from the conduction band minimum of Si. Each of the traps was identified to come from the nitride related trap and the Si-SiO_2 interfacial states (by comparison of the samples – Oxide, Nitride, ONO grown on n-type Si substrate). And the origin of interfacial trap was investigated clearly by SP(Small Pulse) DLTS technique. More details on the experiment will be presented

Kp-050 **Temperature dependence of band gap for $AgGaSe_2$ thin film grown by using hot wall epitaxy** 홍 광준, 유 상하(*조선대학교 물리학과.*) Single crystal $AgGaSe_2$ layers were grown on thoroughly etched semi-insulating GaAs(100) substrate at 420 ℃ with hot wall epitaxy (HWE) system by evaporating $CuAlSe_2$ source at 630 ℃. The crystalline structure of the single crystal thin films was investigated by the photoluminescence and double crystal X-ray diffraction (DCXD). The carrier density and mobility of single crystal $AgGaSe_2$ thin films measured with Hall effect by van der Pauw method are 9.24×10^{16} cm^{-3} and 295 cm^2/V-s at 293K, respectively. The temperature dependence of the energy band gap of the $AgGaSe_2$ obtained from the absorption spectra was well described by the Varshni"s relation, $E_g(T)=1.9501$ eV-$(8.79\times10^{-4}$ eV/K$)T^2/(T+250$ K).

Kp-051 **미소유체 채널(microfluidic channel)을 이용한 PCR chip의 heat-sink 연구** 김 희성, 은 덕수, 공 대영, 정 종현, 조 재범, 방 형희, 유 현준, 장 종민, 류 인식[1], 이 종현(*경북대학교, 전기전자컴퓨터. [1]경동정보대학.*) PCR(Polymerase Chain Reaction)이란 자신이 원하는 DNA의 특정영역을 대량으로 증폭하는 획기적인 기술을 말한다. PCR(Polymerase Chain Reaction)과정에서 특정온도(94℃→55℃→72℃) 컨트롤을 얼마나 정확히 그리고 빠르게 하는 것이 가장 중요하다. 본 논문에서 heat-sink의 역할로서 기존의 팬방식 등이 아니라 미소유체 채널(microfluidic channel)을 사용하여 온도를 얼마나 빠르게 컨트롤 할 수 있는지를 연구하였다. 실리콘웨이퍼(100)에 TMAH를 이용하여 PCR chip의 용량이 4.6㎕를 가지는 챔버를 제작하였다. 직접적인 시료의 온도 컨트롤이 가능하도록 하기 위해서 히터와 센서를 챔버 바닥이 아니라 상판 글라스에 E-beam을 이용하여 증착하였고 polymer bonding 방법을 이용해 결합하였다. 또한 PCR chip의 heat-sink의 역할로서 폭 200㎛, 깊이 350㎛를 가지는 미소유체 채널(microfluidic channel)을 micro-blaster를 이용하여 제작하였고 또한 polymer bonding 방법을 이용해 챔버의 바닥 부분에 결합하였다. 본 연구에서는 미소유체 채널(microfluidic channel)이 있을 때와 없을 때의 온도 변화 특성을 측정하였다.

Kp-052 **Effect of Atomic Hydrogen Plasma Exposure of Si Substrate on The Formation and Light Emission of Porous Silicon** JUNG Yun-Jin, JANG You-Sung, JO Hyun-Ji, YOON Jong-Hwan(*Kangwon National University, Department of Physics.*) Porous silicon was prepared by electrochemical anodization of Si substrate exposed to atomic hydrogen plasma. Hydrogen exposure is shown to result in an increase of photoluminescence (PL) intensity, as well as a significant reduction of pore size. A 30-min H exposure at 150 °C resulted in an increase of the PL intensity by a factor of 4, giving rise to an apparent blueshift, and a decrease of the pore diameter by a factor of 3. These are consistent with enhanced passivation of Si dangling bond defects and enhanced hydrogenation of Si substrate by atomic hydrogen.

Kp-053 **Influence of Atomic Hydrogen Exposure**

on The Photoluminescence of Si Nanocrystals Embedded in SiO_2 JUNG Yun-Jin, JANG You-Sung, JO Hyun-Ji, YOON Jong-Hwan(*Kangwon National University, Department of Physics.*) In this study, we have investigated the effects of atomic hydrogen plasma treatment on the photoluminescence of Si nanocrystals embedded in a silicon dioxide matrix. Si nanocrystals were formed by annealing the SiO_x (x=1.56) films at 1100 °C for 2 hours in high purity(99.999%) nitrogen gas. Hydrogen exposure is shown to result in an gradual increase of emission intensity, followed by a saturation, as well as a redshift of emission spectra. The saturated value of photoluminescence intensity strongly depends on exposure temperature: the higher the temperature, the larger the saturation value. Time-resolved PL measurements are also shown to result in an increase of luminescence life time. It was also observed that the improvement of photoluminescence characteristics was more efficiently improved by atomic hydrogen exposure than molecular hydrogen.

Kp-054 **GaAs 기판 방향에 따른 Ge Nanowire Heteroepitaxy의 특성 연구** 송 만석, 김 영대, 정 재훈, 김 성수, 김 용, TAN H. Hoe[1], JAGADISH Chennupati[1](*동아대학교 물리학과. [1]Department of Electronic Materials Engineering, Research School of Physical Sciences and Engineering, The Australian National University.*) RTCVD(Rapid Thermal Chemical Vapour Deposition)법에 의해 GaAs (001)과 (111) 기판에 각각 heteroepitaxy한 Ge Nanowires(NWs)를 성장하였다. Ge NWs는 VLS(Vapour-Liquid-Solid) 메커니즘을 통해 성장하며, 촉매로는 지름이 50 nm인 Au colloid 용액을, source gas로는 1% GeH_4(in a H_2 mixture)를 사용하였다. Au 입자들을 정전기적으로 고정시키기 위해 poly-L-lysine 용액에 기판을 1분간 담근 후, Au colloid 용액을 살포하였다. Au와 Ge의 공융점 온도 근방인 섭씨 300 - 380도 사이 온도에서 10 Torr 압력에 1시간씩 성장시킨 샘플은 FE-SEM(Field Emission Scanning Microscope)을 이용하여 Ge NWs의 이미지를 관찰하였다. 각 샘플의 평면과 단면 SEM 이미지를 통해 온도에 따른 Ge NWs의 성장 방향과 모양을 분석하였다.

Kp-055 **Precise Resistivity Measurement Independent Of Contact Resistance Influence And Its Appliance.** KIM Daehyun, RYU Hye-yeon, JI Hyun-jin, KIM Gyu-tae(*고려대학교 전기공학과 나노소자연구실.*) A universal four-contact method, has an advantage of non-existence of contact resistance, is demonstrated by the experiments with carbon nanotubes and ZnO. Ti/Au and Pt are tried to compare the influence of contact resistance between two different metals. These metals are selected to make ohmic contact and Schottky contact originated from their different work functions. For precise experiments, Ti/Au and Pt are separately evaporated to form four-contact electrodes on CNTs or ZnO, and they are measured. This method can be applied to universal resistivity measurement for nanotubes and nanowires.

Kp-056 **0.5μm 표준 공정을 이용한 비휘발성 나노결정 플로팅 게이트 nMOSFET의 메모리 특성** 김 민철, 홍 승휘, 김 혜룡, 최 석호, 김 경중[1](*경희대 전자정보대학 물리 및 응용물리 전공. [1]표준과학연구원.*) 이온빔 스퍼터링을 이용하여 고진공 분위기에서 p-type 실리콘 웨이퍼(100)위에 $SiO_2/SiO_x/SiO_2$ 구조를 가지는 게이트 층을 제작한 후 1100℃에서 20분간 열처리를 통하여 실리콘 나노결정을 형성하였다. 산소의 함유량(x=1.4, 1.6)과 플로팅 게이트의 두께(8nm, 12nm)에 변화를 주어 0.5μm CMOS 표준공정에 맞추어 비휘발성 실리콘 나노결정 nMOSFET 메모리 소자를 제작하였다. 쓰기(programming)시에는 전자가 실리콘 웨이퍼로부터 실리콘 나노결정으로 FN(Fowler-Nordheim) 터널링을 통하여 주입되게 된다. 쓰기/지우기(erasing)에서 문턱전압의 이동은 10/100 ms (±23 V)의 조건하에 약 5 V/4.5 V의 이동을 보임을 확인하였다. 내구성(Endurance cycle)의 실험을 통하여 ~10^4 까지 쓰기/지우기의 실험을 한 결과 문턱전압의 이동이 약 0.2 V로 우수한 성능을 보임을 확인할 수 있었다. 전자 저장 능력(Retention time)의 실험은 상온에서 측정하였으며 그 결과로부터 두 가지 현상이 확인되었다. 첫 번째는 플로팅 게이트의 두께가 두꺼울수록 보다 큰 전하 손실률을 보였고 두 번째로 쓰기 상태의 경우 ~10^6 초까지 약 0.7 V의 문턱전압의 손실을 보인 반면 지우기의 경우 약 2.4 V의 손실을 보였다. 이러한 실험의 결과로 메모리 특성에 대한 메카니즘을 논의하고자 한다.

Kp-057 **PECVD방법으로 제작한 a-SiN_x 박막의 발광 특성** 한 문섭, 장 승훈, 고 창훈, 주 지호, 배 명욱, 정 기영, 박 경완[1](*서울시립대학교 물리학과. [1]서울시립대학교 나노과학기술학과.*) 실리콘 기반의 나노구조물은 차세대 전광소자 개발과 응용에 큰 가능성을 보여주고 있다. 본 연구는 Plasma Enhanced Chemical Vapor Deposition (PECVD)을 이용하여 제작한 Silicon-rich silicon nitride (SRSN) 박막의 발광 특성에 관한 것이다.

PECVD 증착 방법을 이용하여 p-type Si(100) 기판 위에 SiH_4와 N_2의 gas 함량비를 달리하면서, a-SiN_x를 제작하였다. 증착 시 플라즈마 RF power는 25W, Working pressure 0.5 torr 및 기판 온도 350°C로써 각각의 조건을 고정하여 증착하였다. 열처리 환경에 따른 특성 변화를 알기 위해서, 증착된 시료를 각각 대기압의 질소 환경과 Ultra High Vacuum (UHV) 환경에서 열처리 하였다. 질소 환경의 열처리는 Furnace를 사용하였고, UHV환경의 열처리는 electron-beam을 이용하였다. 700°C, 800°C, 900°C의 온도에서 각각 10분, 30분 동안 열처리를 하여, 그에 따른Photoluminescence(PL)을 측정하였으며 SiH_4와 N_2의 함량비의 변화, 열처리 온도, 열처리 시간에 따라 발광파장의 PL 특성의 변화를 살펴봄으로써, 증착과 열처리 조건이 PL특성에 어떠한 영향을 미치는지에 대하여 알아보았다. 또한 원자레벨의 결합 구조가 PL특성과 어떠한 관계가 있는지 확인하기 위하여 X-ray photoelectron spectroscopy (XPS) 분석을 이용하였다.

Kp-058 **The effects of acid treatments on the electrical transport characteristics of single-walled carbon nanotubes** KIM Yongsun, YIM Jonghyuk, PARK Ji-Yong(*아주대학교, 에너지시스템학부.*) Acid treatments are often applied to single-walled carbon nanotubes (SWCNTs) for purifications and sidewall functionalizations. In this study, we investigated how the acid treatments affect transport characteristics of SWCNTs. Devices with individual SWCNTs and networks of SWCNTs are fabricated and the transport characteristics before and after the acid treatments are studied by comparing current-voltage(IV) characteristics. Local characterizations using an atomic force microscope, such as electrostatic force microscopy and scanning gate microscopy are also performed to elucidate local changes and their correlations to the IV characteristics observed.

Kp-059 **Diffusion Movement Of Ge Inside Si Of SOI Wafer And Bulk Wafer Via Oxidation** LEE HUNJOO, HONG SEOKHOON[1], LEE GONSUB[2], PARK JEAGUN[3](*한양대학교 전자통신컴퓨터공학부 나노공학과 나노SOI공정연구소. [1]한양대학교 전자통신컴퓨터공학부 전자공학과 나노SOI공정연구소. [2]한양대학교 나노SOI공정연구소. [3]한양대학교 전자통신컴퓨터공학부 나노SOI공정연구소.*) The functional wafer that is different with preexistence bulk wafer is requested as the channel length of n-MOSFET becomes less than 60 nm. The condensation method is the way that is the most trust and economical to make the SGOI wafer. The mechanism of diffusion movement inside Si via oxidation is not find out clearly in the condensation method in spite of a lot of study. If oxidation process is progressed, Si in SiGe reacts with O2 and Ge is accumulated. In case of SiGe layer has initial Ge concentration 20% and 50nm thickness is oxidized, it"s finial concentration is 58.8% and it becomes optimization. However the more oxidation makes the less concentration and Ge profile can not keep the Gaussian distribution because reverse diffusion of Si_sub"s Si is happened and it makes dislocations. On the other hand the structure of SiGe/SOI has opposite result. In initial oxidation Ge profile is graded and dislocations happened because top-Si is thin so Si in SiGe and top-Si layers reacts at the same time. In oxidation process top-Si is disappeared, SiGe and top-Si are one SiGe layer. Diffusion of Ge is not happened anymore because of BOX layer. Ge is condensed and re-arrangement of crystal is happened via the heat in oxidation so SGOI has high quality and concentration is made.
*This work was supported by the Korea Science and Engineering Foundation (KOSEF) through the National Research Lab. Program funded by the Ministry of Science and Technology (No. M10400000436-06J0000-43610).

Kp-060 **Controlled Vapor-Solid Syntheses of NiSi Nanowires and Their Metallic Properties** KIM Cheol-Joo, RYU Kyung-Guk, KANG Kibum, JANG Hyun-Myung, JO Moon-Ho(*Department of Materials Science and Engineering, Pohang University of Science and Technology (POSTECH), San 31, Hyoja-Dong, Nam Gu, Pohang, Gyungbuk 790-784, Korea.*) One-dimensional metallic nanostructures offer challenging opportunities to investigate for their possible applications into interconnects in electronic circuitry and field emitters in field emission display. Among various metallic nanowires, metallic silicide nanowires can be promising candidates, mainly due to the compatibility of their growth with silicon processing technology. Among several transition metal silicides, Ni-silicide are known to possess intrinsically low resistivity at low dimensions compared to the others, thus provides practical advantages. Here we report controlled syntheses of single-crystalline Ni-silicide nanowires at low temperatures (~ 400 °C) by a simple vapor-solid chemical reaction on various substrates, such as SiO_2/Si, glass and Indium-Tin oxide (ITO) substrates.

By employing chemical vapor deposition (CVD) of a SiH_4 gas precursor on predeposited Ni thin films, we have reproducibly directed the dimensionality of Ni-silicides from thin films and nanowires, as well as their phases. In this study, with the close observations of the morphological evolution of Ni-silicide nanowires at the optimized growth conditions, we provide and discuss the nanowire growth mechanism based on one-dimensional Ni diffusion during the vapor-solid reaction at low supersaturation limit. Single-crystalline Ni-silicide nanowires in this study exhibit typical metallic behaviors, and show promising field-emission properties comparable to industrially relevant field-emitters based on carbon nanotube pastes. We suggest that our simple method to spontaneously grow Ni-silicide nanowires by metal induced chemical vapor deposition can provide a practical strategy to fabricate metallic nanostructures based on bottom-up approaches.

Kp-061 **Crystal Orientation Effect on the Electron Mobility in Strained Si grown-on SiGe-on-Insualtor (SGOI) n-MOSFET** MOON HuiChang, BAEK Ji-Young, SHIM Tae-Hun, PARK Jea-Gun(*Nano SOI Process Laboratory, Hanyang University.*) Aggressive scaling of complementary metal-oxide-semiconductor (CMOS) technology requires a high current drivability to speed up the circuit speed. Mobility enhancement by strain and substrate orientation (110) offer the new method to increase drive currents without suffering from gate leakage due to gate dielectric scaling. It has been reported that the electron mobility is highest on (100) substrate while hole mobility is highest on (110) substrate. Out-of-plane effective mass (m_z) is the key parameter that makes the difference in mobility. Many researcher have focused on (100) substrate because it is known that the (100) strained Si SGOI n-MOSFET has 1.6~1.8 higher mobility than bulk MOSFETs. In our study, we investigated the electron mobility of strained Si SGOI n-MOSFETs on (110) substrate. We theoretically calculated that the electron mobility on (110) strained Si SGOI n-MOSFETs was about 1.2 higher than bulk (110) n-MOSFETs. In addition, We demonstrated the effect of strained Si SGOI based on (110) orientated substrate when the high hole mobility was requested. Finally, we researched the possibility that (110) strained Si SGOI would become to be an alternative to CMOS technology.
*This work was supported by the Korea Science and Engineering Foundation (KOSEF) through the National Research Lab. Program funded by the Ministry of Science and Technology (No. M10400000436-06J0000-43610).

Kp-062 **The Influence of Nano-Si Thickness and Ge Concentration on Self-heating Effect in Sub-60 nm Ultra-thin Body Silicon-on-insulator and Strained Si SiGe-on-insulator n-MOSFETs** KIM Seong-Je, LEE Yong-Seon, SHIM Tae-Hun, PARK Jea-Gun(*Nano-SOI Process Laboratory, Hanyang University.*) As the device scale is less than 60 nm, strained Si grown on SiGe-on-insulator (ε-Si SGOI) n-MOSFET which has under 20 nm top Si layer has been introduced. It is a promising device for the next high-speed device technology. Because this shows higher electron mobility resulting from less phonon scattering between conduction valleys. Since ε-Si SGOI n-MOSFETs have buried oxide and $Si_{1-x}Ge_x$ compound material layer, it generate heat during operation by self-heating effect. Consequently, electron mobility and drain current decrease by increasing phonon scattering in the nano-scale device. Our approach was illustrated with a thermal mode, which was validated by self-consistent 2-dimensional numerical simulations. We investigated the self-heating effect considering size effect in ultra-thin body (UTB) structure (~10 nm) through phonon scattering and electron mobility analysis. In addition, we examined the self-heating effect and the electron mobility of ε-Si SGOI n-MOSFET as a function of Ge concentration. It was observed that electron mobility enhancement ratio of ε-Si SGOI was 1.1~1.3 times higher than conventional SOI n-MOSFET under self-heating condition. Finally, we suggested merits, demerits, and improvement technologies.
*This work was supported by the Korea Science and Engineering Foundation (KOSEF) through the National Research Lab. Program funded by the Ministry of Science and Technology (No. M10400000436-06J0000-43610).

Kp-063 **Fabrication of low cost and large area nano stamps using optical lithography** CHOI BumHo, LEE JongHo, KIM YoungBack, YU YunSeop[1](*Energy and Applied optics team, Korea Institute of Industrial technology. [1]Hankyoung National University.*) Nano imprint lithography has been extensively studied due to its

wide variety of application to nano scale semiconductor and display area. Nanometer scale patterns can be successfully defined using nano imprint technology with high throughput and reliability. Although nano imprint lithography can be used to fabricate nano scale devices, it suffer from high cost to define stamps since, in general, nano stamps have been made by electron beam lithography system. In order to apply nano imrpint lithography to mass production, the cost needed to fabricate nano stamps nust be reduced. In this study, we have successfully demonstrate nano stamps using optical lithography and side-wall method. Minimum feature size of 50 nm was defined on 4-inch Si and quartz wafer level using conventional optical lithography technique by controlling process conditions. The nano patterns on stamps was replicated by thermal imprinting and UV embossing on Si substrate. Our study opens up possibility to make low cost, large area nano stamps without nano patterning tools.

Kp-064 **유기 절연막을 이용한 역스태거드 다결정 실리콘 트랜지스터 제작** 안 기완, 박 원훈, 강 동한[1], 오 재환, 배 중호, 천 준혁, 장 진(*경희대학교 정보디스플레이학과. [1]경희대학교 물리학과.*) 최근 차세대 디스플레이로 각광받고 있는 능동형 유기발광 다이오드(AMOLED)의 Back Plane 트랜지스터 제작에 비정질 실리콘(Amorphous Silicon)과 다결정 실리콘(Polycrystalline Silicon)을 이용한 연구가 활발히 진행되고 있다. 두가지 방법은 각각의 장,단점을 가지고 있다. 우선 비정질 실리콘으로 트랜지스터를 제작시 공정 단순화를 통한 재료비 절감효과를 기대할 수 있으나, 비정질 실리콘 고유의 특성변화에 따른 신뢰성 결함으로 장시간 구동시 화면이상을 초래하는 단점이 있다. 반면에 다결정 실리콘으로 트랜지스터를 제작시 10 ~ 400 cm^2/Vs의 높은 전계 효과 이동도(Field Effect Mobility)를 가지게 되므로 유리기판 위에 구동회로까지 집적할 수 있으며, 다결정 실리콘의 우수한 특성 안정성으로 인하여 장시간 구동시에도 안정적인 화면을 구현할 수 있는 장점이 있다. 그러나 제조공정이 복잡하여 수율 감소 및 재료비 증가 등의 단점이 있다. 본 연구에서는 비정질 실리콘과 다결정 실리콘의 장점만을 접목시킨 공정을 적용하여, 공정의 단순화 및 높은 신뢰성의 안정적인 트랜지스터를 제작하였다. 비정질 실리콘의 역스태거드 공정을 기준으로 진행하되, 다결정 실리콘 형성을 위하여 Active층 증착후 Ni금속을 이용한 금속 유도 결정화(Ni-mediated Crystallization)를 진행하였다. 따라서 비정질 실리콘의 단순한 공정의 장점과, 다결정 실리콘의 특성 우수성을 동시에 얻을수 있는 방법을 연구하였다. 또한 Gate 절연물질로는 회전도포를 통한 유기물질 (SOG)을 적용하여, 기존의 무기물질 적용시의 플라즈마를 사용해야 하는 복잡한 공정을 상온에서의 간단한 공정으로 개선 연구 하였다.

Kp-065 **Characteristics of Germanium Thin Films Deposited by Atomic Layer Deposition.** 이 규현, 장 혁규, 이 주영, 김 현창, 송 용원[1](*메카로닉스. [1]한국산업기술대학교.*) Germanium thin film has been used as a buffer layer between Si substrate and compound semiconductor device and is recently applied to PRAM that is gaining public attention as the next generation memory. In this work, we investigated the characteristics of Ge thin films which was prepared from n-$BuGeH_3$ as a precursor and NH_3 as a reactant gas by using atomic layer deposition (ALD). The n-$BuGeH_3$ was synthesized using $GeCl_4$, nBuMgCl and $LiAlH_4$ through two step chemical reaction. Ge precusor with 6N purity was obtained by the fractional distillation. The Ge thin films were grown on 20 nm-thick TiN wafer deposited by a conventional CVD and their physical properties were studied by using XRD, SEM and AES.

Kp-066 **Growth of Carbon Nanotubes on Substrate with a-Si** 유 제황, 김 기서[1], 민 경우, 이 창석, 김 기환, 문 종현, 박 규창, 장 진(*경희대학교, 정보디스플레이학과 및 차세대디스플레이연구센터. [1]경희대학교, 물리학과 및 차세대디스플레이연구센터.*) 탄소나노튜브(CNTs) 는 다양한 형태와 물성을 지닌 특성으로 인하여 나노전자 산업분야로 활발하게 응용되고 있다. 그 중에서도 낮은 임계전계에서의 높은 전자방출 특성으로 전자방출소자(electron emitter) 로의 연구가 활발히 이루어지고 있다. 본 연구팀에서는 실리콘기판 위에 레지스트패터닝법(resist assisted patterning, RAP) 을 이용하여 CNTs 의 선택적 위치제어 성장법을 개발하여 전자소자 응용 가능성을 확인하였다. 본 실험에서는 실리콘기판 대신에 유리기판을 사용하여 CNTs 를 성장함으로써 공정의 저가격으로 인한 다양한 소자로의 상용화가 기대된다. 특히 유리기판에 위치제어 된 CNTs 를 성장하기 위하여 비정질 실리콘(a-Si) 을 촉매 금속의 확산방지 및 전계방출시 저항층으로 이용하였다. 성장온도는 580 ℃ 이하에서 하였고, 반응가스는 아세틸렌(C_2H_2) 을 주입하고 플라즈마화학기상증착법(PECVD) 을 이용하여 15 분간 성장하였다.

Kp-067 **3-단계 성장법을 이용한 GaSb/Si(100)**

박막성장 김 문덕, 노 영균, 박 세린, 오 재응[1], 김 영헌[2](*충남대학교 물리학과. [1]한양대학교 전기전자제어계측공학과. [2]한국표준과학원.*) Sb 기반 화합물 반도체는 고속전자소자 및 장파장 영역의 광소자 응용이 가능한 물질로서 대면적의 값싼 Si 기판위에 성장하려는 연구에 관심이 집중되고 있다. Sb 기반 물질들 중 가장 안정한 물질인 GaSb는 Si(100) 기판과 약 12%의 큰 격자부정합을 가지고 있으며 비극성/극성물질의 계면에서 발생되는 결함에 의해 박막성장에 어려움이 있다. 본 연구에서는 Si(100) 기판위에 molecular beam epitaxy 법으로 성장된 GaSb의 성장 구조에 따른 박막 특성을 조사 하였으며 박막의 구조적 특성 및 광특성을 Reflection high-energy electron diffraction, double crystal x-ray diffraction (DCXRD), atomic force microscopy, scanning electron microscopy, photoluminescence 등으로 조사하였다. 초기 성장 시 격자부정합에 의해 발생되는 3차원 성장과 결함 발생을 줄이기 위해 성장온도를 각각 다르게 하여 적층하는 3-단계 성장법을 사용하는 경우 GaSb 박막의 DCXRD 반치폭이 450 arcsec 로 결정성이 가장 높았으며 GaSb/Si(100) 구조에서 3-단계성장법의 효과에 대해 논의 하였다.

Kp-068 **RHEED 분석을 통한 AlN 성장 조건에 따른 변형 에너지 연구** 김 문덕, 박 세린, 오 재응[1], 김 송강[2], 정 관수[3](*충남대학교 물리학과. [1]한양대학교 전기전자제어계측공학과. [2]중부대학교 정보통신학과. [3]경희대학교 전자공학과.*) Reflection high-energy electron diffraction (RHEED)는 박막 성장 시 결정의 최상층 표면 구조와 박막 성장 과정을 실시간으로 분석할 수 있는 장치이다. RHEED intensity 변화를 이용하여 성장 파라미터에 따른 나노 구조의 성장 과정을 관찰할 수 있으며, 이를 통하여 격자상수의 변화 과정을 분석할 수 있다. 본 연구는 molecular beam epitaxy 법으로 Si(111) 기판 위에 AlN를 성장시켰으며 RHEED를 통하여 성장 파라미터에 따른 변형 에너지를 조사하였다. AlN는 GaN계 기판 성장 시 기판과의 격자부정합 차이를 극복하기 위해 일반적으로 사용되는 완충층이다. Al 흡착과 nitridation으로 변형력이 모두 완화된 AlN 격자상수를 얻을 수 있으며, 이는 nitridation 시간의 영향을 가장 크게 받는 것으로 조사되었다. 또한 기판 온도 550~750 ℃인 경우와 Al 흡착 시간 10~30초인 경우도 nitridation 시간의 영향이 크게 작용하였음을 관찰하였다.

Kp-069 **갈륨비소 기판위에 MBE기술로 자발형성된 나노 크기의 갈륨 금속 덩어리의 구조적 특성** 임 주영, 송 진동[1], 최 원준[1], 양 해석[2], 김 종수[3](*중앙대학교,물리학과;KIST. [1]KIST. [2]중앙대학교,물리학과. [3]광주과학기술원,고등광기술연구소.*) 초고진공의 환경에서 갈륨비소 기판상에 갈륨 금속을 증착하여, 자발형성 나노 금속 덩어리를 형성하여 이의 구조적 특징을 분석한다. 모든 실험은 초고진공 MBE에서 진행되었다. 갈륨비소 기판상의 산화물을 약 600도에서 제거한후, 580도에서 ~100 nm 두께의 갈륨비소 버퍼층을 형성하였다. 기판의 온도를 갈륨 덩어리 형성온도까지 내린 후, 챔버의 진공이 1 x 10^{-9} torr이하로 떨어지기를 기다려, 0.14nm/s의 갈륨비소 성장률의 flux에 해당되는 갈륨 금속을 10초간 주입하였다. 표면에 자발 형성된 나노 크기의 갈륨 금속의 구조적 특성을 측정하기 위해 Atomic force microscope를 사용하였다. 측정 결과에 의하면, 갈륨 형성의 온도(240 ~410도)가 올라감에 따라, 기판상의 나노 갈륨 금속 덩어리의 밀도는 낮아지는 단조감소의 경향이었으나 (800 ~ 20 x 10^8 /cm^2), 높이 및 너비의 크기는 300도 까지는 단조증가의 경향을 보이고 300도 이상에는 단조 감소의 경향을 보였다. 더욱이 380, 410도의 경우에는 가운데가 빈 도너스 모양의 갈륨비소 금속 덩어리의 형태를 보였다. 밀도의 단조 감소는 기판의 온도가 증가함에 따른 표면 갈륨 금속의 이동도가 커져 나타난 현상으로 보이고, 당연히 크기 및 너비도 단조 증가해야 한다. 크기 및 너비의 이상행동의 원인은 기판의 온도가 올라감에 따라 표면의 갈륨비소가 분해되어 비소가 나노 크기의 갈륨 덩어리와 결합되어, 도너스 형태의 모양을 띠게 되는 것으로 판단된다. 본 금속 기판은 이후 5족의 주입을 조절하여 다양한 조성의 양자점을 제작하는 기판으로 이용이 가능하다.

Kp-070 **SiH_4 flow rate dependence of dielectric cap layer induced impurity-free vacancy diffusion of InGaAs/InGaAsP MQWs** 이 희관, 유 재수, 정 관수(*경희대학교 전자전파공학과.*) InGaAs/InGaAsP 다중 양자우물 구조에서 PECVD (plasma enhanced chemical vapor deposition) 공정시 SiH_4 유압을 20 sccm 에서 300 sccm 변화시키면서 증착된 SiO_x와 SiN_x capping층들의 impurity-free vacancy diffusion (IFVD)에 대한 영향을 조사하였다. IFVD에 의한 변화를 관찰하기 위해 상온 PL (photoluminescence)을 사용하였고, spectroscopic ellipsometry에 의한 dielectric층들의 특성을 분석하였다. SiH_4 유압의 변화는 SiO_x와 SiN_x층의 porosity에 영향을 주는데, 낮은 SiH_4 유압이 dielectric 층을 더 porous하게 만든다. 그러한 dielectric 층의 porosity가 양자우물 혼합을 통한 vacancy의 out diffusion을 강화하여 시료의 PL peak 파장을 blueshift 시킨다. 따라서 blueshift의 크기는 SiO_x와 SiN_x dielectric 층의 porosity에 비례하게 되고,

SiH_4 유압의 20 sccm에서 300 sccm으로 변화시키면서 SiO_x capping 층의 경우 850 °C, 30초 동안의 rapid thermal annealing (RTA)후, 그러한 blueshift는 98 nm, SiN_x capping 층의 경우 75 nm 만큼 가변되었다. 또한 20 sccm SiH_4에 의한 증착된 SiO_x capping을 가진 시료가 850 °C, 30초 동안의 RTA후, 138 nm (74 meV)의 blueshift를 나타냈다. 이는 SiH_4 유압을 변화시킨 dielectric층을 이용한 선택적 IFVD의 실현 가능성을 보여준다.

Kp-071 **Optical Characterization of InGaN/GaN Quantum Well Structure with Si-doped Barriers** 한 유대, 박 재규, 이 동한(*충남대학교.*) InGaN/GaN 양자우물은 blue, green, near UV를 효율적으로 발광하기 때문에 UV-LD 나 white LED등 의 제작을 위해 활발한 연구가 진행되고 있다. 하지만, InGaN/GaN 양자우물은 Al_2O_3 기판과 GaN, InGaN 사이의 큰 격자상수 차이에 의한 piezoelectric field와, indium에 의한 강한 localization 때문에 물성을 이해하는데 어려움이 있다. 특성이 좋은 소자를 제작하기 위해서는 물성을 이해하는 것이 반드시 필요하며, 본 연구에서는 Si:GaN barrier가 well내부의 quality, localization 및 piezoelectric field에 어떤 영향을 주는지 조사하였다. 시료는 Si doping이 안된 것과 Si doping 농도가 각각 $2.5 \times 10^{17}/cm^3$, $3 \times 10^{18}/cm^3$인 5주기 InGaN/GaN 양자우물 구조로, MOCVD (metal organic chemical vapor deposition)방법으로 성장하였다. 광학적 특성 분석을 위해 온도나 여기세기에 따른 photoluminescence(PL)를 측정하였으며, femto-second Ti-sapphire laser의 second harmonic generation과 TCSPC(Time correlated single photon counting)를 이용해 시간에 따른 PL(Time reserved PL : TR-PL)을 측정하였다. PL 측정 결과 Si doping 농도가 높을수록 peak이 단파장으로 이동하면서 sharp 한 것을 볼 수 있는데 이를 통해 Si의 농도가 높을수록 excess carrier가 well 내부의 electric field screen에 기여하고 localization이 약해지는 것을 알 수 있다. TR-PL 또한 4 K에서 Si doping 농도가 높을수록 짧아지고 single decay하고 있으며, 이는 excess carrier에 의한 piezoelectric field screening에 의해 hole과 electron간 overlap이 향상되었기 때문이다. 온도가 상승함에 따라 TR-PL을 측정해보면 Si doping농도가 높은 샘플일수록 decay time의 감소폭이 줄어들고 있다. well 내부에 non radiative center의 density가 높을수록 decay time은 큰 폭으로 감소하며 internal efficiency는 낮아진다. 온도에 따른 PL yield 또한 Si doping 농도가 높을수록 저온대비 상온에서 수치가 높아지고 있으며 위의 사실을 뒷받침하고 있다. 본 연구는 LG전자에서 시료를 제공해 주었다.

Kp-072 **Investigation of Self-assembled InAs/AlAs Quantum Dots by Photoreflectance and Photoluminescence.** 심 준형, 조 현준, 고 병수, 김 태훈, 배 인호(*영남대학교 물리학과.*) We study self-assembled InAs quantum dots (QDs) embedded in an AlAs matrix grown by molecular beam epitaxy(MBE) on n-GaAs(100) substrate. Temperature-dependent photoreflectance(PR) and photoluminescence(PL) measurements were carried out in temperature range from 16 to 300 K. At the low temperature, the major features of PL spectra are corresponding to the InAs QDs and GaAs. As the temperature increases, the peak related to InAs QDs are relatively smaller than the peak related to GaAs due to the higher thermal activation energy. In the PR spectra, we found that the InAs wetting layer close to the GaAs band gap. The present results measured by contrast of PR and PL spectra.

Kp-073 **Influence of Ultraviolet Exposure During the Low-Temperature Annealing of GaMnAs Ferromagnetic Semiconductors** KIM Jungtaek, SHIN DongYun, YOO Taehee, KIM Hyungchan, LEE Sanghoon, LIU X.[1], FURDYNA J. K.[1](*Physics Department, Korea University, Seoul Korea. [1]Physics Department, University of Notre Dame IN, USA.*) It has been reported that low-temperature annealing or light illumination significantly changes the magnetic properties of GaMnAs ferromagnetic semiconductor. We have investigated combined effects of thermal and optical treatments by performing annealing of the GaMnAs under ultraviolet (UV) exposure. Two GaMnAs samples were annealed at 250 for 1 hour in air with and without UV exposure. The magnetic properties of the both as-grown and annealed GaMnAs samples were investigated by magnetotransport measurements. The temperature scan of resistance revealed significant increase of Curie temperature (Tc) in both annealed samples. The angular dependence of Planar Hall Effect (PHE) was also measured to investigate magnetic anisotropy property. The cubic (K_c) and uniaxial (K_u) anisotropy constants are obtained from the analysis of angular dependence of planar Hall resistance data using the magnetic free energy equation. The uniaxial anisotropy contribution in the as-grown sample is negligible as compared to cubic one, which results in the easy axes of sample along <100> crystallographic directions. The easy axis initially pinned along <100> directions in as-grown sample changed toward [110] direction in an-

nealed samples indicating increase of uniaxial anisotropy contribution by thermal treatment. Interestingly, the value of K_u/K_c was bigger in the annealed sample with UV exposure than that obtained from annealed sample without UV exposure. This fact clearly indicates that the UV exposure during annealing process significantly affect the magnetic anisotropy properties of GaMnAs ferromagnetic semiconductors.

Kp-074 **Magnetic Anisotropy Properties of GaMnAs Ferromagnetic Semiconductor Under Critical Strain Condition** SON Hyunji, CHUNG Sunjae, YEA Sun-young, LEE Sanghoon, LIU X.[1], FURDYNA J.K.[1](*Physics Department, Korea University, Seoul Korea.* [1]*Physics Department, University of Notre Dame, Notre Dame IN, USA.*) It is known that the magnetic anisotropy properties of GaMnAs strongly depend on the strain caused by the difference in lattice parameters between the GaMnAs layer and the buffer. For example, GaMnAs layer grown on GaAs buffer has in-plane anisotropy due to the compressive strain, while the GaMnAs layer deposited on the materials with larger lattice parameter has out-of-plane anisotropy due to tensile strain. In the GaMnAs with critical strain condition, the transition between in-plane and out-of-plane anisotropy could be manipulated by other external means. To investigate such possibility, we have used GaMnAs film under small tensile strain, which was achieved by growing GaMnAs layer on GaInAs buffer. The planar Hall effect (PHE) measurement revealed that in-plane anisotropy is dominant factor and magnetic easy axes lies along <100> crystallographic directions. The in-plane magnetic anisotropy fields were obtained by analyzing the angular dependence of planar Hall resistance (PHR) based on the magnetic free energy model. Moreover, the transition of magnetic anisotropy from in-plane to out-of-plane was observed when the magnetic field was applied along perpendicular direction to the sample surface. This fact indicates that the magnetic easy axis is changed from in-plane to out-of plane by changing the position of minimum magnetic energy along vertical direction with magnetic field. This study has demonstrated the possibility of controlling the magnetic anisotropy of GaMnAs by external magnetic field.

Kp-075 **Effect of Shape Anisotropy on the Domain Switching Phenomena in (Ga,Mn)As Ferromagnetic Semiconductors** YOO Taehee, SHIN DongYun, KIM Jungtaek, KIM Hyungchan, LEE Sanghoon, LIU X.[1], FURDYNA J.K.[1](*Physics Department, Korea University, Seoul Korea.* [1]*Physics Department, University of Notre Dame, Notre Dame IN, USA.*) In GaMnAs ferromagnetic semiconductors with in-plane magnetic anisotropy, cubic and uniaxial anisotropy constants are the decisive factors in determining the direction of magnetization. A substantial change in the magnetic properties can be introduced by shape anisotropy, which becomes increasingly important as the device size is miniaturized. In order to understand this effect, we have fabricated two Hall bar devices with different channel width, which are 10μm and 300μm, respectively. We have measured angular dependence of planar Hall resistance (PHR), from which the detail informations on the magnetic anisotropy properties were obtained. Interestingly, the magnetization reorientation behavior is observed to be significantly different in the two devices with different size. Specially, the transition from two step to one step switching behavior occurs at different applied field angles in the two devices. This observation clearly indicated the existence of shape anisotropy effect in the smaller sized device. The amount of shape anisotropy constant was obtained from the difference in the switching fields observed for two size Hall bar devices.

Kp-076 **Thickness Dependent Magnetic Properties of GaMnAs Ferromagnetic Semiconductor Film** YEA Sun-young, CHUNG Sunjae, SON Hyunji, LEE Sanghoon, LIU X.[1], FURDYNA J.K.[1](*Physics Department, Korea University, Seoul Korea.* [1]*Department of Physics, University of Notre Dame.*) It has been reported that Curie temperature (Tc) and Coersivity (Hc) depend on sample thickness in GaMnAs film. In this study, we have investigated thickness dependence of magnetic properties of GaMnAs film by studying Planar Hall Effect (PHE) in magnetotransport measurement. First, we have grown 480 nm thick GaMnAS film and applied area selective chemical etching process to achieve 5 different film thicknesses in a single GaMnAs specimen. This sample preparation process guarantees us to eliminate influence of sample to sample fluctuation occurring from different growth runs. The same scale of Hall-bar was patterned on the each layer by using photolithography and chemical wet etching. In order to reduce the effect from non-uniform Mn distribution along the growth direction in the as-grown sample, we also prepared different

thickness of film from annealed GaMnAs sample. We have found very systematic change of both Curie temperature and Coresive field with decreasing sample thickness in both as-grown and annealed sample. This experiment clearly demonstrated the fact that the magnetic properties of GaMnAs film strongly depend on the film thickness.

Kp-077 **Structural and electrical properties of InAlGaN/GaN heterostructures** 김 서군, S. nagarajan, 최 영진, 이 용석, M. Senthil Kumar, 정 상조, 서 은경(*전북대학교 반도체과학기술학과/반도체물성연구소.*) InAlGaN quaternary alloy has emerged as the material for potential application in short wavelength optoelectronic devices. In this study, InAlGaN/GaN heterostructures with various Al compositions have been grown on sapphire substrate using metal organic chemical vapor deposition technique. We have observed the formation of Two-Dimensional Electron Gas (2DEG) at InAlGaN/GaN interface. Atomic force microscopy reveals a smooth surface with formation of hexagonal pits. The size and the density of hexagonal pit increase with increasing Al mole fraction. Due to competitive adsorption between Al, Ga and In atoms, there is a higher Al incorporation efficiency towards InAlGaN quaternary epilayer which leads to decreases the thickness from 100 nm to 40 nm with increasing TMAl flow. When Al increases from 7% to 16%, the sheet carrier density increases due to increase of background donor concentration.
*Acknowledgements: This work was supported by the Korea Research Foundation Grant funded by the Korean Government (MOEHRD)" (KRF-2005-005-J07501).

Kp-078 **Growth and Characterization of $In_{0.22}Ga_{0.78}N$/GaN MQW for green LED with different well thickness** 이 용석, 박 재영, 우 승희, 정 현, 김 희윤, 홍 창희, 서 은경(*전북대학교 반도체과학기술학과/반도체 물성연구소.*) 최근 LCD back-light를 위한 광원으로써 Green LED의 효율을 향상시키기 위한 많은 연구가 진행되고 있다. 본 연구에서는 Green LED의 내부양자효율을 향상시키기 위해 높은 농도의 In 함량을 가진 InGaN well layer의 두께를 변화하여 그에 따른 구조적• 광학적 특성을 연구하였다. 4주기를 갖는 InGaN/GaN MQWs 구조는 MOCVD를 이용하여 성장하였고 InGaN well 두께는 각각 26A°, 28A°, 30A°, 32A°, 34A°로 변화시켰으며 이에 따른 GaN barrier의 두께는 18.5nm로 고정하였다. 측정결과 InGaN well 두께가 증가함에 따라 상온 Photoluminescence 피크 강도는 감소하였으며 피크 위치는 red-shift 하였다. 이에 따른 원인을 HR-XRD, TR-PL 등을 통해 분석하였다.
*Acknowledgements This work was supported by Grant. No. R01-2004-000-10390-0 from the Korea Science and Engineering Foundatation.

Kp-079 **On the Enhanced Light Emission Characteristics of Green InGaN/GaN MQWs with High Temperature GaN Barrier** M. Senthil Kumar, 박 재영, 김 서군, 정 상조, 홍 창희, 이 형재, 서 은경(*전북대학교 반도체과학기술학과/반도체물성연구소.*) Currently, vast interest is being shown on the development of high efficiency InGaN based green light emitters. Because, at high In incorporation in InGaN layer necessary for green emission, the quantum efficiency decreases severely due to the generation of harmful defects like V-pits and also the strong strain induced built-in field in the quantum well. In this report, we have shown that the high temperature GaN barrier growth could improve the structural and optical characteristics of green emitting InGaN/GaN multi-quantum wells. From high resolution x-ray diffraction studies, high temperature barrier growth is found to improve crystalline as well as interface quality of InGaN/GaN super lattices. Also, V-pit density and surface roughness decreased with increase of GaN barrier growth temperature. As a result, an enhancement in the internal quantum efficiency has been observed using low temperature photoluminescence technique.
*Acknowledgements This work was supported by the Korea Research Foundation Grant funded by the Korean Government (MOEHRD)"(KRF-2005-005-J07501).

Kp-080 **Improvement of optical properties of Green InGaN/GaN multi-quantum well with various growth parameters** 우 승희, 박 재영, 김 희윤, 이 용석, 이 형재, 홍 창희, 서 은경(*전북대학교 반도체과학기술학과/반도체물성연구소.*) InGaN/GaN MQW structures are used for active layers in high efficiency LEDs. In this work, we optimized the growth conditions such as growth rate, growth temperature of well and barrier layers, and III/V ratio in order to reduce V-shaped defect and In cluster formation in 4 periods of MQW structures. Structural properties of the grown InGaN/GaN MQWs have been studied by using High Resolution

X-ray diffraction (HR-XRD), and Atomic Force Microscopy (AFM). When the growth temperature increases from 740°C to 910°C, a reduction of V-defect density is observed, it leads to the improvement in internal quantum efficiency. At a low growth rate of MQWs, the photoluminescence (PL) peak intensity is increased.
*This work has supported by Grant No. R01-2004-000-10390-0 from the Korea Science and Engineering Foundation (KOSEF)

Kp-081 **Optical Properties of InAs/GaAs Quantum Dots Heterostructures** 김 준오, 이 상준, 노 삼규, 최 정우[1], 이 규석[2](*한국표준과학연구원 첨단산업측정그룹. [1]경희대학교 전자정보학부. [2]한국전자통신연구원.*) In this work, We report on oscillations in the Photoreflectance (PR) spectra of InAs wetting layer (WL)/GaAs and InAs-QD/ GaAs hetrostructures grown on SI-GaAs substrates by using a molecular beam epitaxy (MBE) technique. An oscillatory feature occurs in the energy range below the bandgap of GaAs, On the other hand, undoped bulk GaAs and InAs WL/GaAs samples grown on SI-GaAs substrates do not show such oscillations. These results estimate that the oscillations in the PR spectra are due to the interference effect of the reflected light beams, one reflected from the interface of GaAs/SI-GaAs substrate and the other reflected from the InAs-QD/GaAs hetrointerface. In addition, Franz-Keldysh oscillation (FKO) were observed in the PR spectra at energy higher than the GaAs band gap. This result indicate that the FKO in the PR spectra are due to the bult-in electric field at the InAs/GaAs hetrointerface.

Kp-082 **Self assembled InAlGaN nanostructures grown by using MOCVD** S. Nagarajan, 최 영진, 우 승희, M. Senthil Kumar, 정 상조, 홍 창희, 서 은경(*전북대학교 반도체과학기술학과/반도체물성연구소.*) InAlGaN offers many possibilities for optoelectronic applications in the blue and ultraviolet emission range. Since band gap and lattice constant can be adjusted independently, the following reduction of strain and defects in the active layer will enhance the characteristics of nitride based devices. In this work, the formation self-assembled InAlGaN nanostructures have been grown by Metal Organic Chemical Vapor Deposition (MOCVD). It is found from atomic force microscopic studies that the size of the nanostructure is controlled by TMAl flow rate. When TMAl flow increases from 1 μmol/min to 10 μmol/min, InAlGaN nanostructure height and width increase from 75 to 91 nm, and 2 to 13 nm, respectively. A maximum density of 2.2 ´10^8 cm^{-2} has been observed for TMAl flow rate of 10 μmol/min. Phase separation in InAlGaN quaternary has been observed for high TMAl flow by using Raman spectroscopy.
* Acknowledgements This work was supported by the Korea Research Foundation Grant funded by the Korean Government (MOEHRD) (KRF-2005-005-J07501).

Kp-083 **Tuning Optical Properties of InAs Quantum Dots with Various InGaAs Structures by Post Growth Rapid Thermal Annealing** PARK Ho Jin, KIM Jongho, KIM Min Soo, JEON Sumin, KIM Jong Su[1], CHO Guan Sik, RYU H. H., JEON Minhyon, LEEM Jae-Young(*Inje University, School of Nano Engineering. [1]Advanced Photonics Research Institute, Nano Photonics Group.*) We have investigated the effects of rapid thermal annealing on the optical properties of the InAs quantum dots (QDs) with different InGaAs structures using photoluminescence (PL). The PL spectra from the InAs QDs subjected to annealing treatment at 750 ℃ in nitrogen ambient showed blue-shift and significant linewidth narrowing of the PL peak, compared with the as-grown samples. It can be attributed to the interdiffusion between the InAs QDs and the InGaAs layer and to the size homogeneity of the QDs. Especially, the InAs QDs deposited between 1-nm-thick $In_{0.15}Ga_{0.85}As$ and 7-nm-thick $In_xGa_{1-x}As$ ($x=0.15$ and $0.05<x<0.25$, respectively), compared with InAs QDs capped by InGaAs/GaAs layers, experience an abnormal variation such as large blue-shift and dramatic decline of PL intensity during annealing process. These results indicate that the optical properties and the crystal qualities of the InAs QDs are greatly dependent on the complex interplay of parameters such as In compositions, positions and thicknesses of InGaAs layers during annealing treatment.

Kp-084 **Dependence of Optical Properties on Temperature in InAs Quantum Dots with Various InGaAs Structures** PARK Ho Jin, KIM Jongho, KIM Do-yeob, KIM Gun Sik, SONG Min Kyeong, CHO Guan Sik, RYU H. H., JEON Minhyon, LEEM Jae-Young, KIM Jin Soo[1], SON J. S.[2](*Inje University, School of Nano Engineering. [1]Chonbuk National University, Division of Advanced*

Materials Engineering. [2]*Kyungwoon University, Department of Visual Optics.*) The dependence of the optical properties on the temperature in self-assembled InAs quantum dots (QDs) with various InGaAs structures, grown by molecular beam epitaxy (MBE), was investigated by photoluminescence (PL). The excited-state transition for the InAs QDs inserted between In-modulation doped combination layers with increasing temperature almost not appeared due to the large energy-level spacing. Temperature-dependent PL shows that the FWHMs of the samples with various InGaAs structures were nearly unchanged with an increase on the temperature up to 200 K, which can be responsible for the linewidth broadening of the QD size distribution and the repopulation process of the thermalized carriers. The thermal activation energy of the electron-hole emission for the InAs QDs with various InGaAs structures was considerably decreased, compared to the InAs QDs without InGaAs layers.

Kp-085 **실리콘 및 사파이어 기판위에 형성된 Eu/O/Si 박막의 결정구조 및 광 특성연구** 김 태근, 김 철민, 김 수진, 신 상훈, 신 영철, 임 시종, 한 철구[1] (*고려대학교 전기전자전파 공학부.* [1]*KETI.*) GaN 기반의 백색 LED(light emitting diodes)는 백열등 및 형광등으로 대표되는 기존의 조명기기들에 비해 80 % 이상의 저 전력 소모와 10~20배 이상의 긴 수명시간을 갖는 장점 등을 바탕으로 하여 차세대 조명기기로 각광받고 있다. GaN 기반의 백색 LED를 만드는 방법 중에서 자외선 LED 위에 삼색(RGB)형광체를 사용하는 방법은 그 형광체의 효율에 따라 LED의 성능이 좌우되는 특징을 갖고 있어 형광체의 효율을 향상시키기 위한 연구가 필요하다. 백색 LED의 형광체로 사용되는 물질 중에서 유로퓸 실리케이트 화합물은 가시광 영역에서 안정적인 광 특성을 갖는다는 장점이 있어 이에 대한 활발한 연구가 진행 중이다. 그러나 실리케이트 화합물의 특성상, 유로퓸 실리케이트의 단결정 성장이 어렵고, EuO와 SiO2를 이용하여 단결정 유로퓸 실리케이트 박막을 성장시키기 위해서는 Eu2SiO4와 EuSiO3는 각각 1800 ℃, 1400 ℃의 높은 온도에서 열처리를 해주어야 하는 문제점들이 있다. 이런 문제점을 해결하기 위해서는 유로퓸 실리케이트에 대한 구조와 특성에 대한 추가적인 연구가 필요하다. 본 논문에서는 R.F. 스퍼터링 법을 이용하여 실리콘과 사파이어위에 증착된 유로퓸 실리케이트 박막의 특성을 X선 회절 패턴(X-ray diffraction Spectroscopy), Auger 전자 분광법(Auger electron spectroscopy), 투과전자현미경(Transmission electron Microscopy), XPS (X-ray Photoelectron Spectroscopy), PL(photoluminescence) 스펙트럼 분석 결과 등을 통하여 결정 구조와 광학적 특성을 조사 하였다.

Kp-086 **Si(111) 기판 위에 성장한 GaN nanorod의 구조적, 광학적 특성분석** 김 문덕, 이 재완, 오 재응[1], 김 송강[2], 정 관수[3], 김 영헌[4](*충남대학교 물리학과.* [1]*한양대학교 전기전자제어계측공학과.* [2]*중부대학교 정보통신 공학과.* [3]*경희대학교 전자공학과.* [4]*한국표준과학연구소.*) III-N 계열 화합물 반도체는 넓은 띠 간격 물질로서 청색, 자외선 광소자 및 고온, 고전압 전자 소자응용이 가능하다. 그 중 GaN nanorod는 충분히 이완된 wurtzite 격자 구조를 갖는다. 본 연구에서는 molecular beam epitaxy 법을 이용하여 Si(111) 기판위에 GaN nanorod를 성장하였으며 scanning electron microscope와 photoluminescence (PL) 및 X-ray diffraction등 을 통하여 구조적, 광학적 특성을 조사하였다. nanorod는 AlN 완충층 위에 성장하였으며 AlN 완충층의 계면 극성에 따라 두 가지 구조로 성장되었다. AlN 완충층 계면이 N-극성일 경우 GaN는 nanorod로 성장되었으며 Ga-극성일 경우 계면에 삽입층이 형성 되었다. 삽입층이 형성된 경우와 형성되지 않은 경우의 PL spectrum은 3.45 eV 부근의 peak 존재와 3.3 eV ~ 3.4 eV 사이의 peak 모양에서 차이를 보인다.

Kp-087 **MBE 법으로 성장된 GaSb 박막의 성장온도에 따른 특성 분석** 김 문덕, 신 윤희, 노 영균, 오 재응[1], 김 동은[1](*충남대학교 물리학과.* [1]*한양대학교 전기전자제어계측공학과.*) Sb 기반 화합물 반도체는 고속전자소자 및 장파장 영역의 광소자 응용이 가능한 물질로서 최근 관심이 집중되고 있는 물질이다. 본 연구에서는 molecular beam epitaxy 법으로 GaAs 기판위에 성장된 GaSb 박막에 대하여 성장온도에 따른 박막 특성을 조사하였다. GaSb 박막의 전기적, 구조적 특성을 Hall 효과 측정, double crystal x-ray diffraction (DCXRD), atomic force microscopy, photoluminescence 등으로 조사하였다. GaSb 박막의 성장온도가 430 ℃ 인 경우 DCXRD 반치폭이 228 arcsec 로 결정성이 가장 좋았다. 또한 성장온도가 500 ℃ 미만에서는 n-GaSb, 500 ℃ 이상에서는 p-GaSb가 성장되었으며 성장온도에 따른 불순물변화에 대하여 논의 하였다.

Kp-088 **InGaN-GaN 발광다이오드의 광특성 향상을 위한 양자우물 하부 구조에 관한 연구** 김 태근, 임 시종, 김 경찬, 김 동호, 이 영수(*고려대학교 전기전자전파공학부.*) 최근 질화물 반도체의 넓은 파장 영역에서의 응용으로 GaN 기반의 레이저 다이오드

(laser diode, LD)나 발광다이오드(light-emitting diode, LED)에 대한 연구가 활발히 수행되고 있다. 이 중 저전력, 고수명, 저가격 및 환경친화성 등과 같은 장점을 갖는 LED 분야에서는 고휘도의 적색, 녹색, 청색 LED가 개발됨으로써 full-color 대형 전광판 뿐만 아니라 LCD(liquid crystal display) 백라이트, 핸드폰, 신호등, 자동차와 더불어 차세대 조명 소자로 주목 받고 있다. 그러나, InGaN/GaN 양자우물 구조는 에너지 밴드 오프셋(energy band offset), 인듐 불균일성(indium non-uniformity), 격자 불일치(lattice-mismatch)로 인한 변형(strain)과 압전장(piezoelectric fields)등과 같은 많은 불확실한 재료 성분(material parameters)을 갖고 있다. 특히, 압전장은 인듐 조성에 따른 변형 정도가 매우 크고, 방출 에너지의 Stark shift를 야기시켜 전위 모양(potential profile)을 깨뜨리고, 광학적 특성을 변형시키기 때문에 이를 감소시키기 위한 연구가 활발히 진행되고 있다. 본 논문은 InGaN-GaN LED의 광특성 향상을 위한 양자우물 하부 구조에 관한 연구로서, 하부구조의 인듐 조성, 두께, 적층 주기에 따른 표면 특성 및 광특성을 조사하였다.

Kp-089 **R-plane 사파이어 기판에 형성된 GaN/InGaN 이종접합구조 형성** 안 형수, 전 헌수, 황 선령, 김 경화, 이 충현, 허 인혜, 홍 상현, 양 민, 김 석환[1], 진 용성[2], 조 인성[2], 이 재학[2], 시 상기[2](*한국해양대학교 나노반도체전공. [1]안동대학교 물리학과. [2]더리즈(주).*) 질화물 반도체의 소자 응용은 현재 양자우물 구조를 이용한 발광소자 (LED : light emitting diode) 제작이 보편화되고 있으며 따라서 비극성 질화물 반도체 박막의 성장은 질화물 양자우물 구조에서 유도되는 분극을 제거하는 가장 중요한 방법으로 인식되고 있다. 분극 현상은 광소자와 전자소자에서 주로 사용되는 이종접합 구조에 있어서 고정전하와 결합하여 소자 내부의 전계를 증가시키고, LED의 활성층으로 많이 이용되고 있는 양자우물 구조에서는 전자와 정공을 분리하여 발광 수명을 감소시킨다. 또한 red shift의 원인이 되며 photon 생성에 있어서도 내부 양자 효율이 크게 낮아지게 된다. 본 연구에서는 HVPE 방법을 이용하여 분극의 영향을 받지 않게 하기 위하여 r-plane 사파이어 기판에 성장온도 변화 (620 ℃에서 820 ℃)에 따른 a-GaN의 구조적인 형상 변화를 관찰하였고, 820 ℃에서 성장된 가장 평탄한 a-GaN 층 위에 GaN/InGaN 이종접합구조를 형성하였다. 이종접합구조는 GaN, InGaN, Mg-doped GaN 층으로 구성되어 있다. 성장방법은 Ga 소스에 In, Mg 등의 금속을 직접 녹여 HCl과 반응시키는 혼합소스 HVPE 방법을 이용하였다. 활성층인 InGaN의 성장온도는 850 ℃이고, 마지막 p-GaN 층은 1050 ℃에서 선택성장 방법을 이용하여 성장하였다. R-plane 사파이어 기판에 성장된 a-GaN의 SEM 측정 결과 성장층의 두께는 대부분의 시료에서 1.4 ㎛ 정도였으며, 5 μm × 5 μm 영역에 대한 AFM (atomic force microscope) 결과에서 RMS (root mean square) 값은 11.5 nm였다. 전극 형성 과정을 거쳐 완성된 GaN/InGaN 이종접합구조는 30 mA의 주입 전류를 통해 EL (electroluminescence)을 측정하였으며, 중심파장은 462 nm 이며 반치폭 (FWHM : full width at half maximum)은 0.67 eV임을 알 수 있었다.

Kp-090 **HVPE 방법에 의해 선택성장된 Si (111) 기판위의 Light-Emitting Diode** 양 민, 이 충현, 황 선령, 김 경화, 전 헌수, 허 인혜, 홍 상현, 안 형수, 김 석환[1], 진 용성[2], 조 인성[2], 이 재학[2], 시 상기[2](*한국해양대학교 나노반도체전공. [1]안동대학교 물리학과. [2]더리즈(주).*) III/V족 질화물 반도체는 높은 열전도도, 강한 기계적 내구성, 화학적 안정성 그리고 우수한 발광 효율 등 많은 장점이 있어 여러 가지 목적의 소자 제작을 위해 이용하려는 연구가 활발하게 진행 되고 있다. 지금까지 반도체 광소자 제작에 있어서 III/V족 질화물 반도체를 성장시키기 위한 기판으로 사파이어나 SiC 기판을 주로 사용하였다. 하지만 사파이어나 SiC 기판은 값이 비싸다는 단점을 가지고 있다. Si 기판과 III/V족 질화물 반도체의 격자상수 및 열팽창계수 차이가 사파이어보다 다소 큼에도 불구하고, III/V족 질화물 반도체의 기판으로써 관심을 모으는 이유는 경제적이고 기존의 Si의 직접회로 공정에 III/V족 질화물 반도체를 쉽게 접목시킬 수 있으며 특성이 우수한 n형, p형 기판을 쉽게 얻을 수 있는 장점이 있기 때문이다. 또한, Si은 열 및 전기 전도도가 사파이어 보다 좋기 때문에 광소자 제작 시 발생하는 열적, 전기적 문제점을 줄일 수 있다. 본 실험에서는 Si (111) 기판 위에 MOCVD 방법으로 GaN를 얇게 성장시킨 후 혼합소스 HVPE 방법을 이용하여 선택성장 (SAG : selective area growth)하여 LED 구조를 성장 시켰다. P형과 n형 도핑물질로서 각각 Mg과 Te을 이용하였으며 클래드층으로 AlGaN 층을 이용하였다. SEM 측정결과 선택성장이 잘 되었음을 알 수 있었고 I-V 측정 결과 turn on 전압은 1 mA에서 3.7 volt 정도이며 저항은 116 Ω 인 특성을 얻었다. 또한, EL 측정 결과 중심파장은 450 nm (1.87 eV)의 특성을 보였다. 이결과로부터 HVPE 방법으로 Si (111) 기판 위에 SAG-AlGaN LED 구조를 제작함으로서 low cost LED chip의 개발 가능성을 확인할 수 있었고 LED 개발 분야에서 경쟁력 강화를 위한 핵심요소 기술의 도출이 가능할 것으로 기대된다.

Kp-091 **Si-doped InGaN 박막의 Si 유량의 변화에 따른 광학적 특성 분석** 정 현, 김 서군, 차 옥

환, 정 문석[1], 변 지수[1], 전 성란[2], 서 은경(*전북대학교 반도체과학기술학과/반도체물성연구소. [1]광주과학기술원 고등광기술연구소. [2]LG전자기술원.*) Quantum well (QW)이나 Super-lattice에 많이 쓰이는 Si-doped InGaN Layer는 높은 Photoluminescence(PL) intensity와 작은 Full Width at Half Maximum (FWHM) 특성을 갖는 것으로 알려져 있다. Si 유량에 따라 달라지는 광학적 요소들을 시분해 발광 특성을 이용하여 그 원인에 대한 접근을 하기 위해 실험을 진행하였다. 본 연구에서는 Metal-Organic Chemical Vapor Deposition (MOCVD)를 이용하여 Sapphire기판 위에 Si-doped InGaN 박막을 성장하였으며, In의 조성비는 11%로 고정하고 이때 Si의 유량을 0.0~1.0sccm 으로 변화시켜주었다. 저온 PL 의 온도 의존성 실험 결과, Si 유량이 많을수록 낮은 온도에서는 확연한 Blue shift 현상을 나타내었다. 또한 Time-Resolved Photoluminescence(TRPL) 측정을 통하여 시간에 따른 발광의 특성변화를 보았으며, 이를 분석하여 Si 유량에 따라 radiative, nonradiative recombination center가 발광에 미치는 영향과 동역학적 성질에 대하여 알아보았다.

*이 논문은 2005년 정부(교육인적자원부)의 재원으로 한국학술진흥재단의 지원을 받아 수행된 연구임(KRF-2005-005-07501)

Kp-092 **혼합소스 HVPE 방법에 있어 성장시간과 소스량의 변화에 따른 에피 특성** 안 형수, 허 인혜, 황 선령, 김 경화, 전 헌수, 이 충현, 홍 상현, 양 민, 김 석환[1], 진 용성[2], 조 인성[2], 이 재학[2], 시 상기[2](*한국해양대학교 나노반도체전공. [1]안동대학교 물리학과. [2]더리즈(주).*) 기존의 HVPE 장치를 이용한 결정 성장은 일반적으로 Ga 소스와 도펀트 소스를 각각 분리하여 장착하는 방법을 사용하기 때문에 장치가 복잡해지고 비용이 많이 드는 문제점이 있다. 그러나 혼합소스 HVPE 방법을 사용하면 Ga 소스에 도펀트를 직접 넣어 포화상태로 만들어 사용하기 때문에 장치가 간단해지며 비용이 적게 드는 장점이 있다. 또한 다양한 도펀트를 사용할 수 있어 n형, p형, 3원 화합물 또는 4원 화합물의 에피성장이 가능하다. 혼합소스 HVPE 방법은 처음 넣은 소스량의 성장 시간이 증가할수록 소스의 변화량에 따라 에피 특성이 변할 수 있는 점이 단점으로 지적되어 왔다. 따라서 본 실험에서는 이러한 것을 고찰하기 위하여 혼합소스에 도펀트를 혼합하여 성장시간에 따른 에피의 도펀트 변화를 관찰하였으며 관측량으로 캐리어 농도를 조사하였다. 한편, Te은 GaAs 화합물 반도체의 n형 도펀트로 가장 많이 사용되는 물질 중의 하나이고, Te이 n형 도펀트로 작용할 때 Si은 3족 원소의 위치에 채워지는 반면에 5족 원소의 자리에 채워지기 때문에 Te이 Si에 비하여 좀 더 효율적으로 도펀트의 역할을 할 수 있다. 따라서 본 연구에서는 캐리어 농도 관찰을 용이하게 하기 위해 n형 도펀트를 이용하였으며 n형 도펀트 중 Te을 사용하여 그 캐리어 농도의 변화를 조사하였다. 모든 실험에서 캐리어 가스로는 N_2를 사용하였고 Te-doped GaN의 성장을 위한 소스 영역의 온도는 900℃ 이며 성장 영역의 온도는 1090℃ 로 유지하였다. 한번 만든 혼합소스로 15개의 시료를 만들었으며 성장된 Te-doped GaN 층은 Hall측정을 하였다. Hall측정에 사용되는 접합에 필요한 전극으로는 In이 사용되었다. 실온에서 Hall측정을 한 결과, n형 전도성을 가지며 sheet 캐리어 농도는 성장시간의 변화에 의해 1.60×10^{14} 에서 3.98×10^{14} /㎠의 범위를 가졌으며 평균 캐리어 농도는 2.66×10^{14} /㎠ 로 조사되었다. 15개의 시료의 총 성장시간은 140분으로 이 시간동안 변화된 캐리어 농도의 변화는 평균 sheet 캐리어 농도에 대해 +1.5 %, -0.6 % 였으며 이 결과 혼합소스 HVPE 방법에 있어 성장시간이 길어질수록 의문시 되었던 에피 특성에는 큰 변화가 없는 것으로 판단된다. 따라서 혼합소스 HVPE 방법은 다양한 성장층을 만들 수 있는 매우 유용한 방법이라고 판단된다.

Kp-093 **GaAs 양자점의 캐리어동력학 연구** 김 종수, 변 지수, 정 문석, 고 도경, 이 종민, 조 남기[1], 박 성준[1], 송 진동[1], 최 원준[1], 이 정일[1](*광주과학기술원 고등광기술연구소. [1]한국과학기술연구원 나노소자연구센타.*) 본 연구에서는 최근 연구되고 있는 droplet 방식으로 AlGaAs (100)면 위에 성장된 GaAs 양자점의 캐리어 동력학을 시분해 photoluminescence (PL) 방법으로 연구하였다. GaAs 양자점의 구조적 특성은 atomic force microscope (AFM)을 이용하여 연구하였으며, 광학적 특성은 펨토초 레이저 (fs-laser)를 이용한 PL 및 시분해 PL (TR-PL)로 분석 하였다. GaAs 양자점의 캐리어동력학은 일반적인 InAs 양자점과 비교하여 분석하였으며, 특히 양자점의 크기에 따른 캐리어수명 시간의 변화를 관측하여 비교분석 하였다.

Kp-094 **Roughened surface LED 구조의 근접장 발광특성 연구** 차 옥환, 정 현, 정 흥섭[1], 정 문석[2], 홍 창희, 서 은경(*전북대학교 반도체물성연구소. [1]LG 이노텍. [2]광주과학기술원 고등광기술연구소*) 본 연구에서는 발광효율을 향상시키기 위한 textured LED 구조의 근접장 발광특성분석을 하였다. 벌집모양 패턴을 형성시킨 sapphire 기판 위에 LED 구조를 성장하였고 그 표면인 p-GaN 층 위를 역피라미드 구조로 마무리하였다. 이러한 patterned sapphire 위에 성장된 textured LED 구조는 빛의 내부 반사와 산란을 감소시키고, 역피라미드 구조에 의해 효과적으로 threading dislocation density가

줄어 carrier를 속박시킴으로써 LED 의 발광효율을 향상시켰다. 또한 시료의 defect 형성에 따른 공간적 발광특성 분포를 알아보기 위하여 UV 근접장 나노광학현미경 (UV-NSOM) 을 이용한 근접장 발광특성분석을 수행하였다. textured 구조에 의한 threading dislocation 분포와 성장된 양자우물의 위치에 따라 공간적 발광분포특성이 관찰되었으며, band-edge와 defect 관련 yellow 발광 스펙트럼을 관찰할 수 있었다.

Kp-095 **Investigations on the Post-Annealing Effects on the Opto-Electronic Properties of Low-Temperature grown GaAs** YOUN Doo-Hyeb, KANG Chul[1], RYU Han-Chul, LEE Seung-Hwan, YOON Suck-Hwang[2], KIM Gil-Ho[2], KANG Kwang-Yong(*ETRI. [1]APRI. [2]SKKU.*) The influence of a post-growth annealing, in the low-temperature grown GaAs (LT-GaAs), on carrier lifetime, structural change of LT-GaAs and coarsening of As-clusters was investigated using high-resolution transmission electron microscopy and photoluminescence. We have studied the structural change and electrical properties such as lattice mismatch and resistance in LT-GaAs. The excess arsenic concentration of LT-GaAs has been determined by the analysis of the intensity and a satellite reflection along with a peak shift of the X-ray Bragg reflection. A systematic study of as-grown and post-growth annealed LT-GaAs, reveals carrier lifetime to be directly related to the excess As incorporation and anneal temperatures. The electrical resistance of LT-GaAs of the LT-GaAs increases with increasing annealing temperature. Post-growth annealing temperature was optimized and terahertz (THz) radiation was generated with photoconductive antennas has been fabricated on low-temperature grown GaAs. THz radiation was not generated at the annealing temperature above 700 °C.

Kp-096 **MOCVD를 이용하여 성장한 InGaN MQWs의 Barrier 두께에 따른 특성분석** 윤 지연, 우 시관, 오 병성(*충남대학교 일반대학원 물리학과.*) InGaN는 에너지 갭이 0.7~3.4 eV 사이의 값을 가진 직접 천이형 반도체이다. 이 물질은 가시광선 영역에서 발광소자, 검출기 및 레이저 다이오드 등으로 사용이 가능하다. 본 연구에서는 GaN 박막위에 InGaN MQWs을 성장하여 XRD 와 PL을 이용하여 박막의 특성을 관찰하였다. MOCVD를 이용하여 사파이어 기판위에 GaN 박막(2 um)를 성장한 후에 InGaN를 성장하였다. 이때 TMGa(7 umol), TMIn(30 umol)로 고정시킨 후 Gan의 barrier 두께를 변화시켜 $In_xGa_{1-x}N$ 시료를 성장하였다. 구조적 특성을 분석하기 위해서 XRD와 고분해능 XRD를 이용하여 시료의 특성을 분석하였다. GaN buffer layer의 XRD 반치폭은 420 arcsec으로 양질의 박막을 얻었으며 그 위에 InGaN을 성장하였다. HRXRD를 이용하여 조성비를 구하였고, MQWs 구조를 관찰할 수 있었다. 또한 저온 PL을 측정하여 InGaN MQWs의 barrier 두께 변화에 따라 밴드관련 피크가 변화해가는 것을 관찰할 수 있었다.

Kp-097 **Growth of GaN Thin Films without Low-temperature Buffer Layers by Hydride Vapor Phase Epitaxy** LEE Sanghwa, CHOE Hyeokmin, OH Taegeon, JEAN Jai Weon, SOHN Yuri, KIM Chinkyo (*Kyunghee University, Dept. of Physics.*) GaN thin films were grown without low-temperature buffer layers by hydride vapor phase epitaxy. Initially nucleated islands on a sapphire substrate merged and no immediate smoothening of the surface was observed. The surface morphology evolved in a different way from that of GaN films grown with low-temperature buffer layers, but the surface was eventually smoothened. The roles of microstructural defects in islands-merging will be discussed.

Kp-098 **Formation of Nitride Nucleation Layers during Nitridation of Sapphire with In Coflow** JEAN Jai Weon, LEE Sanghwa, CHOE Hyeokmin, OH Taegeon, SOHN Yuri, KIM Chinkyo(*Kyunghee University, Dept. of Physics.*) Sapphire substrate was nitridated with an In flow and the formation of nitride nucleation layers was investiaged by utilizing synchrotron x-ray scattering. Depending on the amount of In flow, different nitride nucleation layers were observed. Reciprocal space map revealed an In-flow-dependent strain of nitride nucleation layers.

Kp-099 **Optical Investigation of Quaternary AlInGaN Epilayers and Multiple Quantum Wells grown by a Pulsed Metalorganic Chemical Vapor Deposition** RYU Mee-Yi, CHEN C. Q.[1], KHAN M. Asif[1](*Kangwon National University, Department of Physics. [1]University of South Carolina, Department of Electrical Engineering.*) The recombination mechanisms and optical properties of quaternary AlInGaN epilayers and AlInGaN/AlInGaN multiple quantum wells (MQWs) grown by a novel pulsed metalorganic chemical vapor deposition (PMOCVD) have been investigated by photoluminescence (PL) and

time-resolved PL (TRPL) measurements. The PMOCVD grown AlInGaN samples exhibits a stronger PL intensity, larger blueshift and linewidth broadening with excitation density, and faster decay time with emission energy than those for conventional MOCVD grown AlInGaN samples. These results indicate that the PMOCVD grown AlInGaN samples have more band-tail states than conventional MOCVD grown quaternary samples, which is beneficial to obtain a strong spontaneous emission for UV LEDs. The observed optical properties of PMOCVD grown AlInGaN materials agree well with those in InGaN materials for blue/green LEDs. This indicates that PMOCVD grown quaternary AlInGaN systems are promising materials for the active region of high power deep UV LEDs.

Kp-100 **Self-alignment of GaN Nanograins on Miscut Sapphire Substrates** CHOE Hyeokmin, LEE Sanghwa, JEAN Jai Weon, OH Taegeon, SOHN Yuri, KIM Chinkyo(*Kyunghee University, Dept. of Physics.*) GaN nanograins were grown on a miscut sapphire substrate by hydride vapor phase epitaxy and their alignment behavior was investigated by utilizing synchrotron x-ray scattering. The GaN nanograins were observed to be aligned along the miscut direction, but there was no ordering along the perpendicular direction. Step-induced ordering of nanograins can be used for positioning of nanostructures.

Kp-101 **Photocatalysis of GaN nanowires** 정혜성, 홍 영준[1], LI Yirui, 이 규철[1](*POSTECH, 환경공학부. [1]POSTECH, 신소재공학과.*) GaN is a well-known wide bandgap semiconductor material that means GaN materials can be used as a photocatalyst. Moreover its high flat-band potenail has an advantage for reducing water because photogenerated electrons in the conduction band must have high reduction portential. This material is chemically stable, it implies that GaN can be used even in harsh industrial process. Furthermore by making GaN nanostructured, improved photocatalytic effect has been achieved due to high surface to volume (S/V) ratio. Here we report that GaN nanowires can be a good photocatalyst under harsh conditions. These nanowires were prepared by catalyst-assisted metal-organic chemical vapor deposition (MOCVD) technique. After the growth, photocatalytic effects of GaN nanowires were investigated at different pH conditions in dye-solution. Here UV lamp was used as an optical excitation source. Later, the concentration of the dissolved dye was measured by ultraviolet/visible (UV/VIS) absorption spectroscopy in order to detect the amounts of pollutants degraded during UV light illumination. In the present research investigation of the photocatalytic effect of GaN nanowires at various pH conditions will be carried out. Also report will be made on the enhancement of the photocatalytic effect by using GaN nanowires rather than thin films.

Kp-102 **Anomalous Magnetotransport In AlGaAs/GaAs Double Quantum Well System** YOON Seok Hwang, KANNAN E. S.[1], KIM Gil-Ho[2](*성균관대학교, 정보통신공학부. [1]성균관대학교, 나노과학기술학부. [2]성균관대학교, 정보통신공학부, 성균나노과학기술원.*) We report anomalous magnetotransport in AlGaAs/GaAs double quantum well system (DQW). A novel magnetoresistance oscillation was observed along with the conventional SdH oscillation when the DQW was in single layer configuration. The amplitude of this novel oscillation was found to decrease with increasing magnetic field. No such anomalies are observed when the system evolves into a bilayer. As the carrier densities in the quantum wells are balanced, well developed quantum Hall states appears at anomalous filling factor with a corresponding minima in longitudinal resistivity. These observations are explained on the basis of the predicted existence of electronic mini-bands with mini energy gaps due to the modulation of electron wavefunction by the periodic potential of the DQW.

Kp-103 **Synthesis and Electrical Properties of Catalyst-free Single Crystalline Indium Nitride Nanowire** LEE Sunghun, KIM Jinhee[1], KIM bongsoo[2](*Interdisplinary program for nano science and technology, KAIST. [1]Leading-Edge Technology Group, KRISS. [2]Department of Chemisty, KAIST.*) InN nanowires were synthesized using VS(vapor-solid) method without catalysts. A one-zone chemical vapor deposition technique was used to grow single crystalline InN nanowire under the proper conditions. Scanning electron microscopy showed nanowires with diameters of 40 ~ 60 ㎚ and lengths of 5 ~ 20 ㎛, respectively. The nanowires have coarse morphology. High resolution transmission electron microscopy shows that the as-synthesized InN nanowires grow along the [001] direction with high crystallinity. Nanodevices of

InN nanowire, including source-drain-gate channel, were fabricated by e-beam lithography. I-V characteristics show a linear plot from room temperature to 50 K. Such ohmic I-V characteristics of InN nanowire is consistent with the lower bandgap, 0.65~0.8eV, rather than other Ⅲ-Ⅴ materials. Below 50 K, the device shows typical n-type semiconductor behavior.

Kp-104 **Demonstration of a Two Color 320 x 256 Quantum Dots-in-a-Well Focal Plane Array** 이 상준, 김 준오, 노 삼규, 최 정우[1], KRISHNA Sanjay[2](*한국표준과학연구원. [1]경희대학교. [2]University of New Mexico.*) Infrared photodetectors based on intersubband transitions in nanoscale self assembled quantum dots continue to show potential due to their inherent sensitivity to normally incident light, broad spectral response range, potential for low dark current and long carrier lifetimes due to reduced electron-phonon scattering. As a result of these promising attributes, coupled with the potential for high yield manufacturing processes based on a mature GaAs technology, QD based detectors continue to attract the interest of the infrared detection research community. In the Quantum dots-in-a well (DWELL) heterostructure, InAs quantum dots are placed in a thin InGaAs quantum well that is in turn placed in a GaAs matrix, and the growth issues and the structural and optical characterization techniques were discussed. Two-color DWELL detectors, operating at 78K, with spectral response in the MWIR (λ_{p1} ~ 5㎛) and LWIR (λ_{p2} ~ 10 ㎛) regime have been fabricated in our study. The DWELL QDIP also were fabricated into 320 x 256 focal plane array (FPA) with Indium bumps using standard lithography at UNM. The FPA was hybridized to an Indigo 9705 read-out integrated circuit (ROIC) in collaboration with QmagiQ and tested with a CamIRa^{TM} system manufactured by SE-IR Corp. We have demonstrated that we can operate the device at an intermediate bias (V_b=-1.25 V) and obtain the infrared image of a 300K objecte from the same QD based FPA at 60K.

Kp-105 **GaN LED 전기적 특성 향상을 위한 낮은 결함의 InGaN/GaN MQW 성장** 신 영철, 임 시종, 김 태근, 김 희동, 서 호원(*고려대학교.*) GaN 기반의 LED(light emitting diodes)는 back-lighting과 차세대 조명기기로 각광받고 있으며, 현재 GaN LED 소자의 특성 향상을 위한 연구가 활발히 진행되고 있다. GaN LED는 InGaN/GaN MQW(multiple quantum well)의 활성층으로 구성되어져 있으므로 이러한 활성층에서 결함의 감소가 소자의 특성에 상당한 영향을 주게 된다. 본 연구는 이러한 InGaN/GaN MQW 활성층의 결함 감소를 위하여 성장 온도 및 carrier gas 등의 영향을 연구하였다. 소자의 광 특성 및 구조적 특성은 Photoluminescence 장치 및 원자탐침현미경(atomic force microscope)으로 조사하였으며, 또한 LED 소자의 전기적 및 광 특성을 조사하였다.